

# **The contribution of drug resistant cancer stem cells to paediatric brain tumours**

By

Wiyada Punjaruk, MD.

Thesis submitted to the University of Nottingham  
for the degree of Doctor of Philosophy

October 2010

## Abstract

**Introduction:** Recent studies have revealed that cancer stem cells (CSCs) exist in malignant disease. Additionally, it is proposed that these cells may survive following chemotherapy, and hence contribute to tumour relapse. A significant mechanism of drug resistance in CSCs is believed to be the expression of ATP-binding cassette (ABC) transporters that efflux cytotoxic agents out of cells. The objective of this study was to study the existence of CSCs in a panel of primary paediatric brain tumours (PBTs) and to determine if these were drug resistant via functional ABC transporters.

**Materials and Methods:** The main cell lines characterised were: EPN-2 (primary ependymoma); MED-2 (recurrent medulloblastoma); SPNET-1 [primary CNS primitive neuroectodermal tumour (CNS PNET)]; and a commercial CNS PNET (PFSK-1). Basic characterisation of our cell lines were assessed by Telomeric Repeat Amplification Protocol (TRAP) assay, Terminal Restriction Fragments (TRF) assay, metaphase spread analysis and doubling time. To determine the proportion of cancer stem-like cells in the parental cell lines, CD133 and SOX2 co-staining immunofluorescence was performed and validated by Western blotting analysis. The expression of ABC transporters (ABCB1, ABCC1 and ABCG2) was also investigated by co-staining for CD133 and ABC transporters using immunofluorescence and Western blotting analysis. Flow cytometry was performed to examine ABCB1 function. Four clinically relevant drugs (etoposide, cisplatin, irinotecan and methotrexate) were used to assess the degree of drug resistance of these lines. Clonogenic assay and neurosphere formation assay were then performed to investigate colony survival and the ability of cells to form neurospheres, respectively, after drug treatment. Finally, the potential to increase chemosensitivity by drug treatment in the presence of the ABCB1 inhibitor, Verapamil, was assessed.

**Results:** Basic characterisation results demonstrated that a high level of telomerase activity and maintenance of telomere length was found in all cell lines (grown both as monolayers

and neurospheres). Metaphase spread analysis showed a wide range of aberrant chromosome numbers in PFSK-1 cells whereas our cell lines demonstrated a more stable chromosome number. Neurospheres grew slower than monolayers and monolayers had constant growth rate with increasing passage number. It was found that for each cell line, a small subpopulation (8-12%) of cultured monolayer cells are positive for both CD133 and SOX-2 immunofluorescent staining whilst cultured neurospheres contained 35-45% of co-stained cells. No co-stained cells were identified in the commercial PFSK-1 line and these findings were consistent with the results from Western blotting analysis. Approximately 10% of the parental cell lines comprised cells co-expressing CD133 and ABCB1 or ABCC1 at a low level whilst none of our cell lines were positive for ABCG2. Additionally, the parental cell lines contained a small proportion of cells expressing functional endogenous ABCB1 ( $34 \pm 5.2\%$  in EPN-2,  $26.5 \pm 3.9\%$  in MED-2 and  $13.9 \pm 3.2\%$  in SPNET-1). During multiple rounds of drug treatment, ABCB1 was consistently expressed at a high level throughout and the proportion of functional ABCB1 expressing cells increased in all cell lines almost 2 fold compared to the parental cell lines and the selected control sublines. Whilst ABCC1 expression was gradually upregulated after multiple rounds of treatment but ABCG2 expression remained negative. Drug combined with Verapamil treatment significantly decrease survival rate approximately 5 fold compared to drug treatment alone although the majority of surviving cells were still CD133 and ABCB1 positive.

**Conclusion:** Newly established paediatric cell lines (EPN-2, MED-2 and SPNET-1) represented significant histological and biological features of the original tumours from which they were derived and were stable in standard culture condition for a prolonged period of time. The parental cell lines contained a small proportion of cells expressing endogenous functional ABCB1 at a low level indicating intrinsic drug resistance. After multiple rounds of drug treatment, ABCB1 was the major mechanism of drug resistance in our cell lines. ABCC1 were upregulated later in our cell lines after multiple rounds of drug treatment whereas none of our cell lines expressed ABCG2 during drug treatment.

## Declaration

Except where acknowledged in the text, I declared that this thesis is my own work and is based on research that was undertaken by me in the School of Clinical sciences, Faculty of Medicine and Health Sciences, University of Nottingham during the period 19<sup>th</sup> March 2007 to 29<sup>th</sup> July 2010. Figures obtained from books/papers or results obtained from Dr. Deema Hussein are listed below.

1. Figure 1.1 obtained from McLendon, R.E. *et al*, chapter 3 Ependymal tumours, WHO book (2007)
2. Figure 1.2 obtained from Giangaspero, F. *et al*, chapter 8 Embryonal tumours, Medulloblastoma, WHO book (2007)
3. Figure 1.3 obtained from McLendon, R. E. *et al*, chapter 8 Embryonal tumours, CNS PNET, WHO book (2007)
4. Figure 1.4 obtained from Reifenberger, G. *et al*, chapter 2 Oligodendroglial tumours, WHO book (2007)
5. Figure 1.5 obtained from Kleihues, P. *et al*, chapter 1 Astrocytic tumours, WHO book (2007)
6. Figure 1.6 obtained from Joel, S. (1996)
7. Figure 1.9 and 1.10 obtained from Cepeda, V. *et al* (2007)
8. Figure 1.11 obtained from Smith, N. F. *et al* (2006)
9. Figure 1.12 obtained from Genestier, L. *et al* (2000)
10. Figure 1.13, b obtained from Kos, V. and Ford, R. C. (2009)
11. Figure 1.15 obtained from Ravna, A. W. *et al* (2009)
12. Figure 1.19 and 1.23 obtained from Dean, M. *et al* (2005)
13. Figure 1.21 obtained from Shmelkov, S. V. *et al* (2005)
14. Figure 1.22 obtained from Visvader, J. and Lindeman, G. J. (2008)
15. Figure 3.3 (EPN-1, MED-1, BT-4 and Olig-1) performed by Dr. Deema Hussein
16. Figure 3.4 performed by Dr. Deema Hussein
17. Figure 4.11 performed by Dr. Deema Hussein

**NAME:**

**(Wiyada Punjaruk)**

**ID NUMBER: 4046537**

**DATE: 20<sup>th</sup> October 2010**



## Acknowledgements

First of all, I would like to acknowledge the Royal Thai government that gave me a valuable opportunity to study PhD in England and fully supported me for a whole 4 years although I have to support myself for additional 6 months with difficulties to complete my study. I also would like to thank the Faculty of Medicine, Khon Kaen University, that allow me to leave for study and still hold the position for me.

Importantly, I would like to gratefully acknowledge my supervisor, Dr. Beth Coyle, for all of her support in academic knowledge and research process including mental support, which importantly helped me to stay on this tract. Thanks for her patience with me and her hard work on proving my thesis. I would also like to thank my second supervisor, Dr. Ian Kerr, who always gives me valuable suggestion for my project and helpful correction for my thesis. I would like to thank Dr. Deema Hussein who taught and helped me many techniques at the beginning of my study, Dr. Lisa Storer who helped me throughout my study and positively encourage me during my writing up period and Dr. Ruman Rahman who helped me to set up TRAP and TRF assays. I specifically thank everybody in our group who are very kind and generous, and always give me a good friendship. They also shared their opinion and experience with my difficult situations and sad emotion during my study.

Finally, I would like to delightfully acknowledge my parents, sisters and brothers who always inspire and encourage me to carry on my study, help me every single thing whatever I want and patiently wait for me to come back. Thanks my mother and my sister, P' Noo-Gaw, who daily talk to me and make me feel close to them. Particularly, I would like to thank my special sister, Dr. Pawitra Pulbutr, who is friend, sister, consultant and mother (sometimes), look after me and always share my sadness and happiness. We together passed through many situations in UK both difficulties with tears and happiness with laughing. Without her, I cannot imagine how I can survive here in this lonely country. Thanks for her encouragement throughout my study and during my writing up period.

## Contents

### TITLE

### ABSTRACT

### ACKNOWLEDGEMENTS

### CONTENTS LISTING

<b>Table of Contents</b>	
<b>List of Illustrations</b>	
<b>List of Tables</b>	
<b>List of Appendices</b>	
<b>List of Abbreviations</b>	

<b>CHAPTER 1: GENERAL INTRODUCTION</b>	1-73
<b>1.1 Paediatric brain tumours</b>	3-22
1.1.1 Ependymoma	7
1.1.2 Embryonal tumours	10
1.1.2.1 Medulloblastoma	10
1.1.2.2 Central nervous system (CNS) primitive neuroectodermal tumour (CNS PNET)	14
1.1.3 Oligodendroglioma	16
1.1.4 Glioblastoma multiforme (GBM)	18
<b>1.2 Chemotherapeutic treatment of paediatric brain tumours</b>	23-38
1.2.1 Etoposide	24
1.2.2 Cisplatin	39
1.2.3 Irinotecan	32
1.2.4 Methotrexate	35
<b>1.3 ATP-binding cassette (ABC) transporters</b>	38-54
1.3.1 ABCB1 (MDR1/ P-glycoprotein)	40
1.3.2 ABCC1 (MRP1)	45
1.3.3 ABCG2 (BCRP/ MXR/ ABCP)	49
1.3.4 Substrates and inhibitors of ABCB1, ABCC1 and ABCG2 transporters	52
<b>1.4 Cancer stem cells (CSCs)</b>	54-71
1.4.1 Normal stem cells and cancer stem cells	55
1.4.2 Discovery of cancer stem cells	55
1.4.3 Identification of cancer stem cells	57
1.4.3.1 CD133	59
1.4.3.2 SOX2	64
1.4.4 The model for tumour heterogeneity and propagation	67

1.4.5	Cancer stem cells and drug resistance.....	69
-------	--	----

<b>1.5</b>	<b>What is the contribution of drug resistant CSCs to paediatric brain tumours?.....</b>	<b>71-73</b>
------------	--	--------------

## **CHAPTER 2: MATERIALS AND METHODS..... 74-112**

<b>2.1</b>	<b>Cell culture.....</b>	<b>75-79</b>
------------	--------------------------	--------------

2.1.1	Cell recovery from liquid nitrogen.....	76
2.1.2	Deriving neurospheres from monolayers.....	76
2.1.3	Subculturing cells.....	77
2.1.3.1	Monolayers.....	77
2.1.3.2	Neurospheres.....	77
2.1.3.2.1	Using TrypLE™ select.....	77
2.1.3.2.2	Using mechanical dissociation.....	77
2.1.4	Snap freezing cells.....	78
2.1.4.1	Snap frozen cells for general proposes.....	78
2.1.4.2	Snap frozen cells for microsomal membrane extraction.....	78
2.1.4.2.1	Attached cells.....	78
2.1.4.2.2	Neurospheres.....	78

<b>2.2</b>	<b>Immunofluorescence assay.....</b>	<b>79-82</b>
------------	--------------------------------------	--------------

2.2.1	Immunofluorescent staining of monolayers.....	79
2.2.1.1	Plating monolayer cells on chamber slides.....	79
2.2.1.2	0.4% Paraformaldehyde (PFA) fixation.....	79
2.2.1.3	Single immunofluorescent staining.....	79
2.2.2	Immunofluorescent staining of neurospheres.....	80
2.2.2.1	0.4% Paraformaldehyde (PFA) fixation.....	80
2.2.2.2	Cryostat sectioning of neurospheres.....	81
2.2.2.3	Single immunofluorescent staining.....	81
2.2.3	Double immunofluorescent staining.....	81
2.2.4	Image processing.....	82

<b>2.3</b>	<b>Western blotting analysis.....</b>	<b>82-88</b>
------------	---------------------------------------	--------------

2.3.1	Protein extraction.....	82
2.3.1.1	Standard method for protein extraction from cell pellets.....	82
2.3.1.2	Isolation of microsomal membrane from cell pellets...	83
2.3.1.3	Total cell lysate.....	83
2.3.2	Protein quantification (Bradford assay).....	83
2.3.3	Preparation of Polyacrylamide gel electrophoresis (PAGE).....	84

2.3.4	Sample preparation for gel electrophoresis.....	85
2.3.5	Protein transfer to membrane.....	85
2.3.6	Ponceau staining.....	86
2.3.7	Primary and secondary antibody treatment.....	86
2.3.8	ECL detection.....	87
<b>2.4</b>	<b>DNA extraction.....</b>	<b>88-89</b>
2.4.1	DNA extraction from frozen cell pellets.....	88
2.4.2	DNA extraction from live cell pellets.....	89
<b>2.5</b>	<b>Terminal restriction fragment (TRF) assay or telomere length assay.....</b>	<b>89-92</b>
2.5.1	DNA digestion.....	89
2.5.2	TRF gel electrophoresis.....	90
2.5.3	Denature of DNA.....	90
2.5.4	TRF Southern blot.....	90
2.5.5	Hybridization.....	91
2.5.6	Washing, blocking and anti-DIG-AP treatment.....	91
2.5.7	Detection.....	91
2.5.8	Substrate treatment.....	91
<b>2.6</b>	<b>Haematoxylin and Eosin (H&amp;E) staining.....</b>	<b>92</b>
<b>2.7</b>	<b>Telomere repeat amplification protocol (TRAP) assay.....</b>	<b>92-94</b>
2.7.1	Protein extraction.....	92
2.7.2	Protein quantification.....	93
2.7.3	Addition and amplification of telomere repeats by telomerase.....	93
2.7.4	Telomerase detection.....	94
2.7.5	Quantification of telomerase activity.....	94
<b>2.8</b>	<b>Metaphase spread analysis.....</b>	<b>95</b>
2.8.1	Nocodazole treatment.....	95
2.8.2	Preparation of metaphase spreads from cell culture.....	95
2.8.3	Slide preparation.....	95
<b>2.9</b>	<b>Clonogenic assay.....</b>	<b>96-98</b>
2.9.1	Optimisation of cell density in monolayer cells.....	97
2.9.2	Drug treatment.....	97
2.9.2.1	Plating cells.....	97
2.9.2.2	Drug treatment.....	98
2.9.3	Fixation and counting.....	98
2.9.4	Derivation of IC <sub>50</sub> .....	98
<b>2.10</b>	<b>Cells co-expressing CD133 and ABC transporters detected by FACS analysis.....</b>	<b>99-101</b>
2.10.1	Harvesting cells.....	99
2.10.1.1	Monolayer cells.....	99

2.10.1.2	Neurospheres.....	99
2.10.2	Fixation.....	100
2.10.3	Blocking.....	100
2.10.4	Co-staining immunofluorescence by FACS.....	100
2.10.4.1	Primary antibody treatment.....	100
2.10.4.2	Secondary antibody treatment.....	100
2.10.5	Analysis.....	101
<b>2.11</b>	<b>Functional ABCB1 analysis by FACS.....</b>	<b>101-103</b>
2.11.1	Harvesting cells.....	101
2.11.2	Substrate, inhibitor and primary antibody treatment.....	102
2.11.3	Secondary antibody treatment.....	103
2.11.4	Analysis.....	103
<b>2.12</b>	<b>ABCB1 RNAi transfection.....</b>	<b>103-105</b>
2.12.1	Plating cells for transfection.....	103
2.12.2	ABCB1 SiRNA transfection.....	104
<b>2.13</b>	<b>RNA extraction.....</b>	<b>105-106</b>
2.13.1	Dissociation of nucleoprotein complex.....	105
2.13.2	RNA extraction.....	106
2.13.3	RNA precipitation.....	106
2.13.4	RNA washing.....	106
<b>2.14</b>	<b>Reverse transcriptase polymerase chain reaction (RT-PCR).....</b>	<b>106-108</b>
2.14.1	DNase treatment.....	106
2.14.2	Primer annealing and reverse transcription (cDNA synthesis).....	107
2.14.3	Polymerase Chain Reaction (PCR).....	107
2.14.4	Gel electrophoresis.....	108
<b>2.15</b>	<b>Clonogenic assay: drug treatment combined ABCB1 inhibitor.....</b>	<b>108-112</b>
2.15.1	Plating cells for treatment.....	108
2.15.2	Drug treatment.....	110
2.15.3	Harvesting cells.....	110
2.15.3.1	Colony counting.....	111
2.15.3.2	Cytospin for co-staining immunofluorescence.....	111
2.15.3.3	Neurosphere formation assay.....	112

## **CHAPTER 3: BASIC CHARACTERISTICS OF THE PRIMARY CULTURED PAEDIATRIC CELL LINES AND THEIR ORIGINAL TUMOURS..... 113-131**

<b>3.1</b>	<b>Introduction.....</b>	<b>114-115</b>
<b>3.2</b>	<b>Results.....</b>	<b>116-123</b>

3.2.1	Descriptive data of all primary cultured paediatric and commercial cell lines.....	115
3.2.2	Histopathological features of the original tumours from which 7 cell lines derived.....	118
3.2.3	Metaphase spread analysis.....	122
<b>3.3</b>	<b>Discussion.....</b>	<b>124-131</b>
<b>CHAPTER 4: CHARACTERISATION OF CANCER STEM CELLS.....</b>		<b>132-168</b>
<b>4.1</b>	<b>Introduction.....</b>	<b>133-135</b>
<b>4.2</b>	<b>Results.....</b>	<b>136-154</b>
4.2.1	Primary cultured monolayers and neurospheres of paediatric brain tumour cell lines at early, middle and late passage.....	136
4.2.2	Doubling time.....	138
4.2.3	CD133 and SOX2 co-staining immunofluorescence analysis.....	143
4.2.4	CD133 and SOX2 expression detected using Western blotting analysis.....	148
4.2.5	Telomeric Repeat Amplification Protocol (TRAP) assay.....	150
4.2.6	Terminal Restriction Fragments (TRF) assay or telomere length assay.....	153
<b>4.3</b>	<b>Discussion.....</b>	<b>155-168</b>
<b>CHAPTER 5: IDENTIFICATION AND FUNCTIONAL ANALYSIS OF ABC TRANSPORTERS IN THE PARENTAL CELL LINES.....</b>		<b>169-196</b>
<b>5.1</b>	<b>Introduction.....</b>	<b>170-172</b>
<b>5.2</b>	<b>Results.....</b>	<b>173-191</b>
5.2.1	Co-staining ABC transporters and CD133 immunofluorescence analysis.....	173
5.2.2	Detecting cells co-stained ABC transporters and CD133 by FACS.....	180
5.2.3	ABC transporters expression detected by Western blotting analysis.....	185
5.2.4	Functional analysis of ABC transporters by FACS.....	188
<b>5.3</b>	<b>Discussion.....</b>	<b>192-196</b>
<b>CHAPTER 6: DRUG TREATMENT SELECTED RESISTANT SUBLINES EXPRESSING ABC TRANSPORTERS .....</b>		<b>197-232</b>
<b>6.1</b>	<b>Introduction.....</b>	<b>198-199</b>
<b>6.2</b>	<b>Results.....</b>	<b>201-223</b>
6.2.1	Condition optimised by clonogenic assay.....	201
6.2.2	Neurosphere formation assay after drug treatment.....	203
6.2.3	Immunofluorescence analysis in the parental cell lines after the first round of drug treatment.....	207

6.2.4	Drug treatment selected resistant sublines for downstream drug resistance analysis.....	215
6.2.5	Cellular morphologies of the selected sublines after the multiple rounds of drug treatment.....	216
6.2.6	Co-staining immunofluorescence analysis in the selected sublines after multiple rounds of drug treatment (< 10 and > 10 passages).....	218
6.2.7	The expression of ABC transporters examined by Western blotting analysis.....	220
<b>6.3</b>	<b>Discussion.....</b>	<b>224-232</b>
<b>CHAPTER 7: FUNCTIONAL ANALYSIS ON SELECTED RESISTANT SUBLINES.....</b>		<b>233-271</b>
<b>7.1</b>	<b>Introduction.....</b>	<b>234-235</b>
<b>7.2</b>	<b>Results.....</b>	<b>236-261</b>
7.2.1	Functional analysis of ABC transporters by FACS.....	236
7.2.2	ABCB1 knockdown using RNAi.....	243
7.2.3	Clonogenic assay: drug treatment combined with Verapamil.....	246
7.2.3.1	Surviving colony counting from clonogenic assay.....	246
7.2.3.2	Neurosphere formation assay.....	252
7.2.3.3	Co-staining immunofluorescence in surviving colonies after drug treatment combined with Verapamil.....	255
<b>7.3</b>	<b>Discussion.....</b>	<b>262-271</b>
<b>CHAPTER 8: GENERAL DISCUSSION AND CONCLUSION.....</b>		<b>272-286</b>
<b>REFERENCES.....</b>		<b>287-306</b>
<b>APPENDICES.....</b>		<b>see enclosed CD</b>

## List of Illustrations

Figure 1.1	Histological features of fourth ventricle subependymoma, myxopapillary ependymoma of cauda equine, ependymoma and anaplastic ependymoma.....	9
Figure 1.2	Histological features of different types of medulloblastoma.....	13
Figure 1.3	Histological features of CNS PNETs, cerebral neuroblastomas and ganglioneuroblastomas.....	15
Figure 1.4	Histological features of oligodendrogliomas.....	19
Figure 1.5	Histological features of GBM and variant GBM.....	22
Figure 1.6	The chemical structure of the parental compound (podophyllotoxin) and derivatives; etoposide, etoposide phosphate and Teniposide.....	25
Figure 1.7	Topoisomerase II function.....	27
Figure 1.8	One- and two-drug model of etoposide mechanism.....	28
Figure 1.9	The chemical structures of the platinum group.....	30
Figure 1.10	Cisplatin and DNA formation.....	31
Figure 1.11	Metabolism pathway of irinotecan.....	33
Figure 1.12	Methotrexate chemical structure and intracellular metabolic form of methotrexate.....	36
Figure 1.13	General topology of ABC transporters and 3D figure of NBD.....	41
Figure 1.14	ABCB1 structure.....	43
Figure 1.15	Crystal structure of ABCB1 transporter.....	43
Figure 1.16	The hydrophobic vacuum cleaner model, flippase model and membrane partitioning model.....	46
Figure 1.17	The structure of ABCC1.....	48
Figure 1.18	ABCG2 structure.....	50
Figure 1.19	A model of cancer stem cells and tumour progression in normal stem cells and progenitor cells.....	56
Figure 1.20	Schematic diagram of murine CD133 structure.....	61
Figure 1.21	Genomic organisation of the promoter region of human AC133 and alternative splicing within its 5'-UTR.....	62
Figure 1.22	The location of CD133 and SOX2 expression in postnatal mouse brain.....	67
Figure 1.23	The heterogeneity and propagation of tumours.....	68
Figure 1.24	Models of drug resistance in cancer cells.....	70
Figure 2.1	Testing set for ABCB1 functional analysis.....	102
Figure 2.2	Schematic treatment plan on 6-well plate for clonogenic assay.....	110



Figure 3.1	Histological features of the original tumours from which EPN-1, MED-2, SPNET-1, MED-1 and BT-4 cells were derived.....	120
Figure 3.2	Histological features of tumours from which EPN-2 and Olig-1 were derived.....	121
Figure 3.3	Metaphase spread analysis of EPN-1, EPN-2, MED-1, MED-2, BT-4, Olig-1, SPNET-1 and PFSK-1 cell lines.....	123
Figure 3.4	SNP analysis.....	130
Figure 4.1	The morphology of serially cultured EPN-2, MED-2 and SPNET-1 cell lines as monolayer and neurosphere condition at early, middle and late passage and PFSK-1 cell line.....	137
Figure 4.2	Doubling times at early, middle and late passage number of monolayer and neurosphere from primary cultured cell lines.....	141
Figure 4.3	Doubling time means of monolayers and neurospheres from all primary paediatric cell lines.....	142
Figure 4.4	Co-staining CD133 and SOX2 immunofluorescence in monolayers and neurospheres of primary cultured cell lines and PFSK-1.....	144
Figure 4.5	The percentage of CD133 and SOX2 co-staining cells at early, middle and late passage from monolayers and neurospheres.....	146
Figure 4.6	The percentage of positive co-staining cells in all 7 primary cell lines.....	147
Figure 4.7	Detection of CD133 and SOX2 expression using Western blotting analysis in primary paediatric cell lines.....	149
Figure 4.8	Telomerase activity is present in monolayers and neurospheres of all 7 primary cultured cell lines.....	151
Figure 4.9	The quantification of telomerase activity in EPN-1, EPN-2, MED-1, MED-2, BT-4, Olig-1, SPNET-1 and PFSK-1 cell lines at early passages.....	152
Figure 4.10	TRF assay in monolayers and neurospheres at early, middle and late passages of PFSK-1, SPNET-1, EPN-2 and MED-2 compared with hNSC, U87 and U373 cell lines.....	154
Figure 4.11	An alteration of cell cycle profile in cells grown as neurospheres compared to monolayers.....	157
Figure 5.1	Co-staining CD133 and ABCB1 immunofluorescence in monolayers and neurospheres from EPN-2, MED-2 and SPNET-1 cell lines at early passage number.....	174
Figure 5.2	Co-staining CD133 and ABCC1 immunofluorescence in monolayers and neurospheres from EPN-2, MED-2 and SPNET-1 cell lines at early passage number.....	176

Figure 5.3	Co-staining CD133 and ABCG2 immunofluorescence in monolayers and neurospheres from EPN-2, MED-2 and SPNET-1 cell lines at early passage number.....	178
Figure 5.4	Co-expressing CD133 and ABCB1 cells detected by FACS in monolayers and neurospheres from EPN-2, MED-2 and SPNET-1 cell lines.....	181
Figure 5.5	Co-expressing CD133 and ABCC1 cells detected by FACS in monolayers and neurospheres from EPN-2, MED-2 and SPNET-1 cell lines.....	182
Figure 5.6	Co-expressing CD133 and ABCG2 cells detected by FACS in monolayers and neurospheres from EPN-2, MED-2 and SPNET-1 cell lines.....	183
Figure 5.7	The percentage of cells co-expressing CD133 and ABCB1 or ABCC1 in monolayers and neurospheres from EPN-2, MED-2 and SPNET-1 cell lines at early passage.....	184
Figure 5.8	The expression of ABC transporters in monolayers and neurospheres of EPN-2, MED-2 and SPNET-1 cell lines by Western blotting analysis.....	187
Figure 5.9	ABCB1 functional analysis by FACS in control cells.....	189
Figure 5.10	ABCB1 functional analysis by FACS in monolayers from EPN-2, MED-2 and SPNET-1 cell lines.....	190
Figure 5.11	Proportion of EPN-2, MED-2 and SPNET-1 cells showing functional ABCB1.....	191
Figure 5.12	Drug resistance potential of EPN-1, MED-1, Olig-1 and BT4 to etoposide.....	193
Figure 6.1	Drug inhibitory graphs of etoposide, cisplatin, irinotecan and methotrexate treatment in the EPN-2, MED-2 and SPNET-1 cell line.....	202
Figure 6.2	Neurosphere formation derived from the vehicle control colonies, etoposide and cisplatin treated colonies from EPN-2, MED-2 and SPNET-1 cell lines.....	204
Figure 6.3	Neurosphere formation derived from the vehicle control colonies, irinotecan and methotrexate treated colonies from EPN-2, MED-2 and SPNET-1 cell lines.....	205
Figure 6.4	Neurosphere formation of the vehicle control colonies and 4 drug treatments in EPN-2, MED-2 and SPNET-1 cell lines.....	206
Figure 6.5	Co-staining immunofluorescence analysis in the parental cells of EPN-2 after the first round of etoposide or irinotecan treatment.....	208
Figure 6.6	Co-staining immunofluorescence analysis in the parental cells of MED-2 after the first round of cisplatin or irinotecan treatment.....	210
Figure 6.7	Co-staining immunofluorescence analysis in the parental cells of SPNET-1 after the first round of cisplatin or irinotecan treatment.....	212

Figure 6.8	The cellular morphology of a control subline and selected MED-2 sublines after multiple rounds of drug treatment.....	217
Figure 6.9	ABCB1, ABCC1 and ABCG2 expression determined by Western blotting analysis in selected sublines.....	223
Figure 6.10	Progression expression of ABC transporters by tumour cells after prolonged drug treatment.....	232
Figure 7.1	Optimisation of ABCB1 functional analysis by FACS using HEK-V and HEK-B1.....	237
Figure 7.2	ABCB1 functional analysis in the control subline and selected etoposide and irinotecan EPN-2 sublines.....	239
Figure 7.3	ABCB1 functional analysis in the control subline and selected cisplatin and irinotecan MED-2 sublines.....	240
Figure 7.4	ABCB1 functional analysis in the control subline and selected cisplatin and irinotecan SPNET-1 sublines.....	241
Figure 7.5	ABCB1 functional analysis in the selected EPN-2, MED-2 and SPNET-1 sublines.....	242
Figure 7.6	Optimisation of ABCB1 knockdown using <i>si_ABCB1</i> , <i>si_ABCB1.1</i> and <i>si_ABCB1.2</i> in EPN-2 sublines.....	245
Figure 7.7	Clonogenic assay: Etoposide treatment combined Verapamil reduced colony survival and colony size.....	249
Figure 7.8	Clonogenic assay: Irinotecan treatment combined Verapamil reduced colony survival and colony size.....	250
Figure 7.9	Verapamil combined drug treatment reduced colony formation in the selected EPN-2 sublines.....	251
Figure 7.10	Neurosphere formation from EPN-2, EPN-2_C and EPN-2_E_T1 sublines treated with vehicle, etoposide, or etoposide combined with Verapamil.....	253
Figure 7.11	Neurosphere formation from EPN-2, EPN-2_C and EPN-2_I_T1 sublines treated with vehicle, irinotecan, or irinotecan combined with Verapamil.....	254
Figure 7.12	CD133 and ABCB1 expression in the parental EPN-2 cells after vehicle, etoposide, or etoposide combined Verapamil treatment.....	256
Figure 7.13	CD133 and ABCB1 expression in the EPN-2 control subline after vehicle, etoposide, or etoposide combined Verapamil treatment.....	257
Figure 7.14	CD133 and ABCB1 expression in the EPN-2_E_T1 subline after vehicle, etoposide, or etoposide combined Verapamil treatment.....	258
Figure 7.15	CD133 and ABCB1 expression in the parental EPN-2 cells after vehicle, irinotecan, or irinotecan combined Verapamil treatment.....	259

Figure 7.16	CD133 and ABCB1 expression in the EPN-2 control subline of after vehicle, irinotecan, or irinotecan combined Verapamil treatment.....	260
Figure 7.17	CD133 and ABCB1 expression in the EPN-2_I_T1 subline after vehicle, irinotecan, or irinotecan combined Verapamil treatment.....	261
Figure 8.1	Tumour population in the parental EPN-2 and selected resistant EPN-2 sublines.....	275
Figure 8.2	Drug resistance mechanisms in newly established paediatric brain tumours.....	278
Figure 8.3	Treatment included mutations in surviving cells.....	282

## List of Tables

Table 1.1	The comparison of brain tumours in adults and children.....	4
Table 1.2	WHO grades of CNS tumours.....	6
Table 1.3	Ependymal tumours.....	8
Table 1.4	Embryonal tumours.....	11
Table 1.5	Oligodendroglial tumours.....	17
Table 1.6	Glioblastoma tumour variants.....	21
Table 1.7	Chemotherapeutic drugs used to treat CNS cancers.....	24
Table 1.8	ABC transporters involved in drug resistance.....	42
Table 1.9	Chemotherapeutic drugs and other compounds that interact with ABCB1, ABCC1 and ABCG2 transporters.....	53
Table 2.1	Primary antibodies used in immunofluorescent staining.....	80
Table 2.2	Secondary antibodies used in immunofluorescent staining.....	80
Table 2.3	Effective range of separation of SDS-Polyacrylamide gels.....	85
Table 2.4	Primary and secondary antibodies used in Western blot analysis.....	87
Table 2.5	Preparation of BSA standard concentration for protein quantification.....	93
Table 2.6	PCR Master Mix.....	94
Table 2.7	Drug treatment for clonogenic assay.....	98
Table 2.8	Blocking buffer.....	100
Table 2.9	Primary antibody for FACS co-staining immunofluorescence.....	101
Table 2.10	Reagents for ABCB1 functional analysis by FACS.....	102
Table 2.11	Mixture of SiPORT Amine and Opti-MEM.....	105
Table 2.12	Mixture of ABCB1 SiRNA and Opti-MEM.....	105
Table 2.13	Drug treatment combined with ABCB1 inhibition .....	111
Table 3.1	PFSK-1 commercial cell line details.....	116
Table 3.2	Description of clinical characteristics of the paediatric brain tumours from which cell lines were derived.....	117
Table 3.3	The variation of chromosome number from metaphase spread analysis.....	122
Table 4.1	Mean telomere length of EPN-2, MED-2 and SPNET-1 cell lines.....	154
Table 6.1	Summary of IC <sub>30</sub> , IC <sub>50</sub> and IC <sub>70</sub> of etoposide, cisplatin, irinotecan and methotrexate treated in EPN-2, MED-2 and SPNET-1 cell lines.....	203
Table 6.2	Summary of CD133 and ABC transporters co-expression by immunofluorescence.....	219
Table 7.1	The range of colony size for the etoposide and irinotecan treatment group.....	248
Table 7.2	The details of treatment in the original tumours prior to establishment of cell lines.....	266

## List of Appendices (see enclosed CD)

### **Appendix A: Results**.....308-345

#### **A1: Co-staining immunofluorescence in the parental cell lines after the first round of drug treatment**.....308-313

Figure A1.1 Co-staining CD133 and ABCB1, ABCC1 or ABCG2 immunofluorescence in EPN-2 monolayers after the first round of cisplatin and methotrexate treatment.....	308
Figure A1.2 Co-staining CD133 and ABCB1, ABCC1 or ABCG2 immunofluorescence in MED-2 monolayers after the first round of etoposide and methotrexate treatment.....	310
Figure A1.3 Co-staining CD133 and ABCB1, ABCC1 or ABCG2 immunofluorescence in SPNET-1 monolayers after the first round of etoposide and methotrexate treatment.....	312

#### **A2: Cellular morphologies of the selected sublines after multiple rounds of drug treatment**.....314-315

Figure A2.1 The cellular morphology of a control subline and the selected EPN-2 sublines after multiple rounds of drug treatment.....	314
Figure A2.2 The cellular morphology of a control subline and the selected SPNET-1 sublines after multiple rounds of drug treatment.....	315

#### **A3: Co-staining immunofluorescence in the selected sublines after repeat treatment at early passage (less than 10 passages)**.....316-330

Figure A3.1 Co-staining CD133 and ABCB1 immunofluorescence in the selected EPN-2 sublines treated for less than 10 passages.....	316
Figure A3.2 Co-staining CD133 and ABCC1 immunofluorescence in the selected EPN-2 sublines treated for less than 10 passages.....	317
Figure A3.3 Co-staining CD133 and ABCG2 immunofluorescence in the selected EPN-2 sublines treated for less than 10 passages.....	318
Figure A3.4 Co-staining CD133 and ABCB1 immunofluorescence in the selected MED-2 sublines treated for less than 10 passages.....	319
Figure A3.5 Co-staining CD133 and ABCC1 immunofluorescence in the selected MED-2 sublines treated for less than 10 passages.....	321

Figure A3.6	Co-staining CD133 and ABCG2 immunofluorescence in the selected MED-2 sublines treated for less than 10 passages.....	323
Figure A3.7	Co-staining CD133 and ABCB1 immunofluorescence in the selected SPNET-1 sublines treated for less than 10 passages.....	325
Figure A3.8	Co-staining CD133 and ABCC1 immunofluorescence in the selected SPNET-1 sublines treated for less than 10 passages.....	327
Figure A3.9	Co-staining CD133 and ABCG2 immunofluorescence in the selected SPNET-1 sublines treated for less than 10 passages.....	329
<b>A4: Co-staining immunofluorescence in the selected sublines after repeat treatment at later passage (more than 10 passages).....</b>		<b>331-345</b>
Figure A4.1	Co-staining CD133 and ABCB1 immunofluorescence in the selected EPN-2 sublines treated for more than 10 passages.....	331
Figure A4.2	Co-staining CD133 and ABCC1 immunofluorescence in the selected EPN-2 sublines treated for more than 10 passages.....	332
Figure A4.3	Co-staining CD133 and ABCG2 immunofluorescence in the selected EPN-2 sublines treated for more than 10 passages.....	333
Figure A4.4	Co-staining CD133 and ABCB1 immunofluorescence in the selected MED-2 sublines treated for more than 10 passages.....	334
Figure A4.5	Co-staining CD133 and ABCC1 immunofluorescence in the selected MED-2 sublines treated for more than 10 passages.....	336
Figure A4.6	Co-staining CD133 and ABCG2 immunofluorescence in the selected MED-2 sublines treated for more than 10 passages.....	338
Figure A4.7	Co-staining CD133 and ABCB1 immunofluorescence in the selected SPNET-1 sublines treated for more than 10 passages.....	340
Figure A4.8	Co-staining CD133 and ABCC1 immunofluorescence in the selected SPNET-1 sublines treated for more than 10 passages.....	342
Figure A4.9	Co-staining CD133 and ABCG2 immunofluorescence in the selected SPNET-1 sublines treated for more than 10 passages.....	344
<b>Appendix B: Materials and Methods.....</b>		<b>346-350</b>
<b>B1: Cell culture.....</b>		<b>346</b>
Table B1.1	Cell culture media.....	346
<b>B2: Immunofluorescence analysis.....</b>		<b>346</b>
Table B2.1	Solution for fixation.....	346

Table B2.2	Solution for immunofluorescent staining.....	346
<b>B3: Western blot analysis.....</b>		<b>347</b>
Table B3.1	General solution for Western blotting analysis.....	347
Table B3.2	Lower gel (Resolving gel).....	347
Table B3.3	Upper gel (Stacking gel).....	347
<b>B4: DNA extraction.....</b>		<b>348</b>
Table B4.1	Lysis buffer.....	348
<b>B5: TRF assay.....</b>		<b>348</b>
Table B5.1	Solution for TRF assay.....	348
<b>B6: TRAP assay.....</b>		<b>349</b>
Table B6.1	Solution for TRAP assay.....	349
<b>B7: FACS functional analysis.....</b>		<b>349</b>
Table B7.1	Buffer for FACS.....	349



## List of Abbreviations

7-OH-MTX	7-hydroxy-methotrexate
ABC	ATP-binding cassette
ABCP	ABC transporter in placenta
AML	acute myeloid leukaemia
APC	7-ethyl-10-[4-N-(5 aminopentanoic acid)-1-piperidino] carbonyloxycamptothecin)
APES	aminopropyltriethoxysilane
AT/RT	atypical teratoid/rhabdoid tumour
at-MDR	atypical multidrug resistance
BBB	blood brain barrier
BCRP	breast cancer resistance protein
BSA	serum bovine albumin
BTB	brain tumour barrier
CBTRC	Children's Brain Tumour Research Centre
CCNU	chloroethylcyclohexylnitrocourea
CDDP	<i>Cis</i> -diamminedichloroplatinum (II)
cDNA	complementary DNA
CES	carboxylesterases
<i>cis</i> -DDP	<i>cis</i> -diamminedichloroplatinum (II)
CML	chronic myeloid leukaemia
CNS	central nervous system
CSCs	cancer stem cells
CSF	cerebrospinal fluid
CT	chemotherapy
CYP3A	cytochrome P450 3A
DAMPA	diamino-2, 4-N-10-methylpteroic acid
DAPI	4', 6-diamidino-2-phenylindole
DEPBG	4'-demethylepipodophyllin benzylidene glucoside
DEPC	diethylpyrocarbonate
DFHR	dihydrofolate reductase enzyme
DMSO	dimethyl sulfoxide
DNA	deoxyribonucleic acid
DPBS	Dulbecco's phosphate buffered saline
dsDNA	double stranded deoxyribonucleic acid
dsRNA	double stranded RNA
DTT	dithiothreitol

ECL	enhanced chemiluminescence
EDTA	ethylene diamine tetracetic acid
EGF	epidermal growth factor
EGFR	epidermal growth factor receptor
EM	electron microscopy
ESCs	embryonic stem cells
FACS	fluorescence activated cell sorting
FFPE	formalin-fixed paraffin embedded
FGF	fibroblast growth factor
FPGS	folylpolyglutamate synthesase
GAPDH	glyceraldehyde-3-phosphate dehydrogenase
GBM	glioblastoma multiforme
GFAP	glial fibrillary acidic protein
GSH	glutathione
GS-x	GSH conjugate export pump
GVHD	graft-versus-host disease
HBSS	Hank's balance salt solution
HMG	high mobility group
HRP	horseradish peroxidase enzyme
HSC	haematopoietic stem cell
hTERT	human telomerase reverse transcriptase
IC	inhibitory concentration
ICM	inner cell mass
LICs	leukaemic-initiating cells
LOH	loss of heterozygosity
MACS	magnetic activated cell sorting
MDR	multidrug resistance
MT	metalothioneins
MTT	microtetrazoline
MXP	mitoxantrone-resistance protein
NBD	nucleotide binding domain
NOD-SCID	non-obese diabetic severe combined immunodeficiency
NPC	7-ethyl-10-(4-amino-1-piperidino) carbonyloxycamptothecin
NSCs	neural stem cells
NSE	neuron specific enolase
OCT	optimal cutting temperature
PBTs	paediatric brain tumours
PCR	Polymerase chain reaction

PCV	Procarbazine
PDVF	polyvinylidene fluoride
PFA	paraformaldehyde
P-gp	P-glycoprotein
PNET	Primitive neuroectodermal tumour
prom-rp	<u>prom</u> inin <u>rel</u> ated <u>pr</u> otein
QMC	Queen Medical Centre
RA	rheumatoid arthritis
Rh123	Rhodamine 123
RNAi	ribonucleic acid interference
RT	radiotherapy
RT-PCR	reverse transcriptase PCR
SDS	sodium dodecyl sulfate
SEER	Surveillance, Epidemiology, and End Results
shRNA	short hairpin RNA
siRNA	short interference RNA
SNP	single nucleotide polymorphism
SRR	SOX2 regulatory region
SSC	sodium chloride/sodium citrate
T/E	trypsin/EDTA
TAE	tris-acetate-EDTA
TBS	tris-buffered saline
TBS-T	tris-buffered saline tween-20
TKIs	tyrosine kinase inhibitors
TMD	transmembrane domain
TRAP	Telomeric Repeat Amplification protocol
TRF	Terminal Restriction Fragments
UGT1A	uridine diphosphate-glucuronosyltransferase 1A
UPSW	ultra pure sterile water
WHO	World Health Organisation

---

---

## **Chapter 1**

### **General introduction**

---

---

## Chapter 1: General introduction

Cancer or malignant neoplasm is a group of diseases resulting from dysregulation of cell proliferation, differentiation or cell death and involving alteration of genomic structures and gene expression. The properties most likely to result in mortality among patients are invasiveness (destroying adjacent tissues or organs), aggressiveness (immortal cell division and infinite growth), metastasis (spreading to remote organs via blood circulation, cerebrospinal fluid (CSF) or the lymphatic system). At present, many types of neoplasm are unable to be cured effectively without short or long term adverse reactions in response to aggressive treatments such as surgery, chemotherapy and radiotherapy. Many cancers often relapse even long periods after completion of treatment due to tumour regrowth after treatment failure. This can be due to a number of different factors including incomplete resection of the tumour, metastasis being present at diagnosis and development of resistance to chemotherapy or radiotherapy. This project is focused on the development of resistance to chemotherapy specifically when this resistance encompasses a number of different types of drugs i.e. multidrug resistance.

Cancer stem cells (CSCs), which comprise a small proportion of the tumours/cancers [Ignatova, T. N. *et al* (2002) and Singh, S. K. *et al* (2004)], are proposed to associate with multidrug resistance [Dean, M. *et al* (2001) and Schinkel, A. *et al* (2003)]. Consequently, enormous efforts have been made to improve our understanding of multidrug resistance in CSCs. One of the key drug resistance mechanisms in CSCs is active drug efflux. The ATP-binding cassette (ABC) transporter family is the most important drug efflux transporter believed to play a role in drug resistance in many cancers. This chapter introduces 5 relevant topics, which form the background of this study, before leading to the results and discussions. These are paediatric brain tumours (PBTs), chemotherapeutic treatment in PBTs, ABC transporters, CSCs and drug resistance in paediatric brain tumours.

## 1.1 Paediatric brain tumours

The most common solid neoplasms in children are tumours of the central nervous system (CNS), which are the second most common type of paediatric cancer behind leukaemia, and account for one third of childhood cancers [Pollack, Ian F. (1994), and Stewart, E.S. and Cohen, D.G. (1998)]. The most common PBTs are low grade astrocytomas with all types of astrocytoma accounting for 52% of PBTs. Embryonal tumours or primitive neuroectodermal tumours (PNETs) (the majority of which are medulloblastomas) represent approximately 21% of PBTs, hence, medulloblastoma is the second most common malignant brain tumour in children. Ependymomas and other gliomas account for 9% and 15% respectively [Baldwin, R.T. and Martin, S.P. (2004) and Jay, V. *et al* (2003)].

In western countries, children under 15 years of age diagnosed with cancer account for 2% of all cancer cases. Moreover, the incidence of PBTs in Europe and the United States is estimated at approximately 130 new cases per year per million children [Scotting, P.J. *et al* (2005)]. There are several pieces of evidence supporting the fact that childhood solid tumours are different from adult solid tumours in terms of biology, genetics and environmental influences [Scotting, P.J. *et al* (2005)]. Some tumours develop mainly in children and are uncommon in adults such as neuroblastoma, Wilm's tumour, osteosarcoma, and retinoblastoma [Kline, N.E. and Sevier, N. (2003)]. Several differences between childhood and adult brain tumours are shown in Table 1.1. The majority of children with brain tumours have a much better prognosis than adults with respect to median survival rate. Brain tumours developing in children are generally primary brain tumours, whilst adults often develop tumours that are more aggressive, such as the highly malignant tumour glioblastoma multiforme [Albright, A.L. (1993)]. However, when one compares the prognosis of brain tumours among children, it is revealed that infants and young children with brain tumours fare less well than older children since tumours in young children appear to become biologically aggressive. Surveillance, Epidemiology, and End Results (SEER) data collected from 1985 to 1994 revealed that 5 year survival rates for all CNS cancers was 45% for

**Table 1.1 The comparison of brain tumours in adults and children** [Stewart, E.S. and Cohen, D.G. (1998)].

Comparison of Brain Tumours in Adults and Children		
	Adults	Children (<15yr)
Incidence of primary brain tumours	28,500/yr	2,200/yr
Incidence rate	10.9 per 100,000	3.7-4.1 per 100,000
Survival	20%-30% survival	60% survival
Most common	Metastatic brain tumours	Primary brain tumours
Standard of care	Palliative treatment	Surgery±radiation+chemotherapy

children younger than 1 year, 59% for 1 to 4 years, 64% for 5-9 years, 70% for 10-14 years and 77% for 15-19 years [Gupta, N. *et al.* (2004)]. It has been shown that the older the age of the child developing a brain tumours, the better the prognosis. There are several reasons why this may be the case. Young children are capable of cranial enlargement to compensate for the increase in intracranial pressure from growing brain tumours, resulting in delayed diagnosis. Young children also have less tolerance than older children to complications from surgery and the toxic effects of radiation and chemotherapy. Radiotherapy is commonly avoided or reduced in young children with brain tumours due to the fact that their developing cells are easily affected by radiation. Also the types of tumours are seen varies with age with germ cell tumours seen mainly in teenagers.

Histology type of brain tumours is the most reliable method used to predict the biological behaviour of a neoplasm. It is therefore routinely used to determine treatment options such as manipulation of adjuvant radiation and specific chemotherapy [Kleihues, P. *et al.* (2007)]. Classification of brain tumours is predominantly based on the histological features from light microscopy. In 1979, neuropathologists working under the control of the World Health Organization (WHO) developed a new classification and grading system for brain tumours that was more valuable for treatment evaluation. Since then the classification and grading system for brain tumours had been continuously developed to give more appropriate categories and cover all brain tumours. Presently, the revised WHO classification still classifies brain tumours

predominantly from the evidence of histological findings, which provides a major advantage for diagnosis of brain tumours. PBTs classified according to 4<sup>th</sup> edition of the WHO classification are shown in Table 1.2 [Kleihues, P. *et al.* (2007)].

The grading system in paediatric brain tumours is very important due to the fact that the histological grading of tumours is one of the significant factors indicating the biological behaviour of tumours. Additionally, grading of tumours is an essential factor for treatment consideration in using adjuvant radiation and specific chemotherapy protocols [Pollack, I. F. (1994)]. WHO grades of central nervous system tumours are classified into 4 grades. Grade I describes tumours containing cells with a low proliferative potential and only complete surgical resection is required to cure grade I tumours. Tumours classified as grade II are generally infiltrative and have a low level of proliferative activity. Some grade II tumours are able to develop to a higher grade tumour e.g. low grade diffuse astrocytomas can develop to anaplastic astrocytoma or glioblastoma. Grade III identifies tumours with histological features of malignancy with regard to nuclear atypia and high mitotic activity. These tumours types normally require adjuvant radiation and/or chemotherapy. Grade IV describes tumours that are the most aggressive and hence have the poorest prognosis. Grade IV tumours comprise cytological malignancy characteristics including high mitotic activity, necrosis, rapid pre and postoperative progression and consequently have poor treatment outcome [Rorke, L. B. *et al* (1985) and Louis, D. N. *et al* (2007)].

Only the 5 types of paediatric brain tumour that were used in this study are covered in more depth (ependymoma, medulloblastoma, oligodendroglioma, glioblastoma multiforme and CNS PNET). Each tumour type will be described in terms of histopathological features, incidence, localisation, growth and invasion, genetic abnormalities, and prognosis. There will particular emphasis given to the tumour sub-type from which the cell lines used in this study were derived.



**Table 1.2 WHO grades of CNS tumours** [Kleihues, P. *et al.* (2007)]

Tumours	Grades			
	I	II	III	IV
<b>Astrocytic tumours</b>				
Subependymal giant cell astrocytoma	•			
Pilocytic astrocytoma	•			
Pilomyxoid astrocytoma		•		
Diffuse astrocytoma		•		
Pleomorphic xanthoastrocytoma		•		
Anaplastic astrocytoma			•	
Glioblastoma				•
Giant cell glioblastoma				•
Gliosarcoma				•
<b>Oligodendroglial tumours</b>				
Oligodendroglioma		•		
Anaplastic oligodendroglioma			•	
<b>Oligoastrocytic tumours</b>				
Oligoastrocytoma		•		
Anaplastic oligoastrocytoma			•	
<b>Ependymal tumours</b>				
Subependymoma	•			
Myxopapillary ependymoma	•			
Ependymoma		•		
Anaplastic ependymoma			•	
<b>Choroid plexus tumours</b>				
Choroid plexus papilloma	•			
Atypical choroid plexus papilloma		•		
Choroid plexus carcinoma			•	
<b>Other neuroepithelial tumours</b>				
Angiocentric glioma	•			
Chordoid glioma of the third ventricle		•		
<b>Neuronal and mixed neuronal-glial tumours</b>				
Gangliocytoma	•			
Ganglioglioma	•			
Desmoplastic infantile astrocytoma and ganglioglioma	•			
Anaplastic ganglioglioma			•	
Dysembryoplastic neuroepithelial tumour	•			
<b>Pineal tumours</b>				
Pineocytoma	•			
Pineal parenchymal tumour of intermediate differentiation		•	•	
Pineoblastoma				•
Papillary tumour of the pineal region		•	•	
<b>Embryonal tumours</b>				
Medulloblastoma				•
CNS primitive neuroectodermal tumour (PNET)				•
Atypical teratoid/rhabdoid tumour				•
<b>Tumours of the cranial and paraspinal nerves</b>				
Schwannoma	•			
Neurofibroma	•			
Perineurioma	•	•	•	
Malignant peripheral nerve sheath tumour (MPNST)		•	•	•
<b>Meningeal tumours</b>				
Meningioma	•			
Atypical meningioma		•		
Anaplastic/malignant meningioma			•	
Haemangiopericytoma		•		
Anaplastic haemangiopericytoma			•	
Haemangioblastoma	•			
<b>Tumours of the sellar region</b>				
Craniopharyngioma	•			
Granular cell tumour of the neurohypophysis	•			
Pituitaryoma	•			
Spindle cell oncocytoma of the adenohypophysis	•			

### 1.1.1 Ependymoma

Ependymomas are ependymal tumours, which are classified into 4 subtypes; subependymoma (WHO grade I), myxopapillary ependymoma (WHO grade I), ependymoma (WHO grade II) and anaplastic ependymoma (WHO grade III) (Table 1.3). Ependymomas commonly develop in young children between 3-8 years of age at diagnosis. The majority of Ependymoma cases (90%) are intracranial, whilst the remainder are located in the spinal cord. The most common area in which ependymoma is located is the 4<sup>th</sup> ventricle followed by the spinal cord, the lateral ventricle and the 3<sup>rd</sup> ventricle [Prayson, R. A. (1999)]. Two thirds of paediatric intracranial ependymomas are found in the infratentorial region, hence this is the predominant subtype found in children [Horn, B.N. and Smyth, M. (2004)].

The most frequent genetic abnormality found in 30% of ependymoma is the aberration of chromosome 22 [Hamilton, R. L. and Pollack, I. F. (1997)]. Whilst the most frequent genetic abnormality in spinal ependymoma is monosomy 22, deletions and translocations in chromosome 22q also occur [Huang, B. *et al* (2003)]. Genetic abnormalities, which were commonly found in ependymoma although less frequently, include losses of 6q, 9q, 3p14, 10q23 and 11q [Huang, B. *et al* (2003)]. A description of histology and histological images of all ependymal tumour subtypes are shown in Table 1.3 and Figure 1.1.

In Europe from 1990-1994, 1-year survival and 5-year of children diagnosed with ependymoma were 80% and 55%, respectively. The survival rate in infant is very low (24%). Interestingly, the survival rate then increases in older ages; 44% in 1-4 year age, 68% in 5-9 year age and 75% in 10-14 year age [Reni, M. *et al* (2007)]. Factors indicating prognostic value in ependymoma have been studied in many aspects, however, it is still controversial. Ependymoma, which is diagnosed during the first 2 years of life in children, leads to poor prognosis [Horn, B. *et al* (1999)]. Supratentorial tumours provide a better prognosis than infratentorial tumours whilst spinal tumours also have a better prognosis than intracranial tumours [Emestus, R. I. *et al* (1996)]. The histological grading of tumour also plays a role in prognosis. The histological factors indicating poor prognosis in ependymoma include mitotic

**Table 1.3 Ependymal tumours** [Derived from McLendon, R.E. *et al*, chapter 3, (2007)]

Subtypes of ependymoma	WHO grade	Frequency	Location	Histopathology	Genetics	Prognostic and predictive factors
Subependymoma	I	<ul style="list-style-type: none"> <li>- rare and accounts for approximately 8% of ependymal tumours</li> <li>- more frequent in middle-aged and elderly patients</li> </ul>	<ul style="list-style-type: none"> <li>- fourth ventricle (50-60%) and lateral ventricles (30-40%)</li> </ul>	<ul style="list-style-type: none"> <li>- clusters of isomorphic nuclei in a dense fibrillary matrix of glial processes (Figure 3.1, a and b)</li> </ul>	<ul style="list-style-type: none"> <li>- no consistent cytogenetic information</li> </ul>	<ul style="list-style-type: none"> <li>- good prognosis</li> <li>- surgical removal is usually curative</li> <li>- recurrence reported following incomplete resection</li> </ul>
Myxopapillary ependymoma	I	<ul style="list-style-type: none"> <li>- accounts for 9-13% of ependymal tumours</li> <li>- age ranges between 4 and 82 years</li> <li>- median age of 36 years</li> </ul>	<ul style="list-style-type: none"> <li>- conus medullaris-cauda equina-filum terminale region</li> </ul>	<ul style="list-style-type: none"> <li>- GFAP expressing, cuboidal to elongated tumour cells radially arranged in a papillary manner around vascularised stromal cores (Figure 3.1, c and d)</li> </ul>	<ul style="list-style-type: none"> <li>- no consistent cytogenetic information</li> </ul>	<ul style="list-style-type: none"> <li>- favourable prognosis</li> <li>- more than 10-year survival after total or partial resection</li> <li>- late recurrence and distant metastasis may occur in incomplete resections</li> </ul>
Ependymoma	II	<ul style="list-style-type: none"> <li>- accounts for 6-12% of all intracranial tumours and up to 30% in children younger than 3 years</li> <li>- the most common spinal cord tumour (50-60%) in adults, but rare in children</li> </ul>	<ul style="list-style-type: none"> <li>- most common in the fourth ventricle and spinal cord</li> </ul>	<ul style="list-style-type: none"> <li>- well-delineated, moderately cellular glioma with a monomorphic nuclear morphology</li> <li>- perivascular pseudorosettes and ependymal rosettes (Figure 3.1, e and f)</li> </ul>	<ul style="list-style-type: none"> <li>- 30% have losses at 6q and 9q and aberrations of chromosome 22 eg. monosomy 22, deletions or translocations involving 22q</li> </ul>	<ul style="list-style-type: none"> <li>- children tend to fare worse than adults (probably due to the tumour's location being commonly posterior fossa in children but spinal cord in adults)</li> <li>- supratentorial ependymomas have better survival rates than infratentorial lesions</li> <li>- spinal ependymomas have a better outcome than cerebral lesions, although late recurrences are common</li> </ul>
Anaplastic ependymoma	III	<ul style="list-style-type: none"> <li>- variable incidence data due to uncertainty of histological criteria of malignancy</li> <li>- more frequent in childhood intracranial ependymomas than spinal cord</li> </ul>	<ul style="list-style-type: none"> <li>- intracranial and posterior fossa</li> </ul>	<ul style="list-style-type: none"> <li>- increased cellularity and brisk mitotic activity</li> <li>- perivascular pseudorosettes and pseudopalisading necrosis (Figure 3.1, g and h)</li> </ul>	<ul style="list-style-type: none"> <li>- largely unknown</li> </ul>	<ul style="list-style-type: none"> <li>- poor prognostic indicators include; age below 3 years, anaplasia, incomplete tumour resection and cerebrospinal fluid (CSF) metastasis</li> </ul>

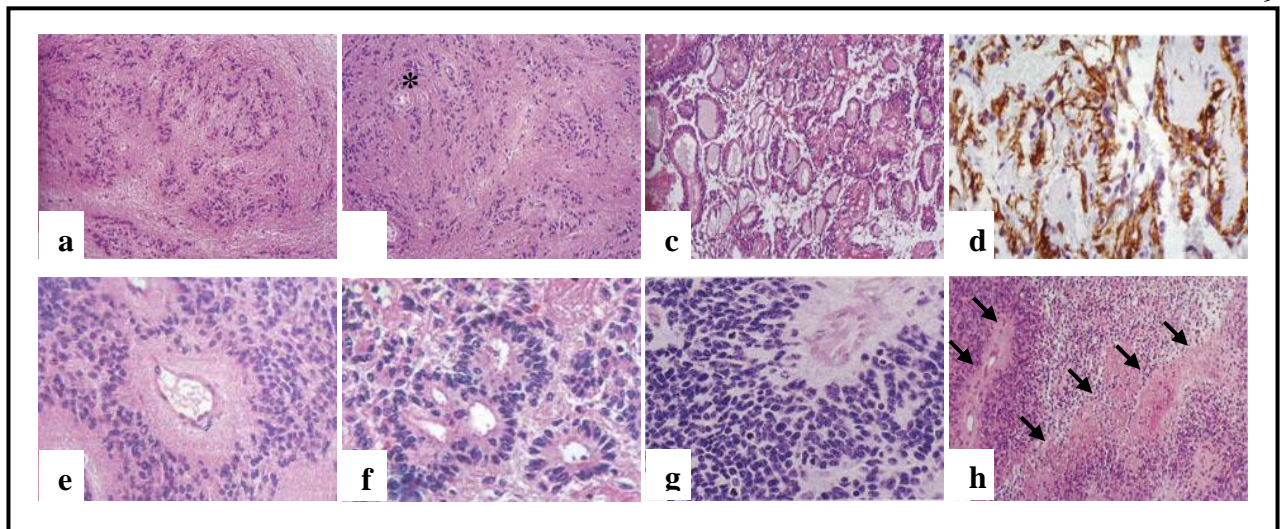


**Figure 1.1 Histological features of fourth ventricle subependymoma, myxopapillary ependymoma of cauda equine, ependymoma and anaplastic ependymoma.**

Subependymomas (a and b) typically arise in the ventricular lumen and present as firm nodules which bulge into the lumen. This tumour is characterised by lobular architecture and clusters of isomorphic nuclei embedded in a dense fibrillary matrix of glial cell processes (a). Clustered nuclei and fibrillary stroma (b) with small cysts (\*) are frequently present. Myxopapillary ependymoma (c and d) commonly arises in the conus medullaris-cauda equine-filum terminale region. Tumour cells are frequently found around vessels with mucoid degeneration (c). Furthermore, this tumour is characterised by GFAP expression of perivascular cells described as cuboidal to elongated tumour cells radially arranged in a papillary manner around vascularised stromal cores (d). Ependymomas (e and f) are able to develop at any site along the ventricular system and spinal cord. The hallmark features of this tumour are perivascular pseudorosettes (e) described as vessels surrounded by ependymal tumour cells with a nuclear-free zone which has thin ependymal processes directed toward the walls of vessels and ependymal rosettes (f) defined as ependymal tumour cells arranged around an empty lumen. Anaplastic ependymomas (g and h) commonly occur in children, particularly in the posterior fossa. Poorly differentiated tumour cells with brisk mitotic activity (g) are frequently described. In addition, foci of necrosis (➤), an area of dead cells without nuclei, are commonly displayed (h) [McLendon, R.E. *et al*, chapter 3, (2007)].

activity, degree of proliferation, foci of hypercellular cells and less differentiated cells [Korshunov, A. *et al* (2004), Kurt, E. *et al* (2006), Schiffer, D. and Giordana, M. T. (1998)].

In this study, the two cell lines, which were derived from patients who were diagnosed with ependymoma, were EPN-1 and EPN-2. The EPN-1 cell line was derived from a patient who had had a 2<sup>nd</sup> relapse and had been treated with chemotherapy and radiation. The tumour tissues were obtained from the 3<sup>rd</sup> surgery. Whilst, the EPN-2 cell line was derived from a primary tumour.

### **1.1.2 Embryonal tumours**

Embryonal tumours were classified by WHO as highly malignant tumours and these tumours are the most common brain tumours in children, accounting for 25% of all children brain tumours [Kleihues, P. *et al* (2000)]. Embryonal tumours are categorised into 3 groups; medulloblastoma, CNS PNET and atypical teratoid/rhabdoid tumour (AT/RT) (Table 1.4). Medulloblastoma and CNS PNET, which were studied in this project, are described in the next section.

#### **1.1.2.1 Medulloblastoma**

Medulloblastomas are the most frequent malignant brain tumour in children. Medulloblastomas originate from granular-cell progenitors located in the external granular layers and also cells situated in the neuroepithelium of the cerebellum [Dahmane, N. and Altaba, A. R. (1999)]. Medulloblastomas are classified as highly malignant (grade IV) tumours by the WHO classification. Approximately 80% of cases arise in the vermis and the median part of cerebellum whilst the remainder arise in the cerebellar hemispheres. Due to the highly malignant capacity of medulloblastoma, remote dissemination may occur in the meninges and cerebrospinal fluid (CSF).

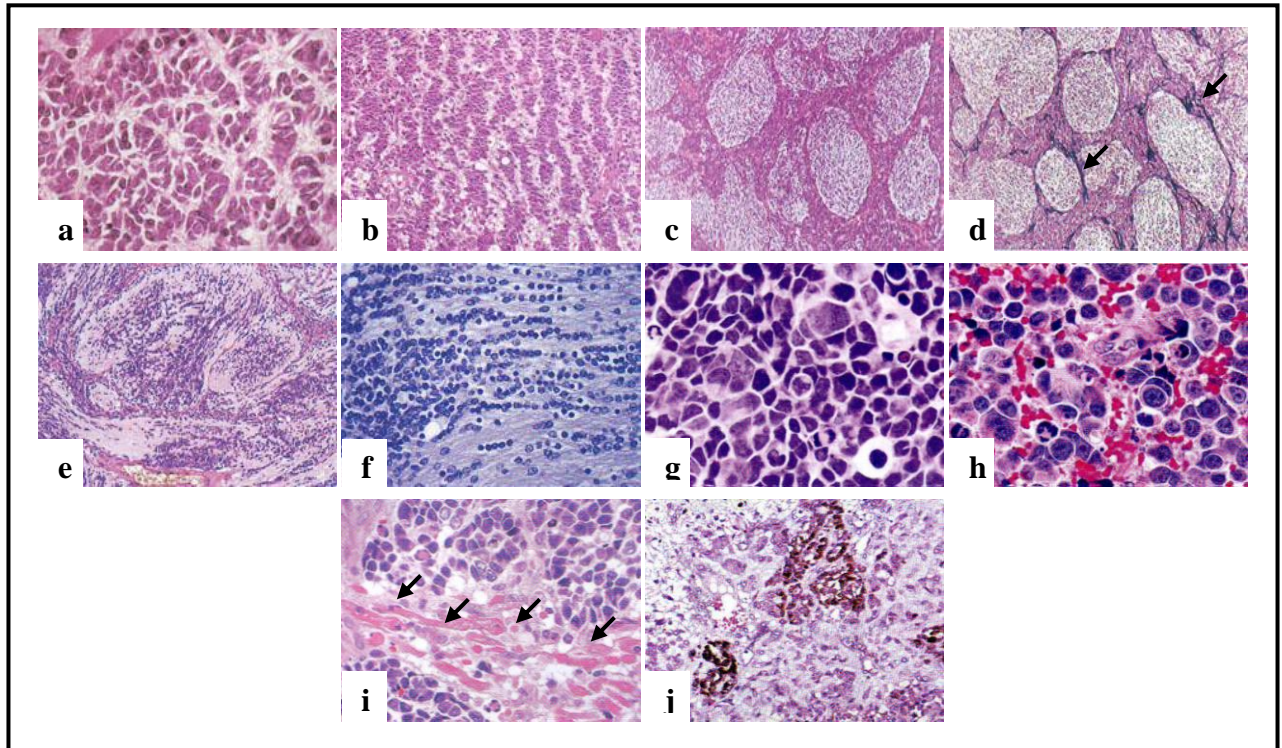
**Table 1.4 Embryonal tumours** [Derived from McLendon, R.E. *et al*, chapter 3, (2007)]

Subtypes of ependymoma	Grade (WHO)	Frequency	Location	Histopathology	Genetics	Prognostic and predictive factors
Medulloblastoma	IV	<ul style="list-style-type: none"> <li>- the most common PBT accounting for 20%</li> <li>- 70% occurs in individuals younger than 16 year</li> <li>- the peak incidence occurs at 7 years of age</li> </ul>	<ul style="list-style-type: none"> <li>- 75% arise in the vermis and project into the 4<sup>th</sup> ventricle</li> </ul>	<ul style="list-style-type: none"> <li>- described as small, round-to-oval cells, tightly packed and poorly differentiated with scanty cytoplasm and dense basophilic nuclei.</li> <li>- Pseudorosettes or Homer-Wright rosettes (&lt;40%) and rhythmic palisading tumours (Figure 3.2) are observed</li> </ul>	<ul style="list-style-type: none"> <li>- isochromosome 17q (<i>i(17)q</i>) present in 30-40% of cases.</li> <li>- both loss of 17p and gain of 17q resulting in <i>i(17)q</i> may also occur independently</li> </ul>	<ul style="list-style-type: none"> <li>- 50-60% of cases are expected to survive and be progression free following treatment.</li> <li>- Children with localised disease and who have received three-drug adjuvant chemotherapy regimen have a better five-year progression-free survival of up to 80% or more</li> </ul>
CNS PNET	IV	<ul style="list-style-type: none"> <li>- rare in children accounting for 2-3% of all PBTs</li> </ul>	<ul style="list-style-type: none"> <li>- commonly arises in cerebral hemispheres and also in pineal region</li> <li>- also found in spinal cord or supracellar region</li> </ul>	<ul style="list-style-type: none"> <li>- described as very poorly differentiated and round regular nuclei with a high nucleus:cytoplasm ratio.</li> <li>- better differentiated CNS PNETs may show more clear neuronal features, with oval to elongated nuclei having vesicular chromatin and nucleoli.</li> </ul>	<ul style="list-style-type: none"> <li>- still unclear</li> <li>- <i>RASSF1A</i> promoter methylation, expression of the <i>Neuro D</i> family of basic helix-loop-helix transcription factors and achaete scute (neurogenic transcription factor with homology to <i>Neuro D</i> genes) are proposed to have a correlation with CNS PNET</li> </ul>	<ul style="list-style-type: none"> <li>- far worse prognosis compared with medulloblastoma</li> <li>- overall 5-year survival rate is 18% but it can increase up to 50-60% after aggressive treatment</li> </ul>
Atypical teratoid/rhabdoid tumour (AT/RT)	IV	<ul style="list-style-type: none"> <li>- rare in children accounting for only 1-2% of all PBTs</li> </ul>	<ul style="list-style-type: none"> <li>- located in both supratentorial (cerebral hemispheres, ventricular system, supracellar region and pineal gland) and infratentorial regions (cerebellar hemispheres, cerebellopontine angle and brain stem)</li> </ul>	<ul style="list-style-type: none"> <li>- the most striking feature: classic rhabdoid features described as eccentrically placed nuclei containing vesicular chromatin, prominent eosinophilic nucleoli, abundant cytoplasm with an obvious eosinophilic globular cytoplasmic inclusion and well-defined cell borders.</li> </ul>	<ul style="list-style-type: none"> <li>- the genetic hallmark is mutation or loss of the <i>INI1</i> (<i>hSNF5/SMARCB1</i>) locus at 22q11.2</li> </ul>	<ul style="list-style-type: none"> <li>- the overall prognosis of AT/RT is poor</li> <li>- one study showed mean survival after surgery of only 11 months</li> </ul>

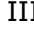

The most common genetic abnormality in medulloblastoma is isochromosome 17q (*i(17)q*) present in 30-40% of cases. Both loss of 17p and gain of 17q resulting in *i(17)q* may also occur independently [Griffin, C. A. *et al* (1988)]. The Sonic-Hedgehog-patched (Shh-Ptch) signalling pathway was also proposed as a significant genetic mutation found in 25% of sporadic human medulloblastomas. Shh-Ptch is the major signalling pathway which regulates the cell-fate determination and proliferation of the external granular layer (EGL) progenitor cells [Zurawel, R. H. *et al* (2000)]. Additionally, Wnt signalling pathway, which regulates the proliferation of EGL progenitor cells, was another important gene abnormality found in 15% of medulloblastoma with nuclear accumulation of  $\beta$ -catenin and GSK3 $\beta$  as the main inhibitory component [Zurawel, R. H. *et al* (1998) and Jia, J. *et al* (2002)]. Medulloblastoma was also discovered to present in rare autosomal dominant familial syndromes including Gorlin syndrome (Naevoid basal cell carcinoma syndrome: NBCCS) found in 4% of patients under 3 years of age, Turcot type 2 found in the setting of familial adenomatous polyposis (FAP) and a germ line *APC* mutations and in 14% of cases of Li-Fraumeni syndrome with a germline *TP53* mutation [Reviewed in Ellison, D. (2002)].

Histologically, medulloblastoma and the other variant medulloblastoma are described in Figure 1.2. Since they are highly malignant, medulloblastomas cannot be reliably be cured by surgery alone. However, it is a chemosensitive and radiosensitive tumour. Therefore, 50-60% of cases are expected to survive and be progression free following treatment. Several studies have proposed a number of prognostic indicators that influence treatment outcomes and median survival rate of patients. None of these indicators have, however, been proved to affect prognosis of medulloblastoma patients in the context of therapeutic trials [Jakacki, R. I. (2005)]. The clinical criteria categorises medulloblastoma into 2 groups of high-risk and standard-risk patients. This might be useful and probably can indicate prognosis of disease. The high-risk patients were identified as diagnosis of disease at age less than 3 years, incomplete surgical resection leaving more than 1.5 cm<sup>2</sup> of residual tumours and presentation of metastasis [Reviewed in Packer, R. J. (1999)]. However, this criteria is not generally accepted.





**Figure 1.2 Histological features of different types of medulloblastoma.**

Medulloblastomas are typically located in cerebellar hemispheres. Hallmark histological features of this tumour are areas of Homer-Wright rosettes (neuroblastic, a), and arrangement of tumour cells in parallel rows described as a rhythmic palisading tumour cells (b). Desmoplastic medulloblastoma have pale nodular areas surrounded by densely packed hyperchromatic cells and reticulin (c) or reticular fibers, a histological term used to describe structural fibers composed of type III collagen staining (  ) shows reticulin-free zones described as pale islands (d). Variant medulloblastoma with extensive nodularity (e and f) was primarily classified as cerebellar neuroblastoma. The histological features were described as expanded lobular architecture with large elongated reticulin-free zones (e) due to the fact that such zones become unusually enlarged and rich in neurophil-like tissue. These zones contain small round neurocytic cells, which are similar to central neurocytoma and exhibit a streaming pattern, in the fibrillary background (f). Anaplastic medulloblastomas are characterised by increased nuclear size and pleomorphism (g). Large cell medulloblastomas show enlarged vesicular nuclei, prominent nucleoli, and moderate cytoplasm (h). Large cell and anaplastic medulloblastomas have substantial cytological overlap, therefore, many studies classify both into a large cell/anaplastic category. Any variant of medulloblastoma which comprises focal rhabdomyoblastic elements is described as medulloblastoma (i). This variant occasionally contains striated muscle fibers (  ) with brisk mitotic activity. Melanocytic medulloblastoma shows melanotic cells commonly appearing as tubular epithelial structures (j). Melanotic tumour cells may also appear in different variants of medulloblastoma [Giangaspero, F. *et al*, chapter 8, (2007)].



The cell lines which derived from medulloblastoma tumours, were MED-1 and MED-2. The MED-1 cell line was established from a primary medulloblastoma, which had not previously been treated. MED-2 was derived from a recurrent medulloblastoma, which had been treated with both chemotherapy and radiation.

#### **1.1.2.2 CNS primitive neuroectodermal tumours (CNS PNET)**

CNS/supratentorial primitive neuroectodermal tumours (CNS PNET/SPNET) are described as PNETs developing in the CNS and spinal cord. CNS PNETs, a group of highly malignant lesions, comprise undifferentiated or poorly differentiated neuroepithelial cells, which may differentiate along neuronal, astrocytic, ependymal, muscular or melanocytic lines. CNS PNETs are rare in children accounting for approximately 2-3% of all PBTs. CNS PNET currently has a far worse prognosis than medulloblastoma (pineoblastoma). [Kuhl, J. *et al.* (2004)].

Several studies have revealed a variety of non-random cytogenetic gains and losses associated with CNS PNETs but not *i(17)q*. These include *RASSF1A* promoter methylation [Chang, Q. *et al* (2005)], expression of the *Neuro D* family of basic helix-loop-helix transcription factors and achaete scute (neurogenic transcription factor with homology to *Neuro D* genes [Rostomily, R. C. *et al* (1997)]). However, there is no evidence, which convincingly confirms genetic abnormalities specifically found in CNS PNETs.

The typical histological features of CNS PNET are described and shown in Figure 1.3. They are difficult to histologically distinguish from medulloblastomas. Therefore, the diagnosis of this tumour is still primarily based on a supratentorial location and the histological features of a predominantly undifferentiated neuroepithelial tumour with focal areas of divergent differentiation. CNS PNET patients have a much worse 5-year survival rate compared to children diagnosed with medulloblastoma especially in children aged under 2 years [Geyer, J. R. *et al* (2005)]. One study demonstrated that the 5-year survival rates of children with CNS PNET or medulloblastoma treated with pre- irradiation chemotherapy were 30% and 57%, respectively [Kühl, J. *et al* (1998)]. Due to the fact that CNS PNETs are commonly located in

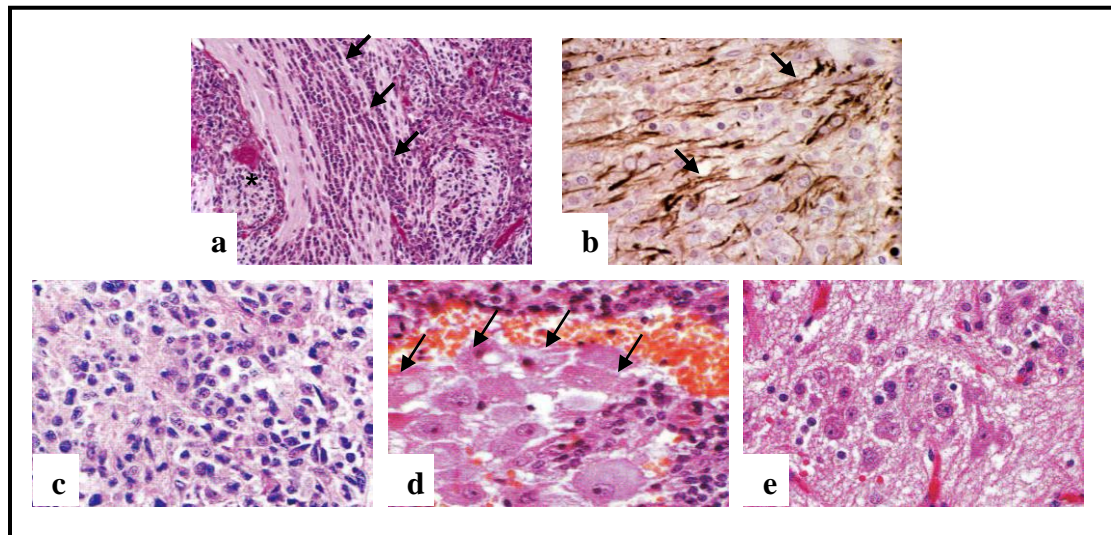


**Figure 1.3 Histological features of CNS PNETs, cerebral neuroblastomas and ganglioneuroblastomas.** Typical histology of PNETs are described as poorly differentiated cells with round regular nuclei and high nucleus:cytoplasm ratios. Tumours with only advanced neuronal differentiation exhibiting a nodular architecture (\*) with typical streaming of tumour cells ( ↘ ) are defined as cerebral neuroblastoma (a). Neurofilament (an intermediate filament which is a major element of the cytoskeleton of axon cytoplasm) staining ( ↘ ) predominantly expresses in tumour cell processes (b). PNETs having better differentiation may show different stages of neuronal differentiation (c). Cerebral neuroblastomas might express cluster of mature ganglion cells (arrows) with poorly differentiated area (d). Tumours having ganglion cells are defined as ganglioblastomas which may show regions of low cellularity with a neuronal phenotype (e) [McLendon, R.E. *et al*, chapter 8, (2007)].

paraventricular, thalamic and hypothalamic regions, they are difficult to resect surgically. In phase II trials, up-front multidrug chemotherapy was used to treat high-risk patients. Complete response plus partial response accounted for 57% in CNS PNET and 67% in medulloblastoma. Children diagnosed with CNS PNETs should be treated with postoperative craniospinal radiotherapy (CSRT) and chemotherapy; due to the fact that, occult microscopic dissemination frequently occurs in patients. Reduction of CSRT or total tumour dose or excluding CSRT may frequently result in fatal outcome [Kühl, J. *et al.* (2004)].

The cell line, which was established from CNS PNET tumour, is SPNET-1. This CNS PNET tumour was a primary tumour which had only been partially resected, then despite adjuvant chemotherapy and radiation the tumour recurred several times.

### **1.1.3 Oligodendroglioma**

Oligodendroglioma belongs to a family of oligodendroglial tumours which includes anaplastic oligodendroglioma, oligoastrocytoma and anaplastic oligoastrocytoma (Table 1.5). Additionally, oligodendroglial tumours range from well-differentiated neoplasms to malignant tumours defined as WHO grade II and III, respectively. Oligodendroglioma rarely occurs in children and represents only 1% of all PBTs diagnosed in children younger than 2 years [Razak, N. *et al* (1998)]. Oligodendroglioma is commonly situated in the cortex and the white matter of the cerebral hemispheres [Kros, J. M. *et al* (1994)]. Bilateral cerebral spreading of oligodendroglioma commonly occurs in patients [Packer, R. J. *et al* (1985)].

The most frequent genetic mutations found in oligodendrogliomas is unbalanced translocation between chromosomes 1 and 19 [t(1;19)(q10;p10)] which appears to be co-deletion of 1p and 19q. 1p and 19q deletion is the hallmark alteration in oligodendrogliomas and is found up to 80% of these cases. Entire loss of one copy of 1p and 19q commonly occurs in patients whilst partial deletions of these regions are infrequent. This genetic abnormality is used to distinguish between glioblastoma, occasionally have similar histology with oligodendroglioma, and oligodendroglioma since it is rare in glioblastoma [Aldape, K *et al* (2007)].

**Table 1.5 Oligodendroglial tumours** [Derived from Reifenberger, G. *et al*, chapter 2, (2007)].

Subtypes of ependymoma	Grade (WHO)	Frequency	Location	Histopathology	Genetics	Prognostic and predictive factors
Oligodendroglioma	II	<ul style="list-style-type: none"> <li>- 2.5% of all primary brain tumours and 5-6% of all gliomas</li> <li>- majority of cases arise in adults (peak incidence 40-45 years of age)</li> <li>- rare in children ( 2% of all brain tumours in patients &lt; 14 years of age)</li> </ul>	<ul style="list-style-type: none"> <li>- in the cortex and white matter of the cerebral hemispheres</li> <li>- 50-60% in the frontal lobe</li> <li>- commonly involves more than one cerebral lobe or bilateral tumour spread</li> </ul>	<ul style="list-style-type: none"> <li>- composed of monomorphic cells with uniform round nuclei and perinuclear halos ("honeycomb appearance"), microcalcifications, mucoid/cystic degeneration and a dense network of branching capillaries</li> </ul>	<ul style="list-style-type: none"> <li>- 80% of cases show co-deletion of chromosomal arms 1p and 19q</li> <li>- other genetic alterations include gain on chromosome 7 and losses on chromosomes 4,6, 11p, 14 and 22q</li> </ul>	<ul style="list-style-type: none"> <li>- typically slowly growing tumours with relatively long survival times</li> </ul>
Anaplastic oligodendroglioma	III	<ul style="list-style-type: none"> <li>- 1.2% of all primary brain tumours and 20-35% of all oligodendroglial tumours</li> <li>- predominant in adults (peak incidence 45-50 years of age)</li> </ul>	<ul style="list-style-type: none"> <li>- in the cerebral hemispheres with a preference at the frontal lobe, followed by the temporal lobe</li> </ul>	<ul style="list-style-type: none"> <li>- rounded hyperchromatic nuclei, perinuclear halos, few cellular process and focal microcalcifications, mitotic activity prominent, gliofibrillary oligodendrocytes and minigemistocytes are frequent</li> </ul>	<ul style="list-style-type: none"> <li>- approximately two thirds of cases have total losses of 1p and 19q</li> <li>- additional chromosomal abnormalities include gains on 7 and 15q, and losses on 4q, 6, 9p, 10q, 11, 13q, 18 and 22q</li> </ul>	<ul style="list-style-type: none"> <li>- combined therapy (chemo-radiotherapy) significantly prolongs progression-free survival (approximately 2-2.5 years) and overall survival times of about 4-5 years</li> </ul>
Oligoastrocytoma	II	<ul style="list-style-type: none"> <li>-reported incidence has been increasing over the last 10 years due to varying pathological criteria and increased recognition</li> <li>- studies report incidence of 1.8% and 19%</li> <li>- usually develop in middle-age between 35-45 years of age</li> </ul>	<ul style="list-style-type: none"> <li>- in cerebral hemispheres</li> <li>- order of site frequency; frontal, temporal, parietal then occipital</li> <li>- cerebellar localization very uncommon</li> </ul>	<ul style="list-style-type: none"> <li>- moderately cellular neoplasms with no or low mitotic activity</li> <li>- microcalcifications and microcystic degeneration may be present</li> <li>- necrosis and microvascular proliferation are absent</li> <li>- neoplastic glial cells with astrocytic or oligodendroglial phenotypes</li> <li>- divided into biphasic (compact) and intermingled (diffuse) variants</li> </ul>	<ul style="list-style-type: none"> <li>- 30-50% characterised by combined loss on chromosome 1p and 19q</li> <li>- 30% have mutations of the <i>TP53</i> gene</li> </ul>	<ul style="list-style-type: none"> <li>- factors associated with longer survival; younger age at operation (&lt; 37 years), gross total tumour resection, postoperative radiotherapy and low Ki-67 levels (index of mitotic activity)</li> </ul>
Anaplastic oligoastrocytoma	III	<ul style="list-style-type: none"> <li>- precise epidemiological data is not available</li> <li>- peaks in the fifth decade (mean at 44 years)</li> </ul>	<ul style="list-style-type: none"> <li>- predominantly in cerebral hemispheres</li> <li>- mostly occur in the frontal lobe followed by the temporal lobe</li> </ul>	<ul style="list-style-type: none"> <li>- oligoastrocytomas with histological features of anaplasia, including nuclear atypia, cellular pleomorphism, high cellularity, and high mitotic activity</li> <li>- microvascular proliferation may be present</li> </ul>	<ul style="list-style-type: none"> <li>- loss of 1p/19q or <i>TP53</i> mutations</li> </ul>	<ul style="list-style-type: none"> <li>- important prognostic markers; necrosis is associated with worse prognosis and 1p loss associated which is improved progression-free and overall survival</li> </ul>

Histological features of oligodendroglioma are described in Figure 1.4. Presently, there are no specific immunohistochemistry markers that are able to identify human oligodendroglial tumours because oligodendrogliomas express many markers similar to other brain tumours such as S-100 protein, the HNK1 (anti-Leu7, CD57) carbohydrate epitope [Nakagawa, Y. (1986)], microtubule-associated protein 2 (MAP2) [Blumcke, I. *et al* (2001)], oligodendrocyte lineage-specific transcription factors (OLIG-1 and OLIG-2) [Riemenschneider, M. J. *et al* (2004)] and SOX10 [Bannykh, S. I. *et al* (2006)]. Therefore, these markers might not help in diagnosis of oligodendroglioma.

A retrospective review of 106 patients diagnosed between 1979-1997 (77 oligodendroglioma and 29 mixed glioma) found that 5- and 10-year survival rates were 71% and 54%, respectively [Olson, J.D. *et al* (2000)]. Factors involved in worse prognosis are necrosis, high mitotic activity, increased cellularity, nuclear atypia, cellular pleomorphism and microvascular proliferation. Low or high expression of Ki-67 indicates low or high grade histology of neoplasms, respectively. Several studies have reported as Ki-67 index over 3-5% as a significant factor involved in worse prognosis [Dehghani, F. *et al* (1998), Heegaard, S. *et al* (1995)].

Olig-1 is the cell line that was derived from an oligodendroglioma tumour. This oligodendroglioma tumour was a primary tumour. This cell line was included in some experiments to compare the results with cell lines (EPN-2, MED-2, SPNET-1 and PFSK-1) and it was mainly studied by Dr. Deema Hussein, Postdoctoral researcher.

#### **1.1.4 Glioblastoma multiforme (GBM)**

Glioblastoma multiforme (glioblastoma, GBM) is rare in children and it preferentially affects adults between 45 and 75 years of age [Ohgaki, H. *et al* (2004)]. The variants of glioblastoma are explained in Table 1.6. GBM may be biologically and clinically subdivided into primary (> 90%) and secondary (< 10%) GBM. Primary GBM develop very rapidly (usually < 3 months) without clinical histopathological evidence of a pre-existing precursor

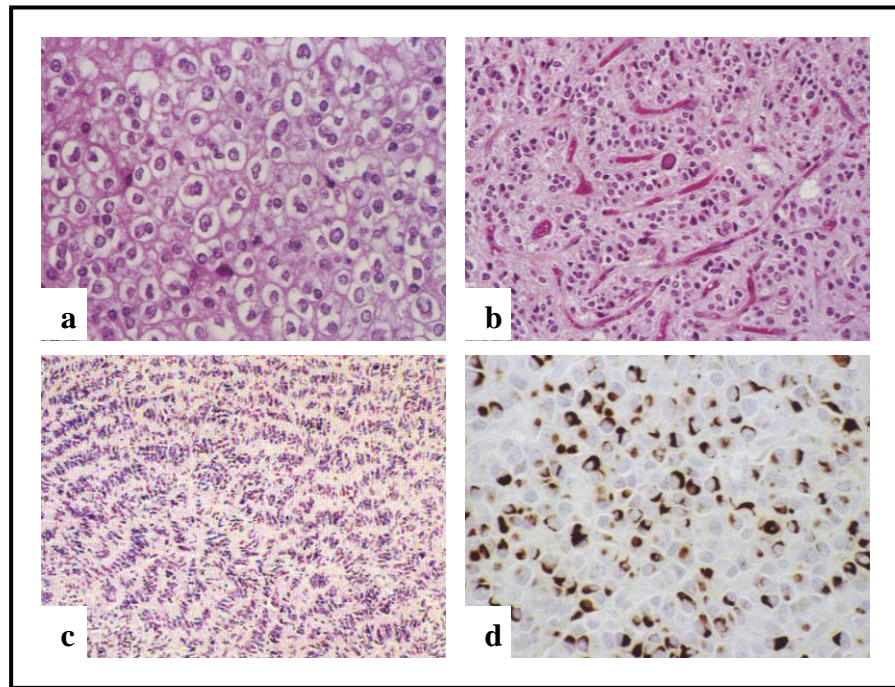


**Figure 1.4 Histological features of oligodendrogliomas.** Tumour cells degenerated by acute swelling result in an enlarged round cell with clear cytoplasm and well defined plasma membrane are described as typical honeycomb pattern (a). Oligodendroglioma normally shows a dense network of branching capillaries which is similar to the pattern of chicken-wire and occasionally causes intratumoural haemorrhage (b). Rare growth of oligodendroglioma as tumour cells form parallel rows with elongated nuclei forming a striking pattern of nuclear palisading (c). Some oligodendrogliomas contains tumour cells with the appearance of small gemistocytes with eccentric cytoplasm which is positive for glial fibrillary acidic protein (GFAP) (d). These cells were identified as minigemistocytes or microgemistocytes [Reifenberger, G. *et al*, chapter 2, (2007)].

lesion. Conversely, secondary GBM gradually develop through progression of diffuse astrocytoma grade II or anaplastic astrocytoma grade III. The prognosis of GBM is extremely poor and survival rates of more than one year and more than 3 years are found in less than 20% and 3%, respectively, of all GBM cases. Secondary GBM has significantly longer survival rate (7.8 months) than that of the primary GBM (4.7 months) [Ohgaki, H. *et al* (2004), Ohgaki, H. and Kleihues, P. (2005)]. Histological features demonstrating necrosis [Burger, P. C. *et al* (1987), Pierallini, A. *et al* (1998)] and genetic alteration of LOH 10q [Ohgaki, H. *et al* (2004)] also correlate with a shorter survival.

There are several genetic abnormalities in GBM including *TP53* mutation, loss of heterozygosity (LOH) on chromosome 10q and 17p, epidermal growth factor receptor (*EGFR*) amplification, *P16<sup>INK4a</sup>* deletion, and *PTEN* mutation. Secondary GBM predominantly have *TP53* mutations (65%), whereas, LOH 10q typically occurs in primary GBM. Patients diagnosed with GBM normally carry a poor prognosis. [von Deimling, A. *et al* (1993)]. GBMs display variable histological features and morphological heterogeneity [Figure 1.5].

BT-4 was the cell line used in this study. It was derived from a primary tumour originally described as a giant cell GBM but rediagnosed as malignant glioneuronal tumour (MGNT) during the course of this study (Hussein *et al* unpublished).

Low grade brain tumours (grade II: Ependymoma and Oligodendroglioma) and high grade brain tumours (grade IV: Medulloblastoma, CNS PNET and Glioblastoma multiforme) were included in this study. These brain tumours include those with low survival rates (medulloblastoma, CNS PNET and GBM) and these that commonly recur after treatment (ependymoma). Chemotherapy is still the standard treatment in many cancers. This is described in the next topic. Presently, the failure of chemotherapeutic treatment due to multidrug resistance in cancers is an unresolved problem.

**Table 1.6 Glioblastoma tumour variants** [Derived from Kleihues, P. *et al*, chapter 1, (2007)].

Variant types of Glioblastoma	Grade (WHO)	Frequency	Location	Histopathology	Genetics	Prognostic and predictive factors
Glioblastoma	IV	<ul style="list-style-type: none"> <li>- the most frequent brain tumour (12-15% of all intracranial tumours)</li> <li>- 60-75% of astrocytic tumours</li> <li>- preferentially affects adults between 45-75 years of age</li> </ul>	<ul style="list-style-type: none"> <li>- the subcortical white matter of the cerebral hemispheres (temporal lobe: 31%, parietal lobe: 24%, frontal lobe: 23%, and occipital lobe: 16%)</li> </ul>	<ul style="list-style-type: none"> <li>- histopathology is extremely variable, with a high degree of cellular ranging from nuclear polymorphism with numerous multinucleated giant cells to monotonous cells</li> <li>- predominant features: poorly differentiated cells, pleomorphic astrocytic tumour cells with marked nuclear atypia and brisk mitotic activity, prominent microvascular proliferation and/or necrosis</li> </ul>	<ul style="list-style-type: none"> <li>- significant genetic alterations combining <i>TP53</i> mutations, loss of heterozygosity (LOH) on chromosomes 10 and 17p and <i>EGFR</i> amplification</li> </ul>	<ul style="list-style-type: none"> <li>- overall survival is extremely poor, less than 20% of patients survive more than one year</li> <li>- predictive factors that associate with poor prognosis such as age &gt; 50 years at diagnosis, presence and extent of necrosis, presence of LOH 10</li> </ul>
Giant cell glioblastoma (GC-GBM)	IV	<ul style="list-style-type: none"> <li>- accounts for up to 5% of glioblastomas and less than 1% of all brain tumours</li> <li>- mean age at clinical manifestation is 41 years</li> </ul>	<ul style="list-style-type: none"> <li>- often located subcortically in the temporal and parietal lobes</li> </ul>	<ul style="list-style-type: none"> <li>- comprised of numerous multinucleated giant cells, smaller fusiform cells and, to a varying extent, a reticulin network</li> <li>- may be heavily lipidized</li> <li>- frequent atypical mitosis and necrosis</li> </ul>	<ul style="list-style-type: none"> <li>- characterised by frequent <i>TP53</i> mutations (75-90% of cases) and <i>PTEN</i> mutations (33%), but typically lacks <i>EGFR</i> amplification/overexpression and homozygous p16 deletion</li> </ul>	<ul style="list-style-type: none"> <li>- carry a poor prognosis but some reports indicate the clinical outcome is better than ordinary glioblastoma (possibly because it is less frequent)</li> </ul>
Gliosarcoma (GS)	IV	<ul style="list-style-type: none"> <li>- accounts for approximately 2% of all glioblastomas</li> <li>- preferentially manifests between ages 40 and 60</li> <li>- rarely occurs in children</li> </ul>	<ul style="list-style-type: none"> <li>- located in the cerebral hemispheres, involving temporal, frontal, parietal and occipital lobes in decreasing order of frequency</li> <li>- rarely occurs in the posterior fossa and spinal cord</li> </ul>	<ul style="list-style-type: none"> <li>- mixed gliomatous and sarcomatous tissue confers a biphasic tissue pattern</li> <li>- epithelial differentiation manifest as carcinomatous features with gland-like or adenoid formations and squamous metaplasia</li> <li>- sarcomatous features of malignant transformation component shows nuclear atypia, mitotic activity and necrosis</li> </ul>	<ul style="list-style-type: none"> <li>- contains <i>PTEN</i> mutations (38-45%), <i>p16<sup>INK4A</sup></i> deletions (38%) and <i>TP53</i> mutations (23-24%)</li> </ul>	<ul style="list-style-type: none"> <li>- has a more favourable prognosis than ordinary glioblastoma</li> </ul>



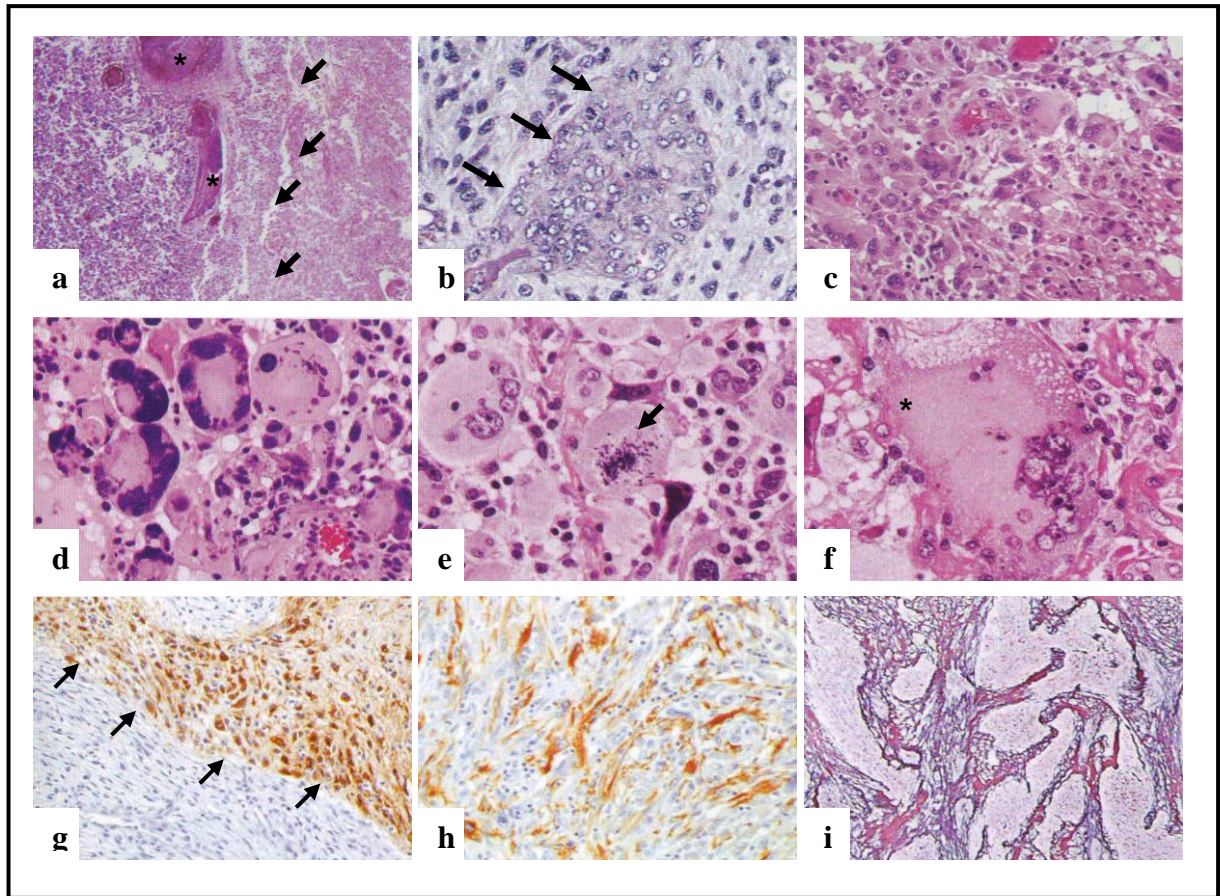


**Figure 1.5 Histological features of GBM and variant GBM.** Glioblastoma “multiforme”, suggests the histopathology of this tumour is variable. GBM shows essential histological characteristics for diagnosis which are a large ischemic necrosis ( ➤ , a) and several large thrombosed tumour vessels (\*, a). Microvascular proliferation with formation of a multilayered ‘glomeruloid tuft’ ( ➤ , b) and a high degree of anaplasia (c) are also significant characteristics for diagnosis. GC-GBM comprise cells of variable size and shape (d) (may measure more than 500µm in diameter), a giant cell with an atypical mitotic figure ( ➤ , e) and a very large multinucleated giant cell (\*, f). GBM are characterised by a biphasic tissue pattern with alternating areas displaying glial and mesenchymal differentiation. GBM typically express strong GFAP expression of gliomatous components geographically separated from sarcomatous tumour cells ( ➤ , g) or GFAP staining cells blended with sarcomatous tumour cells (h). A biphasic tissue pattern may also be displayed as reticulin-rich sarcomatous and reticulin-free gliomatous elements (i) [Kleihues, P. *et al*, chapter 1, (2007)].

## 1.2 Chemotherapeutic treatment of paediatric brain tumours

The general principles of treatment in paediatric brain tumours consist of surgical treatment, radiotherapy and chemotherapy. Surgery is the initial treatment, which provides a tissue biopsy for histologic diagnosis and decreases tumour burden. However, some brain tumours such as diffuse glioma of brain stem or deep-seated tumours are less surgically accessible due to the high risk of destroying vital brain areas. Radiotherapy is essential for some tumours such as medulloblastomas, which frequently disseminate throughout the neuraxis, and glioblastoma multiformes, which are highly aggressive and locally invasive tumours. However, for children ages less than 2 or 3 years radiotherapy is avoided due to the fact that radiation affects the developing nervous system resulting in impaired cognition and memory. Therefore, postoperative chemotherapy is necessary in patient at these ages. Chemotherapy is mandatory treatment in many cancers and commonly used as postoperative treatment [Reviewed in Pollack, I. F. (1994)].

Chemotherapy had been used as a standard treatment of cancers for many years, the outcome after chemotherapy is however still minimal success. Combined treatment of various chemotherapeutic drugs is normally applied to treat patients to avoid multidrug resistance, which is a major problem in cancer treatment and cause of tumour relapse. Multidrug resistance in cancers has been extensively studied in many aspects to understand the biology of drug resistant cancers and improve treatment. Nevertheless, multidrug resistance in cancer cells has not been conquered yet. Novel chemotherapeutic agents have been developed and new derivatives synthesised to improve the quality of treatment and reduce drug toxicity. Many chemotherapeutic agents that have been used to treat brain tumours and chemotherapeutic drugs for CNS cancers, which had been developed within the last two decades, are shown in Table 1.7. With respect to the study undertaken in this thesis 4 common chemotherapeutic drugs (etoposide, cisplatin, irinotecan and methotrexate), which are known to be the substrates of ABC transporters [Szakács, G *et al* (2006)], are described in detail with respect to general information or drug history, chemical structures, mechanisms of action and resistance mechanisms to drugs.

### 1.2.1 Etoposide

Etoposide (VP-16) belongs to the podophyllin group, which has been used in folk medicine for over a thousand years to treat many diseases. Toxicity of podophyllotoxins however was a limitation to their use. The most effective derivative from the Indian *Podophyllum* plant was 4'-demethylepipodophyllin benzyldene glucoside (DEPBG). Later, etoposide (VP-16) and Teniposide (VM-26) were successfully synthesised in 1966 and 1967, respectively. These 2 analogues of DEPBG effectively preserve antineoplastic activity better than previous derivatives [Reviewed in Hande, K. R. (1998)].

**Table 1.7 Chemotherapeutic drugs used to treat CNS cancers** [Bredel, M. (2001)]

<b><i>Chloroethylnitrosoureas (CENUs)</i></b> Carmustine (BNCU) Lomustine (CCNU) Nimustine (ACNU) Semustine (MeCCNU) PCNU HeCNU NB-Fotemustine	<b><i>Antimetabolites</i></b> <b>Methotrexate (MTX)</b> Edatrexate 5-Fluorouracil (5-FU) Cytosine arabinoside (Ara-C) 6-Thioguanine (6-TG) 5-Fluorocytosine (5-FC) Bromodeoxyuridine (BrdU) Iododeoxyuridine (IUDR) Methylprednisolone (MPred)	<b><i>Protein kinase C (PKC) inhibitors</i></b> Tamoxifen Bryostatin 7-Hydroxystaurosporine (UCN-01)
<b><i>Vinca alkaloids</i></b> Vincristine (VCR) Vinblastine (VBL)	<b><i>Alkylating agents</i></b> Temozolomide Procarbazine (PCB) Dacarbazine (DTIC) Thiotepa Chlorambucil Busulfan Melphalan Hydroxyurea (HU) Gemcitabine Spirohydantoin mustard (SHM)	<b><i>Miscellaneous agents</i></b> Difluoromethylornithine (DFMO) Mechlorethamine Nitrogen mustard (HN2)
<b><i>Epipodophyllotoxins</i></b> <b>Etoposide (VP-16)</b> Teniposide (VM-26)		Mitoxantrone Topotecan Etanidazole (ETA) Misonidazole (MISO) <b>Irinotecan (CPT-11)</b> Lovastatin Methylglyoxal bisquanylhydrazide Benznidazole Didemnin B Acivicin
<b><i>Platinum compounds</i></b> <b>Cisplatin (CDDP)</b> Carboplatin		Boswellic acids Thalidomide Eflornithine Piroxantrone
<b><i>Phosphamides</i></b> Cyclophosphamide (CPA) Ifosfamide Mafosfamide	<b><i>Antibiotics</i></b> Doxorubicin Iradubicin Epirubicin Actinomycin D Bleomycin (Bleo) Aziridinylbenzoquinon (AZQ) KRN8602 (MX-2)	<b><i>Hexitol derivatives</i></b> Dibromodulcitol (DBD) Dianhydrogalactitol (DAG)
<b><i>Taxanes</i></b> Paclitaxel Docetaxel		

The four drugs that are the focus of this thesis are highlighted.

## The structure of etoposide

Etoposide is one of the most common drugs used to treat many tumours. It is a semi-synthetic epipodophyllotoxin. Etoposide having molecular weight 588 is weakly soluble in water. Therefore, etoposide phosphate had been developed to improve the solubility. Etoposide phosphate, the prodrug of etoposide which is converted by alkaline phosphatase action in blood, is water soluble. Etoposide phosphate shares the same pharmacokinetics and toxicities as etoposide [Reviewed in Hande, K. R. (1998)]. The chemical structures of the parental compound (podophyllotoxin) including other derivatives; etoposide, etoposide phosphate and teniposide are shown in Figure 1.6.

## The mechanism of action

In all cells, the processes of DNA replication, transcription, chromosomal segregation and DNA recombination require DNA topoisomerase, which comprises 2 types; topoisomerase I and topoisomerase II. Topoisomerase I is required for single strand cuts in DNA whilst topoisomerase II is essential for cutting and passing an intact double helix through a transient double-stranded DNA break (Figure 1.7) [Wang, J. C. *et al* (1971) and Gellert, M. *et al* (1976)]. The main target of etoposide is nuclear topoisomerase II enzyme, which is a

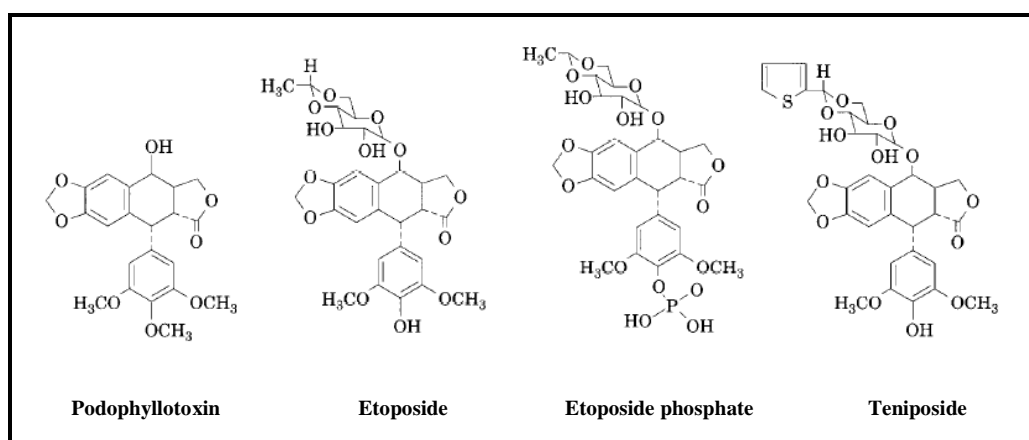


**Figure 1.6 The chemical structure of the podophyllotoxin and derivatives; etoposide, etoposide phosphate and Teniposide.** The figure shows the chemical structures of the original compound (podophyllotoxin) and its derivatives (etoposide, etoposide phosphate and Teniposide) [Adapted from Joel, S. (1996)].

homodimer, consisting of 2 forms; topoisomerase II  $\alpha$  (170 kDa) and topoisomerase II  $\beta$  (180 kDa). Topoisomerase II  $\alpha$  activity is highly increased during DNA replication detected in particular during S and G2 phases of cell cycle and has been correlated with DNA replication whilst topoisomerase II  $\beta$  expression is detected at a low level throughout all phases of cell cycle [Joel, S. (1996)].

The mechanism of etoposide's antineoplastic effects is still poorly understood. Topoisomerase II function requires ATP for catalytic activity and modulation of DNA topology. Etoposide inhibits topoisomerase II function by directly binding to a covalent DNA and topoisomerase II complex resulting in stabilising of this complex. To inhibit topoisomerase II, etoposide interacts with the closed-gate state of topoisomerase II (Figure 1.7) [Chen, A. Y. and Liu, L. F. (1994)]. Stabilisation of the covalent complex toxin causes DNA breaks resulting in cell death.

In 2003, Bromberg and colleagues postulated that there were 2 possible models for etoposide mechanism; one-drug model and two-drug model (Figure 1.8) [Bromberge, K. D. *et al* (2003)]. In the one-drug model etoposide affected on only one scissile bond of DNA but due to a strong communication between the active site of each topoisomerase II promoter, this was effective to cause double-stranded DNA breaks. In contrast, the two-drug model postulated that etoposide was required on both sites of scissile bonds to effectively lead to double-stranded DNA breaks. Drug action on each site worked independently and there was the slightest communication between these 2 topoisomerase II promoters. Therefore, if etoposide action occurs on a single scissile bond, this results in single-stranded DNA breaks [Bromberge, K. D. *et al* (2003)]. In addition, in 1985, DNA breakage and repair were studied in human lung adenocarcinoma cells *in vitro* and the investigators found that single- and double- stranded DNA breakage were detected shortly after both etoposide and Teniposide exposure. After cells were incubated with both drugs for 1 hour then drugs were removed, approximately half of all single- and double- stranded DNA breakages were repaired within 1 hour [Long, B. H. (1985)].

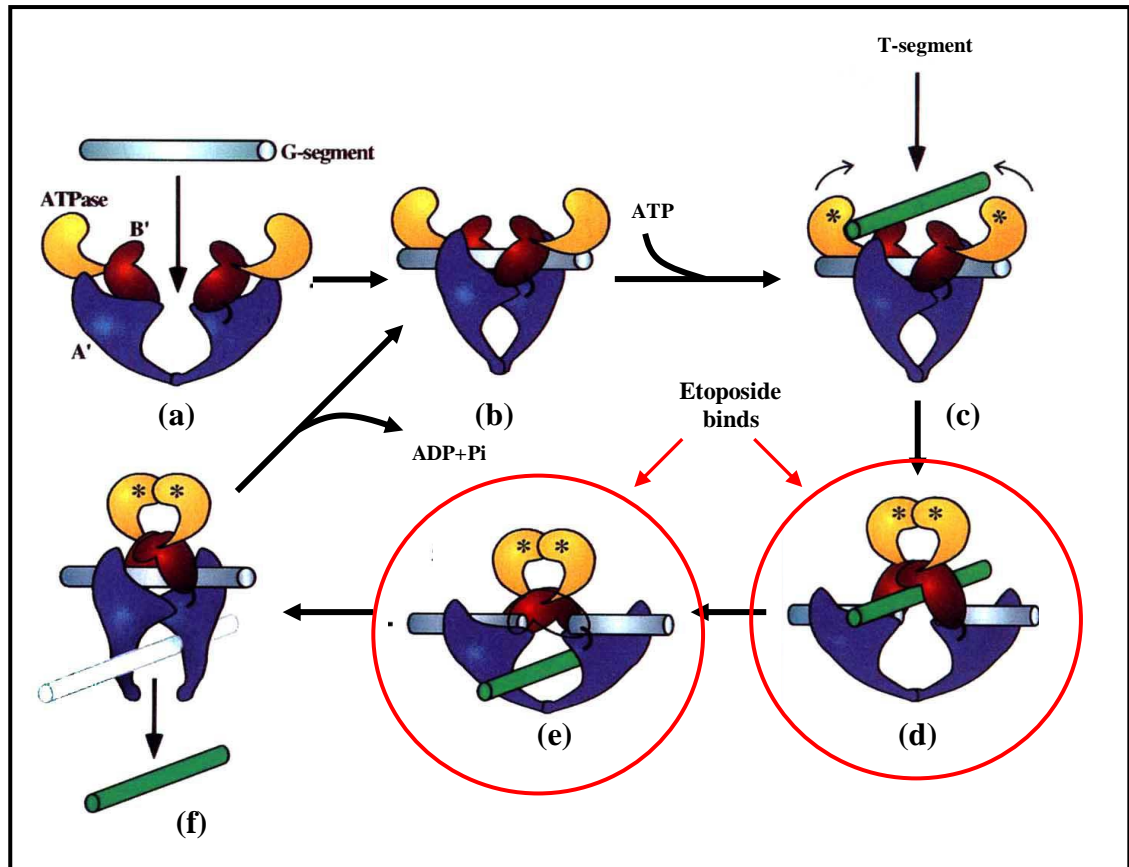


**Figure 1.7 Topoisomerase II function.** Topoisomerase II enzyme is composed of an ATP unit (yellow colour), an A' subfragment (blue colour) and a B' subfragment (red colour) (a). When G-segment DNA (grey rod), which contains the DNA gate, binds to topoisomerase II, it results in modification of the topoisomerase II structure (b) then T-segment DNA passes through (c). Due to binding of ATP unit, G-segment DNA is split into 2 parts by the A' subfragment (d) then the ATP domain dimerises and transported T-segment DNA (green rod) is allowed to pass through the broken G-segment DNA into the central hole (e). G-segment DNA is resealed again and T-segment DNA is transported through the opening of A' subfragment (f). Etoposide inhibits topoisomerase II function by directly binding to DNA and topoisomerase II complex during the close gate stage [d and e] resulting in stabilisation of DNA and DNA breaks [Adapted from Burger, J. M. *et al* (1996)]. Red circles indicate the stage that etoposide binds to topoisomerase II enzyme.

### Resistance mechanisms to etoposide

Two mechanisms of resistance to etoposide have been described; decreased intracellular accumulation of drug and atypical multidrug resistance (at-MDR) [Joel, S. (1996)]. A significant factor, which leads to decreased intracellular accumulation of drug, is the multidrug resistance gene (*MDR1*) and its product P-glycoprotein (ABCB1) [Endicott, J. and Ling, V. (1989)]. Drug resistance has been shown to develop by increasing the expression of P-glycoprotein after cells have been exposed to even one drug and this often results in cross resistance to other drugs of unrelated structure. at-MDR describes any drug resistance

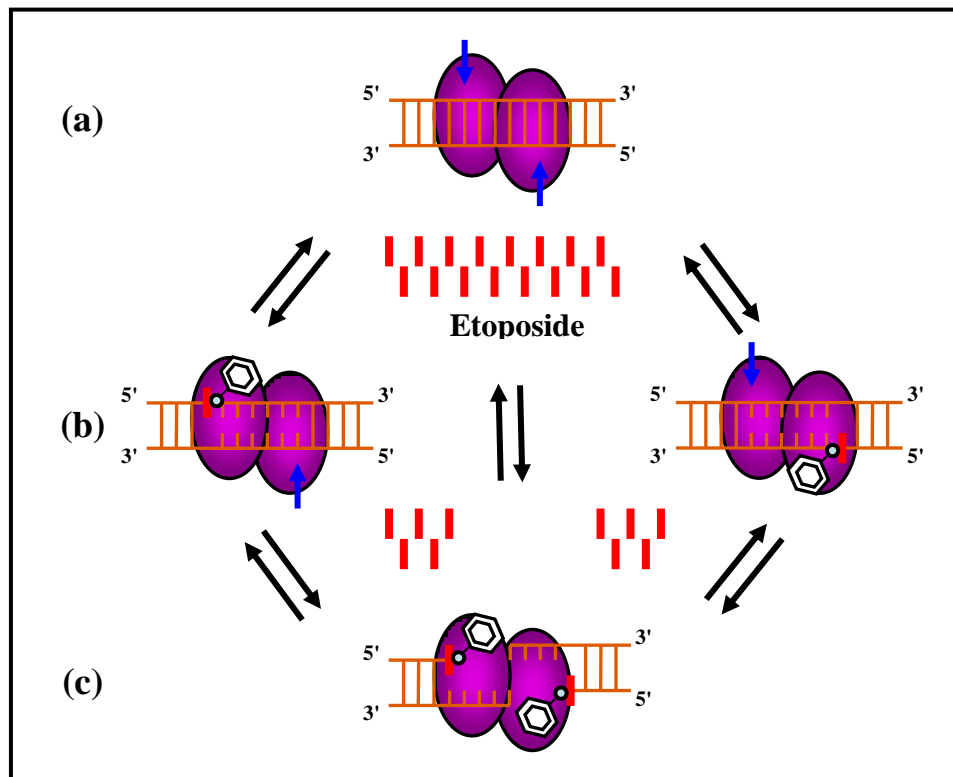


**Figure 1.8 One- and two-drug model of etoposide mechanism.** Etoposide is represented as red rods and blue arrows indicate active sites, to which etoposide binds (a). In the one-drug model etoposide binds to a single scissile (b), which is effective enough to cause double stranded DNA break due to strong communication between 2 scissiles. Whilst the two-drug model proposed that etoposide binds to both scissiles resulting in double stranded DNA break (c). If etoposide binds to a single scissile, this results in single stranded DNA break (b) [Adapted from Bromberg, K. D. *et al* (2003)].



mechanism which does not involve overexpression of P-glycoprotein. Any alteration of topoisomerase II with regard to either a lower level of topoisomerase II enzyme or a mutation of topoisomerase II, which alters ATP binding, can lead to drug resistance [Bugg, B. Y. *et al* (1991)]. This decreases the amount of covalent DNA complex resulting in decreasing etoposide activity. Additionally, lengthening of the cell cycle can reduce etoposide efficacy since etoposide action is specific to S and G2 phases of cell cycle, which contain a very high level of topoisomerase II enzyme [Long, B. H. *et al* (1991)]. Increased DNA repair also leads to drug resistance whereby single- or double-stranded DNA breakage resulting from etoposide treatment can be repaired quickly when etoposide is removed.

### **1.2.2 Cisplatin**

Cisplatin is also known as Dichloroplatinum azanide, Cisplatinum, *Cis*-diamminedichloroplatinum (II) (CDDP) or *cis*-DDP. There are 3 antitumour drugs, which belong to the platinum group, including cisplatin, carboplatin and oxaliplatin. *cis*-DDP were first synthesised in 1845 and is generally known as Peyrone's chloride. In the 1900s, *Cis*-diamminedichloroplatinum (II) and *cis*-DDP forms of platinum were successfully used in treatment of cancer [Reviewed in Lippard, S. J. (1982)]. Later, cisplatin was identified as the main anti-proliferative agent among the platinum group, and was generally used to treat cancer [Review in Cepeda, V. *et al* (2007)].

#### **The structure of cisplatin**

The platinum atom contains 2 nitrogen atoms of the ammine ligands and 2 chloride atoms of *cis*-DDP. The structures of cisplatin and other forms of platinum group including carboplatin, oxaliplatin and biologically inactive transplatin are shown in Figure 1.9. Oxaliplatin is the only member of the platinum group claimed to be able to overcome cisplatin resistance in tumours such as colorectal carcinoma [Reviewed in Cepeda, V. *et al* (2007)].



### The mechanism of action

The main target of cisplatin is gDNA and the N7 atoms of guanine and adenine, which are located on the major groove of the double helix (Figure 1.10, D). There are 2 different forms of binding kinetics between cisplatin and DNA: monofunctional formation (*cis*-[Pt(NH<sub>3</sub>)<sub>2</sub>(H<sub>2</sub>O)]:DNA adducts) (Figure 1.10, C) and bifunctional formation (*cis*-[Pt(NH<sub>3</sub>)<sub>2</sub>]:DNA) (Figure 1.10, A and B). Bifunctional formation can occur by either interstrand (Figure 1.10, B) or intrastrand cross-links (Figure 1.10, A). The majority of cisplatin and DNA formation (60-65%) are 1, 2-d(GpG) intrastrand cross-links although d(ApG) intrastrand cross-links do occur (20-25%). Monofunctional and bifunctional formations result in inhibition of DNA replication and transcription [Payet, D. *et al* (1993)]. Cisplatin results in cell death or inhibition depending on the concentration applied. The effects of cisplatin in G2 arrest and DNA double-strand breaks were studied in murine leukaemic L1210 cells and the results demonstrated that cells were transiently inhibited at G2 phase for 24-48 hours at a lower concentration of cisplatin (1.67 µM) then cells were recovered after drug removal. Whilst the higher concentration of cisplatin (26.67 µM) led to cells arresting at the G2 phase and double stranded DNA breakage, which could not be recovered within 96 hours [Sorenson, C. M. and Eastman, A. (1988)].

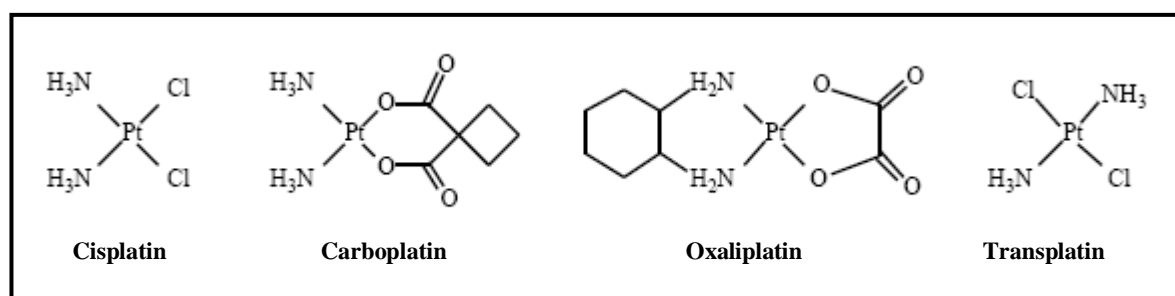


**Figure 1.9 The chemical structures of the platinum group.** The chemical structures of the active derivatives of platinum compound including cisplatin, carboplatin and oxaliplatin and the inactive derivative: transplatin [Cepeda, V. *et al* (2007)].

## Resistance mechanism to cisplatin

The resistance of tumour cells to cisplatin treatment is still an unresolved problem in many types of cancers. At present, many studies have tried to investigate the mechanisms of cisplatin resistance, however, the exact mechanisms to explain cisplatin resistance in tumour cells are not fully understood. Three mechanisms were postulated to be important in cisplatin resistance: decreasing intracellular cisplatin accumulation [Richon, V. M. *et al* (1987), Teicher, B. A. *et al* (1987) and Waud, W. R. (1987)] e.g. overexpression of transporter membrane protein e.g. SQM1 identified in human squamous carcinomas [Bernal, S. D. *et al* (1990)] and CP<sup>R</sup>-200 identified in murine thymic lymphoma sublines [Kawai, K. *et al* (1990)], increasing levels intracellular thiols inactivating cisplatin [Andrews, P. A. *et al* (1985),

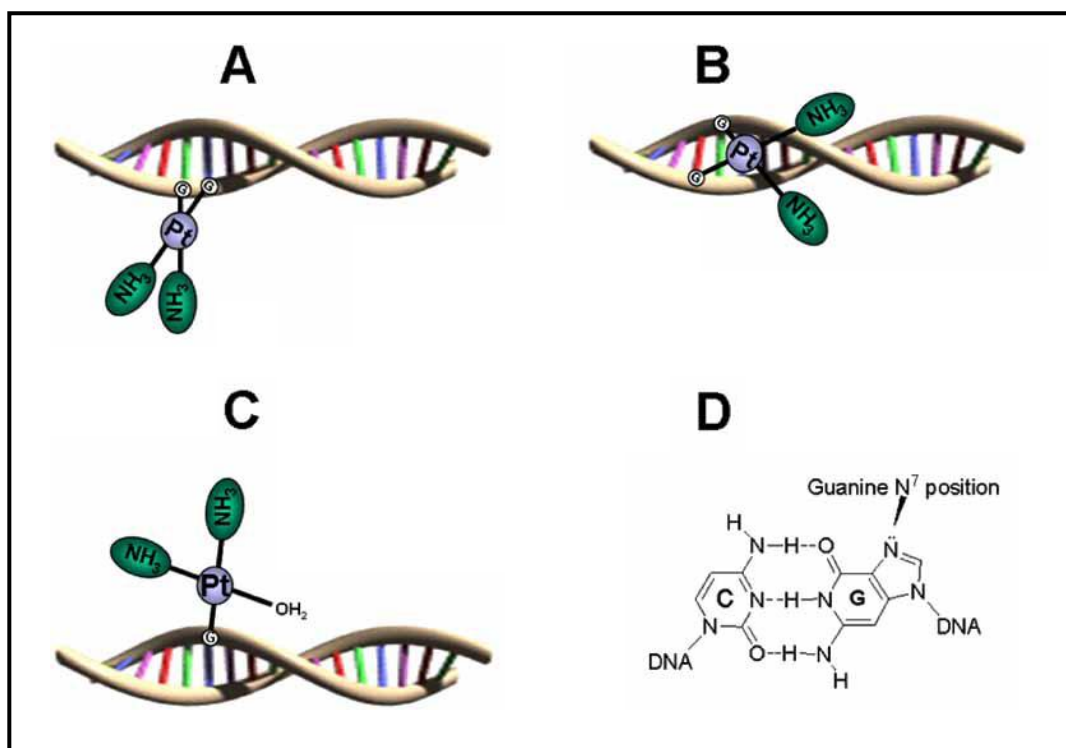


**Figure 1.10 Cisplatin and DNA formation.** Figure demonstrates various binding forms between cisplatin and DNA; bifunctional formation consisting of 2 binding sites of cisplatin within the same DNA strand [intrastrand cross-link (A)] or between 2 DNA strands [interstrand cross-link (B)], monofunctional formation composing one binding site of cisplatin on one DNA strand (C) and the N7 position of Guanine, which is the specific site for cisplatin binding to DNA (D) [Adapted from Cepeda, V. *et al* (2007)].

Hromas, R. A. *et al* (1987), Dabholkar, M. *et al* (1992) and Schilder, R. J. *et al* (1990)] and an increase in DNA repair [Parker, R. J. *et al* (1991), Eastman, A. and Schulte, N. (1988) and Sheibana, N. *et al* (1989)]. However, evidence of these 3 main mechanisms of cisplatin resistance is inconsistent and has not been convincingly confirmed.

### **1.2.3 Irinotecan**

Irinotecan is also known as CPT-11, Camptosar<sup>®</sup> and 7-ethyl-10-[4-(1-piperidino)-1-piperidino] carbonyloxycamptothecin, which is a semisynthetic water soluble analogue of camptothecin. In 1983, camptothecin was primarily discovered and synthesised in Japan [Rothenberg, M. L. (2001)]. Irinotecan, which has a broad spectrum of anticancer treatment, was discovered earlier and applied to treat cancers for many years before the mechanisms of irinotecan action in cancer treatment were revealed [Wall, M. E. *et al* (1966)]. At present, irinotecan is widely used to treat many types of cancers such as colorectal cancers, oesophageal cancers, gastric cancers, non-small-cell and small-cell lung cancers, leukaemia, lymphomas, and CNS cancers [Reviewed in Rothenberg, M. L. (2001)]. Currently, the metabolism of irinotecan is very complicated and it has been extensively studied due to the many enzymes, which are involved in the process of metabolising and converting irinotecan to various forms.

#### **The structure of irinotecan**

The chemical structure of irinotecan is illustrated in Figure 1.11 including its metabolites. Several enzymes metabolise irinotecan to either active or inactive metabolites including cytochrome P450 3A (CYP3A), carboxylesterases (CES) and uridine diphosphate-glucuronosyltransferase 1A (UGT1A). In humans, irinotecan is catalysed by CES to the most potent metabolite: SN-38 (7-ethyl-10-hydroxycamptothecin), which has 100 – 1,000 fold higher potency than the parental compound [Kawato, Y. *et al* (1991)]. CYP3A also plays an important role in the metabolic pathway of irinotecan converting it to inactive metabolites 7-ethyl-10-[4-*N*-(5 aminopentanoic acid)-1-piperidino] carbonyloxycamptothecin (APC) and 7-ethyl-10-(4-amino-1-piperidino) carbonyloxycamptothecin (NPC). Additionally, NPC might

also be metabolised by CES and converted back to SN-38, which is an active metabolite again [Santos, A. *et al* (2000)]. UGT1A is an important enzyme in glucuronidation of SN-38 whereby  $\beta$ -glucuronic acid is conjugated to SN-38 resulting in formation of 10-O-glucuronyl-SN-38 (SN-38G) (Figure 1.11, e). This is the main mechanism to detoxify SN-38 [Iyer, L *et al* (1998)].

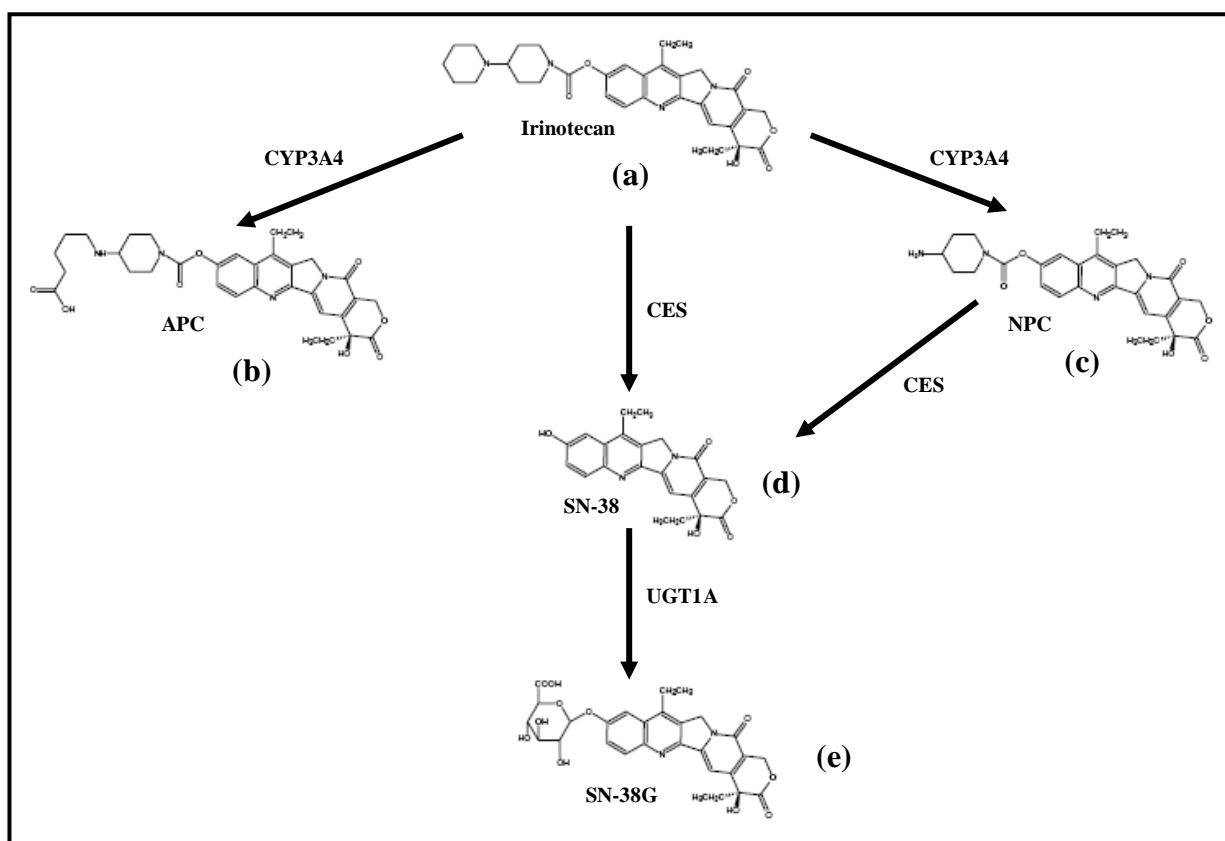


**Figure 1.11 Metabolism pathway of irinotecan.** There are several enzymes involving in metabolism of irinotecan. Irinotecan (a) is converted to an active metabolite (SN-38) (d) by Carboxylesterase (CES). Cytochrome P450 3A (CYP3A) functions to metabolise irinotecan to inactive metabolites; 7-ethyl-10-[4-N-(5 aminopentanoic acid)-1-piperidino] carbonyloxycamptothecin) (APC) (b) and 7-ethyl-10-(4-amino-1-piperidino) carbonyloxycamptothecin (NPC) (c). To detoxify SN-38, which is the most potent metabolite of irinotecan, SN-38 is glucuronised by UGT1A whereby SN-38 is conjugated with  $\beta$ -glucuronic acid resulting in the formation of 10-O-glucuronyl-SN-38 (SN-38G) (e) [Adapted from Smith, N. F. *et al* (2006)].

### **The mechanisms of action**

The main target of irinotecan is DNA topoisomerase I enzyme, which is an important enzyme in reducing DNA twisting and supercoiling, consequently, it is an essential enzyme in the process of DNA transcription, replication and repair recombination. Irinotecan binds reversibly to the DNA-topoisomerase I complex resulting in its stabilisation. This process inhibits resealing of single stranded DNA breaks and prevents accession of the replication fork leading to double stranded DNA breaks ultimately causing cell death. However, irinotecan can only effectively target the DNA-topoisomerase I complex while cells are in the G2 or S phase [Hsiang, Y. H. *et al* (1989)]. Therefore, irinotecan effectively targets proliferating cells particularly in rapidly dividing tissues such as bone marrow cells and intestinal mucosa. Significant adverse effects of irinotecan are myelosuppression and diarrhoea, which limit irinotecan dose for treatment [Rowinsky, E. K. *et al* (1994)]. For excretion of irinotecan and all of its metabolites, the ABC transporter superfamily is the main transporter via a hepatobiliary pathway in faeces [Slatter, J. G. *et al* (2000)].

### **Resistance mechanisms to irinotecan**

Four general mechanisms have been postulated to be involved in irinotecan resistance. The first mechanism is an alteration of pharmacokinetics and metabolism of irinotecan. Any factors, which favour the production of inactive metabolites, result in irinotecan resistance such as overexpression of UGT1A [Takahashi, T. *et al* (1997)] or CYP3A [Gupta, E. *et al* (1997)] and decreasing CES level [van Ark-Otte, J. *et al* (1998)]. The second mechanism is active drug transporters. Many studies have demonstrated that ABC transporters play a role in irinotecan resistance including ABCB1, MRP [Chu, X. Y. *et al* (1999)], cMOAT, MRP2 [Koike, K. *et al* (1997)] and ABCG2 [Maliepaard, M. *et al* (2001)]. The third mechanism is topoisomerase I level, one study reported that a low level of topoisomerase I activity correlated with irinotecan resistance in a resistant cell line compared to parental cell line [Giovanello, B. C. *et al* (1989)]. The last mechanism is topoisomerase I mutations: any mutations that reduce the affinity of irinotecan binding. Mutations of topoisomerase I have

been detected in murine cell lines resistant to irinotecan [Reviewed in Saleem, A. *et al* (2000)].

#### **1.2.4 Methotrexate**

Methotrexate, a folate antagonist, is also known as Amethopterin,  $\alpha$ -Methopterin or MTX. In 1948, aminopterin (2, 4-diaminopteroyl glutamic acid), the original folate antagonist compound, was used to treat lymphocytic leukaemia in children [Farber, S. *et al* (1974)]. Methotrexate is not only used as an antineoplastic but also as anti-inflammatory in treatment of rheumatoid arthritis (RA) [Weinblatt, M. E. *et al* (1985) and Williams, H. J. *et al* (1985)] and psoriasis [Weinstein, G. D. *et al* (1990)]. Additionally, it is used to suppress immune reaction in the prophylaxis of acute graft-versus-host disease (GVHD) [Storb, R. *et al* (1986)]. Currently, methotrexate is extensively used to treat many types of cancers.

#### **The structure of methotrexate**

Basically, polyglutamation occurs intracellularly to convert physiological folates to polyglutamate storage forms in the liver, erythrocytes and various tissues. Folylpolyglutamate synthetase (FPGS) functions to add glutamate groups in gamma linkage to the end carboxyl group of the neighbouring folyl glutamate. Similarly, methotrexate, a folate analogue, is also converted to polyglutamate form (7-hydroxy methotrexate) by polyglutamation in the liver and erythrocytes (Figure 1.12, d) [Baugh, C. M. *et al* (1973) and Jacobs, S. A. *et al* (1977)]. There are other 2 metabolic forms of methotrexate, which have less efficiency in inhibition of DHFR: DAMPA (Figure 1.12, a) and polyglutamated metrotrexate (Figure 1.12, c). The importance of polyglutamation of methotrexate is 1) to intracellularly store any excess methotrexate after binding to dihydrofolate reductase enzyme (DHFR) and thus maintain a high degree of DHFR inhibition even after drug removal [White, J. C. *et al* (1975)] and 2) to increase the affinity of binding to DHFR [Jacobs, S. A. *et al* (1975)]. Unbound methotrexate (MTX-Glu<sub>1</sub>) or MTX-Glu<sub>2</sub> and MTX-Glu<sub>3</sub> are removed from cells, however, MTX-Glu<sub>4</sub> and MTX-Glu<sub>5</sub> are retained in cells for at least 24 hours after drug removal [Jolivet, J. *et al* (1983)].

## The mechanisms of action

The main target enzyme of methotrexate is DHFR, which is an essential enzyme for intracellular folate metabolism. Methotrexate is a potent inhibitor for DHFR resulting in inhibition of DNA synthesis [White and Goldman, (1976)]. The effect of methotrexate has been proposed to depend on the concentration and the stage in the cell cycle. Studies in human peripheral T cells *in vitro* demonstrated that cells were inhibited in their proliferation but were not induced to undergo apoptosis at a high concentration (100  $\mu\text{M}$ ) or a low concentration (0.01  $\mu\text{M}$ ) of methotrexate [Genestier, L. *et al* (1998)]. Whilst Chinese hamster ovary cells underwent apoptosis in response to 128  $\mu\text{M}$  methotrexate [Barry, M. A. *et al* (1990)]. Therefore, the correlation between methotrexate concentration and cell apoptosis

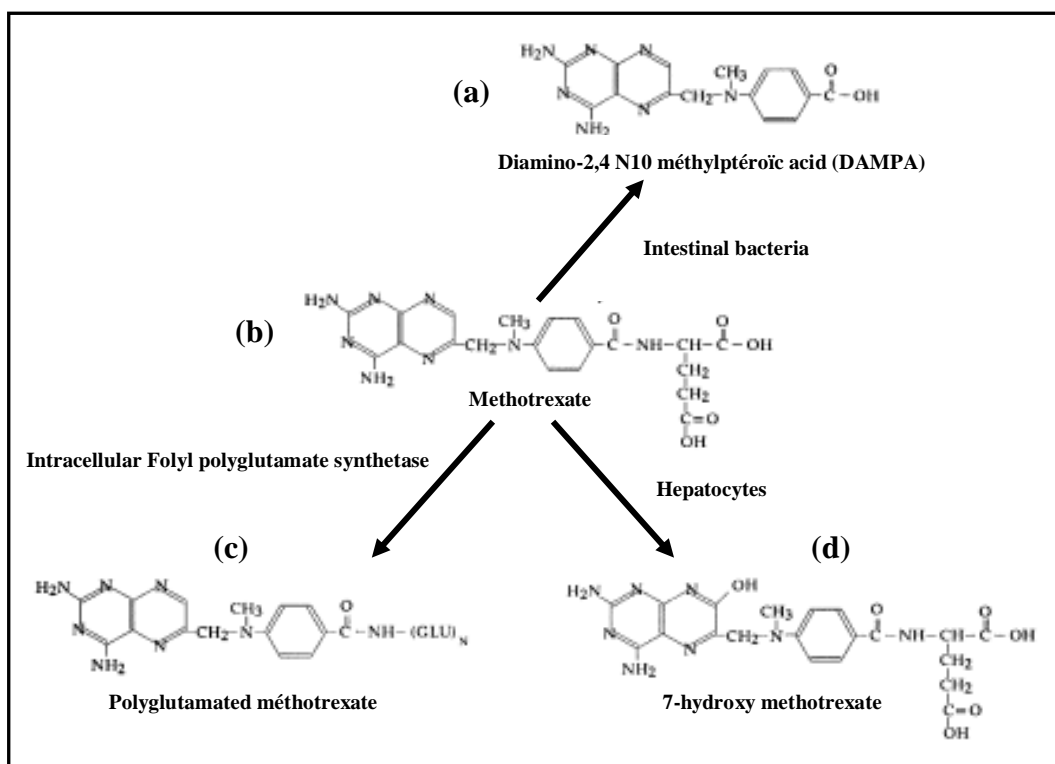


**Figure 1.12 Methotrexate chemical structure and intracellular metabolic form of methotrexate.** Methotrexate (b) is metabolised by intestinal bacteria to Diamino-2,4-N-10-methylpteroic acid (DAMPA) (a) and hydroxylated at 7-position of the pterine ring in hepatocytes to form 7-Hydroxy-methotrexate (7-OH-MTX) (d). The polyglutamation of methotrexate occurs by adding 1 – 4 new glutamyl groups into an unusual gamma-peptide linkage (c) [Reviewed in Genestier, L. *et al* (2000)].

remains unclear due to the fact that methotrexate concentrations from these 2 studies were similar but provided different effects. Cells were only effectively induced to undergo apoptosis by methotrexate while they were in S or G2 phases of cell cycle. Peripheral T cells were induced to stay in G1 phase when they were treated with methotrexate resulting in resistance to methotrexate-induced apoptosis [Genestier, L. *et al* (1998)]. Studies in peripheral blood lymphocytes suggested that the maximum effect of apoptosis were detected after 8 hours of methotrexate exposure and the half-life of methotrexate was approximately 3 days [Genestier, L. *et al* (1998)].

### **Resistance mechanisms to methotrexate**

There are 3 main mechanisms, associated with resistance to methotrexate. An overproduction of DHFR resulting from gene amplification is a common mechanism for acquired methotrexate resistance after drug exposure [Schimke, R.T. (1988) and Srimatkandada, S. *et al* (1989)]. However, an alteration of the ability of methotrexate to bind to DHFR is primarily believed to result in intrinsic resistance, and has been found in different methotrexate resistant cell lines [Jackson, R. C. *et al* (1976)]. Decreasing drug accumulation or increasing drug efflux is the final significant mechanism leading to methotrexate resistance, which correlates with several transporters. Reduced or impaired folate carrier (RFC), an important transporter of folates and folate analogues, leads to methotrexate resistance [Sirotnak, F. M. and O'Leary, D. F. (1991)]. Overexpression of ABC transporters such as ABCC1, MRP2 [Hooijberg, J. H. *et al* (1999)], ABCB1 [Gifford, A. J. *et al* (1998)] and ABCG2 [Volk, E. L. *et al* (2000)] also plays an important role in increasing methotrexate efflux resulting in reduction of methotrexate cytotoxicity. Additional minor mechanisms include impaired polyglutamation resulting from alteration or mutation of FPGS and failed polyglutamation [Chabner, B. A. *et al* (1985)].

In summary, etoposide, cisplatin, irinotecan and methotrexate are common chemotherapeutic drugs used to treat paediatric brain tumours. They have different mechanisms to attack cancer cells causing inhibition of proliferation or apoptosis. However, all chemotherapeutic drugs similarly target proliferating cells. Currently, chemotherapy is still a common treatment



for paediatric brain tumours and it is particularly in children aged less than 2 years, to avoid destroying the developing nervous system with radiation. Chemotherapy regimens commonly comprise more than one drug to attack cancer cells each with different mechanisms, to increase the effectiveness of treatment. However, the outcome of chemotherapy is not as good as expected partially due to the fact that cancer cells develop multidrug resistance. Hence, cancer cells are resistant to many drugs regardless of the types of drugs or drug chemical structure. At present, multidrug resistance in cancers is an unconquered enigma resulting in tumour recurrence, poor prognosis and unsatisfactory treatment outcome. One of the most important mechanisms playing a role in multidrug resistance is active drug efflux by transporters. The ABC transporter family is currently believed to initiate multidrug resistance in many cancers and has been extensively studied and discovered to correlate with multidrug resistance in tumours resulting in failure of chemotherapy.

### **1.3 ATP-binding cassette (ABC) transporters**

Drug resistance in cancers is a multifactorial phenomenon since there is possibly more than one mechanism involved in drug resistance with regard to overexpression of active drug efflux transporters, improved DNA repairing, increased detoxification of drug, decreased drug uptake and altered cell cycle. Overexpression of active drug transporters has been found in many drug resistant cancer cells and it causes resistance to many drugs in different groups or chemical structures. This is known as multidrug resistance. ABC transporters are currently postulated as the most important drug resistance mechanism since these transporters have a broad spectrum of specificity to many substrates and also chemotherapeutic drugs resulting in multidrug resistance. At present, 49 ABC transporters, which correlate with substrate efflux, have been identified in the human genome [Dean, M. *et al* (2001)]. Most ABC transporters have a role in cellular transportation to excrete substrates from cells. Currently, 15 ABC transporters are correlated to chemotherapeutic drug efflux, but only 3 main ABC

transporters (ABCB1, ABCC1 and ABCG2) have been extensively studied and proposed as important in active drug efflux in brain tumours [Schinkel, A. H. *et al* (2003)].

These transporters were named ABC transporters because the structure contains an ATP-binding cassette region which provides energy for this transporter to export intracellular substrates to extracellular spaces [Bunting, K. D. (2002)]. ABC transporters mainly comprise 2 components: transmembrane domain (TMDs) and nucleotide-binding domain (NBD) or ATP-binding region. General ABC topology is demonstrated in Figure 1.13, a. The full length of the ABC transporter structure is normally composed of two homologous halves each containing a 6TMDs and a NBD with the exception of some ABC transporters, which have distinct topologies, such as ABCC1 and ABCG2 described in more detail later. Each domain connects to the other via a flexible linker region, an important part involved in the catalytic activity of the transporter [Bunting, K. D. (2002)]. The NBD is an important unit which hydrolyses adenosine triphosphate (ATP) to provide energy for the transporter to transport substances across membranes. The NBD, an ~200 amino acid residue region, contains 2-domain architecture; a RecA-like catalytic domain and a smaller helical domain. The NBD also comprises a highly conserved region consisting of a Walker A motif, a Walker B motif, and a signature motif (linker peptide or LSGGQ motif) used to classify ABC transporters into seven types which are detected in both normal and malignant cells (ABCA through to ABCG), D-loop, H-loop and Q-loop as shown in Figure 1.13, b [Reviewed in Kos, V. and Ford, R. C. (2009)]. Human ABC transporters involved in drug transportation are as shown in Table 1.8 [Leonard, G. D. *et al* (2003)]. TMDs are the functional unit which selectively effluxes specific substrates including sugars, amino acids, glycans, cholesterol, phospholipids, peptides, proteins, toxins, antibiotics, and xenobiotics [Gottesman, M. M. and Ambudkar, S. V. (2001)]. ABC transporters are not only involved in the efflux of many of these substrates from cells, but are also involved in the excretion of toxic substances from liver, kidneys and the gastrointestinal tract. Furthermore, such transporters protect vital organs, including brain, placenta and testis, from toxic agents penetrating through to these organs [Leonard, G. D. *et al* (2003)].

### 1.3.1 ABCB1

ABCB1 also known as MDR1 or P-glycoprotein (P-gp) was initially discovered in colchicine resistant Chinese hamster ovary cells but it was not present in the wild type cells. These cells also showed cross-resistance to other drugs. This transporter was named P-glycoprotein because it was a glycoprotein that had the ability to alter permeability of cell membrane [Juliano, R. L. and Ling, V. (1976)]. ABCB1 is a large membrane protein comprising more than 1,200 amino acid which has a molecular weight of approximately 170 kDa. ABCB1 is a product of the *ABCB1* (*MDR1*) gene which is located on chromosome 7p21 in humans. The *MDR1* gene is a member of the *MDR* gene family including *MDR2* and *MDR3* genes.

In normal tissues, ABCB1 is detected in human brain located on the luminal membrane of endothelial cells in the blood brain barrier (BBB) and had a very important role in protecting vital organs (brain and spinal cord) from toxic agents [Regina, A. *et al* (2001)]. Additionally, ABCB1 was also located on the transport epithelium of liver, kidney and gastrointestinal tract [Reviewed in Szakács, G. *et al* (2006)].

#### The structure of ABCB1

The 1,280 amino acid polypeptide of ABCB1 consists of two NBDs, two transmembrane domains (TMDs) linked by a 60-70 amino acid linker region with multiple phosphorylation sites and glycosylation sites (GS) [Figure 1.14]. Individual TMDs comprised 6 helices, therefore, ABCB1 consists of 12 helices in total [Loo, T. W. and Clarke, D. M. (1997)]. The current crystal structure of ABCB1 is demonstrated in Figure 1.15 and shows that the ABCB1 structure is an inverted V. Transmembrane helices (TMHs) of ABCB1 correlating to drug efflux are TMH4 and TMH5 associated with TMD2 and TMH10 and TMH11 associated with TMD1. These TMHs are close to the extracellular site contributing to substrate transport [Ravna, A. W. *et al* (2009)]. Transmembrane domains are the regions, which bind to ABCB1 substrates or anticancer drugs and these are hydrophobic (either neutral or positively charge). This binding stimulates ATPase activity of ABCB1 and the 2 ATP binding domains were required for the transport mechanism but these 2 ATP domain did not work simultaneously. The first

ATPase event is proposed to be transport drug across the membrane whilst the second ATPase event is proposed to alter ABCB1 structure ready for the next round of transportation [Ambudkar, S. V. *et al* (1999), Senior, A. E. and Bhagat, S. (1998) and Sauna, Z. E. and Ambudkar, S. V. (2000)].

### ABCB1 and multidrug resistance

ABCB1, the first ABC transporters discovered in both normal tissues and many cancers, has physiological function in the blood brain barrier (BBB) to prevent cytotoxic drugs entering vital organs e.g. brain and spinal cord [Regina, A. *et al* (2001)], and also plays a role in multidrug resistance by efflux of a broad spectrum of drugs in cancer cells overexpressing ABCB1. Therefore, both physiological function and active drug efflux may initiate multidrug resistance in brain tumours. ABCB1 was hence extensively studied with regard to the correlation between ABCB1 and multidrug resistance in brain tumours. Many studies revealed

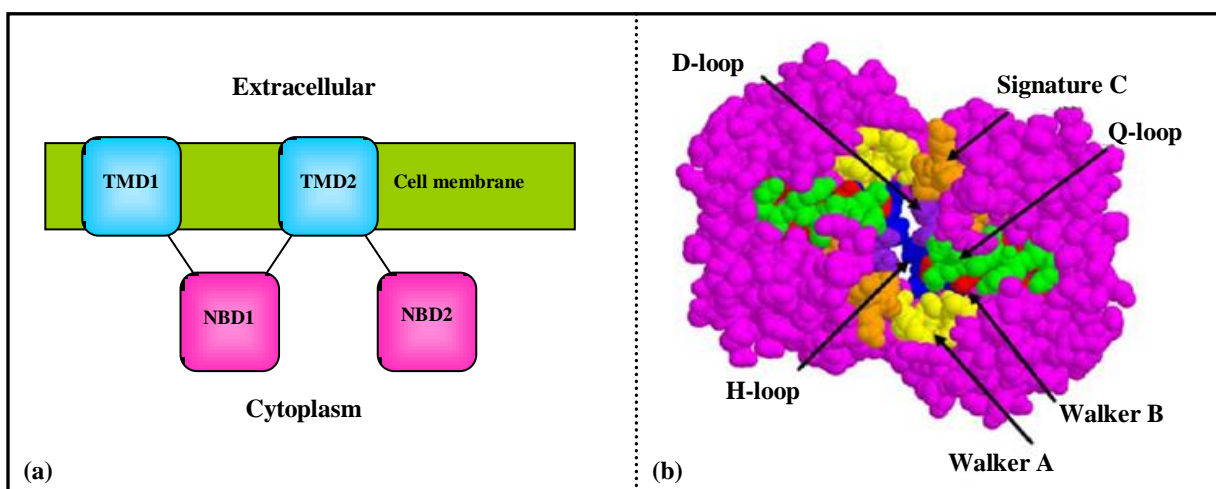


**Figure 1.13 General topology of ABC transporters and 3D figure of NBD.** General topology of ABC transporters comprises two TMDs located in membrane and two NBDs located in cytoplasm (a). ABC region of ABC transporters is composed of three highly conserved regions including Walker A, B motifs and signature C motif including D, H and Q-loop. The highly conserved signature C motif lies between Walker A and B regions (b) [(a): Adapted from Ravna, A. W. *et al* (2009) and (b): Obtained from Kos, V. and Ford, R. C. (2009)].

**Table 1.8 ABC transporters involved in drug resistance** [Adapted from Dean, M. *et al* (2005), Gottesman, M. M. *et al* (2002), Dean, M. *et al* (2001) and Szakacs, G. *et al* (2006)]

Genes	Protein /alias	Location	Chemotherapeutic drugs effluxed by transporter	Other drugs and substrates	Normal location
<b>ABCA2</b>	<b>ABCA2</b>	9q34	Estranustine	Steroid derivatives, lipids	Brain, monocyte
<b>ABCB1</b>	<b>ABCB1 (MDR1)</b>	7p21	Doxorubicin, daunorubicin, vincristine, vinblastine, actinonycin-D, paclitaxel, doetaxel, etoposide, teniposide, bisantrene, homoharmingtonine (STI-571)	Digoxin, saquinivir, neutral and cationic organic compounds, many commonly used drugs	Intestine, liver, kidney, blood-brain barrier
<b>ABCB4</b>	<b>MDR2</b>	7q21.1	Phophatidylcholine, some hydrophobic drugs	Paclitaxel, vinblastine	Liver
<b>ABCB11</b>	<b>BSEP, SPGP</b>	2q24	Paclitaxel	Bile salts	Liver
<b>ABCC1</b>	<b>ABCC1</b>	16p13.1	Doxorubicin, epirubicin, daunorubicin, vincristine, etoposide, colchicine, camptothecins, methotrexate	Glutathione and other conjugates and other conjugates, organic anions, rhodamine, leukotriene C4	Widespread all tissues
<b>ABCC2</b>	<b>MRP2 (cMOAT)</b>	10q24	Vinblastine, cisplatin, doxorubicin, methotrexate, etoposide, vincristine	Similar to ABCC1, non-bile salt organic anions, sulfinpyrazone	Liver, kidney, intestine
<b>ABCC3</b>	<b>MRP3 (MOAT-D)</b>	17q21.3	Teniposide, etoposide, methotrexate, cisplatin, vincristine, doxorubicin	Glucuronate and glutathione conjugates, anti-folates, bile acids	Pancreas, kidney, intestine, liver, adrenal
<b>ABCC4</b>	<b>MRP4 (MOAT-B)</b>	13q32	Methotrexate, thiopurine, 6-mercaptopurine, 6-thioguanine and metabolites	Nucleoside analogues, organic anions, PMEA, cAMP, cGMP	Prostate, testis, ovary, intestine, pancreas, lung
<b>ABCC5</b>	<b>MRP5 (MOAT-C)</b>	3q27	6-mercaptopurine, 6-thioguanine and metabolites	Nucleoside analogues, cyclic nucleotides, organic anions, PMEA, cAMP, cGMP	Widespread
<b>ABCC6</b>	<b>MRP6 (MOAT-E)</b>	16p13.1	etoposide	Anionic cyclic pentapeptide	Liver, kidney
<b>ABCC10</b>		6p21	Vinblastine, vincristine, docetaxel, paclitaxel	Cyclosporin, MK571	
<b>ABCC11</b>	<b>MRP8</b>	16q11-q12	5-fluorouracil	PMEA, cAMP, cGMP	
<b>ABCG2</b>	<b>MXR, BCRP, ABC-P</b>	4q22	Estramustine, mitoxantrone, topotecan, doxorubicin, daunorubicin, irinotecan, imatinib, methotrexate	Anthracyclines, steroid derivatives, lipids, pheophorbide A, Hoechst 33342, rhodamine	Placenta, intestine, breast, liver

BCRP=breast cancer resistance protein, cAMP=cyclic adenosine monophosphate, cGMP=cyclic guanine monophosphate, MDR=multidrug resistance, MRP=multidrug-resistance-associated protein, MXR=mitoxantrone-resistance protein, PMEA=9-[2-(phosphonomethoxy)ethyl]adenine

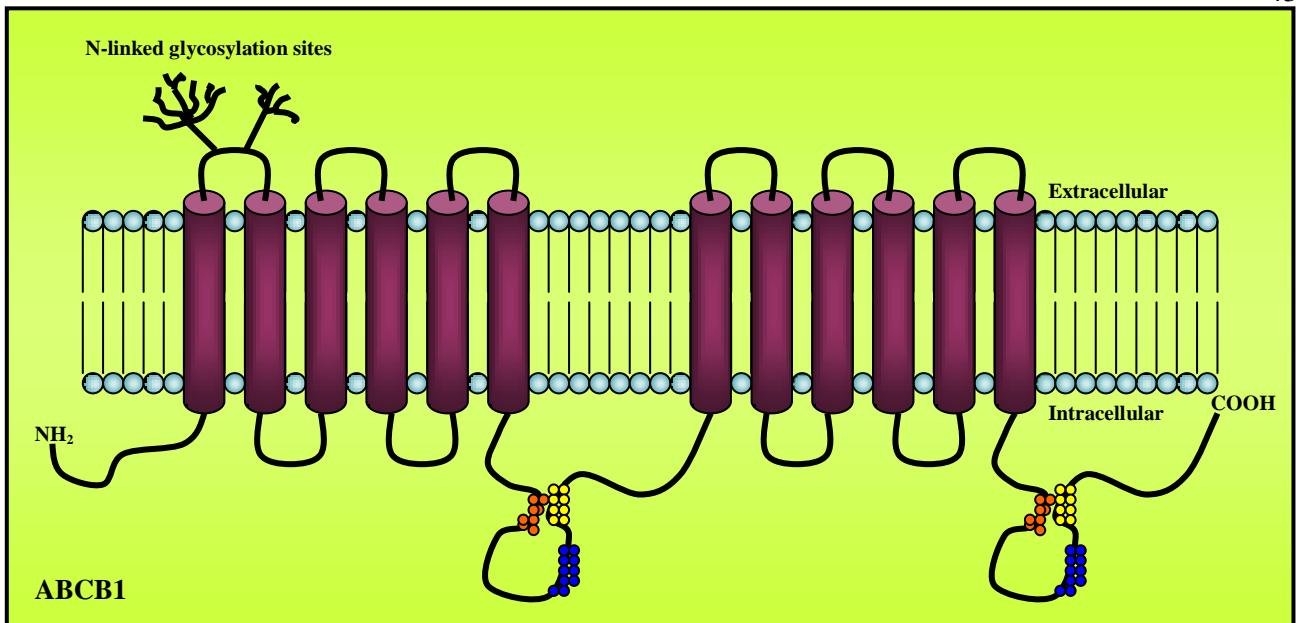


**Figure 1.14 ABCB1 structure.** ABCB1 structure in cell membranes comprises two ABC segments (ATP binding domains or nucleotide binding domains: NBDs), two 6TMDs and glycosylation sites. There are 2 glycosylation sites indicated by branching black lines, which are located in extracellular part of ABCB1. Two 6TMDs are connected by NBDs comprising Walker A ( ● ), Walker B ( ● ) and a signature C motif ( ● ) [Adapted from Löscher, W. and Potschka, H. (2005)].

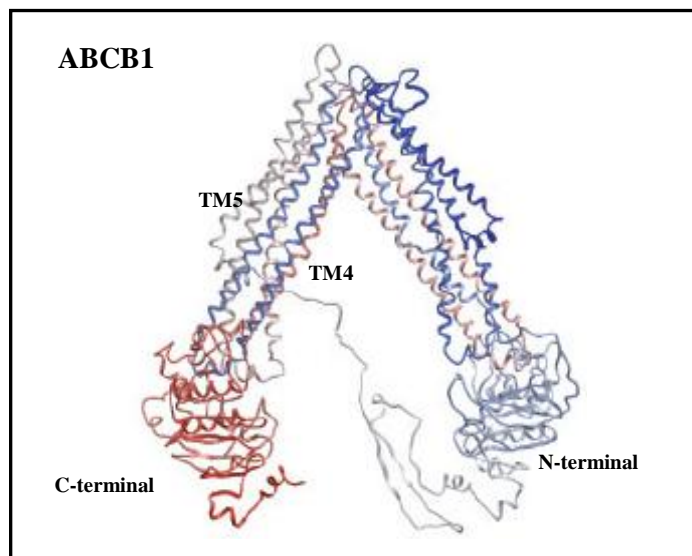


**Figure 1.15 Crystal structure of ABCB1 transporter.** Three dimension structure of ABCB1 is an inverted V shape. In the arm of V shape, NBD1 is associated with TMH1, 2, 3 and 6 of TMD1 and TMH10 and 11 of TMD2 and NBD2 are associated with TMH4 and 5 of TMD1 and TMH7, 8, 9 and 12 of TMD2 [Adapted from Ravna, A. W. *et al* (2009)].

a relationship between ABCB1 and multidrug resistance in many cancer types. However, the multidrug resistance mechanism of ABCB1 in brain tumours is not fully understood. One study demonstrated that ABCB1 was intensely expressed on the luminal surface of endothelial cells of human gliomas, and these endothelial cells expressing ABCB1 probably formed a brain tumour barrier (BTB) which restricts the entrance of chemotherapeutic agents to targeted cells. Therefore, active drug efflux was increased to remove xenobiotics from the brain tumour cells [Tanaka, Y. *et al* (1994)]. A study to investigate the relationship between ABCB1 expression and a grading of astrocytic tumours showed that ABCB1 expression was detected in 31% of low grade astrocytomas and 88% of high grade astrocytomas. This study suggested that ABCB1 expression influenced the prognosis of gliomas, whereby a high expression of ABCB1 may result in increasing chemoresistance [von Bossanyi, P. *et al* (1997)]. In addition, the study of *mdr1a*<sup>(-/-)</sup> mice found that the accumulation of neurotoxic drugs in brain increased up to 80-100 fold when compared with the wild type mice exposed to digoxin, ondancetron, loperamide, paclitaxel, vinblastin and doxorubicin [Schinkel, A. H. *et al* (1994)]. Therefore, a great deal of evidence confirmed that ABCB1 correlated with multidrug resistance. Hence, it was proposed that ABCB1 was overexpressed in drug resistant cancer cells and it reduced drug cytotoxicity by increase drug export into extracellular spaces resulting in decreased intracellular drug accumulation. Additionally, a high level of ABCB1 detected in cancers was associated with high level of chemoresistance resulting in a worse treatment outcome [Ling, V. (1997) and Regina, A. *et al* (2001)].

Hence, ABCB1 is believed to be one of the active drug efflux transporters correlating with multidrug resistance in brain tumours. The function of these transporters is to export cytotoxic drugs to extracellular spaces regardless of the type or structure of drugs resulting in resistance to many chemotherapeutic drugs. This is the reason why the treatment outcome is still poor even though many drugs having different mechanisms of actions are combined in a chemotherapeutic regimen. The mechanism to explain how ABCB1 is able to efflux a broad spectrum of drugs is still unclear. However, 3 mechanisms have been proposed to explain the efflux function of ABCB1. Firstly, the hydrophobic vacuum cleaner model describes that many

lipophilic substrates penetrated into lipid bilayers (outer or inner leaflet) of the cell membrane then these substrates were absorbed by the TMDs of ABCB1 and effluxed into the extracellular spaces prior to the substrate penetrating into cytoplasm (Figure 1.16, a) [Higgins, C. F. and Gottesman, M. M. (1992), Raviv, Y. *et al* (1990, Homolya, L. *et al* (1993) and Shapiro, A. B. *et al* (1997)]. The second “flippase” model describes how ABCB1 functions to translocate substrates from the inner leaflet to the outer leaflet of lipid bilayers resulting in a concentration gradient between the outer and the inner leaflet (Figure 1.16, b). Drug binding sites of ABCB1 can then be exposed to the extracellular medium therefore, drugs are released into extracellular space depending on their hydrophobicity [Higgins, C. F. and Gottesman, M. M. (1992) and Margolles, A. *et al* (1999)]. Finally, the membrane partitioning model explains three different factors involved in drug efflux of ABCB1 transporter: the lipid-waterpartition coefficient ( $K_{lip}$ ), the apparent binding affinity ( $K_d$ ) and the intrinsic binding affinity ( $K_{dlip}$ ). Substrates bind to ABCB1 within the membrane (Figure 1.16, c and d). The lipid-waterpartition coefficient ( $K_{lip}$ ) indicates the ability of the aqueous phase of substrates to penetrate into the lipid bilayers. Therefore, the  $K_{lip}$  value indicates the ability of the membrane to concentrate substrates in the lipid bilayers. The  $K_{lip}$  of ABCB1 is approximately 300 – 20,000 fold that of the substrates concentration in the aqueous solution. The intrinsic binding affinity ( $K_{dlip}$ ) indicates the ability of substrates in binding to the transporter within the membrane. These 2 parameters;  $K_{lip}$  and  $K_{dlip}$ , are an important factors, which influence the apparent binding affinity or the dissociation constant ( $K_d$ ), which is the product of substrates penetrating to the lipid bilayers and the substrates binding to the transporter within the membrane [Eytan, G. D. *et al* (1997)]. Therefore, to overcome drug resistance, drug (lipophilicity) should be reduced resulting in a decrease in drug efflux by ABCB1 and hence the drug will be accumulated in cells.

### 1.3.2 ABCC1

ABCC1 is also known as MDR-associated protein1 (MRP1). The MRP1 gene spans 2.8 kb of DNA, which encodes an approximately 180-195 kDa membrane protein. Currently, 6 other human MRPs have been identified. ABCC1 (ABCC1) is the first MRP member and is located on chromosome 16 at band p13.13-13.12. It is expressed in the plasma membrane of several cells



including erythrocytes and many MDR tumours [Reviewed in Regina, A. *et al* (2001) and Bredel, M. (2001)]. In 1992, Cole and colleagues cloned ABCB1 from the human lung cancer cell line H69AR, which was selected by doxorubicin. Doxorubicin-selected H69AR cells had cross-resistance to many chemotherapeutic drugs but did not express ABCB1 [Cole, S. P. C. *et al* (1992)].

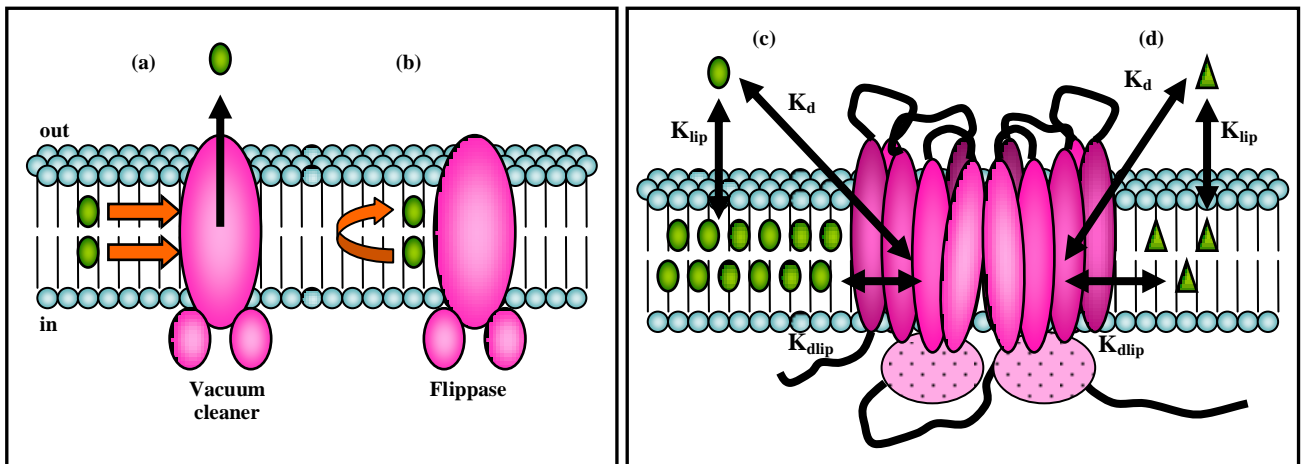


**Figure 1.16 The hydrophobic vacuum cleaner model, flippase model and membrane partitioning model.** The hydrophobic vacuum cleaner model postulated that TMDs of ABCB1 bound to substrates while they penetrated into the lipid bilayers but not into the cytoplasm then the substrates were exported into the extracellular spaces (a). Whilst the flippase model suggests that ABCB1 only translocates the substrates from the inner leaflet to the outer leaflet of lipid bilayers of cell membrane (b). The membrane partitioning model shows 2 different substrates.  $K_{dip}$  is an intrinsic binding affinity, which is determined by the concentration of the substrates in the membrane and is relatively low. Substrates with a high  $K_{lip}$  were able to get into the lipid bilayers with a high concentration compared to the aqueous solution but they will have a low  $K_d$  resulting from a low intrinsic binding affinity (c). Whilst the substrates with a low  $K_{lip}$  results in a low concentration of the substrates in the membrane but they will have a high  $K_d$  resulting from a high intrinsic binding affinity (d) [Adapted from Eckford, P. D. W. and Sharom, F. J. (2009)].

ABCC1 expression is detected in most normal tissue types throughout our body, however, some normal tissues express a high level of ABCC1 including the adrenal gland, bladder, choroid plexus, colon, erythrocytes, kidney, lung, placenta, spleen, stomach, testis, helper T-cells, and both skeletal and cardiac muscle [Flens, M. J. *et al* (1996)]. ABCC1 is also detected in sensitive normal tissues with this protein being located on basal membranes of sertoli cells in testis to protect the germline cells from toxicity and on basolateral membranes in the choroid plexus to protect nervous system tissues from drugs in blood circulation getting into cerebrospinal fluid [Regina, A. *et al* (2001) and Bredel, M. (2001)]. A study in ABCC1 knockout mice found that *mrp*<sup>-/-</sup> mice were viable and fertile with no physiological abnormalities. These mice were more susceptible to etoposide (2 fold) and had increased levels of glutathione (GSH) in tissues of breast, lung, heart, kidney, muscle, colon, testes, bone marrow cells, blood mononuclear leukocytes, and blood erythrocytes. This study indicated that ABCC1 is not essential for growth and development but it does play an important role in drug detoxification and GSH metabolism [Lorico, A. *et al* (1997)].

### **Structure of ABCC1**

The structure of the ABCC1 transporter is similar to MRP2/3/6. It consists of two 6 TMDs, two ATP binding sites, glycosylation sites and an additional amino N-terminal domain with 5TMDs (Figure 1.17). The additional 5TMDs located on the N-terminal domain is a distinct characteristic of the ABCC1 transporter. The 2 ATP binding sites contain highly conserved ABC regions comprising a Walker A, a Walker B and a signature C motif. The two N-linked glycosylation sites are located on the extracellular loops. [Bakos, É. *et al* (1996)].

### **ABCC1 and multidrug resistance**

ABCC1 was found to associate with multidrug resistance similar to ABCB1. It has been proposed that the level of MRP mRNA expression in glioma cells lines relates to the degree of anticancer sensitivity. High levels of MRP expression results in a poor response of cells to many anticancer agents such as etoposide, vincristine and adriamycin. On the contrary, cell lines are less chemoresistant when the level of MRP expression is low. The level of MRP expression might

therefore indicate the degree of chemoresistance. Both ABCB1 and MRP have an influence on the acquired multidrug resistance phenotype [Abe, T. *et al* (1994)].

ABCC1 transports many substrates similar to ABCB1 however, the proposed mechanism of ABCC1 is distinct and different from ABCB1. Both ABCC1 and MRP2 have been studied and it is known that these two proteins are involved in MDR. MRP transporters are organic anion transporters which transport anionic drugs and neutral drugs by conjugating these drugs to acidic ligands (e.g. glutathione (GSH) and glucuronate or sulphate) and exporting them into the extracellular space [Jetlitschky, G. *et al* (1996)]. The principle functions of ABCC1 have been described; first, both hydrophobic and hydrophilic compounds are transported via ABCC1; second, it has an important role in normal physiology in the transportation of drugs across the

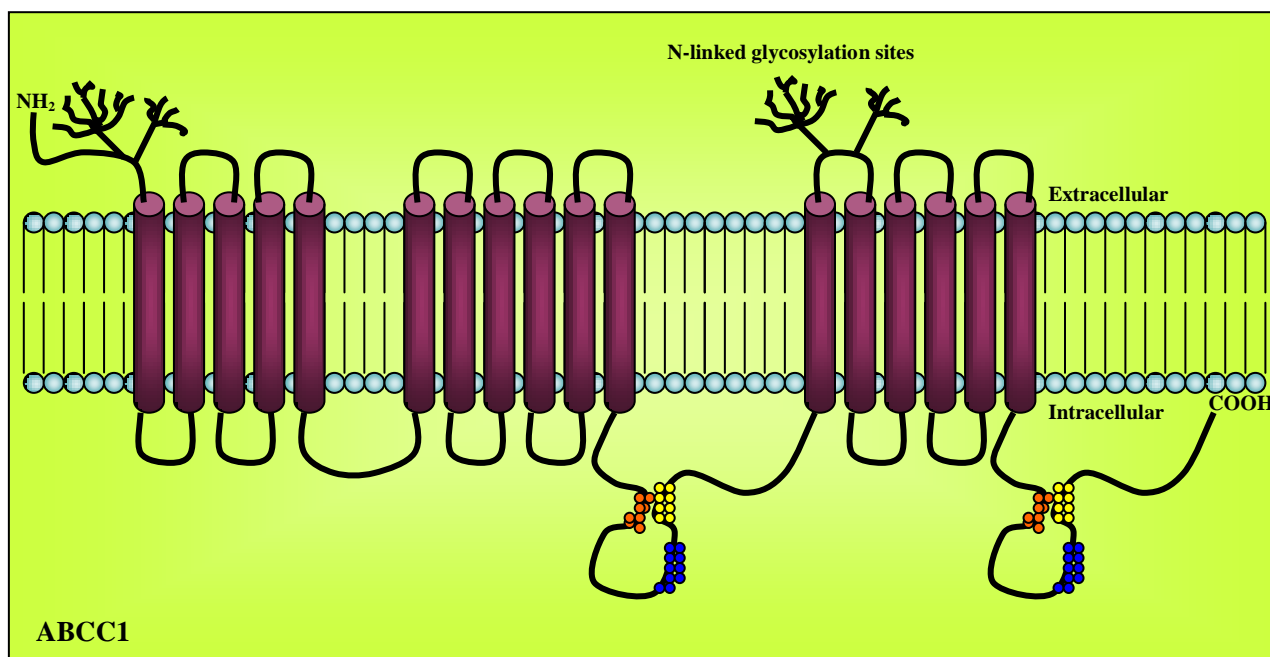


**Figure 1.17 The structure of ABCC1.** ABCC1 structure is similar to ABCB1 (two 6TMDs and 2 NBDs) but ABCC1 consists of an additional 5TMD, which is of unknown function and an extracellular N-terminus whilst the C-terminus of ABCC1 is located intracellularly. There are N-linked glycosylation sites (indicated by black branching lines) on extracellular loops of TMDs. Intracellular NBDs comprise Walker A (●), Walker B (●) and a signature C motif (●) [Adapted from Löscher, W. and Potschka, H. (2005)].

placenta and intestine; third, it is a vital component of the BBB and blood tumour barriers (BTBs) [Reviewed in Bredel, M. (2001)]. A recent mechanism of ABCC1 multidrug resistance was proposed whereby MRP interacted with the glutathione (GSH) -linked enzyme system in drug efflux function. ABCC1 worked as an active anticancer efflux pump by conjugating with GSH called GSH conjugate export pump (GS-x). When drugs enter the cells, they were detoxified by conjugating with GSH-GST to form drug/GSH complexes. These drug/GSH complexes were then removed from cells via the GS-X pump resulting in chemoresistance [Jetlitschky, G. *et al* (1996)].

### **1.3.3 ABCG2**

ABCG2 initially known as the breast cancer resistance protein (BCRP)/mitoxantrone-resistance protein (MXP)/ABC transporter in placenta (ABCP) is located on chromosome 4q22 [Sparreboom, A. *et al* (2003)]. ABCG2 is a membranous transporter protein, which is a 72-kDa protein and comprises 655 amino acids [Bunting, K. D. (2002)]. ABCG2 was initially isolated from the placenta, and is also expressed in many tissues such as the liver, small intestine, colon, lung, kidney, adrenal gland, sweat gland and endothelial of vein and capillaries [Ozvegy-Laczka, C. *et al* (2005)]. ABCG2 is highly expressed in the trophoblast cells of the placenta where it is believed to eliminate toxic metabolites from the foetus and transport nutrients and useful compounds to the foetus via the foetal blood supply [Dean, M. *et al* (2001)]. The ABCG2 knockout study showed that abnormal functions occurred in several tissues such as altered BBB function, intestinal drug absorption, foetal drug exposure and drug induced damage in testicular tubules, choroid plexus epithelium and oropharyngeal mucosa [Sparreboom, A. *et al* (2003)].

The ABCG2 transporter is able to transport large, hydrophobic, both positively and negatively charged molecules. Some substrates transported by ABCG2 are overlapping with ABCB1 and MRP transporters. However, ABCG2 can be distinguished from ABCB1 and ABCC1 in the fact that there are some substrates, which are transported by these two transporters, but are not transported by ABCG2 such as vinblastine, paclitaxel and verapamil (transported by ABCB1),

and calcein (transported by ABCC1) [Huang, Y and Sadee, W. (2006)]. Additionally, mitoxantrone resistant cell lines expressed ABCG2 but did not express ABCB1 or ABCC1 [Dean, M. *et al* (2001)].

### Structure of ABCG2

ABCG2 is called an ABC half transporter because of its structure, which is different from other ABC transporters. ABCG2 structure consists of only one 6TMD and one ATP-binding region (Figure 1.18). The ATP-binding region is located on the amino-terminal side (N) of the TMD whilst in ABCB1 and ABCC1 the NBD is located on carboxy-terminal side (C) of TMD. The half

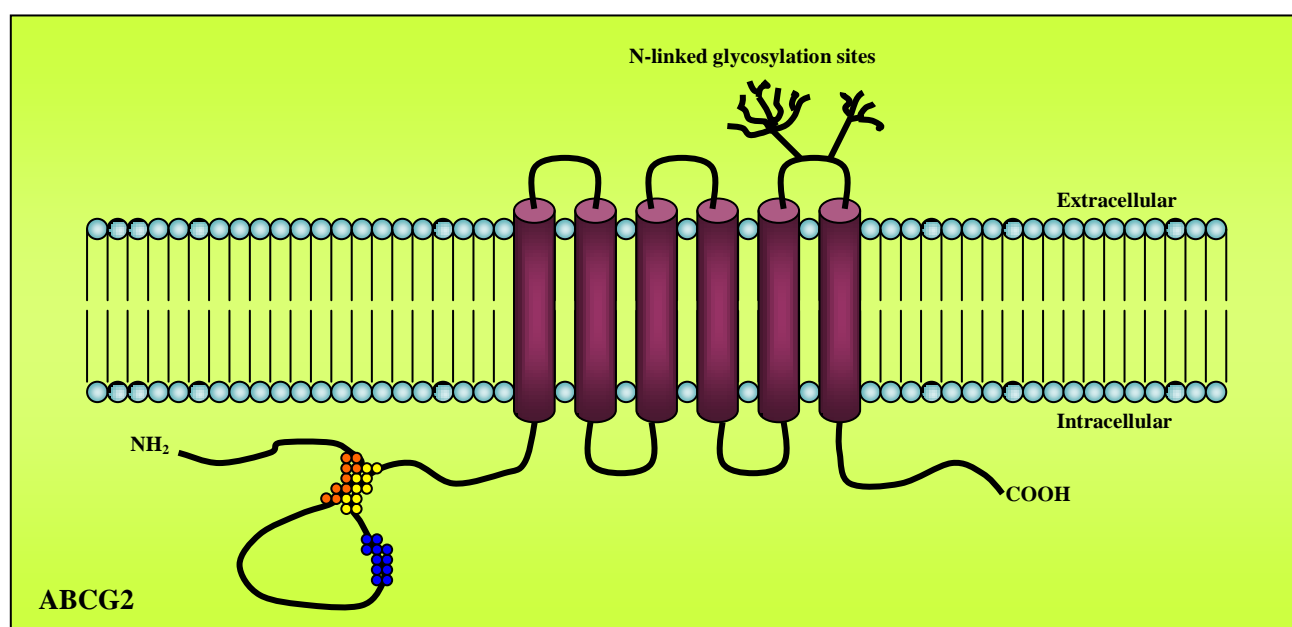


**Figure 1.18 ABCG2 structure.** ABCG2 is a half transporter, which comprises only one 6TMD with a glycosylation site and one ATP-binding region. The ATP-binding region, which provides energy to transport compounds, is located on the N-terminal side in cytoplasm. The position of ATP-binding region of ABCG2 is different from the other ABC transporters, which have this region on C-terminal side. Functional ABCG2 works as a homodimer. There are N-linked glycosylation sites (indicated by black branching lines) on extracellular loops of TMDs. Intracellular NBDs comprise Walker A (●), Walker B (●) and a signature C motif (●) [Adapted from Löscher, W. and Potschka, H. (2005)].

transporter structure of ABCG2 lacks the required 4 domains for function [Gottesman, M. M. *et al* (2002)]. So dimerisation of ABCG2 is believed to be essential to function [Ozvegy-Laczka, C. *et al* (2005)].

### **ABCG2 and multidrug resistance**

ABCG2 was postulated to play a role in chemosistance in many cancers. Resistant cell lines overexpressing ABCG2 were serially selected for a high level of mitoxantrone resistance, these cell lines also had cross-resistance to anthracyclines but they were susceptible to vinca alkaloids or taxanes [Ross, D. D. *et al* (1999)]. ABCG2 is an important multidrug resistant transporter in many cancers [Reviewed in Robey, R. W. *et al* (2007)]. Since, human ABCG2 has been shown to confer resistance to various compounds such as mitoxantrone, methotrexate, topotecan, SN38 and flavopiridol, which are commonly used chemotherapeutic drugs. ABCG2 was also found to be an important identified marker for the stem cell subpopulation; it was overexpressed in human hemotopoietic stem cells (HSCs) and rapidly downregulated with differentiation [Zhou, S. *et al* (2001)]. ABCG2 was therefore proposed as an important mechanism to protect HSCs from cytotoxic agents [Zhou, S. *et al* (2002)]. Also in breast cancer, ABCG2 was functionally overexpressed and played an important role in chemotherapeutic resistance in breast cancer cell lines and hence multidrug resistance in this cancer [Doyle, L. A. *et al* (1998)]. *In vivo* studies also demonstrated that mice with ABCG2 knockout were more sensitive to chemotherapy and depletion of ABCG2 gene did not affect growth and fertility [Jonker, J. W. *et al* (2002) and Zhou, S. *et al* (2002)]. ABCG2 is another important ABC transporters associating with multidrug resistance in many cancers. Human ABCG2 has recently been found to interact with a high binding affinity with tyrosine kinase inhibitors (TKIs), Gleevec/Imatinib (STI-571) and Iressa (ZD 1839). These 3 newly developed anticancer drugs specifically to inhibit malignant cell growth and metastasis formation. Hence inhibition of ABCG2 can enhance the ability of these drugs to kill malignant cells [Reviewed in Sarkadi, B. *et al* (2004)].

At present, ABCG2 drug resistance mechanisms are still unclear, with little known compared to ABCB1 and ABCC1 transporters. There are many unclear issues about ABCG2, and further study is required with regard to the characteristics of the ATP hydrolytic pathway, the location of drug interaction sites, transitions of the protein during translocation of drug and regions involved in conformational coupling. Residue 482 is believed to be situated on the binding site of ABCG2 and to be involved in increased drug recognition by driving mutation of arginine to either glycine or threonine. In a study of R482G, which is an isoform of ABCG2, by Clark *et al* the results obtained that there are 2 different drug binding sites on ABCG2: the first one is for rhodamine 123 and the second one is a [<sup>3</sup>H]-daunomycin site, which is able to recognise at least four other compounds [Clark, R. *et al* (2006)].

#### **1.3.4 Substrates and inhibitors of ABCB1, ABCC1 and ABCG2 transporters**

ABCB1, ABCC1 and ABCG2 are polyspecific because they were able to interact with many substrates. In general, the substrates for ABCB1 are large organic molecules (200-1,900 Da), amphipathic and lipid-soluble in nature with an aromatic ring system. However, not all of ABCB1 substrates have these properties for example some of them have an uncharged or positively charge N atom. ABCC1 has 2 regions for substrate binding; the first one for amphipathic molecules, which is similar to ABCB1 and the second one (a more hydrophilic site) for free glutathione or drug conjugated to glutathione. Similar to ABCC1, ABCG2 is able to transport both positively and negatively charged drugs including sulphates and drugs conjugated to glucuronide. Substrates and inhibitors of ABCB1, ABCC1 and ABCG2 are summarised in Table 1.9 (Reviewed in Eckford P. D. W. and Sharom, F. J. (2009)).

To summarise this section, 3 main ABC transporters (ABCB1, ABCC1 and ABCG2) are confirmed to correlate with multidrug resistance in many cancers. These 3 ABC transporters are overexpressed in resistant cell lines and lead to insensitivity of chemotherapy [Chen, C. J. *et al* (1986), Cole, S. P. C. *et al* (1992) and Doyle, L. A. *et al* (1998)]. Additionally, depletion of either the *ABCB1*, *ABCC1* or *ABCG2* gene resulted in increased chemotherapeutic susceptibility but growth and fertility of mice were not affected indicating that these genes were not essential

**Table 1.9 Chemotherapeutic drugs and other compounds that interact with ABCB1, ABCC1 and ABCG2 transporters** [Derived from Eckford P. D. W. and Sharom, F. J. (2009), Sparreboom, A. *et al* (2003), Nies, A. T. (2007) and Gottesman, M. M. *et al* (2002)]

ABC subfamily	NCBI protein accession no.	Number of amino acids and gene location	Tissues	Substrates	Inhibitors	Physiological substrates
<b>ABCB1</b> (MDR1/ABCB1)	NP_000918	1280 amino acid, chromosome 7p21	Intestine, liver, kidney, placenta, BBB	<b>Anticancer drugs:</b> bisantrone, mitoxantrone, doxorubicin, daunorubicin, topotecan, etoposide, teniposide, paclitaxel, docetaxel, vinblastine, vincristine <b>Fluorescent dyes:</b> Calcein-AM, H33342, rhodamine 123, tetramethylrosamine <b>Natural products:</b> Colchicine, curcuminoids <b>Tyrosine kinase inhibitors:</b> Gefitinib, imatinib mesylate	Biricodar, cyclosporine A, elacridar (GF120918), LY335979, R101933, Valspodar (PSC833), Verapamil, tariquidar (XR9576)	
<b>MRP1</b> (ABCC1)	NP_004987	1531 amino acid, chromosome 16p13.13-13.12	All tissues	<b>Anticancer drugs:</b> Doxorubicin, daunorubicin, topotecan, irinotecan, etoposide, teniposide, vinblastine, vincristine, methotrexate <b>Fluorescent dyes:</b> BCECF, calcein, fluo-3 <b>Glucuronide conjugates:</b> Estradiol-17- $\beta$ -D-glucuronide, etoposide glucuronide, glucuronosylbilirubin, NS-38-glucuronide <b>Natural products:</b> curcuminoids <b>Sulfate conjugates:</b> Dehydroepiandrosterone-3-sulfate, estrone-3-sulfate, sulfatolithocholyl taurine <b>Tyrosine kinase inhibitors:</b> Gefitinib, imatinib mesylate	Biricodar, Cyclosporin A, Glutathione ethacrynic acid, clotrimazole	Estrone 3-sulfate, 17 $\beta$ -Glucuronosyl estradiol, GSH <sup>d</sup> +vincristine, Leukotriene C <sub>4</sub>
<b>ABCG2</b> (BCRP/MXR/ABCP)	NP_004818	655 amino acid, chromosome 4q22	Placenta, intestine, breast, liver	<b>Anticancer drugs:</b> topotecan, irinotecan, etoposide, teniposide, Methotrexate, flavopiridol <b>Fluorescent dyes:</b> BODIPY-prazosin, H33342 <b>Glucuronide conjugates:</b> Estradiol-17- $\beta$ -D-glucuronide <b>Natural products:</b> curcuminoids <b>Sulfate conjugates:</b> Acetaminophen sulfate, dehydroepiandrosterone-3-sulfate, estrone-3-sulfate <b>Tyrosine kinase inhibitors:</b> Gefitinib, imatinib mesylate	CI1033, Fumitremorgin C, GF120918, Ko134, Reserpine, Diethylstilbestrol	Dehydroepiandrosterone sulfate (DHEAS), Estrone 3-sulfate



for mice viability [Jonker, J. W. *et al* (2002), Schinkel, A. H. *et al* (1994) and Zhou, S. *et al* (2002)]. Hence, ABC transporters are a major mechanism for multidrug resistance in cancers. Presently, cancers resistant to chemotherapy are believed to result from a small subpopulation of cells, which can survive after treatment and initiate new tumours resulting in tumour recurrence. This small subpopulation of cells resistant to chemotherapy could be correlated with expression of drug efflux transporters from the ABC transporter family, which protects cancer cells from drug cytotoxicity. A small subpopulation of stem-like cells has recently been discovered in many cancers and these cells may be a significant target for treatment to cure cancers, as discussed in the rest of section.

## **1.4 Cancer stem cells**

Most malignant neoplasms have the capabilities of invasion, progression and metastasis. Current available treatments do not completely eradicate all cancer cells, consequently, many cancers recur within a few or several years after a complete course of treatment. Presently, most patients diagnosed with malignant cancer ultimately have a poor prognosis and fatal outcome. In light of this, many types of cancers have been extensively studied in order to develop a deeper understanding of the pathology of cancer and improve treatment by attacking the right targets. The origin of cancer cells is still obscure and complicated by the fact that cancer populations consist of heterogeneous cells. Studies have shown that not all cancer cell populations are able to sustain formation or growth of tumours. In the last decade, there have been several studies focused on the risk of stem cells in cancer. These aberrant stem-like cells are known as 'cancer stem cells (CSCs)' or 'tumour initiating cells'. Several studies have hypothesised that CSCs, small populations of cancer cells, are the cell of origin from which the primary cancer initiates [Ignatova, T. N. *et al* (2002), Hemmati, H. D. *et al* (2003), Tan, B. T. *et al* (2006), Galli, R. *et al* (2004), Singh, S. K. *et al* (2003 and 2004)]. It is still unknown where cancer stem cells themselves originate from. Importantly, however, cancer stem cells have been hypothesised to be the chemoresistant population resulting in failure of chemotherapy and tumour recurrence.

### **1.4.1 Normal stem cells and cancer stem cells**

Normal stem cells and CSCs have many shared characteristics such as self-renewal, indefinite proliferation and differentiation (although in the case of CSCs this is limited). Therefore, it is important to understand what mechanisms in CSCs, which regulate self-renewal and differentiation, are different from normal stem cells and drive these cells to proliferate and fail to fully differentiate hence forming tumours. The two most likely possible sources from which CSCs originate are normal stem cells and progenitor cells. Due to their observed sharing of many similar characteristics with normal stem cells, CSCs have been proposed to originate from normal stem cells. Normally, stem cells self-renew to maintain themselves and generate restricted progenitors, which ultimately differentiate into the mature cells composing a particular tissue. Genetic mutations are an important factor participating in tumour formation. Normal stem cells have ability to indefinitely proliferate throughout their life span resulting in these cells have been through proliferation process more frequent than progenitor cells which have less ability to proliferate. Therefore, normal stem cells have a higher risk to accumulate genetic mutations than progenitor or differentiated cells. Hence, genetic aberrations occurring in normal stem cells could cause tumour initiation [Reya, T. *et al* (2001) and Pandal, R. *et al* (2003)]. A model of tumour progression in normal stem cells and progenitor cells is showed in Figure 1.19 [Dean, M. *et al* (2005)]. Studies in leukaemia supported the fact that stem cells isolated from acute leukaemia expressed similar markers to normal stem cells and isolated leukaemic cells could differentiate into multiple mature cell lineages similar to normal stem cells [Lapidot, T. *et al* (1994)]. Later studies postulated that CSCs arose from progenitor cells, which acquired the self-renewal capability of stem cells. Hence, CSCs were proposed to be derived from progenitor cells able to generate both self-renewing and non self-renewing progenitor cells [Wagner, K. *et al* (2006)].

### **1.4.2 Discovery of cancer stem cells**

In 1997, the first evidence was discovered that CSCs studied in acute myeloid leukaemia (AML) were a significant component of the tumour bulk [Bonnet, D. and Dick, J. E. (1997)]. Minor populations of leukaemic cells were derived and identified by side-population analysis. This

side-population not only expressed the specific surface marker CD34<sup>+</sup> but also was pluripotent. CD34<sup>+</sup>/CD38<sup>-</sup> populations were established in NOD-SCID mice and new tumours were generated. Additionally, these tumours could be serially established. Furthermore, the phenotypes of these leukaemic-initiating cells (LICs) were very similar to normal hemopoietic stem cells (HSC) [Bonnet, D. and Dick, J. E. (1997)]. Therefore, it is possible that LICs might be derived from normal HSCs. Since then CSCs have also been studied in solid tumours such as breast cancers [Al-Hajj, M. *et al* (2003)], prostate cancers [Collins, A. T. *et al* (2001)] and brain tumours [Singh, S. K. *et al* (2003 and 2004) and Hemmati, H. D. *et al* (2003)]. CSCs of solid tumours express different stem cells markers, for example, tumour-initiating cells of

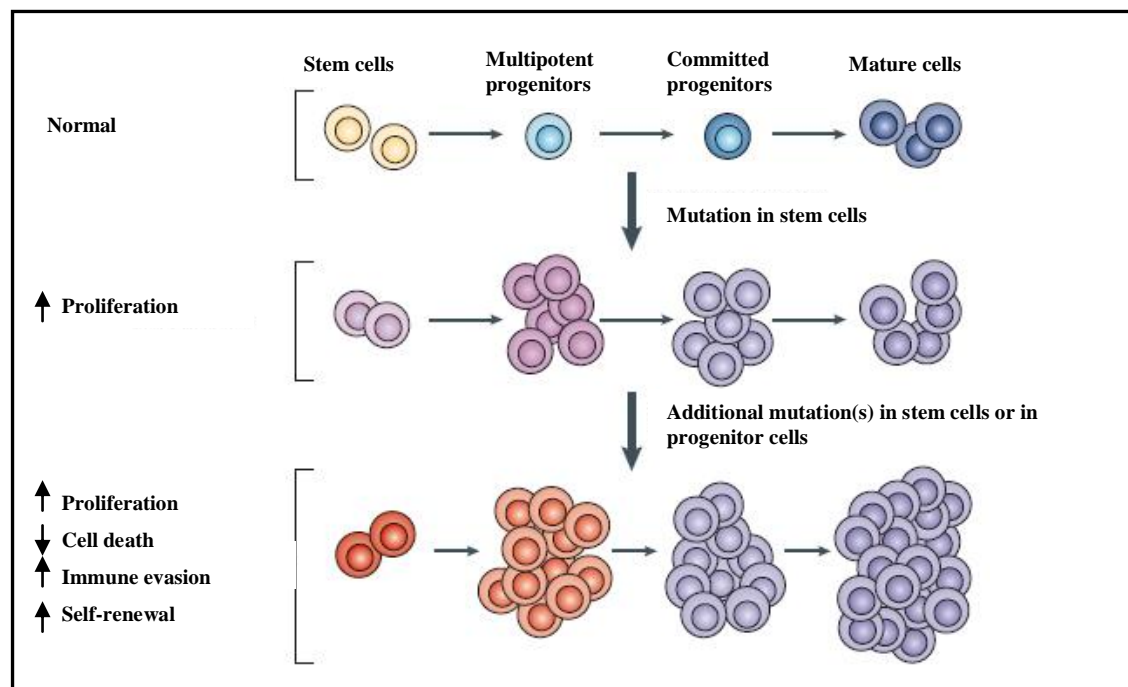


**Figure 1.19 A model of cancer stem cells and tumour progression in normal stem cells and progenitor cells.** Normal stem cells generate progenitors that ultimately differentiated into mature cells. When a mutation occurs in normal stem cells, this results in abnormal proliferation of stem cells leading to a pre-malignant lesion. If further mutation(s) occur in these stem cells or progenitor cells, these cells have more aberrations and acquire more stem cell-like characteristics resulting in increased proliferation, evasion of the immune system, self-renewal and decreased apoptosis. Hence, aberrant normal stem cells or progenitor cells can initiate malignant tumours [Dean, M. *et al* (2005)].

breast cancers express CD44<sup>+</sup>CD24<sup>-</sup>, CD29<sup>hi</sup>CD24<sup>+</sup> and CD49f<sup>+</sup>CD24<sup>+</sup>Sca-1<sup>low</sup> immunophenotypes [Tan, B. T. *et al* (2006)].

The first evidence that supported the existence of stem cell-like cells in human brain tumours was a study that isolated cells from a post-surgery specimen of human glioblastoma multiforme. Isolated cells could be induced to form neurospheres which expressed both neuronal and astroglial markers and had stem cell capacities [Ignatova, T. N. *et al* (2002)]. Hemmati *et al* (2003) also discovered that paediatric brain tumours (PBTs), including medulloblastomas and gliomas, contained stem cell-like cells. Cells derived from these PBTs could be induced to generate neurospheres and when these neurospheres were transplanted into immunodeficient mice, they could initiate tumours, which were able to be serially transplanted, and had the ability to self-renew. These cells could differentiate into both neurons and glial cells (multilineage differentiation) under differentiation conditions and after xenograft into neonatal rat brain. Genes expressed in neural and other stem cells (CD133, SOX2, musashi-1, bmi-1, maternal embryonic leucine zipper kinase, and phosphoserine phosphatase) could be detected in these stem cell-like neurospheres. However, the characteristics of these cells were not exactly the same as normal neural stem cells. Cancer stem-like cells occasionally differentiated into abnormal cells which expressed multilineage markers, hence a heterogeneous tumour might result from these cells [Hemmati, H. D. *et al* (2003)]. Galli *et al* (2004) studied neural-like stem cells derived from adult human glioblastoma multiforme. They found that neural-like stem cells derived from tumour specimen had characteristics of stem cells in terms of multilineage differentiation, capability of neurosphere formation and initiation of tumours recapitulating the original tumours when they were transplanted into immunodeficient mice. Additionally, these neural-like stem cells could be repeatedly isolated and used to initiate neurospheres and new tumours indicating their self-renewal characteristic *in vivo* [Galli, R. *et al* (2004)].

#### **1.4.3 Identification of cancer stem cells**

Many techniques have been developed to effectively identify and isolate brain tumour stem

cells. However, cancer stem cells are still difficult to isolate due to the fact that they are a small population of the tumour. There is no specific antibody to detect these cells at present and none of techniques exclusively isolates cancer stem cells. Cancer stem cells can be identified by the neurosphere assay, side population analysis or stem cell markers. However, the most convincing method to prove the existence of cancer stem cells is serial transplantation by orthotopic transplantation. Cells containing cancer stem cells should be able to re-established tumours, which recapitulate the original tumours, and these cells should preserve self-renewal ability on serial passages.

The neurosphere assay is the simplest method to identify, isolate and expand neural stem cells. The principle of neurosphere assay is that cells are dissociated into single cells in serum free tumour media supplemented with growth factor. Most cells die but only cells, which are responsive to the growth factors, can survive and proliferate to form floating clusters of cells defined as neurospheres. This assay examines the ability of cells to self-renew and proliferate [Reynolds, B. A. and Weiss, S. (1992)].

Side population analysis is based on the principle that cancer stem cells have the capability to extrude the DNA binding dye Hoechst 33342 and flow cytometry is used to detect the level of dye accumulation in cells. Cells with a low level of dye accumulation are identified as side population cells (the putative stem-like population) [Komuro, H. *et al* (2007) and Hadnagy, A. *et al* (2006)].

Markers for cancer stem cells have been generally used to identify and characterise cancer stem cells in multiple solid tumour types. Due to the extensive study of cancer stem cells, many cell surface markers have proved to be effective in identifying populations enriched with cancer stem cells such as CD133 (PROM1), CD44 (PGP1), CD24 (HSA), epithelial cell adhesion molecule [EpCAM (epithelial specific antigen: ESA or TACSTD1)], ALDH1, THY1 (CD90) and ATP-binding cassette B5 (ABCB5) [Reviewed in Visvader, J. E. and Lindeman, G. J. (2008)]. SOX2 is also generally used to identify neural stem cells since SOX2 is an important gene

involving in the maintenance of self-renewal and proliferation of human embryonic stem cells [Fong, H. *et al* (2008)]. SOX2 gene deletion in glioblastoma lead to loss of proliferation and tumourigenicity [Gangemi, R. M. R. *et al* (2009)]. CD133 and SOX2 were hence used to identify cancer stem-like cells in our study.

#### 1.4.3.1 CD133

CD133 was formerly known as human AC133 or human PROML-1 (prominin-1, named after its location on protrusions of the plasma membrane). Human prominin-1 was first isolated from hematopoietic stem cells using a monoclonal antibody to CD34<sup>+</sup> and identified as AC133 (CD133). CD133 belongs to a pentaspan transmembrane glycoprotein family including prominin-2, recently discovered and originally known as prominin related protein (prom-rp). Prominin-2 has also been shown to be expressed in human lung cancer and tumours of the CNS [Mizrak, D. *et al* (2008)]. Human CD133 has 37 exons and encodes a 865 amino acid (aa) protein with a total molecular weight of 120 kDa [Shmelkov, S. V. *et al* (2005)].

CD133 has been used to isolate and study cancer stem cells in many studies. Singh *et al* (2003) sorted CD133<sup>+</sup> and CD133<sup>-</sup> cells by magnetic cell sorting and characterised the properties of these cells. Their results showed that brain tumours originate from cells expressing CD133, with these cells being able to form clusters of neurosphere-like cells, self-renew, proliferate and initiate new tumours which recapitulated the original tumour phenotypes *in vivo*. Normal neural stem cells were also found within CD133<sup>+</sup> populations so it is possible that these normal stem cells are the candidate cells that initiate brain tumours [Singh, S. K. *et al* (2003)]. Singh *et al* (2004) went on to study tumour-initiating cell characteristics from CD133<sup>+</sup> cells isolated from medulloblastoma and glioblastoma. Their study showed that only the CD133<sup>+</sup> subpopulation cells (100 cells were sufficient) could be xenografted into NOD-SCID mice and initiate new tumours which display similar histological features to the original tumours. Additionally, these cells also could be consecutively transplanted. In contrast, CD133<sup>-</sup> cells could not form nodules or masses even after a large number of these cells (100,000 cells) were injected into mouse brain. This demonstrates the self-renewal and recapitulation capacity

of CD133<sup>+</sup> cells. The tumours initiated by CD133<sup>+</sup> cells comprised a small proportion of CD133<sup>+</sup> cells (19-22%) and a large proportion of CD133<sup>-</sup> cells (78-81%). This suggested that CD133<sup>+</sup> cells may produce both CD133<sup>+</sup> and CD133<sup>-</sup> cells in new tumours. Furthermore, xenografted and transplanted tumours expressed similar markers to the original tumours using antibodies to nestin and vimentin (neural precursor cell marker),  $\beta$ III-tubulin and MAP2 (neuronal markers), and GFAP (astrocyte marker). This demonstrated the multilineage differentiation capability of these tumour initiating cells (CD133<sup>+</sup> cells). The immunofluorescent results of their study showed that CD133<sup>+</sup> positive cells accounted for 9-29% of GBM and 6-21% of medulloblastoma which was in accordance with the assay of primary sphere formation *in vitro* [Singh, S. K. *et al* (2004)]. These two studies support the fact that neural stem cell surface marker CD133 can be used to effectively identify cancer stem cells in brain tumours. However, one study revealed that CD133 could not identify cancer stem cells in the C6 glioma cell line since both CD133<sup>+</sup> and CD133<sup>-</sup> cells had characteristics of cancer stem cells. Hoechst 33342 also could not identify side population due to its toxicity to this cell line. Therefore, they concluded that both CD133 and Hoechst 33342 have limitations in identification of cancer stem-like cells in C6 glioma cell line [Shen, G. *et al* (2008)].

### **CD133 structure**

The structure of CD133 [Figure 1.20] consists of an extracellular N-terminal domain, two large glycosylated extracellular loops of 255 and 290 aa, five transmembrane domains, two small intracellular loops of 30 aa each and a cytoplasmic C-terminal domain [Sakariassen, P. *et al* (2007)]. The extracellular loops have eight potential N-glycosylation sites with five located on the first loop and three located on the second loop. The two large extracellular loops and the cytoplasmic C-terminal can be detected by antibodies and epitope insertion analysis [Corbeil, D. *et al* (2001)]. Transcription of CD133 is regulated by five alternative promoters (P1-P5) [Figure 1.21]. Three are located within a CpG-island suggesting that they can be controlled by methylation. The 5'-untranslated region (UTR) comprises 10 exons (A, B, C, D1-3 and E1-4). CD133 transcription is regulated by at least five alternative promoters. There are 8 isoforms of CD133 transcribed depending on which promoters regulate this process. Therefore, different

alternative promoters result in the inclusion of different 5'-UTR exons which may have an influence on splicing of the coding regions. Consequently, different alternative promoters play a role in the expression of prominin-1 isoforms [Shmelkov, S. V. *et al* (2005)]. Due to this variation CD133 isoforms, it is difficult to select an appropriate antibody to identify CD133 in a tissue/tumour of interest.

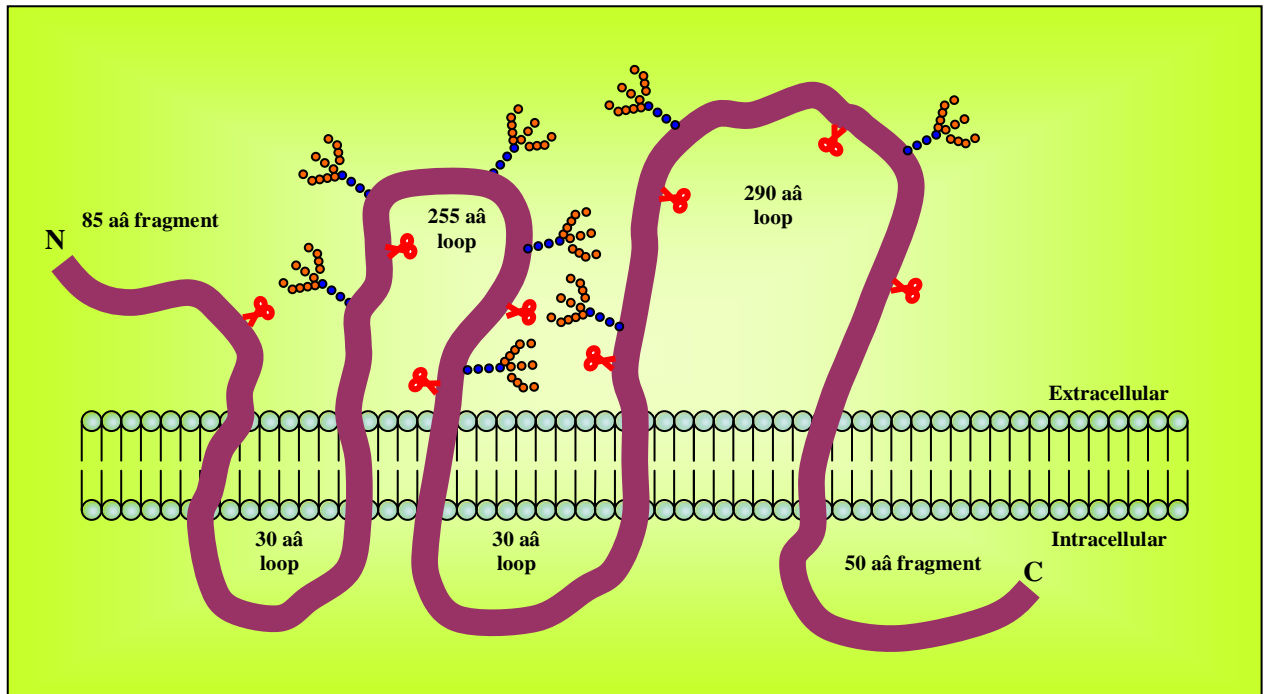


**Figure 1.20 Schematic diagram of murine CD133 structure.** The structure of murine CD133 consists of five transmembrane domains which are located in lipid bilayers of the plasma membrane. Extracellular components of CD133 comprise an 85 aa N-terminal domain and two large glycosylated extracellular loops of 255 and 290 aa which have eight potential N-glycosylation sites (orange-blue forks). Five glycosylation sites exist on the 255 aa loop and three are located on the 290 aa loop. In addition, there are two small intracellular loops of 30 aa each and a cytoplasmic 50 aa C-terminal domain. Red scissors indicates the sites where trypsin can cut CD133 when it is exposed for too long to trypsin solution [Adapted from Sakariassen, P. *et al* (2007)].



### CD133 as a marker

CD133 is normally used as a marker for human haematopoietic stem cells. It is also a very useful marker for normal neural stem cells. Additionally, many undifferentiated cells also express CD133, such as endothelial progenitor cells, foetal brain stem cells, embryonic epithelium, prostatic epithelial stem cells and myogenic cells. Moreover, prominin-1 protein, detected by mAb AC133, is not only restricted to human neural or haematopoietic stem cells but it is also expressed in adult human tissues such as kidneys, mammary gland, trachea, salivary gland and placenta [Florek, M. *et al* (2005)]. Furthermore, some other cancers express CD133 such as retinoblastoma [Maw, M. A. *et al* (2000)], teratocarcinoma [Miraglia, G. *et al* (1997)] and leukaemia [Baersch, G. *et al* (1999)]. CD133, as described previously, has been used

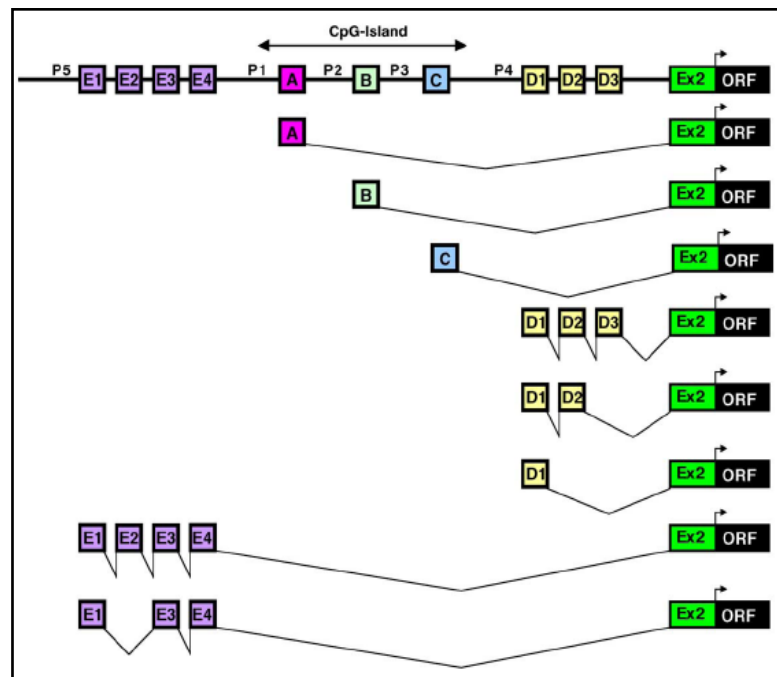


**Figure 1.21 Genomic organisation of the promoter region of human AC133 and alternative splicing within its 5'-UTR.** The diagram shows eight CD133 isoforms due to the regulation of alternative promoters. Five alternative promoters (P1 - P5) influence which particular isoform of CD133 is expressed with alternative promoters being transcription initiation points. The detection of five alternative first exons indicated the existence of these five alternative promoters, P1 (upstream of exon 1A), P2 (upstream of 1B), P3 (upstream of 1C), P4 (upstream of 1D1) and P5 (upstream of 1E1) [Shmelkov, S. V. *et al* (2005)].

as a marker to detect stem cells in several studies [Singh, S. K. *et al* (2003 and 2004) and Hemmati, H. D. (2003)]. In addition, CD133 has been used to study the biology and plasticity of CD133<sup>+</sup> haematopoietic stem cells by Handgretinger *et al* (2003). CD133<sup>+</sup> stem cells were isolated using magnetic activated cell sorting (MACS) from peripheral blood cells of healthy adults. These isolated CD133<sup>+</sup> cells had a high capacity of xenograftment into NOD-SCID mice and gave rise to both adherent and non-adherent cells *in vitro*. Interestingly, the adherent cells lacked CD34 expression and could be induced to develop into stem cells which had a high capability of NOD-SCID engraftment, similar to the original cells. Adherent CD133<sup>+</sup>CD34<sup>-</sup> cells could also produce CD133<sup>+</sup>CD34<sup>+</sup> cells after a short time of culture *in vitro* [Handgretinger, R. *et al* (2003)].

### **CD133 function and application**

The functions of CD133 are not completely understood. One study found that single nucleotide deletion of prominin-1 resulted in retinal degeneration since morphogenesis of photoreceptor disk was impaired [Maw, M. A. *et al* (2000)]. CD133 was proposed to have a function in cell membrane protrusions and be inherited with the apical membrane during asymmetric cell division [Reviewed in Corbeil, D. *et al* (2001)]. This might give a clue to CD133 function. Several studies have characterised CD133 and showed that CD133<sup>+</sup> cells are able to differentiate into both neurons and glial cells, can form neurospheres and be serially transplanted into NOD-SCID mice. Such properties reflect self-renewal and multilineage differentiation of stem cells [Singh, S. K. *et al* (2003 and 2004), Uchida, N. *et al* (2000) and Hemmati, H. D. *et al* (2003)]. CD133 expression has also been used as a prognostic factor or an indicator in cancers. Recently, Zeppernick and colleagues were the first group to demonstrate the correlation between CD133 expression and clinical outcome of glioma patients. They revealed that the proportion of CD133 expressing cells and the presence of positive cell clusters were prognostic factors for glioma patients. Whereby a high proportion of positive cells or a presence of the clusters associated with a high grade of tumour. These 2 prognostic factors also can indicate tumour recurrence, patient survival and tumour progression in particular for WHO grade II and III tumours [Zeppernick, F. *et al* (2008)]. CD133 reactivity

might therefore identify cells with increased tumourigenicity. High CD133 reactivity cells have also been found in the active phase of cell cycle whilst low CD133 reactivity cells were detected in G<sub>1</sub>-G<sub>0</sub> phase suggesting an association with proliferating cells. Therefore, CD133 is a good marker to reflect mitotic activity indicating increasing tumourigenicity as well as identifying a distinct cancer stem cell-like subpopulation. However, recent studies have indicated that the AC133 epitope is not a stable marker whereby high AC133 reactivity cells generate less reactivity of AC133 cells after many passages of culture whilst low AC133 reactivity cells can generate high AC133 reactivity cells after prolonged cultivation [Jaksch, M. *et al* (2008)]. Another complicating factor is the sensitivity of CD133 to cell harvesting agents such as trypsin (Figure 1.20).

#### **1.4.3.2 SOX2**

SOX2, encodes a SRY-related high mobility group (HMG) box transcription factor, which has 90% aa residue identity in its HMG-DNA binding domain to SOX1 and SOX3. SOX2 is a member of the superfamily of SOXB1 transcription factors, consisting of closely related genes including SOX1 and SOX3. SOX2 is normally expressed in neural progenitors and stem cells, which can be found throughout the vertebrate CNS [Graham, V. *et al* (2003)].

#### **SOX2 function and application**

SOX2 protein is expressed in embryonic stem cells (ESCs) and neural stem cells (NSCs), but its function remains unclear. Graham *et al* (2003) studied SOX2's ability to maintain neural progenitor identity. They found that SOX2 plays a role in maintenance of general stem cell properties including self-renewal, proliferation and differentiation into varying progenies [Graham, V. *et al* (2003)]. Similar to human embryonic stem cells, SOX2 is also involved in regulation of self-renewal and pluripotency studied in human embryonic stem cell lines: H1 and H9 [Fong, H. *et al* (2008)]. When SOX2 was knocked down in glioblastoma cell lines, they lost the capability of self-renewal and tumourigenicity [Gangemi, R. M. R. *et al* (2009)]. In addition, inhibition of SOX2 function results in promotion of differentiation of neural progenitor cells, but the inhibitory mechanism of neuronal differentiation by SOX2 is still unclear. A possible

mechanism of SOX2 inhibition of cell differentiation has been proposed whereby SOX2 regulates cells to continuously be maintained in the cell cycle resulting in no differentiation [Graham, V. *et al* (2003)]. SOX1, SOX2 and SOX3 are normally co-expressed in neuroepithelial cells and regulate the development of neural stem cells. SOX2 however, plays a very important role in the regulation of neural development because SOX2 knockout embryos fail to develop embryonic or trophectoderm lineages. Conversely, SOX1 and SOX3 knockout mice can survive and have no defects in the CNS [Episkopou, V. (2005)]. SOX2 has been found to be a marker for ESCs and NSCs. Additionally, SOX2 functionally co-operates with transcription enhancer regions including SOX2 regulatory region 1 (SRR1) and SRR2 identified from ESCs. The function of SRR2 is to enhance the Oct-3/4-SOX2 or Oct-6-SOX2 complex (Oct-SOX enhancers) in ESCs resulting in maintenance of the multipotent capacity of both ESCs and NSCs [Miyagi, S. *et al* (2004)]. SOX2 therefore plays an important role in maintenance of the undifferentiated stage of stem cells.

Masui *et al* (2007) hypothesized that SOX2 collaborates with OCT3/4 to maintain pluripotency of ESCs whereby SOX2 acts as a cofactor of OCT3/4 [Masui, S. *et al* (2007)]. Avilion *et al* (2003) found that SOX2 and OCT4 are co-expressed in early embryonic cells including morula, inner cell mass (ICM), epiblast and germ cells. Therefore, both SOX2 and OCT4 might have a role in the regulation of cell differentiation. Their results showed that the presence of both SOX2 and OCT4 induced epiblast formation whilst their absence resulted in the formation of trophectoderm. In addition, single expression of SOX2 is required to maintain an undifferentiated property of the epiblast whilst extraembryonic endoderm is developed when OCT4 is individually expressed. Furthermore, SOX2 shuttles between nuclei and cytoplasm depending on the stage of cell development. SOX2 is located in nuclei in the early stage of embryogenesis whilst SOX2 is exported to the cytoplasm when embryonic cells progressively develop. SOX2 was stained in both nuclei and cytoplasm [Avilion, A. A. *et al* (2003)]. In the early mouse embryo, SOX2 mRNA expression has been detected in some embryonic cells including inner cell mass, epiblasts, germ cells and trophoblast cells. SOX2 expression was found to be restricted to cells having stem cell characteristics rather than more differentiated

cells [Miyagi, S. *et al* (2004)]. Hence, SOX2 is expressed in cells having stem cell properties whilst being downregulated in cells differentiating into terminal specific mature cells. SOX2 functions to maintain pluripotency and undifferentiated stage of stem cells. Additionally, SOX2 is also one of the important transcription factors involved in reprogramming mature cells (mouse fibroblast) to embryonic stem-like cells alongside Oct3/4, c-Myc and Klf4. These cells had characteristics of embryonic stem (ES) cells in terms of morphology and growth properties, expression of ES markers and initiation of tumour after transplantation [Takahashi, K. and Yamanaka, S. (2006)].

CD133 and SOX2 identify both stem cells and progenitor cells. The location of CD133 and SOX2 expression in brain was not obviously stated because these two markers are expressed in the developing brain and they are down regulated when brain is developed. In both human fetal brain and embryonic mouse brain, it was revealed that both CD133 and SOX2 were expressed in the subventricular zone [Uchida, N. *et al* (2000), Ferri, A. L. M. *et al* (2004) and Pfenninger, C. V. *et al* (2007)]. In human fetal brain, there is evidence revealing that CD133 was expressed in the roof and floor plate of the ventricle and surrounding the central canal [Uchida, N. *et al* (2000)]. In postnatal mouse brain, CD133 and SOX2 co-staining was positive in the ventral wall whereas the dorsal wall of the ventricle expressed SOX2 without CD133 (Figure 1.22) [Ferri, A. L. M. *et al* (2004) and Pfenninger, C. V. *et al* (2007)].

#### **1.4.4 The model for tumour heterogeneity and propagation**

The identity of the cells which initiate and develop brain tumours is not fully understood at present. Currently, there are two models which explain the heterogeneity, initiation and development of tumours [Figure 1.23]. The clonal evolution model describes that any cell (stem cell/progenitor or mature) is able to acquire mutations that provide a growth advantage hence allowing selection of these cells which will continually proliferate and maintain the tumour population (Figure 1.23, a) [Visvader, J. and Lindeman, G. J. (2008)]. This model is similar to the stochastic model in some aspects. The stochastic model suggests that all cancer cells are heterogeneous and have a similar tumourigenic potential to initiate and sustain

tumours. Cells accumulate mutations over a considerable period of time and are induced into CSCs which have capabilities of self-renewal and maintenance of tumour cells [Vescovi, A. L. *et al* (2006)]. The cancer stem cell model or hierarchical model proposes that only a small population of tumour cells, cancer stem cells, is able to generate and sustain the tumour population due to their self-renewal capacity and proliferation whilst the remaining cancer cells are either short-lived progenitors or terminally differentiated cells without stem cell-like characteristics, and with a low potential for continued proliferation (Figure 1.23, b) [Visvader, J. and Lindeman, G. J. (2008)]. The progression of tumours might be based on both of these models of tumourigenesis. Initially, CSC1 generates and maintains the tumour population. When progression of the tumour occurs, CSC2 is selected due to the clonal evolution of CSC1. CSC2 acquires more mutations or epigenetic modifications resulting in generation of a more aggressive tumour. This might indicate that cancer stem cells will gain more and more mutations after many rounds of treatment and these severely aberrant cancer stem cells will generate increasingly aggressive tumours (Figure 1.23, c) [Visvader, J. and Lindeman, G. J. (2008)].

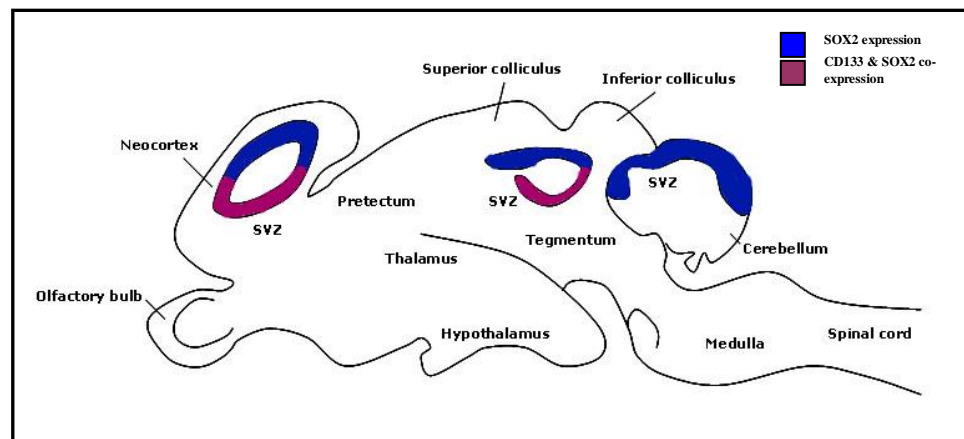


**Figure 1.22 The location of CD133 and SOX2 expression in postnatal mouse brain.**

CD133 and SOX2 expression was present in the subventricular zone (SVZ) of postnatal mouse brain. CD133 and SOX2 co-expression was found in the ventral wall of the ventricle whilst the dorsal wall is positive for SOX2 only.

At present, many genetic mutations have been shown to correlate with brain tumour formation. In astrocytoma, aberrations of *INK4A*, *CDK4*, *RB* and *TP53*, which regulate cell cycle, and *EGFR*, *PDGFR* and *PTEN*, which are growth factor receptor signalling, have all been shown to initiate astrocytoma in mouse models [Reviewed in Furnari, F. B. *et al* (2007)]. Additionally, one study revealed that both neural stem cells and progenitor cells were able to be transformed into high grade glioma cancer cells by depletion of specific tumour suppressor genes. A tamoxifen-inducible *Nestin-cre-ER<sup>T2</sup>* transgene was used to induce these cells to form tumours in mice model. This study confirmed the hypothesis that loss of tumour suppressor genes could lead to tumour formation from both neural stem cells and progenitor cells [Llaguno, S. A. *et al* (2009)].

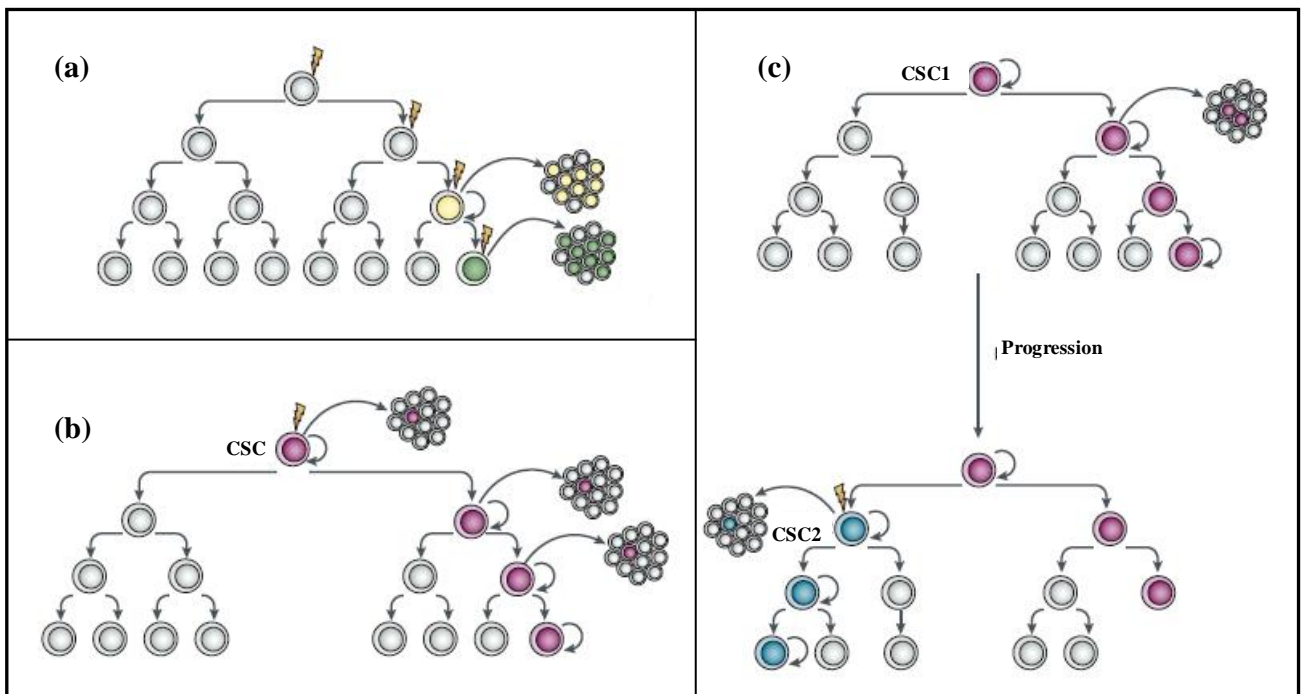


**Figure 1.23 The heterogeneity and propagation of tumours.** The clonal evolution model proposes that all cells have a similar potential to generate a tumour. Cells that have acquired mutations that provide a growth advantage are selected to propagate tumours (a). Whilst the cancer stem cell model postulates that only cancer stem cells can generate and maintain a tumour population (b). For tumour progression, clonal evolution of CSC1 occurs therefore, CSC2 therefore acquires more mutations and is selected to be the prominent population of tumours. The more mutated CSC2 population can then initiate a more aggressive tumour (c) [Visvader, J. and Lindeman, G. J. (2008)].

#### 1.4.5 Cancer stem cells and drug resistance

Drug resistance of cancer cells can occur by either intrinsic or acquired resistance. Drug resistance in cancer cells, which contain a resistant population in the absence of previous exposure to chemotherapeutic drugs, is called intrinsic resistance. Whilst the process whereby a resistant population is developed after chemotherapy resulting from mutation or overexpression of drug target, inactivation or detoxification of drugs or drug removal from cells, is defined as acquired resistance. Cancer stem cells, a small population of tumours, are an important target of treatment since these cells are believed to be chemoresistant and have the ability to re-initiate tumours after treatment. Four models of drug resistance in tumours are presented in Figure 1.24.

The conventional model of acquired drug resistance in cancer cells hypothesised that tumours contained one cell or a small proportion of the tumour population, which gained genetic alterations or mutations after chemotherapy. Consequently, these drug selected resistant cells developed a growth advantage after drug selection resulting in rapid repopulation of tumours and taking over of the whole tumour population (Figure 1.24, a). Stem cells are now widely believed to be responsible for drug resistance in cancer. The second model therefore postulates that tumours contain a small number of cancer stem cells, which are resistant to chemotherapy due to either their quiescent properties, ability to undergo DNA repair or active drug efflux capability by ABC transporters (or a combination of all). Therefore, they are able to survive and reform tumours, which are heterogeneous and share characteristics with the parental tumour (Figure 1.24, b). The third model describes acquired drug resistance, which can be found in patient who have been treated with radiation or exposed to carcinogens for a long period of time or undergone tumour recurrence after chemotherapy. Consequently, cancer stem cells have accumulated genetic mutations or alterations. After treatment, surviving genetically mutated cancer stem cells regenerated progenitor cells containing these genetic mutations. Hence, initiated tumours have different characteristics from the parental tumours (Figure 1.24, c). The final model describes intrinsic drug resistance whereby tumours contain cancer stem cells and various stages of differentiating cells, which are all inherently drug resistant.



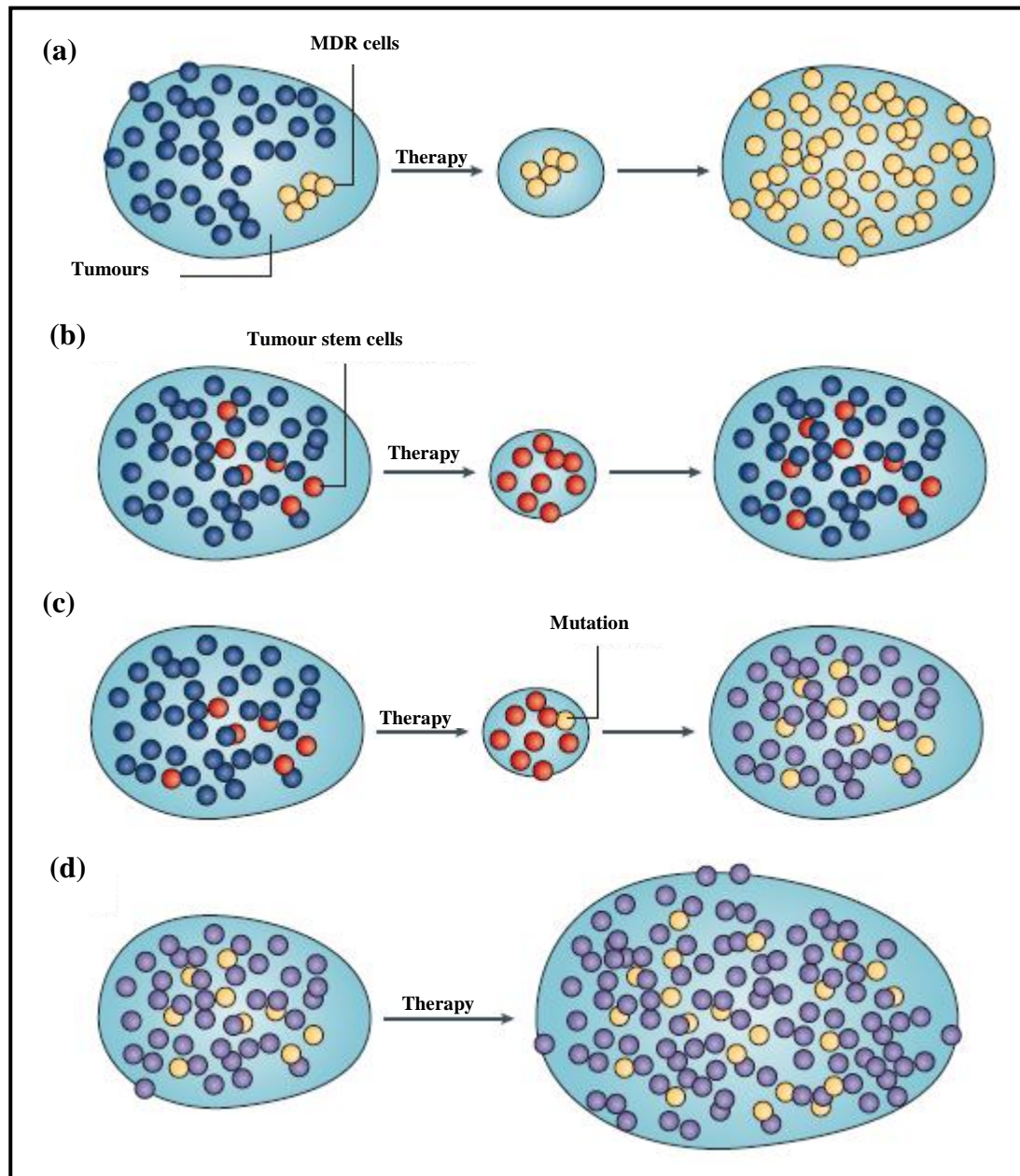


**Figure 1.24 Models of drug resistance in cancer cells.** The conventional model of drug resistance in cancer cells proposes that a small population of cancer cells (blue) containing a genetic alteration (yellow) survives after treatment and regenerates a new tumour (a). A drug resistance model based on cancer stem cells (red) is shown in (b) whereby cancer stem cells survive after treatment and regenerate cancer stem cells and progenitors. The acquired drug resistance model proposes that cancer stem cells (pale yellow) acquire genetic mutations after prolonged treatment resulting in regenerating cancer stem cells containing that genetic mutation and various differentiating progenitors with the same genetic alteration (purple) (c). The last model describe intrinsic drug resistance whereby both cancer stem cells (yellow) and cancer cells (purple) are completely resistant to chemotherapy, consequently, there is no effect on these cells [Dean, M. *et al* (2005)].

Therefore, chemotherapy will not have any effect on these cells and tumour will continue to progress (Figure 1.24, d) [Dean, M. *et al* (2005)]. The cancer population is heterogeneous. It is proposed that a large proportion of the cancer population is comprised of non-tumourigenic cells, which are sensitive to chemotherapy resulting in shrinkage of tumour mass after treatment. However, a small proportion of the cancer population, is chemoresistant and survives after treatment. This small proportion of cancer cells is cancer stem cells. Cancer stem cells were initially identified in acute leukaemia. They were also detected in many brain tumours. An overexpression of ABC transporters in cancer stem cells increased DNA repair and their quiescent nature are important factors in resistance to therapy. With these main characteristics, cancer stem cells surviving after treatment self renew and proliferate to re-initiate the tumour population resulting in tumour relapse. Therefore, cancer stem cells are currently believed to cause chemoresistance in many cancers and hence represent the main target of treatment to ultimately cure malignant diseases in the future.

### **1.5 What is the contribution of drug resistance CSCs to paediatric brain tumours?**

Paediatric brain tumours (PBTs) are the second most common malignant disease in children after leukaemia [Pollack, Ian F. (1994), and Stewart, E.S. and Cohen, D.G. (1998)]. Most PBTs are still devastating diseases since the treatment outcome is not impressively successful and patients also have adverse sequelae after treatment. Although, many treatment options are currently available and new improved drugs are included in chemotherapeutic regimens, the survival rate of patients and prognosis of disease remains poor for many tumour types [Stewart, E.S. and Cohen, D.G. (1998) and Gupta, N. *et al*. (2004)]. Several chemotherapeutic drugs with different mechanisms of action are used in a single regimen to treat patients, however, the clinical outcome is only slightly improved and less effective than expected. The phenomenon whereby PBTs are/become resistant to chemotherapy and commonly have cross-resistance to many chemotherapeutic drugs is currently known as multidrug resistance (MDR).

During the last few decades, MDR has been extensively studied in many malignant diseases. One important drug resistance mechanisms, predominantly found in many drug resistant cancers, involves the ABC transporter family. These transporters function as pumps to extracellularly export many cytotoxic drugs resulting in decreased cellular accumulation of drugs. ABCB1 [Chen, C. J. *et al* (1986)], ABCC1 [Cole, S. P. C. *et al* (1992)] and ABCG2 [Doyle, L. A. *et al* (1998)] have been shown to be predominantly overexpressed in many drug resistant brain tumours and these three transporters have ability to transport various substrates and chemotherapeutic agents regardless of their drug categories or chemical structures. These 3 transporters are therefore obvious candidate for the acquisition of multidrug resistance.

More recently, cancer stem cells (CSCs) have been confirmed to exist as a small proportion of the tumour population [Ignatova, T. N. *et al* (2002), Hemmati, H. D. *et al* (2003), Tan, B. T. *et al* (2006), Galli, R. *et al* (2004), Singh, S. K. *et al* (2003 and 2004)]. The hypothesis being tested here is that CSCs are chemoresistant and they are able to re-initiate tumours after treatment due to their self-renewal and proliferative capability. It is proposed that the main mechanism of MDR in CSCs is active drug efflux by ABC drug transporters although other mechanisms may also protect CSCs from cytotoxic drugs including their quiescent property and capability of DNA repair. Therefore, CSCs are postulated to contribute to MDR in cancers via active drug efflux by ABC drug transporters. As a result, CSCs might be the real target for treatment in many malignant diseases.

The hypothesis being tested in this thesis postulates that paediatric brain tumour cell lines contain a subpopulation of cancer stem cells that use ABC multidrug transporters to efflux chemotherapeutic agents.

The aim of this thesis were therefore to

- characterise newly derived paediatric brain tumour cell lines to demonstrate their clinical relevance

- characterise the cancer stem cell component of these lines
- determine the expression of ABCB1, ABCC1 and ABCG2 in cancer stem cell enriched cultures/cancer stem cells
- test whether it was possible to enrich for ABC expressing cancer stem cells using 4 different chemotherapeutically applied drugs
- test if ABC transporter function can be detected and if inhibition restores chemosensitivity

---

---

## **Chapter 2**

### **Materials and Methods**

---

---

## Chapter 2: Materials and Methods

### 2.1 Cell culture

Generating cell lines from paediatric brain tumours is difficult and often is limited by the size of the tumour tissue available and the ability of dissociated cells to grow under cell culture conditions. This has resulted in a dearth of appropriate model cell lines in which to investigate prognostic targets and develop potential therapies. For several tumour types, such as ependymoma, there are no 'commercially' available cell lines. Others are more readily available, but their relationship to the tumour of origin has not been studied, nor has their retention of CSCs and degree of tumourigenicity. Brain tumour cell lines were derived at the Children's Brain Tumour Research Centre (CBTRC) (EPN-1, EPN-2, MED-1, MED-2, Oig-1 and SPNET-1) and at the University of Birmingham (BT-4) as approved by the Local Research Ethics Committee. The tumours of origin were graded and classified by a pathologist (Professor James Lowe) according to the World Health Organisation (WHO) 2007 classification. All material was obtained and used in accordance with the human tissue act. Additionally, a commercial cell line which is CNS PNET (PFSK-1) was also studied in this project. EPN-2, MED-2 and SPNET-1 cells were successfully cultured in tumour media, whereas PFSK-1 cells were grown in PFSK media as recommended by the ATCC\* (media recipes in appendix B1, Table B1.1). Apart from paediatric brain tumour cells, control cells were also grown to provide positive controls for Western blotting analysis, Fluorescence-activated cell sorting (FACS) and co-staining immunofluorescence. NTERA-2, a commercial cell line derived from a teratocarcinoma, were grown in NTERA media (appendix B1). This cell line was used as a positive control for CD133 expression in Western blotting analysis. HEK cells stably transfected with pcDNA encoding ABCB1, ABCC1, ABCG2 or empty pcDNA were also used as positive and negative controls for Western blotting analysis, FACS and immunofluorescence. These control cell lines were kindly provided by Dr. Ian Kerr. These

\* [www.lgcpromochem-atcc.com](http://www.lgcpromochem-atcc.com)

cells were grown in tumour media containing 500 µg/ml of G418. All cell lines were grown in 75 cm<sup>2</sup> vented flasks containing 20 ml of media and incubated in a standard humidified 5% CO<sub>2</sub> –air incubator at 37°C. Cells were cultured as monolayer cells and subcultured twice a week when cells reached subconfluency. In addition, cells were screened regularly for mycoplasma infection using Venor®GEM-Mycoplasma detection kit (11-1050, Minerva biolabs). The other cell lines, which are EPN-1 (ependymoma), MED-1 (medulloblastoma), BT-4 (glioblastoma multiforme) and Olig-1 (oligodendroglioma), were grown by Dr. Deema Hussein, who kindly provided snap frozen pellets and fixed cells for some experiments.

Monolayers and neurospheres from all cell lines were collected as pellets, snap frozen in liquid nitrogen, then stored at -80°C. A large number of cell pellets were routinely prepared and frozen for future experiments from early, middle and late passage of monolayers and neurospheres. Additionally, the earliest passage numbers of each cell line were frozen by resuspending at one million cells/ml in 10% dimethyl sulfoxide (DMSO) in FBS, and stored in liquid nitrogen for future culture.

### **2.1.1 Cell recovery from liquid nitrogen**

Cryovial tubes containing the designated cell line were removed from the liquid nitrogen bank and rapidly thawed at 37°C. Cells were then immediately transferred to a 75 cm<sup>2</sup> flask containing fresh 20 ml of the appropriate cell culture media and incubated overnight. The media was replaced with fresh media the next day, and cells were incubated until ready for subculture.

### **2.1.2 Deriving neurospheres from monolayers**

Monolayers were induced to form neurospheres by culturing in stem cell media. After trypsinization of monolayers with 1xT/E [1xTrypsin/Ethylene diamine tetracetic acid (EDTA)], 1:20 dilution of trypsinized cells was transferred into 75 cm<sup>2</sup> flask with 20 ml of stem cell media. Neurospheres were usually formed within 48 hours.

### **2.1.3 Subculturing cells**

Cells were subcultured when cells were approximately subconfluent. Normally, this was about 72-96 hours after subculturing when cells were passaged at a 1:20 dilution.

#### **2.1.3.1 Monolayer cells**

Cells were detached from flask using 1xT/E (Fisher, VX15400-054). Cells were washed with Hanks' Balanced Salt Solution (HBSS) (Invitrogen, 14025-050) before adding 2 ml 1xT/E into each flask then incubated in trypsin solution for 5 minutes at 37 °C. Trypsinized cells were harvested by tapping the flask before transferring a small proportion of cells to a new 75 cm<sup>2</sup> flask at a 1:10 or 1:20 dilution with appropriate media.

#### **2.1.3.2 Neurospheres**

##### **2.1.3.2.1 Using TrypLE™ select**

To dissociate neurospheres into single cells, neurospheres were centrifuged at 70xg for 3 minutes then washed with 5 ml of HBSS and centrifuged again to pellet cells. The pellet was resuspended in 1 ml of TrypLE™ select (Invitrogen, 12563-029) for 1 minute with gentle swirling to gently dissociate neurospheres. Dissociated neurospheres were passaged as 1:2 or 1:5 or 1:10 into fresh stem cell media (see appendix B1). Fibroblast growth factor (FGF) (Invitrogen, PHG0026) and epidermal growth factor (EGF) (Invitrogen, 13247-051) were replenished to promote neurosphere growth every 3 or 4 days.

##### **2.1.3.2.2 Using mechanical dissociation**

Neurospheres were also dissociated by mechanical dissociation using pipette. Dissociated neurospheres were filtered through a 40 µm cell strainer (BD Sciences, 352340) into fresh stem cell media.

These two different methods for neurosphere dissociation have different advantages and disadvantages and there was no evidence to confirm which method is better for cell dissociation. Chemical dissociation using TrypLE™ select is a gentle and fast method to dissociate cells. However, the chemical effect of TrypLE™ select might cause cell membrane and protein damage for long term use. This is a very important issue since the protein of interest is located on cell membrane (CD133 and ABC transporters). Mechanical dissociation



using mechanical pipette also effectively singularised cells. However, this method is slightly harsh to cells and probably causes cells lysis resulting in increasing number of death cells. Additionally, cells were required to filter through cell strainer to ensure that they were separated into single cells, therefore, this method is time consuming compared to chemical dissociation method. To avoid taking risk of disadvantages and receiving some advantages of each method, these two different dissociation methods were hence used alternately to dissociate cells. Neurospheres tested in this study were obtained after their first passage from neurospheres.

#### **2.1.4 Snap freezing cells**

##### **2.1.4.1 Snap frozen cells for general purposes**

Monolayers and neurospheres were harvested as described in section 2.1.3. After trypsinization, cells were washed once with HBSS then centrifuged at 70xg for 3 minutes. Cell pellets were resuspended in 1 ml of HBSS and transferred to new eppendorfs. Cells were centrifuged again at 70xg for 3 minutes. HBSS was removed and cell pellets were dropped in liquid nitrogen for snap freezing. Snap frozen pellets were stored at -80 °C until required.

##### **2.1.4.2 Snap frozen cells for microsomal membrane extraction**

###### **2.1.4.2.1 Attached cells**

Cells were detached using a scraper and transferred into 50 ml Falcon tube. Cells were centrifuged at 70xg for 3 minutes then media was removed. Cells were resuspended in fresh media and incubated at 37 °C for 30 minutes to recover surface protein expression. Cells were centrifuged again at the same speed then washed twice with filtered PBS. Cells were resuspended with 1 ml of filtered PBS in an eppendorf tube and centrifuged again. PBS was removed then the pellet was snap frozen in liquid nitrogen and stored at -80 °C until required.

###### **2.1.4.2.2 Neurospheres (cells grown in suspension)**

Cells were transferred into a 50 ml Falcon tube and washed twice with filter PBS. Cells were centrifuged at 70xg for 3 minutes to remove PBS. Cells were then resuspended in filtered

PBS and transferred into an eppendorf tube. Cells were centrifuged again at the same speed to pellet and snap frozen in liquid nitrogen then stored at -80 °C until required.

## **2.2 Immunofluorescence assay**

Indirect immunofluorescence was performed to detect stem cell-like populations and ABC transporter expression in newly established paediatric brain tumour cell lines. This method detects emitted fluorescence from species specific secondary antibodies bound to epitope specific primary antibodies.

### **2.2.1 Immunofluorescent staining of monolayers**

#### **2.2.1.1 Plating monolayer cells on chamber slides**

Monolayers were subcultured as mentioned in section 2.1.3.1. Cells were stained using trypan blue and counted using a haemocytometer. Cells were resuspended in appropriate tumour media and plated at a density of 1,000 cells/ml in 500 µl of media into each chamber of an 8 well slide (VWR international, 734-2126). Cells were incubated for 3 or 4 days until subconfluence before fixation.

#### **2.2.1.2 0.4% Paraformaldehyde (PFA) fixation**

Cells were washed with HBSS then fixed with 200 µl of 0.4% Paraformaldehyde (PFA) for 30 minutes at room temperature. After fixation, 0.4% PFA was removed and fixed cells were covered with 500 µl of HBSS. Fixed cells were stored at 4°C until required.

#### **2.2.1.3 Single immunofluorescent staining**

Fixed cells were washed once with PBS. Non-specific antigens were blocked by incubating cells in 150 µl of an appropriate blocking solution (appendix B2) for 1 hour at room temperature. Blocking solution was removed and cells were incubated in the appropriate primary antibody (Table 2.1) at 4 °C overnight. Following primary antibody incubation, cells were gently washed 3 times with PBS then incubated with the appropriate secondary antibody (Table 2.2) at room temperature for 1 hour. Cells were washed gently twice with PBS. Chambers and gaskets were then removed, and slides were mounted with Vectashield containing 4', 6-diamidino-2-phenylindole (DAPI) (Vector, H-1,200) to stain nuclei. Cells

**Table 2.1 Primary antibodies used in immunofluorescent staining**

Primary antibody	Host species	Dilution	Suppliers
1. CD133 antibody	Rabbit	1:200	Abcam (ab19898)
2. CD133 (C24B9)	Rabbit	1:75	Cell signaling (3663)
3. Human/Mouse SOX2 MAb (Clone 245610)	Mouse	1:75	R&D system (MAB 2018)
4. Anti-P-Glycoprotein Mouse mAb (C219)	Mouse	1:50	Calbiochem (517310)
5. P glycoprotein antibody (4E3)	Mouse	1:50	Abcam (ab10333)
6. Multidrug Resistance Associated Protein (MRPr1) Monoclonal Antibody	Rat	1:50	Signet (SIG-38760)
7. Anti-MultiDrug Resistance Related Protein (clone MRpm6)	Mouse	1:50	Chemicon (MAB4122)
8. BCRP/ABCG2 antibody (BXP-21)	Mouse	1:50	Abcam (ab3380)

**Table 2.2 Secondary antibodies used in immunofluorescent staining**

Secondary antibody	Dilution	Suppliers
1. Alexa fluor <sup>®</sup> 555 goat anti-mouse antibody	1:500	Invitrogen, A21424
2. Alexa fluor <sup>®</sup> 488 goat anti-rabbit antibody	1:500	Invitrogen, A11008
3. Alexa fluor <sup>®</sup> 555 goat anti-rat antibody	1:500	Invitrogen, A21434

were covered with coverslips and sealed with tosylamide-formaldehyde resin (nail varnish).

Slides were wrapped in foil and stored at 4 °C up to 4 weeks until microscopically analysed.

### **2.2.2 Immunofluorescent staining of neurospheres**

#### **2.2.2.1 0.4% Paraformaldehyde (PFA) fixation**

Neurospheres were transferred into 50 ml Falcon tubes and left for 30-40 minutes to naturally settle down at room temperature. Media was carefully removed and neurospheres were washed with 5 ml of HBSS and allowed to settle down again. HBSS was then carefully removed. Neurospheres were then fixed with 0.4% PFA at room temperature for 30 minutes. After fixation, 0.4% PFA was removed and neurospheres were resuspended in 1 ml of 30% sucrose in HBSS. Fixed neurospheres were transferred to new eppendorfs using 10 ml pipette to preserve intact neurosphere and stored at 4 °C until required.

#### **2.2.2.2 Cryostat sectioning of neurospheres**

The Leica CM 1850 cryostat machine was set below -20°C, and the chuck holder gap was filled with optimal cutting temperature (OCT) compound (BDH, 361603E) then left until set. To create a neurosphere block, 10 µl of fixed neurospheres were added to the middle of a 300 µl drop of OCT on the coated chuck holder then left to set. The neurosphere block was cut at a thickness of 8 µm and neurosphere sections were picked up onto 3-Aminopropyltriethoxysilane (APES) coated slides. Neurosphere sections were stored at -20 °C until required.

#### **2.2.2.3 Single immunofluorescent staining**

Cryostat sections of neurospheres were removed from -20 °C and left at room temperature until defrosted. An immunoedge pen (Vector, H-4000) was used to create a border around neurosphere sections. Sections were incubated with an appropriate blocking reagent (appendix B2, Table B2.2) for 1 hour at room temperature. The blocking reagent was removed and sections were incubated with the appropriate primary antibody (Table 2.1) at 4 °C overnight. Following primary antibody incubation, sections were gently washed 3 times with PBS. Sections were then incubated with the appropriate secondary antibody (Table 2.2) at room temperature for 1 hour. Sections were washed gently twice with PBS and mounted with Vectashield containing DAPI (Vector, H-1,200) to stain nuclei. Sections were covered with coverslips and sealed with nail varnish. Slides were wrapped in foil and stored at 4 °C until microscopically analysed.

#### **2.2.3 Double immunofluorescent staining**

The process of double staining IF in both monolayer cells and neurospheres is similar to that of single staining. However, the blocking reagent and antibody solution used for double staining are different as mentioned in appendix B2, Table B2.2. Two primary antibodies were added together as were the anti-mouse or anti-rat and anti-rabbit secondary antibodies.

### **2.2.4 Image processing**

Immunofluorescence slides were observed under a Leica DMRM fluorescent microscope [Nikon: Digital sight-USB (H)] fitted with filters to detect fluorescence omitted by DAPI (blue), Texas red (red) and FITC (green). A Nikon camera and the NIS elements software was used to capture images. Positive cells stained for specific markers (total counted cells range from 600-1,000 cells) were counted by using Adobe Photoshop elements 3.0 with x40 and x100 magnification for monolayer and neurospheres, respectively.

## **2.3 Western blotting analysis**

Western blot analysis was performed to detect the level of protein expression, semi-quantitatively. Proteins were separated based on size by SDS gel electrophoresis, transferred to a membrane and then incubated with a primary antibody. The membrane was then incubated with a secondary antibody, directed against the primary antibody, conjugated to horseradish peroxidase enzyme (HRP). The emitted light from the HRP activity was detected by Enhanced Chemiluminescence (ECL) detection. This technique is fairly effective because of the combination of enzyme label and chemiluminescent detection of peroxidase labelled proteins resulting in a highly sensitivity assay. The HRP enzyme complex bound to the primary antibody catalyzes oxidation of Lumigen PS-3 Acridan substrate in the ECL detection kit, resulting in the generation of acridinium ester intermediates. These intermediates react with peroxide under slight alkaline conditions to produce a sustained, high intensity chemiluminescent signal with maximum emission at 430 nm. This chemiluminescent emission was detected on chemiluminescent film, Kodak<sup>®</sup> BioMax<sup>™</sup> light film (Sigma, Z373508).

### **2.3.1 Protein extraction**

#### **2.3.1.1 Standard method for protein extraction from cell pellets**

Cell pellets, as mentioned in section 2.1.4.2, were removed from -80°C freezer and stored on dry ice. Cells were then resuspended in an appropriate volume (depends on number of cells pelleted, 100-200 µl for  $1-5 \times 10^6$  cells) of ice cold lysis buffer containing 1:50 protease

cocktail inhibitor (appendix B3, Table B3.1). Cells were homogenised using Fisher Scientific PowerGen Model 125 Homogeniser (Fisher Scientific, 14-359-250) for a minute on ice and then incubated at 4°C for 20 minutes on a rocker. After incubation, the cell lysate was centrifuged at 12,470xg for 30 minutes at 4°C then the supernatant solution comprising of extracted protein was transferred into a fresh eppendorf tube and stored at -80°C or the protocol continued with a Bradford assay.

#### **2.3.1.2 Isolation of microsomal membrane from cell pellets**

Cell pellets prepared by the method described in section 2.1.4.2 were removed from -80 °C freezer and placed on dry ice. Cells were resuspended with 250 µl of ice cold lysis buffer containing 1:50 protease cocktail inhibitor (see appendix B3, Table B3.1) and homogenised using the Fisher Scientific PowerGen Model 125 Homogeniser for a minute on ice. Homogenised cells were incubated at 4°C for 20 minutes with agitation. Gentle centrifugation was then performed to remove cell debris at 300xg, 4°C for 3 minutes. Supernatants were transferred to ultracentrifuge tubes for membrane separation. An ultracentrifugation machine (Optima™ Max Ultracentrifuge 130,000 rpm, Beckman Coulter™) was used to centrifuge the supernatant at 100,000xg, 4 °C for 1 hour. After ultracentrifugation, the cytosolic component was transferred to a fresh eppendorf. The microsomal membrane pellets were then resuspended in ice cold PBS containing 1:50 protease cocktail inhibitor and stored at -80°C until used.

#### **2.3.1.3 Total cell lysate**

The initial steps of total cell lysate are similar to the standard method for protein extraction. After incubation on ice, the centrifugation step was omitted to ensure that the protein extracted contained the nuclear fraction. Total cell lysates were used for SOX2 detection and stored at -80 °C until used.

#### **2.3.2 Protein quantification (Bradford assay)**

The concentration of protein was quantified by using a Bradford assay. A range of bovine serum albumin (BSA) standards from 1, 5, 10, 15, 20, 30 and 40 µg/ml (total volume is 1 ml) were prepared using 2 mg/ml stock of BSA (Sigma, B4287) diluted with 1:5 Bio-Rad

protein assay dye reagent (Bio-Rad, 500-0006). To prepare the sample for protein quantification, 5  $\mu$ l of sample was added into 995  $\mu$ l of 1:5 Bio-Rad protein assay dye reagent. Individually, 200  $\mu$ l of the BSA standards and samples were added into 96-well plate and the absorbance was measured at 600 $\lambda$  using a spectrophotometer (MRX II, DYNEX technology). Revelation software for MRX<sup>®</sup> version 5.1.2600.2180 was used to analyse and calculate protein concentration.

Before loading proteins on the gel, protein samples were mixed with sample buffer so that at least 20% volume is sample buffer (appendix B3, Table B3.1). The maximum volume for loading was 15  $\mu$ l when using 0.75 mm spacers or 50  $\mu$ l when using 1.5 mm spacer from Bio-Rad Mini-Protean III system. The sample buffer must have 1:20  $\beta$ -mercaptoethanol freshly added prior to use.

### **2.3.3 Preparation of Polyacrylamide gel electrophoresis (PAGE)**

The Bio-Rad mini Protean III glass plates and spacers were cleaned with 1.5% trigene and 70% ethanol before use. Glass plates and spacers were set into the glass plate casting frame and the casting frame was clamped tightly into the casting stand. Distilled water was added first to ensure that there was no leakage. The lower gel (appendix B3, Table B3.2) then was prepared and immediately added between the glass plates to 2 cm below the top of the smaller glass plate. Butanol was added on top of the lower gel to ensure a smooth surface on setting. The percentage of lower gel prepared for gel electrophoresis depends on the expected size of the proteins to be detected as shown in Table 2.3. The gel was allowed to set at room temperature for approximately 30 minutes then the butanol was removed. A 4% acrylamide upper gel (upper stacking gel, appendix B3, Table B3.3) was prepared and rapidly layered over the top of the lower gel. The comb was carefully inserted into the upper gel and the gel was allowed to polymerize at room temperature for 30 minutes.

**Table 2.3 Effective range of separation of SDS-Polyacrylamide gels** (Sambrook, J. and Russell, D.W. 2001)

Acrylamide concentration (%)	Linear range of separation (kD)
15	10 – 43
12	12 – 60
10	20 – 80
7.5	36 – 94
5	57 – 212

Molar ratio of bisacrylamide:acrylamide is 1:29

#### 2.3.4 Sample preparation for gel electrophoresis

The set gel was placed in an electrode assembly with the smaller glass plate facing inwardly then the assembly was filled with electrode buffer (appendix B3, Table B3.1). If only one gel was to be run, a dummy plate was placed in the opposing slot. To prepare samples for loading, 40 µg – 100 µg of protein was mixed with sample buffer and boiled on a 99°C hot plate for 3 minutes (for microsomal membrane samples, samples were incubated at 37°C for 30-45 minutes (CD133 detection) or at 70°C for 10 minutes (ABC transporters detection). Samples were centrifuged at 12,470xg for 1 minute. The combs were carefully removed and each well was flushed of any gel debris using a needle filled with electrode buffer. Then 12 µl of See blue size marker (Invitrogen, LC5925) was loaded into the first well and 15 µl (for 0.75 mm spacer) or 50 µl (for 1.5 mm spacer) of protein samples was loaded into each subsequent well. The gel was then electrophoresed at 120-150 V until markers in the size range of expected protein were sufficiently separated (approximately 2 or 3 hours at room temperature).

#### 2.3.5 Protein transfer to membrane

Hybond™-P PVDF membrane (Amersham, RPN303F) was activated in 1) methanol for 10 seconds, 2) distilled water for 5 minutes and 3) ice cold transfer buffer (appendix B3, Table B3.1) for at least 10 minutes. The gel was carefully detached from the glass plates and upper gel was removed. The transfer cassette was arranged in the transfer buffer as follow, 1) black gel holder, 2) 2 sponges soaked in transfer buffer, 3) 2 pieces of filter paper, 4) gel,



5) the membrane, 6) 2 pieces to filter paper, 7) 2 sponges soaked in transfer buffer, and 8) white gel holder. Negatively charged proteins (SDS) migrate toward the anode. To transfer the protein to the membrane, the transfer cassette was placed inside the transfer tank with black and white holders facing the negative electrode (black) and the positive electrode (red), respectively. The tank was filled with transfer buffer until the transfer cassette was fully immersed. The transfer was carried out at 100 mA and 25 V overnight at 4°C.

### **2.3.6 Ponceau staining**

Ponceau staining was performed to test whether protein had been successfully transferred to the membrane. If the proteins are transferred onto the membrane, pink bands will appear on the membrane after incubating in the Ponceau solution. The membrane was removed from the transfer cassette and incubated in the 0.1% Ponceau S solution for approximately 1 minute until the pink bands were detected. The membrane was then washed with TBS-T (appendix B3, Table B3.1). Due to the fact that the size markers may fade during incubation steps, the position of markers on the membrane was marked using non-soluble ink.

### **2.3.7 Primary and secondary antibody treatment**

To block non-specific antigens, the membrane was incubated in blocking solution, 5% Marvel milk in TBS-T (appendix B3, Table B3.1), for 1 hour at room temperature on a rocker, then rinsed twice with TBS-T solution. For primary antibody treatment, the membrane was incubated in primary antibody diluted in blocking solution (Table 2.4) overnight at 4°C on the rocker. The membrane was then washed as follows: 1) rinsed twice in 5% Marvel milk in TBS-T, 2) 10 minutes in 5% Marvel in TBS-T, 3) 5 minutes in 5% Marvel in TBS-T twice, and 4) TBS-T for 5 minutes, all performed on the rocker. The membrane was then incubated in secondary antibody diluted in TBS-T (Table 2.4) for 1 hour at room temperature on the rocker. The membrane was then washed as follow: 1) rinsing twice in 5% Marvel in TBS-T, 2) 10 minutes in 5% Marvel in TBS-T, 3) 5 minutes in 5% Marvel in TBS-T twice, 4) TBS-T for 5 minutes and finally, 5) in 1xTBS (appendix B3, Table B3.1) for 5 minutes all performed on the rocker.

### 2.3.8 ECL detection

Peroxidase activity of secondary antibody bound to primary antibody on the membrane was detected by the ECL plus western blotting detection kit (Amersham Bioscience, RPN2132). For 1 blot, the ECL detection reagent was prepared by adding 50 µl of solution B to 2 ml of solution A (Lumigen). The ECL reagent was pipetted to cover the surface of the membrane (protein side up) and incubated for 5 minutes. Excess reagent was removed by blotting the edge of the membrane with tissue paper. The membrane was placed facing side down on a smooth sheet of Saran wrap. Another piece of Saran wrap was placed over the membrane and carefully smoothed to ensure no creases or bubbles were present. The sealed membrane was transferred to a photography cassette. Kodak® BioMax™ light film (Sigma, Z373508) was placed on top of the membrane under dark room condition. Exposure time

**Table 2.4 Primary and secondary antibodies used in Western blot analysis**

Primary antibody	Host Species	Dilution	Secondary antibody	Dilution
<b>CD133</b> (Abcam, ab19898) : detected size 110 kDa : predicted size 97 kDa	Rabbit	1:400	Anti-rabbit HRP (Universal biologicals, A120-101P)	1:2,000
<b>CD133/1 (W6B3C1) pure</b> (Milenyi Biotec, 130-092-395) : detected size 120 kDa : predicted size 95 kDa	Mouse	1:100	Anti-mouse HRP (Cell signaling NEB, 7076)	1:2,000
<b>SOX2</b> (R&D system, MAB2018) : detected size 37 kDa : predicted size 34 kDa	Mouse	1:150	Anti-mouse HRP	1:2,000
<b>SOX2</b> (Cell signaling, 2748) : detected size 35 kDa : predicted size 35 kDa	Rabbit	1:1,000	Anti-rabbit HRP	1:2,000
<b>C219</b> (Calbiochem, 517310) : detected size range from 140 – 170 kDa	Mouse	1:100	Anti-mouse HRP	1:2,000
<b>MRPr1</b> (Signet, SIG-38760) : detected size range from 140 – 190 kDa	Rat	1:100	Anti-rat HRP (Cell signaling NEB, 7077)	1:2,000
<b>BXP-21</b> (Abcam, ab3380) : predicted size 72.3 kDa	Mouse	1:500	Anti-mouse HRP	1:2,000
<b>β-tubulin</b> (Cell signaling, 2128)	Rabbit	1:1,000	Anti-rabbit HRP	1:2,000

varied from approximately 15 seconds to 30 minutes. Finally, the film was developed using an automatic developer machine (Curix 60, Agfa) or manual developing.

## **2.4 DNA extraction**

DNA extraction was performed for single nucleotide polymorphism (SNP) array and TRF (terminal restriction fragments) assay. DNA was extracted from both monolayer and neurosphere cell pellets. Live cell pellets were for SNP array whilst frozen cell pellets were extracted for TRF assay.

### **2.4.1 DNA extraction from frozen cell pellets**

Frozen cell pellets removed from -80°C and kept on dry ice. 500 µl DNA lysis buffer (appendix B4, Table B4.1) containing 2 mg proteinase K (Sigma, P2308) was added to cell pellets. Cell pellets were homogenised for a minute using Fisher Scientific PowerGen Model 125 Homogeniser then incubated on a Thermomixer (Eppendorf) at 37°C, 450 rpm overnight. 700 µl Phenol/chloroform/isoamyl alcohol (25:24:1) (Sigma, 77617) was added to homogenised cells and transferred into the mixtured precentrifuged 2.0 ml Phase Lock Gel (PLG) (5 PRIME, 2302830) tubes. Samples were centrifuged at 16,000xg for 5 minutes allowing the PLG to separate the solution into 2 parts: an upper phase containing nucleic acid and a lower phase. The upper phase solution was transferred into fresh eppendorfs. 100 µg RNase A (Sigma, R6513) was added to upper phase solution and samples were incubated on thermomixer at 37°C for 30 minutes. An equal volume of isopropanol (Fisher, P/7508/17) was added to precipitate DNA then samples were centrifuged at 12,000xg for 5 minutes. The supernatant was removed avoiding the DNA pellet and the pellet was washed twice with 500 µl of 70% ethanol then centrifuged at 12,000xg for 5 minutes. Supernatant was discarded and DNA pellets were left to dry at room temperature. DNA pellets were resuspended with 100 – 200 µl of ultra pure sterile water (UPSW) then incubated on the Thermomixer at 60°C, 450 rpm for 15 minutes then at 37°C, 450 rpm for 1 hour. DNA concentration was determined using Nanodrop (NanoDrop Technologies, INC, NanoDrop® ND-1000 Spectrophotometer). Five micro litres of extracted DNA was mixed with 5 µl gel loading buffer (Sigma, G2526) and run on a 1% agarose MP (Multi purpose agarose) gel (Roche, 11388991001) at 120 V. for 20 minutes to test the quality of DNA and for contaminations.

10 kb hyperladder was loaded as a DNA marker. If there is no contamination, extracted DNA was stored at -80°C.

#### **2.4.2 DNA extraction from live cell pellets**

Live cells were collected from a T75 cm<sup>2</sup> flask using a scraper and washed twice with HBSS. 500 µl DNA lysis buffer (appendix B4, Table B4.1) and 2 mg proteinase K were added to live cell pellets. Pellets were homogenised using the Fisher Scientific PowerGen Model 125 Homogeniser for a minute and incubated on a thermomixer at 37°C, 450 rpm overnight. From this point DNA extraction was the same as from frozen cell pellets as mentioned in section 2.4.1.

### **2.5 Terminal restriction fragment (TRF) assay or telomere length assay**

The telomere length assay was performed to measure any alteration of telomere length in EPN-2, MED-2, SPNET-1 and PFSK-1 cell lines at early, middle and late passages in comparison to normal human stem cell (hNSC) and adult glioblastoma (U87 and U373 cell lines). There is significant difference in doubling time at early passage compared to later passage of neurospheres. It was opposed that alteration of telomere length might be responsible for the longer doubling time of late passage neurospheres.

#### **2.5.1 DNA digestion**

The required DNA amount for this assay was 3 µg resuspended in distilled water (total volume is 16 µl) and mixed with 9 µl of the master mix containing 30 units of Hinf I\*, 30 units of Rsa I\*, 2.5 µl of NEBuffer 2 (Biolabs, B7001S) and 0.5 µl of Rnase A (Sigma, R5000). Samples were incubated at 37°C overnight. This step results in cutting of genomic DNA into small pieces but telomeric DNA and sub-telomeric regions remain intact.

[\* Supplied with Telo TAGGG Telomere Length assay kit (Roche, 12209136001)]

#### **2.5.2 TRF gel electrophoresis**

0.75% agarose gel in 1x TAE solution (appendix B5, Table B5.1) was prepared in gel tray with a 20 lane comb. DIG marker\*, Digoxigenin labelled telomere-specific probe, had to be activated prior to use. Thereby 4 µl of DIG marker was mixed with 12 µl of distilled water and 4 µl of gel loading buffer then the mixture solution was incubated at 65°C for 10 minutes. Digested DNA was mixed with 3 µl of loading buffer before loading and DIG marker also was loaded at the first and last lanes of gel. The gel was initially run at 100 V for 20 minutes then 30 V overnight at room temperature.

(\* Supplied with Telo TAGGG Telomere Length assay kit)

### **2.5.3 Denature of DNA**

The gel was cut at left upper corner and transferred into the tray. Gel was incubated in 0.25 M HCL for 10 minutes to separate double strands of DNA. All steps were performed on shaker at room temperature. The gel was rinsed twice with distilled water before incubating in denaturing solution (appendix B5, Table B5.1) for 15 minutes twice. The gel was rinsed twice with distilled water and incubated in neutralising solution (appendix B5, Table B5.1) for 15 minutes.

### **2.5.4 TRF Southern blot**

DNA was transferred to a positively charged nylon membrane (Roche, 11417240001) in 20x SSC (1.5 litres, appendix B5, Table B5.1). The order of transferring was arranged as following; 1) long blotting paper soaked in 20x SSC prior to used and placed on top the hard plate, 2) gel inverted prior to transfer, 3) Nylon positive charge membrane (cut the same corner as gel), 4) Saran wrap cut around gel border then peeled off to leave the remain on edges of gel, 5) two pieces of soaked 20cm x 20cm blotting paper, 6) two pieces of 10cm x 20cm blue tissue paper, 7) two packs of blue tissue paper placed on top each 10cm x 20cm blue tissue paper, and 8) heavy weight. Bubbles were removed by rolling a pipette across each layer. DNA was transferred overnight at room temperature.

### **2.5.5 Hybridization**

The membrane was placed DNA side up and DNA was linked to membrane using UV cross linker at 120 mJ/cm<sup>2</sup> for 1 minute. The membrane was washed in 50 ml 2x SSC before prehybridisation. The membrane was rolled in the roller bottle and prehybridised in 15 ml DIG Easy (Roche) Hyb TRF solution\* for 1 hour at 42°C in hybridisation machine. For hybridisation, the membrane was incubated in 15 ml DIG Easy (Roche) Hyb TRF solution containing 3 µl of Telomere TTAGGG probe\* (1 µl/5 ml) at 42°C overnight.

(\* Supplied with Telo TAGGG Telomere Length assay kit)

### **2.5.6 Washing, blocking and anti-DIG-AP treatment**

The membrane was washed as follows; 1) twice in 50 ml of 2x SSC containing 0.1% SDS for 5 minutes on shaker at room temperature, 2) twice in 50 ml of 0.2x SSC containing 0.1% SDS for 15 minutes in the roller bottle at 50°C and 3) once washing buffer (appendix B5, Table B5.1) for 5 minutes on shaker at room temperature. The membrane was blocked in 100 ml of blocking solution (appendix B5, Table B5.1) for 30 minutes then incubated in 100 ml of anti-DIG-AP solution (appendix B5, Table B5.1) for 30 minutes on shaker. The membrane was washed twice in 100 ml of washing buffer for 15 minutes on shaker.

### **2.5.7 Detection**

The membrane was incubated in 100 ml of detection solution (appendix B5, Table B5.1) for 5 minutes on shaker at room temperature.

### **2.5.8 Substrate treatment**

The membrane was placed on Saran wrap then CDP substrate solution (supplemented with TRF assay kit) was dropped to cover the membrane. The membrane was wrapped with another piece of Saran wrap then excess solution, bubbles and creases were removed. The sealed membrane was transferred to a photography cassette. Kodak® BioMax™ light film (Sigma, Z373508) was placed on top of the membrane under dark room condition. Exposure time varied from approximately 15 seconds to 30 minutes. Finally, the film was developed using an automatic developer machine (Curix 60, Agfa) or manual developing.

## **2.6 Haematoxylin and Eosin (H&E) staining**

H&E staining was performed on formalin-fixed paraffin embedded (FFPE) tumours to study histological features of tumours. Sections were dewaxed in solutions as following; 1) xylene (Fisher Scientific, X/0250/PB17) for 15 minutes, 2) 100% ethanol for 5 minutes twice and 3) 95% ethanol for 5 minutes twice. Slides were incubated in running tap water to get rid of ethanol and wax. Slides were placed in the rack and agitated in Harris haematoxylin for 7 seconds then washed in running tap water until clear. Slides were agitated in Lithium carbonate until turning blue then washed in running tap water until clear. Slides were soaked in Eosin (Nustain, Department of Pathology, Nottingham, AD046) for 10 seconds then washed in running tap water until clear. Sections were dehydrated in 95% ethanol, 100% ethanol and xylene respectively and sections were mounted by using DePex.

## **2.7 Telomere Repeat Amplification Protocol (TRAP) assay**

The TRAP assay was performed to measure telomerase activity in each cell lines at early, middle and late passage number.

### **2.7.1 Protein extraction**

Snap frozen pellets as mentioned in section 2.1.4 were placed on dry ice. Total protein was extracted by adding 50 µl 1x CHAPS buffer\* containing 200 units/ml RNase inhibitor (Roche, 03335399001). Cell pellets were resuspended by gently pipetting then incubated on ice for 30 minutes. Extracted proteins were snap frozen on dry ice and prepared for protein measurement or stored at -80°C. Protein extraction was diluted with CHAPS buffer at a concentration of 0.1 µg/µl for Polymerase Chain Reaction (PCR) assay.

[\* Supplied with TRAPeze<sup>®</sup> Telomerase Detection Kit (Chemicon, S7700)]

### **2.7.2 Protein quantification**

To determine protein concentration, a BSA standard curve was prepared by serial dilution as shown in Table 2.5. BSA standard concentration from tube A-F was loaded as 25 µl into 96-well plate. Both BSA standard concentrations and samples were prepared as duplication and loaded in 96-well plate. To prepared samples for protein quantification, 1 µl from each sample was diluted in 9 µl of 1x CHAPS buffer then transferred to each well of a 96-well plate. 250 µl of 1:12 diluted Coomassie reagent (appendix B6, Table B6.1) was added into each well of 96-well plate then the absorbance value of protein was analysed using a spectrophotometer at 595-600 nm. Protein concentration was determined from the BSA standard curve using the equation from linear graph.

### 2.7.3 Addition and amplification of telomere repeats by telomerase

A PCR method was performed to add and amplify telomere repeats in samples. The required amount of protein for each PCR reaction is 0.1 µg. 1 µl of 0.1 µg/µl protein extraction was resuspended in 40.6 µl of nuclease-free water. PCR master mix as shown in Table 2.6 was prepared and 8.4 µl was added to each sample. Samples were run in PCR machine as the following cycle conditions:

- 30°C for 30 minutes: 1 cycle (Telomere extension)
- 94°C for 30 seconds, 59°C for 30 seconds: 31 cycles (Amplification of Telomere repeats)

**Table 2.5 Preparation of BSA standard concentration for protein quantification**

<b>Tube</b>	<b>BSA volume (µl) from 2mg/ml stock</b>	<b>CHAPS diluent volume (µl)</b>	<b>Total protein (µg)</b>
<b>A</b>	25 µl BSA stock	25 µl	25
<b>B</b>	25 µl from tube A	25 µl	12.5
<b>C</b>	25 µl from tube B	25 µl	6.25
<b>D</b>	25 µl from tube C	25 µl	3.12
<b>E</b>	25 µl from tube D	25 µl	1.55
<b>F</b>	25 µl from tube E	25 µl	0.775

**Table 2.6 PCR Master Mix**



<b>Solutions</b>	<b>Volume (μl)</b>
1. 10x TRAP buffer	5
2. Ts primer	1
3. Primer mix	1
4. 50x dNTP	1
5. Taq Polymerase	0.4
<b>Total</b>	<b>8.4</b>

#### 2.7.4 Telomerase detection

A 10% polyacrylamide gel (appendix B6, Table B6.1) was cast between gel plates and left to set for 30 minutes. Gel plates were set into electrophoresis tank and filled with gel running buffer (appendix B6, Table B6.1). DNA molecular marker (appendix B6, Table B6.1) was loaded as 10 μl in the first lane of gel. 25 μl of samples were loaded on gel which was run 240 Volts for 90 minutes. The gel was incubated in staining solution (appendix B6, Table B6.1) and agitated on the shaker for 30 minutes in dark. The gel was scanned with FL-2000 gel imager (FUJIFILM) to detect telomerase activity.

#### 2.7.5 Quantification of telomerase activity

The Quantity One software was used to analyse the density of telomerase activity. The density of telomerase activity was assessed by the summation of density measuring from divided 6 boxes covering the telomerase activity and the internal bands were also measured density. The total product of telomerase activity was calculated from the formula as followed.

$$\text{The total product (units)} = \left[ \frac{(\sum A - \sum B) / D_A}{(\sum C - \sum B) / D_B} \right] \times 100$$

A = the density of samples

B = the density of negative control

C = the density of TSR8

D<sub>A</sub> = the density of A internal control band

D<sub>B</sub> = the density of B internal control band

### 2.8 Metaphase spread analysis

The result from Telomere length assay showed 2 different lengths of telomeres (short and long telomere) in both monolayer and neurosphere samples. Long and short telomere lengths are approximately 15 and 4 Kbp respectively. Therefore, cell spread analysis was performed to investigate whether long telomere length resulted from end-fusion of chromosome.

### **2.8.1 Nocodazole treatment**

Cells were subcultured into T75 flasks and incubated until 50-70% confluency (approximately  $2 \times 10^6$  cells). Cells were treated with 0.1  $\mu\text{g/ml}$  Nocodazole (Sigma, M1404) for 16 hours to induce cells in metaphase.

### **2.8.2 Preparation of metaphase spreads from cell culture**

Mitotic rounded cells were collected by tapping the flask several times and checked under the microscope to ensure that all mitotic cells were collected. Floating mitotic cells were transferred to a 50 ml Falcon tube and centrifuged at 800xg for 5 minutes then the supernatant was discarded. Freshly prepared 10 ml of 0.6% Tri-Sodium citrate (Fisher, S/P500/53) (hypotonic solution) was added to pellets while vortexing and incubated at room temperature for 15 minutes to allow cells to absorb the solution and swell. Cells were centrifuged at 800xg for 5 minutes and supernatant was removed. Pellets were fixed 3 times with 6 ml of freshly prepared fixative solution, 3:1 methanol: acetic acid, which was added drop wise while vortexing to each pellet then cells were centrifuged at 800xg for 5 minutes. The process was repeated 3 times before cell pellets were resuspended in 500  $\mu\text{l}$  of fixative and stored at  $-20^\circ\text{C}$ .

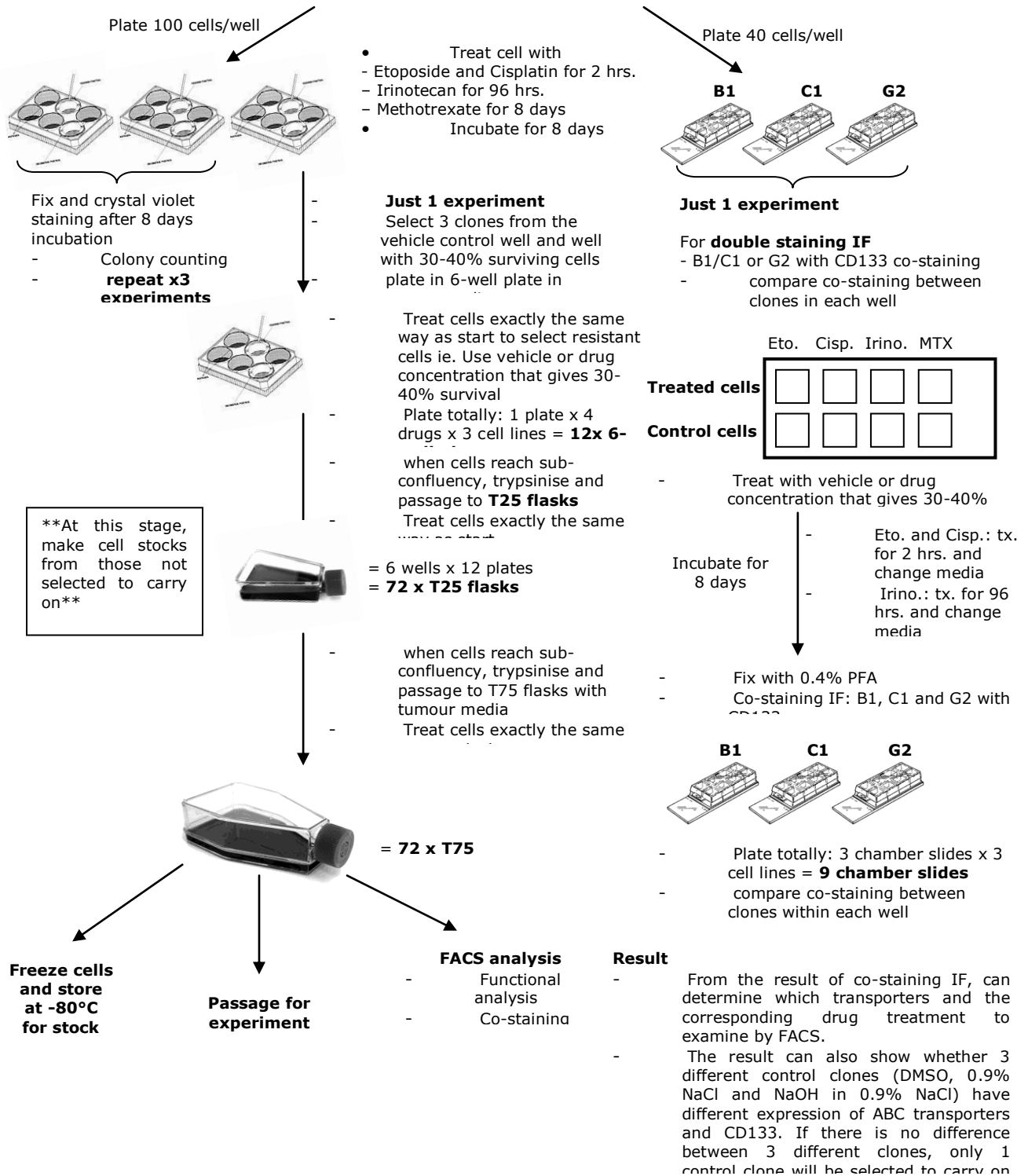
### **2.8.3 Slide preparation**

Slides were incubated in 70% ethanol overnight prior to performing metaphase spread analysis. Slides were washed in distilled water then polished with blue roll paper. Slides were held at a  $30^\circ$  angle to the bench then fixed cells were dropped from approximately 5 inches above slides. Three drops of fixed cells were dropped on each slide then slides were incubated at room temperature until dry. Metaphase cells were examined under the light microscope.

## **2.9 Clonogenic assay**

## Clonogenic plan

### EPN-2, MED-2 and SPNET-1 cell lines (70-80% confluency)



Clonogenic assay was performed to select drug resistant cells after cells were exposed to chemotherapeutic drugs and examine the ability of surviving cells following treatment to form colonies.

### **2.9.1 Optimisation of cell density in monolayer cells**

Cells were plated in 6-well plates at different cell densities to find the most appropriate number of cells to form sufficient countable colonies after 8 day incubation. Cells were trypsinised using 1x Trypsin/EDTA to dissociate cells into single cells. Cells were seeded in tumour media at different cell numbers: 50, 100, 200, 300, 500 and 1,000 cells/well into a 6-well plate. Cells were incubated in 5% CO<sub>2</sub> –air incubator at 37°C for 8 days to allow each single cell to form a colony. Cells were then fixed with 0.4% PFA for 20 minutes and stained with 0.1% crystal violet. A cell density of 100 cells/well provided sufficient well separated single clone for all cell lines and was selected to be used for seeding.

### **2.9.2 Drug treatment**

To determine inhibitory concentration (IC<sub>50</sub>) of chemotherapeutic drugs in paediatric brain tumour cell lines: EPN-2, MED-2 and SPNET-1, cells were treated with 4 different drugs: Cisplatin, Etoposide, Irinotecan and Methotrexate with different concentration. Four different drugs were tested on each of the 3 cell lines in order to identify the appropriated clonogenic range. Several different ranges of drug concentration were tested until a single ranges was identified that would allow the full range of drug response to be determined ideally including IC<sub>0</sub>, IC<sub>30</sub>, IC<sub>50</sub>, IC<sub>70</sub> and IC<sub>90</sub>. Resistant clones were picked from the well giving 30-40% survival and cultured for further investigations: co-expression of ABC transporters and CD133 and functional analysis of ABC transporters using Fluorescence Activated Cell Sorting (FACS).

#### **2.9.2.1 Plating cells**

Monolayer cells were detached using 1xTrypsin/EDTA then passed through the cell strainer to separate cells into single cells. Cells were plated in 6-well plate at 100 cells/well in 3 ml of tumour media and incubated for 4-6 hours in an incubator to allow them attaching the flask.

### 2.9.2.2 Drug Treatment

Cells were observed under a microscope to ensure that cells had attached before treatment. Each cell line was treated with different concentration of Cisplatin, Etoposide, Irinotecan and Methotrexate as shown in Table 2.7 and incubated for 8 days. Each 6-well plate contained the control well and 5 different concentrations of each drug.

### 2.9.3 Fixation and Counting

After 8-day incubation, cells were fixed with 4% PFA for 20 minutes and stained with 0.1% crystal violet for 5 minutes. Cells were then washed 3 times with distilled water to remove crystal violet. Only well separated surviving colonies containing more than 50 cells were counted.

### 2.9.4 Derivation of IC<sub>50</sub>

GraphPad Prism 5 software was used to draw dose-response curve and determine the IC<sub>50</sub> value.

**Table 2.7 Drug treatment for clonogenic assay**

Drug	EPN-2		MED-2		SPNET-1		Drug exposure duration
	Control	Conc. (μM)	Control	Conc. (μM)	Control	Conc. (μM)	
<b>1. Etoposide</b> (Sigma, E1383)	0.08% DMSO	5 10 20 40 80	0.04% DMSO	3 6 12 20 40	0.04% DMSO	3 6 12 20 40	Cells treated with either Etoposide or Cisplatin were incubated for 2 hours then tumour media were replaced with fresh media.
<b>2. Cisplatin</b> (Cisplatin 1 mg/ml Injection from TEVA UK limited)	1.6x10 <sup>-5</sup> % NaCl	0.3 0.75 1.5 3 6	1.6x10 <sup>-5</sup> % NaCl	0.3 0.75 1.5 3 6	2.2x10 <sup>-5</sup> % NaCl	0.5 1 2 4 8	
<b>3. Irinotecan</b> (Sigma, I1406)	0.02% DMSO	0.5 4 8 12 24	0.012% DMSO	0.75 1.5 3 6 12	0.012% DMSO	0.75 1.5 3 6 12	
<b>4. Methotrexate</b> (100mg/ml, Pharmacy, DBL)	1.2x10 <sup>-5</sup> % NaCl +0.42M NaOH	1 nM 5 nM 10 nM 20 nM 30 nM	1.2x10 <sup>-5</sup> % NaCl +0.42M NaOH	1 nM 5 nM 10 nM 20 nM 30 nM	1.2x10 <sup>-5</sup> % NaCl +0.42M NaOH	1 nM 5 nM 10 nM 20 nM 30 nM	Cells treated with Methotrexate were continuously treated for 8 days.

## **2.10 Cells co-expressing ABC transporters and CD133 detected by FACS analysis**

Co-staining CD133 and ABC transporters immunofluorescence by FACS was performed to confirm the data of co-staining immunofluorescence and Western blotting analysis in resistant selected clones. Both immunofluorescence and Western blotting analysis results indicated that resistant selected clone expressed higher proportion of cells expressing CD133 and either ABCB1 or ABCC1. Unfortunately, FACS analysis results showed inconsistent proportion of CD133 and ABC transporters co-stained cells when the experiments were repeated. Therefore, the data from co-staining immunofluorescence FACS were unreliable.

### **2.10.1 Harvesting cells**

Cells were subcultured as monolayers and neurospheres in sufficient T75 flasks to achieve  $2 \times 10^7$  cells/ml for each assay. HEK cells stably transfected with pcDNA encoding either ABCB1 or ABCC1 or ABCG2 were used as positive controls and HEK cells stably transfected with empty pcDNA were used as negative control.

#### **2.10.1.1 Monolayer cells**

Cells were washed with Dulbecco's Phosphate Buffered Saline (DPBS) without  $\text{CaCl}_2$  and  $\text{MgCl}_2$  (Sigma, D8537) and detached from flasks with 2 ml of 10 mM EDTA in DPBS. Cells were incubated for 15 minutes in standard cell culture incubator then gently dissociated using 10 ml pipette to singularise cells. Cells were centrifuged at 800xg for 3 minutes then DPBS was removed. Cells were resuspended in 500  $\mu\text{l}$  of DPBS.

#### **2.10.1.2 Neurospheres**

Neurospheres were centrifuged at 800xg for 3 minutes then media were removed. Neurospheres were washed with 5 ml DPBS then 5 ml of 10 mM EDTA was added into neurospheres to dissociate cells into single cells. Neurospheres were incubated at 37°C on an orbital shaker for 20 minutes. To ensure that cells are singularised, cells were pipetted up and down using 10 ml pipette and centrifuged at 800xg for 3 minutes to remove EDTA. Cells were resuspended in 500  $\mu\text{l}$  of DPBS.

### 2.10.2 Fixation

Cells were fixed with 2% PFA for 30 minutes at room temperature. Cells were gently vortexed while PFA was dropped into the tube. Then  $2 \times 10^6$  cells were equally transferred into FACS tube for ABCB1, ABCC1, ABCG2 detection and also negative controls for each one.

### 2.10.3 Blocking

Cells were centrifuged at 250xg for 3 minutes then PFA was discarded. Cells were blocked with appropriate blocking buffer as described in Table 2.8. Cells were blocked for 15 minutes at room temperature then centrifuged at 250xg for 3 minutes and blocking buffer was removed. Cells were then resuspended in 100  $\mu$ l of DPBS.

### 2.10.4 Co-staining immunofluorescence by FACS

#### 2.10.4.1 Primary antibody treatment

Cells were incubated in the appropriate primary antibody made up in the appropriate blocking buffer (co-staining between ABC transporters and CD133) (Table 2.9) for 1 hour at room temperature. Cells were centrifuged at 250xg for 3 minutes then the primary antibody solution was removed. To remove excess primary antibody, cells were washed once with 100  $\mu$ l blocking buffer.

#### 2.10.4.2 Secondary antibody treatment

Cells were resuspended in 100  $\mu$ l of DPBS and incubated with secondary antibody (Table 2.9) made up in appropriate blocking buffer. For ABCG2 detection, cells were incubated with conjugated ABCG2 primary antibody at this stage. Cells were incubated for 30 minutes at room temperature in dark. After which cells were washed once with 100  $\mu$ l of DPBS then resuspended in 300  $\mu$ l of DPBS.

**Table 2.8 Blocking buffer**

ABC transporters	Blocking buffer
1. ABCB1	2% NGS in DPBS
2. ABCC1	2% NGS + 0.2% Triton X-100 in DPBS
3. ABCG2	2% NGS in DPBS

**Table 2.9 Primary and secondary antibody for FACS co-staining immunofluorescence**

Primary antibody	Supplier	Working concentration	Secondary antibody	Supplier	Working concentration
<b>1. ABCB1: 4E3</b>  <b>CD133</b>	Abcam (Ab10333)	1:50	Anti-Mouse Alexa 647	Invitrogen (A21235)	1:1,000
	Cell signaling (3663)	1:100	Anti-Rabbit Alexa 488	Invitrogen (A11008)	1:500
<b>2. ABCC1: MRPR1</b>  <b>CD133</b>	Signet (SIG-38760)	1:10	Anti-Rat Alexa 647	Invitrogen (A21247)	1:1,000
	Abcam (Ab19898)	1:400	Anti-Rabbit Alexa 488	Invitrogen (A11008)	1:500
<b>3. ABCG2*: 5D3</b>  <b>CD133</b>	R&D system (FAB995P)	1:100	-	-	-
	Cell signaling (3663)	1:100	Anti-Rabbit Alexa 488	Invitrogen (A11008)	1:500

\*ABCG2 primary antibody is conjugated with PE therefore this antibody will be added later when cells reaches secondary antibody treatment step.

### 2.10.5 Analysis

ABC transporters co-stained with CD133 were detected using FACS machine (Cytomics FC500, Beckman Coulter). FACS data were analysed using WinMDI version 2.8 software.

## 2.11 Functional ABCB1 analysis by FACS

Immunofluorescence and Western blotting analysis results showed that the ABCB1 transporter was enriched after drug treatment and consistently expressed at a high level after prolonged treatment. Therefore, functional analysis using FACS was performed to determine whether high level of ABCB1 expression correlated with an increase in function.

### 2.11.1 Harvesting cells

Sufficient cells were subcultured as monolayers to achieve  $2 \times 10^7$  cells/ml for each assay. Cells were washed with DPBS then detached by incubating in 10 mM EDTA in DPBS for 15 minutes in a standard incubator. To ensure that cells are singularised, a 10 ml pipette was used to dissociate cells. Cells were centrifuged at 250xg for 3 minutes then EDTA was removed. Cells were washed once with DPBS and resuspended in FACS buffer (appendix B7, Table B7.1) to achieve  $2 \times 10^7$  cells/ml.



### 2.11.2 Substrate, inhibitor and primary antibody treatment

100  $\mu$ l of cells ( $2 \times 10^6$  cells) were transferred as into each FACS tube as described in figure 2.1 and incubated with Rhodamine123 (ABCB1 substrate), Verapamil (ABCB1 inhibitor) or 4E3 (anti P-glycoprotein) which were made up in FACS buffer, for 30 minutes at 37°C with periodic inversion every 10 minutes. Working concentration of all reagents and testing set were described in Table 2.10 and figure 2.1. Cells were washed twice with FACS buffer and were centrifuged at 250xg for 3 minutes to removed FACS buffer. Then cells were resuspended in 100  $\mu$ l FACS buffer.

**Table 2.10 Reagents for ABCB1 functional analysis by FACS**

Reagents	Supplier	Aim	Working concentration
<b>1. Rhodamine 123</b>	Sigma (R8004)	Substrate	2 $\mu$ M
<b>2. Verapamil</b>	Sigma (V4629)	Inhibitor	20 $\mu$ M
<b>3. 4E3</b> (anti P-glycoprotein)	Abcam (ab10333)	Primary antibody	1:20
<b>4. Alexa Fluor® 647 goat anti-mouse IgG (H+L)</b>	Invitrogen (A21235)	Secondary antibody	1:1,000

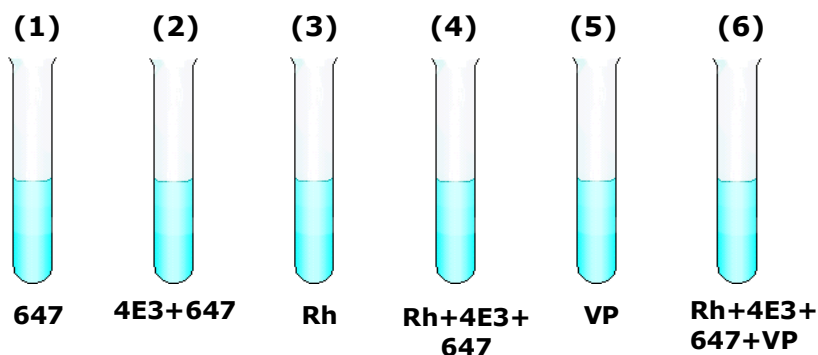


**Figure 2.1 Testing set for ABCB1 functional analysis.** Cells ( $2 \times 10^6$  cell) were equally transferred to each FACS tubes. Each tube was added with different chemicals for different aims: 1<sup>st</sup> tube for background staining of secondary antibody, 2<sup>nd</sup> tube for co-staining detection, 3<sup>rd</sup> tube for Rhodamine123 (Rh) accumulation or efflux determining, 4<sup>th</sup> tube for determining cells, which effluxed Rh and expressed ABCB1, 5<sup>th</sup> tube for determining Verapamil effect and last tubes for determining inhibition effect of Verapamil on cells, which expressed ABCB1 and effluxed Rh.

### **2.11.3 Secondary antibody treatment**

Cells were incubated with the secondary antibody as described in Table 2.10 for 30 minutes on ice in dark. Then cells were washed twice with 100  $\mu$ l FACS buffer and resuspended in 300  $\mu$ l FACS buffer.

### **2.11.4 Analysis**

ABCB1 function was determined by FACS (Cytomics FC500, Beckman Coulter). FACS data was analysed using WinMDI version 2.8 software.

## **2.12 ABCB1 RNAi transfection**

Previous results showed that the ABCB1 transporter was primarily enriched after first treatment in the selected clones and consistently expressed at a high level after prolonged treatment. To prove that ABCB1 transporter is the major mechanism that protects cells from chemotherapeutic cytotoxicity, ABCB1 transporter function was inhibited using Ribonucleic acid interference (RNAi) transfection. After transfection, messenger RNA (mRNA) of ABCB1 will be degraded and protein expression will be absent. If ABCB1 is the major mechanism to protect cells from cytotoxicity, ABCB1 siRNA transfected cells should respond better to drug treatment. Unfortunately, this technique was unsuccessfully optimised to find the appropriate condition for ABCB1 SiRNA transfection into our cell lines. As a result, the clonogenic assay was performed to investigate the effectiveness of ABCB1 inhibition in drug treatment as mentioned later.

### **2.12.1 Plating cells for transfection**

Cells were plated in 24-well plate (EPN-2 cell line and EPN-2 C1 (DMSO) clone =  $20 \times 10^3$  cells/well and EPN-2 T1 Etoposide and Irinotecan clones =  $25 \times 10^3$  cells/well in 1 ml of tumour media) for 24 hours in a standard culture incubator before transfection to achieve 50%-70% confluency.

### 2.12.2 ABCB1 SiRNA transfection

SiPORT Amine (Ambion, AM4503) and Opti-MEM® I + GlutaMAX™ I (Gibco, 51985-026) were warmed to room temperature and mixed together as different concentrations (Table 2.11). The mixture of SiPORT Amine and Opti-MEM was incubated at room temperature for 10-15 minutes. GAPDH or ABCB1 SiRNA was mixed with Opti-MEM as described in Table 2.12. 25 µl of both SiPORT Amine and SiRNA mixture was mixed properly using pipette and incubated at room temperature for 10-15 minute to allow them to form RNA induced silencing complex (RISC). Cells with 450 µl tumour media were added with 50 µl of different concentration of the SiPORT Amine and SiRNA mixture while plate was tilting to avoid directly contact of the mixture to particular cell area. Transfected cells were incubated in 5% CO<sub>2</sub> –air incubator at 37°C for 24 hours. After 6-8 hour incubation, tumour media was replaced with fresh tumour media to avoid cytotoxicity from SiPORT Amine. After 24-hour transfection, cells were harvested and extracted RNA to determine ABCB1 expression using Reverse Transcriptase Polymerase Chain Reaction (RT-PCR).

To optimise the condition for ABCB1 transfection, the transfection experiment was performed to knockdown known highly expressed gene. Therefore, Silencer® GAPDH SiRNA (human) (Ambion, AM4605) (forward GAPDH: TCTGGCCCCCTCTGCTGATGC and reverse GAPDH: GGTGGCAGTGATGGCATGGAC) was used to knockdown GAPDH, which is house keeping gene generally expressed in all cells, to optimise the appropriate condition for ABCB1 transfection. Once the appropriate concentration of GAPDH SiRNA and SiPORT Amine condition can be optimised. The optimised concentration will be applied for ABCB1 transfection.

There are 3 different ABCB1 SiRNAs used to optimise for knocking down ABCB1 expression; *si\_ABCB1* (AACUUUGGCUGCCAUCAUCCA) [Yagüe, E. *et al* (2007)], *si\_ABCB1.1* (GCAAAGAAUAAAGCGACU) and *si\_ABCB1.2* (AGAAAGAACUUGAAAGGUA) from Eurogentec. The condition optimised from GAPDH knockdown however did not effectively knockdown ABCB1 expression in our cell lines. The concentration of SiPORT Amine and ABCB1 SiRNA

**Table 2.11 Mixture of SiPORT Amine and Opti-MEM**

<b>Concentration of SiPort Amine (%v/v) in 500 <math>\mu</math>l</b>	<b>20 <math>\mu</math>M SiPort amine (<math>\mu</math>l)</b>	<b>Opti-MEM 1 (<math>\mu</math>l)</b>
<b>0.1</b>	2.75	135
<b>0.2</b>	5.50	132
<b>0.4</b>	11.00	126.5
<b>0.6</b>	16.5	121
<b>0.8</b>	22	115.5
<b>1.6</b>	44	93.5

**Table 2.12 Mixture of ABCB1 SiRNA and Opti-MEM**

<b>SiRNA (nM) in 500 <math>\mu</math>l</b>	<b>1 nM</b>	<b>5 nM</b>	<b>10 nM</b>	<b>20 nM</b>	<b>40 nM</b>	<b>80 nM</b>	<b>100 nM</b>
<b>20 <math>\mu</math>M Stock SiRNA (<math>\mu</math>l)</b>	0.08	0.41	0.83	1.65	3.3	6.6	8.25
<b>Opti-MEM (<math>\mu</math>l)</b>	82.4	82.1	81.7	80.9	79.2	75.9	74.3

was hence increased up to 1.6%v/v and 100 nM, respectively. Unfortunately, ABCB1 expression in our cell lines could not be knocked down at all. Consequently, drug inhibition, Verapamil, was used to inhibit ABCB1 function instead of SiRNA knockdown.

## **2.13 RNA extraction**

RNA extraction was performed to extract RNA from cells after transfection. RNA was used to determine ABCB1 messenger RNA expression using RT-PCR.

### **2.13.1 Dissociation of nucleoprotein complex**

After 24-hour transfection, tumour media was removed then 200  $\mu$ l of RNA STAT-60™ (TEL-TEST, INC, CS-110) was used to harvest cells. Cells were passed through pipette several times and incubated at room temperature for 5 minutes to complete the dissociation of nucleoprotein complexes.

### **2.13.2 RNA extraction**

To extract RNA, 1:50 chloroform was added into the homogenate. The homogenate was vigorously vortexed for 15 seconds and incubated at room temperature for 2-3 minutes. The homogenate was centrifuged at 12,000xg for 15 minutes at 4°C as resulting in separation into 2 phases: a lower red phenol chloroform phase and the colourless upper aqueous phase containing RNA.

### **2.13.3 RNA precipitation**

The upper aqueous phase was transferred into fresh eppendorf tube and RNA was precipitated by adding an equal volume of 1:2 isopropanol. Samples were incubated at room temperature for 5-10 minutes and centrifuged at 12,000xg for 10-15 minutes at 4°C. A tiny pellet of RNA should be seen at this step.

### **2.13.4 RNA washing**

Supernatants were discarded and RNA pellets were washed once with 200 µl of 75% ethanol. Samples were centrifuged at 7,500xg for 5 minutes at 4°C. Supernatants were removed then RNA pellets were dried by air-drying at room temperature. RNA pellets were resuspended in 25 µl of Diethylpyrocarbonate (DEPC) treated RNase-free water and incubated at 55-60°C for 10-15 minutes to effectively dissolve RNA pellets. RNA concentration was determined by using Nanodrop. RNA samples were stored at -80°C until required.

## **2.14 Reverse transcriptase Polymerase Chain Reaction (RT-PCR)**

### **2.14.1 DNase treatment**

Required RNA amount to process cDNA synthesis is 1,000 ng. Required RNA amount was topped up with DEPC water to 8 µl and mixed with 1 µl of 10x reaction buffer supplied with DNaseI. 1 µl of RQ1 RNase free DNaseI (Promega, M6101). Once DNase was added into RNA

samples, samples were strictly incubated for 15 minutes at room temperature. To stop DNaseI activity, 2 µl of stop solution supplied with DNaseI was immediately added into RNA samples, which were then incubated at 65°C for 10 minutes to inactivated DNase.

#### **2.14.2 Primer annealing and reverse transcription (cDNA synthesis)**

DNase treated RNA samples were combined with 1 µl of Oligo (dT)<sub>18</sub> primer, 4 µl of 5x reaction buffer, 2 µl of dNTP Mix (10 mM each), 1 µl of Ribolock™ RNase inhibitor and 1 µl of RevertAid™ M-MuLV Reverse Transcriptase [all reagents are supplied in RevertAid™ First Strand cDNA Synthesis Kit (Fermentas, K1622)]. To synthesise cDNA, RNA samples were incubated at 42°C for 1 hour and 70°C for 5 minutes. Finally, cDNA samples were diluted by the addition of 40 µl of DEPC water and stored at -20°C until needed.

#### **2.14.3 Polymerase chain reaction (PCR)**

3 µl of cDNA template was mixed with the master mix solution consisting of 1.5 µl of DEPC water, 1.5 µl of forward primer (10 µM), 1.5 of reverse primer (10 µM) and 7.5 µl of Taq (2x Biomixred) (Bioline: Bio-Bio-25005). The mixture was properly mixed and briefly centrifuged before running the PCR programme. The PCR programme used in this study is described below.

- **Normal PCR programme:** initial denaturation at 94°C for 5 minute, at 94°C for 30 seconds, at 60°C (annealing temperature) for 30 seconds, at 72°C for 30 seconds and final extension at 72°C for 5 minutes.
  - **GAPDH detection:** annealing temperature = 60°C, 30 cycles
  - **ABCB1 detection:** annealing temperature = 56°C, 35 cycles
- **Gradient PCR programme:** initial denaturation at 94°C for 5 minute, at 94°C for 30 seconds, at 58°C Δ 10°C (gradient temperature) for 1 minute, at 72°C for 30 seconds and final extension at 72°C for 5 minutes.
  - **Optimisation for ABCB1:** gradient temperature = 53.8°C, 54.3°C, 55.1°C, 56.1°C, 56.8°C, 57.6°C, 58.2°C, 59.6°C, 60.2°C, 61.3°C, and 62.2°C.

#### **2.14.4 Gel electrophoresis**

PCR product (7  $\mu$ l) and ladder marker (10  $\mu$ l) [HyperLadder marker (Bioline: Bio-33025)] were loaded into 2% agarose gel (Invitrogen: 15517-022) containing ethidium bromide (5  $\mu$ l/40 ml). Gel was dissolved and run in 1x TAE buffer at 150 volts for 20 minutes. DNA bands were observed and photographed using the UV light machine (GENEFlash, syngene bioimaging).

#### **2.15 Clonogenic assay: Drug treatment combined ABCB1 inhibition**

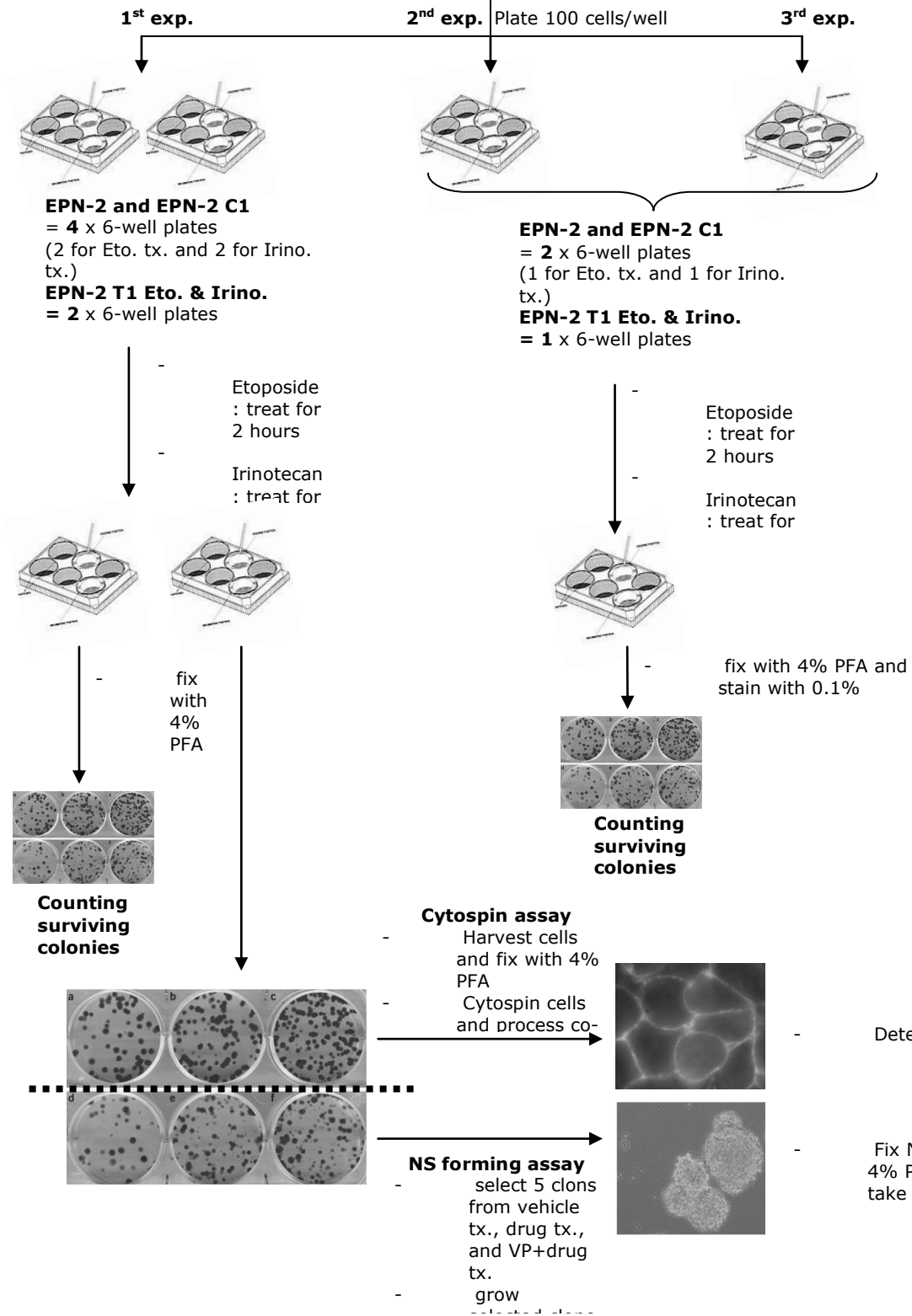
Previous results showed that our cell lines contain approximately 10-12% of cancer stem-like cells in monolayer cells and they were enriched in neurosphere condition. After treatment with drugs, the majority population which survived after treatment was co-stained CD133 and ABCB1 cells. Therefore, ABCB1 transporter probably is the major mechanism which protects these tumour cells from drug toxicity. To prove whether ABCB1 transporter is an essential mechanism for these cells to survive after treatment, verapamil was used as a combined treatment with drug to inhibit ABCB1 function. If the ABCB1 transporter is a major mechanism for these cells to survive, drug treatment combined with verapamil should provide much more effective result than single drug treatment. Based on the FACS result, EPN-2 cell line was selected to be studied. The schematic plan is shown in the next page.

##### **2.15.1 Plating cells for treatment**

Monolayer cells were harvested using 1x Trypsin/EDTA to detach cells and passed through the cell strainer to ensure that cells were separated into single cells. Cells were counted using trypan blue and plated into 6-well plate at 100 cells/well in 2 ml of tumour media. Cells were incubated in 5% CO<sub>2</sub> –air incubator at 37°C for 2-4 hours to allow them to attach on plate properly before treatment.

# Clonogenic assay: Drug treatment combined with ABCB1 inhibition

**EPN-2, EPN-2 C1 (DMSO), EPN-2 T1 Etoposide and EPN-2 T1 Irinotecan (70-80% confluency)**





### 2.15.2 Drug Treatment

Cells were observed under the microscope to ensure that they had attached before treatment. There are 8 different conditions of treatment as shown in Table 2.13. Each condition was prepared in 1 ml of tumour media (total tumour media/well = 3 ml) and transferred into each well of 6-well plate as shown in the figure 2.13. Cells treated with Etoposide were incubated for 2 hours whereas cells treated with Irinotecan were incubated for 96 hours, each in a 5% CO<sub>2</sub> –air incubator at 37°C, then tumour media were replaced with fresh media. Cells were incubated until each colony contained at least 50 cells (6 cell divisions) approximately 6-8 days.

### 2.15.3 Harvesting cells

After 6-8 day incubation, when colonies were properly formed (contain more than 50 cells/clone). There were 3 different assays performed: colony counting to determine the effectiveness of drug treatment combined with verapamil, cytospin for co-staining immunofluorescence to investigate whether surviving clones express ABCB1 or not and neurosphere forming assay to examine the ability of cells to form neurospheres which is one of the CSC characteristics.

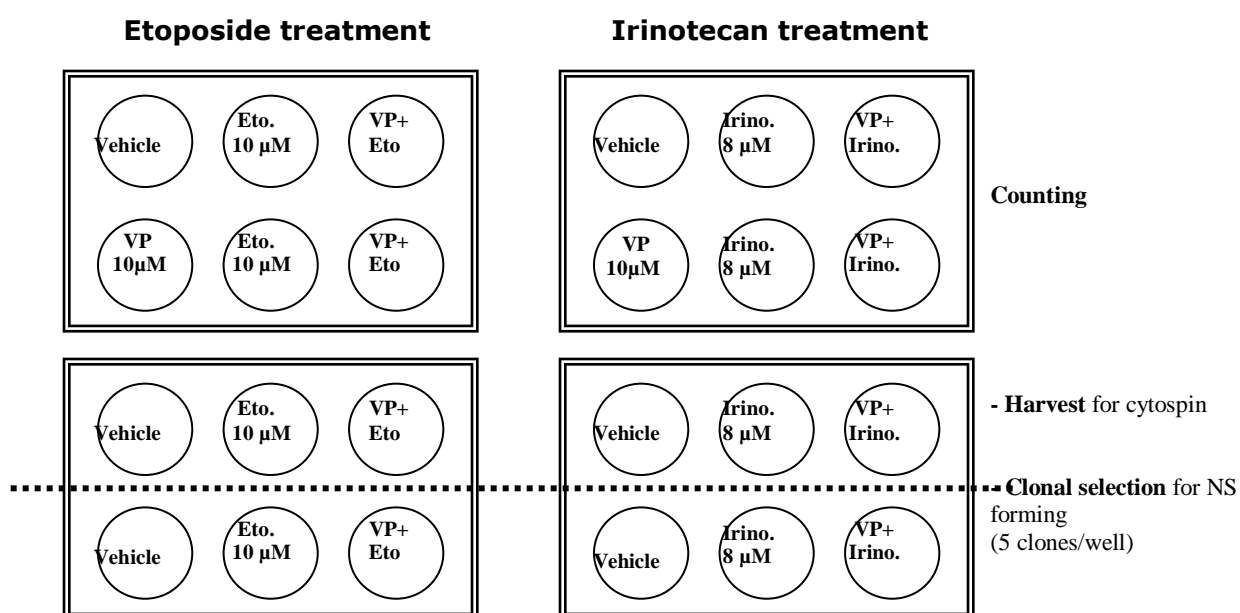


**Figure 2.2 Schematic treatment plan on 6-well plate for clonogenic assay**

### 2.15.3.1 Colony counting

To compare the effectiveness of treatment between single drug treatment and drug treatment combined with verapamil, clonogenic assay was performed. Surviving colonies were counted to determine the effectiveness of drug and combined verapamil treatment.

After 6-8 day incubation, cells were fixed with 4% PFA for 20 minutes and stained with 0.1% crystal violet for 5 minutes. Surviving colonies containing more than 50 cells were counted and compared single drug treatment or drug combined with verapamil treatment with vehicle treatment.

### 2.15.3.2 Cytospin for co-staining immunofluorescence

To determine the expression of ABCB1 after drug and verapamil treatment, cytospin and co-staining immunofluorescence were performed. We hypothesised that surviving colonies probably are 1) cells expressing ABCB1 because of insufficient Verapamil concentration, 2) cells expressing ABCB1, which turn on another mechanism of protection and 3) cells without ABCB1 expression. Therefore, this experiment could not distinguish the population of 1) and 2) resulting in the future study should be performed to further investigate to distinguish these 2 populations. To prove whether surviving cells after drug treatment combined with

**Table 2.13 Drug treatment combined with ABCB1 inhibition**

Treatment	Concentration
1. Vehicle for Etoposide (DMSO)	1:4,000
2. Vehicle for Irinotecan (DMSO)	1:12,500
3. 20 $\mu$ M Verapamil treatment	20 $\mu$ M
4. 10 $\mu$ M Verapamil treatment	10 $\mu$ M
5. 20 $\mu$ M Verapamil + 10 $\mu$ M Etoposide	Verapamil = 20 $\mu$ M
	Etoposide = 10 $\mu$ M
6. 10 $\mu$ M Verapamil + 8 $\mu$ M Irinotecan	Verapamil = 10 $\mu$ M
	Irinotecan = 8 $\mu$ M
7. 10 $\mu$ M Etoposide	10 $\mu$ M
8. 8 $\mu$ M Irinotecan	8 $\mu$ M

verapamil are ABCB1 positive cells or ABCB1 negative cells, that does not need ABCB1 function to protect them but they have different mechanism to survive from drug treatment.

Clonogenic assay for drug treatment combined with verapamil was performed and incubated for 6-8 days. Cells were harvested using 1x Trypsin/EDTA and washed once with HBSS. Cells were centrifuged at 800xg for 5 minutes then HBSS was removed. Cells were fixed with 0.4% PFA for 20 minutes at room temperature then PFA was removed, as much as possible, and cells were resuspended in HBSS. Cytospin was performed using Cytospin machine (Centurion Scientific LTD, 4050 series). Filter papers with a hole and APES slides were fit into the cytopsin bucket and locked with clips. To soak filter paper, 200 µl of HBSS was added into each bucket and centrifuged at 1,000 rpm for 1 minute. 500 µl of fixed cells were then transferred into the cytopsin bucket and centrifuged at 1,000 for 2 minutes. Slides were left to dry at room temperature and stored at -20°C until required. Co-staining CD133 and ABCB1 IF was performed as described in section 2.2.1.

### **2.15.3.3 Neurosphere formation assay**

This assay was performed to determine the ability of surviving cells after chemotherapeutic drugs (Etoposide and Irinotecan) and ABCB1 inhibitor (verapamil) treatment to form neurospheres which is one of significant characteristics of stem cells.

Clonogenic assay was performed as mentioned earlier in section 2.15. After 6-8 days treatment, 5 clones were microscopically identified and selected using a P10 Gilson's pipette, from each condition. Selected clones were induced to form neurospheres in 24-well plates containing 1 ml of stem cell media with EGF and FGF for 3-4 days. To ensure that cells were initially dissociated into single cells, a P1000 Gilson's pipette was used to singularise cells. Neurospheres were fixed with 0.4% PFA for 20 minutes. Neurosphere forming images were captured using a dissecting microscope by Digital Sight D3 U1, Nikon camera and ACT-2U software, Version 1.61.136.292.

---

---

## **Chapter 3**

**Basic characteristics of the primary cultured paediatric cell  
lines and their original tumours**

---

---

## **Chapter 3: Basic characteristics of the primary cultured paediatric cell lines and their original tumours**

### **3.1 Introduction**

The most common solid neoplasms in children are tumours of the central nervous system (CNS) accounting for approximately one third of childhood cancers and they are the second most common paediatric cancers behind leukaemia [Pollack, I. F. (1994), and Stewart, E.S. and Cohen, D.G. (1998)]. The most common paediatric brain tumours (PBTs) are low grade astrocytomas accounting for 52% and the embryonal tumours (the majority of which medulloblastomas) are the second most common, accounting for 21%. The less frequently occur PBTs are glioblastoma multiforme and ependymoma accounting for 15% and 9%, respectively [Baldwin, R.T. and Martin, S.P. (2004) and Jay, V. *et al* (2003)]. PBTs studied in this project were newly established from 5 different tumour types, which were obtained from patients diagnosed with ependymomas (EPN-1 and EPN-2), medulloblastomas (MED-1 and MED-2), CNS PNETs (SPNET-1), giant cell glioblastoma multiformes (BT-4) and oligodendrogliomas (Olig-1). The commercial cell line (PFSK-1) was also included. The five different tumour types studied in this project are all common PBTs, many of which show drug resistance after treatment leading to tumour relapse. All high grade tumours (WHO grade IV) including medulloblastoma, CNS PNET and GBM have less susceptibility to treatment and have high mortality rate. Low grade tumours (WHO grade II) include ependymomas, which have a tendency to recur locally, and oligodendrogliomas, which are sensitive to chemotherapy. Oligodendrogliomas were included to compare with the other tumours, which are frequently resistant to chemotherapy. Ependymomas and medulloblastomas comprised both primary (EPN-2 and MED-1) and recurrent tumours (EPN-1 and MED-2), although these are unpaired (i.e. the recurrent cell line EPN-1 and the primary EPN-2 are derived from different patients). To confirm the diagnosis, Haematoxylin and Eosin staining is performed on all tumour samples after surgery.

Histological features are able to indicate the cellular characteristics of tumours and are important in the tumour grading system. Each type of tumour demonstrates different hallmarks of histological features for example the hallmarks of ependymomas are perivascular pseudorosettes and true ependymal rosettes whereas common histological features of medulloblastomas are pseudorosettes or Homer-Wright rosettes and rhythmic palisading cells [Hart, M. N. *et al* (1973)]. Details of common histological features of each tumour type are described in the General Introduction.

Haematoxylin and Eosin staining confirmed the tumour type from which the cell lines were established and analysis of their genomic variability was established with a chromosomal count. Normal somatic cells normally have 46 chromosomes (diploidy) whilst normal sex cells contain only 23 chromosomes (haploidy). Cancer cells, which are aberrant cells, are expected to have variable number of chromosomes. Cytogenetic analysis in children brain tumours have been less frequently carried out than in adult brain tumours due to many limitations [Bhattacharjee, M. B. *et al* (1997)]. Specific genetic abnormality patterns were observed in some brain tumours. Isochromosome 17q and loss of chromosome 22 were commonly observed in PNETs whilst there were no convincing evidence to support a specific genetic alteration in ependymomas [Bhattacharjee, M. B. *et al* (1997)]. Karyotyping of chromosomes is a major method to screen for chromosome abnormalities and highly specialised assay, and was not performed in our study. To get a basic idea how variable our cell lines with respect to a variation of chromosome numbers, metaphase spread analysis was performed on monolayers from all cell lines at early passage. To determine variation of chromosome numbers, chromosomes were counted from 100 cells and means of chromosome numbers were calculated. This gave some inspection of a degree of chromosome number variation in our cell lines. Therefore, basic characterisation of newly established paediatric brain tumour cell lines were assessed in term of Haematoxylin and Eosin staining to describe histology of tumours and metaphase analysis to determine a variation of chromosome numbers.

## 3.2 Results

### 3.2.1 Descriptive data of all primary cultured paediatric and commercial cell lines

Primary cultured cell lines EPN-1 and EPN-2 (ependymoma), MED-1 and MED-2 (medulloblastoma), SPNET-1 (CNS PNET) and Olig-1 (oligodendroglioma) were obtained from the Children's Brain Tumour Research Centre (CBTRC) cell line bank, University of Nottingham. BT-4 (glioblastoma multiforme) was donated by Dr. Andrew Peet, University of Birmingham. The commercial cell line, PFSK-1, was obtained from LGC promochem (CRL-2060™). Details of all cell lines are described in Table 3.1 and Table 3.2. EPN-2, MED-1, SPNET-1, BT-4 and Olig-1 cell lines were obtained from first surgery (primary tumours) while EPN-1 and MED-2 cell lines are from recurrent tumours which relapsed after treatment. Dr. Lisa Storer who has the responsibility to produce and maintain the CBTRC cell line bank kindly provided all cell line stocks for this study.

**Table 3.1 PFSK-1 commercial cell line details** [Product description from [www.lgcpromochem-atcc.com](http://www.lgcpromochem-atcc.com) (cited 17 November 2007)]

Name of cell line	Diagnosis	Source	Characteristics of cells
<b>1. PFSK-1</b>	Malignant primitive neuroectodermal tumour	- male Caucasian, 22 months of age - tumour located in cerebral hemisphere - obtained from LGC promochem	<b>Comments:</b> express the intermediate filament protein, nestin, and are positive for neuron specific enolase (NSE). : lack characteristics of terminally differentiated neurons or glia. : loss of heterozygosity for multiple loci on chromosome 17. : neither c-myc nor N-myc is amplified or re-arranged. <b>Doubling time:</b> 30 hours

**Table 3.2 Description of clinical characteristics of the paediatric brain tumours from which cell lines were derived**

Name of cell line	Diagnosis	Age at diagnosis	Origin of tumour	Surgical resection status and treatment	Follow up (months)	Outcome	Metastatic status
<b>1. EPN-1</b> [Figure 3.1]	Recurrent ependymoma, WHO grade II	13 years 6 months	- located in right parietal lobe - sample was obtained from 3 <sup>rd</sup> surgery	- complete surgical resection - repeat surgery at relapse - 3 cycles of CT: Vincristine, Cyclophosphamide and Etoposide and focal RT then 3 cycles of PCV prior to 3 <sup>rd</sup> surgery	111 (from 1 <sup>st</sup> operation)	Deceased	M0
<b>2. EPN-2</b> [Figure 3.2]	Ependymoma, WHO grade II	3 years 6 months	- located in fourth ventricle - primary tumour	- Macroscopic resection - UKCCSG infant ependymoma study	20	Alive	M0
<b>3. MED-1</b> [Figure 3.1]	Medulloblastoma, WHO grade IV	3 years 5 months	- located in cerebellum - primary tumour	- partial surgical resection - High dose Cyclophosphamide. UK infant Medulloblastoma protocol posterior fossa RT	8	Deceased	M0
<b>4. MED-2</b> [Figure 3.1]	Recurrent medulloblastoma, WHO grade IV	10 years 6 months	- metastatic to supratentorial compartment (bilateral frontal lobes)	- partial surgical resection - POG 3021 regimen: CT and craniospinal RT prior to surgery from which this line was derived	42 (from 1 <sup>st</sup> operation)	Deceased	M2 at relapse
<b>5. SPNET-1</b> [Figure 3.1]	CNS PNET, WHO grade IV	5 years 1 month	- located in left frontal lobe - primary tumour	- partial surgical resection - Headstart CT and high dose Carboplatinum+Thiotepa after surgery - Local relapse at 13 months after the 1 <sup>st</sup> operation: repeat surgery and craniospinal RT. Further local relapse 4 months post RT	21	Deceased	M0
<b>6. Olig-1</b> [Figure 3.2]	Oligodendroglioma, WHO grade II	6 years 7 months	- located in right fronto-temporo-parietal lobe - primary tumour	- Subtotal surgical resection - PCV: Procarbazine, CCNU and Vincristine - progression high dose Carboplatin+Etoposide - Repeat surgery – Focal RT 54Gy)	24	Alive	M0
<b>7. BT-4</b> [Figure 3.1]	Giant cell glioblastoma multiforme, WHO grade IV	4 years 3 months	- located in frontal lobe of cerebral hemisphere - primary tumour	- partial surgical resection - Cisplatin – Temozolomide x 6 courses (Partial response) - Repeat surgery – focal RT	52	Alive	M0

CT=Chemotherapy, RT=Radiotherapy, PCV=Procarbazine, CCNU (Chloroethylcyclohexylnitrocourea) (eg. Lumustine) and Vincristine



### **3.2.2 Histopathological features of the original tumours from which 7 cell lines were derived**

Haematoxylin & Eosin staining was performed on sections from all original brain tumours to identify type of tumour and evaluate grading based on WHO criteria 2007. EPN-1 and EPN-2 cell lines were derived from WHO grade II ependymomas. EPN-2 was derived from a primary tumour. The EPN-1 cell line was however obtained from the 3<sup>rd</sup> surgery after the second tumour relapse. Hence, this cell line was derived after the patient had been treated with focal radiotherapy and 3 cycles each of two chemotherapy regimens prior to the third surgery (Table 3.2). The EPN-1 tumour was originally diagnosed as an ependymoma but tumour Haematoxylin and Eosin staining from the 3<sup>rd</sup> surgery showed dense networks of branching capillaries (Figure 3.1, a) which are a predominant characteristic of oligodendroglioma. Therefore, electron microscopy (EM) was performed to confirm the original diagnosis. This showed ependymal cilia (Figure 3.1, b) which is the characteristic electron microscopic feature of ependymoma. EPN-2 tumour Haematoxylin and Eosin staining showed monomorphic nuclear morphology characterised by round to oval nuclei with 'salt and pepper appearance' (Figure 3.2, a). In addition, perivascular pseudorosettes (Figure 3.2, b) and ependymal rosettes (Figure 3.2, b), typical histological features of ependymoma were observed. Neuroblastic rosette or perivascular pseudorosette (Figure 3.2, c) are described as vessels surrounded by ependymal tumour cells with a nuclear-free zone which has thin ependymal processes directed toward the walls of vessels.

MED-1 and MED-2 tumours were diagnosed as medulloblastoma tumours, WHO grade IV. MED-1 was derived from a primary tumour located in cerebellum. Haematoxylin and Eosin staining of MED-1 showed classical features of medulloblastoma described as densely packed round to oval or carrot shaped cells with highly hyperchromatic nuclei surrounded by scanty cytoplasm (Figure 3.1, g). MED-2 was a recurrent tumour and surgical and radiological evidence found that this tumour had metastasised to supratentorial compartment. MED-2 patient had been treated with POG 3021 regimen (chemotherapy and craniospinal radiotherapy) prior to surgery. Haematoxylin and Eosin staining showed round to oval hyperchromatic nuclei surrounded by

scanty cytoplasm. Additionally, a rhythmic palisading of tumour cells (Figure 3.1, c) defined as arrangement of tumour cells into parallel rows was observed. Neuroblastic rosettes (Homer Wright rosettes) which are observed in less than 40% of cases (Figure 3.1, d) were also observed in this patient.

The SPNET-1 cell line was derived from a CNS PNET, WHO grade IV. This tumour was located in left frontal lobe. Histological features of SPNET-1 tumour from Haematoxylin and Eosin staining showed cells with round regular nuclei and high nucleus:cytoplasm ratios (Figure 3.1, e). Furthermore, mitotic cells labelled with arrows were observed (Figure 3.1, f).

The BT-4 cell line was derived from a giant cell glioblastoma multiforme, WHO grade IV tumour. This tumour was located in frontal lobe of the cerebral hemisphere. Haematoxylin and Eosin staining of BT-4 tumour showed a high degree of nuclear polymorphism with multinucleated giant cells and vascular proliferation (Figure 3.1, h).

The Olig-1 tumour of origin was diagnosed as oligodendroglioma tumour, WHO grade II. This tumour was located in the right fronto-temporo-parietal lobe. Haematoxylin & Eosin staining of Olig-1 tumour showed monomorphic cells with uniform round nuclei and perinuclear halos (Honeycomb appearance) (Figure 3.2, d). Dense networks of branching capillaries were also observed (Figure 3.2, e) in this tumour, as were microcalcifications (Figure 3.2, f).

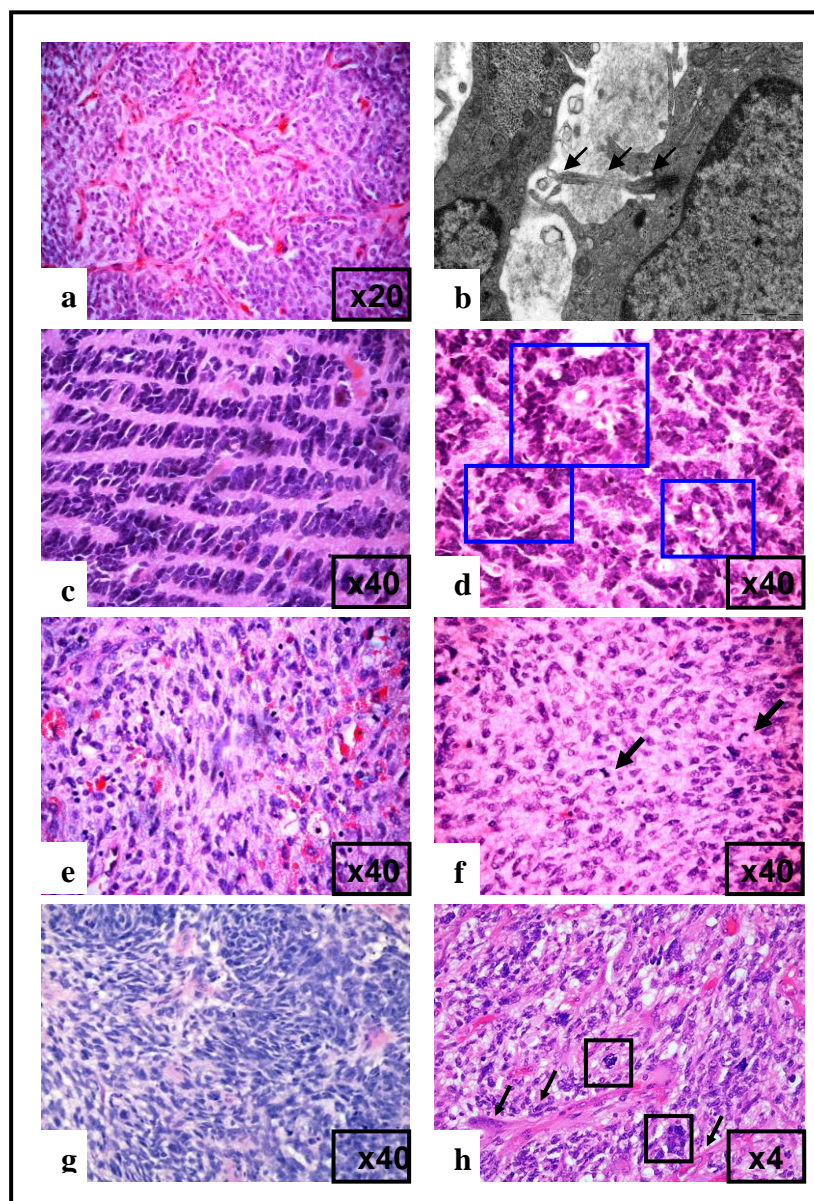


**Figure 3.1 Histological features of the original tumours from which EPN-1, MED-2, SPNET-1, MED-1 and BT-4 cells were derived.** EPN-1 tumour Haematoxylin and Eosin staining showed dense networks of branching capillaries, a classical feature of oligodendroglioma tumour at x20 magnification (a). Therefore, electron microscopy was performed and showed ependymal cilia which is hallmark feature for ependymoma indicated by arrows (b). MED-2 Haematoxylin and Eosin staining at x40 magnification showed a rhythmic palisading of tumour cells (c) and neuroblastic rosettes (d) indicated by blue boxes. Haematoxylin and Eosin staining of SPNET-1 tumour showed cells with regular round nuclei and high nucleus:cytoplasm ratios (e) and mitotic cells (f) indicated by arrows at x40 magnification. MED-1 Haematoxylin and Eosin showed densely packed round to oval or carrot shaped cells with highly hyperchromatic nuclei surrounded by scanty cytoplasm (x40) (g). BT-4 Haematoxylin and Eosin staining showed significant histological features for diagnosis of giant cell glioblastoma multiforme comprising of nuclear polymorphism, multinucleated giant cells (black boxes) and vascular proliferation (arrows) (x40) (h).

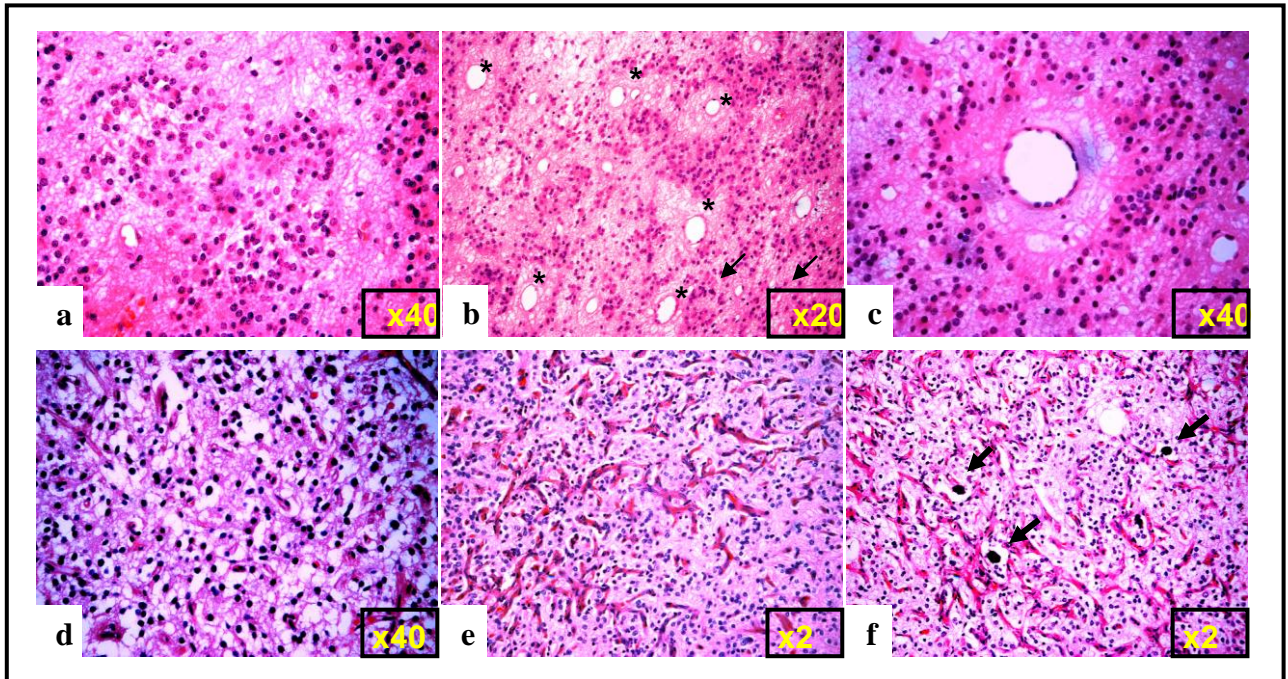


**Figure 3.2 Histological features of tumours from which EPN-2 and Olig-1 were derived.** EPN-2 Haematoxylin and Eosin staining is shown in the top row (a – c). The classical histological features of ependymoma are clearly visible; salt and pepper appearance (a), perivascular pseudorosettes (\*, b and c) and ependymal rosettes (↙, b). Histological features of Olig-1 tumour were showed in the bottom row (d – f). Haematoxylin and Eosin staining of Olig-1 showed a honey comb appearance (d), branching capillaries (e) and microcalcification indicated by arrows (f).

### 3.2.3 Metaphase spread analysis

To study chromosomal variation in cultured tumour cell lines, metaphase spread analysis was performed on EPN-2, MED-2, SPNET-1 and PFSK-1 cell lines. Cells cultured as monolayers were blocked in metaphase using Nocodazole. Metaphase cells then were harvested and dropped onto slides and observed under the microscope. Chromosome numbers were counted from 100 cells for each cell line. Metaphase spread analysis results are shown in Table 3.3 and Figure 3.3. Primary cultured cell lines (EPN-2, MED-2 and SPNET-1) demonstrated less variation of chromosome number when compared to the commercial cell line (PFSK-1) (Table 3.3 and Figure 3.3). When the size of chromosomes was evaluated, all 3 primary cultured cells contained the expected range in chromosome size whereas PFSK-1 cell line mostly contained chromosomes of the same size (Figure 3.3).

Metaphase analysis results from EPN-1, MED-1, BT-4 and Olig-1 cells shown in Figure 3.3 were produced by Dr. Deema Hussein. These 4 primary cell lines also showed a low level of variation of chromosome numbers (Figure 3.3); EPN-1 (20-82), MED-2 (22-84), BT-4 (33-113) and Olig-1 (30-89) and the majority of cells contained 40-45 chromosomes/cell. Therefore, our 7 primary cultured cells had less variation of chromosome numbers when compared to the commercial cell line.

**Table 3.3 The variation of chromosome number from metaphase spread analysis**

Cell line	Chromosome number				STDEV
	Max.	Min.	Median	Mean	
<b>EPN-2</b>	76	23	45	44.73	7.04
<b>MED-2</b>	62	27	38	39.55	6.78
<b>SPNET-1</b>	66	25	44	44.28	4.88
<b>PFSK-1</b>	132	7	47	45.26	21.76



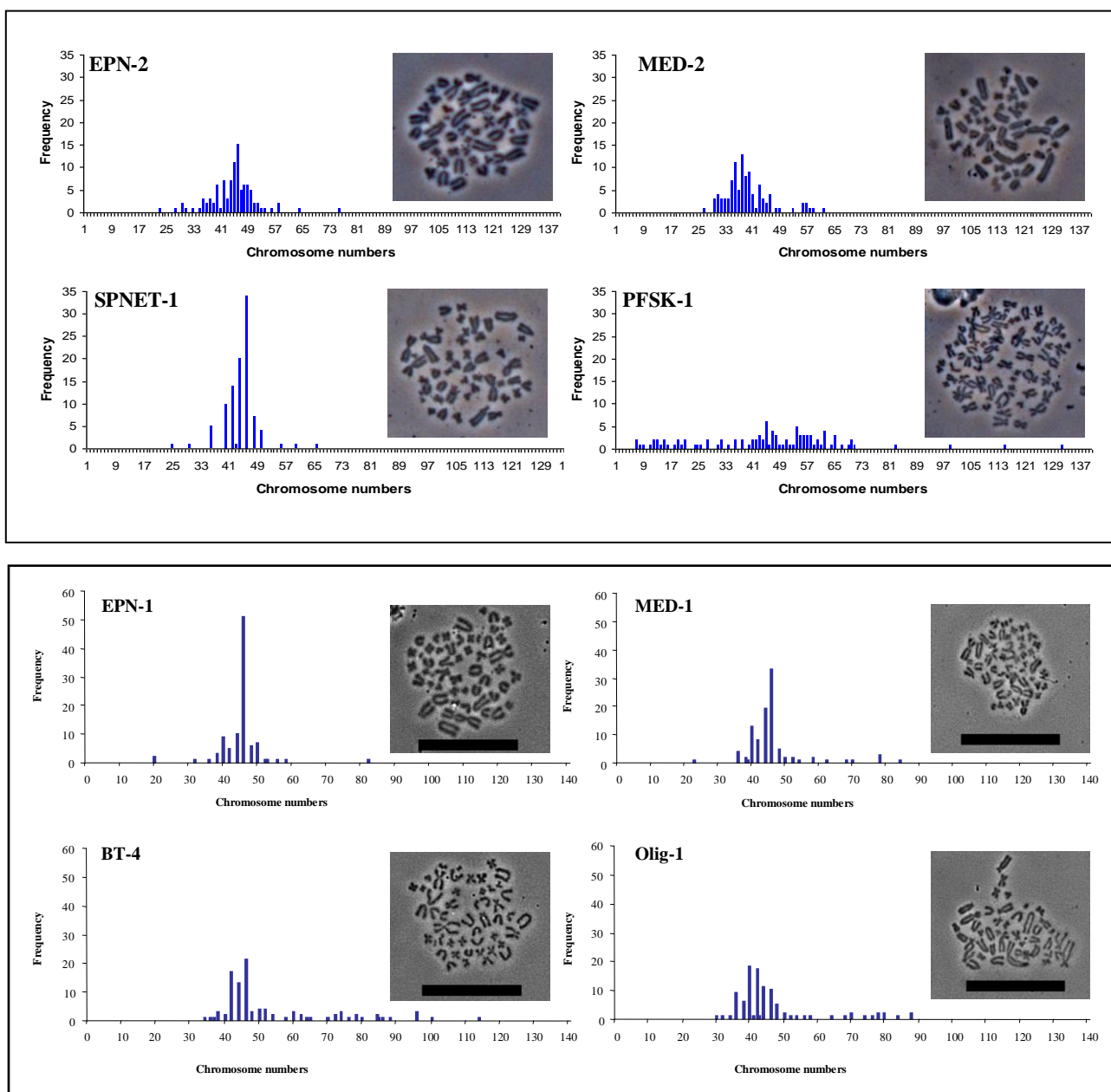


**Figure 3.3 Metaphase spread analysis of EPN-1, EPN-2, MED-1, MED-2, BT-4, Olig-1, SPNET-1 and PFSK-1 cell lines.** Monolayers were treated with Nocodazole to block cells in metaphase. After treatment, cells were fixed and observed under the microscope. The result showed that metaphase cells from EPN-2 (23-76, mean = 44.73, STDEV = 7.04), MED-2 (27-62, mean = 39.55, STDEV = 6.78) and SPNET-1 (25-66, mean = 44.28, STDEV = 4.88) have a less variable chromosome number than those from PFSK-1 (7-132, mean = 45.26, STDEV = 21.76). The majority of chromosome numbers from the other 4 cell lines range from 40-50.

### 3.3 Discussion

#### High and low grade tumours were included in this study

Seven primary cultured cell lines; EPN-1, EPN-2, MED-1, MED-2, SPNET-1, BT-4 and Olig-1 were included in this study as well as the commercial cell line; PFSK-1. All 8 cell lines were categorised into 5 types of tumours; Ependymoma (EPN-1 and EPN-2), Medulloblastoma (MED-1 and MED-2), CNS PNET (SPNET-1 and PFSK-1), Glioblastoma multiforme (BT-4) and Oligodendroglioma (Olig-1). These 5 different brain tumours covered the most common malignant CNS tumours which occur in children and they were also defined as different grading by WHO criteria 2007 into high grade tumours; WHO grade IV (MED-1, MED-2, SPNET-1, BT-4 and PFSK-1) and lower grade tumours; WHO grade II (EPN-1, EPN-2 and Olig-1). Although ependymomas are classified as grade II tumours, they behave aggressively in terms of high rate of recurrence after treatment and having chemoresistance [Messahel, B. *et al* (2009)]. Cell lines derived from Ependymoma and Medulloblastoma were generated from both primary tumours (EPN-2 and MED-1) and recurrent tumours (EPN-1 and MED-2) whilst SPNET-1, BT-4 and Olig-1 were established from the corresponding primary tumours. Only 3 cell lines; EPN-2, MED-2 and SPNET-1 were the focus of this PhD. The others were studied by Dr. Deema Hussein and have been included for completeness so that comparisons can be made.

The high grade tumours; medulloblastoma, CNS PNET and glioblastoma multiforme were selected to study because they are common types of paediatric brain tumours (PBTs) which are still resistant to chemotherapy and relapse after complete treatment resulting in poor prognosis. Medulloblastoma is the most common brain tumour occurring in children accounting for 25% of all PBTs and it has a poor prognosis. However, the 5-year survival rate has currently been increased because of improved treatment resulting in 60% of cases were cured with a combination treatment of neurosurgery and adjuvant radiotherapy and chemotherapy [Polkinghorn, W. R. and Tarbell, N. J. (2007)]. Nevertheless, the survivors

still have long sequelae resulting from treatments. At least 30% of those, who do not respond to treatment, present with disseminated lesion and the majority of cases are younger children [Packer, R. J. and Vezina, G. (2008)]. 10-15% of these cases have no response to therapy and die within 2 years of diagnosis. Hence, it is believed that these high-risk medulloblastoma patients are intrinsically resistant to chemotherapy [Johnsen, J. I. *et al* (2009)]. Both patient tumours, which generated the MED-1 and MED-2 cell lines, were classified as a high risk medulloblastoma with regard to partial surgical resection (MED-1 and MED-2), metastasis to supratentorial compartment (MED-2) and young age at diagnosis (MED-1). CNS PNET rarely occurs in children and locates in different region compared with medulloblastoma but they share some similar histological features. However, CNS PNET is more aggressive and unsusceptible to current chemotherapy resulting in far worse prognosis compared to medulloblastoma [Johnsen, J. I. *et al* (2009)]. GBM is also a very aggressive tumour and patients have a very poor prognosis. The median survival time was approximately 1 year after diagnosis and only 29% - 37% of patients survived for 18 month [Shapiro, W. R. *et al* (1989)]. This tumour is still highly resistant to combination treatment between chemotherapy and radiotherapy. These high grade tumours are very high malignant brain tumours and have aggressively metastatic characteristics within the neuroaxis. Particularly, CNS PNETs are recognised to have more locally aggressive invasion than medulloblastoma and the outcome of treatment is worsen in CNS PNET. Glioblastoma also rapidly spread through the contralateral hemisphere resulting in a very poor prognosis. Therefore, these highly resistant tumours were studied and characterised to provide useful data to overcome drug resistance in the future.

Low grade tumours were also included in this study. Ependymomas were included because these have a tendency to recur locally. This tumour is the third most common of PBTs accounting for 12%. Although advanced diagnosis using neuroimaging and treatments including neurosurgery and adjuvant therapy are available, the overall survival rate in ependymoma patients is still poor (39-64% for 5-year survival rate) [Zacharoulis, S. *et al* (2007)]. The prognosis is poorer after relapse and only 25% of patients survive after a first



relapse [Messahel, B. *et al* (2009)] indicating the acquisition of drug and radiotherapy resistance in this tumour. Oligodendrogliomas were included because these tumours respond well to therapy, and these will provide a comparison of the characteristics of tumours susceptible to chemotherapy with chemoresistant tumours. Therefore, this study included both high and low grades tumours for downstream analysis. Studying the characteristics in several types of tumours provides much more useful data and describes basic information from representative cell lines. The comparison of the similarities and differences among cell lines will hopefully promote understanding of the differences between high grade and low grade tumours or between primary and recurrent tumours.

**All primary cultured cell lines demonstrated common histological features of tumours from which they were established.**

It was important prior to undertaking this analysis to make sure that the cell lines being studied were representative of these tumour types and had not been altered in culture. At the beginning, all cell lines were basically characterised (>30 in the CBTRC bank) then the most interesting cell lines were further investigated. Haematoxylin and Eosin staining is a reliable standard method and simple to perform. The classification of tumour presently still relies on Haematoxylin and Eosin staining observed under the light microscope. This technique is an initial screening and routinely used in the pathological department for diagnosis of tumour samples. Therefore, Haematoxylin and Eosin staining was performed on our original tumours to classify and confirm the original diagnosis. Histological features from each cell line are shown in Figure 3.1 and 3.2 and the descriptions of Haematoxylin and Eosin results are also mentioned in section 3.2.2. All primary cultured cell lines showed classical histological features of the corresponding tumours from which they were derived with the exception of EPN-1 cell line. This cell line was derived from the third surgery and the patient had been treated with several complete courses of chemotherapy and radiation prior to surgery. Haematoxylin and Eosin staining, which was processed on the corresponding formalin-fixed, paraffin-embedded (FFPE) sample from the third surgery, did

not show classic ependymoma histological features. In contrast, the histological feature showed capillary branching, which is commonly found in oligodendroglioma (Figure 3.1, a). However, specific characteristic of ependymoma was observed using EM assay, which showed ependymal cilia (Figure 3.1, b). Hence, EM assay result confirmed that ependymoma is the final diagnosis for this tumour. Haematoxylin and Eosin results therefore indicated that all 7 cell lines would be expected to present specific representative characteristics of each tumour type hence justifying their inclusion in this study.

**Huge variation of chromosome number was observed in PFSK-1 whilst all paediatric primary culture cell lines contained less variation.**

Human chromosome number was first described in 1923 by Painter, T. However, the right chromosome number (46) was discovered by Tjio, J. H. and Levan, A. in 1956. In 1958, human chromosome number was studied in different 13 human samples from different organs and also derived samples, which were grown *in vitro*. Tjio and Puck found that chromosome numbers of 46 were found in 99.9% from almost 2,000 cells whilst the frequency of tetraploidy was observed at less than 3% [Tjio, J. H. and Puck, T. T. (1958)]. Therefore, normal human chromosome number is stable at 46 and has a very narrow range of chromosome number. Many previous studies found a variation of chromosome number in brain tumours. Griffin, C. A. and colleagues studied the chromosome abnormalities in paediatric brain tumours; 6 astrocytomas, 10 CNS PNETs, 2 atypical teratoid tumours, 1 mixed glioma, 1 ependymoma and 1 meningioma. Their data showed that chromosome numbers of CNS PNET and ependymoma ranging from 41-100 and 43-46, respectively [Griffin, C. A. *et al* (1988)]. Additionally, karyotype data studied in paediatric brain tumours found that there were a variation of chromosome numbers in tumour cells; 50-285 in glioblastoma multiforme, 36-91 in medulloblastoma [Aganmolis, D. P. and Malone, J. M. (1995)], 50-77 in ependymoma [Sainati, L. *et al* (1996)]. A huge variation of chromosome numbers and chromosomal abnormalities were found in aggressive tumours such as glioblastoma multiforme or medulloblastoma while low grade tumour or untreated tumour

have normal karyotype and less variation of chromosome numbers [Aganamol, D. P. and Malone, J. M. (1995), Sainati, L. *et al* (1996) and Bhattacharjee, M. B. *et al* (1997)]. So cancer cells are expected to have abnormal chromosome numbers compared to normal cells. Hence, a simple metaphase spread analysis was performed to investigate the range of chromosome numbers in our cell line when they were cultured in standard tumour media for a certain period (early passage, < 25) compared to the commercial cell line. All cell lines were cultured as monolayer cells in standard tumour media supplemented with 15% fetal bovine serum apart from PFSK-1 cell line, which was cultured in specific media, recommended by ATCC. Analysis results showed that chromosome numbers of our 7 primary cell lines have less variation than the commercial cell line, PFSK-1 (Figure 3.3) and the descriptive statistical data for EPN-2, MED-2, SPNET-1 and PFSK-1 are shown in Table 3.3. The majority of cells are diploid giving a mean of 40-50, some cells are in the lower range but the majority are higher. This was particularly the case for BT-4, the giant cell GBM, and is in-keeping with Griffins results [Griffin, C. A. *et al* (1988)]. Additionally, the PFSK-1 line data was much more widely spread with more homogeneity in chromosome length indicating that this line had altered greatly in culture whilst our cell lines retained the expected variation in chromosome length.

Metaphase analysis results revealed that all 7 paediatric primary cultured cell lines had a narrow range of chromosome number whilst PFSK-1 had a huge variation of chromosome number (7-132, STDEV = 21.76). Hence, a variation of chromosome numbers commonly occurred in tumour cells, the results from metaphase analysis of our cell lines correlated to the previous studies. The majority of chromosome numbers from our primary cell lines ranged from 30-50 while the chromosome numbers of PFSK-1 cell line generally spread from 7 to 132. Therefore, our cell lines contained much narrow range of chromosome numbers than the commercial cell line. Although PFSK-1 cells were able to form colonies (17%) in agar [Fults, D. *et al* (1992)] and also initiated new tumours when they were transplanted into mice brain within 4 weeks [Fults, D. *et al* (1992)], this cell line had been continuously cultured in RPMI medium supplemented with 10% fetal calf serum for over 2 years (85

passages) after establishment from patient. However, it was not clear what passage was provided commercially. Additionally, PFSK-1 was described as hypotetraploid at passage 59 (karyotype: 81, XXYY, t(Xp;8q), del(1)(p22), -2, -3, del(4)(p14), -5, -8, -9, -9, -13, -13, -14, -16, -20, -22, +mar and at passage 75: 84, XXY, -Y, t(Xp;8q), del(1)(p22), -3, del(4)(p14), -9, -10, -13, -14, -14, -16, -22) with loss of chromosome 17 occurring during establishment [Fults, D. *et al* (1992)]. Based on the establishment history of PFSK-1 and our findings, this indicated that PFSK-1 were unstable in culture condition whilst our cell lines were more stable in preserving a narrow chromosome number range. Hence, PFSK-1 was not a good cancer cell line model for PBT research. To complete this assay and extract more useful information, karyotype assay should be performed to determine the abnormalities of chromosomes from each tumour type and define whether the increase in chromosome numbers is hyperdiploidy or tetraploidy.

**Monolayers from all cell lines preserved alterations of chromosomal copy number from the corresponding original tumours.**

Single nucleotide polymorphism analysis (SNP; Affymetrix 500K arrays) was performed on monolayers from 5 primary paediatric cell lines (EPN-1, EPN-2, BT-4, MED-2 and SPNET-1) including the corresponding original tumours and were analysed by Dr. Deema Hussein to determine whether monolayer culture conditions are able to preserve a significant DNA copy number aberration, which is detected in the original tumour samples from which they were derived. The SNP results demonstrated that significant DNA copy number aberrations detected in the original tumours were present in both monolayer and neurosphere culture conditions of all cell lines (Figure 3.4, and data not shown). The chromosomal copy number of the recurrent ependymoma derived EPN-1 cell lines showed gain in regions 1q32.1, 2q32.1, 6p21.33, 11q23.3, 14q11.2, and 17q21.2, which have been reported previously that these aberrations were found in ependymoma tumour [Taylor, M. D. *et al* (2005)]. The primary ependymoma derived EPN-2 cell line demonstrated gain of chromosomal copy number in regions 2p23.1, 2q14.2, 3p14.2, 6q25.3, 7q32.3, 17q12, and loss in 15q11.2.

Ependymoma tumour has been reported to contain an amplification of 3p14.2 [Taylor, M. D. *et al* (2005)]. Chromosomal copy number aberrations in region 1q32.1 and changes in chromosome 7, which were detected in BT-4 cell lines, have also been reported to be found in other glioblastoma tumours [The Cancer Genome Atlas Research Network (2008)]. Gain of chromosomal copy number in region 1p34.2 and loss in 8p23.1 were recently reported as an aberration in medulloblastoma and were present in MED-2 cell line [Northcott, P. A. *et al* (2009)]. The aberrations of chromosome copy number, which are commonly detected in CNS PNETs, are gain of 1q21.3, 2p24.1, and 6p22.1 (unpublished data Suzanne Miller). These aberrations were also preserved in SPNET-1 cell line. In accordance with Haematoxylin and Eosin, metaphase analysis and SNP results, our cell lines were able to preserve important characteristics from the original tumours from which they were derived and they were stable in culture conditions.

In summary, patient tumours showed the hallmark of histological features of the corresponding tumours which they were diagnosed. Our cell lines contained less variation of chromosome number than the commercial cell line and they also preserved significant genetic aberrations from the corresponding original tumours from which they were derived. To examine the existence of CSCs in our cell lines, characterisation of CSCs was studied in Chapter 4.

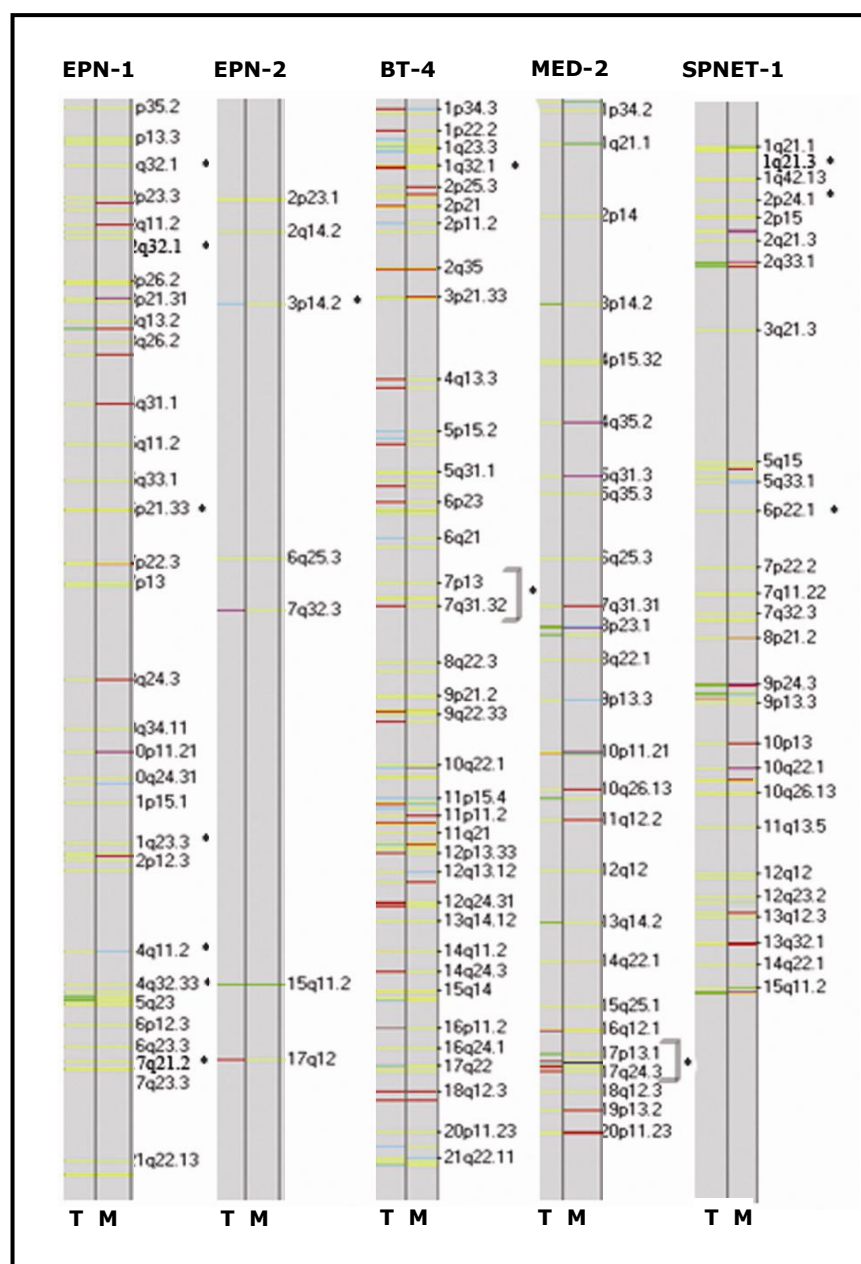


**Figure 3.4 SNP analysis.** SNP analysis was performed on monolayers (M) from EPN-1, EPN-2, BT-4, MED-2 and SPNET-1 cell lines at early passages (less than 25 passages) compared with the original tumours (T) from which they were derived. The results demonstrate that a significant DNA copy number aberrations detected in the original tumours were present in both monolayer culture conditions of all cell lines [The results obtained from Dr. Deema Hussein].

---

---

## **Chapter 4**

### **Characterisation of cancer stem cells**

---

---

## Chapter 4: Characterisation of cancer stem cells

### 4.1 Introduction

The previous chapter described basic characterisation of 5 different paediatric brain tumours including ependymomas, medulloblastomas, CNS PNETs, GMBs and oligodendrogliomas that had been successfully established in tumour media supplemented with serum. Additionally, the results from Chapter 3 demonstrated that Haematoxylin & Eosin staining from tumour specimens, from which paediatric brain tumour cell lines were generated for this study, displayed significant histological features of tumours that they were diagnosed. SNP analysis results also confirmed that significant genetic abnormalities found in the original tumours were preserved in culture. Additionally, our cell lines were more stable in culture than the commercial cell line (PFSK-1) in term of having less variation of chromosome numbers demonstrated by metaphase analysis.

At present, a major unresolved problem of malignancy including paediatric brain tumours is multidrug resistance resulting in tumour relapse and high mortality. Causes of drug resistance in malignancy have been extensively studied. Cancer stem cells, discovered a decade ago, were postulated to be an important cause of drug resistance. Cancer stem cells are a small population of tumour cells and currently are believed to resist to chemotherapy resulting in surviving after treatment and initiating new tumours causing tumour relapse. Cancer stem cells were firstly discovered in a small population of acute myeloid leukaemia (AML) using side-population analysis. These cells initiated new tumours when they were transplanted into NOD-SCID mice [Tan, B. T. *et al* (2006)]. The first evidence supporting the existence of cancer stem cells in brain tumours was discovered in human glioblastoma multiforme. The isolated cells resembled normal neural stem cells in formation of clones and neurospheres and expressing neuronal and astroglial markers [Ignatova, T. N. *et al* (2002)]. In later studies, medulloblastomas and gliomas were also shown to contain cancer stem-like



cells, which were induced to form neurospheres. These neurospheres initiated new tumours when they were transplanted into mouse brain and they were able to be serially passaged. Neurospheres could be induced to differentiate into both neurons and glial cells under differentiation conditions. These cells shared some characteristics with normal neural stem cells and they occasionally differentiated into abnormal cells possibly explaining tumour generation [Hemmati, H. D. *et al* (2003)]. Neural stem-like cells have also been discovered in adult glioblastoma multiforme. These cells had multilineage differentiation and generated new tumours after transplantation. These neural stem-like cells isolated from initiated tumours were used to form neurospheres, which were serially transplanted into mice and formed new tumours [Galli, R. *et al* (2004)].

To study cancer stem cells, many studies used different stem cell markers to identify and isolate these cells and methods used to isolate cells were also different. Singh and colleagues used CD133 to isolate cancer stem-like cells using magnetic cell sorting. CD133<sup>+</sup> cells were able to initiate tumour, which was recapitulate the original tumours when they were transplanted, these cells had the abilities to form neurospheres, self-renew and proliferate [Singh, S. K. *et al* (2003)]. In a later study, Singh and colleagues found that tumours, which were initiated from CD133<sup>+</sup> cells, contained a small proportion of CD133<sup>+</sup> cells (19-22%) and a majority population of CD133<sup>-</sup> cells (78-81%). Therefore, they suggested that CD133<sup>+</sup> cells were able to produce both CD133<sup>+</sup> cells and CD133<sup>-</sup> cells in initiated tumours [Singh, S. K. *et al* (2004)]. SOX2 is also generally used as a stem cell marker due to the fact that SOX2 is a nuclear transcriptional factor, which is normally expressed in embryonic stem cells and neural stem cells [Graham, V. *et al* (2003)]. Since then, many laboratories extensively studied cancer stem cells in brain tumours to understand the mechanisms of drug resistance, which may open the door to overcoming drug resistance in adult and paediatric brain tumours.

The aim of this Chapter is to characterise cancer stem cells in newly established paediatric brain tumour cell lines. One of the significant characteristics of cancer stem cells is

neurosphere formation [Tan, B. T. *et al* (2006), Ignatova, T. N. *et al* (2002) and Galli, R. *et al* (2004)]. To test ability in formation of neurospheres, all cell lines normally grown as monolayers in tumour media were induced in stem cell media to form neurospheres at early, middle and late passages. CD133 and SOX2 were used as stem cell markers to identify cancer stem cells in our cell lines by co-staining immunofluorescence and Western blotting analysis. Since CD133 [Singh, S. K. *et al* (2003) and (2004)] and SOX2 [Graham *et al* (2003) and Miyagi, S. *et al* (2004)] have been generally used as a stem cell markers. Identification of cancer stem cells was performed in both monolayer and neurospheres conditions to compare the proportion of cancer stem cells in different culture conditions. Additionally, the assay was performed at early, middle and late passages to determine any alteration of cancer stem cell proportion when cell lines were serially passages. Western blotting analysis was performed to investigate CD133 and SOX2 expression at protein level and validate the immunofluorescence data.

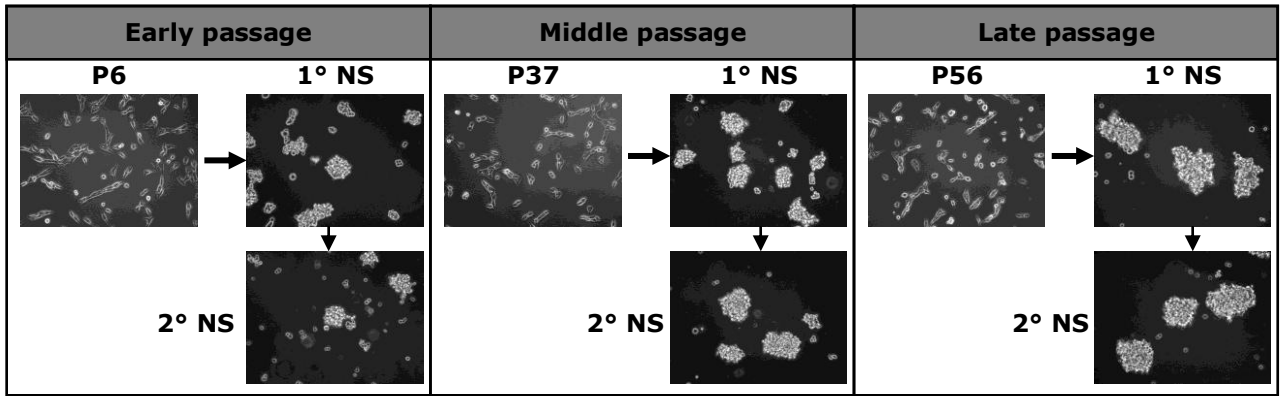
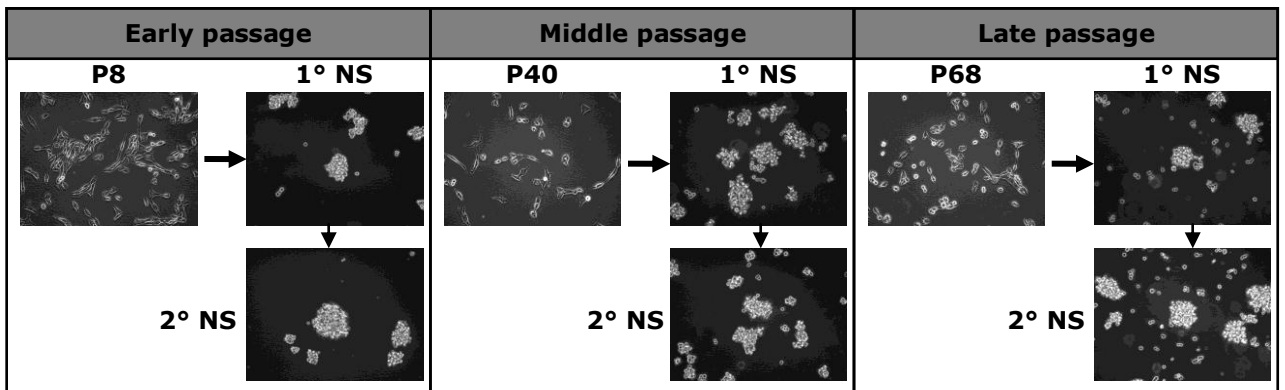
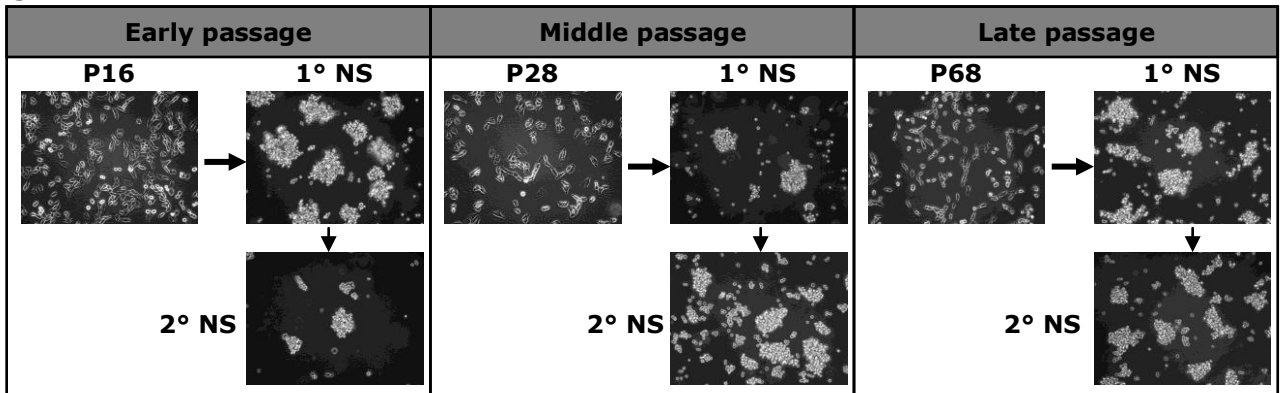
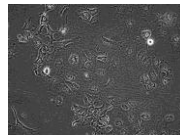
Telomerase activity and telomere maintenance have been postulated as significant factors to preserve immortality in cancer cells. Telomerase activity is also a feature of normal stem cells. Telomeres are usually maintained in malignant cells and 85-90% of these cells are telomerase positive [Bryan, T. M. and Cech, T. R. (1999)]. To demonstrate activation of telomerase in our cell lines, the Telomeric Repeat Amplification Protocol (TRAP) assay was performed in both monolayers and neurospheres from all cell lines. Telomere length was also assessed using the Terminal Restriction Fragment length (TRF) assay in our cell lines in both monolayers and neurospheres at early, middle and late passages to investigate telomere maintenance and determine any alteration of telomere length at different time points.

## 4.2 Results

### 4.2.1 Primary cultured monolayers and neurospheres of paediatric brain tumour cell lines at early, middle and late passage

There were 7 cell lines studied in the overall project. However, only 3 cell lines were the subject of my experiments; EPN-2, MED-2 and SPNET-1. The remainder were studied by Dr. Deema Hussein, a Post Doctoral researcher. Cell line stocks from the CBTRC liquid nitrogen bank were recovered as described in section 2.1.1 and cultured as monolayers in tumour media. All cell lines were successfully grown in tumour media. PFSK-1 cells were initially cultured in the standard tumour media however, they failed to survive in this media. They had to be cultured in media specifically recommended by LGC Promochem for this cell type.

All primary culture paediatric cell lines used in this study were serially subcultured as monolayers in standard tumour media supplemented with serum up to at least 80 passages. Neurospheres were continuously re-established from monolayer cells and cells from both growth conditions were collected at different passages for experiments. Morphological features of cultured monolayers and neurospheres from each cell line at early, middle and late passage are shown in Figure 4.1. When PFSK-1 cells were cultured in stem cell media, they attached to the flask and did not form neurospheres even after 7 days of incubation. Therefore, under these conditions the PFSK-1 cell line could not be induced to form neurospheres. The morphological features of all cell lines were not visibly changed even when they were serially subcultured at late passage. All cell lines were also still able to be induced to form neurospheres even at late passage number. The passage numbers of monolayers and neurospheres were matched as close as possible prior to analysis. The passage number was separated into 3 categories; early passage (less than 25), middle passage (26-50) and late passage (more than 50). The number next to cell line names indicates the passage number, which is continually counted when cells are subcultured. For neurospheres, the passage number, which is initially induced from monolayers, is designated as primary neurosphere (1° NS) and when 1° NS was passaged, they are called secondary neurospheres (2° NS). All experiments were always performed on 2° NS.

**EPN-2****MED-2****SPNET-1****PFSK-1**

Failed to  
form NS

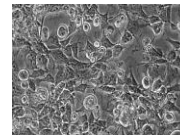


**Figure 4.1 The morphology of serially cultured EPN-2, MED-2 and SPNET-1 cell lines as monolayer and neurosphere condition at early, middle and late passage and PFSK-1 cell line.** This figure shows the morphology of cultured cell lines at different time points when they were serially subcultured as monolayers. All cell lines were stably grown in tumour media even at very late passages and the morphology did not obviously change when the passage number increased. Primary neurospheres were formed when monolayers were induced in stem cell media at any passage number. Secondary neurospheres were also able to be properly formed when primary neurospheres were passaged. Neurosphere sizes range from 30 – 100  $\mu\text{m}$ .

### 4.2.2 Doubling time

EPN-2, MED-2 and SPNET-1 cell lines were serially subcultured as monolayers and passaged to form neurospheres whereas PFSK-1 monolayers were unable to be induced to form neurospheres. To determine the growth characteristic of cultured cell lines when they were continually passaged for a long period of time, a doubling time assay was performed on both monolayers and neurospheres (with the exception of PFSK-1). The doubling time of all cell lines was determined at early, middle and late passage number to study the variation in doubling time when cells were serially subcultured for a long period of time. The doubling time is the amount of time that cells require to double in number. The doubling time results are shown in Figure 4.2. The formula used to calculate the doubling time is shown below.

$$T_d = (T_2 - T_1) \times \frac{\log 2}{(Q_2 - Q_1)}$$

$T_d$  = Doubling time (hour)

$T_1$  = Time when cells were plated

$T_2$  = Time that cells reached subconfluency

$Q_1$  = Original cell numbers that were plated

$Q_2$  = Final cell numbers

Doubling times of all cell lines were examined at early, middle and late passage number in both monolayers and neurospheres. To compare the difference of the doubling time at different passages or between monolayers and neurospheres, unpaired student T-test was performed. PFSK-1, a commercial cell line, had the longest doubling time (mean  $\pm$  SEM)  $32.1 \pm 1.2$  hours when compared to other monolayers ranging from 20.3 - 23.5 hours (Figure 4.2). One way Anova was used to compare the difference in doubling time at early, middle and late passage number. Doubling times at early, middle and late passage of this cell line were not significantly different ( $p = 0.158$ ). Therefore, this cell line had a consistent growth rate even when they were serially subcultured for a long period of time.

The results in Figure 4.2 show that each cell line has a different characteristic growth pattern. The average doubling times of EPN-2 monolayers and neurospheres were  $20.6 \pm 1.1$  and  $38.4 \pm 2.3$ , respectively and they were significantly different ( $p < 0.001$ ). As passage numbers increased, the doubling time of monolayers remained constant at all passages ( $p > 0.05$ ) as shown in Figure 4.2 (a). On the contrary, the doubling time of neurospheres apparently increased when passage numbers increased and they are significantly different between early, middle and late passages ( $p = 0.001$ ). At all passage numbers of EPN-2 cells, the average doubling time of neurospheres was significantly higher than the monolayers [Figure 4.2, (a)] (unpair student T-tests,  $p < 0.01$ ).

The average doubling times of MED-2 monolayers and neurospheres were  $23.5 \pm 1.6$  and  $25.4 \pm 2.4$ , respectively. The average doubling time of neurospheres was higher than that of monolayers however there was no significant difference ( $p > 0.05$ ) and the average doubling times of neurospheres were not consistently higher than monolayers at early, middle and late passages. Monolayer doubling times remained constant when passage numbers increased ( $p > 0.05$ ). Whilst, the doubling time of neurospheres increased when passage numbers increased and they were significantly different ( $p < 0.001$ ) at early, middle and late passages [Figure 4.2, (b)].

The average doubling time of SPNET-1 monolayers and neurospheres were  $20.3 \pm 1.5$  and  $24.9 \pm 2.0$ , respectively and there was no difference between them ( $p > 0.05$ ). The average doubling times of neurospheres at early, middle and late passages were not consistently higher than that of monolayers. The doubling times of both monolayers and neurospheres decreased when passage numbers increased. The doubling times among monolayer group at early, middle and late passages were not different ( $p > 0.05$ ) whilst there were significant difference in neurosphere group ( $p < 0.001$ ) [Figure 4.2, (c)].

Each paediatric cell line showed different characteristics and patterns in doubling time when these cells were serially subcultured over a long period of time. However, the average

doubling times showed a similar pattern among EPN-2, MED-2 and SPNET-1 cell lines when compared between monolayers and neurospheres [Figure 4.2 (a-c)]. The average of doubling times of neurospheres was higher than monolayer cells. However, only the EPN-2 cell line showed significantly different doubling time in neurospheres compared to monolayers ( $p < 0.001$ ). Additionally, the average of doubling times at early, middle and late passages in monolayers from all cell lines was consistent whilst they were variable in neurospheres.

When merging the data from all 7 cell lines (Figure 4.3), it can be seen that the mean doubling time in neurospheres was higher than monolayers in all cell lines. However, only EPN-1, EPN-2, MED-1 and Olig-1 neurospheres had significantly higher mean of doubling times compared to monolayers.

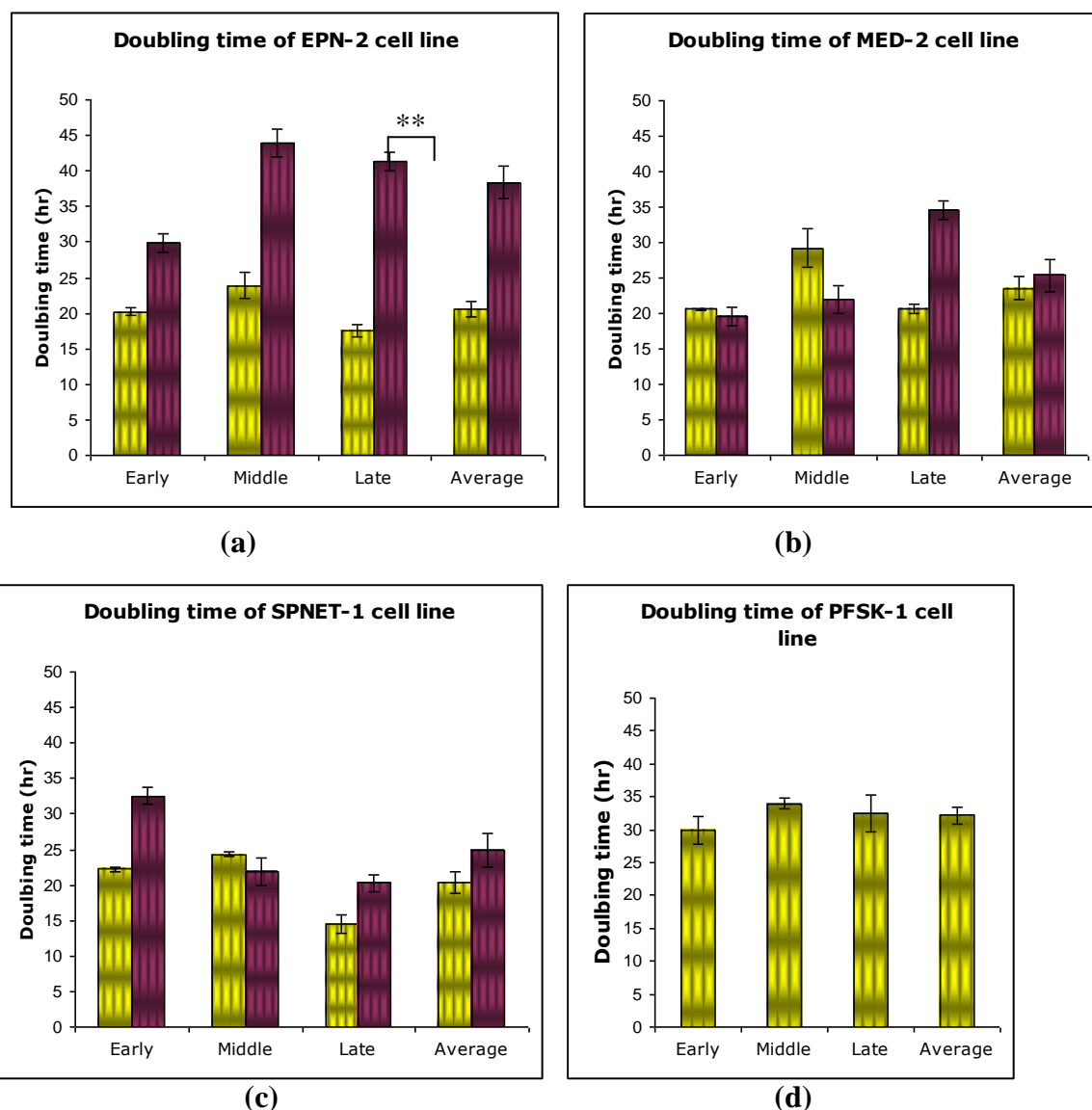


**Figure 4.2 Doubling times at early, middle and late passage number of monolayer and neurosphere from primary cultured cell lines.** Doubling times of EPN-2, MED-2, SPNET-1 and PFSK-1 cell lines at early, middle and late passage are shown in (a), (b), (c) and (d), respectively [ ■ = monolayers, ■ = neurospheres]. The average doubling time of all cell lines showed similar patterns whereby neurospheres had longer doubling times than monolayers. The doubling times of neurospheres from EPN-2 were significantly higher than monolayers at all passages (a). This was not the case for the MED-2 (b) and SPNET-1 (c) cell lines since the comparison between monolayers and neurospheres at different passages was variable. However, doubling times of monolayers from all cell lines were fairly stable at all passage numbers. PFSK-1 cell line also showed a constant growth rate throughout all passages (d).



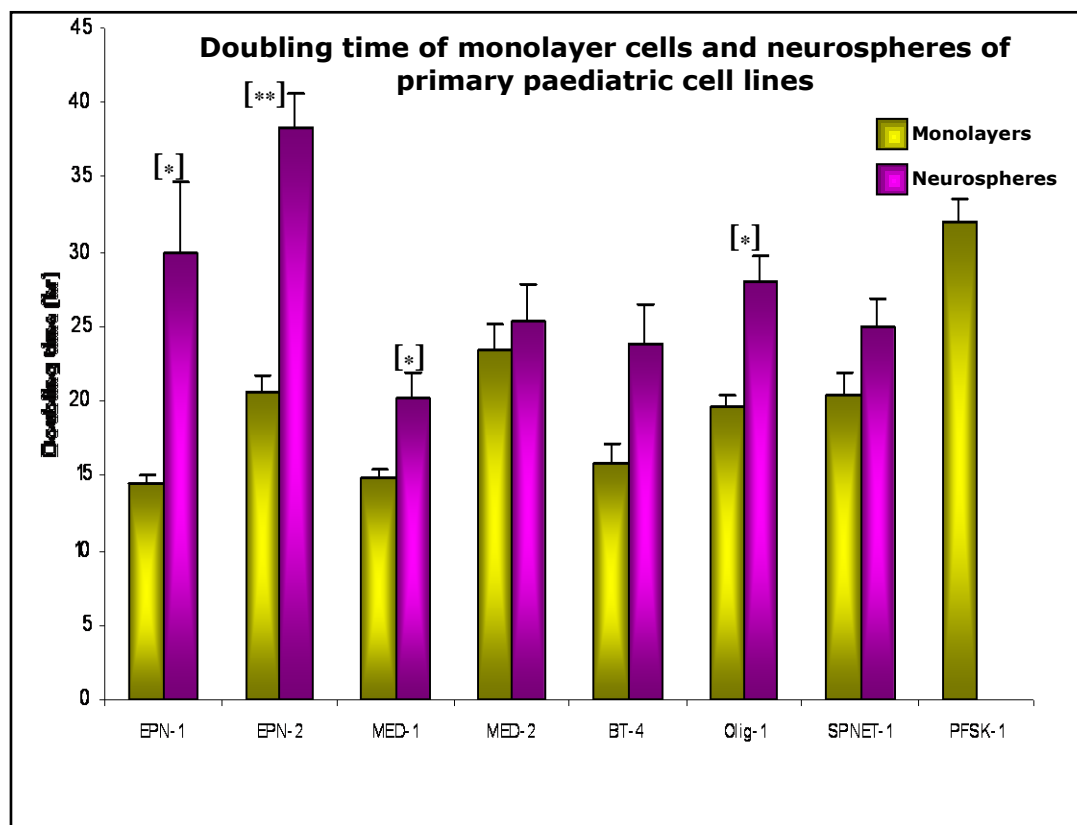


**Figure 4.3 Doubling time means of monolayers and neurospheres from all primary paediatric cell lines.** This graph shows doubling time means from all 7 cell lines including 4 data sets obtained from Dr. Deem Hussein. Neurosphere doubling times of all cell lines were higher than monolayers however, only the doubling times of EPN-1, EPN-2, MED-1 and Olig-1 cell lines were significantly longer than that of monolayers ( $** = p < 0.01$ ,  $* = p < 0.05$ ). PFSK-1 cell line had the longest doubling time than the other cell lines among monolayers whereas the longest neurosphere doubling time was found in EPN-2 cell line. Interestingly, the pattern of neurosphere growth rate was distinctively observed in EPN-1 and EPN-2 cell lines. Neurospheres of ependymoma from which EPN-1 and EPN-2 cell lines were derived had a significant slower growth rate than that of monolayers.

#### 4.2.3 Co-staining CD133 and SOX2 immunofluorescence analysis

Co-staining immunofluorescence was performed to study the existence of a cancer stem cell-like population in primary cultured cell lines under both monolayer and neurosphere conditions. For monolayer conditions, cells were grown in serum supplemented tumour media which supported cells to normally proliferate whilst neurosphere conditions, serum-free media, promoted cells to proliferate without differentiation. Neurosphere conditions were expected to contain a higher percentage of stem cell-like cells since many studies supported that these conditions can preserve characteristics of cancer stem cells [Reynold, B. A. and Weiss, S. (1992) and Lee *et al* (2006)]. Co-staining immunofluorescence was also performed at different time points: early, middle and late passage to determine whether increasing passage number affects the proportion of stem cell-like cells in each condition or not. CD133 and SOX2, which are commonly used to study cancer stem cells, were used as stem cell markers.

The immunofluorescence results shown in Figure 4.4 are representative images from each cell line. Positive co-staining CD133 and SOX2 immunofluorescence was defined as obvious membranous staining of CD133 antibody (green signal) and nuclear or cytoplasmic staining of SOX2 antibody (red signal). Positive co-staining cells were counted as stem cell-like cells as shown in Figure 4.4. Cells were counted at x40 and x100 magnification for monolayers and neurospheres, respectively and more than 600 cells were counted to determine the proportion of stem cell-like cells in each condition for all cell lines. Immunofluorescence results showed no CD133 positive cells in PFSK-1 monolayer cells (Figure 4.4). As previously mentioned, PFSK-1 monolayer cells could not be induced to form neurospheres, which is one of significant characteristic of stem-like cells, when they were grown in stem cell media. Therefore, it was concluded that based in these criteria there was no stem cell-like population in PFSK-1 cell line.

Co-staining immunofluorescence results in primary cultured cell lines (EPN-2, MED-2 and SPNET-1) showed that positive co-staining cells were observed in both monolayer and

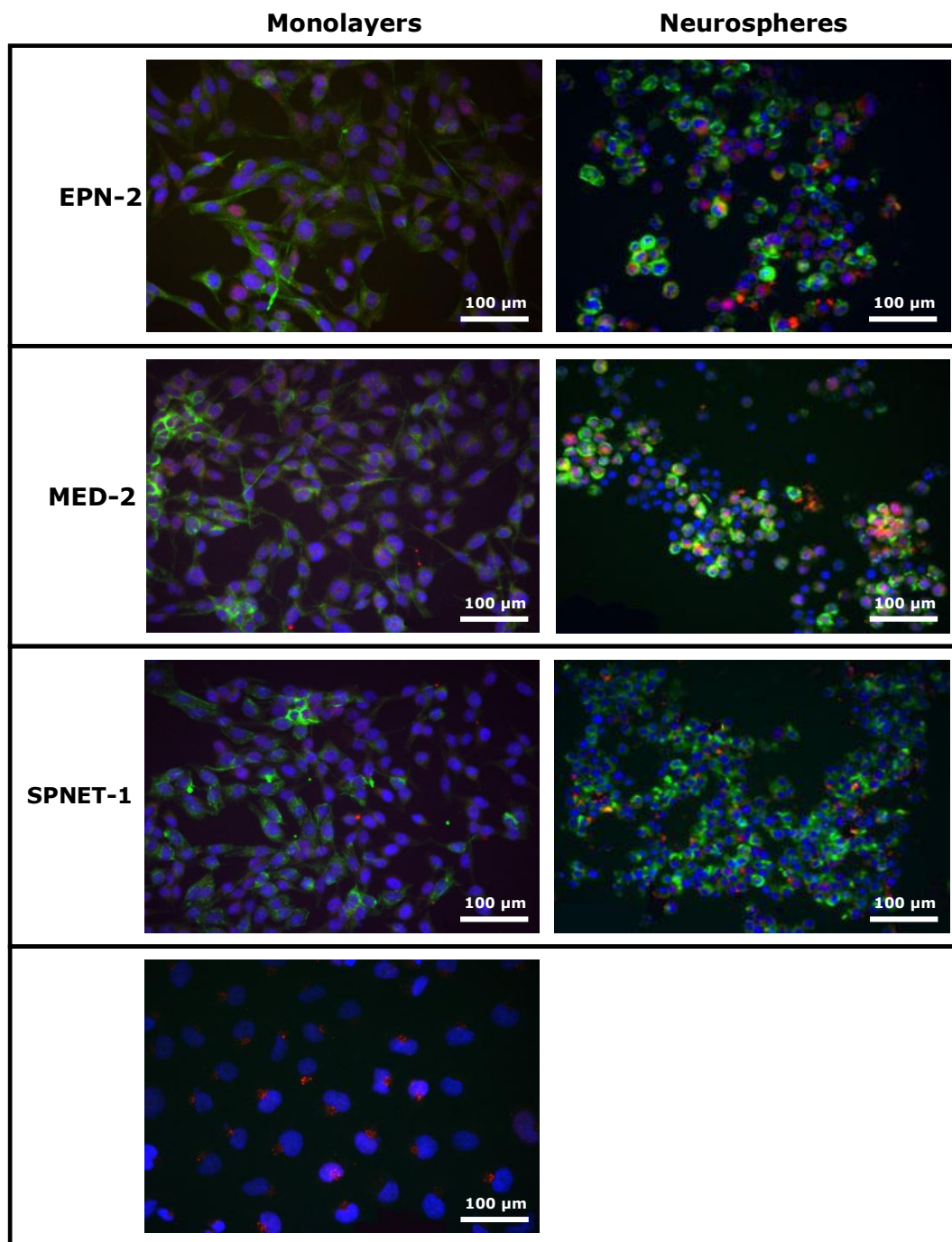


**Figure 4.4 Co-staining CD133 and SOX2 immunofluorescence in monolayers and neurospheres of primary cultured cell lines and PFSK-1.** Co-staining immunofluorescence results of EPN-2, MED-2 and SPNET-1 cells showed typical double staining cells described as membranous staining of CD133 (1:200, green signal) and nuclear staining of SOX2 (1:75, red signal). PFSK-1 cells were negative for CD133 and SOX2 staining. Approximately 40-50% of co-stained CD133 and SOX2 cells were detected in neurospheres as shown in the right column whereas in monolayer cultured cells co-staining CD133 and SOX2 represented only 10-15% of the total (left column).

neurosphere conditions (Figure 4.4). However, monolayer conditions for all of the cell lines contained a smaller proportion of co-staining cells (~10-15%) (Figure 4.4, left column) than neurosphere conditions where almost half of neurosphere population were positive for CD133 and SOX2 (~30-45%) (Figure 4.4, right column). Hence, the neurosphere population comprised a larger proportion of cells co-staining CD133 and SOX2 than monolayers. Therefore, cells grown under neurosphere conditions were enriched with stem cell-like cells when compared to monolayer conditions.

All 3 primary cell lines (EPN-2, MED-2, SPNET-1) showed a similar pattern of co-staining CD133 and SOX2 with increased passage number, namely that the proportion of positive co-staining cells decreased (Figure 4.5). The proportion significantly decreased in EPN-2 cell line (monolayers  $p < 0.05$ , neurospheres  $p < 0.01$ ) and SPNET-1 cell line (monolayers and neurospheres  $p < 0.05$ ), whilst there was no significant decreasing in both monolayers and neurospheres of MED-2 cell line (monolayers  $p = 0.40$ , neurospheres  $p = 0.21$ ). The percentage of positive co-staining cells was higher in neurospheres (almost 4 fold) when compared to monolayers; EPN-2 (monolayer =  $10.3 \pm 1.3$ , neurosphere =  $37.5 \pm 4.0$ ), MED-2 (monolayer =  $10.6 \pm 1.1$ , neurosphere =  $37.9 \pm 2.5$ ) and SPNET-1 (monolayer =  $9.6 \pm 1.1$ , neurosphere =  $35.6 \pm 2.8$ ).

To study the proportion of stem cell-like cells in paediatric brain tumour cell lines, not only the main 3 cell lines were investigated but the other 4 cell lines at early passage (EPN-1, MED-1, BT-4 and Olig-1) were also included in this assay to determine the proportion of cancer stem-like cells in all primary cell lines (Figure 4.6). The average proportion of positive co-staining cells across all 7 cell lines was then evaluated. The proportion of positive cells was significantly higher in neurospheres ( $p < 0.01$ ) ranging from 30-40% compared to monolayers comprising of 8-12% positive cells (Figure 4.6). Additionally, there was no correlation between the proportion of stem cell-like population and types of tumours (primary or recurrent) or grading in both monolayers and neurospheres (Figure 4.6).

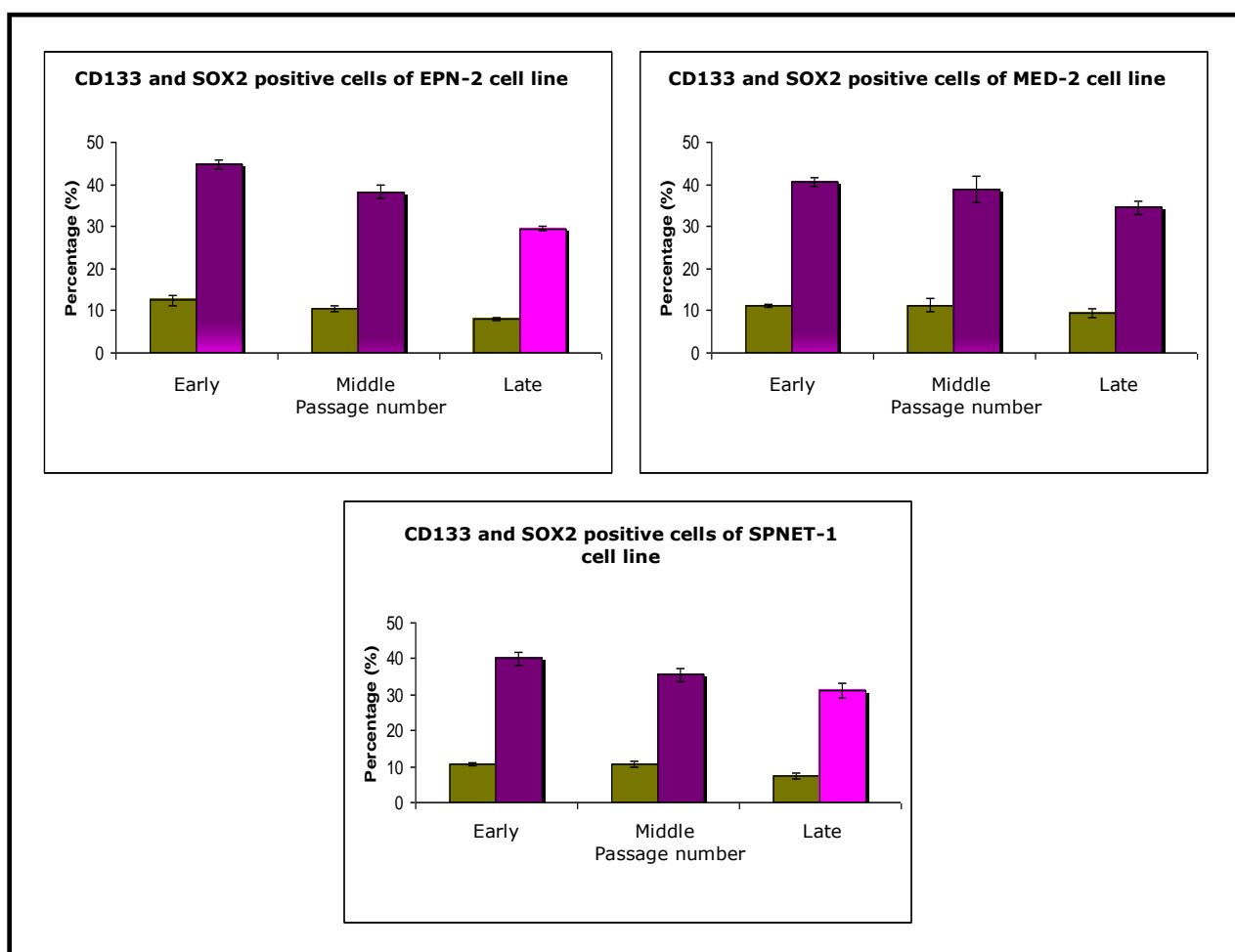


**Figure 4.5 The percentage of CD133 and SOX2 co-staining cells at early, middle and late passage from monolayers and neurospheres.** CD133 and SOX2 co-staining was performed at early, middle and late passage number of EPN-2, MED-2 and SPNET-1 monolayers (■) and neurospheres (■). All cell lines expressed similar characteristics of CD133 and SOX2 expression with increasing passage number. The percentage of CD133 and SOX2 co-expressing cells slightly decreased in both monolayer culture and neurosphere culture when passage numbers increased. Monolayer cells and neurospheres expressed CD133 and SOX2 in approximately 10% and 35-45%, respectively. Decline of co-staining cells was clear in neurospheres when passage number increased. The proportion of cells co-expressing CD133 and SOX2 in neurospheres was nearly 4 fold higher than monolayers from all cell lines at any passages.

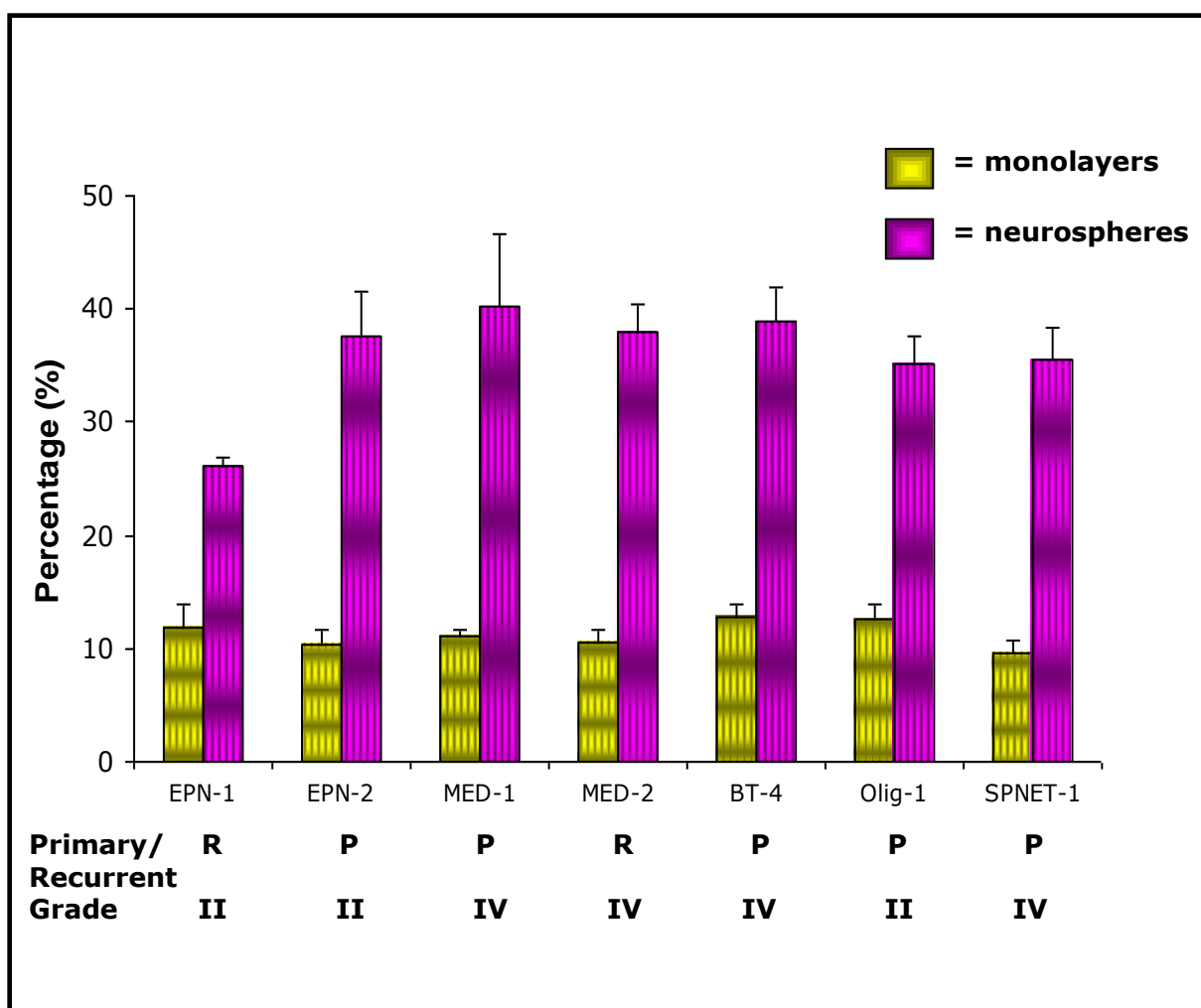


**Figure 4.6 The percentage of positive co-staining cells in all 7 primary cell lines.**

This graph shows the average percentage of positive co-staining CD133 and SOX2 cells from EPN-1, EPN-2, MED-1, MED-2, BT-4, Olig-1 and SPNET-1 cell lines in both monolayer and neurosphere culture at early passage. Neurospheres from all cell lines contained 30-45% positive co-staining cells whilst there were only 8-12% positive cells in monolayers. EPN-1 and MED-2 cell lines were recurrent tumours (R) whereas the others were primary tumours (P). The percentage of co-staining cells either in monolayers or neurospheres from all cell lines had no correlation with the grading (I-IV) or type of tumour (primary or recurrent tumour).

#### **4.2.4 CD133 and SOX2 expression detected using Western blotting analysis**

To validate the data from co-staining immunofluorescence, Western blotting analysis was performed to detect CD133 and SOX2 expression in the 3 primary cultured cell lines (EPN-2, MED-2 and SPNET-1) and the commercial cell line (PFSK-1) in both monolayer and neurosphere conditions at early passage. This assay was performed to confirm whether neurospheres expressed higher level of CD133 and SOX2 than monolayers. CD133 expression was detected from the membranous fractions whilst SOX2 expression was detected from total cell lysates retaining the nuclear and cytoplasmic fractions.

NTERA-2 cells, which expressed a high level of CD133 at ~120 kDa (Figure 4.7) were used as a positive control and were compared to the CD133 expression in monolayers and neurospheres of EPN-2, MED-2, SPNET-1 and PFSK-1 cell lines. The detected size of CD133 in our cell lines was ~140 kDa probably due to additional glycosylation. Western blotting analysis showed that neurospheres from all 3 primary cultured cell lines expressed higher levels of glycosylated CD133 when compared to their monolayers. In the light of the negative immunofluorescence for PFSK-1, it seems possible that the bands observed on Western blotting analysis may represent non-specific reaction of the antibody.

NTERA-2 cells were also used as a positive control for SOX2 expression. A SOX2 band of 37 kDa was detected in NTERA-2 cells as expected. SOX2 expression was detected at a very low level in all cell lines including the positive control (NTERA-2) whereas PFSK-1 cells gave a strong positive band of SOX2 (Figure 4.7). The protein extraction process was optimised and different methods to extract the appropriate fraction enriched with nuclei and cytoplasm were attempted. Additionally, different SOX2 antibodies were tested. Unfortunately, despite these changes the level of SOX2 detected in our cell lines and the NTERA-2 control remained too low for effective detection by Western blotting.

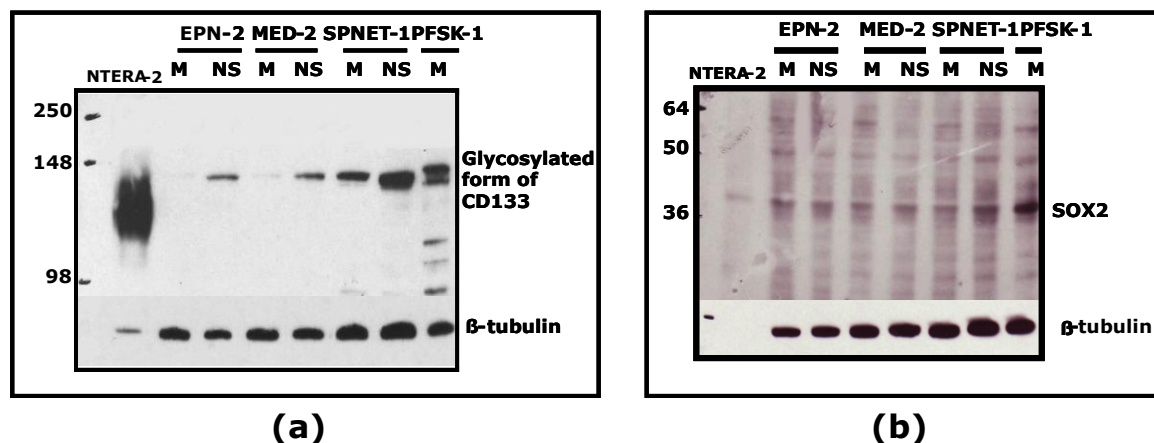


**Figure 4.7 Detection of CD133 and SOX2 expression using Western blotting analysis in primary paediatric cell lines.** NTERA-2 cells were used as positive control and highly expressed CD133 when detected with the Miltenyi CD133 antibody (1:100). CD133 expression was detected in the membrane fraction and CD133 expression in neurospheres (NS) showed stronger intensities than monolayers (M). This data correlated to co-staining immunofluorescent data. NTERA-2 cells were also used as a positive control for SOX2. SOX2 antibody, R&D system (1:150), detected an equally low level of SOX2 expression in all samples. However, PFSK-1 cells highly expressed SOX2 when compared to other cell lines. Loading controls detected by  $\beta$ -tubulin are also shown. The membrane fraction samples were loaded 60  $\mu$ g/well and total cell lysate samples were loaded 100  $\mu$ g/well whilst NTERA-2 cell extraction was loaded 5  $\mu$ g/well. Membranes were incubated in primary antibody for overnight at 4°C.



#### 4.2.5 Telomeric Repeat Amplification Protocol (TRAP) assay

Maintenance of telomere length is an important mechanism for tumour cells to survive beyond the limited cell division that occurs in normal cells. A significant factor that extends the length of telomere in cancer cells is the enzyme telomerase. This enzyme is activated in cancer cells to extend telomere length, thus these cancer cells can escape from senescence and apoptosis resulting in indefinite cell division. Telomerase may also remain active if a stem cell has been transformed [Lee, J, *et al* (2006)]. Therefore, the TRAP assay was performed to study telomerase activity. Positive telomerase activity will indicate that the active telomerase is maintaining telomere length in these cancer cells.

The TRAP assay was performed to determine the degree of activation of telomerase activity in monolayers and neurospheres from all 7 primary cultured cell lines; EPN-1, EPN-2, MED-1, MED-2, BT-4, Olig-1 and SPNET-1 at early passage (Figure 4.8). Human neural stem cells (hNSCs), adult glioblastoma cells (U87), PFSK-1 and the positive control supplied with the TRAP kit were all used as positive controls. The TRAP assay was independently repeated 3 times then telomerase activity was quantified using the Quantity One software to analyse the level of telomerase activity (Figure 4.9). A representative figure is shown in Figure 4.8. Telomerase products were seen as incremental 6 bp ladder bands starting from 50 bp (Figure 4.8). Internal positive control bands detected at 36 bp were also seen in individual samples (Figure 4.8, bottom bands). All positive controls expressed high telomerase activity and telomerase processivity was also detected in all cell lines, both monolayers and neurospheres. The quantitative data shown in Figure 4.9 allows comparison of processivity between monolayers and neurospheres from each cell line. The TRAP assay showed that the telomerase activity was present in both monolayers and neurospheres of all cell lines with EPN-1, EPN-2 and MED-1 cell lines showing high processivity of telomerase in both monolayers and neurospheres. Neurospheres from BT-4 and SPNET-1 cell lines have visibly higher telomerase processivity than that of monolayers, whilst MED-2 (grade IV recurrent tumour) and Olig-1 (grade II primary tumour) have low levels of telomerase activity in both conditions. However, telomerase activity was consistently active in both monolayers and

neurospheres of all cell lines in all 3 individual experiments. There is no significant difference in telomerase activity between monolayers and neurospheres from all cell lines (unpaired student T-test). Tumour grade and recurrence status suggests that there is no correlation with the degree of telomerase processivity.

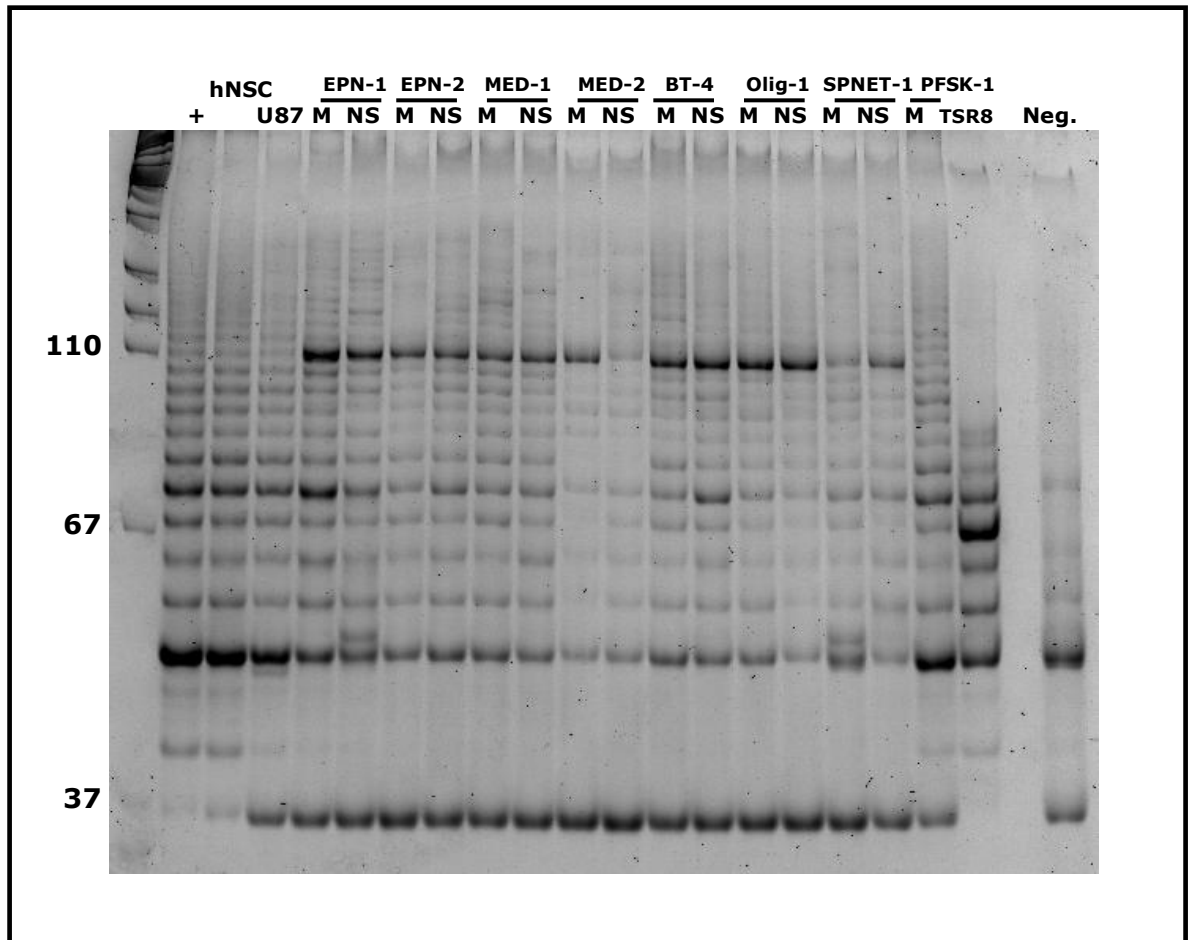


**Figure 4.8 Telomerase activity is present in monolayers and neurospheres of all 7 primary cultured cell lines.** Telomerase products are shown as incremental 6 bp ladder bands starting from 50 bp. The positive controls were human neural stem cells (hNSCs), adult glioma cells (U87) and PFSK-1 all of which have high telomerase processivity. Telomerase was consistently active in monolayers (M) and neurospheres (NS) derived from EPN-1, EPN-2, MED-1, MED-2, BT-4, Olig-1 and SPNET-1 cell lines in 3 individual experiments (a representative figure is shown). Additional controls were the telomerase positive cells (+), TSR8 PCR control template and the lysis buffer only sample (Neg.). The internal positive control product is seen at 36 bp. Samples were loaded 0.01 µg/well.

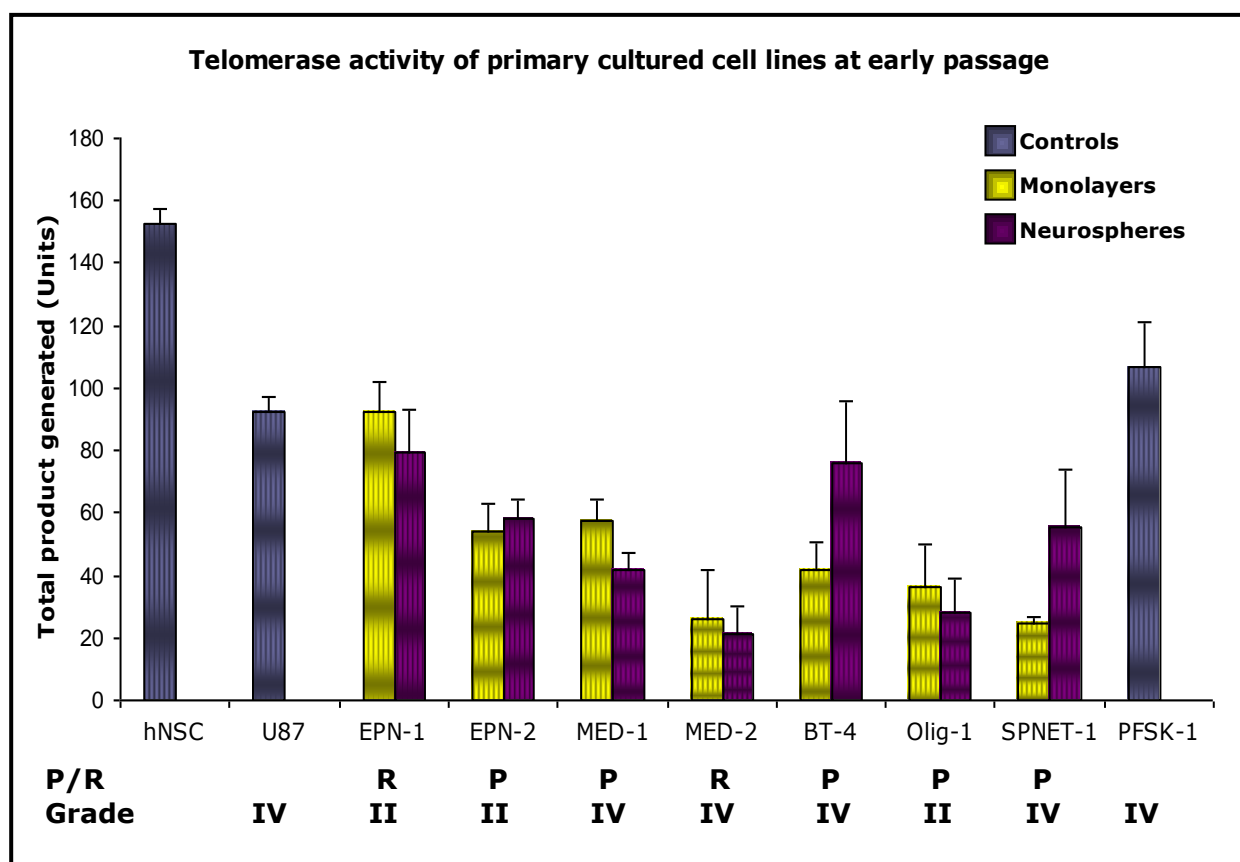


**Figure 4.9 The quantification of telomerase activity in EPN-1, EPN-2, MED-1, MED-2, BT-4, Olig-1, SPNET-1 and PFSK-1 cell lines at early passages.** Telomerase activity was quantified from the density of telomerase processivity using the Quantity one software. The quantification data of telomerase activity from all cell lines are shown in the graph to allow comparison of the processivity between monolayers and neurospheres. Monolayers of the EPN-1 cell line, a recurrent (R) ependymoma, have the highest telomerase activity while the MED-2 cell line, a recurrent medulloblastoma, has the lowest level of telomerase activity. Neurospheres from EPN-2, a primary (P) ependymoma, BT-4 and SPNET-1 cell lines have a higher telomerase processivity than that of monolayers but it is not statistically significant ( $p$  value = 0.738, 0.199 and 0.167, respectively). Additionally, the processivity compared between monolayers and neurospheres from all cell lines was not significantly different (unpair student T-test,  $p$  value > 0.05). The analysis of the total product was described in section 2.7.5.

#### 4.2.6 Terminal Restriction Fragments (TRF) assay or Telomere length assay

Telomere length of normal somatic cells is shorter after each round of the cell cycle and this mechanism limits the number of cell division [Harley, C. B. and Futcher, A. B. (1990)]. When the length of telomere becomes too short (crisis), cells will go into senescence or undergo apoptosis. However, this mechanism is aberrant in tumour cells where tumourigenic cells can escape from senescent and apoptotic processes. The Terminal Restriction Fragment (TRF) assay complements the TRAP assay and was performed to investigate whether the telomere length is maintained in our primary cultured cell lines.

The TRF assay was performed on monolayers and neurospheres of EPN-2, MED-2, SPNET-1 and PFSK-1 cell lines at early, middle and late passage number. hNCS, U87 and U373 (both adult glioblastoma cells) were used as positive controls. Telomere length was detected as a smear shown in Figure 4.10. Mean telomere length was analysed using the Quantity One software and the data are shown in table 4.1. hNSC had the longest telomere length (8.6 kbp) while telomere length of U87 and U373 was 5.7 and 3.9 kbp, respectively. The telomere length in our cell lines ranged from 4-8 kbp. Mean telomere length of neurospheres (NS) was shorter than monolayers (M) in EPN-2 ( $M=5.8\text{kb}\pm0.2$  and  $NS=4.5\text{kb}\pm0.2$ ) and MED-2 cell lines ( $M=6.3\text{kb}\pm0.8$  and  $NS=6\text{kb}\pm0.6$ ) (Table 4.1), whilst a shorter mean telomere length was observed in monolayers from SPNET-1 compared to neurospheres ( $M=6\text{kb}\pm0.51$  and  $NS=6.62\text{kb}\pm0.85$ ) (Table 4.1). However, this did not reach statistical significance (Table 4.1). Telomere length was maintained in both monolayers and neurospheres of all cell lines at all passages. Thus, consistent with the TRAP assay data it appears that the 7 cell lines are all able to perpetuate their telomeres at a length suitable for cell survival.

**Table 4.1 Mean telomere length of EPN-2, MED-2 and SPNET-1 cell lines**

Cell line	Telomere length (kb)		Independent student t-test ( <i>p</i> value)
	Monolayer	Neurosphere	
<b>EPN-2</b>	5.8±0.2	4.5±0.4	0.055
<b>MED-2</b>	6.3±0.8	6.0±0.6	0.801
<b>SPNET-1</b>	6.0±0.5	6.6±0.8	0.572
<b>PFSK-1</b>	5.4±0.2	-	-

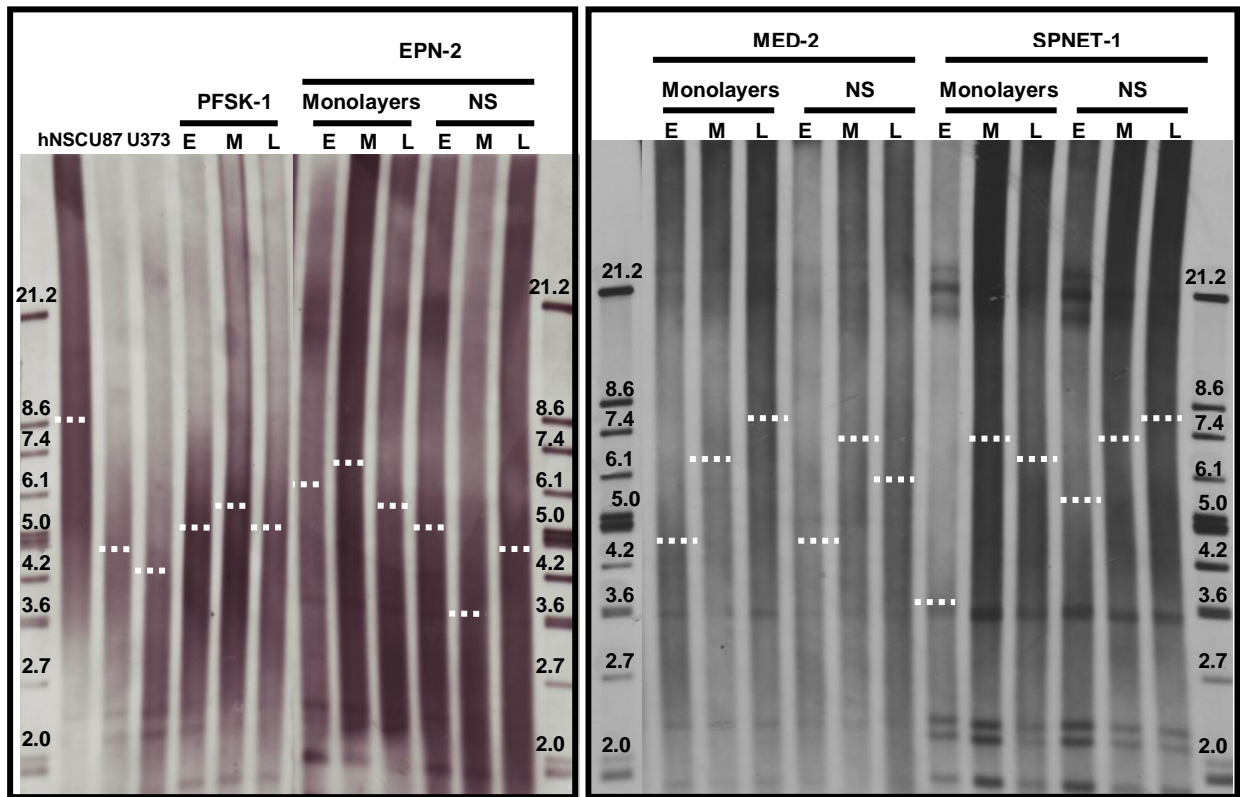


**Figure 4.10 TRF assay in monolayers and neurospheres at early, middle and late passages of PFSK-1, SPNET-1, EPN-2 and MED-2 compared with hNSC, U87 and U373 cell lines.** Telomere length was determined in monolayers and neurospheres (NS) from EPN-2, MED-2, SPNET-1 and PFSK-1 at early (E), middle (M) and late (L) passages. hNSC has the longest length of telomeres whereas the other cell lines have telomere length range between 3.6 – 7.4 kbp. Telomere length was still maintained in all cell lines even at late passages. White dotted lines indicate mean of telomere in each cell line as assigned by Quantity One.

### 4.3 Discussion

#### **Our cell lines cultured as standard monolayers were more stable than neurosphere conditions.**

Cell lines studied in this project were derived from paediatric patients diagnosed with brain tumours; ependymoma (EPN-2), medulloblastoma (MED-2) and CNS PNET (SPNET-1), which were the main focus of this project. The commercial cell line, PFSK-1, was also included in this project. The PFSK-1 cell line however needed specialised culture media, recommended by LGC Promochem, because they could not survive in the much simpler tumour media and they could not be induced to form neurospheres in stem cell media. Due to the limitation of consecutive subculture in neurospheres, we could not serially subculture cells as neurospheres for prolonged propagation. They could be continuously subcultured with our experiment terminating at passage number 6. At this stage they became harder to dissociate and re-establish, a feature also recognised by other groups and prolonged culture of neurospheres also caused changes in proliferation kinetics, gene expression and cell adhesion [Morshead, C. M. *et al* (2002)]. All cell lines hence were cultured as monolayers and they have been continually passaged for up to 80 passages with regular growth rate (constant doubling times) and similar cellular morphology with increasing passage numbers (Figure 4.1.). Additionally, neurospheres were routinely generated from monolayers and monolayers were effectively induced to form neurospheres within 48 hours even at late passages (Figure 4.1.). The immunofluorescence results also demonstrated that all cell lines expressed stem cell markers (CD133 and SOX2) in both monolayer and neurosphere conditions at all passages. The proportion of cells co-expressing CD133 and SOX2 in monolayers was consistent even in late passage (up to 80 passages) (Figure 4.4 and 4.5). In addition, significant genetic abnormalities commonly found in the original tumours were preserved in our cell lines both monolayers and neurospheres from SNP analysis (Chapter 3). Metaphase spread analysis results from Chapter 3 also demonstrated that our monolayers had less variation of chromosome numbers compared to PFSK-1 indicating more

stability of cell lines. Therefore, these results suggested that our cell lines were stably preserved during prolonged culture under monolayer conditions, standard tumour media supplemented with serum. Monolayer conditions also conserved the characteristic of cancer stem cell in neurosphere formation and preserved significant characteristics of the original tumours. A previous study also demonstrated that human neural stem cells, which were grown as adherent monolayer cells, had stem cell characteristics and their property was stable even when they were continuously subcultured as adherent cells for long periods [Daadi, M. M. *et al* (2008)].

The failure to establish neurospheres from PFSK-1 monolayer cells is probably explained from the study of Lee, J. *et al* (2006). They proposed that there are *de novo* genetic and/or epigenetic changes in cells which have been cultured in serum condition (DMEM media containing 10% FBS) for a long period. PFSK-1 is a commercial cell line, which was established from a 22-month old boy diagnosed with undifferentiated PNET. These cells had been cultured in RPMI media supplemented with 10% fetal calf serum for over 2 years (85 passages). Initially, PFSK-1 cells were able to form neurospheres in gel and initiate new tumours when they were transplanted into mice brain. It was concluded therefore that the PFSK-1 cell line had characteristics of neuroepithelial stem cells. However, this cell line had lost the heterozygosity on chromosome 17 at passage 39 and 73 during an establishment in culture [Fulfs, D. *et al* (1992)]. These findings suggest instability of the PFSK-1 cell line and also supported the findings of Lee *et al* study. In our hands, PFSK-1 could not form neurospheres in stem cell media and they were negative for CD133. Based on the evidence from Fulfs *et al* and our findings, it is concluded that PFSK-1 was not stable in prolonged culture and they had lost a property of stem cells during continuous subculture in media supplemented with serum. Hence, our cell lines were more stable in monolayer conditions than the commercial cell line, PFSK-1.

## Neurosphere grew slower than monolayers indicating containing more quiescent cells.

To determine any alteration of growth rate with increasing passage numbers, doubling time analysis was performed at early, middle and late passage numbers of monolayers and neurospheres. Our results demonstrated that monolayer doubling time was constant even when passage number increased whilst neurosphere doubling time was variable. Additionally, neurosphere doubling time was longer than monolayer although this was not significant in many cases. These findings indicated that neurospheres grew slower than monolayers possibly due to increasing CSCs, which are spending longer time in  $G_0G_1$  phase of the cell cycle. Cell cycle analysis performed by Dr. Deema Hussein, a post doctoral researcher, showed that the proportion of cells in  $G_0G_1$  phase was significantly increased in neurospheres ( $p < 0.001$ ) when compared to the monolayers, with a corresponding decrease in S phase cells ( $p < 0.001$ ) (Figure 4.11). Hence, the presence of a larger

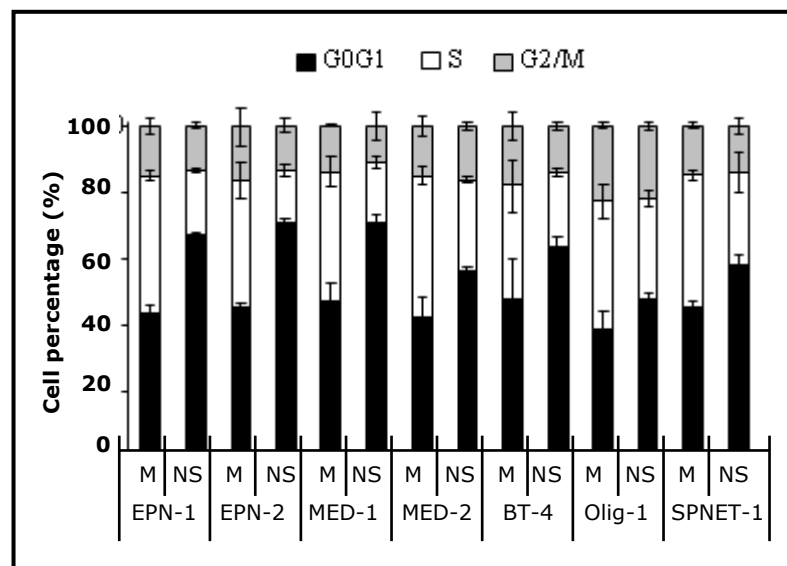


**Figure 4.11 An alteration of cell cycle profile in cells grown as neurospheres compared to monolayers.** Monolayers (M) and neurospheres (NS) from EPN-1, EPN-2, MED-1, MED-2, BT-4, Olig-1 and SPNET-1 cell lines were examined cell cycle profile using flow cytometry. Cell cycle profile results demonstrated that a proportion of cells in  $G_0G_1$  phase had increased in neurospheres compared to the corresponding monolayers. An increase in a proportion of cell in  $G_0G_1$  is consistent with the slower growth in neurospheres [The result was obtained from Dr. Deema Hussein].



proportion of neurosphere derived cells in the  $G_0G_1$  phase of the cell cycle suggests the presence of an increased proportion of quiescent cells, a recognised feature of stem cells [Cotsarelis, G. *et al* (1990) and Li, L. *et al* (2010)]. Previous studies also supported the finding of slower growing neurospheres in neural stem cells derived from a subventricular zone of a newborn mouse. Nestin positive cells, which indicated neural stem cells present in a quiescent state, were found in neurosphere culture condition indicating slow cycling cells. They hence concluded that neural stem cells cultured as neurospheres remained in quiescent state [Ma, B. F. *et al* (2006)]. Our findings were similar to the previous study performed by Alam and colleagues. They studied a murine neural stem cell line and found that neurospheres were slowly cycling cells and the majority (65-70%) population were in  $G_1$  state whilst a very small proportion of cells were found in  $G_2/M$  state. 20% of population were always observed in  $G_0$  phase. They also discovered that prolonged continuous culture (more than 60 days) affected the cell cycle kinetics. The proportion of cells in  $G_2/M$  phase increased in the later passage [Alam, S. *et al* (2004)]. Quiescent cells or slow cycling cells ( $G_0$ ) are important cells in maintenance of self-renewal property of stem cells or preserve stemness in hematopoietic stem cells. These cells were normally located in niche when they were activated to be active cycling cells, they moved out of the niche [Arai, F. *et al* (2004)]. Another possibility for slower growth is different cell growth form. These 2 conditions were due to growth in different media; monolayers were grown in media supplemented with serum and neurospheres were grown as floating clusters of cells in serum free media supplemented with EGF and FGF. Large neurospheres may have an inadequate oxygen and nutrient supply to the centralized cells. As a result, apoptosis and necrosis could occur in the neurospheres, resulting in slowing down and termination of neurosphere growth [Zhdanov, V. P. and Kasemo, B. (2004)]. Monolayer cells grown as single layers should not have depletion of oxygen and nutrients. We did however try to control for this by routinely culturing neurospheres ever 3-4 days in order to keep their size minimal ( $< 100 \mu m$  in diameter). Additionally, the difficulty of dissociation in neurospheres leads to clumping of cells. Therefore, these cells were not included when they were counted using hemocytometer. When the doubling time was calculated using the formula in page 141, this

underestimated cell number of neurospheres resulted in longer doubling time compared to monolayers.

**Neurosphere conditions were enriched for CSCs but CSCs were maintained in monolayer conditions.**

It has been generally accepted that the tumour cell population is heterogeneous and not all tumour cells have the characteristics of cancer stem cells, which are able to regenerate new tumours. Only a subpopulation of cells is capable of initiating tumours and this population is believed to resist chemo- or radiotherapy [Guo, W. *et al* (2006), Nakano, I. *et al* (2006) and Singh, S. K. *et al* (2004)]. Therefore, to investigate whether our paediatric primary cell lines contain cancer stem cells, co-staining immunofluorescence and Western blotting analysis were performed.

Immunofluorescence results confirmed a consistent proportion of cells co-expressing CD133 and SOX2 (8-12%) in monolayers at early, middle and late passages (Figure 4.4 and 4.5) and these cells were effectively induced to form neurospheres at any passages. Therefore, monolayer conditions can constantly maintain the proportion of cancer stem-like cells at all passages for a long period. This was true of all the 3 tumour types under analysis in this and the wider study (ependymoma, medulloblastoma, CNS PNET, Oligodendroglioma and malignant glioneuronal tumour). A previous study demonstrated that human neural stem cells, which were grown as adherent monolayer cells, express molecular features of stem cells such as nestin, vimentin and radial glial markers and have a symmetrical mode of cell division. The stem cell characteristics of these adherent cells were stable even when they were continuously subcultured as adherent cells for long periods [Daadi, M. M. *et al* (2008)]. Additionally, neural stem cells derived from embryonic stem cells, fetal forebrain and adult forebrain, were successfully cultured as adherent monolayer cells. These adherent cells rapidly grow and maintain the characteristics of stem cells including clonogenicity, homogeneity and symmetrical division. They are also an enrichment resource of pure stem

cells [Pollard, S. M. *et al* (2006)]. However, there was a discrepancy between adherent and non-adherent culture in maintenance of cancer stem cell characteristics. Several previous studies used neurospheres to study the characteristics and properties of cancer stem cells [Shiras, A. *et al* (2007), Chen, L. *et al* (2007), Merkel, F. T. *et al* (2004), Lee, J. *et al* (2006), Calabrese, C. *et al* (2007), Inagaki, A. *et al* (2007), Hansford, L. M. *et al* (2007), Singh, S. K *et al* (2003 and 2004)]. These studies found that neurospheres have the properties of stem cells including self-renewal, proliferation, multilineage differentiation and expression of several stem cell markers. In addition, isolated neurospheres express neuroepithelial stem cell markers including nestin, an intermediate filament protein. The characteristics of stem cells could be maintained while culturing the cells as floating cell clusters (neurospheres) [Reynold, B. A. and Weiss, S. (1992)]. Cells, derived from a primary GBM and grown as neurospheres under serum free neurobasal media supplemented with bFGF and EGF, can maintain their potential of self-renewal and ability of multiple lineage differentiation. Additionally, these cells expressed similar genes to NSCs and parental GBM cells, and maintained genetic stability over serial culture for a long period. In contrast, adherent cells cultured under DMEM media containing 10% FBS lost the properties of stem cells and could not maintain tumourigenic characteristics. The genetic profiles of these cells were totally different from NSCs and their parental tumour cells [Lee, J. *et al* (2006), Yuan, X. *et al* (2004)]. In addition, Fael Al-Mayhany *et al* claimed that the Cambridge protocol, which comprised 2 phases; derivation and propagation phases, was an effective method to derive tumour initiating cells from glioblastoma. They combined spheroid and monolayer culture in the Cambridge protocol to achieve the most effective yield of derivation and they revealed that this method successfully derived cell lines from glioblastoma (100%) and these cell lines also conserved parental genomic profiles [Fael Al-Mayhany, T. M. *et al* (2009)]. However, when the underlying metabolic events and biological features were analysed to investigate the maintenance of stem cell properties of both adherent and non-adherent cultured cells. It was found that both adherent and non adherent cells could preserve the stem cell characteristics over several passages [Inagaki, A. *et al* (2007)].

Hence, there are two different methods; monolayer and neurosphere conditions, to maintain stem cell characteristics in culture.

Additionally, neurospheres, induced from adherent (monolayer) cells, were enriched with stem-like cells. Approximately 35-45% of neurospheres were positive for stem cell markers; CD133 and SOX2 (Figure 4.4 and 4.5). The proportion of CD133 and SOX2 co-stained cells was significantly higher in neurospheres (35-45%) than in monolayers (8-12%) ( $p < 0.001$ ). The presence of an increased proportion of cells expressing CD133 in neurospheres compared to monolayers was confirmed by Western blotting analysis (Figure 4.7) whereas SOX2 expression detected by Western blotting analysis was low and did not appear to alter in any of the cell lines. In addition, a 4-fold increase in cells co-expressing CD133 and SOX2 was correlated with the immunofluorescence and FACS data performed by Dr. Deema Hussein. These FACS and immunofluorescence data also showed that a higher proportion of cells expressing nestin was observed in neurospheres from EPN-1 and EPN-2 cell lines ( $18 \pm 1.6$  and  $16.7 \pm 3.1$ , respectively) compared to monolayers ( $4.9 \pm 0.6$  and  $4.6 \pm 0.6$ , respectively). Similarly, flow cytometry data also demonstrated a higher proportion of nestin positive cells in neurospheres ( $11.1 \pm 2.2$ ) compared to monolayers ( $3.8 \pm 0.7$ ). Taken these all data together, it was convincingly confirmed that neurosphere conditions were enriched with cancer stem-like cells approximately 4-fold compared to monolayer conditions.

The PFSK-1 cell line failed to form neurospheres and immunofluorescence showed that there were no positive CD133 cells in PFSK-1 cells (Figure 4.4) (also confirmed by Dr. Deema Hussein, personal communication). However, the adherent PFSK-1 cells that grew in stem cell media were not examined for the expression of stem cell markers. Due to that fact that there were no CD133 positive cells present under monolayer growth conditions, however, PFSK-1 cells grown under neurosphere condition should be negative for CD133.

### **Co-stem cell marker (CD133 and SOX2) effectively identified CSCs in our cell lines.**

Based on the hypothesis of cancer stem cell characteristics, appropriate stem cell markers should identify a subpopulation, which has the capabilities of self-renewal, multilineage differentiation and tumour initiation *in vivo*. CD133 was originally recognized as a marker for human haematopoietic stem cells and neural stem cells. However, CD133 mRNA is also expressed in normal human tissues including mammary gland, trachea, salivary gland, placenta pancreas, digestive tract and testes [Mizrak, D. *et al* (2008)]. Currently, CD133 has been generally used as stem cell marker to identify the cancer stem cell subpopulation and many studies have provided evidence to support the effectiveness of CD133 in cancer stem cell identification. For example a study in human epithelial basal cells, supported the fact that AC133 identified a rare population, which showed 2 essential characteristics of epithelial stem cells in terms of higher proliferation *in vitro* and complete differentiation into prostatic like-acini *in vivo* [Richardson, G. D. *et al* 2004)]. AC133<sup>+</sup>CD34<sup>+</sup>CD3<sup>-</sup> cells, sorted from human fetal liver cells, had the capability to differentiate into astrocytes and neural cells [Hao, H. N. *et al* (2003)]. Additionally, CD133 antigens were rapidly down regulated when Caco-2 cells (colon carcinoma cell line) differentiated [Corbeil, D. *et al* (2000)]. Cells expressing AC133 isolated from human brain tumour cell lines significantly increased the capability of cells to initiate tumour when they were transplanted into non-obese diabetic-severe combined immunodeficient (NOD-SCID) mouse brain [Singh, S. K. *et al* (2004)] whereas cells without AC133 or AC141 expression had less tumourigenic capacity [Günther, H. S. *et al* (2008)]. In addition, AC133 co-expressed with other stem cell markers was used in many studies to specify cancer stem cells. Uchida *et al* found that cells expressing AC133 and AC141 but not CD34 and CD45 isolated from human fetal brain tissues formed neurospheres and differentiated into both neurons and glial cells *in vitro*. When these cells were transplanted into immunodeficient neonatal mice, they had high potential of tumour initiation, proliferation, migration and neural differentiation [Uchida, N. *et al* (2000)]. There were, however, also some findings revealed a weakness and limitation of using CD133 to identify cancer stem cells. Sakariassen *et al* examined the reliability of each technique in the

detection of stem cells and stated that false positive and a wide range of data could occur. For example, quantitative reverse transcriptase polymerase chain reaction (qRT-PCR) showed a huge variance of CD133 mRNA expression probably due to the presence of multiple isoforms and immunofluorescent results showed unexpected staining location in positive cells. CD133 staining is difficult possibly due to the presence of trypsin sensitive cytoplasmic loops and the high levels of intracellular expression. [Sakariassen, P. *et al* (2007)]. Beier *et al* revealed that CD133<sup>+</sup> and CD133<sup>-</sup> cells, which sorted from primary and secondary glioblastoma tumours by FACS, showed similar tumourigenic potential when they were engrafted into nude mice. They found that CD133<sup>-</sup> subpopulation also had infinite self-renewal and pluripotency capacity where these cells were able to differentiate into neurons, astrocytes and oligodendrocytes [Beier, D. *et al* (2007)]. Clément *et al* also studied CD133 in glioblastoma and they supported that CD133<sup>+</sup> and CD133<sup>-</sup> cells sorted by flow cytometry showed similar stem cell potential. They also suggested that FACS technique was not effective enough to isolated cancer stem cells, which can preserve long term self-renewal capacity, and CD133 was insufficient to detected entire cancer stem cells [Clément, V. *et al* (2009)]. Hence, there is a controversy in using CD133 alone to identify cancer stem cell population. However, there are several currently available stem cell markers for detection of cancer stem cells. For example SOX2 (MAB2018 R&D system®) was raised against recombinant human SOX2 at 135-317 amino acids. SOX2 is a transcription factor, which is important in the designation of neural stem cell fate. In addition, SOX2 is highly expressed in neuroepithelial stem cells and neural stem/progenitor cells. It was recognised as embryonic or neural stem cell marker [Miyagi, S. *et al* (2006)]. Nestin, which is neural stem cell marker, is also commonly used to identify cancer stem cells [Singh, S. K. *et al* (2004) and Wu, A. *et al* (2008)]. Nestin was used to identify CSCs in brain tumours (medulloblastoma and glioma) [Hemmati, H. D. *et al* (2003)]. Therefore, double staining of two stem cells markers is probably more convincing than single staining of one stem cell marker. Co-staining CD133 and SOX2 hence were used as stem cell markers to identify cancer stem-like cells in our primary cell lines. Co-staining immunofluorescence analysis was performed and the data were also validated by Western blotting analysis. CD133 antibody

(ab19898 abcam®) binds to C-terminus of human CD133. In our study, immunofluorescence staining of CD133 and SOX2 showed the correct sites of staining whereby positive signal was identified from membranous staining and nuclear or cytoplasmic staining, respectively. Our immunofluorescence data were consistent with co-staining immunofluorescence data performed by Dr. Deema Hussein using CD133 co-stained Nestin to identify cancer stem cells. CD133 co-stained with Nestin was also used to identify cancer stem cells in brain tumours [Singh, S. K. *et al* (2004) and Wu, A. *et al* (2008)]. The results showed high enrichment of CSCs in neurospheres almost 4 fold than in monolayers. Therefore, using 2 stem cell markers in CSC identification provided convincing results and CD133 and SOX2 effectively identified CSCs in our cell lines.

**Telomere length was maintained and telomerase was activated in our cell lines at any passages.**

The TRAP assay, which determined the level of telomerase activity, was performed on monolayers and neurospheres from 7 primary paediatric cultured cell lines. The TRAP results showed that telomerase processivity was positive in both monolayers and neurospheres from all cell lines (Figure 4.8 and 4.9). Telomerase activity is negative in normal brain tissues [Siyuan, L. *et al.* (1998) and Nakatani, K. *et al.* (1997)]. Although, to obtain more convincing results, normal brain samples should have been included in the TRAP assay as a negative control. Our results showed further that there was no correlation between telomerase activity and tumour progression or tumour grading in our cell lines and there was no consistent correlation between TRAP processivity and culture conditions between monolayers and neurospheres. Currently, the correlation between telomerase activity and tumour progression or tumour grading is not confirmed and remains controversial. One previous study showed that telomerase activity in gastric carcinoma was detected in large size tumours, those at an advanced stage and metastatic whereas at an early stage of gastric cancer telomerase activity was negative. In addition, telomerase positive cases had a shorter survival time than negative cases. However, telomerase activity was not always

positive in advanced stages of gastric cancer [Hiyama, E. *et al.* (1995)]. In contrast, in brain tumours, telomerase activity was detected in both high and low grade tumours (glioblastoma multiforme, oligodendroglioma and anaplastic astrocytoma). Positive processivity detected in anaplastic astrocytoma indicated that a tumour was more likely to transform to a higher grade tumour; glioblastoma multiforme. This study concluded that telomerase activity was associated with tumour progression [Langford, L. A. *et al.* (1995)]. Our TRAP results indicated that there was no correlation between a degree of telomerase activity and tumour grading of tumour progression, however, to make a strong conclusion, the TRAP assay should be performed on the same cell lines derived from the original tumours at different stage of tumour progression in term of primary tumour and relapse tumour. So that the level of telomerase activity can be compared when tumours have progression. These samples were, however, not available for us to compare the level of telomerase activity at different stages of tumours. It would also be important to increase the sample size for each type of tumour under analysis.

A TRF assay was also performed to determine telomere length in monolayers and neurospheres from EPN-2, MED-2, SPNET-1 and PFSK-1 cell lines at early, middle and late passages (Figure 4.10 and Table 4.1). Although, TRF assays were independently repeated many times, however, good quality results were only derived from 2 experiments. The TRF assay confirmed that telomeres were maintained in monolayers and neurospheres from all cell lines at all passages. Didiano *et al.* determined telomere length in PNET cell lines and found that telomere length ranged from 5 – 12.1 kbp [Didiano, D. *et al.* (2004)]. This data is consistent with our findings, which showed the telomere length ranging from 4.78 – 7.6 kbp in SPNET-1 and MED-2 cell lines. Another study revealed that all recurrent ependymomas demonstrated a high level of telomerase activity and telomere lengthening was observed in the majority (71%) of these tumours compared to the corresponding primary tumours [Ridley, L. *et al.* (2008)]. However, we could not indicate whether the maintenance of telomere length in our cell lines are shortening or lengthening since data on the original tumour or the primary tumour specimens were not available to make a comparison. Based



on evidence that telomere length detected in fetal brain and adult brain (32 – 76 years) was  $11.9 \pm 1.5$  and  $10.5 \pm 0.5$  kbp, respectively [Allsopp, R. C. *et al.* (1995)], telomere length was maintained at a short length in our cell lines since it was shorter than 10 kbp. The pattern of telomere length smear of our cell lines was different from the controls, hNSC, U87 and U373. The TRF results showed heterogeneous telomere length smears, which contained short and long telomere length. The heterogeneous telomere length pattern, which is the characteristic of ALT cell lines, was previously found in late passages where cells have gone through crisis [Yeager, T. R. *et al.* (1999)]. Therefore, this evidence suggested that our cell lines have gone through crisis since early passages (< 25) and ALT probably was the major mechanism to maintain telomere length in our cell lines. As a result, our cell lines still survived with no change of cellular morphology even they have been passaged up to 80 passages. Additionally, Didiano *et al.* found that telomerase positive PNET cells had shorter telomere length than telomerase negative cells. This data indicated that the maintenance of telomere length in PNET cells does not always depend on the upregulation of telomerase activity but it possibly resulted from ALT mechanism [Didiano, D. *et al.* (2004)]. Therefore, telomerase activation might not be the only mechanism to maintain telomere length in cancers. It is also possible that different mechanisms could be operating in different tumour subpopulation.

The correlation between telomerase activity and telomere length was evaluated to see whether a high telomerase activity is found in cell lines having a short telomere length. A previous study, which determined telomerase activity and telomere length in cancer cells, revealed that telomere length of cancer cells was maintained at homeostasis was short where cancer cells had limiting amount of telomerase [Cristofari, G. and Lingner, J. (2006)]. However, telomerase activity did not correlate with telomere length in our cell lines with regard to tumour grading, tumour types whether primary or recurrence or history of treatment. This might be because the different telomere length maintenance mechanisms possibly activated in different types of tumours. Didiano *et al.* also found that there was no correlation between telomerase activity and telomere length in PNET cell lines but their data

showed that human telomerase reverse transcriptase (hTERT) mRNA expression significantly correlated with telomerase activity [Didiano, D. *et al* (2004)]. In addition, telomere length is not the only factor, which determines telomeric function. It has also been found that telomeric dysfunction can be detected in cells with long telomere length [Hemann, M. T. *et al* (2001)]. Taking all the TRF and TRAP results together, the results indicated that telomeres were maintained and telomerase activity was present at all passages in all cell lines both monolayers and neurospheres. However, there was no correlation between telomere length and telomerase processivity.

Due to the fact that telomerase activity and telomere length were not the main aim of this project, experiments were not performed to study in depth about these topics. However, there were several interesting points, which should be studied to complete the data. Firstly, normal childhood brain samples should be included in both the TRAP and TRF assay to compare the level of telomerase activity and the length of telomere. Secondly, a telomerase inhibitor could be used to inhibit telomerase activity then telomere length determined to see whether telomere length is affected when telomerase activity is absent. This will prove which cell lines use telomerase activity as a major mechanism to maintain telomere length. The TRF assay using Southern blotting analysis is standard method to determine telomere length where the black smear on the blot represents mean of telomere length from a whole DNA, which is extracted from samples. This is the limitation of this technique, which only shows the mean telomere length from all chromosomes. In fact, each chromosome contains variation of telomere length and the shortest telomere length will activate telomerase to elongate that telomere or other dysfunctional telomere [Hemann, M. T. *et al* (2001)]. For future study, Q-FISH technique could be performed to determine telomere length because this technique is able to show individual telomere length from each cell and distinguish between ALT pattern (variation of telomere length) and telomerase pattern (equal telomere length). Additionally, the TRF and TRAP assay should be performed on the original tumours obtained from patients to determine the preservation of original characteristic in cell lines, which have been serially passaged in tumour media. Pulse field electrophoresis could also

have been used to give better resolution of heterogeneous telomere length smears. Finally, clonal analysis could have been used to determine if different tumour subpopulation are using different mechanisms to maintain their telomeres.

---

---

## **Chapter 5**

**Identification and functional analysis of ABC transporters in  
the parental cell lines**

---

---

## **Chapter 5: Identification and functional analysis of ABC transporters in the parental cell lines**

### **5.1 Introduction**

In Chapter 4, co-staining immunofluorescence analysis of the parental cell lines demonstrated that monolayers and neurospheres from our cell lines (EPN-2, MED-2 and SPNET-1) contained approximately 8-12% and 35-45% of cells co-expressing CD133 and SOX2, respectively, consistent with previous findings by Singh and colleagues in medulloblastoma [Singh, S. K. *et al* (2003)]. This indicated that neurosphere culture conditions were able to enrich for cells co-expressing CD133 and SOX2 (cancer stem-like cells) when compared to the monolayers. Western blotting results also confirmed a higher expression level of CD133 detected in neurospheres compared to monolayers. Therefore, our cell lines contain a small but detectable proportion of cancer stem-like cells. To study drug resistance in our cell lines, these cell lines were investigated for the expression of functional ABC transporters.

Conventional chemotherapy remains an essential treatment for several types of cancers. In some types of cancer, patients diagnosed with malignancy and first treated with chemotherapy, are seen to respond to treatment, resulting in tumour mass being shrunken in size. Nonetheless, tumour relapse will occur in a sizeable proportion of patients within a few years or many years after the first treatment, resulting from drug resistance of targeted cells. Chemotherapeutic drug resistance occurring in cancer cells is broadly categorised as being either acquired and intrinsic drug resistance. Acquired drug resistance is observed after cancer cells are treated with many rounds of chemotherapeutic agents. It is believed to occur from accumulated genetic mutation or alteration after each cycle of chemotherapy resulting in these cells become resistant to drugs. Drug resistance which is originally present in cancer cells prior to treatment is intrinsic drug resistance. Drug resistance in cancer cells is commonly multidrug resistance (MDR). A unique characteristic of MDR is that resistant cells are able to have cross-

resistance to many chemotherapeutic drugs regardless of structure of drugs or drug exposure experience. Although, chemotherapeutic regimens comprise multiple drugs with different targets, effectiveness of treatment cannot be improved. Therefore, multidrug resistance is still a major problem of chemotherapeutic treatments resulting in failure of treatment and relapsed cancers. At present, researchers are attempting to understand the mechanism of drug resistance of cancer. Many mechanisms lead to MDR, however, members of the adenosine triphosphate-binding cassette (ABC) transporter family are at least partly responsible for MDR [Goldie, J.H. (2001)].

Current knowledge about drug transporters involved in drug resistance has been obtained from extensive studies into ABCB1, ABCC1 and ABCG2. ABCB1 was initially detected in several types of cancer, with colon, kidney, adrenocortical and hepatocellular cancers having high levels of expression [Fojo, A. T *et al* (1987)]. ABCC1 was also highly expressed in human cancers e.g. leukaemias, oesophageal carcinoma and non-small-cell lung cancers [Nooter, K. *et al* (1995)]. ABCG2 was discovered later and identified by methoxantrone resistance without ABCB1 or ABCC1 expression [Dean, M. *et al* (2001)]. ABCG2 was highly expressed in breast cancer and postulated to associate with drug resistance [Doyle, L. A. *et al* (1998)]. Therefore, the correlation between high levels of ABCB1, ABCC1 or ABCG2 expression and drug resistance was extensively studied in many types of cancers. In leukaemia, ABCB1 was detected in only one third of patients diagnosed with acute myelogenous leukaemia (AML), and highly expressed in approximately half of relapsed cases of AML. Additionally, it was found that a high level of ABCB1 expression was correlated with poor prognosis and ineffective response to treatment by patients [Gottesman, M. M. (2002)]. Poor treatment outcome of breast cancer [Trock, B. J. *et al* (1997)] and highly doxorubicin resistant sarcoma [Abolhoda, A. *et al* (1999)] were also correlated with high levels of ABCB1 expression. The level of ABCC1 mRNA expression also related to a degree of chemoresistance in glioma resulting in poor treatment outcome [Bredel, M. (2001)]. ABCG2 expression had an impact on prognosis and clinical chemoresistance studied in acute myeloid leukaemia (AML) [Wilson, C. S. *et al* (2006) and van den Heuvel-Eibrink, M. M. *et al* (2002)]. The patient having the poorest prognosis was found to have both ABCB1 and

ABCG2 co-expression [Benderra, Z. *et al* (2004)]. Therefore, ABCB1, ABCC1 and ABCG2 play an important role in drug resistance in many cancer types.

CSCs, proven to exist in brain tumours, may be the population that survives following treatment hence targeting these cells could improve chemotherapy. We hypothesised that ABC transporters might be an important mechanism for drug resistance in cancer stem cells. Therefore, as part of our studies of drug resistance in our paediatric brain tumour cell lines, endogenous ABC transporter expression was determined by immunofluorescence, Western blotting and flow cytometry. The assays were performed in monolayers and neurospheres to compare the proportion of cells co-expressing CD133 and ABC transporters between these 2 culture conditions. The existence of endogenous ABC transporter expression co-stained with CD133 was coupled with drug export assays to examine ABC transporter function. The presence of co-expressing cells with functional drug exporters would be consistent with our hypothesis regarding CSCs being able to survive drug treatment.

## 5.2 Results

### 5.2.1 Co-staining ABC transporters and CD133 immunofluorescence analysis

Co-staining immunofluorescence was performed on 3 primary cultured cell lines; EPN-2, MED-2 and SPNET-1 at early passage (<25). Monolayers and neurospheres were co-stained with antibodies to CD133 and either ABCB1, ABCC1 or ABCG2. Human embryonic kidney (HEK) cells stably transfected with vector expressing ABCB1, ABCC1 or ABCG2 were used as positive controls. Positive control cells showed a high expression of ABC transporters defined as clear membranous staining with ABC transporter antibodies (Figure 5.1, 5.2 and 5.3). Positive ABCB1 or ABCC1 cells co-stained with CD133 were detected in both monolayers and neurospheres of all 3 cell lines. In general, monolayers showed a low level of co-expression whereas neurospheres expressed ABCs and CD133 at a higher level and also the proportion of co-expressing cells was larger in neurospheres compared to monolayers (Figure 5.1, 5.2 and 5.3). However, there were some populations which singly stained for CD133 or ABC transporters in both monolayers and neurospheres of all cell lines. ABCG2 expression was not detected in any of the cell lines. Although, ABCG2 antibody positivity was detected in SPNET-1 neurospheres, this positive signal was nuclear instead of membranous staining. Therefore, this positive signal was defined as non-specific for ABCG2 since only protein located on the plasma membrane could function as a drug transporter.



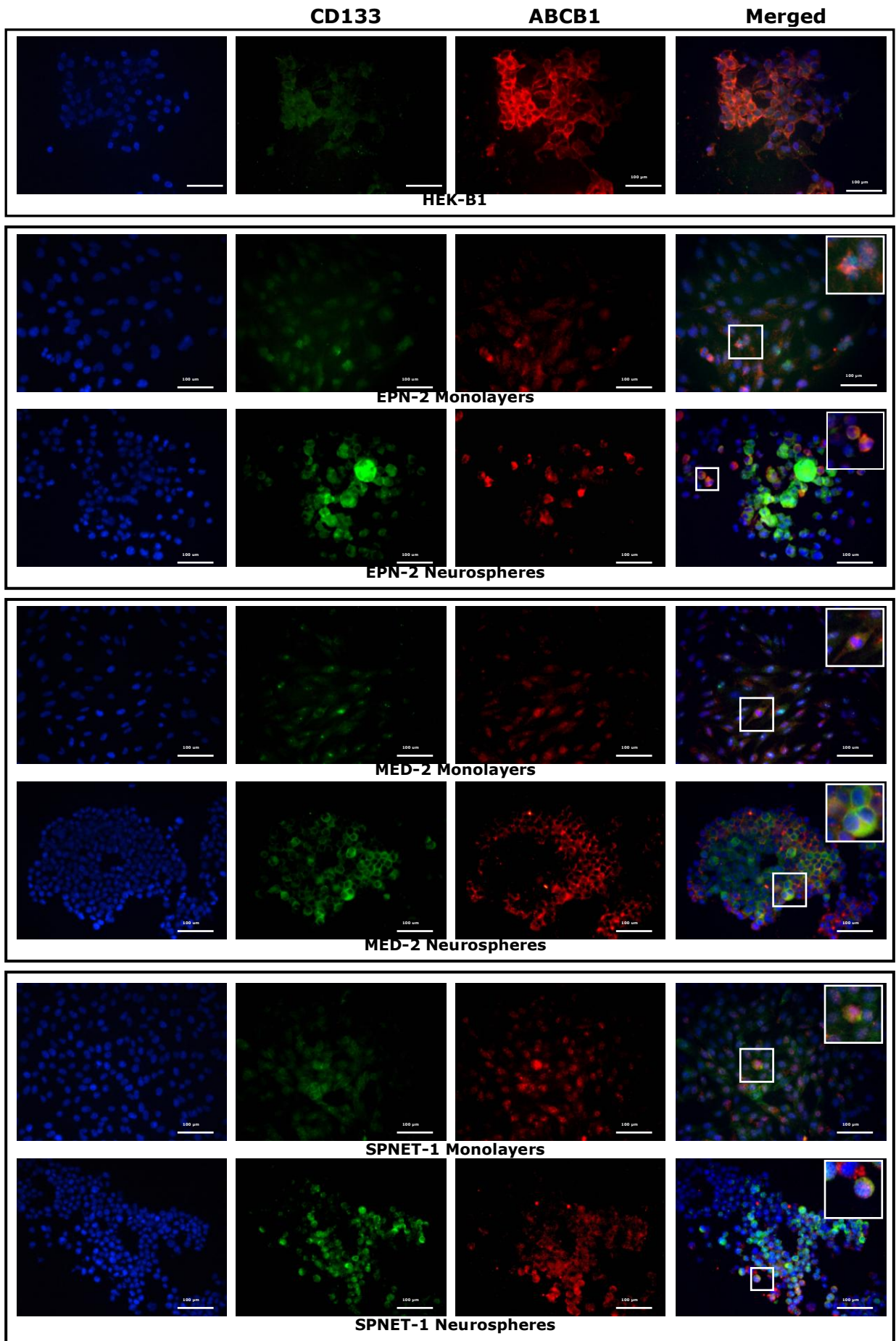


**Figure 5.1 Co-staining CD133 and ABCB1 immunofluorescence in monolayers and neurospheres from EPN-2, MED-2 and SPNET-1 cell lines at early passage number.**

HEK-B1 cells were used as a positive control and they highly expressed ABCB1, which clearly showed membranous staining. Monolayers and neurospheres from EPN-2, MED-2 and SPNET-1 cell lines were detected with antibodies against CD133 and ABCB1 and images were captured at x40 magnification. Cells expressing membranous CD133 and ABCB1 were detected in both monolayers and neurospheres from all 3 cell lines. Co-staining CD133 and ABCB1 cells were detected at a higher proportion in neurospheres and were more intensely stained compared to monolayers. Single staining; DAPI staining nuclei (blue), CD133 (green) and ABCB1 (red), and merged images are shown. The white boxes in the merged images show an example of co-staining cells and merged images are enlarged for clarity (x2-3). (Scale bars = 100  $\mu$ M)

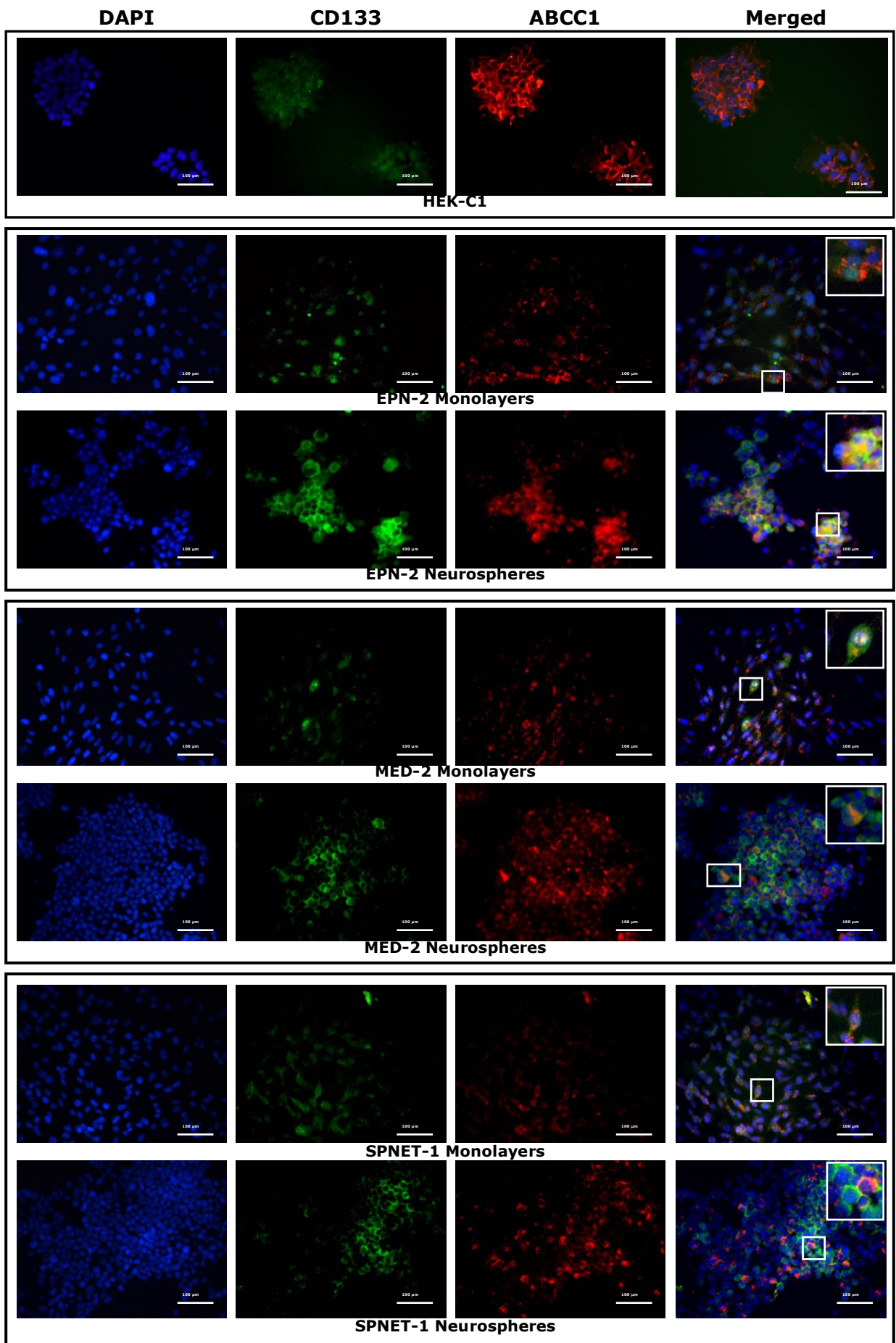


**Figure 5.2 Co-staining CD133 and ABCC1 immunofluorescence in monolayers and neurospheres from EPN-2, MED-2 and SPNET-1 cell lines at early passage number.** A high level of clear membranous staining of ABCC1 was detected in the HEK-C1 positive control cells. Both monolayer and neurosphere cells from all 3 cell lines were positive for antibodies against CD133 and ABCC1. In each case a higher proportion of CD133 and ABCC1 co-staining cells was detected in neurospheres when compared to monolayers. Similar to co-staining CD133 and ABCB1 results, cells grown as neurospheres had membranes which were entirely co-stained CD133 and ABCC1 antibodies. White boxes in each merged image show representative co-staining cells and merged images are enlarged for clarity (x2-3). Immunofluorescence results are shown as single staining images (DAPI [blue], CD133 [green] and ABCC1 [red]) and merged images; all images were captured at x40 magnification. (Scale bars = 100  $\mu$ M)



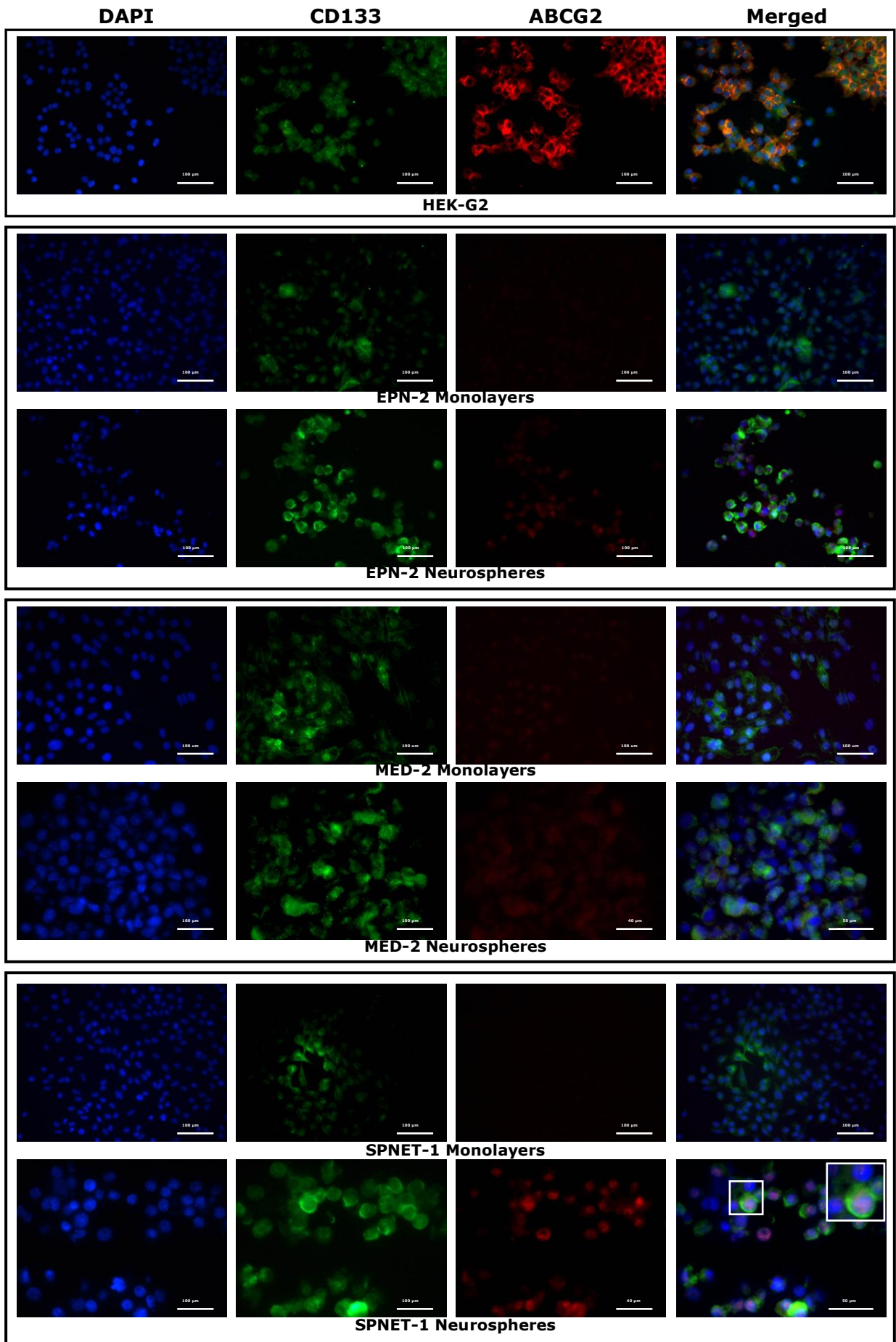


**Figure 5.3 Co-staining CD133 and ABCG2 immunofluorescence in monolayers and neurospheres from EPN-2, MED-2 and SPNET-1 cell lines at early passage number.**

HEK-G2 cells were used as a positive control and they showed a high level of membranous staining detected with ABCG2 antibody. Monolayers and neurospheres from EPN-2, MED-2 and SPNET-1 cell lines were co-stained with antibodies against CD133 and ABCG2. CD133 membranous staining was detected in both monolayers and neurospheres but ABCG2 staining was negative in all cell lines apart from SPNET-1 neurospheres. However, positive ABCG2 staining in the SPNET-1 neurospheres was nuclear staining. The white box in the merged image shows co-staining cells. This figure shows single staining images of DAPI (blue), CD133 (green) and ABCG2 (red) and merged images. All images shown in this figure were captured at x40 magnification apart from neurospheres from MED-2 and SPNET-1 cell lines which were captured at x100 magnification. (Scale bars = 100  $\mu$ M and 40  $\mu$ M)

### **5.2.2 Detecting cells co-stained for ABC transporters and CD133 by FACS**

The results from previous immunofluorescence analysis showed that neurospheres contained a larger proportion of cells co-expressing CD133 and ABCB1 or ABCC1 than monolayers. Additionally, no cells co-expressing CD133 and ABCG2 were detected in either monolayers or neurospheres. To validate the data from co-staining immunofluorescence, FACS was performed.

The proportion of fixed cells co-stained with antibodies against CD133 and ABCB1, ABCC1 or ABCG2 was detected by flow cytometry in early passage monolayers and neurospheres from EPN-2, MED-2 and SPNET-1 cell lines. The assay was individually repeated 3 times and included either HEK-B1, HEK-C1 and HEK-G2 cells as positive controls or HEK-V cells as negative controls. Representative figures from each sample are shown in Figures 5.4 – 5.6 and the percentage of co-expressing cells is shown in Figure 5.7. FACS results showed that our cell lines, especially when grown as neurospheres, were not well suited to this assay. Even in positive control cells, the percentage of co-expressing cells showed considerable variation. In addition, HEK-V cells (empty vector) sometimes displayed a high proportion of co-expressing cells similar to positive cells, in contrast to expectation. FACS results from 3 independent experiments showed a huge variation of co-staining percentage especially in neurospheres as shown in Figure 5.7. To illustrate the unreliability of FACS data, the proportion of cells expressing CD133 by FACS was compared to the proportion of co-staining CD133 and SOX2 by immunofluorescence. The immunofluorescence results showed that neurospheres were enriched 4-5 fold for cells expressing CD133 and SOX2. In contrast, over 50% of cells expressed CD133 detected by FACS in both monolayers and neurospheres (Figure 5.4 - 5.6) and, there is no 4 fold increase in the proportion of cells expressing CD133 in neurospheres compared to monolayers. The large degree of error (Figure 5.7) also indicated that this method was unreliable and Western blotting analysis was consequently performed to detect ABC transporter expression.

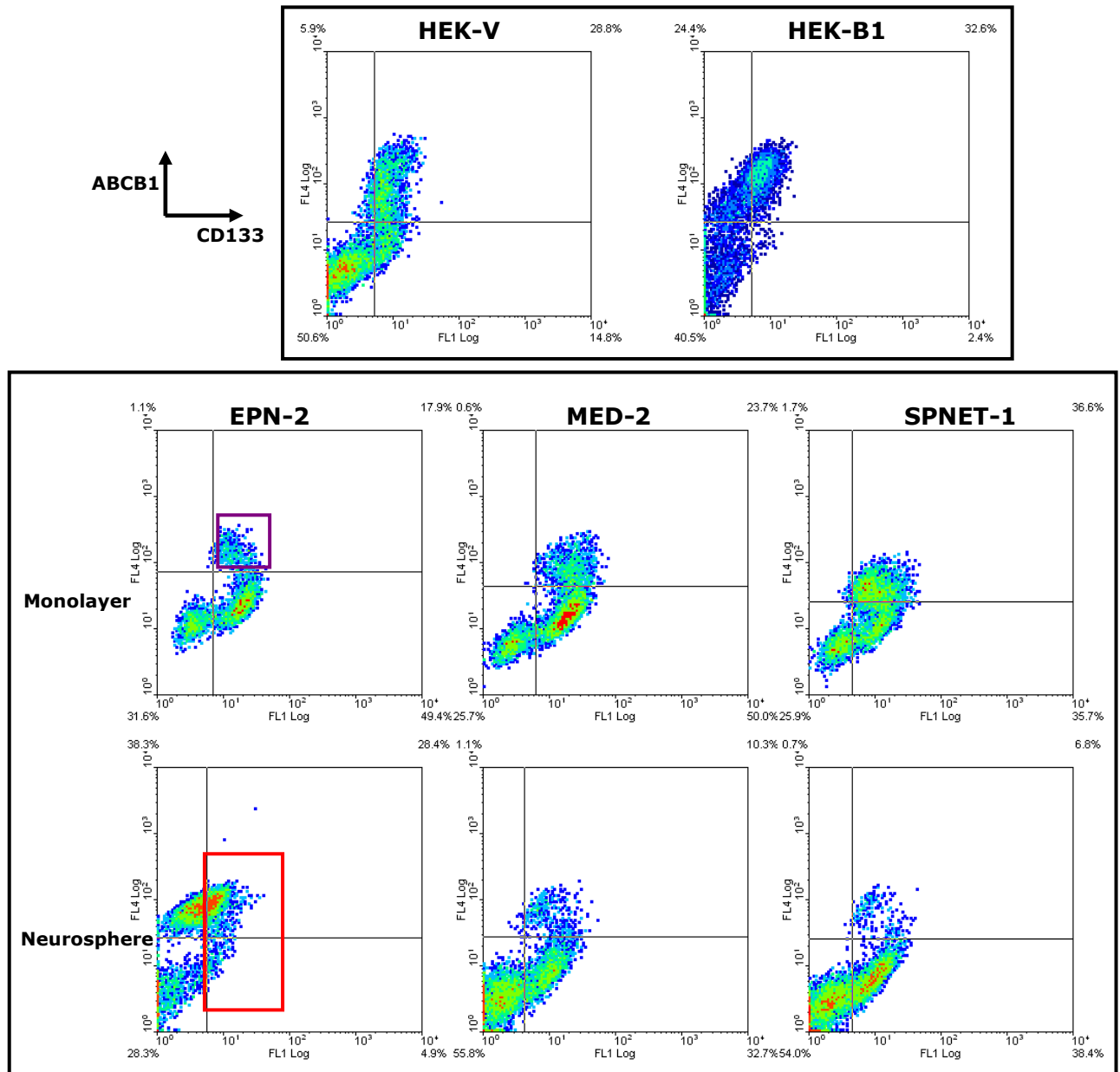


**Figure 5.4 Co-expressing CD133 and ABCB1 cells detected by FACS in monolayers and neurospheres from EPN-2, MED-2 and SPNET-1 cell lines.** Co-expression of CD133 and ABCB1 was detected in almost 50% in HEK-V cells similar to HEK-B1 cells on every occasion. Cells co-expressing CD133 and ABCB1 indicated in purple box sometimes were higher in neurospheres than monolayers (EPN-2) but sometimes they were higher in monolayers than neurospheres (MED-2 and SPNET-1). Cells expressing CD133 indicated in red box were detected at a very high proportion in all cell lines. Number of events included in the experiments was 5,000 – 10,000. The results were gated based on the consistent negative controls of samples (secondary antibody alone) since the results from HEK-V and HEK-B1 showed higher intensities of co-expression. Cells co-expressing CD133 and ABCB1 displayed in the right upper quadrant indicated cancer stem-like cells expressing ABCB1.



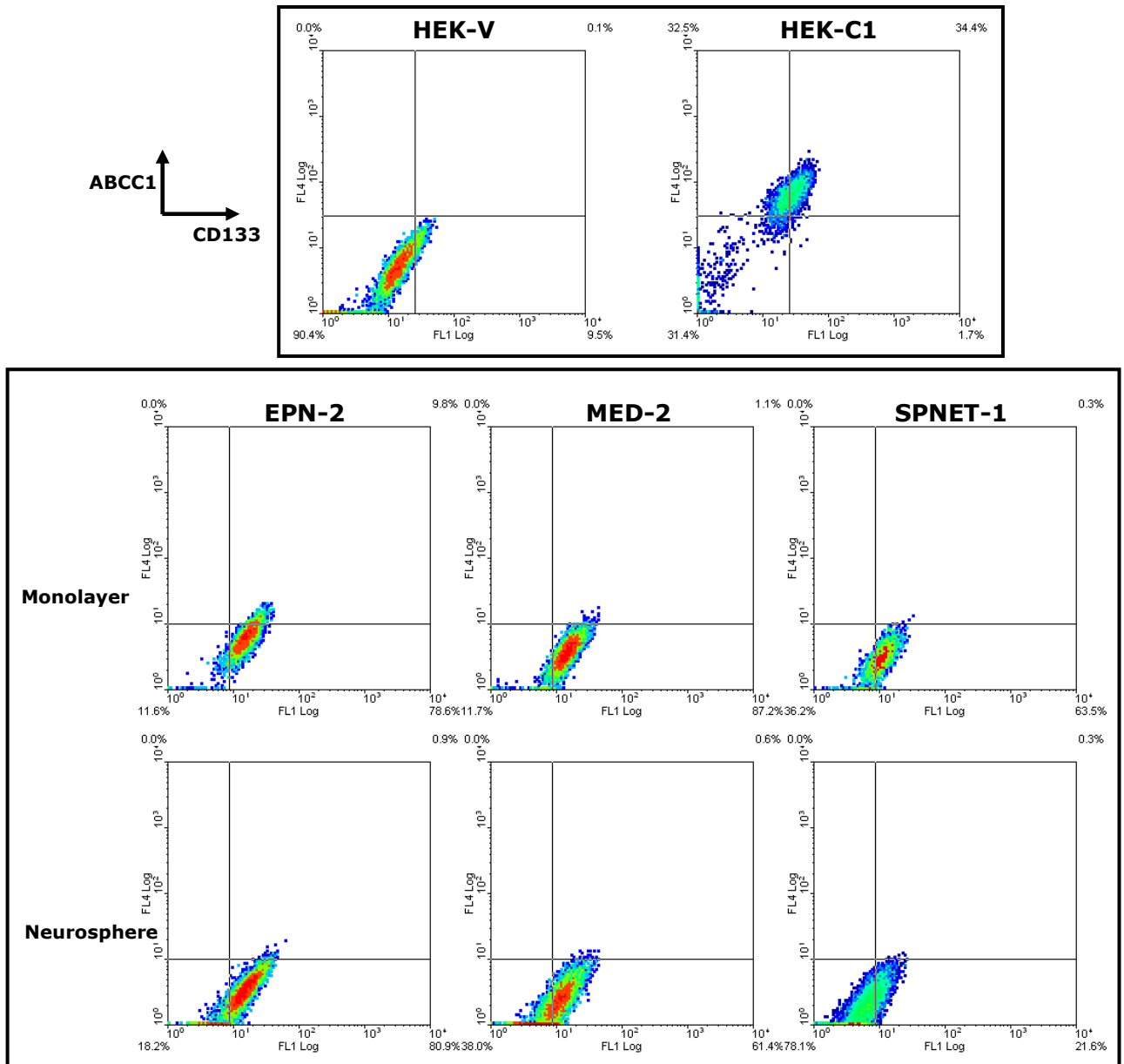


**Figure 5.5 Co-expressing CD133 and ABCC1 cells detected by FACS in monolayers and neurospheres from EPN-2, MED-2 and SPNET-1 cell lines.** This figure shows the best result of co-staining from HEK-C1 and HEK-V cells. CD133 and ABCC1 co-expressing cells of HEK-V were detected at similar proportion to HEK-C1 cells on some occasions. Cells co-expressing CD133 and ABCC1 were detected at a very low proportion in all cell lines whereas CD133 expressing cells were detected at more than 50% in both monolayers and neurospheres from all cell lines.

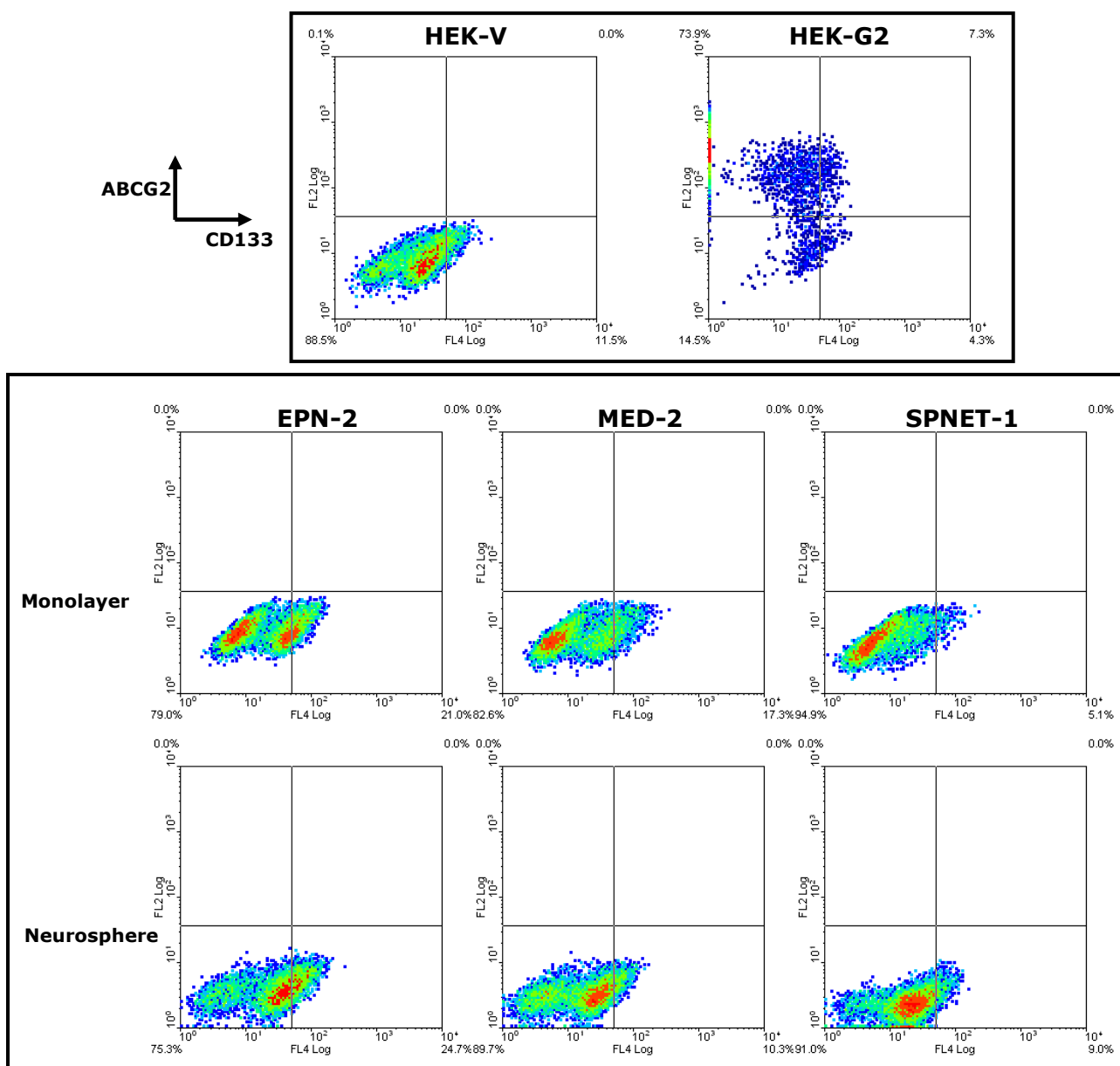


**Figure 5.6 Co-expressing CD133 and ABCG2 cells detected by FACS in monolayers and neurospheres from EPN-2, MED-2 and SPNET-1 cell lines.** HEK-G2 cells used as a positive control contained approximately 80% ABCG2 expressing cells. There were no CD133 and ABCG2 co-expressing cells detected in HEK-V cells (negative control) as expected. Co-expression of CD133 and ABCG2 was negative in both monolayers and neurospheres from all cell lines and the result was consistent from 3 independent experiments.

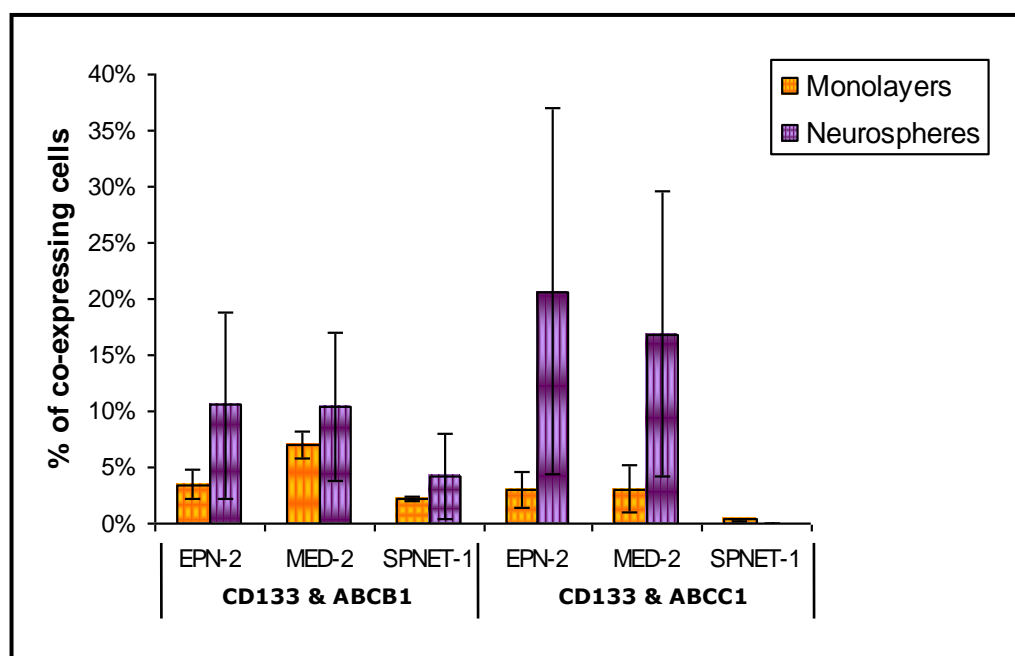


**Figure 5.7 The percentage of cells co-expressing CD133 and ABCB1 or ABCC1 in monolayers and neurospheres from EPN-2, MED-2 and SPNET-1 cell lines at early passage.** Graph shows the mean percentage of cells co-expressing CD133 and ABCB1 or ABCC1 from 3 independent experiments but co-expression of CD133 and ABCG2 was consistently negative from all 3 experiments so the data are not included in this figure. The proportion of cells in neurosphere samples showed extensive variation and also less variation was observed in monolayers. Therefore, the data show unacceptable variation, as discussed in the text.

### 5.2.3 ABC transporters expression detected by Western blotting analysis

Due to the dissimilarity between data obtained from immunofluorescence analysis and flow cytometry in detection of cells co-expressing CD133 and ABC transporters, Western blotting analysis was performed to validate the results. To confirm whether neurospheres express higher levels of ABC transporters than monolayers, ABC transporters expression was detected from the microsomal membrane fraction, where functional ABC transporters should be located, of both monolayers and neurospheres by Western blotting analysis. Microsomal membrane fractions had previously been shown to be enriched for CD133 expression (Figure 4.7, a, Chapter 4).

The microsomal membrane fraction was extracted from monolayers and neurospheres of EPN-2, MED-2 and SPNET-1 cell lines at early passage. HEK cells stably transfected with vector expressing ABCB1 (HEK-B1), ABCC1 (HEK-C1) or ABCG2 (HEK-G2) were used as positive controls whereas the negative control in each case was HEK cells stably transfected with empty vector (HEK-V). ABCB1 and ABCC1 proteins were detected at ~140 kDa in the appropriate controls and also in our cell lines (Figure 5.8, a and b). Neurospheres of all 3 cell lines showed a higher intensity of ABCB1 and ABCC1 expression compared to monolayers in agreement with immunofluorescence analysis. ABCG2 protein was detected at ~72 kDa in controls whereas the only positive bands detected in our cell lines were ~200 kDa (Figure 5.8, c). This may have resulted from unresolved dimers of ABCG2 transporters or the aggregation of ABCG2 protein. As ABCG2 dimerisation is stabilised by an inter-chain disulphide bridge, additional steps were taken to investigate whether the 200 kDa species could represent ABCG2. Among these was the incubation of sample additionally containing urea, dithiothreitol (DTT) and higher than normal concentrations of  $\beta$ -mercaptoethanol. However, the observed bands could not be reduced to 72 kDa and they were still detected at ~200 kDa in our cell lines. The sequence used to derive the ABCG2 antibody was screened against human protein databases using standard protein-protein BLAST (blast p) to find sequences with a high degree of similarity and hence other proteins that may have been detected. Eight different isoforms of human ABCG2 protein, which have expected size ranging from 68-72 kDa, were identified as a number of

other members of ABC transporter subfamily G and several other proteins of unrelated function to ABC transporter. Under all electrophoresis conditions HEK-G2 showed a 72 kDa band whereas the cell lines did not show this reactivity. The identity of the 200 kDa sequences remains unknown but it seems impossible that it represents ABCG2 (in agreement with immunofluorescence analysis which showed no expression of ABCG2).

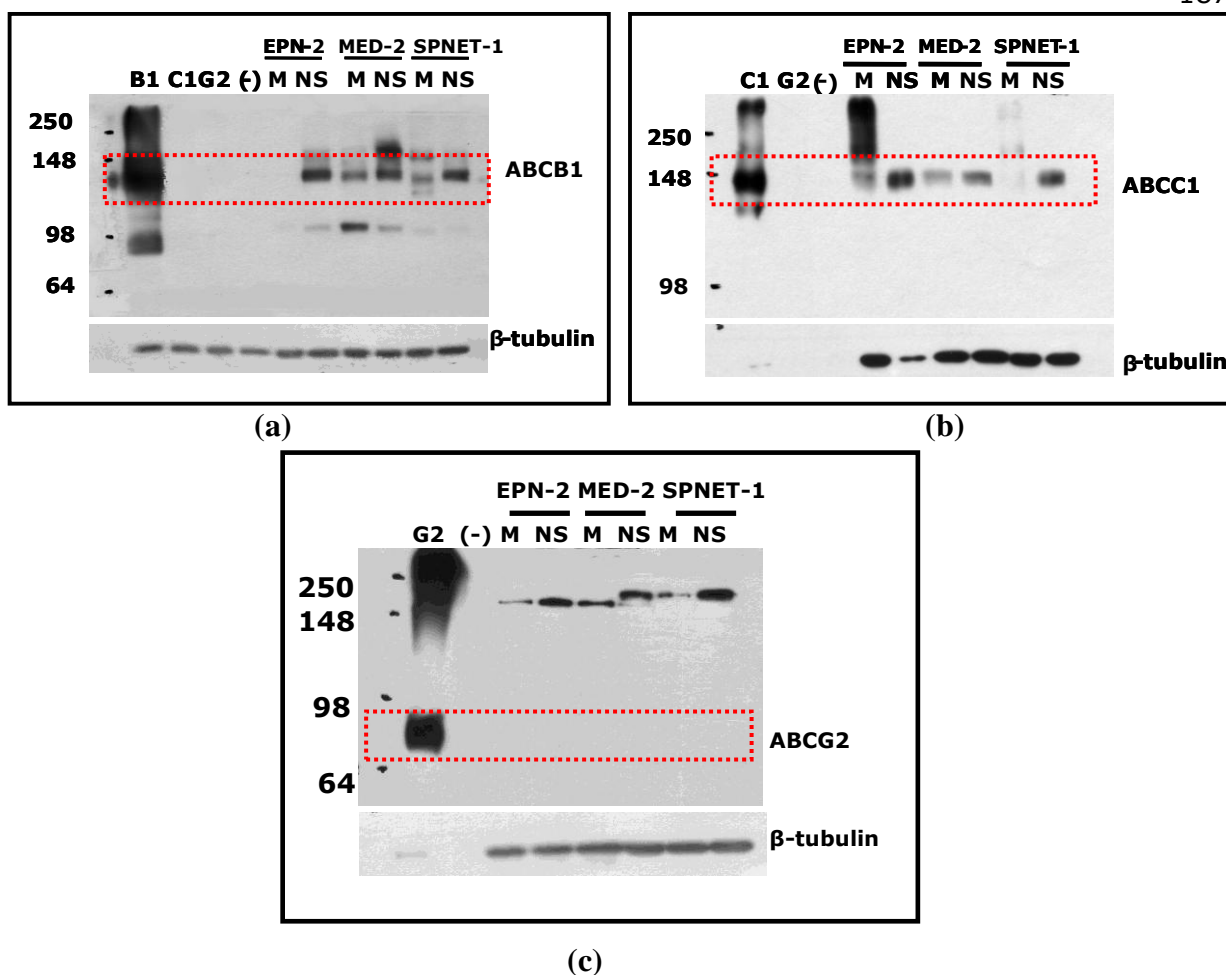


**Figure 5.8 The expression of ABC transporters in monolayers and neurospheres of EPN-2, MED-2 and SPNET-1 cell lines by Western blotting analysis.** ABCB1, ABCC1 and ABCG2 expression was detected in membranous fractions of all 3 cell lines in both monolayers (M) and neurospheres (NS). HEK cells stably transfected with ABCB1 (B1), ABCC1 (C1) or ABCG2 (G2) were used as a positive control for each blot. In each case 40  $\mu$ g of membrane fractions was loaded alongside a much reduced amount of HEK control cells [2  $\mu$ g B1, 5  $\mu$ g C1 and G2, and 10  $\mu$ g of empty vector (-)]. Neurospheres showed higher intensity bands representing ABCB1 and ABCC1 expression compared to monolayers. Only the G2 control showed the expected 72 kDa band. A larger ~200 kDa protein was detected in both monolayers and neurospheres. This was deemed to be non-specific. A huge band at more than 250 kDa in HEK-G2 was occasionally present in some blots resulting from protein aggregation. The  $\beta$ -tubulin loading control is shown at the bottom of each blot.

#### 5.2.4 Functional analysis of ABC transporters by FACS

Both co-staining immunofluorescence and Western blotting results were consistent in that all 3 cell lines; EPN-2, MED-2 and SPNET-1 contained a cancer stem cell-like population and expressed ABCB1 and ABCC1 in both monolayers and neurospheres. To prove cells are expressing functional ABC transporters, drug export analysis using FACS were performed. Initially, export assays for ABCB1 and ABCC1 was performed but parallel studies (described in Chapter 6) indicated that ABCB1 is the major functional efflux mechanism and thus only ABCB1 data is presented here. Rhodamine 123 (Rh123), a fluorescence lipophilic cationic dye, was used as a fluorescent ABCB1 substrate and the extrusion of this by ABCB1 was inhibited using Verapamil (calcium channel blocker). Verapamil is believed to inhibit ABCB1 function by competitively binding to ABCB1 transporter or via an allosteric effect [Qian, X. D. and Beck, W. T. (1990)].

ABCB1 functional analysis was performed on monolayers of EPN-2, MED-2 and SPNET-1 cell lines at early passage. HEK cells stably transfected with vector expressing ABCB1 (HEK-B1) and empty vector (HEK-V) were used as positive and negative controls, respectively. Cells harvested from monolayers were incubated with Rh123 to determine the proportion of cells able to extrude the dye. Cells expressing ABCB1 were able to extrude Rh123 and hence showed a low level of Rh123 accumulation by FACS (Figure 5.9, HEK-B1, Rh123), whereas non-ABCB1 expressing cells accumulated Rh123 and showed a high level of Rh123 by FACS (Figure 5.9, HEK-V, Rh123). If cells expressing ABCB1 are incubated with both Rh123 and Verapamil, export of Rh123 is inhibited and cells accumulate Rh123. FACS analysis therefore detected a high level of Rh123 in these cells (Figure 5.9, HEK-B1, Rh123+VP). As expected, Verapamil does not affect the level of Rh123 in non-ABCB1 expressing cells (Figure 5.9, HEK-V, Rh123+VP). Similar data showed that EPN-2, MED-2 and SPNET-1 cell lines contained a population of cells which were able to extrude Rh123 and that this extrusion was inhibited after incubation in Verapamil resulting in Rh123 accumulation. The results demonstrated that the 3 cell lines comprised a different proportion of functional ABCB1 cells;  $34 \pm 5.2\%$  in EPN-2,  $26.5 \pm 3.9\%$  in MED-2 and  $13.9 \pm 3.2\%$  in SPNET-1 as shown in Figure 5.10 and 5.11.

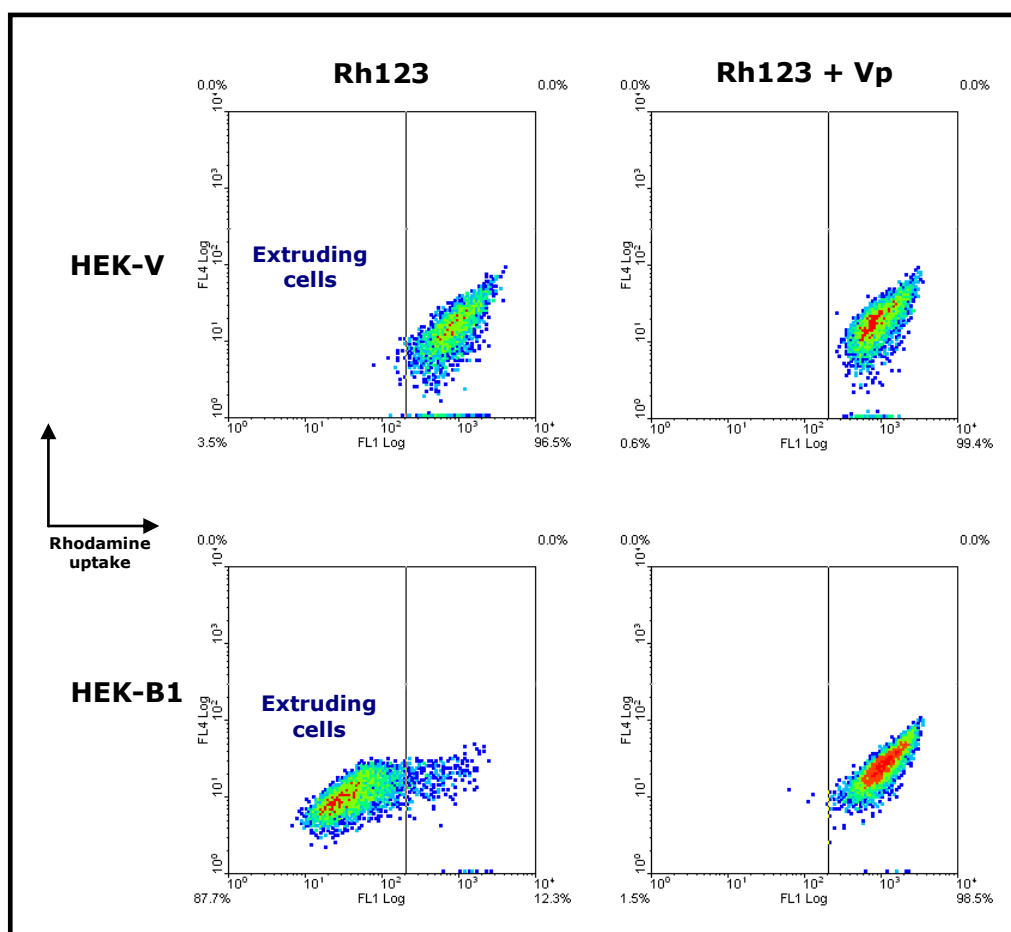


**Figure 5.9 ABCB1 functional analysis by FACS in control cells.** ABCB1 function was analysed in HEK cells stably transfected with ABCB1 (HEK-B1, positive control) and empty vector (HEK-V, negative control). HEK-V cells clearly gave a negative result whereby all cells accumulated Rhodamine 123 (Rh123) and Verapamil (VP) had no effect on these cells. The majority of HEK-B1 cells (88%) had a low level of Rh accumulation after cells were incubated in Rh123 and this extrusion of Rh123 was inhibited by Verapamil resulting in cells accumulating Rh123 and shifting to the right panel. This figure shows data representative of 3 independent experiments. All experiment included 5,000 – 10,000 events. Cells in the left panel indicate efflux function of ABCB1. For the positive control cells, the gate was set based on the results from HEK-V cells.



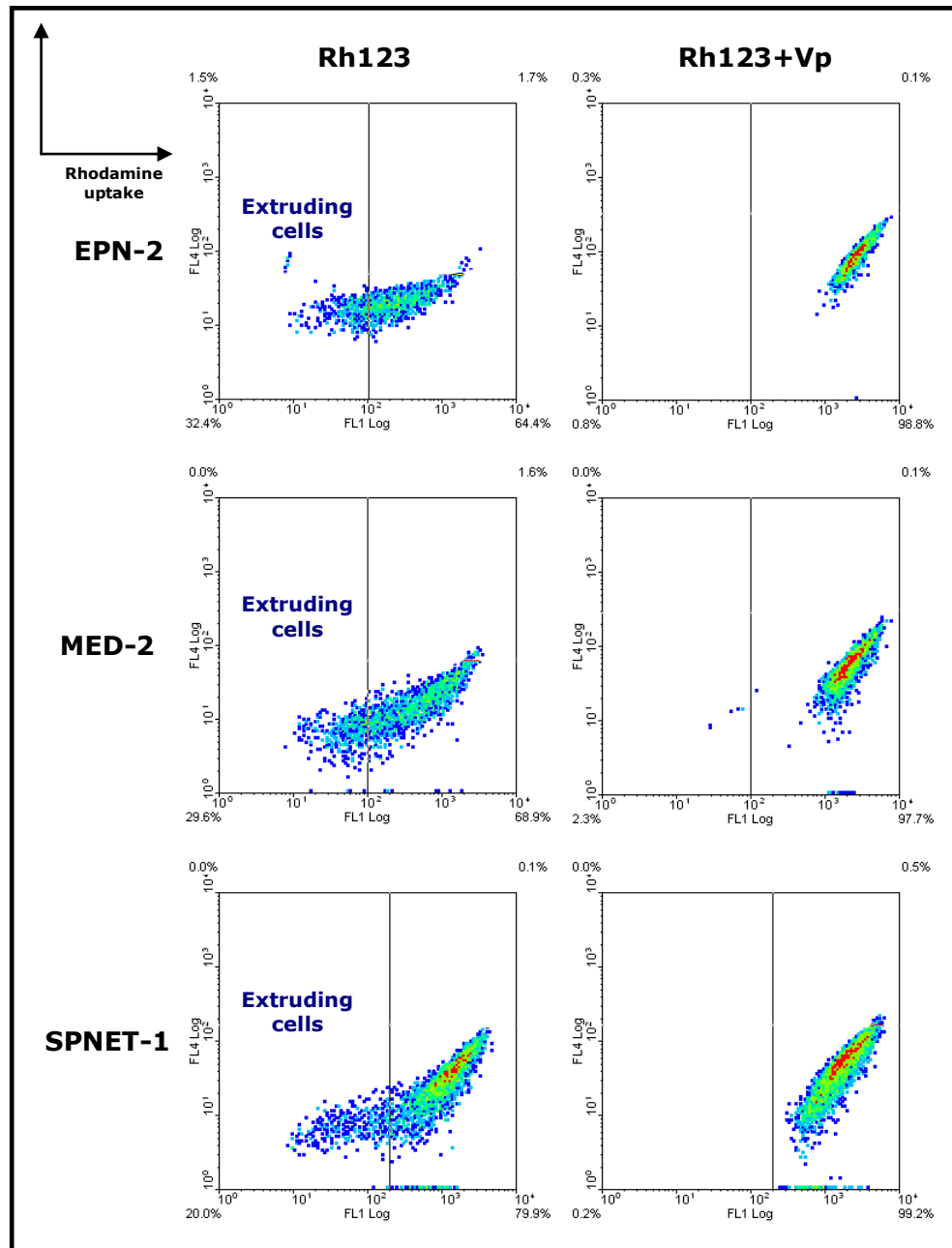


**Figure 5.10 ABCB1 functional analysis by FACS in monolayers from EPN-2, MED-2 and SPNET-1 cell lines.** Cells harvested from monolayers from the 3 cell lines were incubated in Rh123 with or without Verapamil. FACS results showed that all 3 cell lines contained cells extruding Rh123; 32.4% in EPN-2, 29.6% in MED-2 and 20% in SPNET-1 (left panel). All Rh123 extruding cells were inhibited by Verapamil as shown in the right panel. ABCB1 functional analysis hence showed that all 3 cell lines contained functional ABCB1 cells which were completely blocked by Verapamil. This figure shows data representative of 3 independent experiments. For all cell lines, the gate was set based on the results from sample incubated in the secondary antibody only corresponding to each cell line.

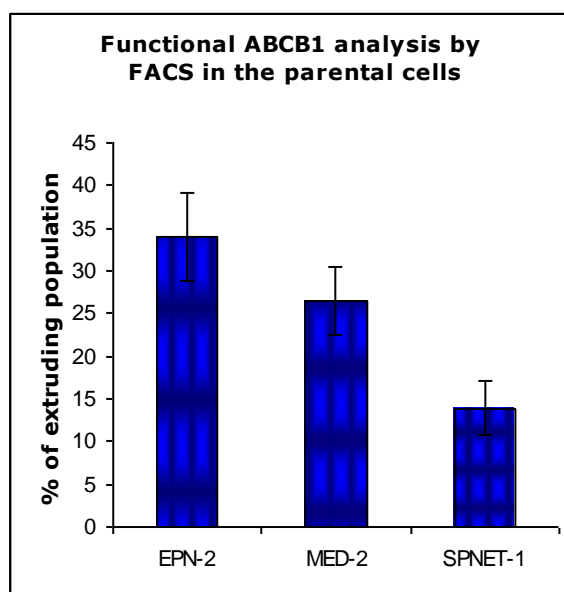


**Figure 5.11 Proportion of EPN-2, MED-2 and SPNET-1 cells showing functional ABCB1.**

The graph shows the percentage of cells extruding Rhodamine 123 (Rh123) detected by FACS from EPN-2, MED-2 and SPNET-1 cell lines. Data represents the (SEM) mean of 3 independent experiments. EPN-2 cell line contained the highest number of endogenous functional ABCB1 cells whilst the lowest number was observed in SPNET-1 cell line.

### 5.3 Discussion

#### **A low level of co-expression of CD133 and ABCB1 or ABCC1 suggests intrinsic drug resistance in parental paediatric brain tumour cell lines.**

Immunofluorescence results (CD133 co-stained with ABCB1, ABCC1 or ABCG2) demonstrated that monolayers from the parental EPN-2, MED-2 and SPNET-1 cell lines contained a small proportion of cells co-expressing a low level of CD133 and ABCB1 or ABCC1 (~10% by estimation) (Figure 5.1 and 5.2), whilst a larger proportion of cells co-expressing a higher level of CD133 and ABCB1 or ABCC1 (~20-30% by estimation) (Figure 5.1 and 5.2) was detected in neurospheres. Cells co-expressing CD133 and ABCG2 were not detected in any parental cell lines when grown both monolayers and neurospheres (Figure 5.3). Calatuzzolo and colleagues studied the expression of ABCB1 and ABCC1 in adult human glioma and found that glioma tissues derived from patients and primary cultures of gliomas as monolayers contained a high proportion of cells expressing ABCC1 whilst ABCB1 was detected at a low proportion. They suggested that ABCC1 probably was a significant drug resistant transporter in glioma tumours [Calatuzzolo, C. *et al* (2005)]. Based on our data at this stage, neither the proportion of cells expressing ABCB1 or ABCC1, nor the level of ABCB1 or ABCC1 expression is obviously different in our cell lines. Our data suggested that the parental cell lines contained a small proportion of cells expressing endogenous ABCB1 and ABCC1 at a similar low level. The difference in the level of ABC transporter expression after drug treatment is the focus of Chapter 6. A higher level of ABCB1, ABCC1 and CD133 expression in neurospheres was confirmed by Western blotting analysis (Figure 5.8, a and b and Figure 4.7, a) and a lack of ABCG2 expression was also confirmed as shown in Figure 5.8, c. For detection of ABCB1, different ABCB1 antibodies were used with respect to 4E3 antibody used in immunofluorescence and C219 antibody used in Western blotting analysis and the results from these 2 techniques were consistent. Similarly, MRPr1 and MRPr6 antibodies were available in our laboratory for ABCC1 detection. MRPr1 was used in immunofluorescence analysis whereas either MRPr1 or MRPr6 was used in Western blotting

analysis and these 2 antibodies showed similar results. The agreement of Western blotting and immunofluorescence analysis affords confidence in the conclusion that a low level of co-expression is observed in monolayers and is enriched under conditions promoting neurosphere formation consistent with enrichment of a drug resistant cell population in neurospheres.

In agreement with this, neurospheres from EPN-1, MED-1, BT-4 and Olig-1 cell lines contained a higher proportion of cancer stem-like cells (cells co-expressing CD133 and SOX2) than that of monolayers (Figure 4.6), and these neurospheres have greater etoposide resistance (Figure 5.12). Similarly, a higher proportion of cells co-expressing CD133 and ABCB1 or ABCC1 was detected in neurospheres when compared to monolayers. Hemmati and colleagues also studied neural stem-like cells in paediatric brain tumours including medulloblastomas and gliomas. They revealed similar results, which demonstrated that the large proportion of neurospheres derived from 4 different medulloblastoma tumours

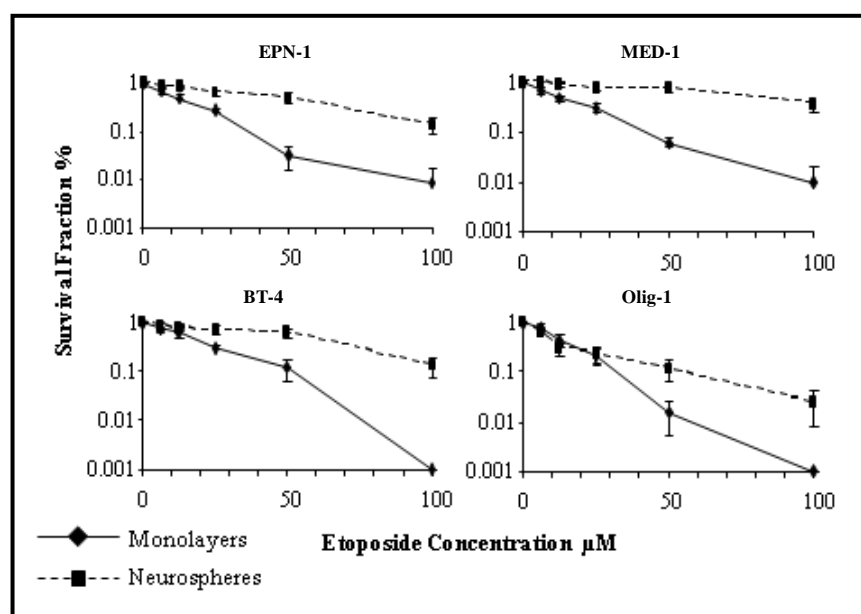


**Figure 5.12 Drug resistance potential of EPN-1, MED-1, Olig-1 and BT4 to etoposide.** The potential of drug resistance tested by clonogenic assay revealed that neurospheres from all cell lines were significantly more resistant to etoposide than monolayers with the exception of Olig-1 (EPN-1  $p < 0.001$ , BT-4  $p < 0.001$  and MED-1  $p < 0.001$ ) (performed by Dr. Deema Hussein).

expressed the stem cell marker nestin (>45%; detected by immunocytochemistry), whilst differentiating conditions demonstrated a lower proportion of nestin positive cells (<20%) [Hemmati, H. D. *et al* (2003)]. Although they used a different stem cell marker (nestin rather than CD133 and SOX2) and a different technique (immunocytochemistry versus immunofluorescence) to detect stem-like cells in paediatric brain tumours, their results and our results demonstrated similar findings i.e. neurosphere growth conditions promote a higher proportion of cancer stem-like cells. Our ABC transporter expression here supports the presence of intrinsic drug resistance in EPN-2, MED-2 and SPNET-1.

Quantification of the percentage of cells expressing CD133 and ABC transporters was attempted by FACS; however, a huge variation in the percentage of cells co-expressing CD133 and ABC transporters was detected in each independent experiment in particular for neurosphere samples (Figure 5.7). Therefore, the percentage of cells co-expressing CD133 and ABC transporters detected by flow cytometry could not be reliably established. Since the principle of FACS is to detect the immunofluorescence signals from a single cells passing through the machine, both monolayers and neurospheres were required to be dissociated into single cells prior to processing FACS analysis. The difficulty in cell dissociation possibly results from the following factors. Since the proteins of interest are located on the membrane, cells need gentle dissociation to avoid destroying the antigens. In particular to CD133, this may be more critical as anti-CD133 antibodies can detect cytoplasmic CD133 rather than membranous CD133, if the plasma membrane is broken down resulting from too harsh dissociation. As a result, our results showed a high proportion of cells expressing CD133 (Figure 5.4 – 5.6), which is an overestimate compared to data from immunofluorescence (Figure 5.1 – 5.3) and Western blotting analysis (Figure 4.7, a). However, if cells were too gently singularised to preserve membranous protein, clumped cells are present and these may not only conceal expression but they may be excluded from the FACS counter. Consequently, the number of cells expressing interesting protein will be underestimated. Gentle dissociation agent had been used to singularise cells e.g. Ethylenediaminetetraacetic acid (EDTA). Monolayers were easily dissociated into a single cell

using 10 mM EDTA in DPBS whilst neurospheres proved more difficult to singularise even after incubation in 10 mM EDTA in DPBS on a rotator for up to 30 minutes. EDTA is a strong chelator for calcium and other divalent cations such as magnesium resulting in digestion of the extracellular matrix or weakening of cell-dish adhesion. Using EDTA to detach cells from flasks is a gentle method and membranous antigens are preserved. However, a disadvantage of using EDTA is its slow action [Hara, M. *et al* (2001) and Corver, W. E. *et al* (1995)]. To improve the quality of dissociation in neurosphere samples, gentle enzymatic dissociation agents had been tried. Alfazyme and Accutase were both assessed to their ability to singularise cells for FACS analysis by Dr. Deema Hussein. However, these 2 gentle enzymatic dissociation agents failed to prepare a good quality of single cells. For the future study, an effective cell dissociation should be properly optimised to obtain a higher yield of viable single cells and a lesser destruction of membranous antigens.

### **Parental cell lines contained endogenous functional ABCB1**

Since we hypothesised that cancer stem cells expressing ABC transporters play an important role in drug resistance of paediatric brain tumours, functional analysis by flow cytometry was performed. Based on the co-staining immunofluorescence data, it was only expected that around 15% of our cells would extrude Rhodamine 123 (Rh123). Since, parallel analysis of drug selected sublines/clones indicated that ABCB1 function was paramount (Chapter 7), only the function of this transporter was assessed. ABCB1 functional analysis demonstrated that parental cancer stem-like cells express functional endogenous ABCB1. The highest proportion was observed in EPN-2 ( $34 \pm 5.2$ ) whilst SPNET-1 parental cells demonstrated the lowest proportion ( $13.9 \pm 3.2$ ), and MED-2 parental cells contained  $26.5 \pm 3.9$  of cells extruding Rh123. The proportion of cancer stem-like cells and level of endogenous functional ABCB1 did not appear to correlate with tumour grade, type of tumour nor whether they were primary or recurrent. The grade II, primary EPN-2 cell line contained the highest proportion of endogenous functional ABCB1 whilst grade IV MED-2 and SPNET-1 cell lines contained a

lower proportion. This could however only be properly assessed on a larger sample size to make a strong conclusion.

An additional question is how appropriate the choice of substrate is?, van der Sandt and colleagues compared the specificity between doxorubicin and Rh123 in cell lines derived from a pig kidney and Caco-2 cell line derived from a human colon carcinoma. They found that Rh123 was able to be transported by both ABCB1 and the organic cation carrier system whilst doxorubicin was transported only by ABCB1. Therefore, the results from studying ABCB1 function in cell lines containing the organic cation carrier system using Rh123 as an ABCB1 substrate should be interpreted carefully. They suggested that doxorubicin seems to be more specific and appropriated to be a substrate for ABCB1 transporters in ABCB1 functional analysis [van der Sandt, I. C. J. *et al* (2000)]. However, we do not know whether our paediatric cell lines contain the organic cation carrier system or not. In addition to this our initial analyses indicate that our cell lines are highly resistant to doxorubicin (Dr. Deema Hussein, personal communication). Currently, a third generation of ABCB1 inhibitors has been discovered and these inhibitors are more specific and have less toxicity. Additionally, they do not alter the level of other cytotoxic drugs, which are used as combined treatment. The third generation of ABCB1 inhibitors includes tariquidar and elacridar (GF120918). A third generation of ABCB1 inhibitors is also recommended to be used in future ABCB1 functional analysis for more specificity.

At this point, it has been known that the parental cell lines contained a small proportion of cancer stem-like cells expressing functional ABCB1 and neurosphere conditions enriched for CSCs expressing functional ABCB1. Active drug efflux transporters had been known to correlate with multidrug resistance in particular to ABC transporter family. Therefore, to prove that the endogenous functional ABCB1 expressed in the parental cell lines plays a role in drug resistance indicating intrinsic drug resistance, drug resistance analyses were performed and the results are shown in Chapter 6.

---

---

## **Chapter 6**

**Drug treatment selected resistant sublines expressing ABC  
transporters**

---

---



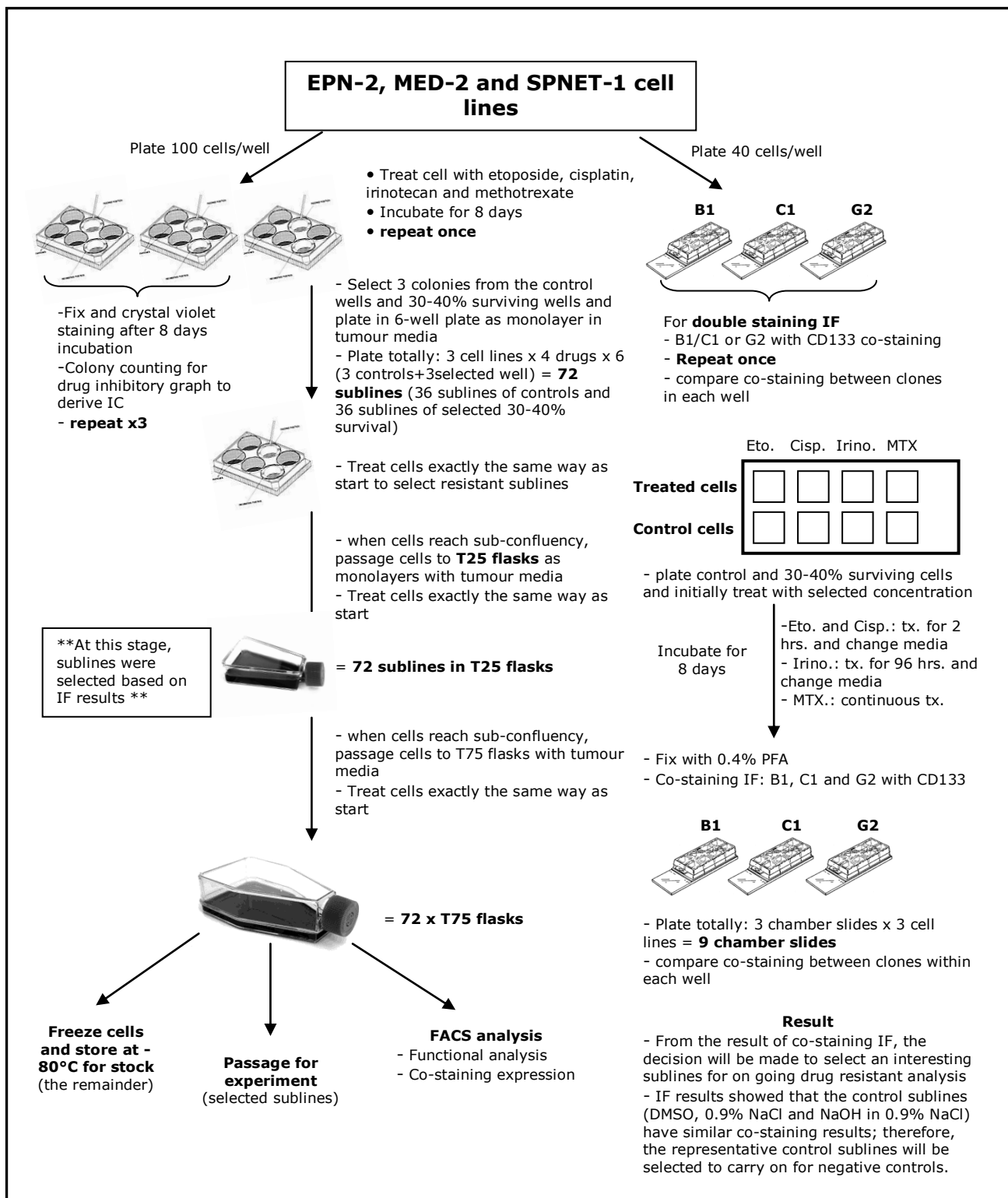
## **Chapter 6: Drug treatment selected resistant sublines expressing ABC transporters**

### **6.1 Introduction**

Although chemotherapy is a main standard treatment for brain tumours, a failure of treatment frequently occurs in patients resulting in tumour relapse and poor prognosis. Drug resistance frequently manifests as a resistance to many drugs, regardless of chemical structures, which is called multidrug resistance (MDR). Many mechanisms can lead to MDR, however, one important mechanism is active drug efflux pumps on the membranes of cancer cells. The ABC transporter family is currently postulated to be an important factor involved in the mechanism of drug resistance in cancer stem cells. Multidrug resistance is still a big obstacle and an unresolved problem for chemotherapy in many cancers. Currently, there are 49 ABC transporter proteins identified in human [Reviewed in Dean, M. *et al* (2001)]. Only 3 ABC transporters are overexpressed in both drug resistant cultured cell lines and drug resistant tumours in patients. ABCB1, ABCC1 and ABCG2 transporter are the main ABC transporters associated with MDR. P-gp (MDR1 or ABCB1) was first discovered in 1976 in Chinese hamster ovary cell lines selected for colchicine resistance. These cells were not only resistant to colchicine but they also had less permeability to other compounds [Juliano, R. L. and Ling, V. (1976)]. Later, a human small-cell lung cancer cell line (H69) that had been selected for doxorubicin resistance (but which did not express ABCB1) showed cross-resistance to many anticancer agents including anthracyclines, vinca alkaloids and epipodophyllotoxins; leading to the identification of MRP1 (ABCC1) [Cole, S. P. C. *et al* (1992)]. More recently, the human breast cancer cell line (MCF-7) was selected for doxorubicin resistance in the presence of verapamil to inhibit ABCB1 function. However, this cell line was still resistant to doxorubicin without ABCB1 and ABCC1 expression [Chen, Y. N. *et al* (1990)]. Later, a drug resistant transporter in this cell line was identified by several groups independently as BCRP/ABCG2/MXR/ABCP [Doyle, L. A. *et al* (1998), Miyake, K. *et al*

(1999) and Allikmets, R. *et al* (1998)]. To study drug resistance in paediatric brain tumour cell lines, a clonogenic assay was performed to select sublines showing resistance to etoposide, cisplatin, irinotecan and methotrexate for ongoing drug resistance analysis. These 4 drugs have different targets and mechanisms of actions. The main target of etoposide is nuclear topoisomerase II enzyme, which is homodimer, consisting of 2 forms; topoisomerase II  $\alpha$  (170 kDa) and topoisomerase II  $\beta$  (180 kDa). The effect of etoposide involves in topoisomerase II since it is highly increased during DNA replication detected in particular to S and G2 phases of cell cycle [Joel, S. (1996)]. Cisplatin exert toxic effects through interacting with gDNA, although much of the drug binds to non-DNA target: the tripeptide glutathione (GSH) and other thiol-containing biomolecules such as metallothioneins (MT) [Reviewed in Cepeda, V. *et al* (2007)]. Irinotecan forms a covalent DNA-topoisomerase I complex by binding to this complex, which is a reversible reaction resulting in stabilisation of the DNA-topoisomerase I complex, preventing the processing of replication forks leading to double stranded DNA breaks and causing cell death [Hsiang, Y. H. *et al* (1989)]. Methotrexate is a potent inhibitor for DHFR, which results in inhibition of DNA synthesis [White and Goldman, (1976)]. All 4 drugs similarly target proliferating or cycling cells. Etoposide, irinotecan and methotrexate were known to be substrates for ABCB1, ABCC1 and ABCG2 transporters and these 3 drugs can be transported by these transporters. Whilst there was evidence supporting the fact that cisplatin was specifically transported by ABCC2 [Reviewed in Szakács, G. *et al* (2006)]. After drug treatment, the selected resistant sublines were investigated to determine whether ABC transporters were the major mechanisms of drug resistance. The expression of ABCB1, ABCC1 and ABCG2 and CD133 was assayed in the selected resistant sublines at different time points to determine whether alteration of expression occurred during prolonged drug treatment. The expression of these transporters was assayed by the immunofluorescence and Western blotting analysis. Additionally, the selected resistant sublines were induced in stem cell media to form neurospheres, to confirm retention of a key stem cell property.

## Clonogenic assay plan



## 6.2 Results

### 6.2.1 Condition optimised by clonogenic assay

To study the contribution of ABCB1, ABCC1 and ABCG2 to drug resistance of cancer stem cells, 4 chemotherapeutic drugs commonly used to treat brain tumours and known to be substrates of ABC transporters; etoposide, cisplatin, irinotecan and methotrexate were applied to the 3 primary cultured cell lines; EPN-2, MED-2 and SPNET-1. All processes for clonogenic assay and immunofluorescence analysis for selection of on going resistant sublines are demonstrated in the schematic plan (page 202). A range of drug concentrations was selected, based on current literature, for the clonogenic assay [Cisplatin [Sorenson, C. M. and Eastman, A. (1988)], methotrexate [Barry, M. A. *et al* (1990)], etoposide [Ermakova, S. P. *et al* (2006)] and irinotecan [Pollack, I. F. *et al* (1999)]. The aim was to derive a concentration curve and identify the inhibitory dose 0, 30%, 50%, 70% and 90%. Once the optimal range had been identified for each drug on each cell line, the experiment was repeated 3 times under these conditions.

The percentage of surviving cells was plotted against log concentration of drug using GraphPad Prism software to determine  $IC_{30}$ ,  $IC_{50}$  and  $IC_{70}$  of each drug. Dose response curves for each cell line were obtained by fitting the data points to the linear quadratic equation and all graphs of etoposide, cisplatin, irinotecan and methotrexate are shown in Figure 6.1. All IC values are also summarised in Table 6.1. From this assay, the concentration which achieved 30-40% surviving cells was selected to treat cells for downstream analysis.  $IC_{30}$ ,  $IC_{50}$  and  $IC_{70}$  values derived from drug inhibitory response graph are shown in Table 6.1. However, the concentrations, selected to treat cells for ongoing analysis, were those of the 30-40% survival well from the clonogenic assay shown in brackets in Table 6.1.

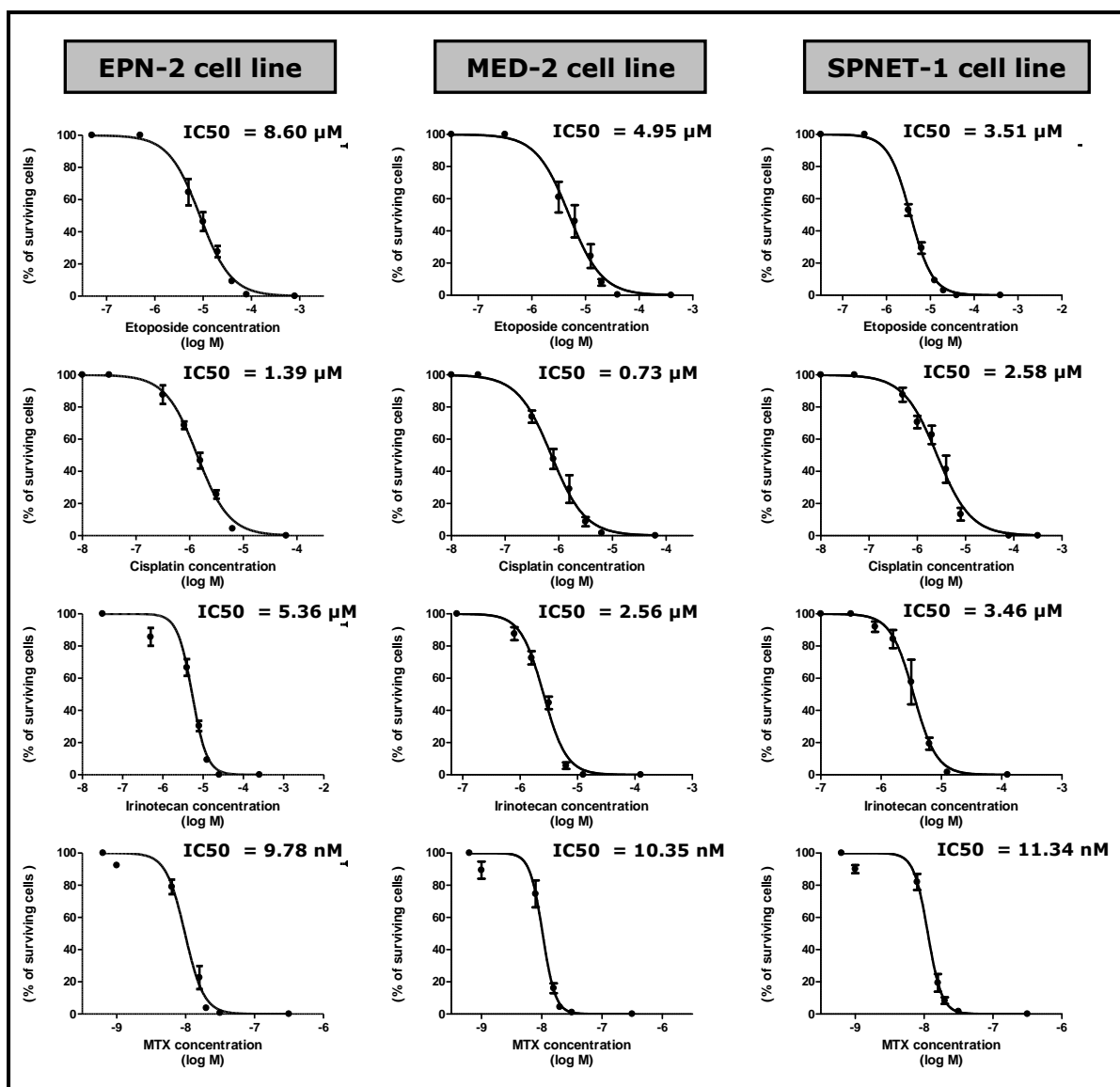


**Figure 6.1 Drug inhibitory graphs of etoposide, cisplatin, irinotecan and methotrexate treatment in the EPN-2, MED-2 and SPNET-1 cell line.** To find the  $IC_{30}$ ,  $IC_{50}$  and  $IC_{70}$  values of these drugs in the EPN-2, MED-2 and SPNET-1 cell line, they were treated with an appropriate range of concentrations of etoposide, cisplatin, irinotecan and methotrexate and percentages of surviving cells were plotted against  $\log[\text{drug concentration}]$ . All 3 IC values are described in table 6.1. Error bars represent the SEM of 3 independent experiments.

**Table 6.1 Summary of IC<sub>30</sub>, IC<sub>50</sub> and IC<sub>70</sub> of etoposide, cisplatin, irinotecan and methotrexate treated in EPN-2, MED-2 and SPNET-1 cell lines**

Drug treatment	IC	IC value		
		EPN-2	MED-2	SPNET-1
<b>Etoposide</b>	IC <sub>30</sub>	4.7 $\mu$ M	2.6 $\mu$ M	2.2 $\mu$ M
	IC <sub>50</sub>	8.6 $\mu$ M	4.95 $\mu$ M	3.5 $\mu$ M
	IC <sub>70</sub>	15.8 $\mu$ M (20 $\mu$ M)	8.8 $\mu$ M (6 $\mu$ M)	5.7 $\mu$ M (6 $\mu$ M)
<b>Cisplatin</b>	IC <sub>30</sub>	0.75 $\mu$ M	0.39 $\mu$ M	1.3 $\mu$ M
	IC <sub>50</sub>	1.39 $\mu$ M	0.73 $\mu$ M	2.58 $\mu$ M
	IC <sub>70</sub>	2.43 $\mu$ M (3 $\mu$ M)	1.3 $\mu$ M (1.5 $\mu$ M)	5.0 $\mu$ M (4 $\mu$ M)
<b>Irinotecan</b>	IC <sub>30</sub>	3.6 $\mu$ M	1.7 $\mu$ M	2.4 $\mu$ M
	IC <sub>50</sub>	5.36 $\mu$ M	2.56 $\mu$ M	3.46 $\mu$ M
	IC <sub>70</sub>	7.6 $\mu$ M (8 $\mu$ M)	3.8 $\mu$ M (3 $\mu$ M)	4.9 $\mu$ M (6 $\mu$ M)
<b>Methotrexate</b>	IC <sub>30</sub>	7.3 nM	8.2 nM	9.3 nM
	IC <sub>50</sub>	9.78 nM	10.35 nM	11.34 nM
	IC <sub>70</sub>	12.9 nM (15 nM)	12.6 nM (15 nM)	14.0 nM (15 nM)

### 6.2.2 Neurosphere formation assay after drug treatment

Surviving colonies were initially examined for their ability to form neurospheres as this is one of the characteristics of cancer stem cells. Six selected colonies from the clonogenic assay were dissociated into single cells in stem cell media. Neurosphere formation was observed under the microscope and counted. Both colonies from the vehicle treated and the drug treated well were able to form neurospheres following etoposide, cisplatin and irinotecan treatment (Figure 6.2 and 6.3). Methotrexate treated surviving colonies, however, formed smaller neurospheres (containing 10-20 cells) when compared to the other conditions. The average number of neurospheres formed was determined from the 6 dissociated colonies. Since each colony selected to form neurospheres contained different cell numbers ranging from 50-200 cells, it is difficult to carry out statistical analysis on the data. However, an attempt was made to select equal size colonies from each condition. Drug treated cells generally formed smaller colonies than the control especially methotrexate treated cells which formed very small colonies containing less than 50 cells even after incubating for 8 days. The average number of neurospheres formed from each condition is shown in Figure 6.4. Control treated cells of SPNET-1 cell line formed the highest number of neurospheres while methotrexate treated cells formed the lowest number of neurospheres. Both control and treated conditions could form neurospheres apart from methotrexate treated cells which probably required a longer time to form proper neurospheres.

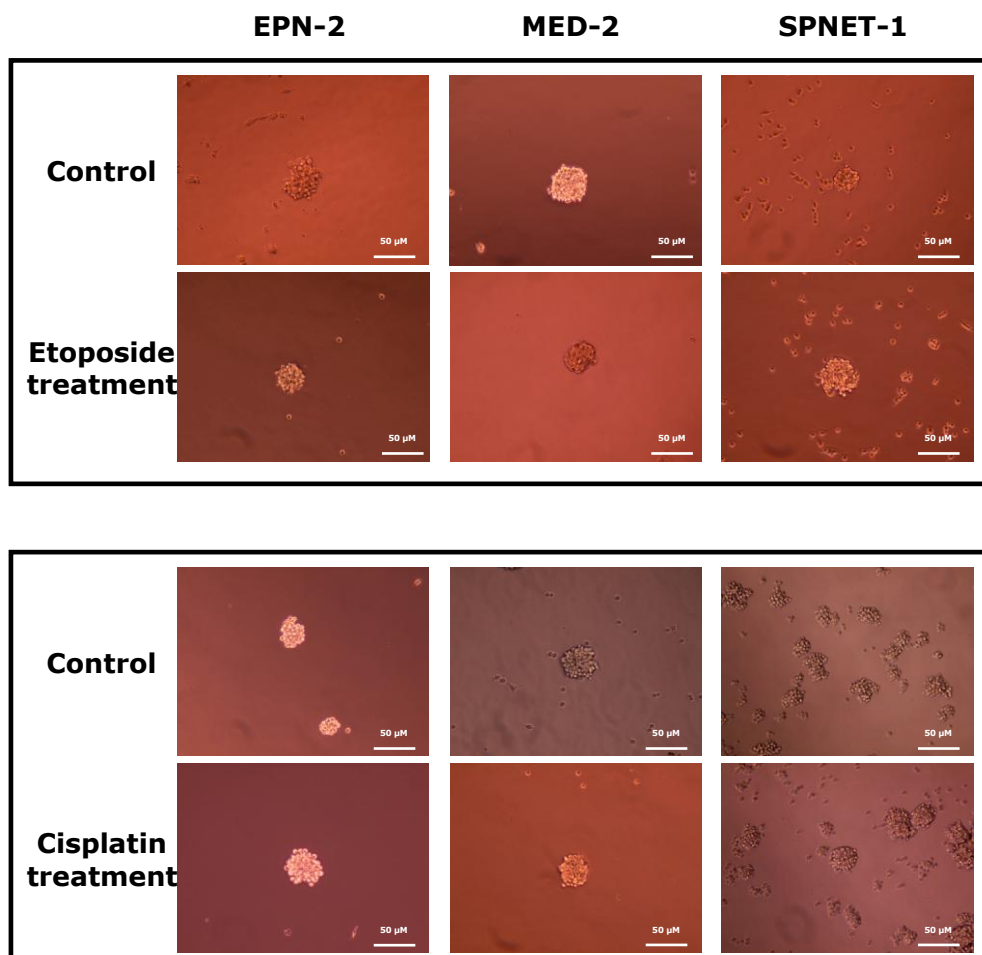


**Figure 6.2 Neurosphere formation derived from the vehicle control colonies, etoposide and cisplatin treated colonies from EPN-2, MED-2 and SPNET-1 cell lines.**

This figure shows neurospheres, which were formed from microscopically selected single colonies, dissociated into single cells and grown in stem cell media for 3-4 days. Colonies derived from all conditions, both the vehicle control and treated conditions, were able to form neurospheres. (Scale bar = 50 µm)

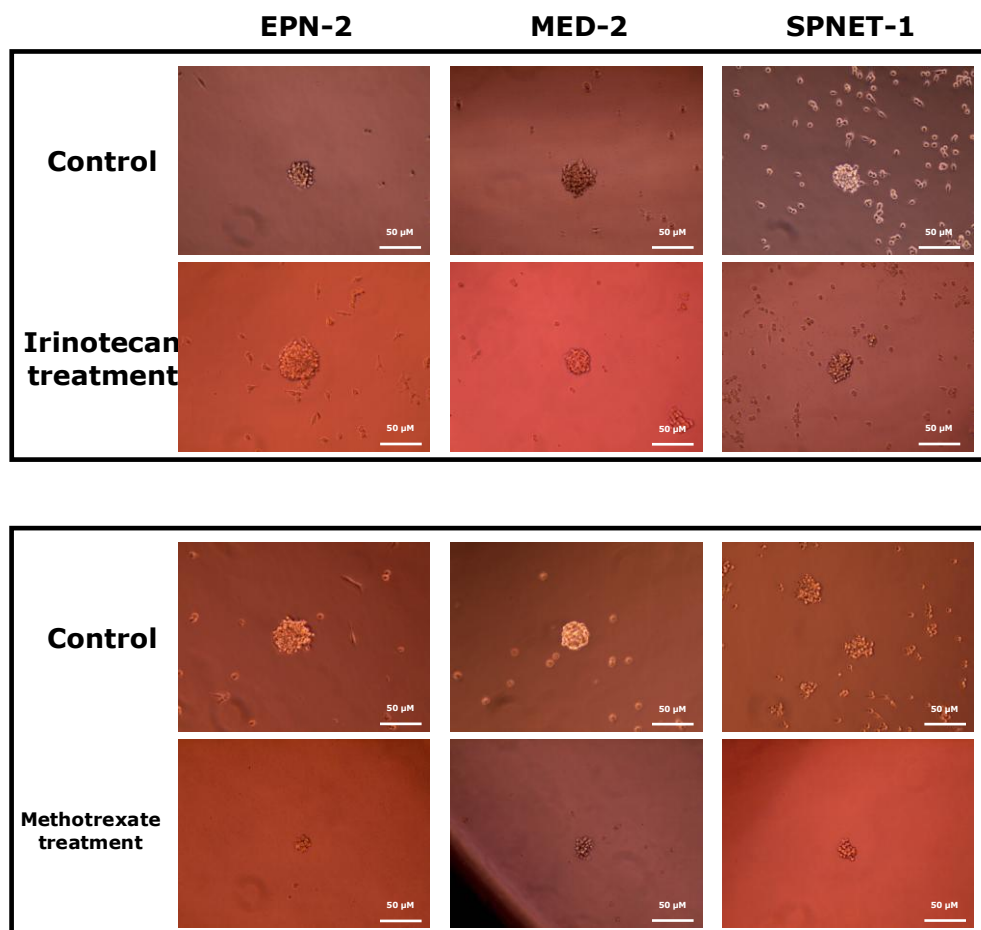


**Figure 6.3 Neurosphere formation derived from the vehicle control colonies, irinotecan and methotrexate treated colonies from EPN-2, MED-2 and SPNET-1 cell lines.** Both the vehicle control colonies and irinotecan treated colonies could readily form neurospheres after 3-4 days incubation which contained more than 50 cells/neurosphere. Whilst methotrexate treated colonies formed tiny neurospheres containing less than 50 cells. (Scale bar = 50 µm)



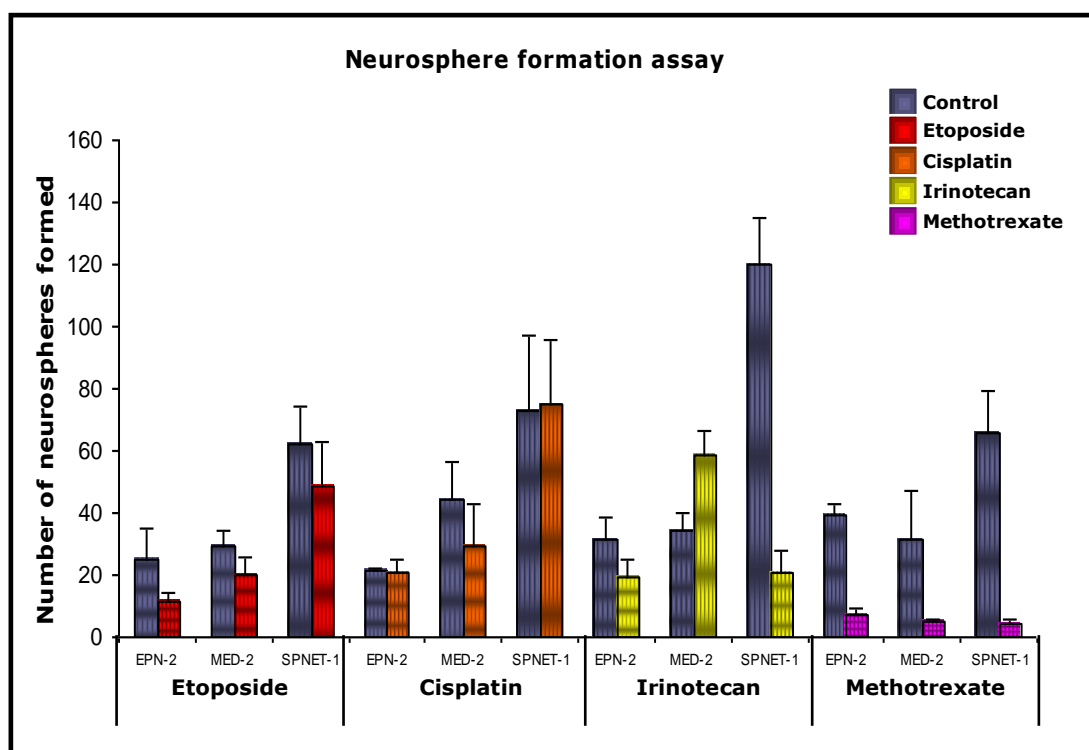


**Figure 6.4 Neurosphere formation of the vehicle control colonies and 4 drug treatments in EPN-2, MED-2 and SPNET-1 cell lines.** The average number of neurospheres formed from each condition is demonstrated in the graph. All conditions were able to readily form neurospheres with the exception of methotrexate treated colonies which formed the lowest numbers of neurospheres. The average numbers of neurospheres could not be directly compared between the vehicle control and the treated conditions because each selected clone contained a different number of cells when they were dissociated in stem cell media. However, neurosphere formation ability was affected in irinotecan treated SPNET-1 colonies and methotrexate colonies of all cell lines since a number of neurosphere formation of these colonies was less than the control colonies.

### **6.2.3 Immunofluorescence analysis in the parental cell lines after the first round of drug treatment**

Previous results confirmed that the parental EPN-2, MED-2 and SPNET-1 cell lines contained a cancer stem cell-like population expressing functional ABCB1 transporter. To investigate whether these parental cell lines can be enriched for cells expressing ABC transporters after drug treatment, the clonogenic assay was performed in chamber slides and the parental cells seeded as single cells were treated with each of the drugs (etoposide, cisplatin, irinotecan and methotrexate) at the concentration determined to give 30-40% survival. CD133 and ABC transporter co-staining immunofluorescence was then performed to determine co-expression of CD133 and ABC transporters after the first round of drug treatment. Immunofluorescence results from selected sublines after the first round of treatment are shown in Figure 6.5 - 6.7 and non-selected subline results are shown in the appendix section (Figure A1.1 –A1.3).

Co-staining immunofluorescence in the parental cells of EPN-2, MED-2 and SPNET-1 cell lines showed a low level of CD133 and ABCB1 or ABCC1 co-expression and a low proportion of co-expressing cells whilst none of our cell lines was positive for CD133 and ABCG2 co-expression (Chapter 5, Figure 5.1, 5.2 and 5.3). After the first round of drug treatment, co-expression of CD133 and ABCB1 was detected in all drug surviving sublines from all cell lines treated with etoposide, cisplatin, irinotecan or methotrexate. Whereby a high level of co-expression was observed in surviving cells treated with etoposide or irinotecan in EPN-2 cell line, irinotecan or methotrexate in MED-2 cell line and etoposide or methotrexate in SPNET-1 cell line. Conversely, EPN-2 treated with cisplatin or methotrexate, MED-2 treated with cisplatin or etoposide and SPNET-1 treated with cisplatin or irinotecan co-expressed a low level of CD133 and ABCB1. A high level of CD133 and ABCC1 co-expression was only detected in SPNET-1 treated with irinotecan whilst EPN-2 treated with each of 4 drugs co-expressed at a low level. On the contrary, co-expression of CD133 and ABCC1 was not found in any sublines of MED-2 cell line.

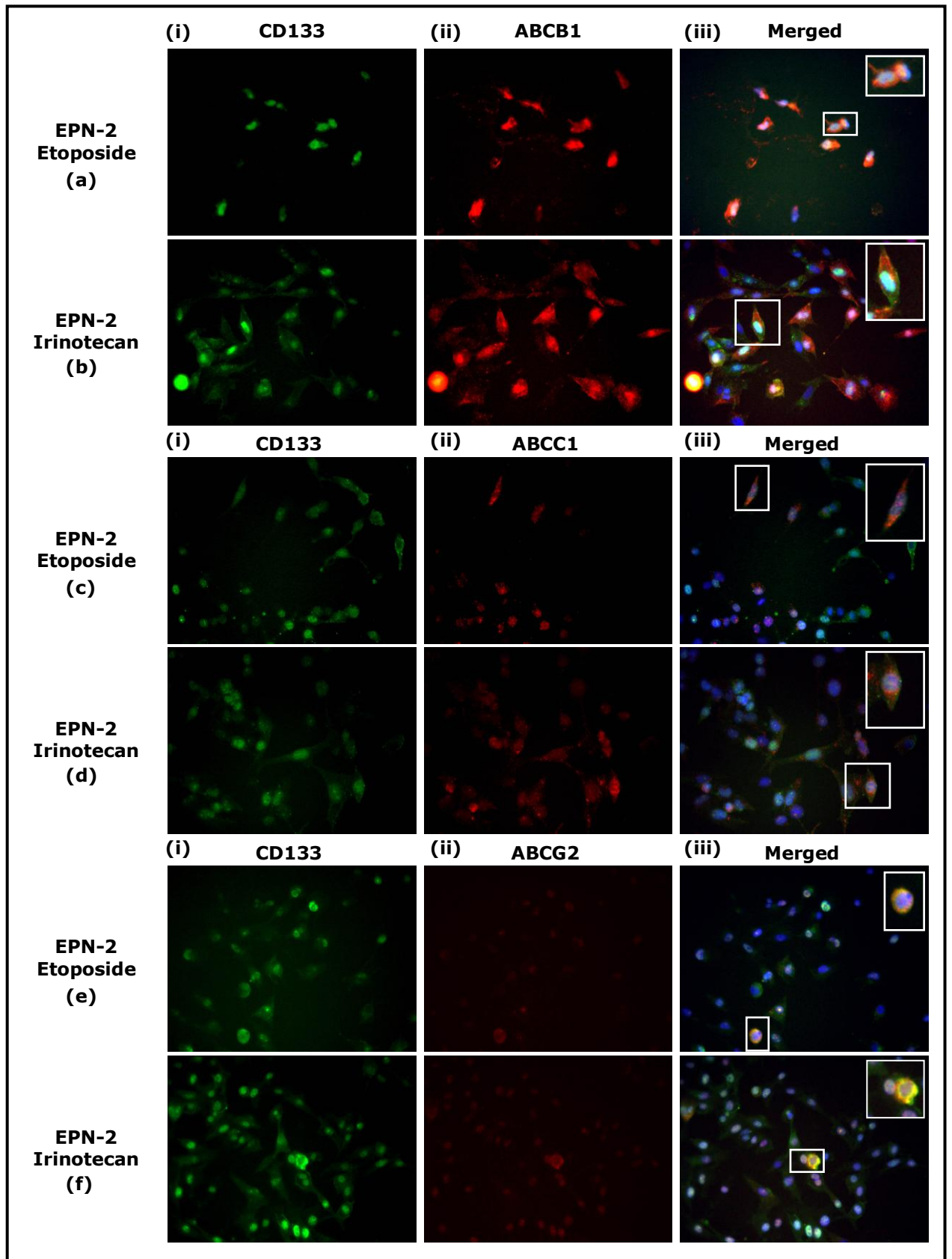


**Figure 6.5 Co-staining immunofluorescence analysis in the parental cells of EPN-2 after the first round of etoposide or irinotecan treatment.** After the first round of etoposide or irinotecan treatment, the co-staining immunofluorescence results showed a large proportion of cells co-expressing CD133 and ABCB1 at a high level [a and b] whilst a low proportion of cells co-expressing CD133 and ABCC1 or ABCG2 were detected at a low level [c – f]. The parental cells of EPN-2 were seeded as single cells (40 cells) in chamber slides then cells were treated with etoposide or irinotecan. Single cells were incubated for 8 days to form colonies. For merged images, a co-staining cell has been enlarged (x2-3) for clarity.

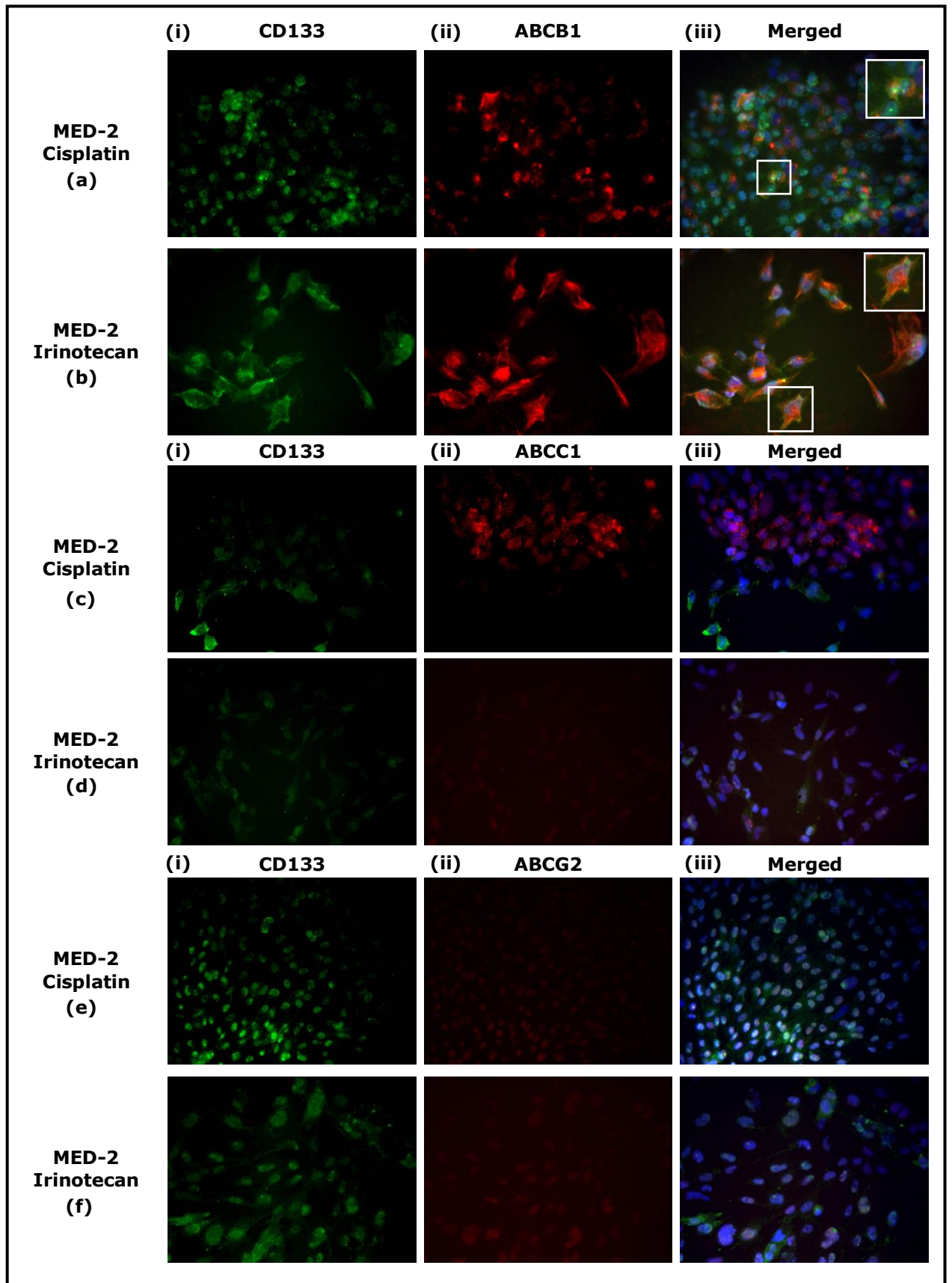


**Figure 6.6 Co-staining immunofluorescence analysis in the parental cells of MED-2 after the first round of cisplatin or irinotecan treatment.** After the first round of cisplatin or irinotecan treatment was applied to MED-2 parental cells, a large proportion of cells co-expressing CD133 and ABCB1 at a high level was observed in MED-2 treated with irinotecan [b] while a smaller proportion of cells co-expressing CD133 and ABCB1 was detected in MED-2 after cisplatin treatment [a]. Surviving MED-2 colonies after neither cisplatin nor irinotecan treatment were positive for CD133 and ABCC1 or ABCG2 co-expression [d – f]. For each treatment a co-staining cell has been enlarged (x2) for clarity.

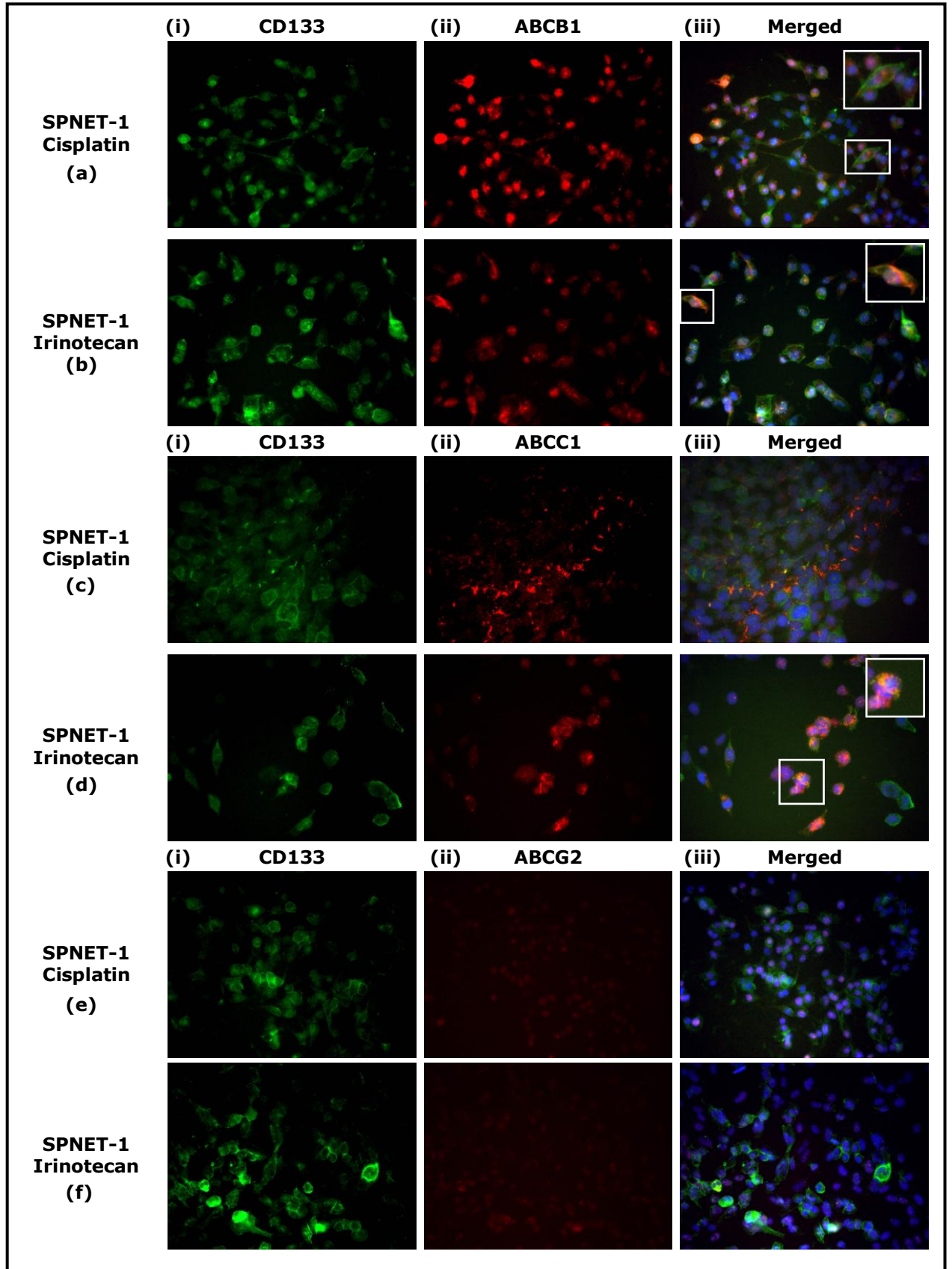
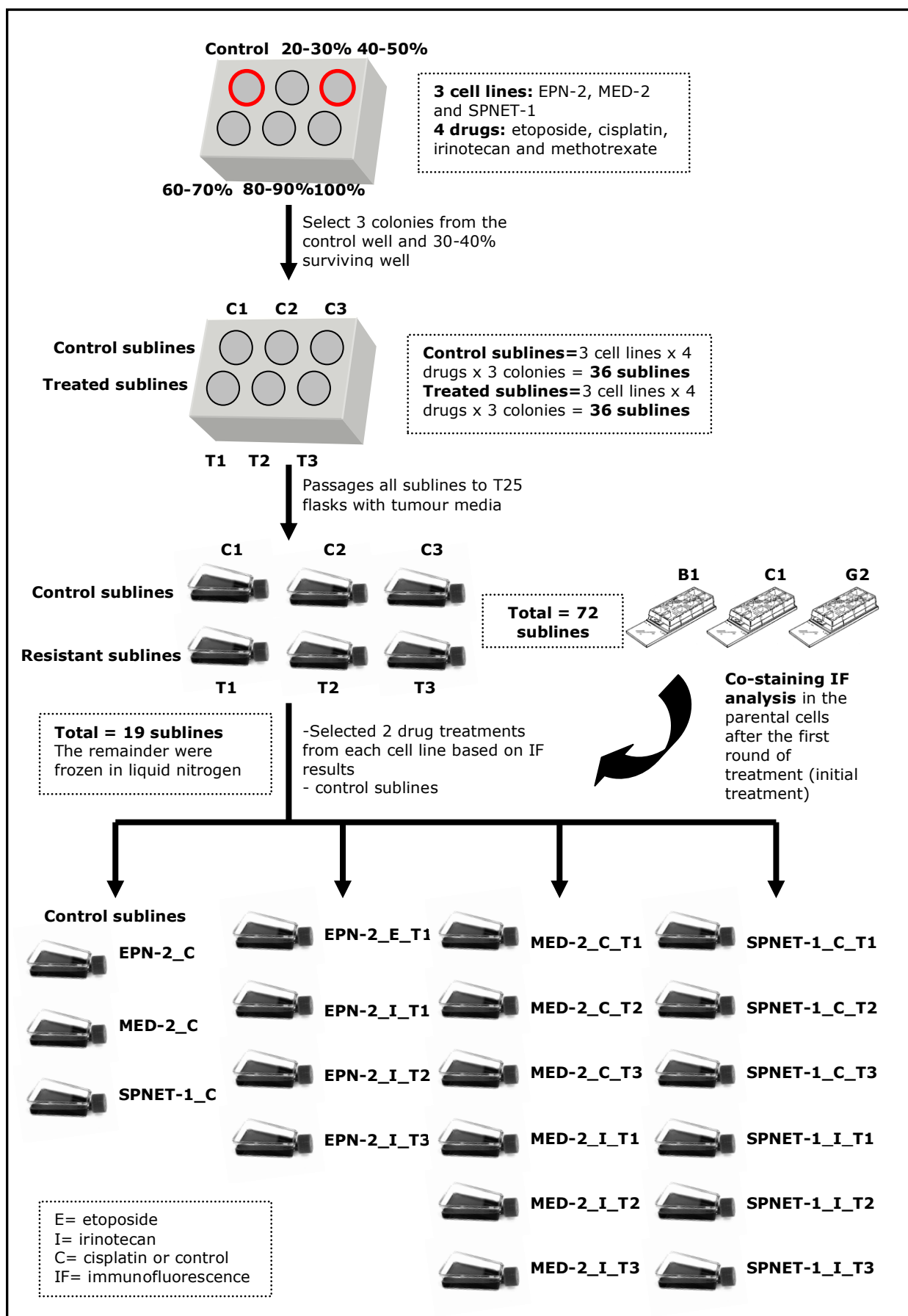


**Figure 6.7 Co-staining immunofluorescence analysis in the parental cells of SPNET-1 after the first round of cisplatin or irinotecan treatment.** After cells were treated with the first round of cisplatin or irinotecan, cells co-expressing CD133 and ABCB1 were detected after either cisplatin or irinotecan treatment [a and b]. Surviving irinotecan SPNET-1 colonies displayed co-expression of CD133 and ABCC1 at a high level [d] whilst surviving cisplatin SPNET-1 colonies demonstrated cells single expressing either CD133 or ABCC1 [c]. No surviving colonies of SPNET-1 were positive for CD133 and ABCG2 co-expression after cisplatin and irinotecan treatment [e and f]. For each treatment a co-staining cell has been enlarged (x2) for clarity.



## Drug treatment of selected resistant sublines



#### **6.2.4 Drug treatment selected resistant sublines for downstream drug resistance analysis**

The schematic work plan as shown in previous page demonstrates that there are 72 sublines in total after colony selection from clonogenic assay. It was unmanageable to carry on analysis on all 72 sublines in parallel with regard to time limitation. Therefore, to slim down the number of sublines for on going drug resistance analysis, co-staining immunofluorescence analysis was performed to determine any alteration of CD133 and ABC transporters co-expression after the first round of drug treatment in the parental EPN-2, MED-2 and SPNET-1 cell lines. We were interested in studying drug resistant cells containing a high proportion of cells co-expressing CD133 and ABC transporters at a high level. Therefore, any drugs, which selected sublines enriched with cells co-expressing CD133 and any ABC transporters after the first round of treatment, were carried on to select drug resistant sublines for downstream drug resistance analysis. Since there was no CD133 and ABCG2 co-expression detected in any surviving colonies, sublines enriched with a high level of CD133 and ABCB1 and/or CD133 and ABCC1 co-expression were selected for downstream of drug resistance analysis. Hence, there were totally 16 sublines selected with respect to EPN-2\_E\_T1, EPN-2\_I\_T1-T3, MED-2\_C\_T1-T3, MED-2\_I\_T1-T3, SPNET-1\_C\_T1-T3 and SPNET-1\_I\_T1-T3 as shown in the schematic work plan. Since the immunofluorescence results of the control sublines treated with different vehicle controls were similar, a representative control subline was selected for each cell line with regard to EPN-2\_C, MED-2\_C and SPNET-1\_C.

### **6.2.5 Cellular morphologies of the selected sublines after multiple rounds of drug treatment**

EPN-2, MED-2 and SPNET-1 selected sublines were then serially passaged as monolayers in tumour media and treated with the designated drugs. Sublines were treated at every passage and the duration of the treatment depended on the drugs: 2 hours for etoposide and cisplatin and 96 hours for irinotecan.

Since the cellular morphologies of the control sublines and the selected sublines from all cell lines showed similar features, only representative sublines are demonstrated in Figure 6.8 and the other selected sublines can be found in the appendix (Figure A2.1 and A2.2). All control sublines were a homogeneous population, which contained cells of a similar size and regular shape, whilst all selected sublines comprised 2 different populations; one was homogeneous population, which was similar to the vehicle control sublines and another was large multinucleated cells with an irregular shape. Additionally, selected sublines grew slower than the control sublines. For etoposide treatment of the EPN-2 cell line, EPN-2\_E\_T2 and T3 were effectively damaged and struggling to survive after treatment. Only EPN-2\_E\_T1 was able to survive and be serially passaged although it grew slowly taking 3x longer to double the number of cells than the parental EPN-2 cells (Figure A2.1).

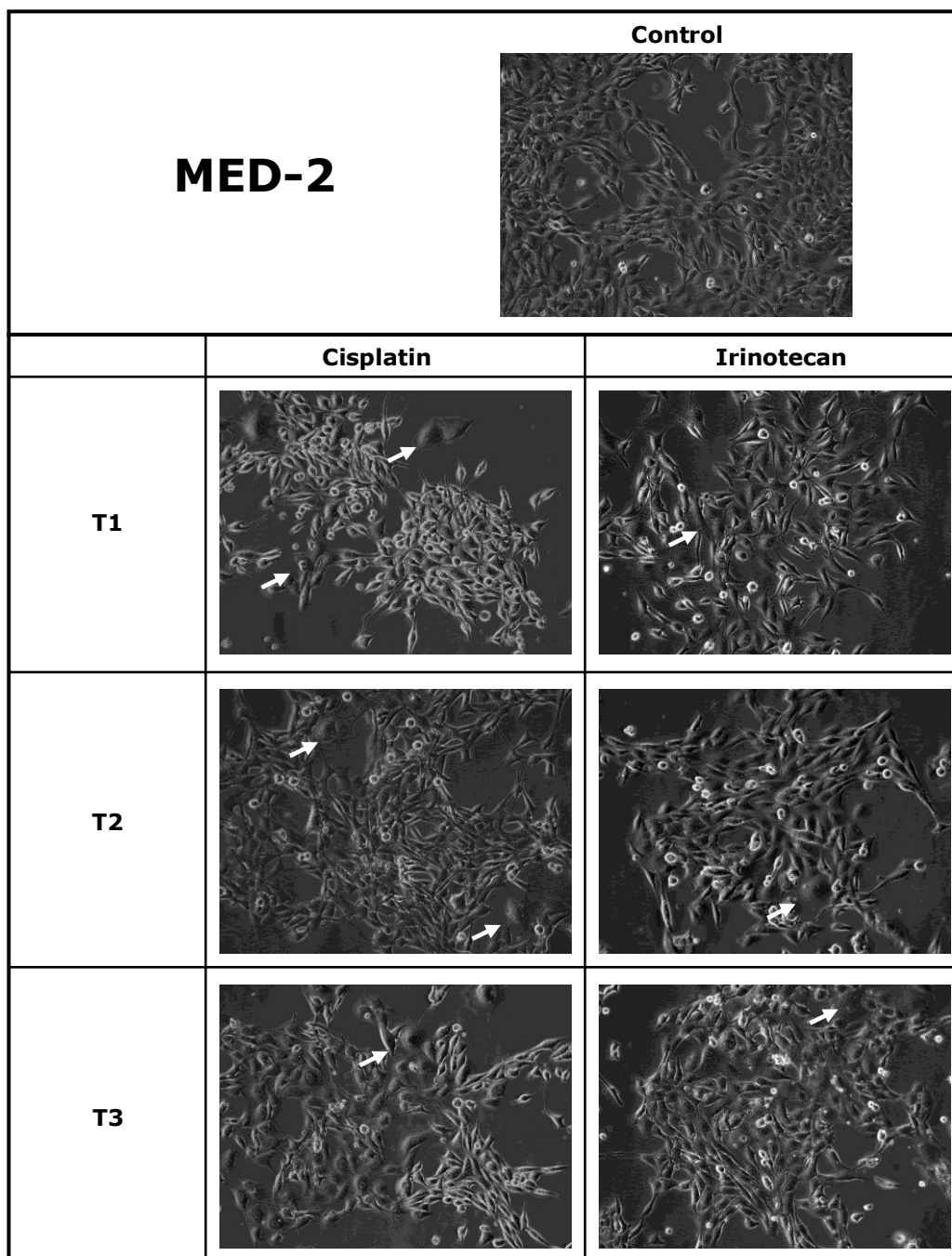


**Figure 6.8 The cellular morphology of a control subline and selected MED-2 sublines after multiple rounds of drug treatment.** All selected MED-2 sublines survived and were serially passaged after cisplatin or irinotecan treatments. The control sublines comprised a homogeneous population similar to the control sublines from EPN-2 and SPNET-1 cell line. Whilst the major cell population in each selected MED-2 sublines consistent with both EPN-2 and SPNET-1 cell lines was similar to the control subline and the remainder were large irregular cells as indicated by white arrows.

### **6.2.6 Co-staining immunofluorescence analysis in the selected sublines after multiple rounds of drug treatment (< 10 and > 10 passages)**

Previous results showed co-expression of CD133 and ABC transporters in the parental cell lines and the parental cell lines after the first round of drug treatment. After the first round of treatment, ABCB1 was obviously expressed at a high level in most surviving sublines and a large proportion of cells co-expressing CD133 and ABCB1 was observed. Low levels of CD133 and ABCC1 or ABCG2 co-expression and a small proportion of CD133 and ABCC1 or ABCG2 co-expressing cells were observed in some surviving sublines. Based on the immunofluorescence results after the first round of drug treatment, some surviving sublines were selected to study for on going drug resistance. To determine any alteration of CD133 and ABC transporters co-expression after continual drug treatment at every passage, co-staining immunofluorescence was performed on selected sublines at < 10 and > 10 passages of drug treatment. All immunofluorescence results are shown in Figure A3.1 – A3.9 and A4.1 – A4.9 of the appendix. The data are also summarised in tabular form (Table 6.2) and the subsection below references representative images. The average score from 3 selected sublines was presented ranging from (-) to (++++). The proportion of cells co-expressing CD133 and ABC transporters was scored using a sliding scale such that the highest score is (++++), which indicated selected sublines containing more than 80% of cells co-expressing CD133 and ABC transporters whereas no co-expressing cells were scored as (-) as described below the table. Sublines indicated with black blocks were not selected for further analysis.

After multiple rounds of drug treatment, all selected sublines were consistently enriched with a large proportion of cells co-expressing CD133 and ABCB1 at a high level throughout drug treatment. On the contrary, most selected sublines were negative for CD133 and ABCC1 co-expression after the first round and < 10 passages of drug treatment then a large proportion of cells co-expressing CD133 and ABCC1 at a high level was detected in most selected sublines after > 10 passages of treatment. There were some selected sublines, which inconsistently co-expressed CD133 and ABCC1 during drug treatment including irinotecan

**Table 6.2 Summary of CD133 and ABC transporters co-expression by immunofluorescence.**

Cell line	Treatment	Treatment								
		ABCB1			ABCC1			ABCG2		
		1 <sup>st</sup>	<10	>10	1 <sup>st</sup>	<10	>10	1 <sup>st</sup>	<10	>10
<b>EPN-2</b>	Cisplatin	+			-			-		
	Etoposide	++++	++++	++++	-	-	++++	+	+	++
	Figure	6.5	A3.1	A4.1	6.5	A3.2	A4.2	6.5	A3.3	A4.3
	Irinotecan	++++	++++	+++	+	-	++++	+	+	+++
	Figure	6.5	A3.1	A4.1	6.5	A3.2	A4.2	6.5	A3.3	A4.3
	Methotrexate	++			+			-		
<b>MED-2</b>	Cisplatin	++++	+++	+++	-	+	-	-	-	+
	Figure	6.6	A3.4	A4.4	6.6	A3.5	A4.5	6.6	A3.6	A4.6
	Etoposide	++			-			-		
	Irinotecan	++++	++++	+++	-	-	++	-	++	+++
	Figure	6.6	A3.4	A4.4	6.6	A3.5	A4.5	6.6	A3.6	A4.6
	Methotrexate	+++			-			-		
<b>SPNET-1</b>	Cisplatin	++++	+++	+++	-	-	-	-	+	+++
	Figure	6.7	A3.7	A4.7	6.7	A3.8	A4.8	6.7	A3.9	A4.9
	Etoposide	+++			-			-		
	Irinotecan	+++	++++	+++	++	-	+++	-	+++	++++
	Figure	6.7	A3.7	A4.7	6.7	A3.8	A4.8	6.7	A3.9	A4.9
	Methotrexate	++			-			-		

- no CD133 and ABC transporters co-expression

+ very low co-expression (less than 10%)

++ moderate co-expression (10-50%)

+++ high co-expression (50-80%)

++++ very high co-expression (more than 80%)

 clones not selected for further analysis

EPN-2, cisplatin MED-2 and irinotecan SPNET-1 sublines. Noticeably, cisplatin SPNET-1 sublines were negative for CD133 and ABCC1 co-expression throughout drug treatment. Co-expression of CD133 and ABCG2 was detected in few selected sublines after the first round of drug treatment then a proportion of cells co-expressing CD133 and ABCG2 was gradually increased after multiple rounds of drug treatment.

From Table 6.2, the overall results of the immunofluorescence with regard to alteration of the proportion of co-expressing cells after repeated treatment can be seen. ABCB1 was the only one transporter, which was consistently present in a high proportion of co-expressing cells throughout drug treatment whilst ABCC1 was inconsistently expressed in some selected sublines and ABCG2 was present later after multiple rounds of drug treatment. Due to the fact that co-staining immunofluorescence was performed once at each passage, to decide which transporter should be the focus of further drug resistance analysis, Western blotting results were simultaneously evaluated to select the most interesting transporter for downstream analysis, as demonstrated in the next section.

### **6.2.7 The expression of ABC transporters examined by Western blotting analysis**

To validate the results from immunofluorescence assay, Western blotting analysis was performed to obtain a further qualitative measure of ABC transporter expression. Western blotting analysis was carried out after the immunofluorescence and the functional analysis by FACS, therefore, selected sublines treated with drug for more than 10 rounds were used to detect ABC transporters expression. The expression of ABC transporters was detected in microsomal membrane fraction extracted from snap frozen cell pellets of all 16 selected sublines including 3 control sublines. HEK-B1, HEK-C1 and HEK-G2 cells were used as positive controls and HEK-V was used as negative control (see section 5.2.1). Representative blots are shown in Figure 6.9.

In the EPN-2 cell line, a strong band representing ABCB1 was detected in HEK-B1 and all selected sublines at ~140 kDa [Figure 6.9, a, (i)]. Although, the positive ABCB1 bands detected by Western blotting in HEK-B cells and selected clones demonstrated 2 different sizes: 140 and 130 kDa [Figure 6.9, a-c, (i)], these 2 different sizes of ABCB1 were different forms of ABCB1. Due to the fact that C219 antibody can detect both glycosylated and nonglycosylated forms of ABCB1 [Arceci, R. J. *et al* (1993)]; fully glycosylated form was detected at 140 kDa (upper bands) and nonglycosylated form was detected at 130 kDa (lower bands). Noticeably, most of selected clones demonstrated doublets of glycosylated and nonglycosylated forms of ABCB1, whilst ABCB1 detected in the vehicle control clones was a single bands (nonglycosylated form, 130 kDa). The highest intensity of ABCB1 expression was detected in EPN-2\_I\_T1. The level of ABCB1 expression detected in all selected EPN-2 sublines was higher than those of the control sublines, which displayed a low intensity band [Figure 6.9, a, (i)]. ABCC1 protein was also detected at ~140 kDa in both HEK-C1 control cells and in the all sublines. The ABCC1 blot shows that ABCC1 expression was detected in all selected sublines and also in the control subline [Figure 6.9, a, (ii)]. However, the intensity of ABCC1 expression detected in treated clones was visibly higher than that of the control subline. The highest intensity of ABCC1 expression was observed in EPN-2\_E\_T1. For ABCG2 expression, ABCG2 protein was detected at ~72 kDa in HEK-G2 cells whereas only a non-specific 200 kDa band was detected in our sublines [Figure 6.9, a, (iii)].

In selected MED-2 sublines, results from 3 independent experiments showed that the level of ABCB1 expression observed in the selected sublines was higher than that of the control sublines with the exception of the MED-2\_C\_T1 expressing at a very low level [Figure 6.9, b, (i)]. The highest level of ABCB1 expression was observed in the MED-2\_C\_T2. A number of different sized bands representing different degrees of ABCB1 glycosylation were detected in the HEK-B1 control and also in the selected sublines. The ABCC1 blot shows that all sublines expressed ABCC1 [Figure 6.9, b, (ii)], with the selected sublines expressing a higher level of



ABCC1 than the control subline. For ABCG2, non-specific bands at ~200 kDa were detected in all clones [Figure 6.9, b, (iii)].

The Western blotting results showed that most selected SPNET-1 sublines expressed ABCB1 and level of ABCB1 expression was higher than the control subline with the exception of the SPNET-1\_C\_T2, which did not express ABCB1 [Figure 6.9, c, (i)]. While the highest level of ABCB1 expression was observed in the SPNET-1\_C\_T1. ABCC1 expression was detected in all selected sublines and in each case was higher than that of the control subline [Figure 6.9, c, (ii)]. The SPNET-1\_I\_T1 and T2 expressed the highest level of ABCC1 expression. For ABCG2, non-specific bands were detected at ~200 kDa in all selected sublines, the control subline and even in HEK-V cells. Only HEK-G2 was positive [Figure 6.9, c, (iii)].

The enrichment of ABCB1 in all selected sublines after multiple rounds of drug treatment was entirely confirmed by both Western blotting and immunofluorescence analysis. A high level of ABCC1 expression in all selected sublines was mostly consistent with the immunofluorescence results demonstrating ABCC1 enrichment after prolonged drug treatment in most selected sublines. On the contrary, ABCG2 expression detected by Western blotting analysis was inconsistent with the immunofluorescence results. Whereby, Western blotting results showed no ABCG2 expression in any selected sublines whilst immunofluorescence results demonstrated an enrichment of ABCG2 after multiple rounds of drug treatment.

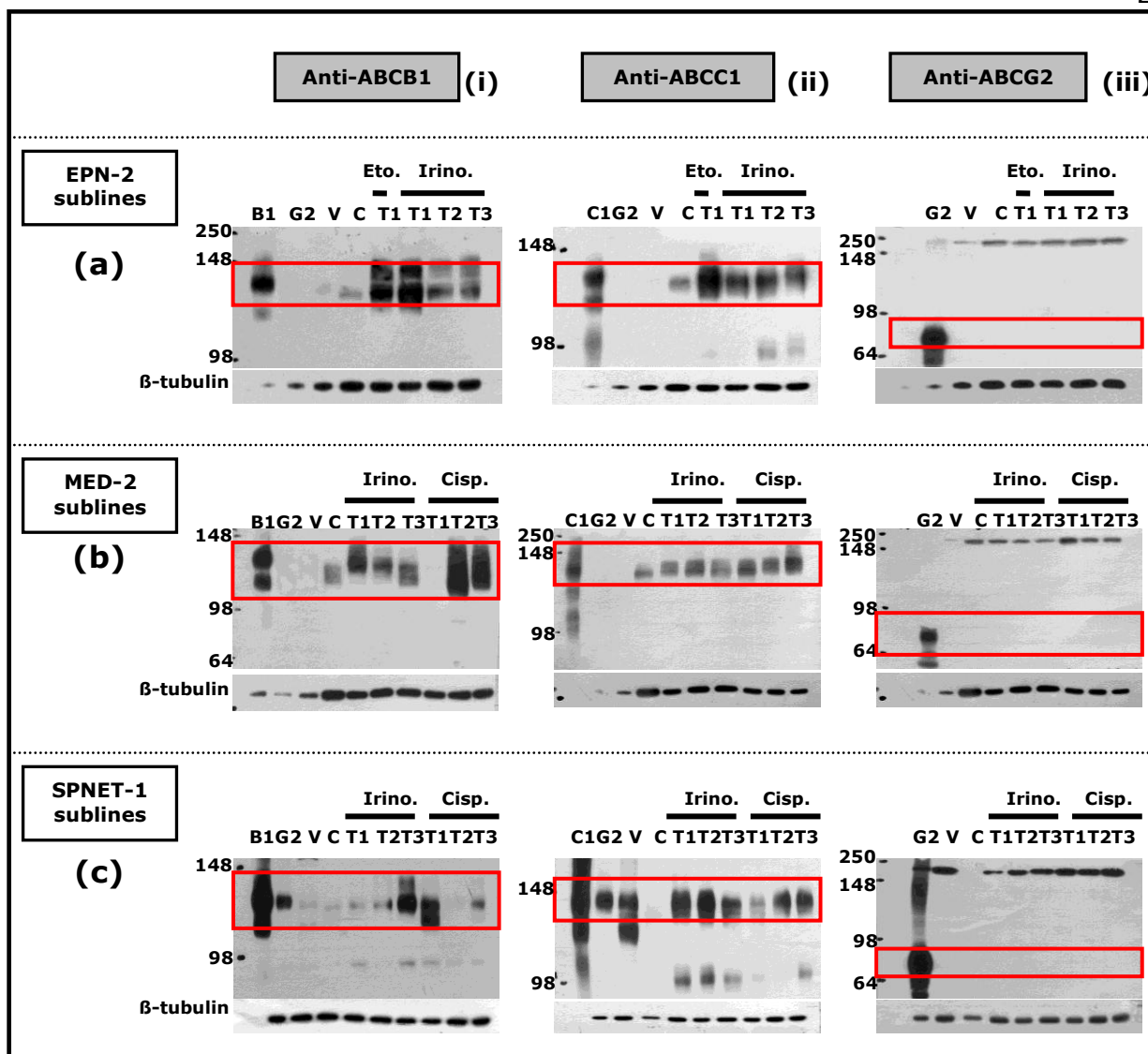


**Figure 6.9 ABCB1, ABCC1 and ABCG2 expression determined by Western blotting analysis in selected sublines.** HEK-B1 (B1), HEK-C1 (C1) and HEK-G2 (G2) were used as positive controls for the expression of ABCB1, ABCC1 and ABCG2, respectively and HEK-empty vector (V) was used as a negative control. Most selected EPN-2, MED-2 sublines expressed a higher ABCB1 than the control sublines [a and b, (i)] whilst only some selected SPNET-1 sublines demonstrated a higher ABCB1 [c, (i)]. A higher ABCC1 expression was detected in all selected sublines compared to the corresponding control sublines [a, b and c, (ii)]. Conversely, no ABCG2 expression was detected in any selected sublines [a, b and c, (iii)]. Microsomal membrane fractions were loaded 40  $\mu$ g/lane with the exception of the positive controls loaded 5  $\mu$ g/lane and the negative control loaded 10  $\mu$ g/lane. 1:100 C219 or MRPm6 and 1:500 BXP-21 antibodies (overnight incubation at 4°C) were used as primary antibody to detected ABCB1, ABCC1 and ABCG2, respectively. 1:2,000 corresponding secondary antibodies were incubated with samples for 1 hour at room temperature. Expected bands were indicated within the red boxes.

## 6.3 Discussion

Co-staining immunofluorescence was the main assay used to determine which sublines were selected for on going drug resistance analysis and the decision was made based on an enrichment of CD133 and ABCB1 or ABCC1 in sublines after the first round of drug treatment since none of our sublines expressed ABCG2. The process of subline selection was described in page 216 and subline nomenclature is also explained. From the clonogenic assay,  $IC_{50}$  of etoposide, cisplatin, irinotecan and methotrexate was determined and it was in a similar range (nM -  $\mu$ M). Drug treatment selected surviving cells having cancer stem cell characteristic i.e. an ability to form neurospheres. Methotrexate affected the ability of surviving cells from all selected sublines to form neurospheres. Both immunofluorescence and Western blotting analysis confirmed that ABCB1 was consistently expressed at a high level in cancer stem-like cells of the selected sublines and it persisted at a high level throughout drug treatment, whilst ABCC1 was upregulated after multiple rounds of drug treatment. On the contrary, no CD133 and ABCG2 co-expressing cells were detected in any selected sublines. Additionally, cellular morphologies of all selected sublines after multiple rounds of drug treatment were heterogeneous.

### **Paediatric brain tumours can be treated.**

The clonogenic assay or colony formation assay is extensively used to determine cell survival *in vitro* after drug treatment or radiation. The principle of the clonogenic assay is based on the ability of single cells in forming colonies containing at least 50 cells [Franken, N. A. P. *et al* (2006)]. The clonogenic assay was suitable for colony selection rather than the microtetrazoline (MTT) assay because surviving colonies after treatment can be achieved from clonogenic assay and these colonies can be selected to culture for further drug selection. In contrast MTT assay does not provide colonies because this technique determines cell survival by measuring the reduction of tetrazolium salts to a formazan end-product and it requires a short incubation. Consequently, single cells do not have enough

time to form colonies and some drugs require a long period of time for treatment e.g. 96 hours for irinotecan or continuous treatment for methotrexate [Berridge, M. V. *et al* (1996)]. Hence, the clonogenic assay was performed for colony selection in our study and cells were treated with chemotherapeutic drugs to select drug resistant sublines. Chemotherapeutic agents used to select drug resistant sublines in our study were etoposide, cisplatin, irinotecan and methotrexate, which are common chemotherapeutic drugs used in treatment of paediatric brain tumours [Grossman, S. A. *et al* (2003), Packer, R. J. *et al* (1999) and Grundy, R. G. *et al* (2007)] and they had been clinically used to treat brain tumours of the type from which our cell lines derived. Additionally, all these 4 chemotherapeutic drugs were known to be substrates of ABCB1, ABCC1 and ABCG2 transporters [Guo, A. *et al* (2002), Reviewed in Borst, P. *et al* (2000) and Reviewed in Szakács, G. *et al* (2006)]. Our selected sublines were selected by multiple rounds of treatment with each of these 4 drugs.

The clonogenic assay results demonstrated that survival rates decreased when drug concentration was increased (Figure 6.1). Therefore, this indicated that there were some cancer cells susceptible to drug treatment and this might suggest that paediatric brain tumour can be treated. Colonies formed after drug treatment indicated that surviving single cells had proliferation capability. To evaluate a degree of drug resistance in our cell lines, IC<sub>50</sub> values derived from drug treatment in our cell lines were compared to IC<sub>50</sub> values from other studies. IC<sub>50</sub> values of etoposide and methotrexate in lung cancer cell line (INER-51) grown as monolayers were 2.2 µM and 800 nM, respectively [Valeria, P. L. and Raúl, B. R. (2005)]. IC<sub>50</sub> values of etoposide and methotrexate in our cell lines ranged from 3–9 µM and 9–11 nM, respectively. Comparing IC<sub>50</sub> values with this study, our cell lines were far more sensitive to methotrexate than INER-51 cell line whilst our cell lines and INER-51 had similar sensitivity to etoposide. IC<sub>50</sub> values of irinotecan in 2 human glioma cell lines were 3.4 µM and 7.2 µM, respectively and these findings were consistent with the results from our cell lines (5.36 µM) [Gomez-Manzano, C. *et al* (2006)]. IC<sub>50</sub> of cisplatin in endometrial adenocarcinoma cell lines 0.7 µM in prostate cancer cell lines 6.7 µM – 16.7 µM, the findings in our cell lines (1.39 µM) were in between the ranges of these 2 studies [Rantanen, V. *et al*

(1994) and Cummings, M. *et al* (2006)]. Different cell lines from different laboratories found different ranges of  $IC_{50}$  values of drugs. These might depend on the characteristics of cancer cell lines with regard to the aggressiveness, grading or treatment history and analysis methods used to determine  $IC_{50}$ . There seems to be no correlation between grade or type of tumours and the  $IC_{50}$  in our cell lines. Using the  $IC_{70}$  values drug resistant sublines were selected for downstream drug resistance analysis. Therefore, we have tried to imitate the situation, which occurs in patient when they are treated with chemotherapeutic drugs, in selecting a concentration that is effective enough to decrease the number of cancer cells but without accompanying toxic effects. The concentration, which gave 30-40% of survival, was hence designated to select resistant cells for ongoing drug resistance analysis.

The results from clonogenic assay demonstrated that the number of surviving colonies was decreased with increasing concentration of drugs. This suggested that paediatric brain tumours can be treated by chemotherapy whereby sensitive cancer cells are killed by cytotoxic drugs, however, resistant cells can still survive after treatment and form colonies. Since our cell lines had intrinsic drug resistance from endogenous ABCB1 and ABCC1 expression, any alteration of ABC transporters expression was determined after the first round and after multiple rounds of drug treatment. This topic is discussed later.

### **ABCB1 was consistently expressed and persisted throughout drug treatment.**

The immunofluorescence results in Chapter 5 indicated that the parental cell lines (EPN-2, MED-2 and SPNET-1) contained a low proportion of cells co-expressing CD133 and ABCB1 or ABCC1 whereby a proportion of co-expressing cells was observed higher in neurospheres than monolayers. Cells co-expressing CD133 and ABCG2 were not observed in any parental lines. To study further drug resistance analysis, these cells were treated with drug to select drug resistant sublines. To determine any alteration of levels of CD133 and ABC transporters co-expression and proportions of co-expressing cells, co-staining immunofluorescence analysis was performed on the parental cell lines after the first round of treatment and the

selected sublines after multiple rounds of treatment with respect to < 10 rounds and > 10 rounds (Appendix A3.1 – A3.9 and A4.1 – A4.9). Additionally, the immunofluorescence data were also validated by Western blotting analysis performed on the selected sublines after >10 rounds of treatment (Figure 6.9). Interestingly, only the ABCB1 transporter was primarily detected in all cell lines at a high level of expression but low proportion after the first round of treatment whilst ABCC1 or ABCG2 transporters were observed in some treated sublines at a very low proportion (Figure 6.5 – 6.7 for selected sublines and Appendix section A1.1 – A1.3 for non-selected conditions). After multiple rounds of drug treatment, ABCB1 was consistently expressed at a high level and persisted throughout drug treatment whilst the proportion of cells co-expressing CD133 and ABCC1 and the level of co-expression were increased after many rounds of treatment. In contrast, there was no ABCG2 expression detected in any selected sublines, which was confirmed by Western blotting analysis. These results might suggest that ABCB1 transporter expression was the major drug resistance mechanism in our cell lines. Taking all results together, these indicated that drug treatment selected for cancer stem-like cells expressing ABCB1 and/or ABCC1 and ABCC1 expression was also upregulated later in these sublines after many rounds of drug selection. However, we could not conclude whether resistant sublines contained cells co-expressing ABCB1 and ABCC1 after many round of treatment because ABCB1 and ABCC1 co-staining immunofluorescence was not performed in the resistant sublines. To select drug resistant sublines, cells were treated with a single cytotoxic drug. However, resistant cells expressed at least 2 ABC transporters, as previously observed [Reviewed in Szakács, G *et al* (2006)]. Although, there was no evidence to support a specific upregulation of ABCB1 in etoposide, cisplatin, irinotecan and methotrexate treatment, ABCB1 was the main transporter selected after multiple rounds of drug treatment in our cell lines and ABCC1 transporter was only upregulated after many rounds of treatment. A similar increase had been reported in breast carcinoma where ABCB1 expressing cells increased with increasing passages of drug treatment (doxorubicin and taxol) and correlated with poor clinical of drug resistance. [Mechetner, E. *et al* (1998)]. It might be concluded that ABCB1 transporter has an important role in drug resistance in our cell lines because of the consistently high expression

of ABCB1 seen throughout drug treatment. To prove that ABCB1 is an essential mechanism, which plays a role in drug resistance, in our cell lines, ABCB1 functional analysis now needs to be performed to examine whether ABCB1 expressed in our cell lines is functional. This analysis of ABCB1 is described and discussed in Chapter 7. For future study, to make a strong conclusion from the immunofluorescence analysis, the analysis should be repeated at least 3 times. Although the immunofluorescence analysis had no repetition (although it was carried out at different passages), Western blotting analysis was independently repeated at least 3 times to validate the results from the immunofluorescence analysis.

### **Drug treatment selected cancer stem-like cells.**

The Neurosphere formation assay was performed to determine the ability of surviving cells after drug treatment to form neurospheres indicating stem cell-like behaviour [Bez, A. *et al* (2003)]. The number of neurospheres formed, which is shown in Figure 6.4, demonstrated that not only the selected sublines can form neurosphere, but the control sublines can also form neurospheres. Therefore, not only drug treatment can select resistant cancer stem cells but the clonogenic assay itself can also select stem cells. Due to the fact that clonogenic assay is based on an ability of single cells to form colonies, these single cells must have an ability to proliferate and produce at least 50 progenitor cells/colony [Franken, N. A. P. *et al* (2006) and Snyder, E. Y. *et al* (1992)]. Our data supported the fact that surviving colonies selected from the clonogenic assay have stem cell characteristics since all colonies selected from the clonogenic assay were able to form neurospheres. Additionally, co-staining immunofluorescence results also demonstrated that a proportion of CSCs co-expressing CD133 and ABCB1 was increased after multiple rounds of drug treatment. This also supported the fact that drug treatment selected CSCs.

The neurosphere formation results also interestingly demonstrated that colonies surviving from methotrexate treatment could not form distinct neurospheres (Figure 6.3) whilst cells, which were treated with etoposide, cisplatin, irinotecan and also the vehicle control, were

able to form neurospheres (Figure 6.2 and 6.3). The size of neurospheres formed from methotrexate treated clones was smaller and there were many single cells in methotrexate treatment wells, which could not form neurospheres, floating in stem cell media (data not shown). This was potentially a selection effect of methotrexate on the growth of cancer stem cells. The surviving single cells might require a longer time to recover from methotrexate cytotoxicity. However, we did not prove this point. Hence, these results suggested that methotrexate possibly inhibited cancer stem cell behaviour in formation of neurospheres, whilst the other drugs did not have any effect on cancer stem cell's ability to form neurospheres. For future study, methotrexate sublines should be incubated longer in stem cell media to prove that these cancer stem cells can recover after drug removal and ultimately form neurospheres.

### **Heterogeneity of tumour cell population after multiple rounds of drug treatment.**

Cellular morphologies of selected sublines from EPN-2, MED-2 and SPNET-1 cell lines (Figure 6.1 and Figure A2.1 and A2.2) demonstrated that the control sublines from all of the cell lines showed a homogeneous population (Figure 6.1 and Figure A2.1 and A2.2, control) similar to monolayers from the parental cell lines (Chapter 4, Figure 4.1). On the contrary, the selected sublines contained a heterogeneous population; the majority of population was similar to the homogeneous population seen in the control sublines and a small proportion was large cells with an irregular shape and multinucleated (Figure 6.1 and Figure A2.1 and A2.2, T1 – T3). Noticeably, an increasing a proportion of large cells was observed in later passage (data not shown). This indicated that drug affected the morphology of cells as it selected the resistant population after each round of treatment.

For etoposide EPN-2 sublines, only the T1 subline survived and could be continuously grown whilst both T2 and T3 sublines were very sick with only a few huge irregular cells (data not shown), remaining alive but unable to proliferate even after 2 weeks. This result indicated that not all selected resistant sublines were similar. Each subline was possibly generated



from different cancer stem cell. The heterogeneity of cancer stem cells was observed in glioblastoma multiforme [Beier, D. *et al* (2007)] and breast cancers [Wright, M. H. *et al* (2008)]. The phenotype heterogeneity was found in primary glioblastoma multiforme, which comprised at least 2 different cancer stem cells with respect to CD133<sup>+</sup> and CD133<sup>-</sup>. These 2 CSCs had different genetic profiles and biological growth patterns [Beier, D. *et al* (2007)]. Additionally, *Brca1*-deficient mouse mammary tumours comprised heterogeneous cancer stem cells with respect to CD44<sup>+</sup>CD24<sup>-</sup> and CD133<sup>+</sup>. These 2 different CSCs had no overlapping population [Wright, M. H. *et al* (2008)]. Therefore, these 2 sublines, which could not survive after drug treatment, might originate from drug sensitive cancer stem cells in which genetic alteration might occur during mitosis whilst drug resistant cancer stem cells generate surviving clones [Fukasawa, K. *et al* (1997)].

Based on the results from immunofluorescence analysis at different time points and Western blotting analysis, the population of selected sublines after drug treatment was heterogeneous and we have hypothesised that there were at least 3 different populations of selected sublines. Firstly, a population, which was negative for both CD133 and ABC transporters, can survive after treatment by other drug resistance mechanisms without ABC transporters. Secondly, a population expressing CD133 indicating CSCs also used other mechanisms to survive from drug cytotoxicity. Thirdly, a population co-expressing CD133 and ABCB1 indicating CSCs expressing ABCB1 and ABCB1 transporters functionally effluxed drug out of cells to survive after drug treatment. Drug resistant CSCs expressing ABCB1 can also upregulate ABCC1 when they were repeatedly treated for many rounds of treatment. Three different populations of selected clones after treatment are shown in Figure 6.10.

This chapter demonstrated that multiple rounds of drug treatment selected cancer stem cells overexpressing ABCB1 and ABCC1 was also gradually upregulated. An overexpression of ABCB1 in surviving resistant sublines was confirmed by both co-staining immunofluorescence and Western blotting analysis. However, we have not known yet determined whether CSCs overexpressing ABCB1 are functional and lead to drug resistance

in our cell lines. Therefore, drug efflux function of ABCB1 in CSCs was examined in Chapter 7 to prove that enrichment of ABCB1 in CSCs after drug treatment contributes to multidrug resistance.

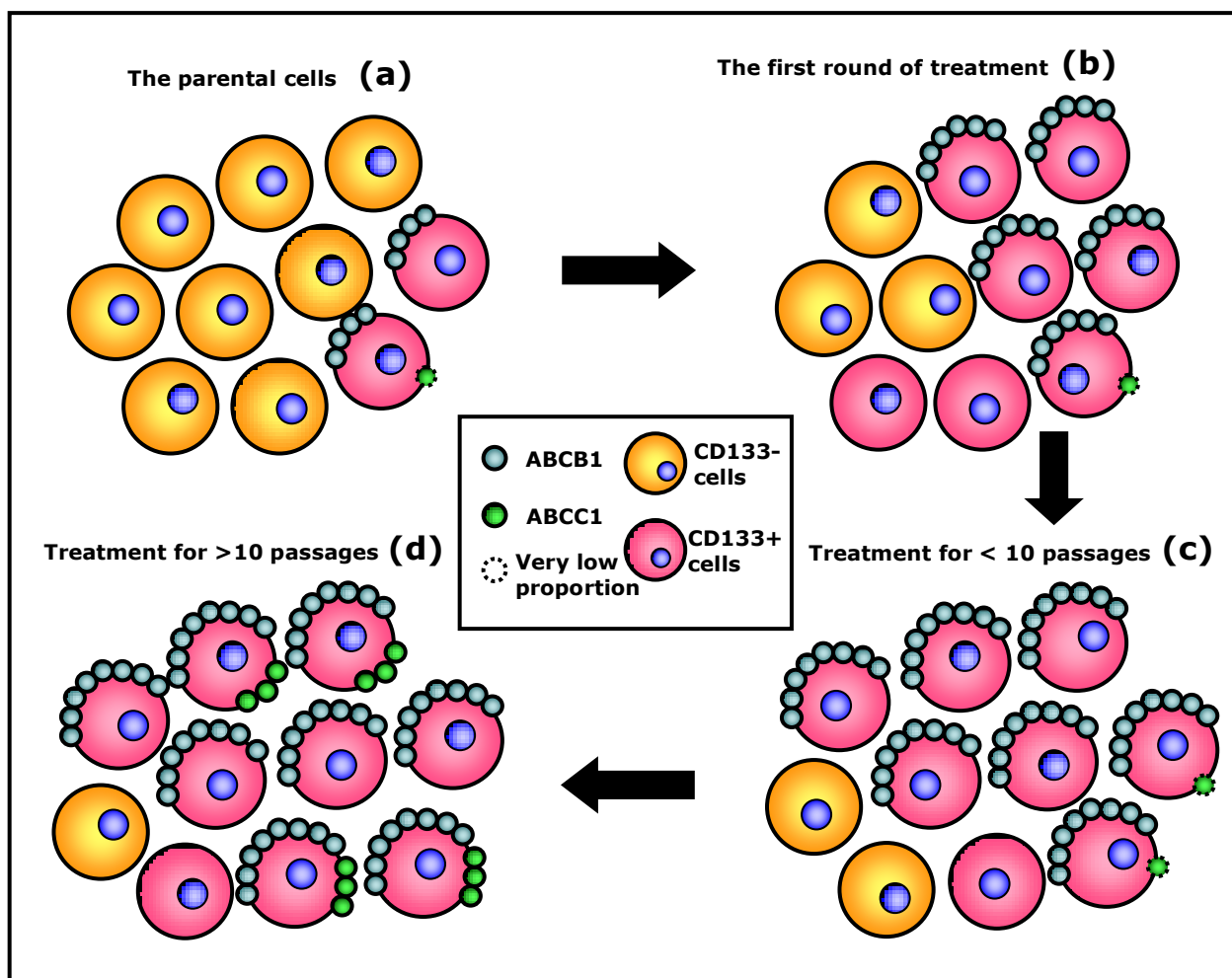


**Figure 6.10 Progression expression of ABC transporters by tumour cells after prolonged drug treatment.** Originally, our cell lines already contained a low proportion of cells expressing ABCB1 (a). After the first treatment, almost half of the tumour cells co-expressed a high level of CD133 and ABCB1 whilst ABCC1 was co-expressed with CD133 on a very few cells (b). Almost half of tumour cells comprised CD133<sup>-</sup> cells or CD133<sup>+</sup> cells without ABC expression (b). When tumour cells had been repeatedly treated, the proportion of cells co-expressing CD133 and ABCB1 (c) was higher and tumour cells expressed ABCB1 at a high level throughout drug treatment. Tumour cells also upregulated ABCC1 later in a smaller proportion of cells when compared to ABCB1 (d).

---

---

## **Chapter 7**

### **Functional analysis on selected resistant sublines**

---

---

## Chapter 7: Functional analysis on selected resistant sublines

### 6.2 Introduction

A major problem of cancers, including paediatric brain tumours, is the failure of chemotherapeutic treatment since cancer cells develop drug resistance to not only a single drug but also many drugs regardless to chemical structure or drug target. This phenomenon is known as multidrug resistance. There are many mechanisms leading to multidrug resistance in cancers however, one of the most important drug resistance mechanisms in many cancers is active drug efflux transporters. ABC transporters are the most significant active transporter mediating multidrug resistance in human cancers. The first ABC transporter discovered to correlate with drug resistance was ABCB1 (P-gp or MDR1). In normal tissues, ABCB1 is present in the blood brain barrier (BBB), which protects brain and spinal cord from cytotoxic drug [Regina, A. *et al* (2001)] and also in the luminal epithelium of liver, kidney and gastrointestinal tract [Cordon-Cardo, C. *et al* (1990)]. ABCB1 is a broad spectrum drug effluxor/effluxing agent capable of transporting natural agents and chemotherapeutic drugs such as vinblastine, paclitaxel, doxorubicin, mithoxantrone, etoposide, actinomycin D, methotrexate and topotecan [Reviewed in Schinkel, A. H. and Jonker, J. W. (2003)]. In the last few decades, attempts have been made to reverse MDR by developing drugs which have more specific inhibition of drug resistant transporters. Other methods to inhibit ABCB1 function had been developed, however, none of the current methods is able to completely reverse MDR. RNAi technology has offered some promise to improve treatment in multidrug resistant cancer cells. RNAi is based on a 21 – 25 nucleotide long double stranded RNA (dsRNA), which is able to trigger a gene silencing mechanism in a specific sequence manner. The RNAi technique comprises 2 different methods; transient and stable RNAi. Transient RNAi is based on transfection of short interference RNA (siRNA) whilst stable RNAi can be achieved by introducing short hairpin RNA (shRNA), encoded by expression vectors, into mammalian cells. The RNAi technique has been extensively studied

both *in vitro* and *in vivo* and it might potentially be applied for cancer treatment. Therefore, RNAi had been attempted to reduce ABCB1 mRNA in our cell lines for investigation of ABCB1 role in drug resistance.

The results from previous chapter suggested that the majority of our cell lines were susceptible to *in vitro* drug treatment; etoposide, cisplatin, irinotecan and methotrexate. Neurosphere formation assay performed on selected resistant clones revealed that all resistant clones were able to form neurospheres with the exception of methotrexate treated clones. Additionally, ABCB1 was possibly the main drug resistance mechanism in our cell lines since ABCB1 was consistently expressed at a high level throughout drug treatment whilst cells expressing ABCC1 were increased after many rounds of treatment. None of the selected clones expressed ABCG2. As a result of a consistent high expression of ABCB1 after treatment, ABCB1 transporter was focused on for ongoing study in this chapter. In this chapter, ABCB1 transporter function was hence determined by FACS using Rh123 and Verapamil as a substrate and inhibitor for ABCB1, respectively. Although there are many inhibitors of ABCB1 such as verapamil, the phenothiazines, quinidine, quinacrine, quinine, amiodarone, several neuroleptics, tamoxifen, progesterone, cyclosporine A, dexverapamil, dextiguldipine, GF-902128, PSC-833 and VX-710, an assessment of the efficacy of ABCB1 inhibition *in vivo* indicated that these drugs provided a weak potency in ABCB1 inhibition and caused side effect at a high dose [Reviewed in Gottesman, M. M. *et al* (2002)]. Since there is excellent evidence to support that Verapamil was able to successfully inhibit *in vitro* ABCB1 function [Tsuruo, T. *et al* (1981)], Verapamil was used to inhibit ABCB1 in our study. To demonstrate that the ABCB1 transporter was responsible for the observed drug resistance, inhibition of ABCB1 expression was also attempted using SiRNA transfection. Clonogenic assays were performed to compare the effectiveness of single drug treatment and combined drug treatment with Verapamil. Surviving resistant clones from the clonogenic assay were selected to determine the ability to form neurospheres. Finally, co-staining immunofluorescence was performed to determine the proportion of cells co-expressing CD133 and ABCB1 in surviving clones after treatment.

## 6.3 Results

### 7.2.1 Functional analysis of ABC transporters by FACS

#### **ABCB1 functional analysis was optimised in the positive and negative controls**

ABCB1 functional analysis by FACS was performed on all selected sublines. Rhodamine 123 (Rh123) and Verapamil were used as ABCB1 substrate and inhibitor, respectively. HEK-V cells stably transfected with empty vector and HEK-B1 cells stably transfected with vector expressing ABCB1 were included as negative and positive controls, respectively, for ABCB1 transporter function, and allow simple illustration of the data. FACS results showed that all HEK-V cells accumulated Rh123 and hence showed a high level of Rh123 fluorescence [Figure 7.1, a, (ii)]. As expected, when such cells were incubated with both Rh123 and Verapamil, the Rh123 accumulation was unaffected [Figure 7.1, a, (iii)]. HEK-B1 cells on the other hand were able to efflux Rh123 and therefore the majority of cells failed to accumulate Rh123 [Figure 7.1, b, (ii)]. In contrast, when HEK-B1 cells were incubated in both Rh123 and Verapamil, efflux function was inhibited resulting in all formerly extruding cells accumulating Rh123 and shifting to the right panel [Figure 7.1, b, (iii)]. The results for both the positive and the negative control therefore showed that ABCB1 functional analysis by FACS was fully optimised.

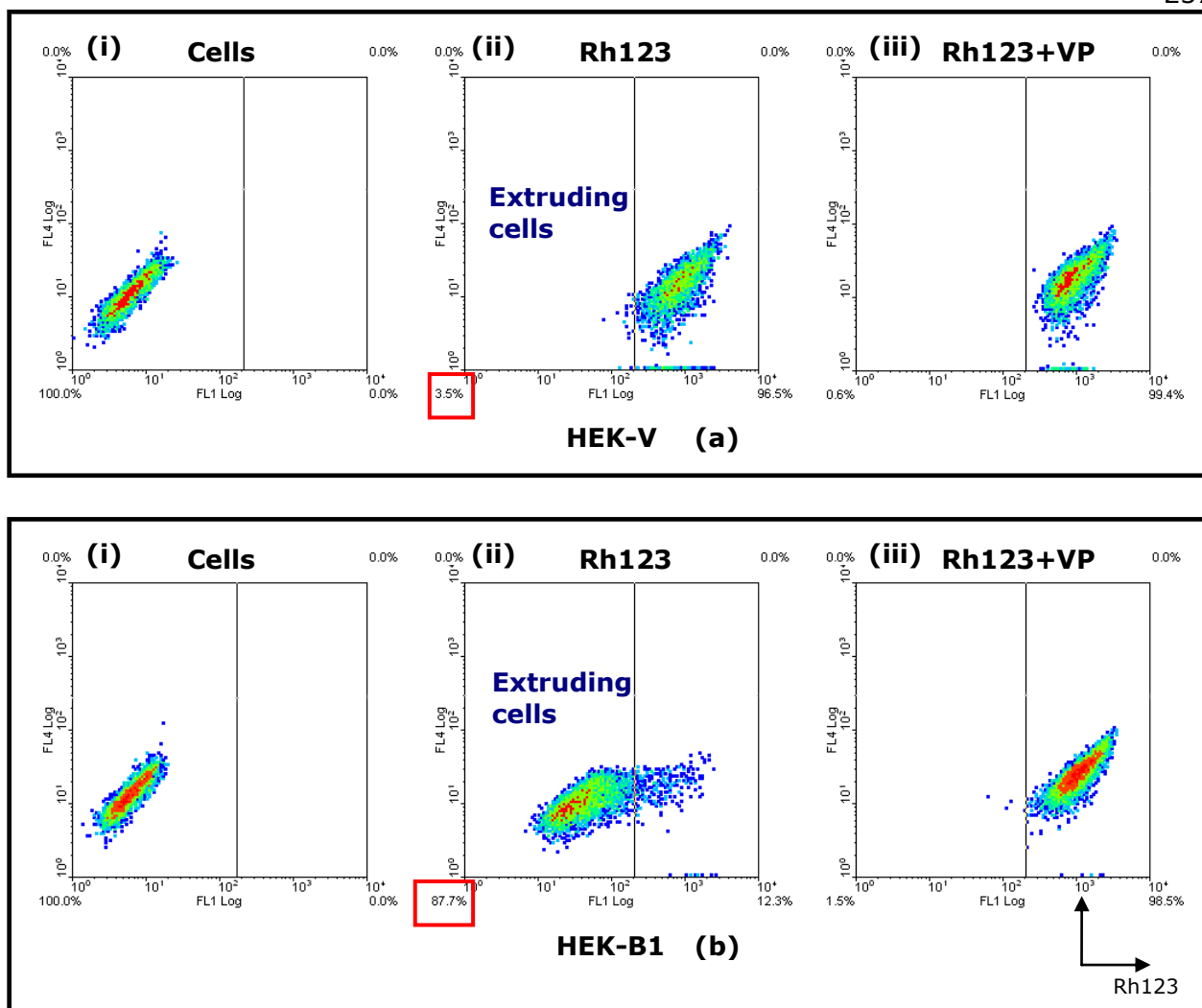


**Figure 7.1 Optimisation of ABCB1 functional analysis by FACS using HEK-V and HEK-B1.** HEK-empty vector (HEK-V) cells were used as a negative control (a). When HEK-V cells were incubated in Rhodamine 123 (Rh123), these cells could not efflux Rh123 resulting in Rh123 accumulation. Most of HEK-V cells hence shifted to the right panel [a, (ii)]. When HEK-V cells were incubated in Verapamil (VP), these cells were not affected [a, (iii)]. HEK-B1 cells highly expressing ABCB1 transporter effluxed Rh123 when they were incubated in Rh123 therefore the majority of cells stayed in the left panel [b, (ii)]. When ABCB1 transporter was inhibited by VP, most of HEK-B1 cells accumulated Rh123 and as a result these cells shifted to the right lower quadrant [b, (iii)]. 5,000-10,000 events of each sample were included in the functional analysis. Rh123 fluorescence wave length was 515 nm. The concentration of Rh123 and Verapamil used was 2  $\mu\text{M}$  and 20  $\mu\text{M}$ , respectively. The numbers in the red boxes indicates the proportion of cells extruding Rhodamine 123.



**ABCB1 functional analysis was performed on the selected resistant sublines**

ABCB1 functional analysis results showed that the control sublines from all 3 cell lines contained a small proportion of extruding cells, and that this extrusion was inhibited by Verapamil (Figure 7.2, 7.3 and 7.4, a). The highest proportion of cells expressing functional ABCB1 in the control sublines was found in EPN-2 ( $32.7 \pm 13.1\%$ ) and the proportions observed in MED-2 and SPNET-1 were  $6.7 \pm 0.8\%$  and  $3.9 \pm 1.7\%$ , respectively. The proportions of functional ABCB1 cells found in the control sublines were consistent with the corresponding parental cell lines (Chapter 5, Figure 5.10 and 5.11).

ABCB1 functional analysis by FACS was also performed on selected sublines from EPN-2, MED-2 and SPNET-1 cell lines. Representative results of ABCB1 functional analysis in the control sublines and selected sublines are shown in Figure 7.2, 7.3 and 7.4. For the EPN-2 cell line, the percentage of cells expressing functional ABCB1 transporters was increased approximately 2 fold in the selected etoposide and irinotecan EPN-2 sublines when compared to the parental cell line and the control sublines (Figure 7.2, b and c) from  $\sim 35\%$  to  $>75\%$  (Figure 7.2, a – c and Figure 7.5). Similarly, the average percentage of Rh123 extruding cells from both selected MED-2 and SPNET-1 sublines was approximately 2 fold higher than the parental cells and the control sublines (Figure 7.3 – 7.5). In this case there was apparently greater variability with the percentage of functional extrusion in selected MED-2 and SPNET-1 sublines ranging from 19% to  $>60\%$  and 8% to 35%, respectively, whilst constant percentage of these cells was found in the selected EPN-2 sublines ranging from 75% - 85% (Figure 7.5). Noticeably, the proportion of extruding cells in the selected SPNET-1 sublines was lower than that of both the selected EPN-2 and MED-2 sublines.

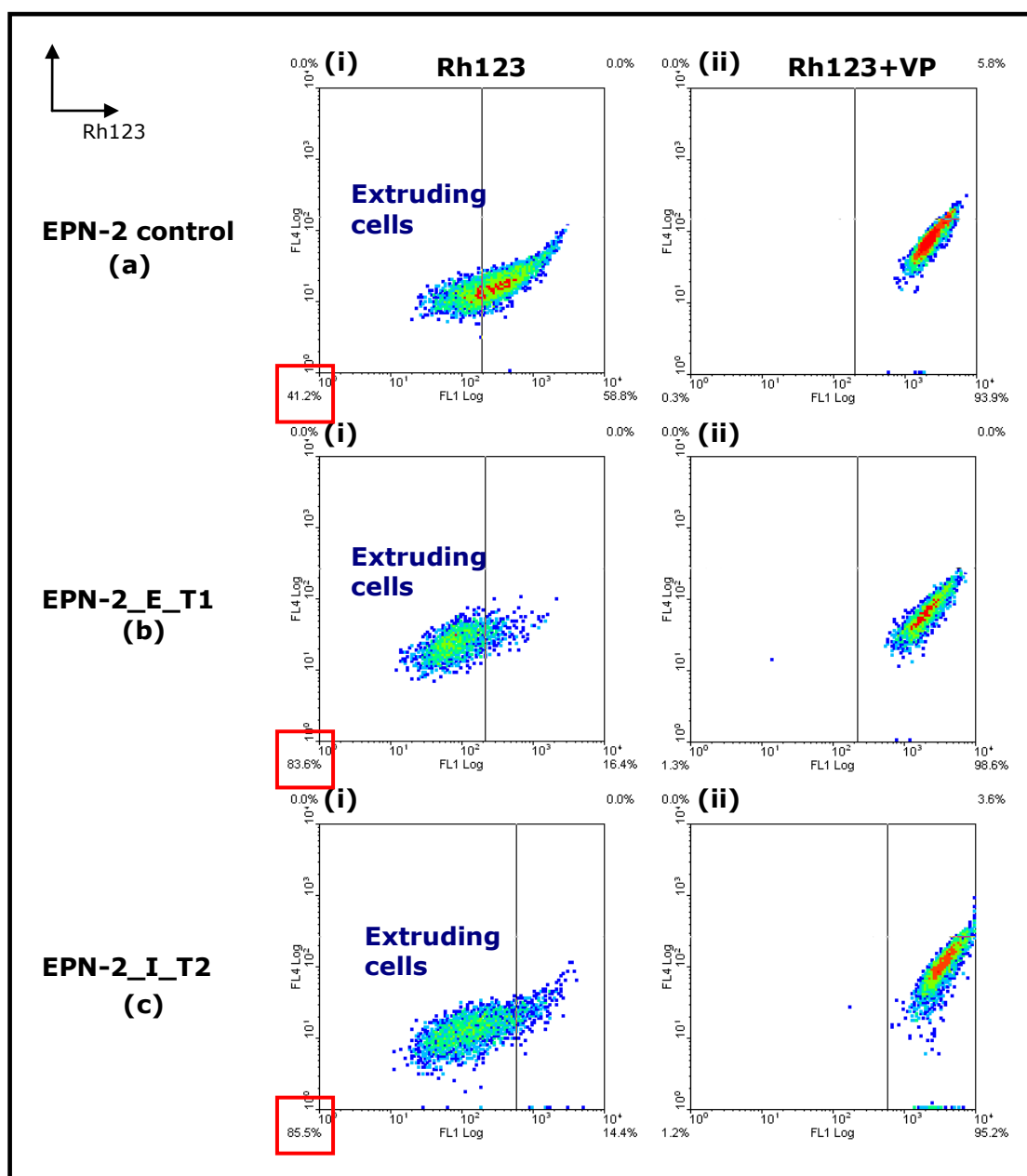


**Figure 7.2 ABCB1 functional analysis in the control subline and selected etoposide and irinotecan EPN-2 sublines.** This figure shows representative results from the control subline, EPN-2\_E\_T1 and EPN-2\_I\_T2 subline. The experiments were independently repeated 3 times as described in Figure 7.1. The proportion of extruding cells, which were inhibited by Verapamil (VP) in representative selected EPN-2 sublines [b and c, (i) and (ii)] was obviously higher than that of the control subline approximately 2 fold [a, (i) and (ii)]. The numbers in the red boxes indicates the proportion of cells extruding Rhodamine 123.

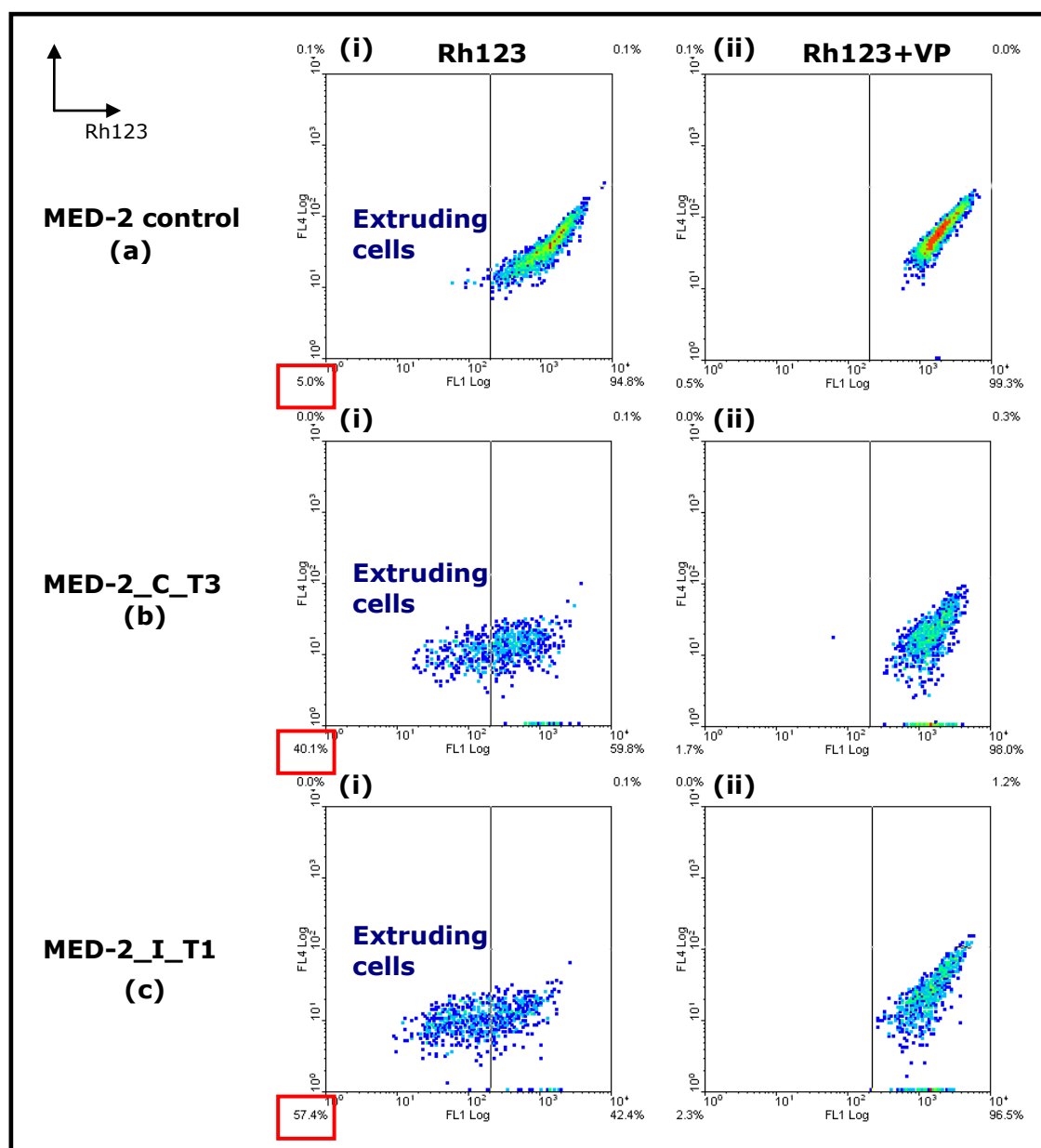


**Figure 7.3 ABCB1 functional analysis in the control subline and selected cisplatin and irinotecan MED-2 sublines.** A very low proportion of cells extruding Rh123, which were inhibited by Verapamil, was detected in the control subline [a, (i) and (ii)] whilst both selected cisplatin and irinotecan MED-2 subline comprised a higher proportion of extruding cells [b and c, (i) and (ii)] ~2 fold. All cells extruding Rh123, in the left panel, were inhibited by Verapamil resulting in they shifted to the right panel after they were incubated in Rh123 and Verapamil [b and c, (i) and (ii)]. The numbers in the red boxes indicates the proportion of cells extruding Rhodamine 123.

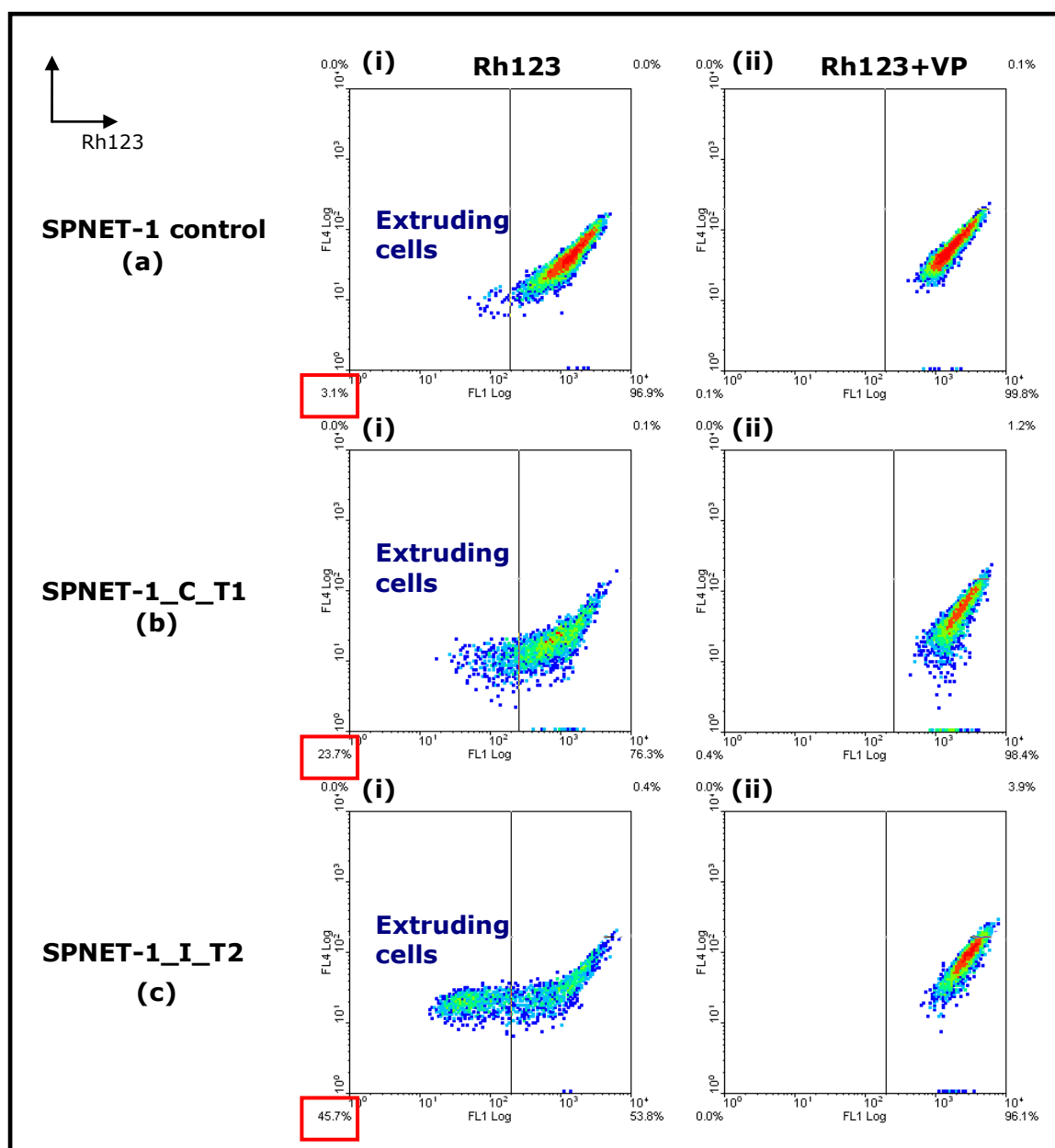


**Figure 7.4 ABCB1 functional analysis in the control subline and selected cisplatin and irinotecan SPNET-1 sublines.** Representative SPNET-1\_C\_T1 and SPNET-1\_I\_T2 sublines are shown. Similar to the results from selected EPN-2 and MED-2 sublines, a higher proportion of cells extruding Rh123, which were inhibited by Verapamil, were detected in all selected SPNET-1 sublines [b and c, (i) and (ii)] compared to that of the control subline [a, (i) and (ii)]. The numbers in the red boxes indicates the proportion of cells extruding Rhodamine 123.

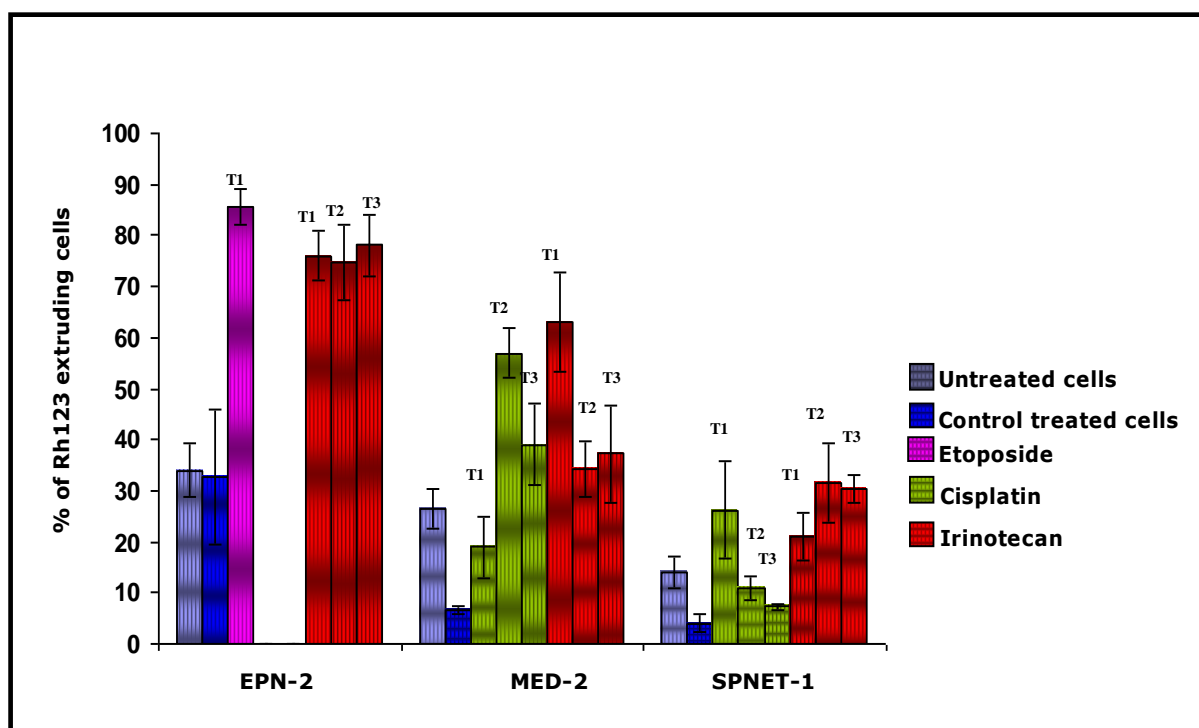


**Figure 7.5 ABCB1 functional analysis in the selected EPN-2, MED-2 and SPNET-1 sublines.** ABCB1 functional analysis by FACS was individually repeated 3 times. This graph shows the mean percentage of cells extruding Rh123, which were inhibited by Verapamil (VP). In EPN-2 cell line, the parental cells and the control subline contained a high proportion of extruding cells ~35% whilst the proportion almost doubled after drug treatment with etoposide or irinotecan (75-85%). The parental cells and the control sublines of MED-2 and SPNET-1 cell lines comprised a lower proportion of extruding cells than the control subline of EPN-2. However, the proportion of those cells was still increased almost 2 fold after drug treatment compared to the parental cell lines although not to as great an extent as in EPN-2 cell line. The proportion of extruding cells was homogeneous in the selected EPN-2 sublines whilst there was a variation detected in the selected MED-2 and SPNET-1 sublines. EPN-2\_E\_T2 and T3 sublines were not included in this analysis because these 2 sublines failed to survive after the second round of etoposide treatment.

All cell lines contained cells expressing functional ABCB1 transporters and the proportion of cells was visibly upregulated after drug treatment. The selected EPN-2 sublines comprised the highest percentage of cells expressing functional ABCB1 whilst the lowest percentage was observed in the selected SPNET-1 subline. After drug treatment, the percentage of functional ABCB1 transporter was increased 2-3 fold in most selected sublines when compared to the parental cells or the control sublines. Interestingly, the EPN-2 cell line comprised a high endogenous percentage of cells expressing functional ABCB1 in the parental cells (34%) and the highest percentage (75-85%) was consistently found in all selected EPN-2 sublines whilst the percentage of those cells in the other 2 cell lines was largely variable. Therefore, the selected EPN-2\_E\_T1 and EPN-2\_I\_T1 sublines were selected for further drug resistance analysis.

### **7.2.2 ABCB1 knockdown using RNAi**

To further substantiate that ABCB1 transporter function is an essential mechanism for our selected sublines to survive after multiple rounds of drug treatment, ABCB1 knockdown using RNAi was performed to inhibit ABCB1 function. The plan was then to treat with drug and determine the efficacy of treatment after ABCB1 inhibition. Three different SiRNAs; *si\_ABCB1*, *si\_ABCB1.1* and *si\_ABCB1.2*, were tested on the EPN-2\_E\_T1 and EPN-2\_I\_T1 sublines using SiPort Amine as the transfection agent. Since the growth characteristics of each selected subline are different, transfection conditions were optimised independently for each selected subline. To optimise the appropriate condition for ABCB1 transfection in each cell line, GAPDH, a housekeeping gene generally found in all cells, was initially used to test the varying conditions for transfection (data not shown). The parental EPN-2 cells (EPN-2) and the control EPN-2 subline (EPN-2\_C), which contained a low proportion of functional ABCB1 cells, were initially tested. 24 hours after GAPDH transfection, cells were harvested and RNA was extracted. The PCR results showed no expression of GAPDH in some conditions [(1) SiRNA of GAPDH = 10 nM, SiPORT = 0.1 %v/v and (2) SiRNA of GAPDH = 1 nM, SiPORT = 0.4 %v/v]. These 2 conditions were applied to transfect GAPDH SiRNA (as a control) and 3 different ABCB1 SiRNAs in the control subline of EPN-2. GAPDH and ABCB1

expression were however present in all conditions after the transfection. It was thought that therefore, each SiRNA probably required specific conditions to be transfected into each subline. All 3 ABCB1 SiRNAs (*si\_ABCB1*, *si\_ABCB1.1* and *si\_ABCB1.2*) were then transfected into EPN-2 cells and the EPN-2\_C subline with vary concentrations of ABCB1 SiRNA (range 1 – 20 nM) and SiPORT Amine (range 0.1 – 0.4 %v/v). The concentration of SiRNA and SiPort Amine were varied in each well of a 24-well plate and a total of 30 different conditions were tested. 24 hours after transfection, cells were harvested and RNA was extracted. RT-PCR was performed to examine the level of ABCB1 knockdown. However, the representative results showed that ABCB1 expression was still detected in all samples (Figure 7.6). Even if the concentration of SiPORT Amine and SiRNA was further increased, ABCB1 transporter still could not be knocked down. Since, ABCB1 SiRNA transfection was unsuccessful, the clonogenic assay using drug combined with Verapamil was performed instead because Verapamil effectively inhibited ABCB1 function in functional analysis by FACS from the previous chapter.

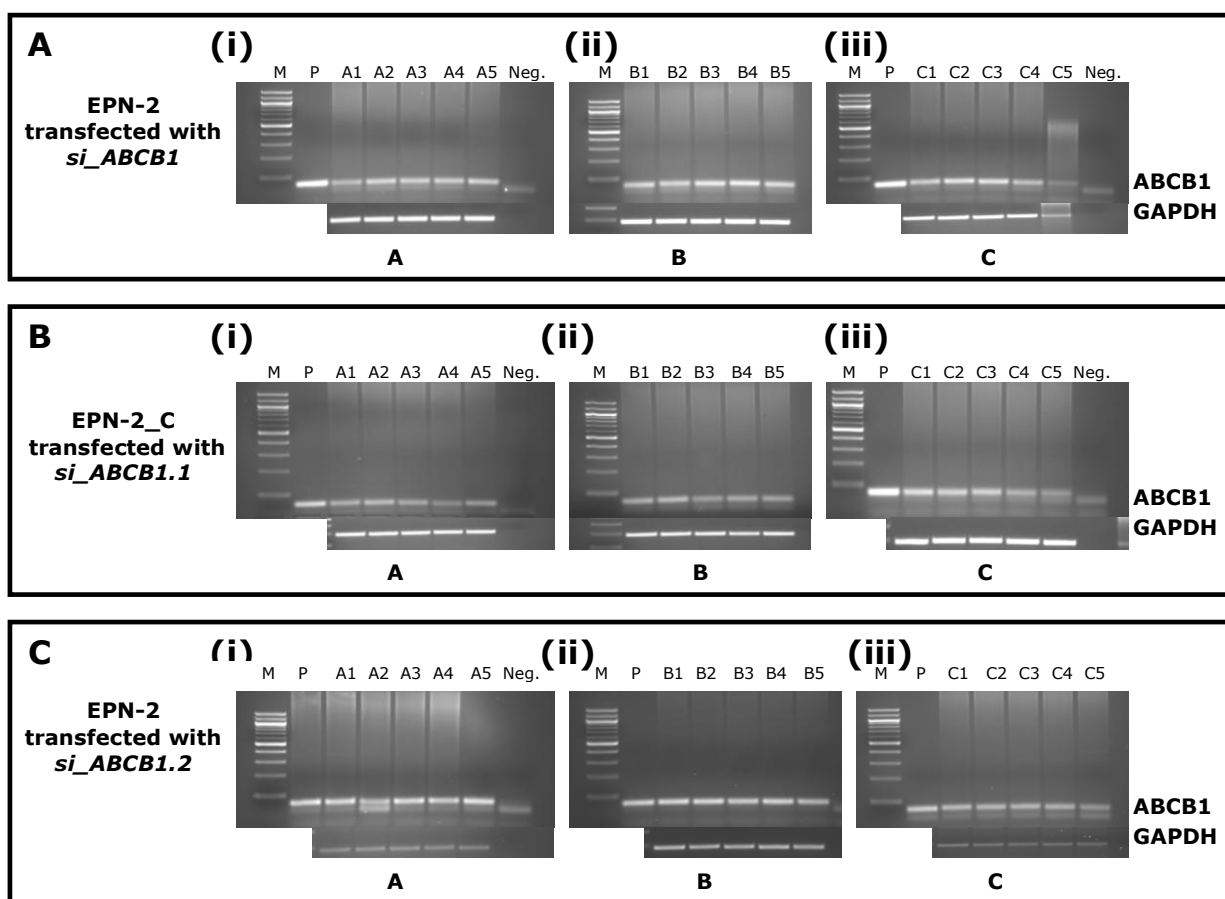


**Figure 7.6 Optimisation of ABCB1 knockdown using *si\_ABCB1*, *si\_ABCB1.1* and *si\_ABCB1.2* in EPN-2 sublines.** The parental EPN-2 cells were transfected with either *si\_ABCB1* or *si\_ABCB1.2* while the EPN-2\_C subline was transfected with *si\_ABCB1*. All 3 different SiRNAs of ABCB1 transporters were transfected with different concentration of SiPORT Amine and SiRNA. A1 was the lowest concentration of both SiPORT Amine and SiRNA (0.2 %v/v and 10 nM, respectively) whereas C5 was the highest concentration (0.6%v/v and 100 nM, respectively). PCR results showed that the 80 bp bands representing ABCB1 expression were still detected in all samples even in the highest concentration of SiPORT amine and SiRNA [C5 lanes, A, B and C (iii)]. Loading controls detected by GAPDH are shown at the bottom of each blot. [M = 100 bp ladder marker and P = control plasmid for ABCB1 cDNA].



### 7.2.3 Clonogenic assay: drug treatment combined with Verapamil

Since ABCB1 knockdown could not be reduced reliably by SiRNA, functional knockdown with Verapamil was performed, because it was previously effective to inhibit ABCB1 function in functional ABCB1 analysis by FACS (as seen in Figure 7.2 – 7.4), to determine whether reducing ABCB1 function affected the ability of cells to withstand drug in a clonogenic assay. This clonogenic assay was performed on the parental cells, the control sublines, EPN-2\_E\_T1 and EPN-2\_I\_T1 sublines. This experiment essentially consisted of 3 assays; the clonogenic assay for surviving colony counting, a neurosphere formation assay and co-staining immunofluorescence. For the clonogenic assay, the parental cells, the control sublines and selected sublines were treated with vehicle (negative control), Verapamil alone (10  $\mu$ M), drug alone (concentration which achieved 30-40% survival: etoposide = 20  $\mu$ M and irinotecan = 8  $\mu$ M) and drug combined with Verapamil (10  $\mu$ M). The surviving colonies were counted to determine the efficacy of Verapamil when it was combined with drug treatment. The neurosphere formation assay was then performed to determine whether surviving resistant colonies have the characteristics of cancer stem cells. Additionally, co-staining CD133 and ABCB1 immunofluorescence was performed on resistant surviving colonies to investigate whether these surviving cells expressed the ABCB1 transporter and the neural stem cell marker (CD133).

#### 7.2.3.1 Surviving colony counting from clonogenic assay

The morphology of the colonies formed is shown in Figure 7.7 and 7.8. To determine the cytotoxic effect of Verapamil on colony formation, colony numbers and colony size of Verapamil treated cells were compared in preliminary experiments with cells treated with the vehicle. Two different concentrations (10 and 20  $\mu$ M) of Verapamil were tested based on a previous study [Anderle, P. *et al* (1998)] and our own functional analyses (section 7.2.1). The results showed that there was no difference in survival between 10  $\mu$ M Verapamil and the vehicle treatment in any of the cell types [Figure 7.7 and 7.8, (i) and (ii)]. Whilst 20  $\mu$ M Verapamil treatment resulted in cellular toxicity, consequently, colony numbers decreased when compared to the vehicle treatment (data not shown). Since, 10  $\mu$ M Verapamil

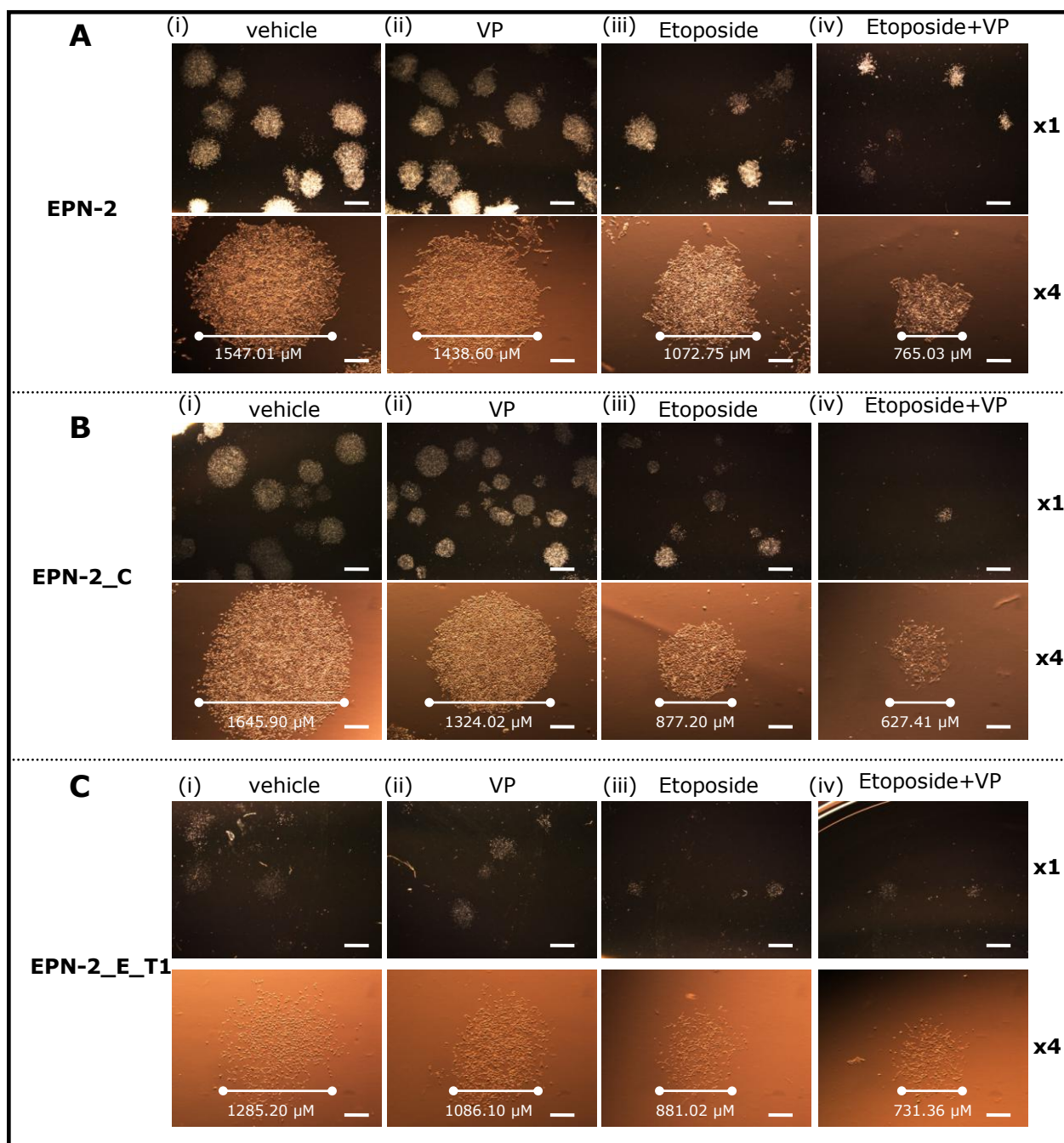
treatment had no effect on cell survival or colony formation, this concentration was selected for drug combination analysis. Basically, both EPN-2\_E\_T1 and EPN-2\_I\_T1 sublines formed smaller colonies in the vehicle and Verapamil treatment when compared to the parental cells (EPN-2) and the control subline (EPN-2\_C). This difference became more pronounced when EPN-2\_E\_T1 and EPN-2\_I\_T1 sublines were treated with etoposide or irinotecan, the numbers of colonies formed visibly decreased and colony size was smaller when compared to those of vehicle and Verapamil treated cells [Figure 7.7 and 7.8, (iii)]. The number of colonies formed and colony size were significantly reduced when cells were treated with drug combined with Verapamil [Figure 7.7 and 7.8, (iv)]. Representative images are present in Figure 7.7 and 7.8 and the size of representative clones is also indicated. For the etoposide and irinotecan treatment groups, the range of colony formed size is described in Table 7.1. Hence, drug combined with Verapamil effectively reduced the number of surviving colonies and in formation of a smaller colony. Figure 7.9 shows the percentage of surviving cells treated with single drug compared with surviving cells treated with drug combined with 10  $\mu$ M Verapamil. The percentage of surviving colonies after treatment with drug and Verapamil was significantly reduced when compared to single drug treatment (unpair student T-test,  $p < 0.01$ ) (Figure 7.9). The survival rate was reduced approximately 4 fold in drug combined Verapamil treatment. Therefore, Verapamil enhanced the efficacy of etoposide and irinotecan to kill cancer cells.

**Table 7.1 The range of colony size for the etoposide and irinotecan treatment group**

Treatment group	Clone	Treatment	The range of colony size ( $\mu$ M)
Etoposide	1. EPN-2	Vehicle	760 – 1,500
		VP	800 – 1,500
		Eto.	450 – 1,400
		Eto. + VP	500 – 1,200
	2. EPN-2_C	Vehicle	640 – 1,600
		VP	650 – 1,400
		Eto.	300 – 1,100
		Eto. + VP	240 – 750
	3. EPN-2_E_T1*	Vehicle	840 – 1,400
		VP	530 – 1,100
		Eto.	260 – 970
		Eto. + VP	230 – 1,300
Irinotecan	1. EPN-2	Vehicle	540 – 1,500
		VP	400 – 1,800
		Eto.	260 – 1,000
		Irino. + VP	260 – 600
	2. EPN-2_C	Vehicle	420 – 1,800
		VP	370 – 1,100
		Eto.	270 – 700
		Irino. + VP	200 – 400
	3. EPN-2_E_T1*	Vehicle	300 – 1,000
		VP	300 – 1,100
		Eto.	270 – 580
		Irino. + VP	220 – 730

VP = Verapamil, Eto. = Etoposide, Irino. Irinotecan

\*the colonies formed were less dense than the other conditions as shown in Figure 7.7 and 7.8, c.

**Etoposide treatment**

**Figure 7.7 Clonogenic assay: Etoposide treatment combined Verapamil reduced colony survival and colony size.** Colonies formed after the vehicle and Verapamil treatment in both the parental cells (EPN-2) and the control subline (EPN-2 C) was not visibly different [A and B, (i) and (ii)] so Verapamil did not affect the cells' ability to form colonies. In EPN-2, EPN-2\_C1 and EPN-2\_E\_T1 subline, numbers of colonies formed were decreased and colony size was smaller after etoposide treatment [A – C, (iii)] with particular to after etoposide treatment combined with Verapamil [A – C, (iv)]. EPN-2\_E\_T1 subline formed a smaller colony in all conditions when compared to the others [C, (i) – (iv)]. Images show the morphologies of colonies formed after different treatments at x1 and x4 magnification. Colony size is also shown in all representative colonies. (Scale bar = 1,000  $\mu\text{m}$  for x1 and 250  $\mu\text{m}$  for x4)

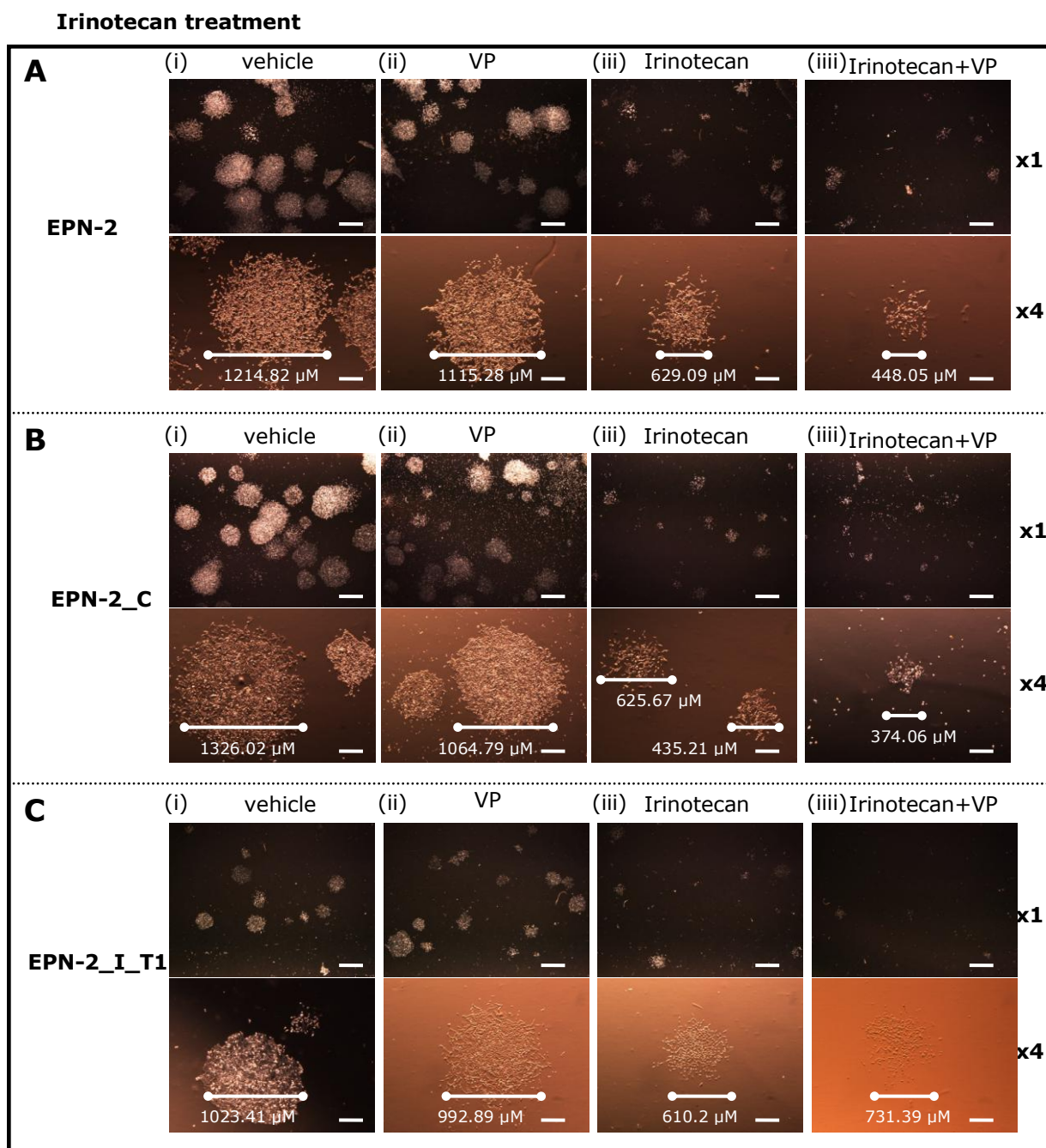


**Figure 7.8 Clonogenic assay: Irinotecan treatment combined Verapamil reduced colony survival and colony size.** Similar to previous results, there was no difference between the vehicle and Verapamil treatment [A – C, (i) and (ii)]. When cells were treated with irinotecan, colony size was obviously smaller and colony formation numbers declined [A – C, (iii)] in particular to when cells were treated with irinotecan combined with Verapami [A – C, (iv)]. Additionally, cells appeared to be struggling to survive and form colonies. Similar to the EPN-2\_E\_T1 and the EPN-2\_I\_T1 sublines consistently formed smaller colonies in all conditions when compared to the others [C, (i) – (iv)]. Colony size is also shown in all representative colonies. (Scale bar = 1,000  $\mu\text{M}$  for x1 and 250  $\mu\text{M}$  for x4)

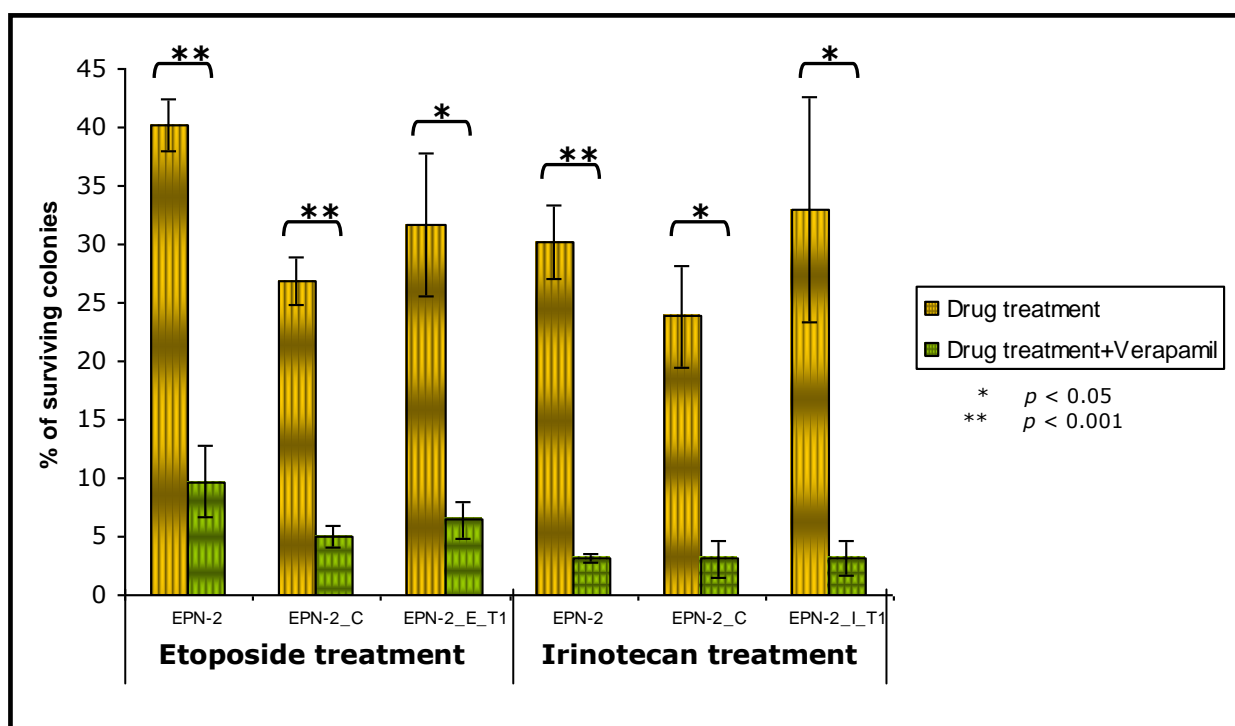


**Figure 7.9 Verapamil combined drug treatment reduced colony formation in the selected EPN-2 sublines.** This graph shows the percentage of surviving colonies compared between single drug treatment and drug treatment combined with Verapamil. The concentration of drug used was that expected to result in survival of 30-40% of colonies (20  $\mu$ M etoposide and 8  $\mu$ M irinotecan), single and combined treatments were carried out using 10  $\mu$ M Verapamil. Drug treatment combined with Verapamil demonstrated significantly increased efficacy over the single drug treatment. The percentage of surviving colonies was significantly reduced [ $p < 0.001$  (\*\*) and  $p < 0.05$  (\*)] when cells were treated with both drug and Verapamil. However, a small proportion of colonies still survive after treatment.

### **7.2.3.2 Neurosphere formation assay**

Five colonies were selected from each condition to perform a neurosphere formation assay by growing them in stem cell media for 4 days. Neurosphere formation is illustrated in Figure 7.10 and 7.11. The parental cells and the control sublines were able to form nice neurospheres after they were treated with vehicle, etoposide, or etoposide with Verapamil as shown in Figure 7.10. Whilst single cells and tiny neurospheres comprising 5-10 cells were observed in EPN-2\_E\_T1 subline (Figure 7.10), these would presumably form larger neurospheres if they were incubated longer. For irinotecan treatment, effective neurosphere formation was observed in EPN-2 and EPN-2\_C sublines treated with vehicle and irinotecan whilst single cells were observed when they were treated with irinotecan and Verapamil (Figure 7.11). In EPN-2\_I\_T1 subline, they could not form neurospheres after any treatments (Figure 7.11). However, a group comprising 5-10 cells was observed and they potentially could form neurospheres with longer incubation.

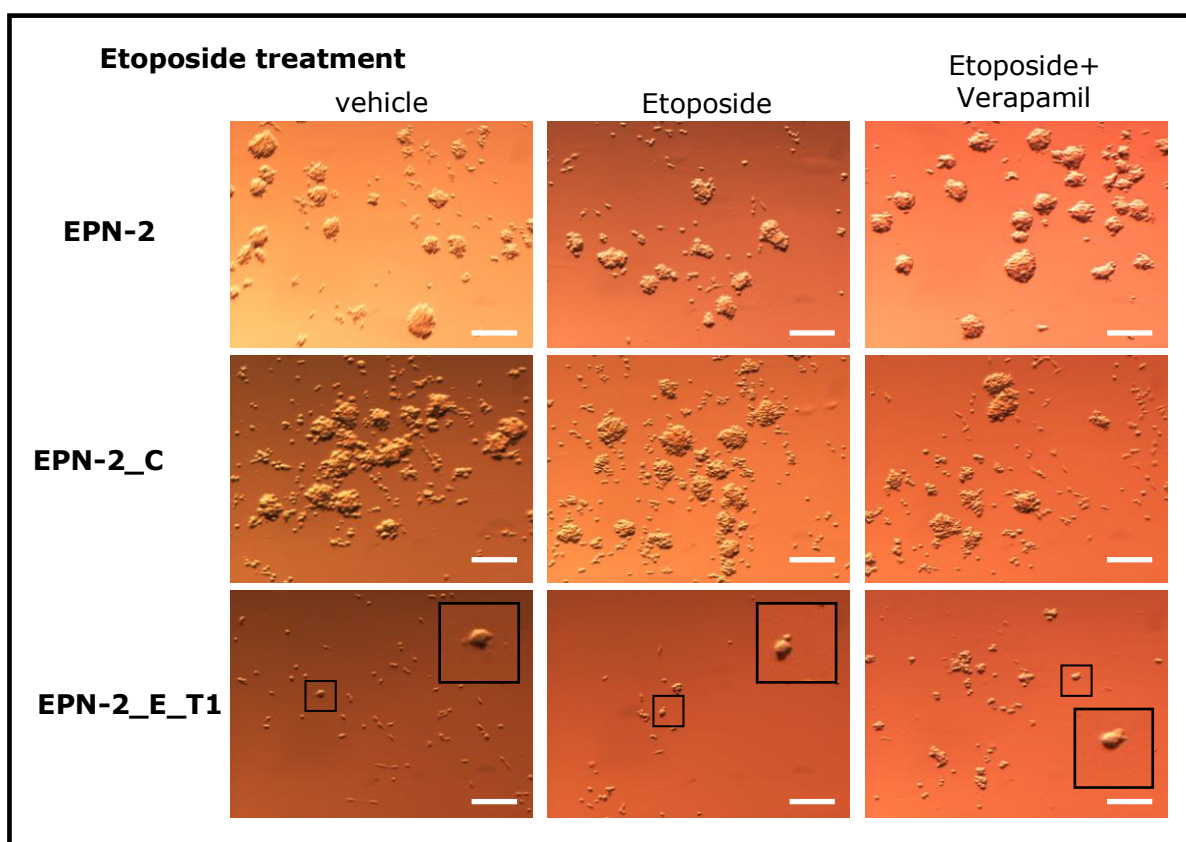


**Figure 7.10 Neurosphere formation from EPN-2, EPN-2\_C and EPN-2\_E\_T1 sublines treated with vehicle, etoposide, or etoposide combined with Verapamil.** Five colonies from each condition were selected to grow in stem cell media to determine neurosphere formation capability. Both EPN-2 and EPN-2\_C sublines were able to form neurospheres in all conditions whilst the EPN-2\_E\_T1 subline could not form neurospheres. However, very tiny neurospheres, which comprised 5-10 cells, not single cells were visible (boxed region). If these cells are incubated longer in stem cell media, they will probably be able to form neurospheres. Cells in the small boxed regions have been enlarged (x2) for clarity, which is demonstrated by the large boxed region. (Scale bar = 100  $\mu$ m)



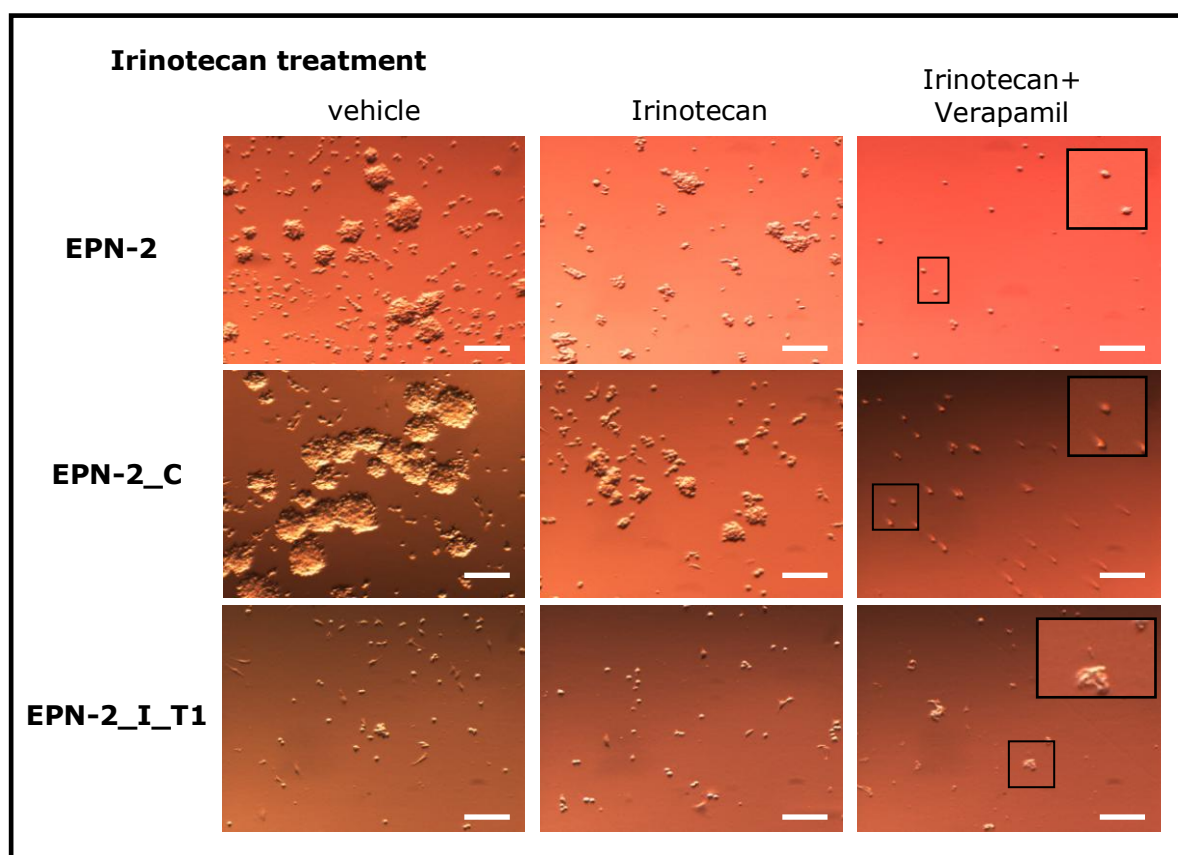
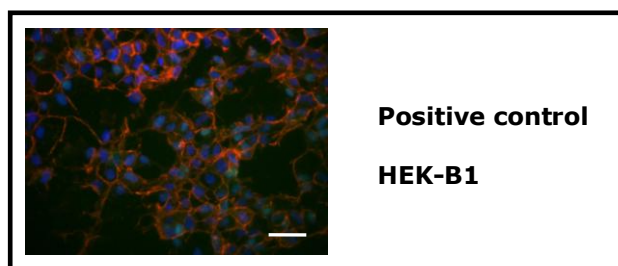


**Figure 7.11 Neurosphere formation from EPN-2, EPN-2\_C and EPN-2\_I\_T1 sublines treated with vehicle, irinotecan, or irinotecan combined with Verapamil.** Both EPN-2 and EPN-2\_C subline could form neurospheres when they were treated with vehicle or irinotecan whilst they were unable to form neurospheres after irinotecan treatment combined with Verapamil. In EPN-2\_I\_T1 subline, they could only form neurospheres when they were treated with vehicle. When they were treated with irinotecan or irinotecan combined with Verapamil, they formed very small neurospheres. Cells in the small boxed regions have been enlarged (x2) for clarity, which is demonstrated by the large boxed region. (Scale bar = 100  $\mu$ m)

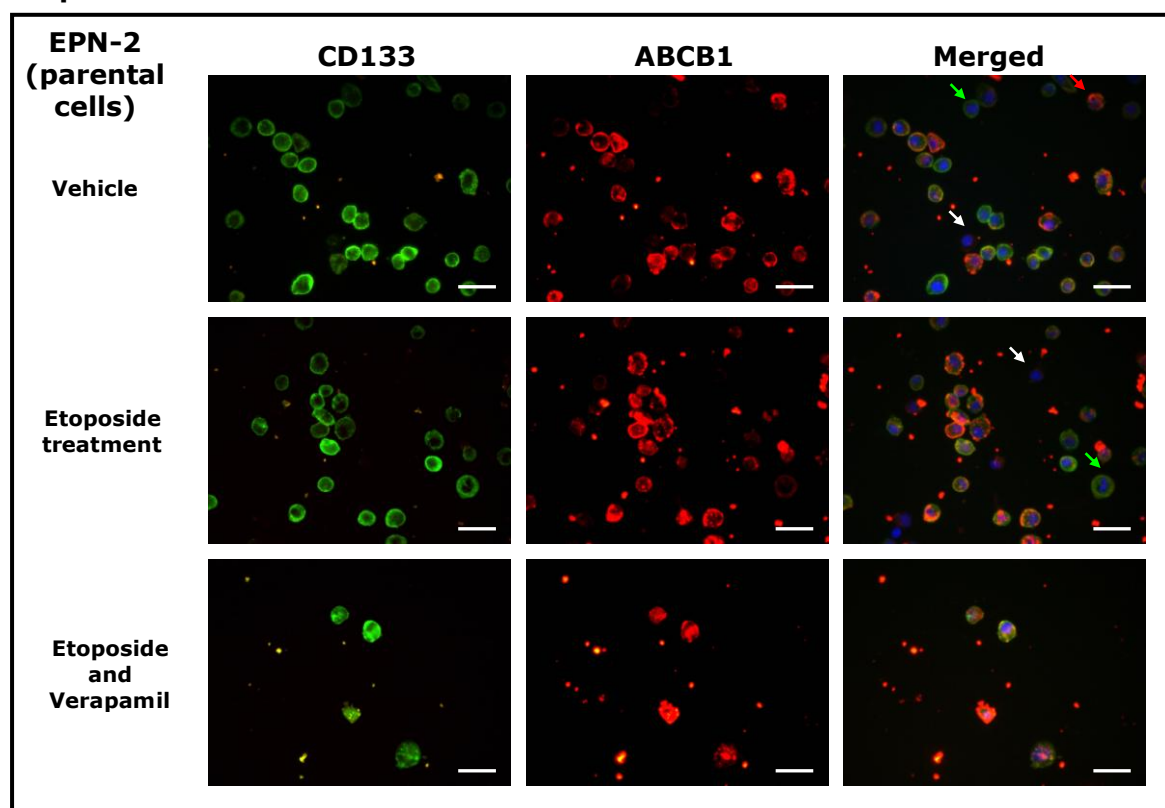
### **7.2.3.3 Co-staining immunofluorescence in surviving colonies**

#### **after drug treatment combined with Verapamil**

In order to examine marker expression, surviving colonies from clonogenic assay were harvested and cytopun onto slides, prior to immunofluorescence assay to determine CD133 and ABCB1 co-expression. Noticeably, the number of surviving cells after drug treatment or drug combined Verapamil treatment was visibly lower than that of vehicle or Verapamil alone, again demonstrating the combined effect of drug and Verapamil in cell survival. Co-staining CD133 and ABCB1 immunofluorescence results are presented in Figure 7.12 – 7.17 and show that the majority of surviving cells co-expressed CD133 and ABCB1 at a high level after all treatments. However, cells expressing CD133 or ABCB1 alone were detected in the control sublines whilst for cells treated with drug alone or drug combined Verapamil cells expressing CD133 or ABCB1 alone were rarely detected (Figure 7.12 – 7.17). The immunofluorescence results of the etoposide treatment group are shown in Figure 7.12 – 7.14 whereas Figure 7.15 – 7.17 shows the results from irinotecan treatment group.

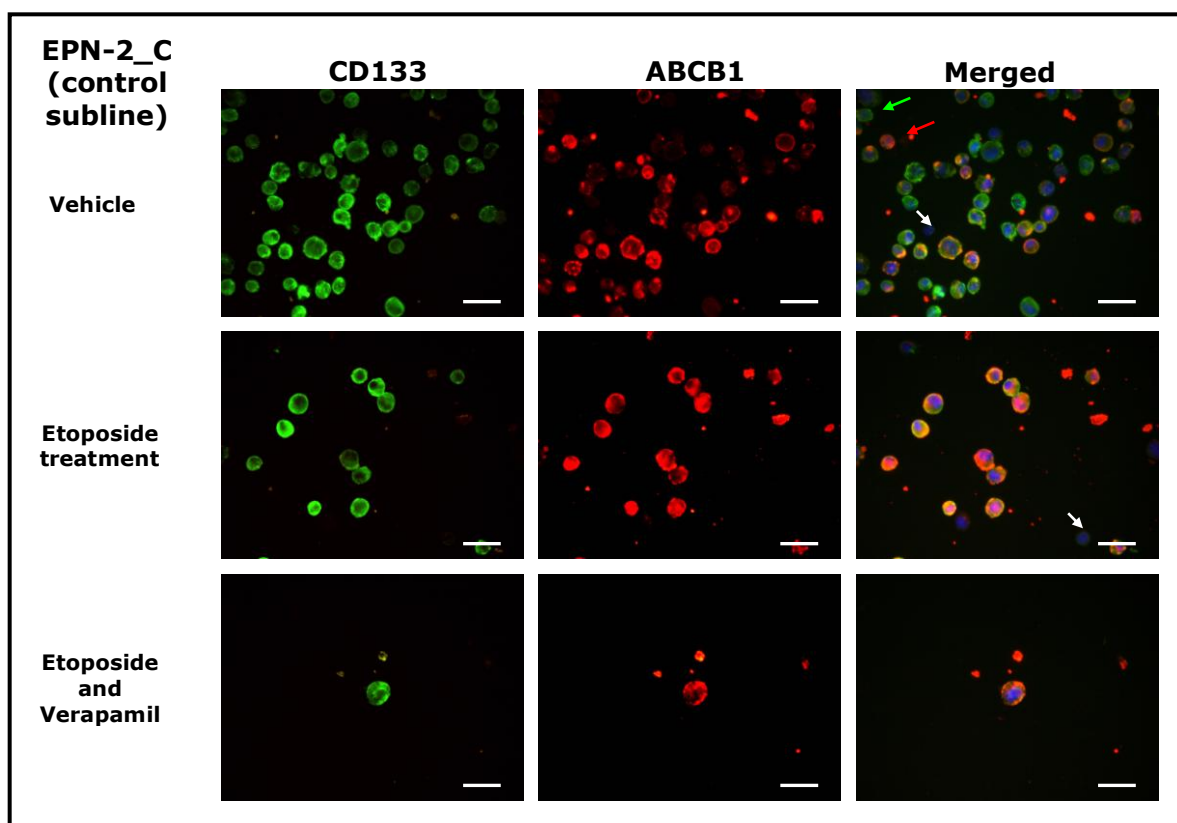


### Etoposide treatment

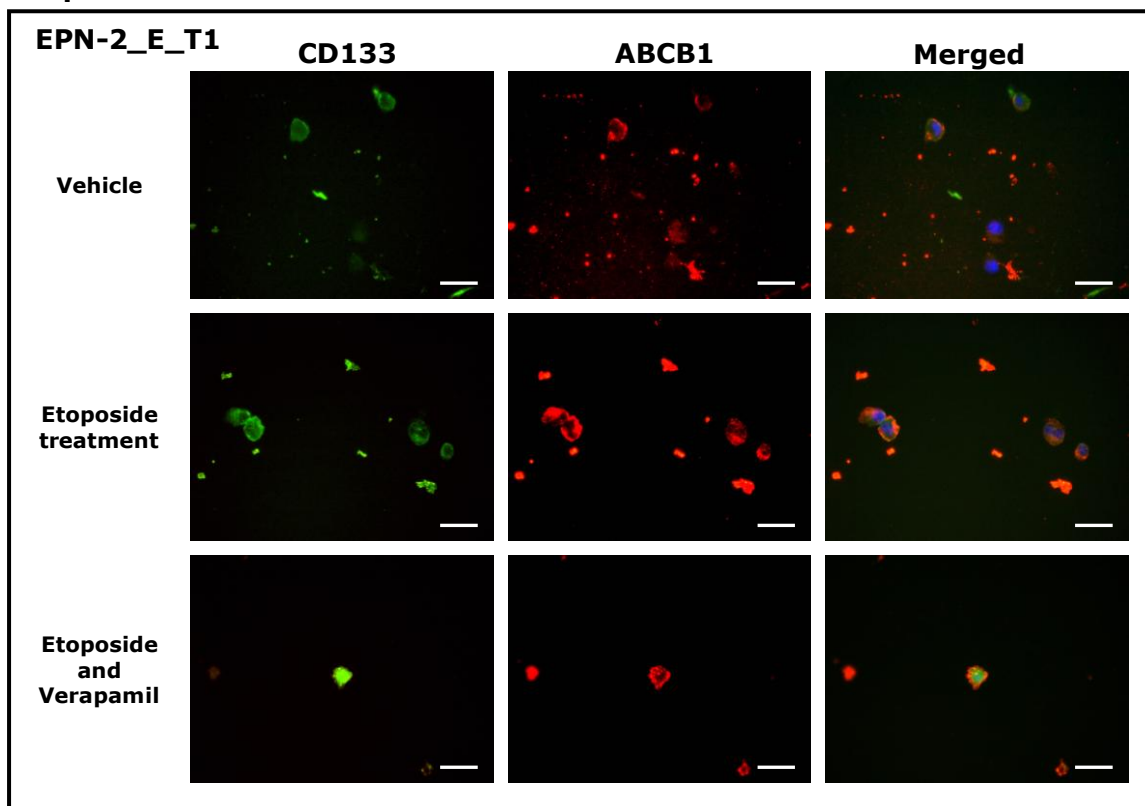


**Figure 7.12 CD133 and ABCB1 expression in the parental EPN-2 cells after vehicle, etoposide, or etoposide combined Verapamil treatment.** The EPN-2 parental cells were treated with vehicle, etoposide, or etoposide combined Verapamil and were harvested then cytospun. CD133 and ABCB1 co-expression was detected in all surviving cells. The majority of surviving cells co-expressed CD133 and ABCB1 at a high level after any treatment, although a small proportion of surviving cells was observed expression of CD133 or ABCB1 alone. (Scale bar = 25  $\mu$ m) (green arrows indicates cells expressing CD133 alone, red arrows indicates cells expressing ABCB1 alone and white arrows indicates cells not expressing CD133 or ABCB1)

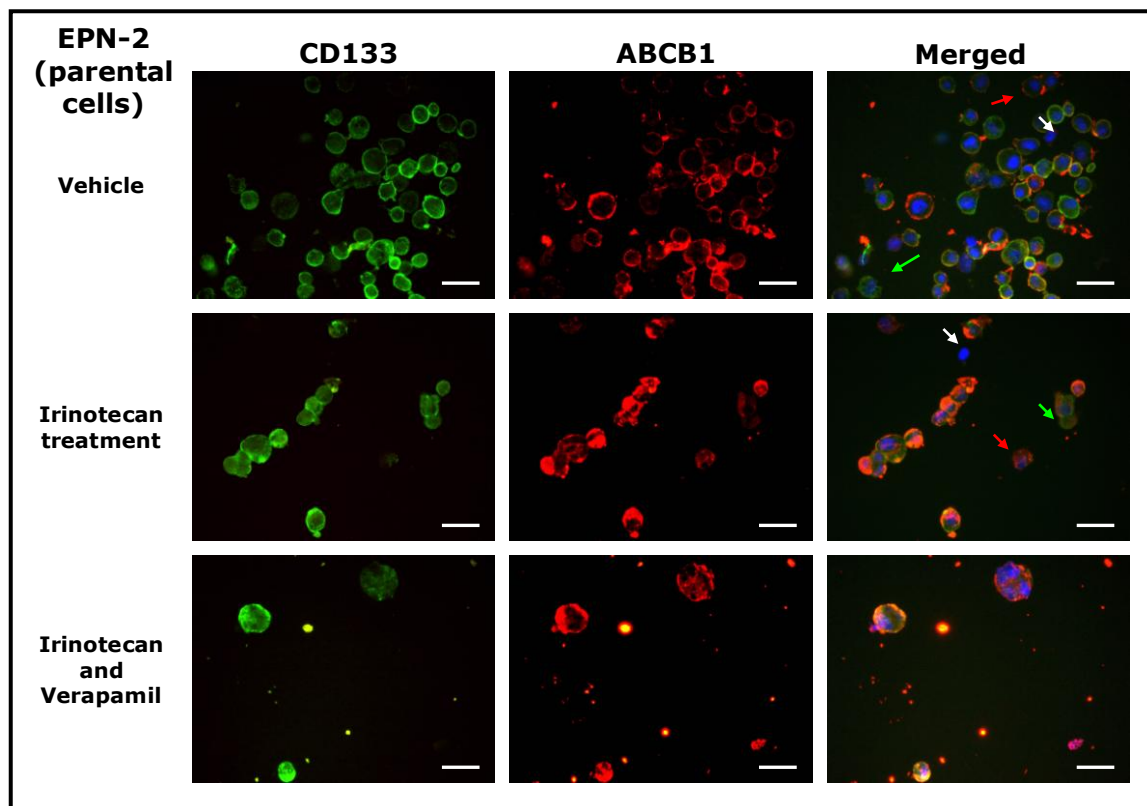
### Etoposide treatment



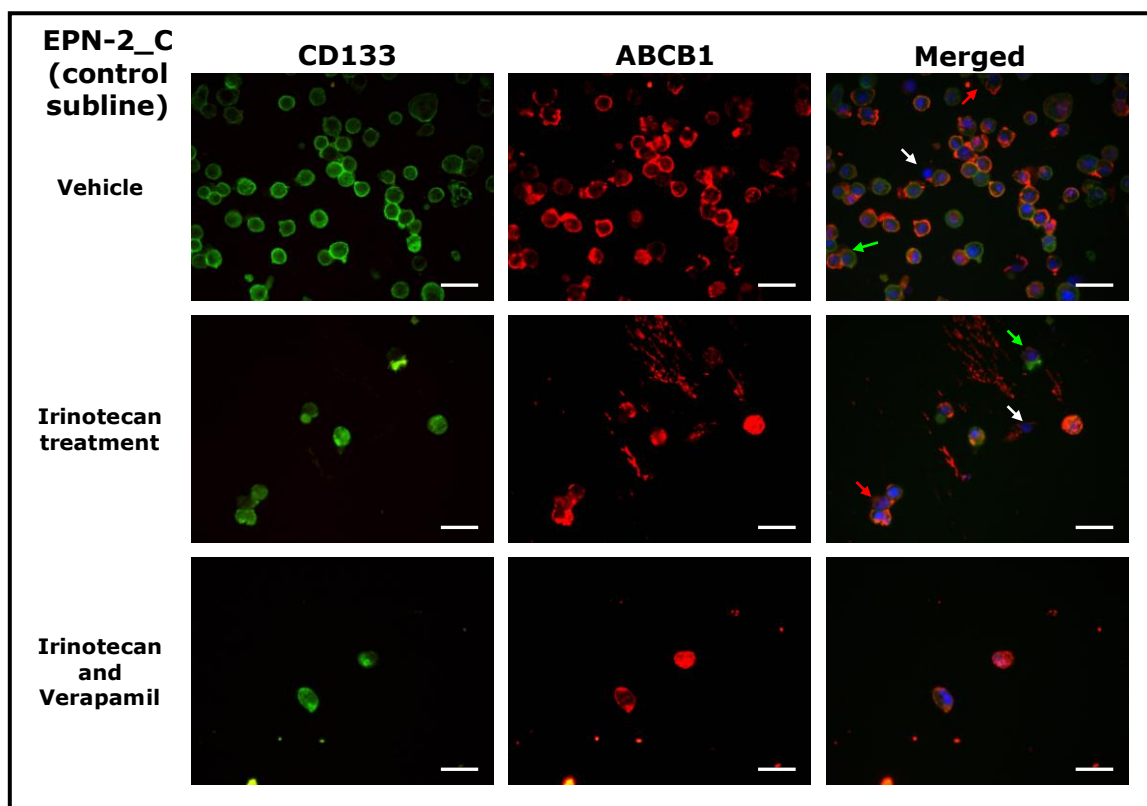
**Figure 7.13 CD133 and ABCB1 expression in the EPN-2 control subline after vehicle, etoposide, or etoposide combined Verapamil treatment.** A high level of CD133 and ABCB1 co-expression was detected in all surviving cells after all treatments. However, cells expressing CD133 alone were detected in the vehicle treatment. A higher proportion of cells expressing CD133 or ABCB1 was detected in cells treated with the vehicle whilst a large proportion of cells observed in etoposide or etoposide combined with Verapamil co-expressed CD133 and ABCB1. (Scale bar = 25  $\mu$ m) (green arrows indicates cells expressing CD133 alone, red arrows indicates cells expressing ABCB1 alone and white arrows indicates cells no co-expressing CD133 and ABCB1)

**Etoposide treatment**

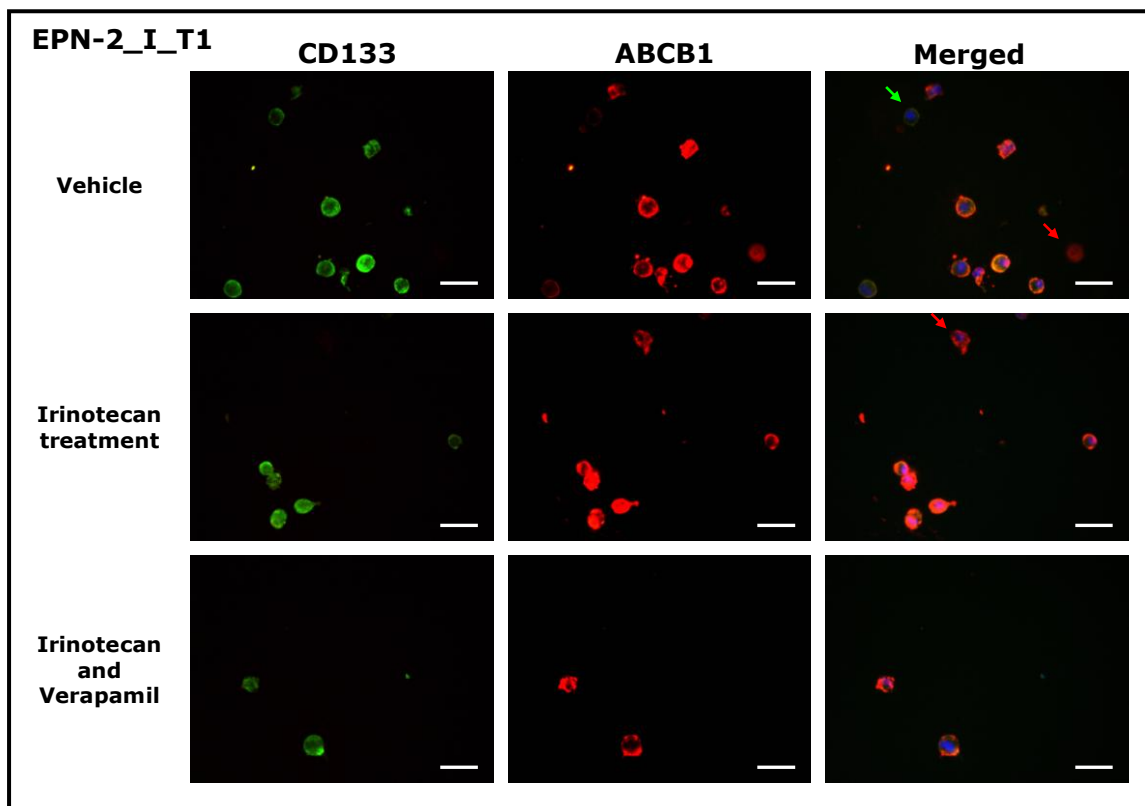
**Figure 7.14 CD133 and ABCB1 expression in the EPN-2\_E\_T1 subline after vehicle, etoposide, or etoposide combined Verapamil treatment.** Cells co-expressing a high level of CD133 and ABCB1 were observed after all treatments. Even after etoposide combined Verapamil treatment, surviving cells still highly co-expressed CD133 and ABCB1. Because the increased effect of etoposide, cell number of EPN-2\_E\_T1 subline after treatment was lower than those of the parental cells and the control subline. (Scale bar = 25  $\mu$ m) All cells are co-expressing although some faintly after vehicle treatment.

**Irinotecan treatment**

**Figure 7.15 CD133 and ABCB1 expression in the parental EPN-2 cells after vehicle, irinotecan, or irinotecan combined Verapamil treatment.** A high level of CD133 and ABCB1 co-expression was observed in most of surviving cells after all treatments. All cells treated with irinotecan combined Verapamil co-expressed CD133 and ABCB1 whereas some of surviving cells after vehicle or irinotecan treatment expressed CD133 or ABCB1 alone. (Scale bar = 25  $\mu$ m) (green arrows indicates cells expressing CD133 alone, red arrows indicates cells expressing ABCB1 alone and white arrows indicates cells no co-expressing CD133 and ABCB1)

**Irinotecan treatment**

**Figure 7.16 CD133 and ABCB1 expression in the EPN-2 control subline of after vehicle, irinotecan, or irinotecan combined Verapamil treatment.** The results were similar to etoposide treatment group whereby cells co-expressing CD133 and ABCB1 were detected at a high level after all treatments. Some of surviving cells after the vehicle treatment expressed CD133 or ABCB1 alone. (Scale bar = 25  $\mu$ m) (green arrows indicates cells expressing CD133 alone, red arrows indicates cells expressing ABCB1 alone and white arrows indicates cells no co-expressing CD133 and ABCB1)

**Irinotecan treatment**

**Figure 7.17 CD133 and ABCB1 expression in the EPN-2\_I\_T1 subline after vehicle, irinotecan, or irinotecan combined Verapamil treatment.** A high level of CD133 and ABCB1 co-expression was observed in surviving cells after all treatments. However, single CD133 expression was observed in vehicle treatment and single ABCB1 expression was observed in etoposide alone treatment. (Scale bar = 25  $\mu$ m) (green arrows indicates cells expressing CD133 alone, red arrows indicates cells expressing ABCB1 alone and white arrows indicates cells no co-expressing CD133 and ABCB1)



### 7.3 Discussion

**Cancer stem cells overexpressing functional ABCB1 were selected after many rounds of drug treatment in our cell lines.**

In the previous chapter, the expression of ABC transporters and CD133 was assessed after drug treatment and the results suggested that ABCB1 was the main transporter that might be responsible for drug resistance in our cell lines. Simultaneously, ABCC1 was also gradually upregulated during prolonged drug treatment whilst no ABCG2 expression was observed in any selected sublines throughout drug treatment. Therefore, ABCB1 was focused and further studied for drug resistance. In this chapter, ABCB1 function was assessed to prove that ABCB1 expressing cells, which were increased after drug treatment, were functionally able to respond to drug treatment.

Flow cytometry was performed to assess ABCB1 function using Rhodamine 123 (Rh123) as a substrate and Verapamil as an inhibitor. The results demonstrated that the proportion of cells extruding Rh123 in selected sublines was 2-3 fold higher than the parental and the control sublines (Figure 7.5). These results correlated with the immunofluorescence results from Chapter 6, which showed that cells co-expressing a high level of ABCB1 and CD133 were observed at a large proportion in all selected sublines after multiple rounds of drug treatment whilst the parental cell lines contained a smaller proportion of cells co-expressing ABCB1 and CD133 at a low level of expression. Taken together, our parental cell lines contained endogenous ABCB1 and ABCC1 at a low level of expression. Therefore, this might indicate intrinsic drug resistance in our cell lines. After drug treatment, ABCB1 was the major functional drug resistance transporter observed in the selected sublines indicative of further acquired drug resistance. This increase in ABCB1 is comparable to previous observation made both in other cell lines and in clinical samples. ABC transporters can be found in resistant cell lines selected by single drug treatment. For example, cell lines treated with Doxorubicin specifically selected for cells overexpressing ABCB1 and ABCC1, yet this

cell line also had cross-resistance from ABCC2 and ABCG2 overexpression [Szakács, G. *et al* (2006)]. Increasing ABCB1 after *in vitro* treatment contributed to failure of chemotherapeutic treatment and also correlated with the degree of drug resistance in breast cancer cell lines [Mechetner, E. *et al* (1998)]. Therefore, ABCB1 is an important transporter, playing a role in drug resistance in many cancers. In our cell lines, functional ABCB1 expressing cancer stem cells were selected after many rounds of drug treatment.

Rh123 and Verapamil were used as substrate and inhibitor, respectively, in ABCB1 functional analysis. Therefore, the accuracy of this assay depends on the specificity of substrate and inhibitor to ABCB1 transporter. If the inhibitor and substrate have less specificity to ABCB1 transporter, the results might be an under- or overestimate and have less accuracy to represent ABCB1 function. However, Rh123 and Verapamil are commonly used to study ABCB1 function. Rhodamine 123 is a fluorescent dye and is extensively used as substrate for ABCB1 to study ABCB1 efflux function [Lee, J. S. *et al* (1994), Fontaine, M. *et al* (1996) and Hsing, S. *et al* (1992)]. However, there is at least one report that ABCC1 transporter is also able to efflux Rh123 but less effectively than ABCB1 transporter [Twentyman, P. R. *et al* (1994)]. Therefore, to interpret the result using Rh123 as substrate to examine ABCB1 function, efflux results might not directly represent ABCB1 function but it possibly results from ABCC1 function too. In our cell lines, the major transporter was ABCB1 however, ABCC1 was upregulated after more than 10 rounds of treatment. Therefore, Rh123 efflux capability in our cell lines might be slightly overestimated from additional efflux function of ABCC1 transporter. To avoid the effect from ABCC1 function, we performed all experiments on samples at the early passages. Doxorubicin was reported to be a more specific ABCB1 substrate than Rh123 [van der Sandt, I. C. J. *et al* (2000)]. Our cell lines were highly resistant to Doxorubicin, therefore, Doxorubicin could not be used as substrate in our cell lines [Dr. Deema Hussein, personal communication]. One study reported that Rhodamine 123 was a poor ABCB1 substrate compared to other forms of rhodamine dyes. They revealed that tetramethylrosamine had superior quality than other rhodamine dyes as a substrate for ABCB1 [Eytan, G. D. *et al* (1997)]. In 1981, Verapamil was confirmed to be able to effectively

overcome ABCB1 function *in vitro* (leukaemic cell line and Vincristine-resistant subline) and *in vivo* (Vincristine-resistant tumour bearing mice) [Tsuruo, T. *et al* (1981)]. Later, Verapamil was generally adapted as an ABCB1 inhibitor to study ABCB1 function [Homolya, L. *et al* (1993), Muller, C. *et al* (1994), Yu, X. N. *et al* (2008) and Pauli-Magnus, C. *et al* (2000)]. Additionally, Verapamil combined with chemotherapeutic drugs treatment increased survival rate in patients diagnosed with breast cancer or non-small lung cell cancer [Belpomme, D. *et al* (2000) and Millward, M. J. *et al* (1993)]. Therefore, Verapamil can effectively inhibit ABCB1 function, and there is clinical evidence to support the advantage of using Verapamil treatment. However, Verapamil is also able to inhibit ABCC1 function but it is not a potent ABCC1 inhibitor compared to VX-710 (Biricodar) [Germann, U. A. *et al* (1997)]. Verapamil is a “first generation” ABCB1 inhibitor (see introduction of Chapter 7). Currently, the third generation of ABCB1 inhibitor had been developed to increased specificity to ABCB1 and decrease toxicity e.g. LY335979 (zosuquidar), XR9576 (tariquidar), GF120918 (elacridar) and OC144-093 (ontogen). In future studies, the third generation might be tested to more specifically inhibit ABCB1 function for drug resistance analysis and reduce associated to toxicity. However, to determine ABCB1 function, it is important to select a more specific inhibitor for ABCB1 rather than attempting to select specific substrate for ABCB1 due to the fact that ABCB1 has broad spectrum substrates and chemotherapeutic agents.

From Figure 7.5, the proportion of cells extruding Rh123 in the selected sublines was approximately 2-3 fold higher than the corresponding parental cells and control sublines. However, the highest proportion of cells extruding Rh123 in the selected sublines and the control sublines were observed in EPN-2 cell lines. Noticeably, a homogeneous proportion of such cells was observed in the selected EPN-2 sublines. In contrast, a varying proportion was observed in both MED-2 and SPNET-1 cell lines. This might be because each tumour originates from different cell types resulting in different characteristics of cancer cells in maintaining tumour population. Radial glia cells are postulated to be the cells of origin of ependymomas [Popleton, H. and Gilbertson, R. J. (2007)]. Since more than 80% of gene

expression observed in ependymoma from supratentorial region were similar to radial glia cells from corresponding region and that cancer cells with self-renewal and multipotent capacity derived from ependymoma share a similar immunophenotype (CD133<sup>+</sup>/Nestin<sup>+</sup>/RC2<sup>+</sup>/BLBP<sup>+</sup>) with radial glia cells [Taylor, M. D. *et al* (2005)], it is believed that radial glia cells have characteristics very close to stem cells. On the other hand, granule-cell progenitors located in the external granular layer (EGL) of the cerebellum are currently proposed as the cell of origin of medulloblastoma [Kadin, M. E. *et al* (1970) and Marino, S. *et al* (2000)]. Therefore, ependymoma originates from cells, which have characteristics very close to stem cells in comparison to medulloblastoma, which originates from more differentiated progenitor cells. Consequently, a larger proportion of population in EPN-2 possibly was cancer stem cells whilst medulloblastoma population might contain a large proportion of more differentiating progenitor cells and a small proportion of cancer stem cells. For CNS PNET, due the rarity of disease and difficulty in diagnosis because the histology is similar to medulloblastoma, the evidence of CNS PNET cell of origin is not available. Since cancer stem cells were selected more and more for purity after many rounds of drug treatment and they had capacity to maintain themselves and also generate progenitors. On the contrary, more differentiating progenitor cells could not survive after multiple rounds of drug selection resulting from these cells have a limitation of proliferation and self-renewal. Hence, a larger proportion of cancer stem cells expressing functional ABCB1 was observed in the selected EPN-2 sublines, which originates from radial glia cells.

In this study, there is no correlation between the proportion of functional ABCB1 cancer stem cells and grade or type of tumours or whether they were primary or recurrent. The EPN-2 cell line was obtained from a grade II primary ependymoma tumour without treatment prior to surgery, and the selected EPN-2 sublines contained the highest number of cells extruding Rh123, approximately 80-90%. On the other hand, SPNET-1 cell line is derived from grade IV primary CNS PNET tumour and MED-2 cell line is derived from grade IV recurrent medulloblastoma. These 2 selected sublines contained a lower number of cells extruding Rh123 (~30-60%) than the selected EPN-2 subline. Many significant factors (e.g.

the origin of tumour, tumour grading, treatment history and primary or recurrent tumour) might have an influence on the characteristics of each cell line and also indicate different response to drug treatment in our cell lines. The data of these significant factors are summarised in table 7.2. Among these 3 cell lines, although the EPN-2 cell line was derived from a low grade tumour (grade II Ependymoma) and had not been treated prior to surgery, they contained the highest proportion of cancer stem-like cells expressing functional ABCB1. Based on these findings we would predict that the patient from which EPN-2 was derived would be likely to relapse however this was the only tumour to be completely resected and the patients still alive.

**ABCB1 was responsible for drug resistance in our cell lines and Verapamil significantly increased drug cytotoxic effect.**

The previous results demonstrated that ABCB1 expression increased in the selected sublines after multiple rounds of drug treatment was functional. These results suggested that ABCB1 possibly was responsible for drug resistance in our cell lines. Therefore, to support ABCB1 as a significant mechanism protecting cells from drug toxicity, ABCB1 function was inhibited and survival rate was observed after drug treatment compared to the control cells. The clonogenic assay showed that drug combined with Verapamil treatment significantly decreased survival colony numbers (approximately 8-10 fold) compared to drug treatment

**Table 7.2 The details of treatment in the original tumours prior to establishment of cell lines.**

Cell line	The original tumour	WHO grade	Primary or Recurrent	Treatment prior to surgery	Degree of surgery
<b>EPN-2</b>	Ependymoma	II	Primary	None	Macroscopic resection
<b>MED-2</b>	Medulloblastoma	IV	Recurrent	Chemotherapy POG 3021 regimen (Cisplatin, Lomustine, Vincristine) and craniospinal radiation	Partial
<b>SPNET-1</b>	CNS PNET	IV	Primary	None	Partial

alone (Figure 7.9). Additionally, the size of colonies treated with drug combined Verapamil was far smaller and also the density of colony cells was far less than colonies treated with vehicle or Verapamil alone (Figure 7.7 and 7.8). Therefore, these results suggested that Verapamil effectively increased cytotoxic effect of drugs and ABCB1 was the main drug resistance mechanism to protect cells from drug treatment in the majority of our cell lines. Hsiang *et al* showed that a low concentration (1  $\mu$ M) irinotecan inhibited mouse lymphoblastic leukaemic cells in G2 resulting in a longer cell cycle and hence a slower growth rate [Hsiang, Y. H. *et al* (1989)]. Interestingly, Verapamil was able to completely inhibit ABCB1 function in flow cytometry (section 7.2.1) whilst this is not the case for clonogenic assay. This might be because of the instability of Verapamil in clonogenic assay. For FACS, to determine an efflux function of ABCB1, selected sublines were incubated with Rh123 and Verapamil for 2-3 hours. Conversely, after single cells in clonogenic assay were incubated with drugs and Verapamil, they were further incubated to allow colony formation for at least 7 days. Another possibility is that these surviving cells have other drug resistance mechanism rather than ABCB1 drug resistant transporter such as improved DNA repair mechanism, increase drug detoxification and metabolism, intracellular change of drug target and alteration of cell cycle. As a result they can survive after drug treatment.

Verapamil effectively inhibited ABCB1 function in both FACS and clonogenic assays. However, the inhibition seemed less effective in clonogenic assay as discussed above. SiRNA of ABCB1 was also attempted to reduce the expression of ABCB1 mRNA in our cell lines resulting in silencing ABCB1 function. However, the optimal conditions for ABCB1 SiRNA transfection were not achieved. Three different ABCB1 SiRNAs were tested with multiple different combinations of SiPORT Amine and SiRNA. There were 2 potential factors influencing successfulness of ABCB1 inhibition using SiRNA. Firstly, the selected sublines overexpressed an extremely high level of ABCB1 after drug selection compared to the parental cell lines or the control sublines. Resistant cell lines selected from drug treatment always expressed a very high level of ABC transporters and the level was far higher than the level in patients [Yagüe, E. *et al* (2004)]. This ABCB1 overexpression was far higher than

that detected in the parental line (Figure 5.1 – 5.3). Even if we have tried to use the earliest passage of the selected EPN-2 sublines, these sublines still contained a very high proportion of cells co-expressing CD133 and ABCB1, as confirmed by immunofluorescence analysis, and a high proportion of cells extruding Rhodamine 123 (ABCB1 substrate) detected by flow cytometry. The endogenous level of ABCB1 was also high in both the parental cells and the control sublines. This may have made it difficult to silence ABCB1 function in the EPN-2 cell line. Secondly, SiRNA may have been ineffective due to the short duration of RNAi stability from transfected synthetic siRNA as opposed to the long half-life of ABCB1 protein (14-17 hours) [Muller, C, *et al* (1995)]. Therefore, SiRNA may not have lasted long enough to result in knockout of ABCB1 protein levels. In recent studies, short hairpin RNA (ShRNA) has been applied to silence ABCB1 expression because ShRNA is more effective than SiRNA in RNA interference [Yu, J. Y. *et al* (2002)]. Yu *et al* studied RNA interference using SiRNA and ShRNA in mammalian cells and revealed that ShRNA was more effective in inhibition of GFP expression than SiRNA. This is because to inhibit a target gene, duplex formation is required. ShRNA forms a duplex by folding back itself, which can occur quickly and efficiently whilst SiRNA requires another strand of SiRNA to form duplex. Additionally, ShRNA can be stably expressed in cells so that it is more effective to target a long half-live ABCB1 gene. For long-lived proteins such as ABCB1 it may therefore be important to use shRNA since it is faster acting and more stable. It may also be necessary to stable integrate the shRNA to achieve knockdown [Yagüe, E. *et al* (2004)]. In recent studies, shRNA of ABCB1 has been attempted to decrease ABCB1 mRNA expression in our cell line with some early promise (Dr. Beth Coyle, personal communication). An additional problem was that our clones, which have different growth characteristic, required different conditions (the proportion of SiPORT Amine and SiRNA) for transfection. Therefore, the optimal condition for ABCB1 knockdown in our cell lines should be optimised in every single cell line. To increase the effectiveness of SiRNA in silencing of ABCB1 function, using two or more specific SiRNA can improve the gene silencing effect compared to a single SiRNA [Ji, J. *et al* (2003)]. Therefore, combined SiRNAs should be attempted to silence ABCB1 expression in the future and flow cytometry might be performed to determine the level of ABCB1 expression after

knocking down. Flow cytometry might have higher sensitivity than the conventional RT-PCR to determine the level of ABCB1 silencing.

**Irinotecan affected the ability of cells to form neurospheres after the initial treatment.**

The neurosphere formation assay showed that capability to form neurospheres of the selected EPN-2 sublines was affected after they were treated with multiple rounds of etoposide (11 rounds). Whilst, irinotecan combined with Verapamil affected the ability of EPN-2, EPN-2\_C and EPN-2\_I\_T1 sublines to form neurospheres, although they were treated with the first round of irinotecan. Sublines repeatedly treated with irinotecan obviously could not form neurospheres after any treatments.

After the clonogenic assay, resistant colonies were selected from each condition to assess the ability of cells to form neurospheres. In Figure 7.10, colonies selected from multiple rounds of etoposide treatment (11 rounds) failed to form neurospheres whilst colonies selected from the parental cells and the control subline, which had been treated for the first round of etoposide, still have ability to form neurospheres. Therefore, this suggested that prolonged treatment of etoposide affected the ability of cells to form neurospheres. In contrast, the ability of cells to form neurospheres was affected in all colonies selected from any conditions of EPN-2 cell lines, even in the cell lines that had been treated with the first round of irinotecan (Figure 7.11). Hence, this suggested that the ability of cells to form neurospheres was affected even after a single round of irinotecan combined with verapamil treatment. Therefore, in our cell lines, prolonged etoposide treatment affected the ability of cells to form neurospheres whilst irinotecan inhibited cells to form neurospheres after the first round of treatment. In Chapter 6, it was also shown that the first round of methotrexate treatment in the parental cell lines affected neurosphere formation ability of cells. Therefore, we hypothesised that methotrexate might be able to target cancer stem cells. For irinotecan,



it may be that, irinotecan is able to target cancer stem cells even after the first round of treatment when it was enhanced to be intracellularly accumulated by Verapamil.

### **Surviving cells after drug combined Verapamil treatment expressed ABCB1.**

After clonogenic assays, surviving cells were examined for CD133 and ABCB1 co-expression. This experiment was performed to identify whether surviving cells were positive or negative for ABCB1 after ABCB1 function has been inhibited by verapamil and cells were treated with cytotoxic drugs. If the majority of surviving cells are negative for ABCB1, this possibly suggests that these cells originally have other drug resistance mechanism to survive after treatment. However, this is not the case for our cell lines, since the immunofluorescence results demonstrated that *most of the surviving cells* expressed ABCB1 at a high level (Figure 7.12 – 7.17). Therefore, this suggests 2 possibilities. Firstly, surviving ABCB1 cells simultaneously developed other drug resistance mechanisms during many rounds of drug selection resulting in survival from drug cytotoxicity even though ABCB1 function was inhibited. Additional ABC transporters can be upregulated in cells after selection with a single drug [Szakács, G. *et al* (2006)]. Our cell lines possibly upregulate other transporters after longer drug exposure; e.g. ABCC1 as found in selected sublines after prolonged drug treatment, or maybe ABCG2, and it may be that even if their expression is not detected, there is some function of ABCC1 and ABCG2 in these cells. However, the expression of other survival mechanisms is also a distinct possibility. Secondly, the concentration of Verapamil may not have been high enough to inhibit ABCB1 function in cells expressing a very high level of ABCB1. Consequently, a small proportion of these cells would survive. Since 10  $\mu$ M and 20  $\mu$ M of Verapamil were tested prior performing clonogenic assay, a concentration between 10-20  $\mu$ M might completely inhibit ABCB1 function in clonogenic assay without cytotoxicity. A previous study reported that 2.2 – 6.6  $\mu$ M of Verapamil was enough to effectively inhibit ABCB1 function in Vincristine-resistant leukaemic cell line [Tsuruo, T. *et al* (1981)]. Hence, our cell lines might have a higher degree of drug resistance resulting in a very high level of ABCB1 expression, consequently, Verapamil might be required higher

concentration to completely inhibit ABCB1 efflux function in our cell lines. For future study, concentrations of Verapamil between 10-20  $\mu$ M may be tested to inhibit ABCB1 function in clonogenic assay. Third generation ABCB1 inhibitors are currently being utilised in the laboratory to more selectively inhibit ABCB1. To assess the effectiveness of ABCB1 inhibition, drug conjugated with immunofluorescence might be used to determine drug uptake. There are many interesting points to investigate further for future study to understand the behaviour and mechanism of drug resistance in cancer cells. These are discussed in the final chapter.

---

---

## **Chapter 8**

### **General discussion and conclusion**

---

---

## Chapter 8: General discussion and conclusion

**Hypothesis:** Paediatric brain tumour cell lines contain a subpopulation of cancer stem cells that use ABC multidrug transporters to efflux chemotherapeutic agents.

This hypothesis was based on the findings that cancer stem cells have been discovered as a small proportion of cells in various types of cancers including brain tumours and these cells are believed to be chemoresistant based on them sharing characteristics with stem cells. Other features in common with normal stem cells are a capacity for self-renewal, proliferation and multipotency which together provide a high potential for these cells to re-initiate tumours after treatment. ABC transporters, in particular to ABCB1, ABCC1 and ABCG2 have been postulated as a major drug resistance mechanism in cancers and these transporters have been demonstrated to be expressed by stem cells and CSCs. Therefore, CSCs expressing ABC transporters may promote multidrug resistance in cancers. Our cell lines were derived from 5 different brain tumours including WHO grade II and IV. These selected tumours represent tumours that are either highly resistant to chemotherapy or have a high potential to recur. Therefore, it is necessary to explore the root of chemoresistance in these tumour types since this might lead the way to open a window of hope to cure these malignant diseases in the future.

Since all cell lines included in this study are newly established, their basic characteristics were first investigated to ensure the quality of cell lines. The results demonstrated that our cell lines are stable in prolonged culture conditions and able to preserve significant genetic aberrations from the original tumours as shown in Chapter 3 and 4. Hence, our cell lines reliably represent the characteristics of the original tumours from which they were derived. Additionally, all of our cell lines were able to rapidly form tumours when they were orthotopically transplanted into immune-compromised mice. The gross immunohistological characteristics of these orthotopic xenografts recapitulated the corresponding original tumours. This indicated that our cell lines contained tumourigenic cells (Hussein, D. *et al*, unpublished data).

The key findings in this study are summarised here. The data have shown that neurosphere culture conditions enriched for cancer stem-like cells expressing ABCB1 or ABCC1 relative to monolayer conditions. Telomere length was maintained and telomerase was active in both monolayer and neurosphere conditions at different passages. The results also demonstrated that the parental cell lines contained a small proportion of CSCs expressing a low level of ABCB1 and ABCC1 but not ABCG2. However, experimental analyses revealed that ABCB1 was the major active drug transporter in our cell lines. The results indicated that our parental cell lines had intrinsic drug resistance via functional ABCB1 expressed in CSCs (less than 30%). In downstream drug resistance analysis, ABCB1 was consistently detected at a high level of expression in a large proportion of cells throughout prolonged drug treatment and was functional. Whilst ABCC1 was upregulated later, after more than 10 rounds of drug treatment. Interestingly, none of our treated cells expressed ABCG2 during drug treatment. Drug treatment selected cells overexpressing functional ABCB1 in our cell lines and they were enriched approximately 2 fold compared to the controls. The survival rate of colonies was significantly reduced when cells were treated with drug combined with a specific ABCB1 inhibitor (Verapamil) and these surviving colonies still expressed ABCB1 at a very high level. Taking all these results together, CSCs expressing functional ABCB1 contribute to multidrug resistance in these newly derived paediatric brain tumour cell lines.

Two main techniques were performed to identify subpopulations in our cell lines including co-staining immunofluorescence and Western blotting analysis. The immunofluorescence assay identified cancer stem-like cells by CD133 and SOX2 co-staining and cancer stem-like cells expressing ABC transporters by CD133 and ABC transporters (ABCB1, ABCC1 or ABCG2) co-staining. Western blotting analysis was also performed to confirm the expression of CD133, SOX2 and ABC transporters in our cell lines. Whilst functional analysis of ABCB1, based on cells extruding Rh123, was determined by flow cytometry. A cartoon depicting the identified subpopulations in the EPN-2 cell line is drawn in Figure 8.1. Subpopulations of tumour were identified into 3 groups; cells extruding Rh123, cells co-expressing CD133 and SOX2 and cells

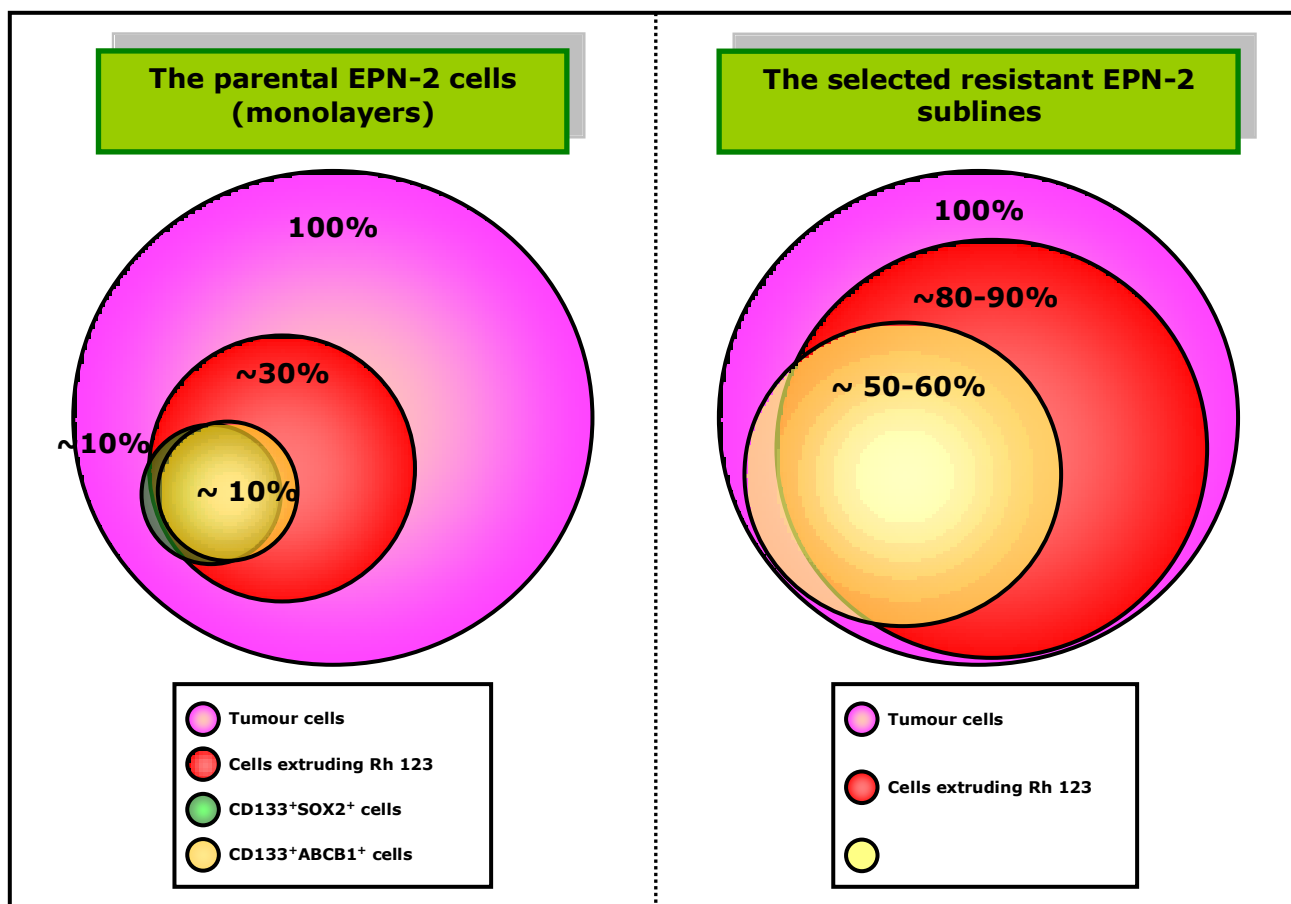


**Figure 8.1 Tumour population in the parental EPN-2 and selected resistant EPN-2 sublines.** The model of tumour population was proposed based on all results from this thesis. In the parental EPN-2 cell line, cells extruding Rh123 accounted for approximately one-third of the population and roughly only 1 in 4 of these cells co-expressed CD133 and SOX2 (~8%) while 1 in 3 of these cells co-expressed CD133 and ABCB1 (~10%). Hence, only about 8% of tumour population that were able to extrude Rh123 co-expressed CD133, SOX2 and ABCB1. Therefore, the parental cell line comprised approximately 8% cancer stem-like cells expressing functional ABCB1. The remaining 22% of cells that were actively extruding Rh123 are predicted to be early progenitor cells (a). After many rounds of drug treatment, cells extruding Rh123 were significantly increased almost 3 fold and cells co-expressing CD133 and ABCB1 were also increased nearly 6 fold compared to the parental cells (b). In the total population, however, in each case a proportion of cells fails to extrude Rh123 (purple). Drug treatment selected for drug resistant cancer stem cells leading to a subsequent increase in drug resistant progenitors (red circle alone without yellow).

coexpressing CD133 and ABCB1. All CD133 cells were SOX2 positive and the majority of these also expressed ABCB1, however a tiny proportion (about 2%) of cells expressed ABCB1 alone. Both the CD133/SOX2/ABCB1 and the ABCB1 only population would be expected to extrude Rh123. These estimated proportions of subpopulations were used to designate partitioning of the whole population pre- and post many rounds of drug selection by comparing the selected resistant EPN-2 subline to the parental EPN-2 line. After many rounds of drug treatment, the proportion of both cells extruding Rh123 and cells co-expressing CD133 and ABCB1 were increased approximately 3 fold and 6 fold, respectively (Figure 8.1, a and b). Cells expressing CD133, SOX2 and functional ABCB1 accounted for about 8% and this subpopulation was enriched up to 50% after drug treatment. This indicated that drug treatment enriched CSCs expressing functional ABCB1 approximately 6 fold in EPN-2 cell line. However, more than half of cells extruding Rh123 were negative for CD133 and ABCB1, suggesting that drug treatment enriched for drug resistant CSCs resulting in a corresponding increase in drug resistant progenitors. The proportion of functional ABCB1 cells extruding Rh123 (Figure 8.1, red) was larger than the proportion of cells co-expressing CD133 and ABCB1 (Figure 8.1, yellow). Although Rh123 can also be transported by ABCC1 (but less effectively) [Twentyman, P. R. *et al* (1994)] possibly resulting in the increase of the Rh123 extruding population, the specific ABCB1 inhibitor, Verapamil, was used to inhibit ABCB1 function hence ABCB1 function is still the most likely reason for this extrusion. It might also be possibly that the sensitivity of the immunofluorescence analysis, which was optimised based on HEK-B1 cells stably expressing an extremely high level of ABCB1, could not detect cells expressing a low level of CD133 and/or ABCB1. These low levels ABCB1 cells would still extrude Rh123, consequently, the proportion of functional ABCB1 cells detected by flow cytometry could be larger than the proportion of CD133 and ABCB1 co-expressing cells detected by immunofluorescence analysis. Additionally, multiple rounds of drug treatment may have selected drug resistant CSCs resulting in an increase in the progenitor population, which has reduced ABCB1 expression. It has previously been reported that the expression of CD133 reduces in differentiating cells [Kania, G. *et al* (2005)] and a similar decrease in ABCB1 expression may also occur.

Four different drugs (Etoposide, Cisplatin, Irinotecan and Methotrexate) were used to select drug resistant sublines for downstream drug resistance analysis. These 4 drugs have different targets and mechanisms of action. However, all 4 drugs target proliferating cells. Our cell lines are highly proliferative as seen from their doubling times (Chapter 4), therefore, when EPN-2, MED-2 and SPNET-1 cell lines were treated with these drugs, the majority of cells were affected leading to death. Whilst a small proportion of cells still survived and formed colonies in clonogenic assay and neurospheres in neurosphere formation assay after drug removal. Hence, this small population was drug resistant and had cancer stem cell characteristics. A previous study performed by Dr. Deema Hussein, a postdoctoral researcher in our group, examined 2 other potential drug resistance mechanisms enriched in CSCs from our cell lines; quiescence of CSCs and an elevation of DNA repair (Figure 8.2). Quiescent or non-cycling cells are found in the  $G_0$  phase of the cell cycle.  $G_0$  cells have been directly isolated from chronic myeloid leukaemia. These cells had stem cell properties with regard to generating leukaemic progenitors and were able to form new tumours after transplantation [Holyoake, T. *et al* (1999)]. Hence, it was proposed that surviving resistant sublines were generated from cancer stem cells, which had undergone quiescence resulting in them escaping from drug effects and surviving after treatment. Dr. Hussein demonstrated that neurospheres, which were enriched with CSCs, contained a higher proportion of  $G_0G_1$  cells than monolayers (64% and 44%, respectively). Cells isolated from these neurospheres from our cell lines (EPN-1, MED-1 and BT-4 cell lines) were more resistant to Etoposide treatment than monolayers. However, the cell cycle profile of nestin positive cancer stem cells showed that nestin positive cells were found in all phases of the cell cycle and only 21% of nestin positive cells were found in  $G_0G_1$ . Based on these findings, we proposed that although cells grown under neurosphere conditions cycle slowly, the majority of nestin positive CSCs are still cycling and hence quiescence does not appear to be a major mechanism of drug resistance. Dr. Hussein also used the comet assay to demonstrate that DNA damage was reduced faster over time in neurospheres compared to monolayers. This result suggested that neurospheres, containing more CSCs, had better DNA repair than monolayers. This assay also revealed an increase in DNA damage after initial



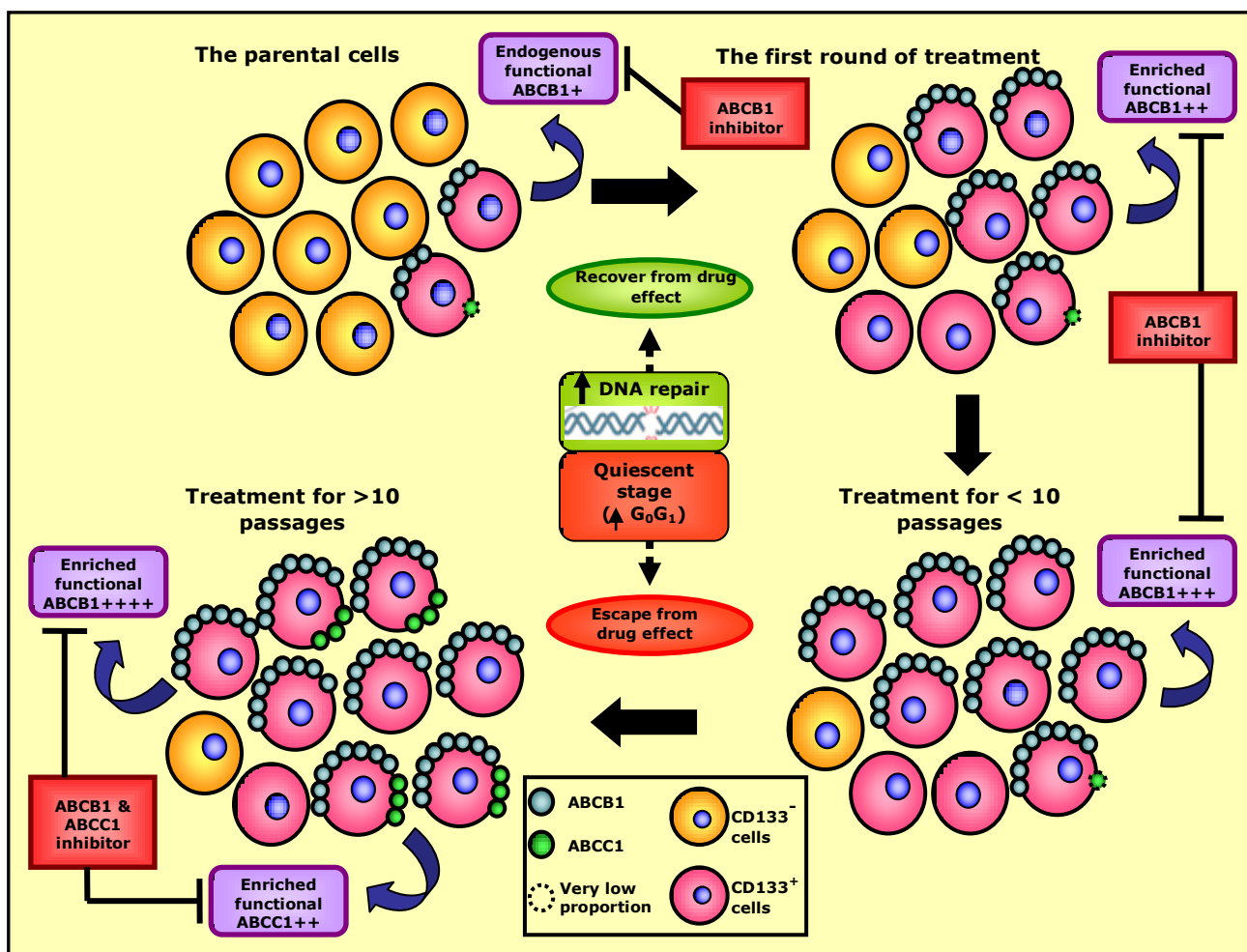


**Figure 8.2 Drug resistance mechanisms in newly established paediatric brain tumours.** This schematic figure shows possible drug resistance mechanisms in our cell lines. It is proposed that the tumour population is heterogeneous and contains different proportions of subpopulations at different time points after drug treatment. Two other minor mechanisms of drug resistance: DNA repair and quiescence are also shown. If drug uptake is sufficiently increased the cell will be unable to repair the damage and we believe the quiescence is a minor mechanism in our cells. An alteration of the main drug resistance mechanism in our cell lines was observed during drug treatment. The parental cell lines originally contained endogenous functional ABCB1, which indicated an intrinsic drug resistance. After prolonged drug treatment, drug treatment selected CSCs expressing functional ABCB1 resulting in cells consistently enriched for functional ABCB1 expression throughout drug treatment. Whilst ABCC1 was upregulated later after many rounds of drug treatment. Hence, using an ABCB1 inhibitor combined drug treatment might improve the effectiveness of treatment, however, using ABCB1 inhibitor in the later stages of treatment might be less effective resulting from further increasing functional ABCB1 and other transporters.

treatment in monolayers compared to neurospheres (35.3% and 15.8%, respectively). These findings support the fact that drug extrusion is the first point of protection in these cells.

My study revealed that functional ABCB1 in CSCs was a major drug resistance mechanism in EPN-2, MED-2 and SPNET-1 cell lines resulting in consistent high expression of ABCB1 throughout drug treatment (Figure 8.2). To confirm functional ABCB1 in our cell lines correlated with drug resistance, the clonogenic assay was performed and the results revealed that survival rate of colonies was significantly reduced in the EPN-2 line after drug treatment combined with an ABCB1 inhibitor as shown in Chapter 7. In the EPN-2, MED-2 and SPNET-1 cell lines, the results demonstrated that the level of ABCB1 expression was increased after the initial treatment and the level of ABCB1 expression and proportion of ABCB1<sup>+</sup> cells were consistently high during prolonged drug treatment. Whilst ABCC1 was only upregulated after many rounds of drug treatment. These findings were the same for each of the 4 drugs. This is a commonly found feature of multidrug resistant cells whereby after treatment with a single drug not only the transporter that specifically exported that drug was increased but other transporters were also upregulated [Szakács, G. *et al* (2006)]. The data presented hence suggests that the main ABC transporter in our cell lines is ABCB1 and it functions as an active drug transporter, pumping drugs out of cells resulting in a decrease in intracellular drug accumulation. From figure 8.1 and 8.2, it is suggested that the resistant CSCs will be selected more and more after multiple rounds of drug treatment. Consequently, the tumour will be enriched with drug resistant CSCs. Hence, it is necessary to develop the means to overcome ABC transporter mediated multidrug resistance.

Figure 8.2 demonstrates how the outcome of treatment can be improved by using a highly specific ABCB1 inhibitor combined with chemotherapy at the beginning of treatment when the proportion of resistant CSCs is low and it is possible to overcome drug resistance compared to the late stage of treatment, when multiple drug efflux transporters will be enriched in resistant CSCs. Therefore, if the amount of drug accumulated in cells is high enough to cause cytotoxic effect in the first round of treatment, it might be sufficient to target all of the CSCs. Hence, a

specific ABCB1 inhibitor should be combined with chemotherapy at the beginning of treatment based on the findings of this thesis, however, these needs to be tested in animal models. The ABCB1 inhibitor used in our study was Verapamil. Verapamil, a calcium channel blocker, is a first generation ABCB1 inhibitor and has less specificity compared to later generations. The second generation of inhibitor e.g. Valspodar increased the level of chemotherapeutic agents 6-8 fold in brain, kidney, liver and plasma [Fellner, S. *et al* (2002)]. Unfortunately, it also interacted with cytochrome P450 enzymes resulting in delayed drug elimination and as a result increased drug toxicity in normal cells [Wandel, C. *et al* (1999)]. Current third generation ABCB1 inhibitors include elacridar (GF 120918) and tariquidar (XR 9576) which have been demonstrated to have reduced side effects and improved effectiveness. Several *in vivo* studies have demonstrated that elacridar co-application with chemotherapeutic agents significantly increased level of drugs in brain higher than plasma level [Edwards, J. E. *et al* (2002) and Huisman, M. T. *et al* (2003)]. Additionally, it was able to selectively reverse ABCB1 transporter effects at the blood brain barrier. Paclitaxel co-administered with elacridar or tariquidar was highly accumulated in brain compared to plasma level and less systemic cytotoxic effects were observed than with valspodar [Hubensack, M. *et al* (2008)]. Therefore, these third generation ABCB1 inhibitors have better efficacy, higher specificity to inhibit ABCB1 in blood brain barrier and less systemic cytotoxicity, and are therefore potentially highly useful for clinical application.

The clonogenic assay results using drugs combined with Verapamil treatment demonstrated that a small proportion of cells survived and were able to form colonies (and therefore were not quiescent) and also neurospheres. The results were different from our expectation because our cell lines had ABCB1 as a major drug resistance mechanism therefore, when ABCB1 function was inhibited, all cells were expected be destroyed and die. Verapamil concentration however may also not have been high enough but the higher concentration that was able to inhibit HEK-B1 (20  $\mu$ M) was toxic to our cells. Elacridar as described above has a higher potency to inhibit ABCB1 function than Verapamil and it may more effectively kill drug resistant cells although our preliminary results still show some cells surviving (David Carrier, personal communication).

Therefore, several possible protective mechanisms have been postulated in Figure 8.3. After multiple rounds of drug selection, the cell population contains a large proportion of CSCs overexpressing ABCB1 and a small proportion of CSCs without ABCB1 expression and non-CSCs. When the line was treated with cytotoxic drug, both CSCs and CSCs overexpressing ABCB1 can survive and regenerate (Figure 8.3, a). Three possible explanations for surviving cells after drug combined Verapamil treatment have been considered in Figure 8.3. Surviving CSCs could have been negative for ABCB1 expression (Figure 8.3, a and b), which was not the case for our study. In the first pathway, surviving CSCs may have used other drug resistance mechanism(s) to protect themselves from cytotoxic drugs with the exception of ABCB1 and re-initiated a heterogeneous cell population containing CSCs and progenitor cells (Figure 8.3, b). The second pathway proposes that some surviving CSCs acquired mutation(s) resulting in regeneration of a cell population containing mutated CSCs, CSCs and progenitor cells (Figure 8.3, c). Our cell lines, however, fit with the last possibility. We hypothesised that CSCs overexpressing ABCB1 were able to survive after treatment, since these cells acquired genetic mutation(s) possibly resulting in alteration of drug binding sites or they developed other drug resistance mechanisms to protect themselves. Hence, CSCs containing other drug resistance mechanism(s) also survived. This second type of CSC reinitiated a cell population consisting of mutated CSCs overexpressing ABCB1 and progenitor cells (Figure 8.3, d). The results obtained in this study were consistent with pathway d. Due to further genetic mutations occurring after multiple rounds of drug treatment in CSCs overexpressing ABCB1, they were not be affected with drug treatment. This might indicate that surviving resistant CSCs will acquire more genetic aberrations or mutations after multiple rounds of drug treatment resulting in the generation of more aggressive and highly drug resistant tumours.

In our cell lines, it is proposed that mutated CSCs overexpressing ABCB1 were able to survive after drug treatment co-application with ABCB1 inhibitor as shown in Figure 8.3, c. Normally, the DNA-mismatch repair (MMR) process functions to detect DNA damage that has occurred in cells and damaged DNA will be repaired if the damage is not too serious. When DNA damage reaches a certain threshold, which is over the limitation of MMR to repair, the excess damaged

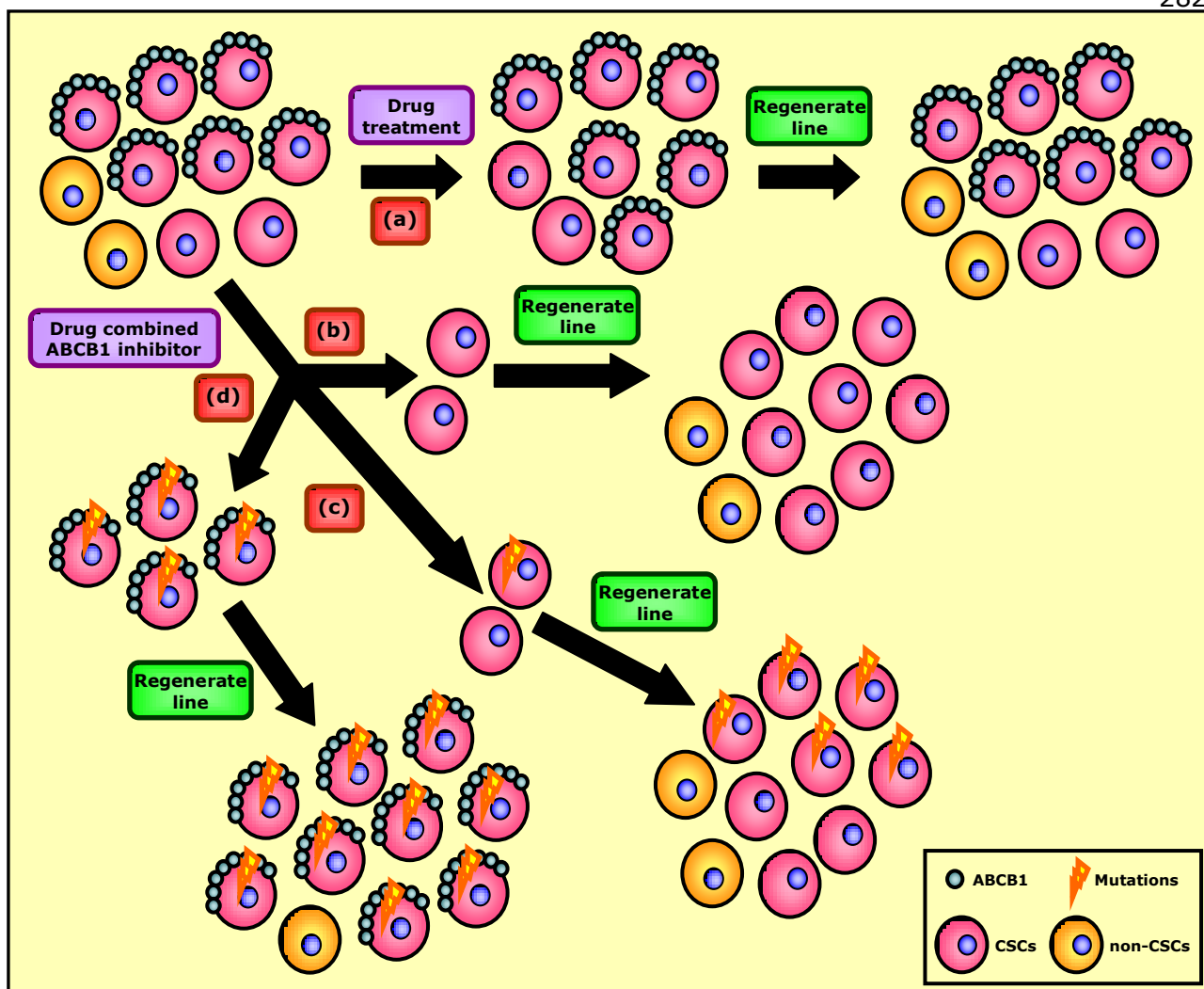


**Figure 8.3 Treatment included mutations in surviving cells.** Cancer cells treated with multiple rounds of drug comprise 3 different subpopulation; CSCs, CSCs overexpressing ABCB1 and non-CSCs. Some possible subpopulations resulting after single drug treatment or drug combined with Verapamil treatment are demonstrated. It is proposed that single drug treatment at the  $IC_{70}$  only destroyed non-CSCs whilst CSCs and CSCs expressing ABCB1 survived and regenerated the line (a). At least 3 possibilities are postulated here after drug combined Verapamil treatment. In (b), CSCs with other drug resistance mechanism survived and regenerated the cell population. In (c), CSCs applied an undefined survival mechanism but some CSCs acquired mutations and they initiate mutated CSCs, CSCs and progenitor cells (c). The last possibility shows that CSCs expressing ABCB1 acquired further mutation allowing them to survive and regenerate a heterogeneous cell population (d). This latter mechanism is most consistent with our findings.

DNA causes the cell to undergo programmed cell death. However, some resistant cells may have impaired MMR resulting in damaged DNA remaining undetected. For example resistant cells having impaired MMR are resistant to temozolomide treatment. Temozolomide transfers a methyl group to DNA at  $N^7$  position of guanine, which is the most common site, followed by  $O^3$  position of adenine and  $O^6$  position of guanine [Denny, B. J. *et al* (1994)]. However, cells with impaired MMR cannot recognise damaged DNA resulting in cells with damaged DNA being able resist to methylation and the cytotoxic effects of temozolomide [Liu, L. *et al* (1996)]. A similar phenomenon might occur in CSCs overexpressing ABCB1 surviving after etoposide or irinotecan combined verapamil treatment. DNA might have some degree of damage in these cells but due to depletion of MMR, CSCs overexpressing ABCB1 having damaged DNA could not be recognised and these cells could survive resulting in generating more aberrant cells (Figure 8.3, d). Some studies have supported the fact that drug resistance to etoposide [Aebi, S. *et al* (1996)] and cisplatin [Lage, H. *et al* (1999)] can result from depletion of MMR. Therefore, drug resistance in CSCs overexpressing ABCB1 might be similar to the mechanism of drug resistance to temozolomide.

In summary, the parental cell lines had intrinsic drug resistance via a low level of endogenous functional ABCB1. A basic level of drug resistance may also have been provided by elevated DNA repair and quiescence in CSCs. However, functional ABCB1 in CSCs is the main drug resistance mechanism in our cell lines. Many rounds of drug treatment selected cancer stem-like cells overexpressing functional ABCB1 and cancer stem-like cells expressing ABCC1 were also ultimately upregulated after serial drug treatment. There is also evidence for selection of another protective mechanism after prolonged treatment. Based on the data presented here it is therefore important to include ABCB1 inhibitors at the start of chemotherapy and to investigate other potential survival mechanisms. Other mechanisms correlating to drug resistance in cancer cells include intracellular alteration or mutation changing drug targets, binding sites and increase detoxification mechanism such as increase level of glutathione ( $\gamma$ -glutamylcysteinylglycine, GSH) and depletion of DNA-mismatch repair.

## Future studies

- **Animal models:** Drug combined with Verapamil treatment can be attempted to treat brain tumour xenografts in animal models. For future study, an immunodeficient mouse might be orthotopically transplanted with our cell lines into mouse brain leading to brain tumour development. Immunofluorescence analysis on xenografted tumours can be used to investigate the expression of stem cell markers and ABC transporters. Mice can then be intravenously treated with Verapamil to inhibit ABCB1 function following by chemotherapeutic agents or drug/Verapamil alone. The appropriate dose of Verapamil and drugs might be derived from the concentrations used *in vitro* treatment from this thesis or from other *in vivo* studies. To determine the efficacy of treatment, size of tumour can be measured, as will the level of drug in brain, liver, kidney and plasma to evaluate the distribution of drug. There is a study using novel compound of ABCB1 inhibitor (FG020318) combined with chemotherapeutic drugs to reverse ABCB1 function *in vitro* and *in vivo*. The ability of FG020318 in ABCB1 reversal was determined by MTT assay and flow cytometry. They found that FG020318 significantly increased chemosensitivity of MCF-7/adr cells and KBv200 cells [Chen, L. M. *et al* (2004)].

- **Using the third generation ABCB1 inhibitor:** Elacridar and tariquidar are the third generation ABCB1 inhibitor. These two drugs should be used to inhibit ABCB1 in treatment combining with chemotherapeutic agents. Elacridar and tariquidar can be tested both *in vitro* similar to our studies when using Verapamil as ABCB1 inhibitor and *in vivo* as mentioned earlier. For *in vitro* studies, clonogenic assay might be performed to investigate colony survival after treatment, flow cytometry can determine function of the inhibitor and immunofluorescence/Western blotting analysis or flow cytometry can examine any alteration of stem cell markers and ABC transporters. In preliminary experiments of our study performed using elacridar combined with etoposide or irinotecan treatment in our cell lines, cancer cells were effectively killed, however, a small proportion of cells still survived after combine treatment.

- **Investigation of other drug resistance mechanisms:** There are many drug resistance mechanisms in cancer cells. Other ABC transporters (ABCC1 and ABCG2) might be investigated functionally by flow cytometry in our cell lines, although the expression is low or absent as detected by immunofluorescence analysis due to the sensitivity of this technique. For future study, flow cytometry might be performed to investigate function of ABCC1 (Calcein as substrate and biricodar or cyclosporine A as inhibitor) and ABCG2 (BODIPY-prazosin or Hoechst 33342 as substrate and fumitremorgin as inhibitor). The level of glutathione (GSH) should be determined in our cells since increasing GSH can lead to increase drug detoxification. DNA mismatch repair (MMR) system might also be the resistance mechanism in our cell lines therefore mapping gene associating to human MMR system might be investigated in our cell lines such as *hMSH2* [Reenan, R. A. G. and Kolodner, R. D. (1992), *hMLH1* [Bronner, C. E. *et al* (1994), *hPMS2* [Nicolaidis, N. C. *et al* (1994)], *hMSH3* [Fujii, H. and Shimada, T. (1989)] and *hMSH6* [Papadopoulos, N. *et al* (1995)]. Other DNA repair mechanisms should also be investigated.

- **Using shRNA to knockdown ABCB1:** shRNA has also been found to reduce ABCB1 mRNA expression resulting in inhibition of ABCB1 function [Yagüe, E. *et al* (2004)]. SiRNA knockdown of ABCB1 was unsuccessful. Therefore, shRNA, which is more stable than SiRNA, should be optimised in our cell lines for future study. Real time PCR should be used to determine the degree of ABCB1 knockdown, since only a proportion of cells will be affected so a more sensitive assay is required.

- **More samples should be included:** To make a stronger conclusion, more brain tumour cell lines should be included.

- **Different time points of treatment:** *In vitro* and *in vivo* treatment might be attempted in our cell lines for future study to prove that using specific ABCB1 inhibitor combined with drug treatment at an early stage provides an advantage over inhibition after many rounds of treatment. *In vitro* study, cell viability analysis might be compared at



different time points after cells are serially treated with drug combined specific ABCB1 inhibitor. *In vivo* study, cell lines might be transplanted into brain of immunodeficient mouse to generate tumours. Mouse can be intravenously treated with drug combined specific ABCB1 inhibitor then biomarker will be determined by magnetic resonance spectroscopy (MRS) to examine treatment response [Mirbahai, L. *et al* (2010)].

## References

- Abe, T. et al (1994) Possible involvement of multidrug-resistance-associated protein (MDR) gene expression in spontaneous drug resistance to vincristine, etoposide and adriamycin in human glioma cells. *International Journal of Cancer* 1994; 58(6): 860-864
- Abolhoda, A. et al (1999) Rapid activation of MDR1 gene expression in human metastatic sarcoma after in vivo exposure to doxorubicin. *Clinical Cancer Research* 1999; 5: 3352-3356
- Aebi, S. et al (1996) Loss of DNA mismatch repair in acquired resistance to cisplatin. *Cancer Research* 1996; 56: 3087-3090
- Aganamol, D. P. and Malone, J. M. (1995) Chromosomal abnormalities in 47 paediatric brain tumours. *Cancer Genetics and Cytogenetics* 1995; 81: 125-134
- Alam, S. et al (2004) Cell cycle kinetics of expanding populations of neural stem and progenitor cells in vitro. *Biotechnology and Bioengineering* 2004; 88(3): 332-347
- Albright, A.L. (1993) Pediatric brain tumors. *A Cancer Journal for Clinicians* 1993; 43: 272-288
- Al-Hajj, M. et al (2003) Prospective identification of tumorigenic breast cancer cells. *PNAS* 2003; 100(7): 3983-3988
- Al-Hajj, M. et al. (2004) Therapeutic implications of cancer stem cells. *Current Opinion in Genetics & Development* 14 : 43-47
- Allikmets, R. et al (1998) A human placenta-specific ATP-binding cassette gene (ABCP) on chromosome 4q22 that is involved in multidrug resistance. *Cancer Research* 1998; 58: 5337-5339
- Allsopp, R. C. et al (1995) Telomere shortening is associated with cell division in vitro and in vivo. *Experimental Cell Research* 1995; 220: 194-200
- Ambudkar, S. V. et al (1999) Biochemical, cellular and pharmacological aspects of the multidrug transporter. *Annual Review of Pharmacology and Toxicology* 1999; 39: 361-398
- Anderle, P. et al (1998) P-glycoprotein (P-gp) mediated efflux in Caco-2 cell monolayers: The influence of culturing conditions and drug exposure on P-gp expression levels. *Journal of Pharmaceutical Sciences* 1998; 87(6): 757-762
- Andrews, P. A. et al (1985) Differential potentiation of alkylating and platinating agent cytotoxicity in human ovarian carcinoma cells by glutathione depletion. *Cancer Research* 1985; 45: 6250-6253
- Arai, F. et al (2004) Tie2/Angiopoietin-1 signaling regulates hematopoietic stem cell quiescence in the bone marrow niche. *Cell* 2004; 118: 149-161
- Arceci, R. J. et al (1993) Monoclonal antibody to an external epitope of the human mdr1 P-glycoprotein. *Cancer Research* 1993; 53: 310 - 317
- Avendano, C. and Menendez, J. C. (2002) Inhibitors of multidrug resistance to antitumor agents (MDR). *Current Medicinal Chemistry* 2002; 9(2): 159-193
- Avilion, A. A. et al (2003) Multipotent cell lineages in early mouse development depend on SOX2 function. *Genes & Development* 2003; 17: 126-140
- Baer, K. et al (2007) Sox-2 is expressed by glial and progenitor cells and Pax-6 is expressed by neuroblasts in the human subventricular zone. *Experimental Neurology* 2007; 204: 828-831
- Baersch, G. et al (1999) Expression of AC133 and CD117 on candidate normal stem cells populations in childhood B-cell precursor acute lymphoblastic leukaemia. *British Journal of Haematology* 1999; 107: 572-580
- Bakos, É. et al (1996) Membrane topology and glycosylation of the human multidrug resistance-associated protein. *The Journal of Biological Chemistry* 1996; 271(21): 12322-12326

- Baldwin, R.T. and Martin, S.P. (2004) Epidemiology of brain tumors in childhood-a review. *Toxicology and Applied Pharmacology* (2004); 199: 118-131
- Bannykh, S. I. et al (2006) Oligodendroglial-specific transcriptional factor SOX10 is ubiquitously expressed in human gliomas. *Journal of Neuro-Oncology* 2006; 75: 115-127
- Bao, S. et al (2006) Glioma stem cells promote radioresistance by preferential activation of the DNA damage response. *Nature* 2006; 444: 756-760
- Barry, M. A. et al (1990) Activation of programmed cell death (apoptosis) by cisplatin, other anticancer drugs, toxins and hyperthermia. *Biochemical Pharmacology* 1990; 40: 2353-2362
- Bates, S.E. et al. (1996) Clinical reversal of multidrug resistance. *Stem Cells* 14 : 56-63
- Baugh, C. M. et al (1973) Polyglutamylation metabolites of methotrexate. *Biochemical and Biophysical Research Communications* 1973; 52(1): 27-34
- Bayer, M. et al (2005) Identification and characterization of Iporin as a novel interaction partner for rab I. *BMC Cell Biology* 2005; 6(15): 1-15
- Beier, D. et al (2007) CD133(+) and CD133(-) glioblastoma-derived cancer stem cells show differential growth characteristics and molecular profiles. *Cancer Research* 2007; 67: 4010-4015
- Belpomme, D. et al (2000) Verapamil increases the survival of patients with anthracycline-resistant metastatic breast carcinoma. *Annals of Oncology* 2000; 11: 1471-1476
- Benderra, Z. et al (2004) Breast cancer resistance protein and P-glycoprotein in 149 adult acute myeloid leukemias. *Clinical Cancer Research* 2004; 10: 7896-7902
- Bernal, S. D. et al (1990) Reduced membrane protein associated with resistance of human squamous carcinoma cells to methotrexate and cis-platinum. *Molecular and Cellular Biochemistry* 1990; 95(1): 61-70
- Berridge, M. V. et al (1996) The biochemical and cellular basis of cell proliferation assays that use tetrazolium salts. *Biochemica* 1996; 4: 15-20
- Bez, A. et al (2003) Neurosphere and neurosphere-forming cells: morphological and ultrastructural characterization. *Brain Research* 2003; 993: 18-29
- Bhattacharjee, M. B. et al (1997) Cytogenetic analysis of 120 primary paediatric brain tumours and literature review. *Cancer Genetics and Cytogenetics* 1997; 97: 39-53
- Birch, B. D. et al (1996) Frequent type 2 neurofibromatosis gene transcript mutations in sporadic intramedullary spinal cord ependymomas. *Neurosurgery* 1996; 39: 135-140
- Blinks, S. P. and Dobrota, M. (1990) Kinetics and mechanism of uptake of platinum-based pharmaceuticals by the rat small intestine. *Biochemical Pharmacology* 1990; 40(6): 1329-1336
- Blumcke, I. et al (2001) Distinct expression pattern of microtubule-associated protein-2 in human oligodendrogliomas and glial precursor cells. *Journal of Neuropathology Experimental Neurology* 2001; 60: 984-993
- Bonnet, D. and Dick, J. E. (1997) Human acute myeloid leukemia is organized as a hierarchy that originates from a primitive hematopoietic cell. *Nature Medicine* 1997; 3(7): 730-737
- Bredel, M. (2001) Anticancer drug resistance in primary human brain tumors. *Brain Research Reviews* 2001; 35: 161-204
- Bromberge, K. D. et al (2003) A two-drug model for etoposide action against human topoisomerase II. *The Journal of Biological Chemistry* 2003; 278(9): 7406-7412
- Bryan, T. M. and Cech, T. R. (1999) Telomerase and the maintenance of chromosome ends. *Current Opinion in Cell Biology* 1999; 11: 318-324

- Bryan, T. M. et al (1995) Telomere elongation in immortal human cells without detectable telomerase activity. *European Molecular Biology Organisation Journal* 1995; 14: 4240-4248
- Bryan, T. M. et al (1998) Telomere length dynamics in telomerase-positive immortal human populations. *Experimental Cell Research* 1998; 239: 370-378
- Bugg, B. Y. et al (1991) Expression of a mutant DNA topoisomerase II in CCRF-CEM human leukemic cells selected for resistance to teniposide. *Proceeding of the National Academy of Sciences USA* 1991; 88: 7654-7658
- Bunting, K. D. (2002) ABC transporters as phenotypic markers and functional regulators of stem cells. *Stem Cells* 2002; 20: 11-20
- Burger, J. M. et al (1996) Structure and mechanism of DNA topoisomerase II. *Nature* 1996; 379: 225-232
- Burger, P. C. et al (1987) Patient age histologic features, and length of survival in patients with glioblastoma multiforme. *Cancer* 1987; 59: 1617-1625
- Calabrese, C. et al (2007) A perivascular Niche for Brain tumor stem cells. *Cancer Cell* 2007; 11: 69-82
- Calatozzolo, C. et al (2005) Expression of drug resistance proteins P-gp, MRP1, MRP3, MRP5 and GST- $\Pi$  in human glioma. *Journal of Neuro-Oncology* 2005; 74: 113-121
- Cepeda, V. et al (2007) Biochemical mechanisms of Cisplatin cytotoxicity. *Anti-Cancer Agents in Medicinal Chemistry* 2007; 7: 3-18
- Chabner, B. A. et al (1985) Polyglutamation of Methotrexate. *The Journal of Clinical Investigation* 1985; 76: 907-912
- Chang, Q. et al (2005) Promoter hypermethylation profile of RASSF1A, FHIT, and sFRP1 in intracranial primitive neuroectodermal tumours. *Human Pathology* 2005; 36: 1265-1272
- Chaudhary, P. M. and Roninson, I. B. (1991) Expression and activity of P-glycoprotein, a multidrug efflux pump, in human hematopoietic stem cells. *Cell* 1991; 66: 85-94
- Chen, A. Y. and Liu, L. F. (1994) DNA topoisomerase: essential enzymes and lethal targets. *Annual Review of Pharmacology and Toxicology* 1994; 34: 191-218
- Chen, L. et al (2007) Precancerous stem cells have the potential for both benign and malignant differentiation. *PLoS ONE* 2007; 3(e293): 1-16
- Chen, Y. N. et al (1990) Characterization of adriamycin-resistant human breast cancer cells which display overexpression of a novel resistance-related membrane protein. *The Journal of Biological Chemistry* 1990; 265(17): 10073-10080
- Chen, L. M. et al (2004) Reversal of P-gp mediated multidrug resistance in-vitro and in-vivo by FG020318. *The Journal of Pharmacy and Pharmacology* 2004; 56(8): 1061-1066
- Chu, G. (1994) Cellular response to cisplatin. *The Journal of Biological Chemistry* 1994; 269(2): 787-790
- Chu, X. Y. et al (1999) Active efflux of CPT-11 and its metabolites in human KB-derived cell lines. *Journal of Pharmacology and Experimental Therapeutics* 1999; 288: 735-741
- Clark, R. et al (2006) Multiple drugbinding sites on the R482G isoform of the ABCG2 transporter. *British Journal of Pharmacology* 2006; 149: 506-515
- Clément, V. et al (2009) Limits of CD133 as a marker of glioma self-renewing cells. *International Journal of Cancer* 2009; 125: 244-248
- Cole, S. P. C. et al (1992) Overexpression of a transporter gene in a multidrug-resistant human lung cancer cell line. *Science* 1992; 258: 1650-1654

- Collins, A. T. et al (2001) Identification and isolation of human prostate epithelial stem cells based on  $\alpha 2\beta 1$ -integrin expression. *Journal of Cell Science* 2001; 114: 3865-3872
- Corbeil, D. et al (2000) The human AC133 hematopoietic stem cell antigen is also expressed in epithelial cells and targeted to plasma membrane protrusions. *The Journal of Biological Chemistry* 2000; 275(8): 5512-5520
- Corbeil, D. et al (2001) Prominin: A story of cholesterol, plasma membrane protrusions and human pathology. *Traffic* 2001; 2: 82-91
- Cordon-Cardo, C. et al (1990) Expression of the multidrug resistance gene product (P-glycoprotein) in human normal and tumor tissues. *The Journal of Histochemistry and Cytochemistry* 1990; 39(9): 1277-1287
- Corver, W. E. et al (1995) Limited loss of nine tumor-associated surface antigenic determinants after tryptic cell dissociation. *Cytometry* 1995; 19: 267-272
- Cotsarelis, G. et al (1990) Label-retaining cells reside in the bulge area of pilosebaceous unit: implications for follicular stem cells, hair cycle, and skin carcinogenesis. *Cell* 1990; 61: 1329-1337
- Cristofari, G. and Lingner, J. (2006) Telomere length homeostasis requires that telomerase levels are limiting. *European Molecular Biology Organization* 2006; 5(3): 565-574
- Daadi, M. M. et al (2008) Adherent self-renewable human embryonic stem cell derived neural stem cell lines: Functional engraftment in experimental stroke model. *PLoS ONE* 2008; 3(2): 1-9
- Dabholkar, M. et al (1992) Determinants of cisplatin sensitivity in non-malignant non-drug-selected human T cell lines. *Mutation Research/DNA Repair* 1992; 274(1): 45-56
- Dahmane, N. and Altaba, A. R. (1999) Sonic hedgehog regulates the growth and patterning of the cerebellum. *Development* 1999; 126: 3089-3100
- Dean, M. et al (2001) The human ATP-binding cassette (ABC) transporter superfamily. *Genome Research* 2001; 11: 1156-1166
- Dean, M. et al (2005) Tumour stem cells and drug resistance. *Nature Reviews* 2005; 5: 275-284
- Dehghani, F. et al (1998) Prognostic implication of histopathological, immunohistochemical and clinical features of oligodendrogliomas: a study of 89 cases. *Acta Neuropathologica* 1998; 95: 493-504
- Denny, B. J. et al (1994) NMR and molecular modelling investigation of the mechanism of activation of the antitumor drug temozolomide and its interaction with DNA. *Biochemistry* 1994; 33: 9045-9051
- Didiano, D. et al (2004) Telomere maintenance in childhood primitive neuroectodermal brain tumours. *Neuro-Oncology* 2004; 1-8
- Dirks, P. B. et al (1996) Supratentorial primitive neuroectodermal tumours in children. *Journal of Neuro-Oncology* 1996; 29: 75-84
- Doyle, L. A. et al (1998) A multidrug resistance transporter from human MCF-7 breast cancer cells. *PNAS* 1998; 95(26): 15665-15670
- Duncan, J. A. and Hoffman, H. J. (1995) Intracranial ependymomas. In Kaye, A. H. and Lows, E. R. (eds.) (1995) *Brain Tumours* Churchill Livingstone: Edinburgh; 493-504
- Eastman, A. and Schulte, N. (1988) Enhanced DNA repair as a mechanism of resistance to cis-diamminedichloroplatinum(II). *Biochemistry* 1988; 27(13): 4730-4734
- Ebert, C. et al (1999) Molecular genetic analysis of ependymal tumours: NF2 mutations and chromosome 22q loss occur preferentially in intramedullary spinal ependymomas. *The American Journal of Pathology* 1999; 155: 627-632
- Eckford, P. D. W. and Sharom, F. J. (2009) ABC efflux pump-based resistance to chemotherapy drugs. *Chemistry Reviews* 2009; 109: 2989-3011

- Edwards, J. E. et al (2002) GF120918, a P-glycoprotein modulator, increases the concentration of unbound amprenavir in the central nervous system in rats. *Antimicrobial Agents and Chemotherapy* 2002; 46(7): 2284-2286
- Ellison, D. (2002) Review: Classifying the medulloblastoma: insights from morphology and molecular genetics. *Neuropathology and Neurobiology* 2002; 28: 257-282
- Ernestus, R. I. et al (1996) Prognostic relevance of localization and grading in intracranial ependymoma of childhood. *Child's Nervous System* 1996; 12: 522-526
- Endicott, J. and Ling, V. (1989) The biochemistry of p-glycoprotein mediated multidrug resistance. *Annual Reviews of Biochemistry* 1989; 58: 137-171
- Episkopou, V. (2005) SOX2 functions in adult neural stem cells. *TRENDS in Neurosciences* 2005; 28(5): 219-221
- Ermakova, S. P. et al (2006) (-)-Epigallocatechin gallate overcomes resistance to etoposide-induced cell death by targeting the molecular chaperone glucose-regulated protein 78. *Cancer Research* 2006; 66: 9260-9269
- Eytan, G. D. et al (1997) Efficiency of P-glycoprotein-mediated exclusion of rhodamine dyes from multidrug-resistant cells is determined by their passive transmembrane movement rate. *European Journal of Biochemistry* 1997; 248: 104-112
- Fael Al-Mayhany, T. M. et al (2009) An efficient method for derivation and propagation of glioblastoma cell lines that conserves the molecular profile of their original tumours. *Journal of Neuroscience Methods* 2009; 176: 192-199
- Farber, S. et al (1974) Temporary remissions in acute leukemia in children produced by folic acid antagonist...Aminopterin. *Cancer Journal for Clinicians* 1974; 24: 297-305
- Farr-Jones, M. A. et al (1999) Improved technique for establishing short term human brain tumor cultures. *Journal of Neuro-Oncology* 1999; 43: 1-10
- Fellner, S. et al (2002) Transport of paclitaxel (Taxol) across the blood-brain barrier in vitro and in vivo. *Journal of Clinical Investigation* 2002; 110(9): 1309-1318
- Ferri, A. L. M. et al (2004) SOX2 deficiency neurodegeneration and impaired neurogenesis in the adult mouse brain. *Development* 2004; 131(15): 3805-3819
- Fire, A. et al (1998) Potent and specific genetic interference by double-stranded RNA in *Caenorhabditis elegans*. *Nature* 1998; 391(6669): 806-811
- Fisher, P.G. (2004) 'Chapter5: Embryonal tumors'. In Gupta, N. (eds) (2004) *Pediatric CNS Tumors*. Berlin: Springer-Verlag Berlin Heidelberg 83-105
- Flens, M. J. et al (1996) Tissue distribution of the multidrug resistance protein. *American Journal of Pathology* 1996; 148(4): 1237-1247
- Florek, M. et al (2005) Prominin-1/CD133, a neural and hematopoietic stem cell marker, is expressed in adult human differentiated cells and certain types of kidney cancer. *Cell Tissue Research* 2005; 319: 15-26
- Fojo, A. T. et al (1987) Expression of a multidrug-resistance gene in human tumors and tissues. *PNAS* 1987; 84: 265-269
- Fong, H. et al (2008) Regulation of self-renewal and pluripotency by SOX2 in human embryonic stem cells. *Stem Cells* 2008; 26: 1931-1938
- Fontaine, M. et al (1996) Use of rhodamine 123 to examine the functional activity of P-glycoprotein in primary cultured brain microvessel endothelial cell monolayers. *Life Sciences* 1996; 59(18): 1521-1531

- Franken, N. A. P. et al (2006) Clonogenic assay of cells in vitro. *Nature Protocols* 2006; 1(5): 2315-2319
- Fukasawa, K. et al (1997) Genomic instability and apoptosis are frequent in p53 deficient young mice. *Oncogene* 1997; 15: 1295-1302
- Fults, D. et al (1992) Establishment and characterisation of a human primitive neuroectodermal tumour cell line from the cerebral hemisphere. *Journal of neuropathology and Experimental neurology* 1992; 51(2): 272-280
- Galli, R. et al (2004) Isolation and characterization of tumorigenic, stem-like neural precursors from human glioblastoma. *Cancer Research* 2004; 64: 7011-7021
- Gangemi, R. M. R. et al (2009) SOX2 silencing in glioblastoma tumor-initiating cells causes stop of proliferation and loss of tumourigenicity. *Stem Cells* 2009; 27: 40-48
- Gellert, M. et al (1976) An enzyme that introduces superhelical turns into DNA. *Proceedings of the National Academy of Sciences USA* 1976; 73: 3872-387
- Genestier, L. et al (1998) Immunosuppressive properties of Methotrexate: Apoptosis and clonal deletion of activated peripheral T cells. *Journal of Clinical Investigation* 1998; 102(2): 322 - 328
- Germann, U. A. et al (1997) Chemosensitization and drug accumulation effects of VX-710, Verapamil, cyclosporine A, MS-209 and GF120918 in multidrug resistant HL60/ADR cells expressing the multidrug resistance-associated protein MRP. *Anti-Cancer Drugs* 1997; 8: 141-155
- Geyer, J. R. et al (2005) Multiagent chemotherapy and deferred radiotherapy in infants with malignant brain tumours: a report from the Children's Cancer Group. *Journal of Clinical Oncology* 2005; 23(30): 7621-7631
- Giangaspero, F. and Wiestler, O.D. (2004) 'Chapter5: Pathology and molecular classification'. In Walker, D.A. (eds) (2004) *Brain and Spinal Tumors of Childhood*. London: A Hodder Arnold Publication 80-91
- Giangaspero, F. et al. (2007) 'Chapter 8: Embryonal tumours'. In Louis, D.N. (eds) *WHO Classification of Tumours of the Central Nervous System*. Lyon: World Health Organization 131-149
- Gifford, A. J. et al (1998) P-glycoprotein-mediated methotrexate resistance in CCRF-CEM sublines deficient in methotrexate accumulation due to a point mutation in the reduced folate carrier gene. *International Journal of Cancer* 1998; 78: 176-181
- Giovanella, B. C. et al (1989) DNA topoisomerase I-targeted chemotherapy of human colon cancer in xenografts. *Science* 1989; 246: 1046-1048
- Goldie, J.H. (2001) Drug resistance in cancer: A perspective. *Cancer and Metastasis Reviews* 20: 63-68
- Gomez-Manzano, C. et al (2006) Delta-24 increases the expression and activity of topoisomerase I and enhances the antglioma effect of irinotecan. *Clinical Cancer Research* 2006; 12(2): 556-562
- Gottesman, M. M. (2002) Mechanisms of cancer drug resistance. *Annual Review of Medicine* 2002; 53: 615-627
- Gottesman, M. M. et al (2002) Multidrug resistance in cancer: Role of ATP-dependent transporters. *Nature Reviews* 2002; 2: 48-58
- Gottestman, M. M. and Ambudkar, S. V. (2001) Overview: ABC transporters and human disease. *Journal of Bioenergetics and Biomembranes* 2001; 33(6): 453-458
- Graham, V. et al (2003) SOX-2 functions to maintain neural progenitor identity. *Neuron* 2003; 39: 749-765
- Greenberg, H.S. et al. (1999) 'Chapter1: Brain tumor classification, grading, and epidemiology'. *Brain Tumors*. New York: Oxford University Press 1-26

- Griffin, C. A. et al (1988) Chromosome abnormalities in paediatric brain tumours. *Cancer Research* 1988; 48: 175-180
- Grossman, S. A. et al (2003) Phase III study comparing three cycles of infusional carmustine and cisplatin followed by radiation therapy with radiation therapy and concurrent carmustine in patients with newly diagnosed supratentorial glioblastoma multiforme: Eastern cooperative oncology group trial 2394. *Journal of Clinical Oncology* 2003; 21(8): 1485-1491
- Grotzer, M. A. et al (2001) MYC messenger RNA expression predicts survival outcome in childhood primitive neuroectodermal tumor/medulloblastoma. *Clinical Cancer Research* 2001; 7: 2425-2433
- Grundy, R. G. et al (2007) Primary postoperative chemotherapy without radiotherapy for intracranial ependymoma in children: the UKCCSG/SIOP prospective study. *Lancet Oncology* 2007; 8: 696-705
- Günther, H. S. et al (2008) Glioblastoma-derived stem cell-enriched cultures form distinct subgroups according to molecular and phenotypic criteria. *Oncogenes* 2008; 1;27(20): 2897-2909
- Guo, W. et al (2006) Cancer stem cells. *Paediatric Research* 2006; 59: 59R-64R
- Gupta, E. et al (1997) Modulation of glucuronidation of SN-38, the active metabolite of irinotecan by valproic acid and Phenobarbital. *Cancer Chemotherapy and Pharmacology* 1997; 39: 440-444
- Gupta, N. et al. (2004) 'Introduction'. in Gupta, N. (eds) (2004) *Pediatric CNS Tumors*. Berlin: Springer-Verlag Berlin Heidelberg 1-6
- Hadnagy, A. et al (2006) SP analysis may be used to identify cancer stem cell populations. *Experimental Cell Research* 2006; 312: 3701-3710
- Hakin-Smith, V. et al (2003) Alternative lengthening of telomeres and survival in patients with glioblastoma multiforme. *The Lancet* 361: 836-838
- Hamilton, R. L. and Pollack, I. F. (1997) The molecular biology of ependymomas. *Brian Pathology* 1997; 7: 807-822
- Hande, K. R. (1998) Etoposide: Four decades of development of a topoisomerase II inhibitor. *European Journal of Cancer* 1998; 34(10): 1514-1521
- Handgretinger, R. et al (2003) Biology and plasticity of CD133+ hematopoietic stem cells. *Annals New York Academy of Sciences* 2003; 996: 141-151
- Hansford, L. M. et al (2007) Neuroblastoma cells isolated from bone marrow metastases contain a naturally enriched tumor-initiating cell. *Cancer Research* 2007; 67(23): 11234-1124
- Hao, H. N. et al (2003) Fetal human hematopoietic stem cells can differentiate sequentially into neural stem cells and then astrocytes in vitro. *Journal of Hematotherapy Stem Cell Research* 2003; 12: 23-32
- Hara, M. et al (2001) Noninvasive detachment of cells on cells. *Materials Science and Engineering* 2001; 17: 107-112
- Harley, C. B. and Futcher, A. B. (1990) Telomeres shorten during ageing of human fibroblasts. *Nature* 1990; 345: 458-460
- Hart, M. N. et al (1973) Primitive neuroectodermal tumors of the brain in children. *Cancer* 1973; 32(4): 890-897
- Heegaard, S. et al (1995) Proliferating cell nuclear antigen and Ki-67 immunohistochemistry of oligodendrogliomas with special reference to prognosis. *Cancer* 1995; 76: 1809-1813
- Hemann, M. T. et al (2001) The shortest telomere, not average telomere length, is critical for cell viability and chromosome stability. *Cell* 2001; 107: 67-77
- Hemmati, H. D. et al (2003) Cancerous stem cells can arise from pediatric brain tumors. *PNAS* 2003; 100(25): 15178-15183



- Hemminki, K. et al (2003) Cancers in the first-degree relatives of children with brain tumours. *The British Journal of Cancer* 2003; 83: 407-411
- Henson, J. D. et al (2002) Alternative lengthening of telomeres in mammalian cells. *Oncogene* 2002; 21: 598-610
- Higgins, C. F. and Gottesman, M. M. (1992) Is the multidrug transporter a flippase? *Trends in Biochemical Sciences* 1992; 17(1): 18-21
- Hiraga, S. et al (1998) Telomerase activity and alterations in telomere length in human brain tumours. *Cancer Research* 1998; 58: 2217-2125
- Hiyama, E. et al (1995) Telomerase activity in gastric cancer. *Cancer Research* 1995; 55: 3258-3262
- Holzer, A. K. et al (2004) The Copper influx transporter human copper transport protein 1 regulates the uptake of cisplatin in human ovarian carcinoma cells. *Molecular Pharmacology* 2004; 66(4): 817-823
- Homolya, L. et al (1993) Fluorescent cellular indicators are extruded by the multidrug resistance protein. *The Journal of Biological Chemistry* 1993; 268(29): 21493-21496
- Honde, K. R. (1998) Etoposide: Four decades of development of a topoisomerase II inhibitor. *European Journal of Cancer* 1998; 34(10): 1514-1521
- Hooijberg, J. H. et al (1999) Antifolate resistance mediated by the multidrug resistance proteins MRP1 and MRP2. *Cancer Research* 1999; 59: 2532-2535
- Hoon, P. J. et al (2008) Sox2 expression in brain tumors: A reflection of the neuroglial differentiation pathway. *The American Journal Surgical Pathology* 2008; 32(1); Abstract
- Horn, B. et al (1999) A multi-institutional retrospective study of intracranial ependymoma in children: identification of risk factors. *Journal of Pediatric Hematology/Oncology* 1999; 21: 203-211
- Horn, B.N. and Smyth, M. (2004) 'Chapter4: Ependymoma'. In Gupta, N. (eds) (2004) *Pediatric CNS Tumors*. Berlin: Springer-Verlag Berlin Heidelberg 65-81
- Hromas, R. A. et al (1987) Glutathione depletion reverses cisplatin resistance in murine L1210 leukemia cells. *Cancer Letter* 1987; 34(1): 9-13
- Hsiang, Y. H. et al (1989) DNA topoisomerase I-mediated DNA cleavage and cytotoxicity of camptothecin analogues. *Cancer Research* 1989; 49: 4385-4389
- Hsing, S. et al (1992) The function of Gp170, the multidrug-resistance gene product, in the brush border of rat intestinal mucosa. *Gastroenterology* 1992; 102(3): 879-885
- Huang, B. et al (2003) Human dpendymomas reveal frequent deletions on chromosome 6 and 9. *Acta Neuropathologica* 2003; 106: 357-362
- Huang, Y. and Sadee, W. (2006) Membrane transporters and channels in chemoresistance and -sensitivity of tumor cells. *Cancer Letters* 2006; 239; 168-182
- Hubensack, M. et al (2008) Effect of the ABCB1 modulators elacridar and tariquidar on the distribution of paclitaxel in nude mice. *Journal of Cancer Research and Clinical Oncology* 2008; 134: 597-607
- Huisman, M. T. et al (2003) Assessing safety and efficacy of directed P-glycoprotein inhibition to improve the pharmacokinetic properties of saquinavir coadministered with ritonavir. *The Journal of Pharmacology and Experimental Therapies* 2003; 304(2): 596-602
- Ignatova, T. N. (2002) Human cortical glial tumors contain neural stem-like cells expressing astroglial and neuronal markers in vitro. *GLIA* 2002; 39; 193-206
- Inagaki, A. et al (2007) Long-term maintenance of brain tumor stem cell properties under at non-adherent and adherent culture conditions. *Biochemical and Biophysical Research Communications* 2007; doi:10.1016/j.bbrc.2007.07.037

- Ishida, S. et al (2002) Uptake of the anticancer drug cisplatin mediated by the copper transporter Ctr1 in yeast and mammals. *Proceedings of National Academy of Sciences* 2002; 99(22): 14298-14302
- Iyer, L. et al (1998) Genetic predisposition to the metabolism of irinotecan (CPT-11). Role of uridine diphosphate glucuronosyltransferase isoform 1A1 in the glucuronidation of its active metabolite (SN-38) in human liver microsomes. *Journal of Clinical Investigation* 1998; 101: 847-854
- Jackson, R. C. et al (1976) Intrinsic resistance to methotrexate of cultured mammalian cells in relation to the inhibition kinetics of their dihydrofolate reductases. *Cancer Research* 1976; 36: 1991-1997
- Jacobs, S. A. et al (1975) Letter: Altered plasma pharmacokinetics of methotrexate administered intrathecally. *The Lancet* 1975; 1(7904): 465-466
- Jacobs, S. A. et al (1977) Accumulation of methotrexate diglutamate in human liver during methotrexate therapy. *Biochemical Pharmacology* 1977; 26: 2310-2313
- Jakacki, R. I. (2005) Treatment strategies for high-risk medulloblastoma and supratentorial primitive neuroectodermal tumours. *Journal of Neurosurgery* 2005; 102: 44-52
- Jaksch, M. et al (2008) Cell cycle dependent variation of a CD133 epitope in human embryonic stem cell, colon cancer and melanoma cell lines. *Cancer Research* 2008; 68(19): 7882-7886
- Jamieson, E. R. and Lippard, S. J. (1999) Structure, recognition, and processing of Cisplatin-DNA adducts. *Chemistry Review* 1999; 99: 2467-2498
- Jay, V. et al (2003) 'Chapter7: Tumours of the central nervous system and eye'. In Cullinane, C.J. (eds) (2003) *Molecular Biology and Pathology of Paediatric Cancer*. New York: Oxford University Press 136-154
- Jayawickreme, D. P. et al (1995) Intracranial ependymomas in childhood: a report of 24 cases followed for 5 years. *Child's Nervous System* 1995; 11: 409-413
- Jenkin, D. K. et al (1990) Posterior fossa medullo-blastoma in childhood: treatment results and a proposal for a new staging system. *International Journal of Radiation Oncology, Biology, Physics* 1990; 19: 265-274
- Jergil, B. and Ekblad, L. (2001) Plasma membranes: methods for preparation. *Encyclopedia of Life Sciences* 2001; 1-2
- Jetlitschky, G. et al (1996) Transport of glutathione, glucuronate and sulfate conjugates by the MRP gene-encoded conjugate export pump. *Cancer Research* 1996; 56: 988-994
- Ji, J. et al (2003) Enhanced gene silencing by the application of multiple specific small interfering RNAs. *Federation of European Biochemical Societies Letters* 2003; 552: 247-252
- Jia, J. et al (2002) Shaggy/GSK3 antagonizes Hedgehog signalling by regulating Cubitus interruptus. *Nature* 2002; 416: 548-552
- Joel, S. (1996) The clinical pharmacology of etoposide: an update. *Cancer Treatment Reviews* 1996; 22: 179-221
- Johansson, C. B. et al (1999) Identification of a neural stem cell in the adult mammalian central nervous system. *Cell* 1999; 96: 25-34
- Johnsen, J. I. et al (2009) Embryonal neural tumours and cell death. *Apoptosis* 2009; 14: 424-438
- Johnstone, A. P. and Thorpe, R. (1996) 'Chapter 1: Basic techniques' *Immunochemistry in Practice*. 3rd edition Oxford: Blackwell Sciences 1-34
- Jolivet, J. and Chabner, B. A. (1983) Intracellular pharmacokinetics of methotrexate polyglutamates in human breast cancer cells. Selective retention and less dissociable binding of 4-NH<sub>2</sub>-10-CH<sub>3</sub>-Pteroylglutamate<sub>4</sub> and 4-NH<sub>2</sub>-10-CH<sub>8</sub>-Pteroylglutamate<sub>5</sub> to dihydrofolate reductase. *The Journal of Clinical Investigation* 1983; 72: 773-778

- Jonker, J. W. et al (2002) The breast cancer resistance protein protects against a major chlorophyll-derived dietary phototoxin and protoporphyrin. *PNAS* 2002; 99(24): 15649-15654
- Juliano, R. L. and Ling, V. (1976) A surface glycoprotein modulating drug permeability in Chinese hamster ovary cell mutants. *Biochimica et Biophysica Acta (BBA) - Biomembranes* 1976; 455(1): 152-162
- Kadin, M. E. et al (1970) Neonatal cerebella medulloblastoma originating from the fetal external granular layer. *Journal of Neuropathology and Experimental Neurology* 1970; 29: 583-600
- Kania, G. et al (2005) Somatic stem cell marker prominin-1/CD133 is expressed in embryonic stem cell-derived progenitors. *Stem Cells* 2005; 23: 791-804
- Kawai, K. et al (1990) Identification of a membrane glycoprotein overexpressed in murine lymphoma sublines resistant to cis-diamminedichloroplatinum (II). *The Journal of Biological Chemistry* 1990; 265(22): 13137-13142
- Kawato, Y. et al (1991) Intracellular roles of SN-38, a metabolite of the camptothecin derivative CPT-11, in the antitumour effect of CPT-11. *Cancer Research* 1991; 51: 4187-4191
- Kleihues, P. et al (2000) World Health Organization Classification of Tumours of the Nervous System: *Pathology and Genetics*. 2000 Lyon: IARC Press
- Kleihues, P. et al. (2007) 'Chapter 1: Astrocytic tumours'. In Louis, D.N. (eds) *WHO Classification of Tumours of the Central Nervous System*. Lyon: World Health Organization 14-52
- Kleihues, P. et al. (2007) 'WHO grading of tumours of the central nervous system'. In Louis, D.N. (eds) *WHO Classification of Tumours of the Central Nervous System*. Lyon: World Health Organization 10-11
- Kline, N.E. and Sevier, N. (2003) Solid tumors in children. *Journal of Pediatric Nursing* 18(2): 96-102
- Koike, K. et al (1997) A canalicular multispecific organic anion transporter (cMOAT) antisense cDNA enhances drug sensitivity in human hepatic cancer cells. *Cancer Research* 1997; 57: 5475-5479
- Komuro, H. et al (2007) Identification of side population cells (stem-like cell population) in pediatric solid tumor cell lines. *Journal of Pediatric Surgery* 2007; 42: 2040-2045
- Korshunov, A. et al (2004) This histologic grade is a main prognostic factor for patients with intracranial ependymomas treated in the microneurosurgical era. *Cancer* 2004; 100: 1230-1237
- Kos, V. and Ford, R. C. (2009) The ATP-binding cassette family: a structural perspective. *Cellular Molecular Life Science* 2009; 66: 3111-3126
- Kros, J. M. et al (1994) Oligodendroglioma: the Rotterdam-Dijkzigt experience. *Neurosurgery* 1994; 34: 959-966
- Kühl, J. et al (1998) Pre-radiation chemotherapy of children and young adults with malignant brain tumours: results of the German pilot trial HIT '88/'89. *Klinische Pädiatrie* 1998; 210: 227-233
- Kühl, J. et al. (2004) 'Chapter16: Embryonic tumors'. In Walker, D.A. (eds) (2004) *Brain and Spinal Tumors of Childhood*. London: A Hodder Arnold Publication 314-330
- Kurt, E. et al (2006) Identification of relevant prognostic histopathologic features in 69 intracranial ependymomas, excluding myxopapillary ependymomas and subependymomas. *Cancer* 2006; 106: 388-395
- Lage, H. et al (1999) Expression of DNA repair proteins hMSH2, hMSH6, hMLH1, O6-methylguanine-DNA methyltransferase and N-methylpurine-DNA glycosylase in melanoma cells with acquired drug resistance. *International Journal of Cancer* 1999; 80: 744-750
- Langford, L. A. et al (1995) Telomerase activity in human brain tumours. *Lancet* 1995; 346: 1267-1268

- Langford, L. A. et al (1997) Telomerase activity in ordinary meningiomas predicts poor outcome. *Human Pathology* 1997; 28; 416-420
- Lapidot, T. et al (1994) A cell initiating human acute myeloid leukaemia after transplantation into SCID mice. *Nature* 1994; 367(6464): 645-648
- Lederman, S. et al (1992) Identification of a novel surface protein on activated CD4+ T cells that induces contact-dependent B cell differentiation (Help). *Journal of Experimental Medicine* 1992; 175; 1091-1101
- Lee, A. et al (2005) Isolation of neural stem cells from the postnatal cerebellum. *Nature Neuroscience* 2005; 8(6); 723-729
- Lee, J. et al (2006) Tumor stem cells derived from glioblastomas cultured in bFGF and EGF more closely mirror the phenotype and genotype of primary tumors than do serum-cultured cell lines. *Cancer Cell* 2006; 9: 391-403
- Lee, J. S. et al (1994) Rhodamine efflux patterns predict P-glycoprotein substrates in the national cancer institute drug screen. *Molecular Pharmacology* 1994; 46: 627-638
- Leemhuis, T. et al (1996) Isolation of primitive human bone marrow hematopoietic progenitor cells using Hoechst 33342 and Rhodamine 123. *Experimental Hematology* 1996; 24(10); 1215-1224
- Leonard, G. D. et al (2003) The role of ABC transporters in clinical practice. *The Oncologist* 2003; 8; 411-424
- Li, L. et al (2010) Coexistence of quiescent and active adult stem cells in mammals. *Science* 2010; 327: 542-545
- Li, M.H. et al (2005) Molecular genetics of supratentorial primitive neuroectodermal tumours and pineoblastoma. *Neurosurgical Focus* 2005; 19: 1-17
- Ling, V. (1997) Multidrug resistance: molecular mechanisms and clinical relevance. *Cancer Chemotherapy Pharmacology* 1997;40; S3-S8
- Lippard, S. J. (1982) New chemistry of an old molecule: cis-[Pt(NH<sub>3</sub>)<sub>2</sub>Cl<sub>2</sub>]. *Science* 1982; 218: 1075-1082
- Liu, L. et al (1996) Mismatch repair mutations override alkyltransferase in conferring resistance to temozolomide but not to 1, 3-bis(2-chloroethyl)nitrosourea. *Cancer Research* 1996; 56: 5375-5379
- Llaguno, S. A. et al (2009) Malignant astrocytomas originate from neural stem/progenitor cells in a somatic tumor suppressor mouse model. *Cancer Cell* 2009; 16: 45-56
- Lois, C. and Buylly, A. A. (1994) Long-distance neuronal migration in the adult mammalian brain. *Science* 1994; 264(5162); 1145-1148
- Long, B. H. (1985) Single- and double-strand DNA breakage and repair in human lung adenocarcinoma cells exposed to Etoposide and Teniposide. *Cancer Research* 1985; 45: 3106-3112
- Long, B. H. et al (1991) Mechanisms of resistance to etoposide and teniposide in acquired resistant human colon and lung carcinoma cell lines. *Cancer Research* 1991; 51: 5275-5283
- Loo, T. W. and Clarke, D. M. (1997) Identification of residues in the drug-binding site of human P-glycoprotein using a thiol-reactive substrate. *The Journal of Biological Chemistry* 1997; 272(51): 31945-31948
- Lorico, A. et al (1997) Disruption of the murine MRP (Multidrug Resistance Protein) gene leads to increased sensitivity to Etoposide (VP-16) and increased levels of glutathione. *Cancer Research* 1997; 57: 5238-5242
- Löscher, W. and Potschka, H. (2005) Drug resistance in brain diseases and the role of drug efflux transporters. *Nature Reviews* 2005; 6; 591-602

- Louis, D. N. et al (2007) The 2007 WHO classification of tumours of the central nervous system. *Acta Neuropathologica* 2007; 114: 97-109
- Ma, B. F. et al (2006) Slower cycling of nestin-positive cells in neurosphere culture. *Developmental Neuroscience* 2006; 17: 377-381
- MacDonald, T. J. et al (2003) Advances in the diagnosis, molecular genetics, and treatment of paediatric embryonal CNS tumours. *The Oncologist* 2003; 8: 174-186
- Mader, R. M. et al (1991) Instability of the anticancer agent Etoposide under in vitro culture conditions. *Cancer Chemotherapy and Pharmacology* 1991; 27(5): 354-360
- Maliepaard, M. et al (2001) Circumvention of breast cancer resistance protein (BCRP)-mediated resistance to camptothecins in vitro using non-substrate drugs or the BCRP inhibitor GF120918. *Clinical cancer Research* 2001; 7: 935-941
- Mao, Q. and Unadkat, J. D. (2005) Role of the breast cancer resistance protein (ABCG2) in drug transport. *The American Association of Pharmaceutical Scientist Journal* 2005; 7(1); E118-E133
- Margolles, A. et al (1999) The purified and functionally reconstituted multidrug transporter LmrA of *Lactococcus lactis* mediates the transbilayer movement of specific fluorescent phospholipids. *Biochemistry* 1999; 38(49): 16298-16306
- Marino, S. et al (2000) Induction of medulloblastomas in p53-null mutant mice by somatic inactivation of Rb in the external granular layer cells of the cerebellum. *Genes Development* 2000; 14: 994-1004
- Masui, S. et al (2007) Pluripotency governed by Sox2 via regulation of Oct3/4 expression in mouse embryonic stem cells. *Nature Cell Biology* 2007; 9; 625-635
- Maw, M. A. et al (2000) A frameshift mutation in prominin (mouse)-like 1 causes human retinal degeneration. *Human Molecular Genetics* 2000; 9(1): 27-34
- McDevitt, C. A. et al (2009) Purification and structural analyses of ABCG2. *Advanced Drug Delivery Reviews* 2009; 61: 57-65
- McLendon, R.E. et al. (2007) 'Chapter 3: Ependymal tumours'. In Louis, D.N. (eds) (2007) *WHO Classification of Tumours of the Central Nervous System*. Lyon: World Health Organization 69-80
- McLendon, R.E. et al. (2007) 'Chapter 8: Central nervous system primitive neuroectodermal tumours'. In Louis, D.N. (eds) *WHO Classification of Tumours of the Central Nervous System*. Lyon: World Health Organization 141-146
- Mechetner, E. et al (1998) Levels of multidrug resistance (MDR1) P-glycoprotein expression by human breast cancer correlate with in vitro resistance to taxol and doxorubicin. *Clinical Cancer Research* 1998; 4: 389-398
- Meeker, A. K. et al (2004) Telomere length abnormalities occur early in the initiation of epithelial carcinogenesis. *Clinical Cancer Research* 2004; 10; 3317-3326
- Meister, A. and Anderson, M. E. (1983) Glutathione. *Annual Review of Biochemistry* 1983; 52: 711-760
- Melton, D. A. and Cowan, C. (2004) "'Stemness": Definitions, Criteria, and Standards' In Lanza, R. (eds) *Handbook of Stem Cells: volume 1 Embryonic stem cells*. USA: Elsevier Academic Press xxv-xxxi
- Merkel, F. T. et al (2004) Radial glia give rise to adult neural stem cells in the subventricular zone. *PNAS* 2004; 101(50); 17528-17532
- Messahel, B. et al (2009) Relapsed intracranial ependymoma in children in the UK: patterns of relapse, survival and therapeutic outcome. *European Journal of Cancer* 2009; 45: 1815-1823
- Millward, M. J. et al (1993) Oral Verapamil with chemotherapy for advanced non-small cell lung cancer: a randomised study. *British Journal of Cancer* 1993; 67: 1030-1035

- Miraglia, G. et al (1997) A novel five-transmembrane hematopoietic stem cell antigen: Isolation, characterization, and molecular cloning. *Blood* 1997; 12: 5013-5021
- Miyagi, S. et al (2004) The SOX-2 regulatory regions display their activities in two distinct types of multipotent stem cells. *Molecular and Cellular Biology* 2004; 24(10); 4207-4220
- Miyagi, S. et al (2006) The Sox2 regulatory region 2 functions as a neural stem cell-specific enhancer in the telencephalon. *The Journal of Biological Chemistry* 2006; 281(19); 13374-13381
- Miyake, K. et al (1999) Molecular cloning of cDNAs which are highly overexpressed in mitoxantrone-resistant cells: demonstration of homology to ABC transporter genes. *Cancer Research* 1999; 59: 8-13
- Mizrak, D. et al (2008) CD133: molecular of the moment. *Journal of Pathology* 2008; 214; 3-9
- Morshead, C. M. et al (2002) Hematopoietic competence is a rare property of neural stem cells that may depend on genetic and epigenetic alterations. *Nature Medicine* 2002; 8(2): 268-273
- Muller, C. et al (1994) Verapamil decreases P-glycoprotein expression in multidrug-resistant human leukemic cell lines. *International Journal of Cancer* 1994; 56(5): 749-754
- Muller, C. et al (1995) P-glycoprotein stability is affected by serum deprivation and high cell density in multidrug resistant cells. *Journal of Cellular Physiology* 1995; 163: 538-544
- Nakagawa, Y. (1986)] Immunohistochemical characterization of oligodendrogliomas: an analysis of multiple markers. *Acta Neuropathologica* 1986; 72: 15-22
- Nakano, I. et al (2006) Brain tumour stem cells. *Paediatric Research* 59; 54R-58R
- Nakatani, K. et al (1997) The significant role of telomerase activity in human brain tumours. *American Cancer Society* 1997; 80(3); 471-476
- Neuzil, J. et al (2007) Tumour-initiating cells vs. cancer 'stem' cells and CD133: What's in the name? *Biochemical and Biophysical Research Communications*: 2007; 355: 855-859
- Nies, A. T. (2007) The role of membrane transporters in drug delivery to brain tumours. *Cancer Letters* 2007; 245: 11-29
- Nooter, K. et al (1995) Expression of the multidrug resistance-associated protein (MRP) gene in human cancers. *Clinical Cancer Research* 1995; 1; 1301-1310
- Northcott, P. A. et al (2009) Multiple recurrent genetic events converge on control of histone lysine methylation in medulloblastoma. *Nature Genetics* 2009; 41: 465-472
- Nykanen, A. et al (2001) ATP requirements and small interfering RNA structure in the RNA interference pathway. *Cell* 2001; 107: 309-321
- Ohgaki, H. and Kleihues, P. (2005) Population-based studies on incidence, survival rates, and genetic alterations in astrocytic and oligodendroglial gliomas. *Journal of Neuropathology and Neurology* 2005; 64: 479-489
- Ohgaki, H. et al (2004) Genetic pathways to glioblastoma: a population-based study. *Cancer Research* 2004; 64: 6892-6899
- Olson, J.D. et al (2000) Long-term outcome of low-grade oligodendroglioma and mixed glioma. *Neurology* 2000;54:1442-1448
- Ozvegy-Laczka, C. et al (2005) Function-dependent conformational changes of the ABCG2 multidrug transporter modify its interaction with a monoclonal antibody on the cell surface. *The Journal of Biology Chemistry* 2005; 280(6); 4219-4227
- Packer, R. J. (1999) Childhood medulloblastoma: progress and future challenges. *Brain and Development* 1999; 21: 75-81

- Packer, R. J. and Vezina, G. (2008) Management of and prognosis with medulloblastoma: therapy at a crossroads. *Archives Neurology* 2008; 65: 1419-1424
- Packer, R. J. et al (1985) Oligodendroglioma of the posterior fossa in childhood. *Cancer* 1985; 56: 195-199
- Pardal, R. et al (2003) Applying the principles of stem-cell biology to cancer. *Nature Reviews* 2003; 3: 895-902
- Parker, R. J. et al (1991) Acquired cisplatin resistance in human ovarian cancer cells is associated with enhanced repair of cisplatin-DNA lesions and reduced drug accumulation. *Journal of Clinical Investigation* 1991; 87: 772-777
- Pauli-Magnus, C. et al (2000) Characterization of the major metabolites of Verapamil as substrates and inhibitors of P-glycoprotein. *The Journal of Pharmacology and Experimental Therapeutics*. 2000; 293(2): 376-382
- Payet, D. et al (1993) Instability of the monofunctional adducts in cis-[Pt(NH<sub>3</sub>)<sub>2</sub>(N7-N-methyl-2-diazapyrenium)CI]<sup>2+</sup>-modified DNA: rates of cross-linking reactions in cis-platinum modified DNA. *Nucleic Acids Research* 1993; 21(25): 5846-5851
- Pendergrass, T.W. et al (1987) Eight drugs in one day chemotherapy for brain tumors: experience in 107 children and rationale for preirradiation chemotherapy. *Journal of Clinical Oncology* 1987;5:1221-1231
- Perez, R. P. (1998) Cellular and molecular determinants of Cisplatin resistance. *European Journal of Cancer* 1998; 34(10): 1535-1542
- Pesheva, P. et al (1998) Murine microglial cells express functionally active galectin-3 in vitro. *Journal of Neuroscience Research* 1998; 52: 49-57
- Pfenninger, C. V. et al (2007) CD133 is not present on neurogenic astrocytes in the adult subventricular zone, but no embryonic neural stem cells, ependymal cells, and glioblastoma cells. *Cancer Research* 2007; 67(12):5727-5736
- Pierallini, A. et al (1998) Radiological assessment of necrosis in glioblastoma: variability and prognostic value. *Neuroradiology* 1998; 40: 150-153
- Polkinghorn, W. R. and Tarbell, N. J. (2007) Medulloblastoma: tumorigenesis, current clinical paradigm, and efforts to improve risk stratification. *Nature Clinical Practice Oncology* 2007; 4: 295-304
- Pollack, I. F. (1994) Current Concept: Brain tumours in children. *The New England Journal of Medicine* 331(22): 1,500-1,507
- Pollack, I. F. et al (1995) Intracranial ependymomas of childhood: long-term outcome and prognostic factors. *Neurosurgery* 1995; 37: 655-666
- Pollack, I. F. et al (1999) Potent topoisomerase I inhibition by novel silatecans eliminates glioma proliferation in vitro and in vivo. *Cancer Research* 1999; 59:4898-4905
- Pollard, S. M. et al (2006) Adherent neural stem (NS) cells from fetal and adult forebrain. *Cerebral Cortex* 2006; 16: 112-120
- Poppleton, H. and Gilbertson, R. J. (2007) Stem cells of ependymoma. *British Journal of Cancer* 2007; 96: 6-10
- Prayson, R. A. (1999) Clinicopathologic study of 61 patients with ependymoma including MIB-1 immunohistochemistry. *Annals of Diagnostic Pathology* 1999; 3(1): 11-18
- Qian, X. D. and Beck, W. T. (1990) Binding of an optically pure photoaffinity analogue of verapamil, LU-49888, to P-glycoprotein from multidrug-resistant human leukemic cell lines. *Cancer Research* 1990; 50: 1132-1137

- Raviv, Y. et al (1990) Photosensitized labelling of a functional multidrug transporter in living drug-resistant tumor cells. *The Journal of Biological Chemistry* 1990; 265(7): 3975-3980
- Ravna, A. W. et al (2009) Binding site of ABC transporter homology models confirmed by ABCB1 crystal structure. *Theoretical Biology and Medical Modelling* 2009; 6(20) doi:10.1186/1742-4682-6-20
- Razak, N. et al (1998) Pediatric oligodendrogliomas. *Pediatric Neurosurgery* 1998; 28: 121-129
- Regina, A. et al (2001) Multidrug resistance in brain tumors: Roles of the blood-brain barrier. *Cancer and metastasis reviews* 2001; 20; 13-25
- Reifenberger, G. (2007) 'Chapter 2: Oligodendroglial tumours'. In Louis, D.N. (eds) *WHO Classification of Tumours of the Central Nervous System*. Lyon: World Health Organization 54-67
- Reni, M. et al (2007) Ependymoma. *Clinical Reviews in Oncology/Hematology* 2007; 63; 81-89
- Reubinoff, B. E. et al (2000) Embryonic stem cell lines from human blastocysts: somatic differentiation in vitro. *Nature Biotechnology* 2000; 18; 399-404
- Reya, T. et al (2001) Stem cells, cancer, and cancer stem cells. *Nature* 2001; 414(6859): 105-111
- Reynolds, B. A. and Weiss, S. (1992) Generation of neurons and astrocytes from isolated cells of the adult mammalian central nervous system. *Science* 1992; 255: 1707-1710
- Richardson, G. D. et al (2004) CD133, a novel marker for human prostatic epithelial stem cells. *Journal of Cell Science* 2004; 117; 3539-3545
- Richon, V. M. et al (1987) Multiple mechanisms of resistance to cis-diamminedichloroplatinum (II) in murine leukemia L1210 cells. *Cancer Research* 1987; 47: 2056-2061
- Ridley, L. et al (2008) Multifactorial analysis of predictors of outcome in pediatric intracranial ependymoma. *Neuro-Oncology* 2008; 10(5): 675-689
- Riemenschneider, M. J. et al (2004) Expression of oligodendrocyte lineage genes in oligodendroglial and astrocytic gliomas. *Acta Neuropathologica* 2004; 107; 277-282
- Robertson, P. L. et al (1998) Survival and prognosis factors following radiation therapy and chemotherapy for ependymomas in children: a report of the Children's Cancer Group. *Journal of Neurosurgery* 1998; 88: 695-703
- Robey, R. W. et al (2007) ABCG2: determining its relevance in clinical drug resistance. *Cancer Metastasis* 2007; 26: 39-57
- Rodda, D. J. et al (2005) Transcriptional regulation of Nanog by OCT4 and SOX2. *The Journal of Biological Chemistry* 2005; 280(26); 24731-24737
- Rorke, L. B. et al (1985) Revision of the World Health Organization Classification of brain tumours for childhood brain tumours. *Cancer* 1985; 56: 1869-1886
- Ross, D. D. et al (1999) Atypical multidrug resistance: Breast cancer resistance protein messenger RNA expression in mitoxantrone-selected cell lines. *Journal of the National Cancer Institute* 1999; 91(5): 429-433
- Rostomily, R. C. et al (1997) Expression of neurogenic basic helix-loop-helix genes in primitive neuroectodermal tumours. *Cancer Research* 1997; 57: 3526-3531
- Rothenberg, M. (2001) Irinotecan (CPT-11): recent developments and future directions-colorectal cancer and beyond. *Oncologist* 2001; 6: 66-80
- Rowinsky, E. K. et al (1994) Phase I and pharmacological study of the novel topoisomerase I inhibitor 7-ethyl-10-[4-(1-piperidino)-1-piperidino]carbonyloxycamptothecin (CPT-11) administered as a ninety-minute infusion every 3 weeks. *Cancer Research* 1994; 54: 427-436



- Sagar, J. et al (2007) Role of stem cells in cancer therapy and cancer stem cells: a review. *Cancer Cell International* 2007; 7(9): 1-11
- Sainati, L. et al (1996) Cytogenetics of pediatric central nervous system tumors. *Cancer Genetics and Cytogenetics* 1996; 91: 13-27
- Sakariassen, P. et al (2007) Cancer stem cells as mediators of treatment resistance in brain tumours: status and controversies. *Neoplasia* 2007; 9(11): 882-892
- Saleem, A. et al (2000) Mechanisms of resistance to camptothecins. *Annals New York Academy of Sciences* 2000; 922: 46-55
- Sambrook, J. and Russell, D. W. (2001) 'Appendix 8: Commonly used techniques in molecular cloning.' *Molecular Cloning: A Laboratory Manual*, Third edition. China: Cold spring harbour laboratory press, New York A8.40-A8.55
- Sano, T. et al (1998) Telomerase activity in 144 brain tumour. *British Journal of Cancer* 1998; 77: 1633-1637
- Santos, A. et al (2000) Metabolism of Irinotecan (CPT-11) by CYP3A4 and CYP3A5 in humans. *Clinical Cancer Research* 2000; 6: 2012-2020
- Sarkadi, B. et al (2004) ABCG2-a transporter for all seasons. *FEBS Letters* 2004; 567: 116-120
- Sauna, Z. E. and Ambudkar, S. V. (2000) Evidence for a requirement for ATP hydrolysis at two distinct steps during a single turnover of the catalytic cycle of human P-glycoprotein. *PNAS* 2000; 97: 2515-2520
- Scanlon, K. J. (1991) Cisplatin resistance in human cancers. *Pharmacology Therapy* 1991; 52: 385-406
- Scharenberg, C. W. et al (2002) The ABCG2 transporter is an efficient Hoechst 33342 efflux pump and is preferentially expressed by immature human hematopoietic progenitors. *Blood* 2002; 99(2): 507-512
- Schiffer, D. and Giordana, M. T. (1998) Prognosis of ependymoma. *Child's Nervous System* 1998; 14: 357-361
- Schilder, R. J. et al (1990) Metallothionein gene expression and resistance to cisplatin in human ovarian cancer. *International Journal of Cancer* 1990; 45(3): 416-422
- Schimke, R.T. (1988) Gene amplification in cultured cells. *The Journal of Biological Chemistry* 1988; 263(13): 5969-5992
- Schinkel, A. H. and Jonker, J. W. (2003) Mammalian drug efflux transporters of the ATP binding cassette (ABC) family: an overview. *Advanced Drug Delivery Reviews* 2003; 55: 3-29
- Schinkel, A. H. et al (1994) Disruption of the mouse *mdr1a* P-glycoprotein gene leads to a deficiency in the blood-brain barrier and to increased sensitivity to drugs. *Cell* 1994; 77: 491-502
- Schinkel, A. H. et al (1995) Absence of the *mdr1a* P-glycoprotein in mice affects tissue distribution and pharmacokinetics of dexamethasone, digoxin, and cyclosporine A. *Journal of Clinical Investigation* 1995; 96: 1698-1705
- Schinkel, A. H. et al (1995) Multidrug resistance and the role of P-glycoprotein knockout mice. *European Journal of Cancer* 1995; 31A(7/8): 1294-1298
- Scotting, P.J. et al. (2005) Childhood solid tumours: a developmental disorder. *Nature Reviews* 2005; 5: 481-488
- Sell, S. (2004) 'Chapter 1: Stem cells.' In Sell, S (ed) (2004), *Stem Cells Hand Book*. New Jersey: Humana Press Inc., 1-18

- Sell, S. (2004) Stem cell origin of cancer and differentiation therapy. *Oncology Hematology*. 2004: 51; 1-28
- Senior, A. E. and Bhagat, S. (1998) P-glycoprotein shows strong catalytic cooperativity between the two nucleotide sites. *Biochemistry* 1998; 37: 831-836
- Shapiro, A. B. et al (1997) P-glycoprotein-mediated Hoechst 33342 transport out of the lipid bilayer. *European Journal of Biochemistry* 1997; 250: 115-121
- Shapiro, W. R. et al (1989) Randomized trial of three chemotherapy regimens and two radiotherapy regimens in postoperative treatment of malignant glioma. *Journal of Neurosurgery* 1989; 71: 1-9
- Shay, J. W. and Bacchetti, S. (1997) A survey of telomerase activity in human cancer. *European Journal of Cancer* 1997; 33; 787-791
- Sheibana, N. et al (1989) DNA repair in cells sensitive and resistant to cis-diamminedichloroplatinum(II): host cell reactivation of damaged plasmid DNA. *Biochemistry* 1989; 28(7): 3120-3124
- Shiras, A. et al (2007) Spontaneous transformation of human adult nontumorigenic stem cells to cancer stem cells is driven by genomic instability in a human model of glioblastoma. *Stem Cells* 2007; 25; 1478-1489
- Shmelkov, S. V. et al (2005) AC133/CD133/Prominin-1. *The International Journal of Biochemistry & Cell Biology* 2005; 37; 715-719
- Singh, S. K. et al (2003) Identification of a cancer stem cell in human brain tumours. *Cancer Research* 2003; 63; 6821-5828
- Singh, S. K. et al (2004) Cancer stem cells in nervous system tumours. *Oncogene* 2004; 23; 7267-7273
- Singh, S. K. et al (2004) Identification of human brain tumour initiating cells. *Nature* 2004; 432; 396-401
- Sirotnak, F. M. and O'Leary, D. F. (1991) The issues of transport multiplicity and energetics pertaining to methotrexate efflux in L1210 cells addressed by an analysis of Cis and Trans effects of inhibitors. *Cancer Research* 1991; 51: 1412-1417
- Siyuan, L. et al (1998) Telomerase activity in human gliomas. *Neurosurgery* 1998; 42(5); 1120-1124
- Slack, J. M. W. (2006) 'Chapter13: Tissue organization and stem cells.' *Essential Developmental Biology*: second edition. Italy: Blackwell Publishing Ltd. 179-198
- Slatter, J. G. et al (2000) Pharmacokinetics, metabolism, and excretion of Irinotecan (CPT-11) following I.V. infusion of [(14)C]CPT-11 in cancer patients. *Drug Metabolism and Disposition* 2000; 28: 423-433
- Smelkov, S. V. et al (2004) Alternative promoters regulate transcription of the gene that encodes stem cell surface protein AC133. *Blood* 2004; 103(6); 2055-2061
- Smith, N. F. et al (2006) Pharmacogenetics of irinotecan metabolism and transport: An update. *Toxicology in Vitro* 2006; 20: 163-175
- Snyder, E. Y. et al (1992) Multipotent neural cell lines can engraft and participate in development of mouse cerebellum. *Cell* 1992; 68: 33-51
- Sorenson, C. M. and Eastman, A. (1988) Mechanism of cis-diamminedichloroplatinum(II)-induced cytotoxicity: role of G2 arrest and DNA double-strand breaks. *Cancer Research* 1988; 48: 4484-4488
- Sparreboom, A. et al (2003) Pharmacogenomics of ABC transporters and its role in cancer chemotherapy. *Drug Resistance Update* 2003; 6: 71-84

- Srimatkandada, S. et al (1989) Amplification of a polymorphic dihydrofolate reductase gene expressing an enzyme with decreased binding to methotrexate in a human colon carcinoma cell line, HCT-8R4, resistant to this drug. *The Journal of Biological Chemistry* 1989; 264(6): 3524-3528
- Stewart, E.S. and Cohen, D.G. (1998) Central nervous system tumours in children. *Seminars in Oncology Nursing* 14(1): 34-42
- Storb, R. et al (1986) Marrow transplantation for severe aplastic anemia: Methotrexate alone compared with a combination of methotrexate and cyclosporine for prevention of acute graft-versus-host disease. *Blood* 1986; 68(1): 119-125
- Svenson, T. and Roos, G. (2009) Telomere length as a biological marker in malignancy. *Biochimica et Biophysica Acta* 2009; doi: 10.1016/j.bbadis.2009.01.017
- Szakács, G et al (2006) Targeting multidrug resistance in cancer. *Nature Reviews: Drug Discovery* 2006; 5: 219-234
- Tabori, U. et al (2006) The role of telomere maintenance in the spontaneous growth arrest of paediatric low-grade gliomas. *Neoplasia* 2006; 8(2): 136-142
- Takahashi, K. and Yamanaka, S. (2006) Induction of pluripotent stem cells from mouse embryonic and adult fibroblast cultures by defines factors. *Cell* 2006; 126: 663-676
- Takahashi, T. et al (1997) The role of glucuronidation in 7-hydroxycamptothecin resistance in vitro. *Japanese Journal of Cancer Research* 1997; 88: 1211-1217
- Tan, B. T. et al (2006) The cancer stem cell hypothesis: a work in progress. *Laboratory Investigation* 2006; 86; 1203-1207
- Tanaka, Y. et al (1994) Ultrastructural localization of P-glycoprotein on capillary endothelial cells in human gliomas. *Virchows Archiv.* 1994: 425; 133-138
- Taylor, M. D. et al (2005) Radial glia cells are candidate stem cells of ependymoma. *Cancer Cell* 2005; 8: 323-335
- Teicher, B. A. et al (1987) Characterization of a human squamous carcinoma cell line resistant to cis-diamminedichloroplatinum (II). *Cancer Research* 1987; 47: 388-393
- The Cancer Genome Atlas Research Network (2008) Comprehensive genomic characterization defines human glioblastoma genes and core pathways. *Nature* 2008; 455: 1061- 1068
- Tjio, J. H. and Puck, T. T. (1958) The somatic chromosomes of man. *Proceedings of the National Academy of Sciences* 1958; 44(12): 1229-1237
- Trock, B. J. et al (1997) Multidrug resistance in breast cancer: a meta-analysis of MDR1/gp170 expression and its possible functional significance. *Journal of the National Cancer Institute* 1997; 89(13): 917-931
- Tsuruo, T. et al (1981) Overcoming of Vincristine Resistance in P388 Leukemia in Vivo and in Vitro through Enhanced Cytotoxicity of Vincristine and Vinblastine by Verapamil. *Cancer Research* 1981; 41(5): 1967-1972
- Tunici, P. et al. (2006) Brain tumour stem cells: New targets for clinical treatment? *Neurosurgical Focus* 20(4) : 1-7
- Twentyman, P. R. et al (1994) A comparison of rhodamine 123 accumulation and efflux in cells with P-glycoprotein-mediated and MRP-associated multidrug resistance phenotypes. *European Journal of Cancer* 1994; 30(9): 1360-1369
- Uchida, N. et al (2000) Direct isolation of human central nervous system stem cells. *PNAS* 2000; 97(26); 14720-14725

- Valeria, P. L. and Raúl, B. R. (2005) Changes in P-glycoprotein activity are mediated by the growth of a tumour cell line as multicellular spheroids. *Cancer Cell International* 2005; 5:20 doi:10.1186/1475-2867-5-20
- van Ark-Otte, J. et al (1998) Determinants of CPT-11 and SN-38 activities in human lung cancer cells. *British Journal of Cancer* 1998; 77: 2171-2176
- van den Heuvel-Eibrink, M. M. et al (2002) Increased expression of the breast cancer resistance protein (BCRP) in relapsed or refractory acute myeloid leukemia (AML). *Leukemia* 2002; 16: 833-839
- van der Sandt, I. C. J. et al (2000) Specificity of doxorubicin versus rhodamine-123 in assessing P-glycoprotein functionality in the LLC-PK1, LLC-PK1:MDR1 and Caco-2 cell lines. *European Journal of Pharmaceutical Sciences* 2000; 11: 207-214
- Vescovi, A. et al (2006) Brain tumour stem cells. *Nature Reviews* 2006; 6: 425-426
- Visvader, J. E. and Lindeman, G. J. (2008) Cancer stem cells in solid tumours: accumulating evidence and unresolved questions. *Nature Reviews Cancer* 2008; 8: 755-768
- Volk, E. L. et al (2000) Methotrexate cross-resistance in a mitoxantrone-selected multidrug-resistant MCF7 breast cancer cell line is attributable to enhanced energy-dependent drug efflux. *Cancer Research* 2000; 60: 3514-3521
- von Bossanyi, P. et al (1997) Immunohistochemical expression of P-glycoprotein and glutathione S-transferases in cerebral gliomas and response to chemotherapy. *Acta Neuropathologica* 1997; 94: 605-611
- von Deimling, A. et al (1993) Subsets of glioblastoma multiforme defined by molecular genetic analysis. *Brain Pathology* 1993; 3: 19-26
- Wagner, K. et al (2006) Absence of the transcription factor CCAAT enhancer binding protein  $\alpha$  results in loss of myeloid identity in bcr/abl-induced malignancy. *PNAS* 2006; 103(16): 6338-6343
- Wall, M. E. et al (1966) Plant antitumor agents. I. The isolation and structure of camptothecin, a novel alkaloidal leukemia and tumor inhibitor from *Camptotheca acuminata*. *Journal of the American Chemical Society* 1966; 88: 3888-3890
- Wandel, C. et al (1999) P-glycoprotein and cytochrome P-450 3A inhibition: dissociation of inhibitory potencies. *Cancer Research* 1999; 59(16): 3944-3948
- Wang, J. C. et al (1971) Interaction between DNA and E. coli: protein omega. *Journal of Molecular Biology* 1971; 55: 523-533
- Waud, W. R. (1987) Differential uptake of cis-diamminedichloroplatinum (II) by sensitive and resistant murine L1210 leukemia cells. *Cancer Research* 1987; 47: 6549-6555
- Weigmann, A. et al (1997) Prominin, a novel microvilli-specific polytopic membrane protein of the apical surface of epithelial cells, is targeted to plasmalemmal protrusions of non-epithelial cells. *PNAS* 1997; 94: 12425-12430
- Weinblatt, M. E. et al (1985) Efficacy of low-dose methotrexate in rheumatoid arthritis. *New England Journal of Medicine* 1985; 312(13): 818-822
- Weinstein, G. D. et al (1990) Cytotoxic and immunologic effects of methotrexate in psoriasis. *The Journal of Investigative Dermatology* 1990; 95(5 suppl): 49S-52S
- White, J. C. and Goldman, I. D. (1976) Mechanism of action of methotrexate: IV. Free intracellular methotrexate required to suppress dihydrofolate reduction to tetrahydrofolate by Ehrlich ascites tumor cells in vitro. *Molecular Pharmacology* 1976; 12: 711-719
- White, J. C. et al (1975) The mechanism of action of methotrexate. III. Requirement of free intracellular methotrexate for maximal suppression of ( $^{14}\text{C}$ ) formate incorporation into nucleic acids and protein. *Molecular Pharmacology* 1975; (11)3: 287-297

- Williams, H. J. et al (1985) Comparison of low-dose oral pulse methotrexate and placebo in the treatment of rheumatoid arthritis. A controlled clinical trial. *Arthritis and Rheumatism* 1985; 28(7): 721-730
- Wilson, C. S. et al (2006) Gene expression profiling of adult acute myeloid leukemia identifies novel biologic clusters for risk classification and outcome prediction. *Blood* 2006; 108(2): 685-696
- Wolf, N. S. et al (1993) In vivo and in vitro characterization of long-term repopulating primitive hematopoietic cells isolated by sequential Hoechst 33342-rhodamine 123 FACS selection. *Experimental Hematology* 1993;21(5); 614-622
- Wright, M. H. et al (2008) Brca1 breast tumors contain distinct CD44+/CD24- and CD133+ cells with cancer stem cell characteristics. *Brain Cancer Research* 2008; 10: R10-R26
- Wu, A. et al (2008) Persistence of CD133+ cells in human and mouse glioma cell lines: detailed characterization of GL261 glioma cells with cancer stem cell-like properties. *Stem cells and Development* 2008; 17; 173-184
- Yagüe, E. et al (2004) Complete reversal of multidrug resistance by stable expression of small interfering RNAs targeting MDR1. *Gene Therapy* 2004; 11: 1170-1174
- Yeager, T. R. et al (1999) Telomerase-negative immortalized human cells contain a novel type of promyelocytic leukemia (PML) body. *Cancer Research* 1999; 59: 4175-4179
- Yu, J. Y. et al RNA interference by expression of short-interfering RNAs and hairpin RNAs in mammalian cells. (2002) *PNAS* 2002; 99(9): 6047-6052
- Yu, X. N. et al (2008) Reversion of P-glycoprotein-mediated multidrug resistance in human leukemic cell line by Carnosic acid. *Chinese Journal of Physiology* 2008; 51(6): 348-356
- Yuan, X. et al (2004) Isolation of cancer stem cells from adult glioblastoma multiforme. *Oncogene* 2004; 23: 9392-9400
- Zacharoulis, S. et al (2007) Outcome for young children newly diagnosed with ependymoma, treated with intensive induction chemotherapy followed by myeloablative chemotherapy and autologous stem cell rescue. *Pediatric Blood Cancer* 2007; 49: 34-40
- Zam, Z. S. et al (1980) Isolation of the plasma membrane from corneal endothelial cells. *Research in Vision and Ophthalmology* 1980; 19(6): 648-652
- Zeppernick, F. et al (2008) Stem cell marker CD133 affects clinical outcome in glioma patients. *Clinical Cancer Research* 2008; 14(1): 123-129
- Zhao, X. et al (2004) 'Neurogenesis in adult brain: understanding its mechanism and regulation' In Gage, F. H. (eds) *Stem Cells in the Nervous System: Functional and Clinical Implications* Germany: Springer-Verlag Berlin Heidelberg 1-24
- Zhdanov, V. P. and Kasemo, B. (2004) Stimulation of the growth of neurospheres. *Europhysics Letters* 2004; 68(1): 134-140
- Zhou, S. et al (2001) The ABC transporter Bcrp1/ABCG2 is expressed in a wide variety of stem cells and is a molecular determinant of the side-population phenotype. *Nature Medicine* 2001; 7: 1028-1034
- Zhou, S. et al (2002) Bcrp1 gene expression is required for normal numbers of side population stem cells in mice, and confers relative protection to mitoxantrone in hematopoietic cells in vivo. *PNAS* 2002; 99(19): 12339-12340
- Ziembar, M. I. and Casatelli, C. (1994) Cytogenetic investigation of four low grade glioma. *Review of Brazilian Cytogenetics* 1994; 17(3): 331-337

---

---

# Appendix

---

---

## Appendix A: Results

### A1: Co-staining immunofluorescence in the parental cell lines after the first round of drug treatment

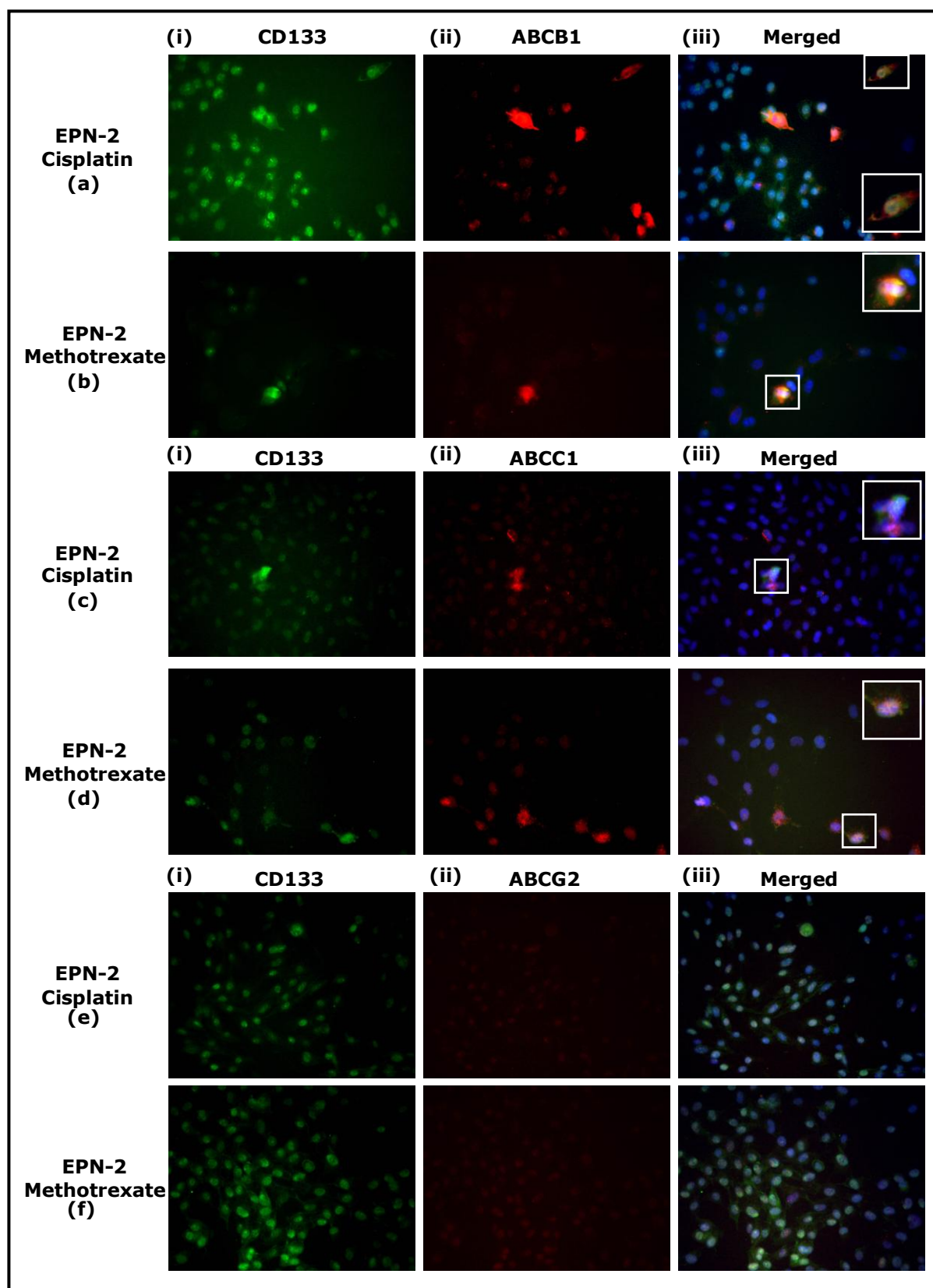


**Figure A1.1 Co-staining CD133 and ABCB1, ABCC1 or ABCG2 immunofluorescence in EPN-2 monolayers after the first round of cisplatin and methotrexate treatment.** After the first treatment of cisplatin and methotrexate, a low proportion of cells co-expressing CD133 and ABCB1 or ABCC1 at a low level was observed [a – d, (i) – (iii)] whereas treated EPN-2 cells were negative for CD133 and ABCG2 co-staining [e and f, (i) – (iii)]. When compared to etoposide and irinotecan treatment, which showed distinctive results of CD133 and ABCB1 co-expression, cisplatin and methotrexate were not selected to treat EPN-2 cells for further analysis, cisplatin and methotrexate EPN-2 cells were hence frozen down in liquid nitrogen. For each treatment a co-staining cell has been enlarged (x2) for clarity.



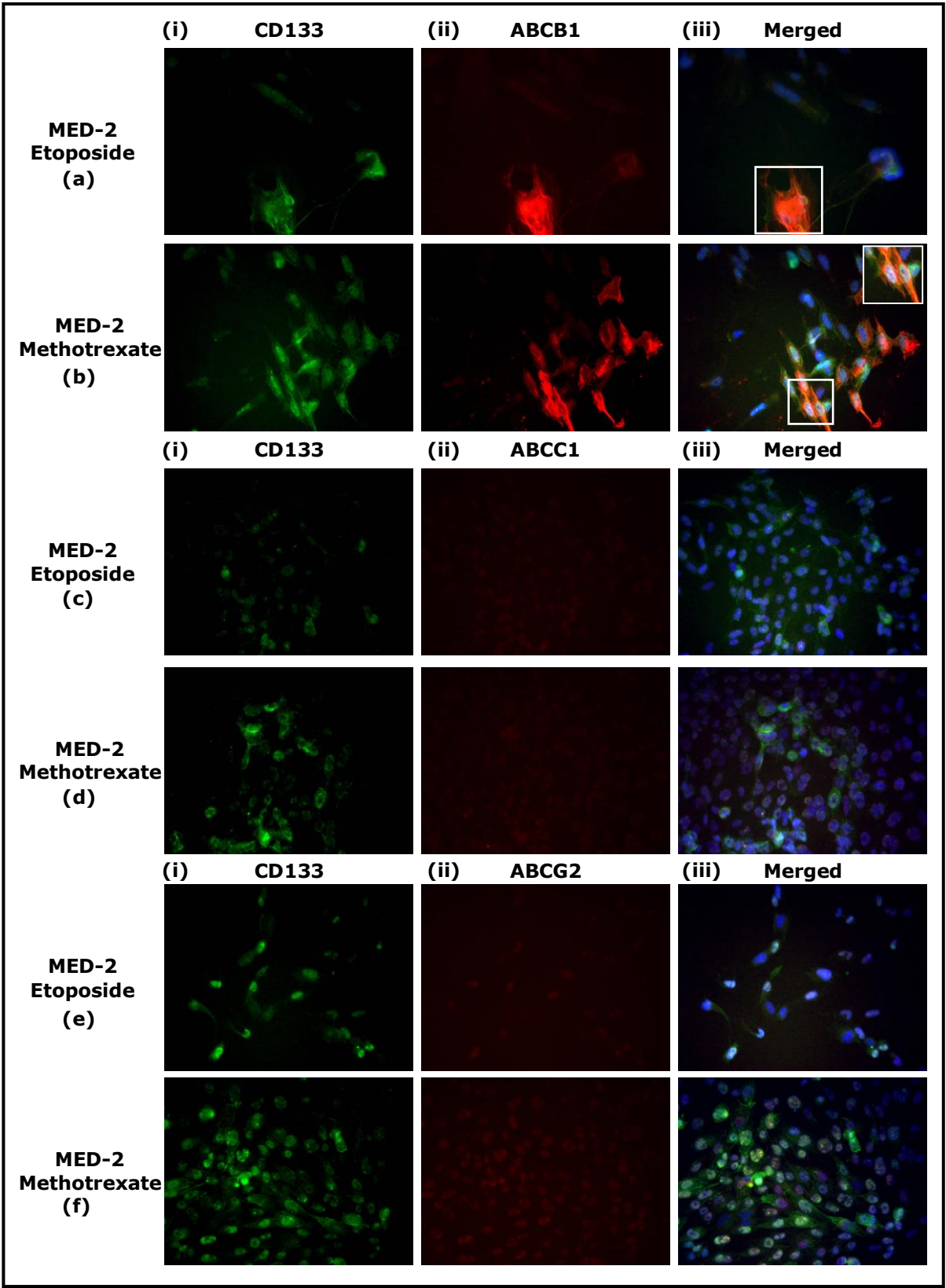


**Figure A1.2 Co-staining CD133 and ABCB1, ABCC1 or ABCG2 immunofluorescence in MED-2 monolayers after the first round of etoposide and methotrexate treatment.** Cells co-expressing CD133 and ABCB1 at a high level were detected in MED-2 treated with etoposide and methotrexate [a and b, (i) – (iii)]. etoposide treated MED-2 displayed a giant co-expressing cell [a, (i) – (iii)]. No CD133 and ABCC1 or ABCG2 co-expressing cells were observed after these 2 treatments [c – f, (i) – (iii)]. MED-2 cells after etoposide and methotrexate treatment were not selected for further analysis and they were frozen down in liquid nitrogen for future study. For each treatment a co-staining cell has been enlarged (x2) for clarity.

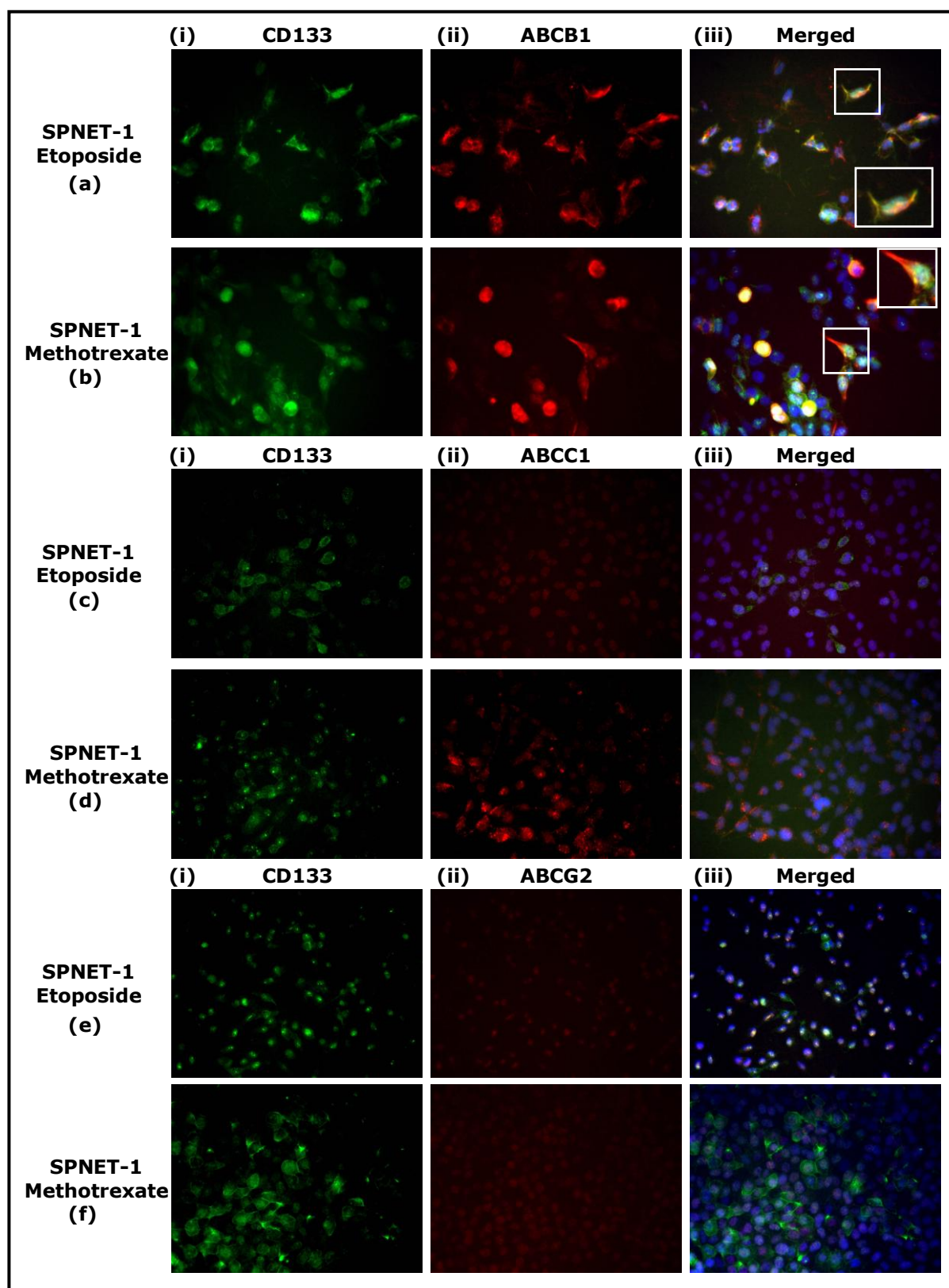


**Figure A1.3 Co-staining CD133 and ABCB1, ABCC1 or ABCG2 immunofluorescence in SPNET-1 monolayers after the first round of etoposide and methotrexate treatment.** SPNET-1 cells after etoposide treatment displayed cells co-expressing CD133 and ABCB1 at a low level [a, (i) – (iii)] whereas a low proportion of cells expressing ABCB1 at a high level were observed in cells treated with methotrexate [b, (i) – (iii)]. No cells co-expressing CD133 and ABCC1 or ABCG2 were present after these 2 treatments [d – f, (i) – (iii)]. Therefore, SPNET-1 cells after etoposide and methotrexate treatment were not carried on for further analysis and they were frozen down in liquid nitrogen as a stock for future study. For each treatment a co-staining cell has been enlarged (x2) for clarity.

**A2: Cellular morphologies of the selected sublines after multiple rounds of drug treatment**

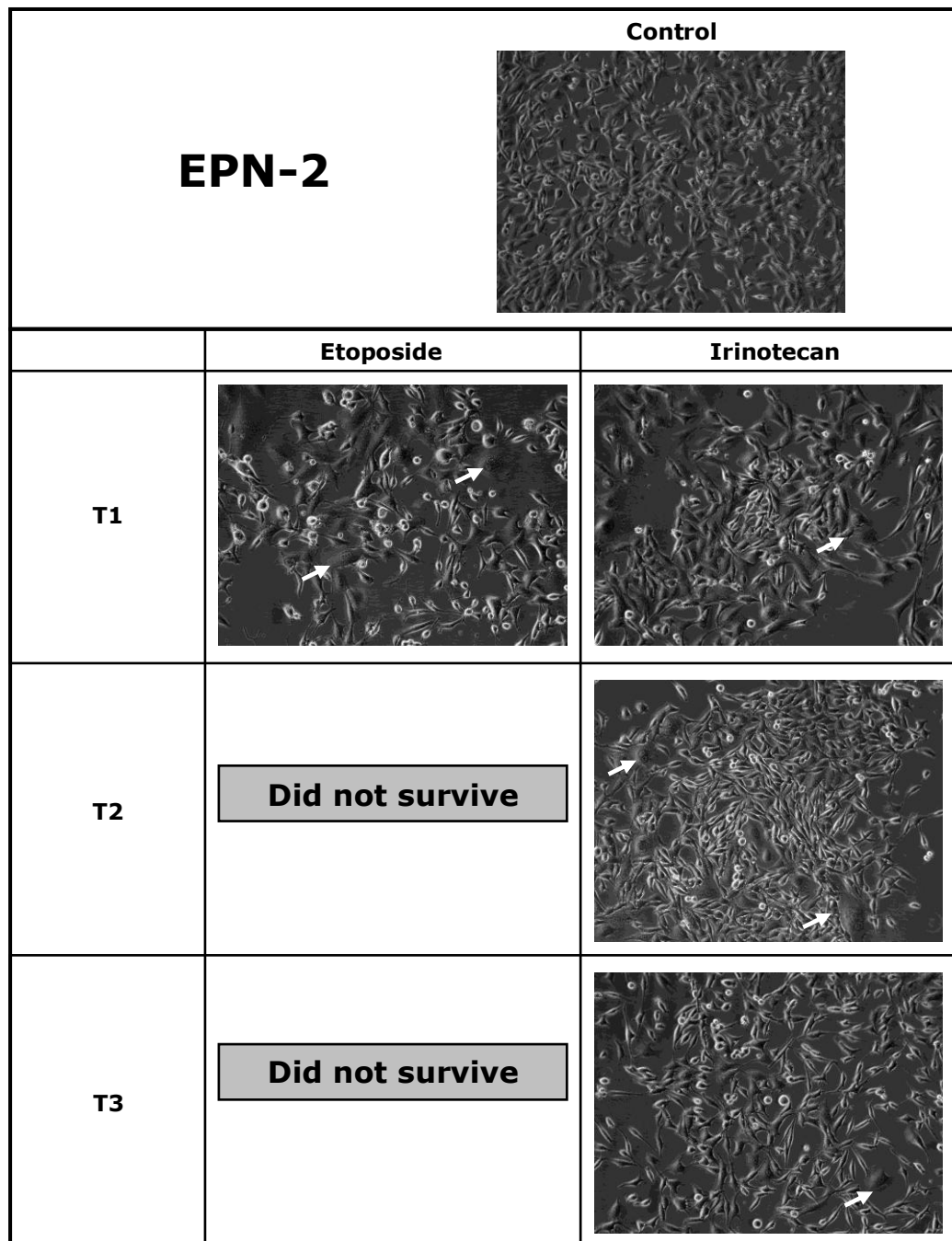


**Figure A2.1 The cellular morphology of a control subline and the selected EPN-2 sublines after multiple rounds of drug treatment.** The control subline comprised a homogeneous population of cells with similar shape and size. The majority of cells in the selected EPN-2 sublines were similar to the control subline, whilst the remainder were large multinucleated cells indicated by white arrows. The selected etoposide EPN-2 sublines were struggling to survive after repeated treatments, consequently, EPN-2\_E\_T1 and T2 failed to grow. Both etoposide and irinotecan EPN-2 sublines grew slower than the control sublines in particular to the etoposide EPN-2 sublines.

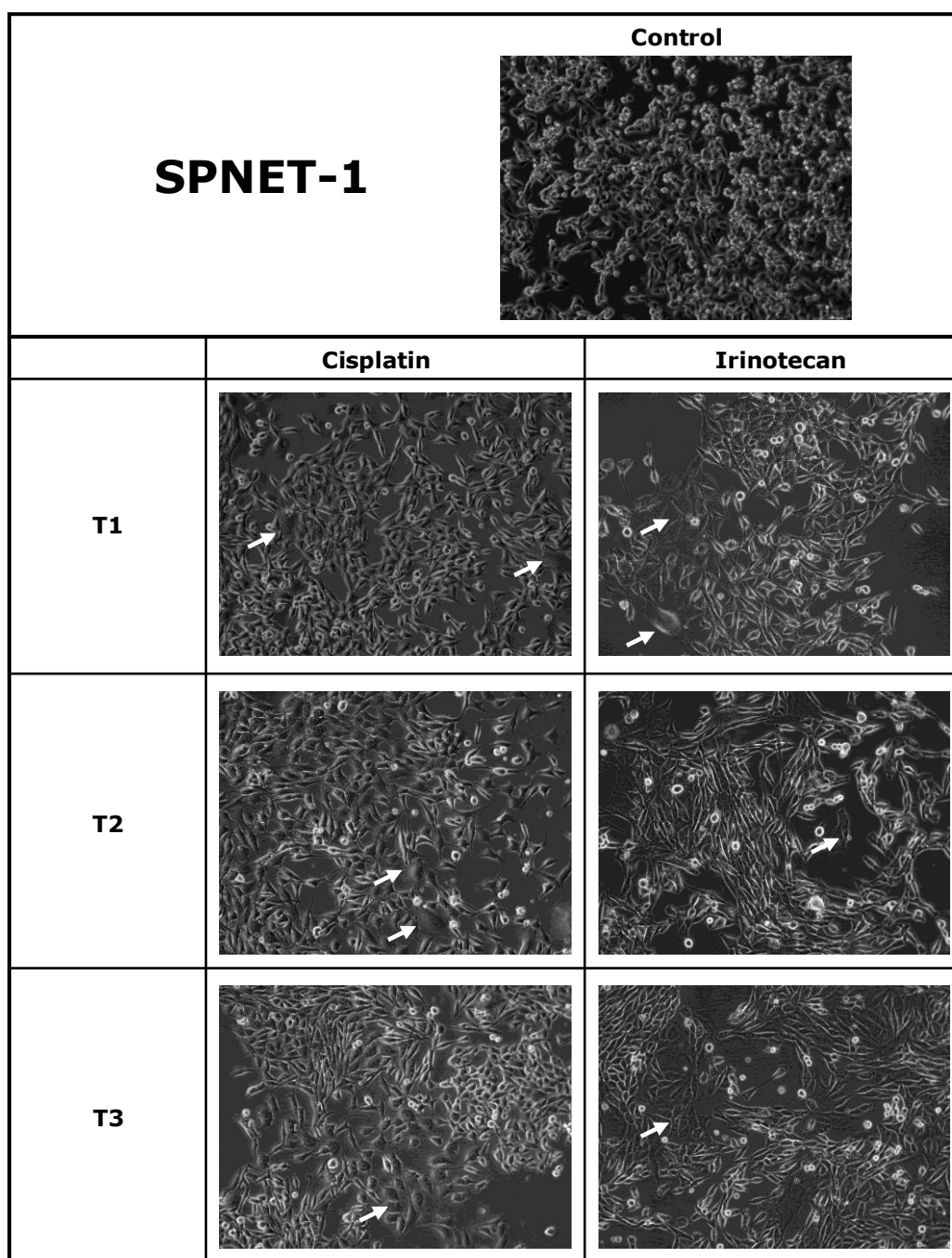


**Figure A2.2 The cellular morphology of a control subline and the selected SPNET-1 sublines after multiple rounds of drug treatment.** Similar to the selected EPN-2 and MED-2 sublines, a homogeneous population was observed in the control sublines. Two different cell morphologies were observed in all selected SPNET-1 sublines: a small proportion of cells, which was large irregular cells (indicated by white arrows) and the majority of cells, which were homogeneous.



**A3: Co-staining immunofluorescence in the selected sublines after repeat treatment at early passage (less than 10 passages)**

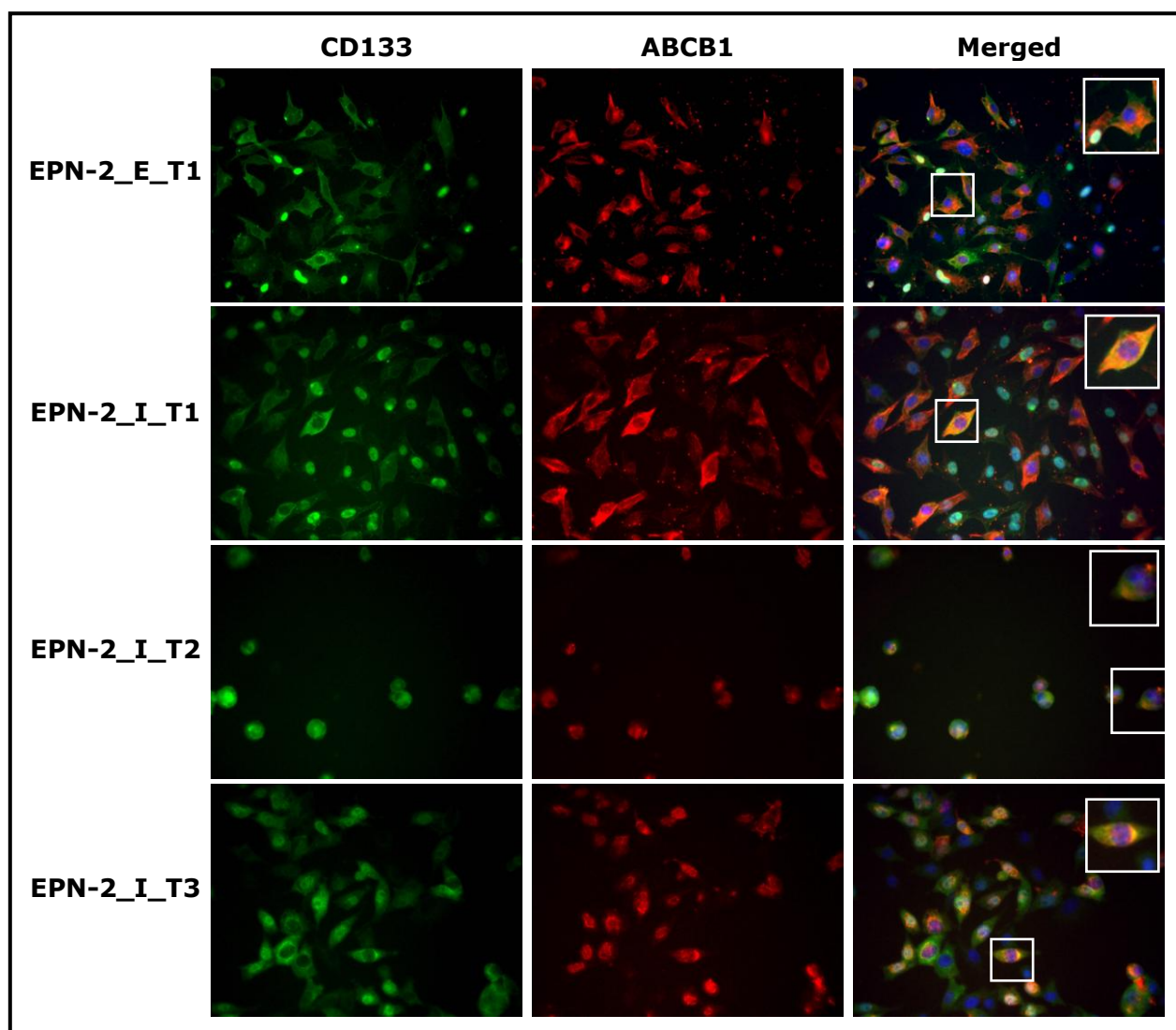


**Figure A3.1 Co-staining CD133 and ABCB1 immunofluorescence in the selected EPN-2 sublines treated for less than 10 passages.** Co-staining immunofluorescence results after first round of treatment showed that a high level of CD133 and ABCB1 co-expression was observed in EPN-2 after all drug treatments. Cells co-expressing CD133 and ABCB1 were consistently observed in all selected EPN-2 sublines. Thereby, all selected EPN-2 sublines expressed a high level of CD133 and ABCB1 co-expression and contained a large proportion of cells co-expressing CD133 and ABCB1 after treatment especially in the EPN-2\_E\_T1 and EPN-2\_I\_T1 sublines. For each treatment a co-staining cell has been enlarged (x2) for clarity.

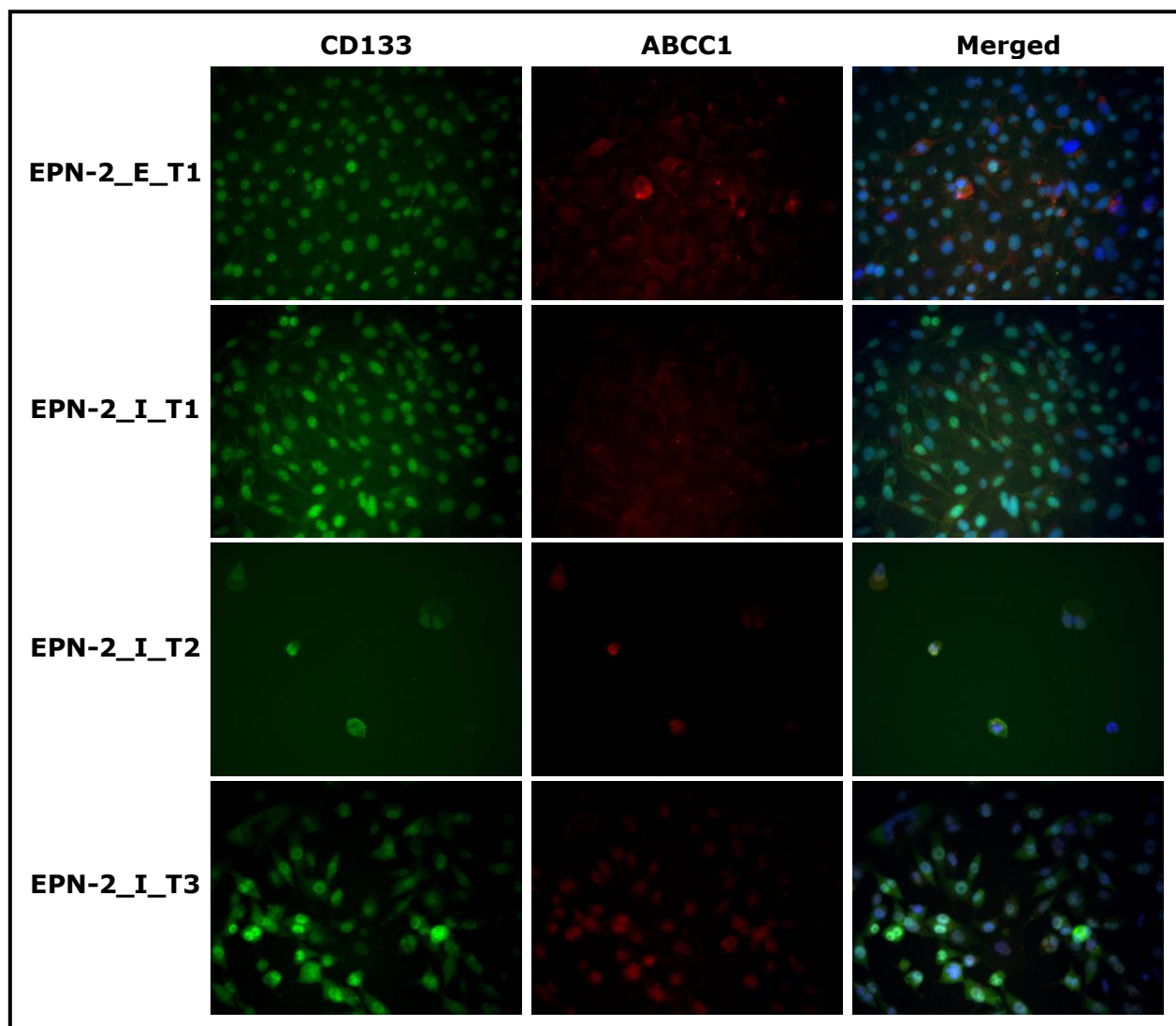


**Figure A3.2 Co-staining CD133 and ABCC1 immunofluorescence in the selected EPN-2 sublines treated for less than 10 passages.** None of the selected EPN-2 sublines co-expressed CD133 and ABCC1. CD133 expression was observed in all selected EPN-2 sublines but these cells were not co-stained with ABCC1. Some cells expressing ABCC1 were detected in the EPN-2\_E\_T1 subline but there was no CD133 co-staining.



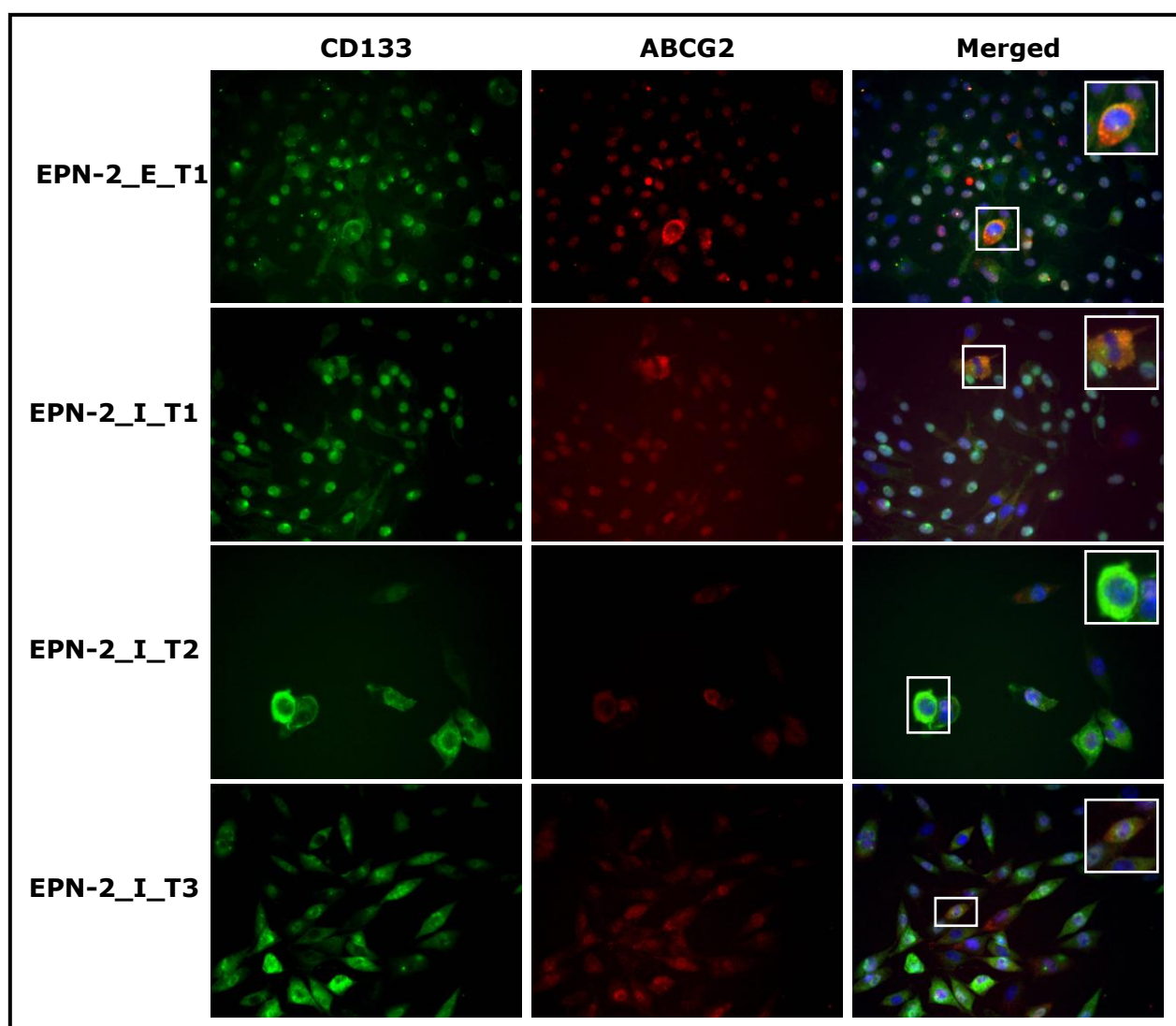


**Figure A3.3 Co-staining CD133 and ABCG2 immunofluorescence in the selected EPN-2 sublines treated for less than 10 passages.** After the first round of etoposide and irinotecan treatment, EPN-2 monolayers co-expressed a low level of CD133 and ABCG2. After many rounds of treatment, a low CD133 and ABCG2 co-expression level and a low proportion of cells co-expressing CD133 and ABCG2 were observed in all selected EPN-2 sublines. For each treatment a co-staining cell has been enlarged (x2) for clarity.

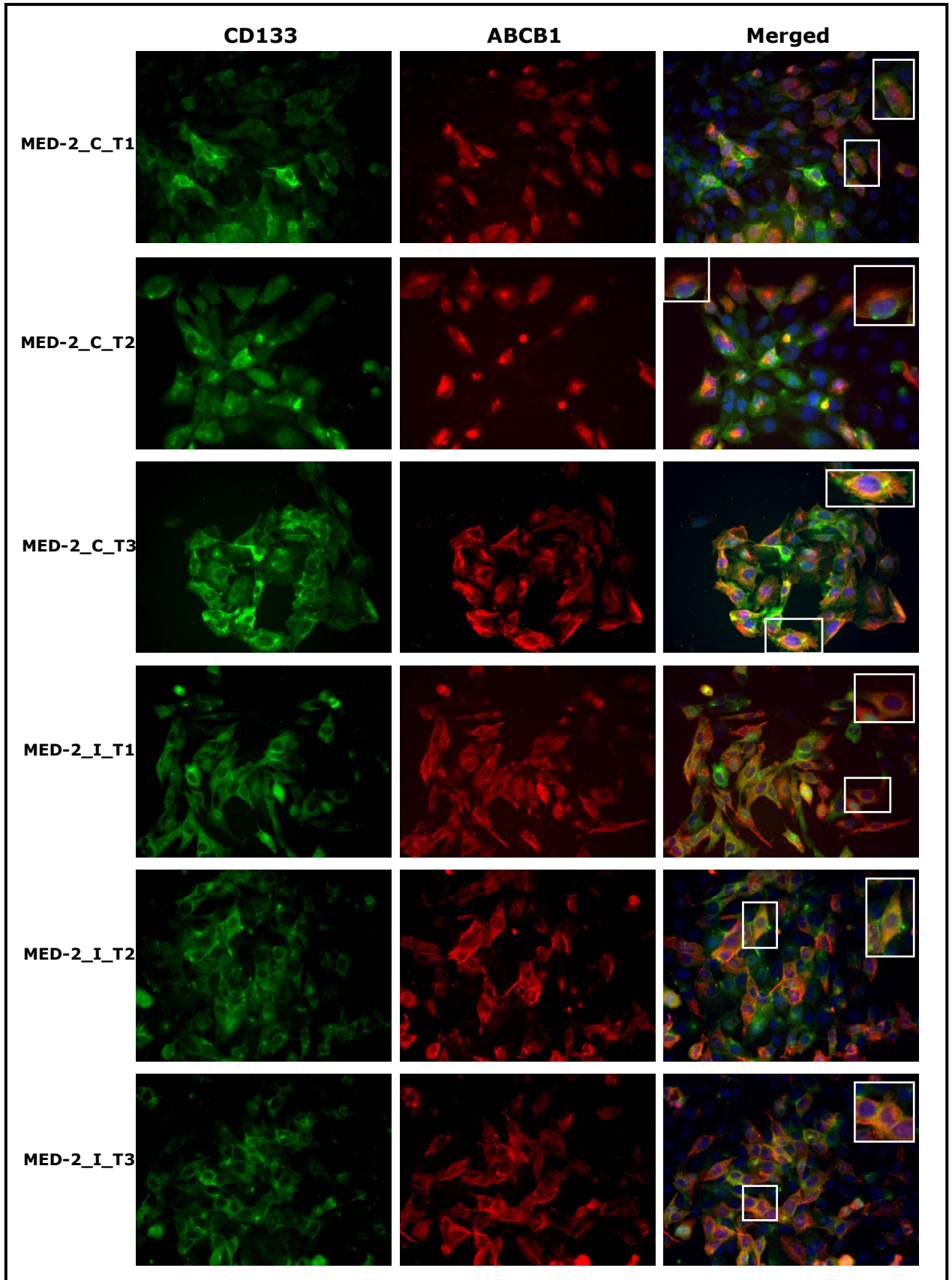


**Figure A3.4 Co-staining CD133 and ABCB1 immunofluorescence in the selected MED-2 sublines treated for less than 10 passages.** All selected MED-2 sublines expressed high levels of CD133 and ABCB1 and contained a high proportion of CD133 and ABCB1 co-expressing cells. Similar to previous co-staining immunofluorescence results, after the first round of treatment, cells co-expressing CD133 and ABCB1 were detected in MED-2 monolayers after cisplatin and irinotecan treatment. For each treatment a co-staining cell has been enlarged (x2) for clarity.

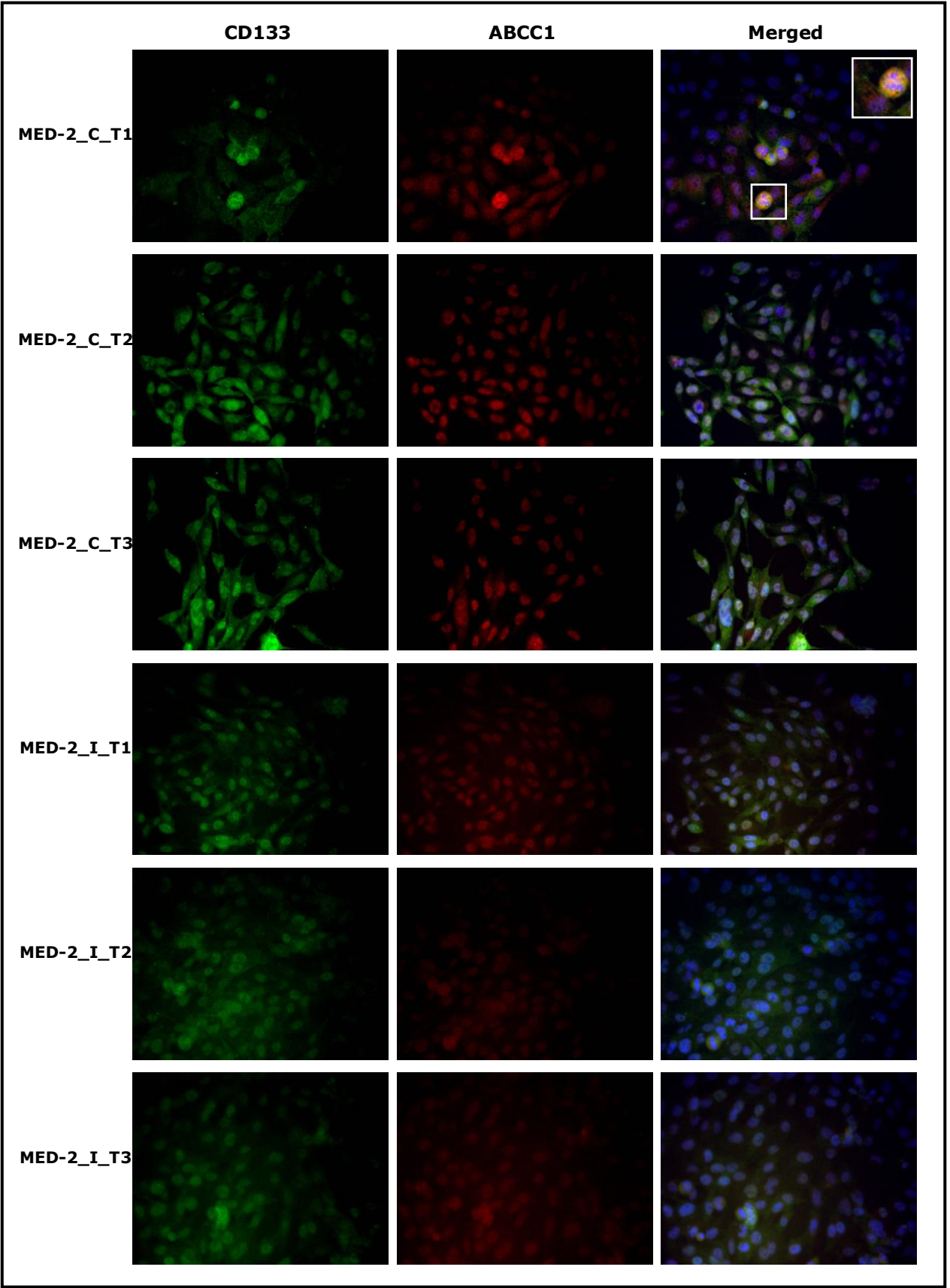


**Figure A3.5 Co-staining CD133 and ABCC1 immunofluorescence in the selected MED-2 sublines treated for less than 10 passages.** Co-staining immunofluorescence results previously showed no cells co-expressing CD133 and ACBC1 in MED-2 monolayers after the first round of cisplatin and irinotecan treatment. After multiple rounds of treatment, all selected MED-2 sublines were still negative for CD133 and ABCC1 co-staining with the exception of MED-2\_C\_T1 subline, which contained some cells expressing CD133 and ABCC1. For each treatment a co-staining cell has been enlarged (x2) for clarity.



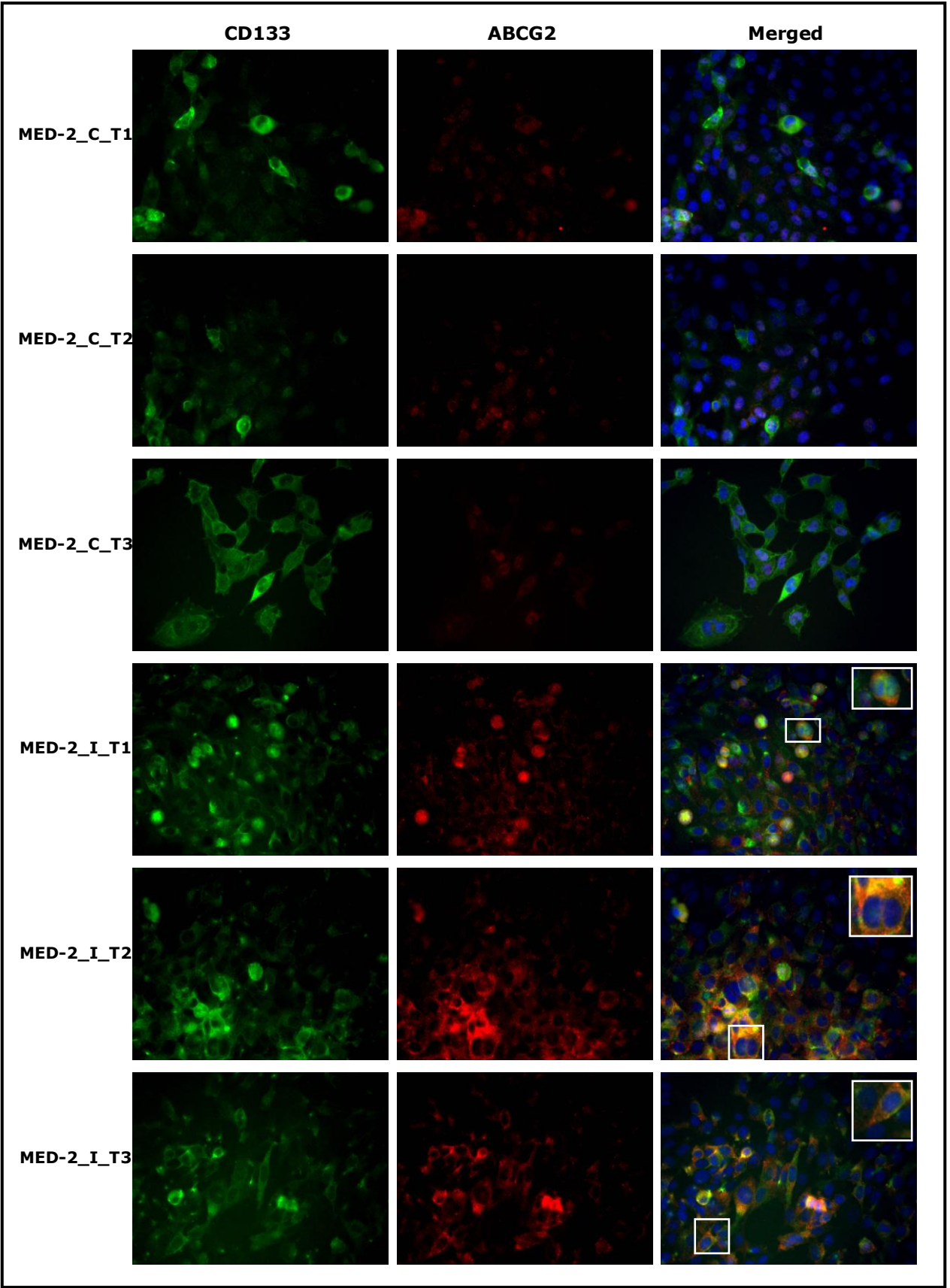


**Figure A3.6 Co-staining CD133 and ABCG2 immunofluorescence in the selected MED-2 sublines treated for less than 10 passages.** Similar to the previous immunofluorescence after the first round of treatment, the selected cisplatin MED-2 sublines were negative for CD133 and ABCG2 co-staining. However, cells expressing CD133 were still observed in all selected MED-2 sublines. Interestingly, CD133 and ABCG2 co-expressed cells were detected in all selected irinotecan MED-2 sublines while they were previously negative for CD133 and ABCG2 co-staining after the first round of treatment. For each treatment a co-staining cell has been enlarged (x2) for clarity.

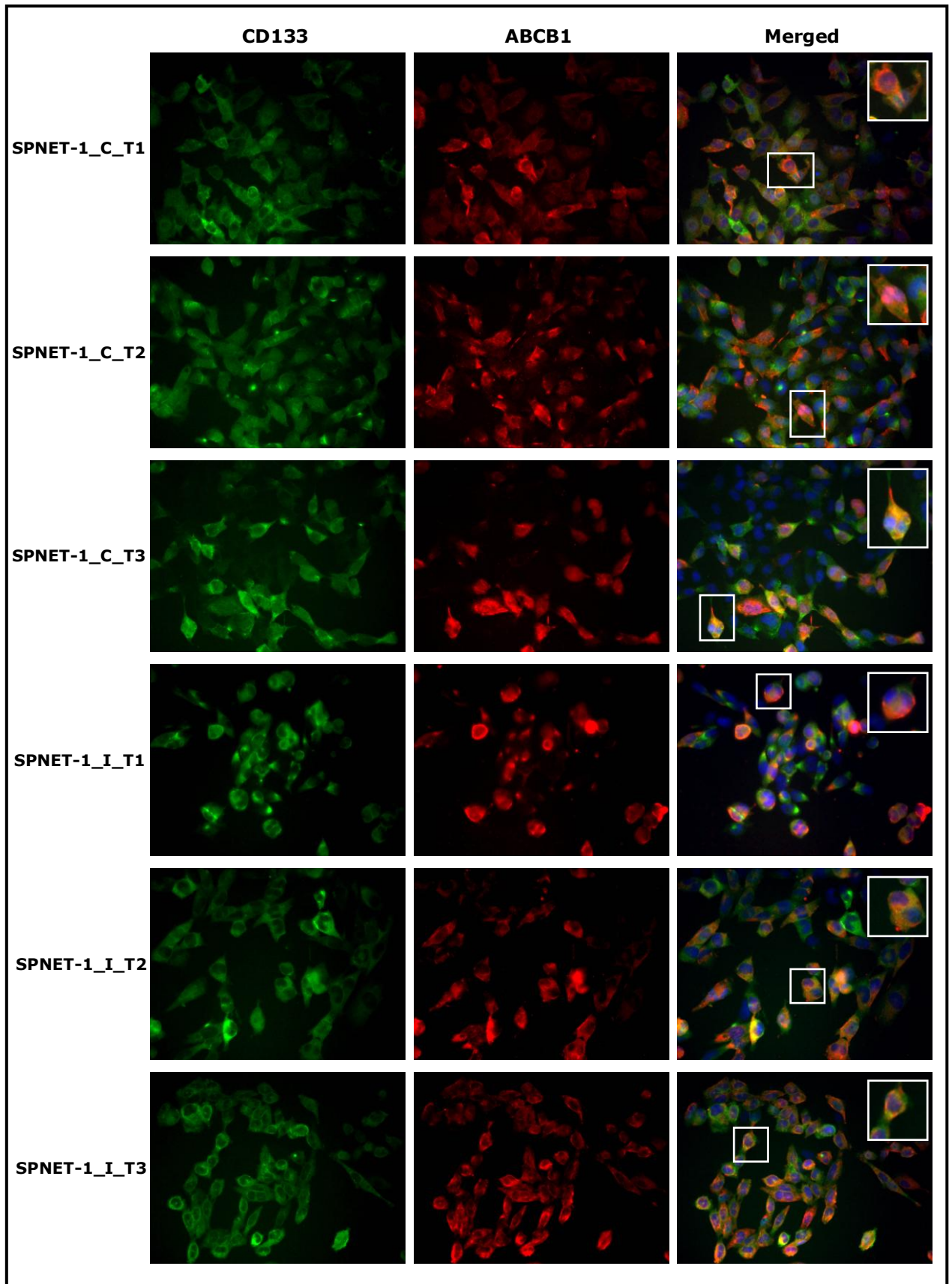




**Figure A3.7 Co-staining CD133 and ABCB1 immunofluorescence in the selected SPNET-1 sublines treated for less than 10 passages.** CD133 and ABCB1 co-expressed cells were obviously observed in all selected SPNET-1 sublines and they were consistently detected at a high level of expression after the first round of treatment. For each treatment a co-staining cell has been enlarged (x2) for clarity.

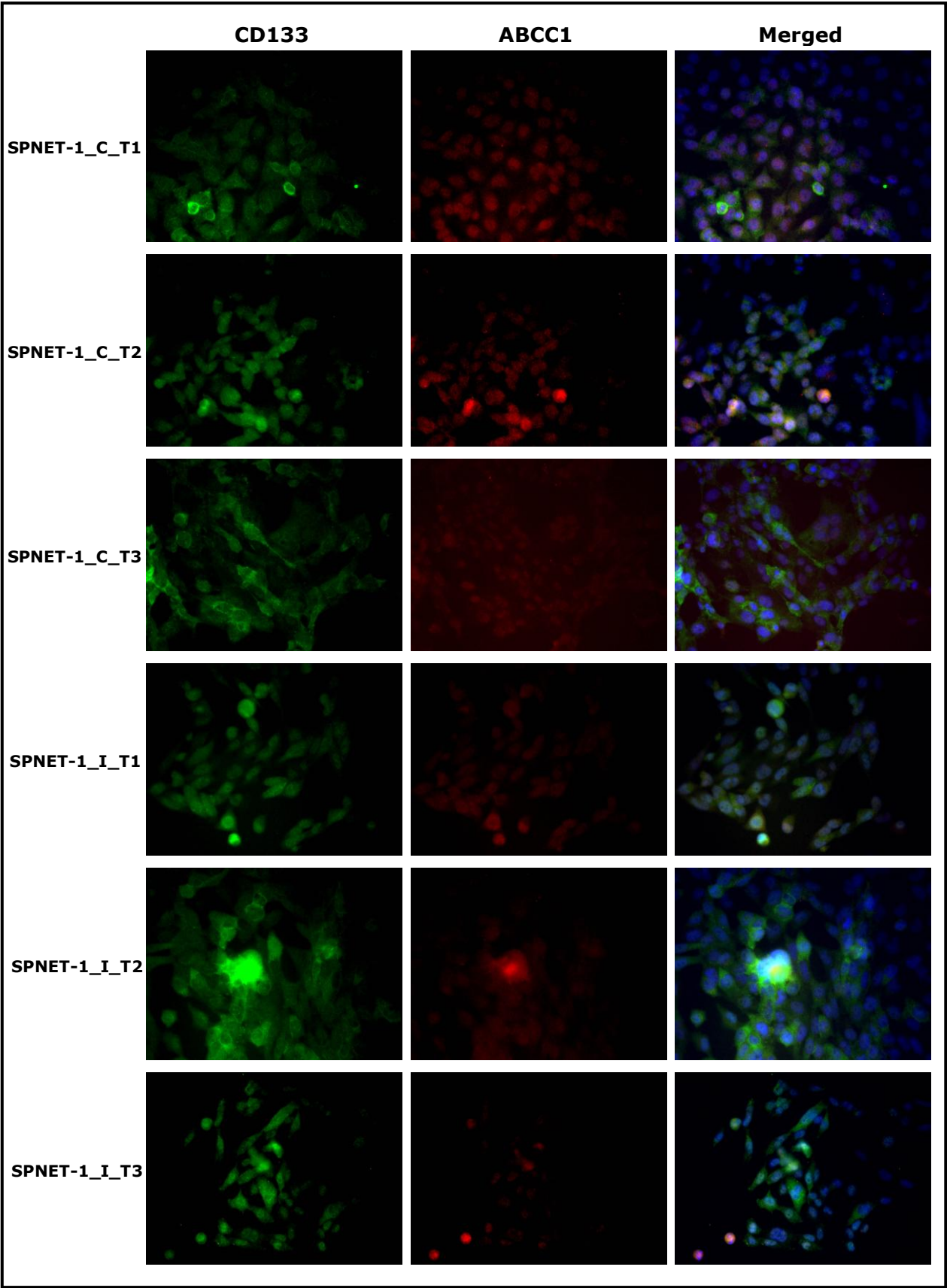


**Figure A3.8 Co-staining CD133 and ABCC1 immunofluorescence in the selected SPNET-1 sublines treated for less than 10 passages.** All selected SPNET-1 sublines were negative for CD133 and ABCC1 co-staining whilst SPNET-1 monolayers treated with irinotecan previously expressed a low level of CD133 and ABCC1 expression after the first round of treatment. CD133 expression was still observed in all sublines.

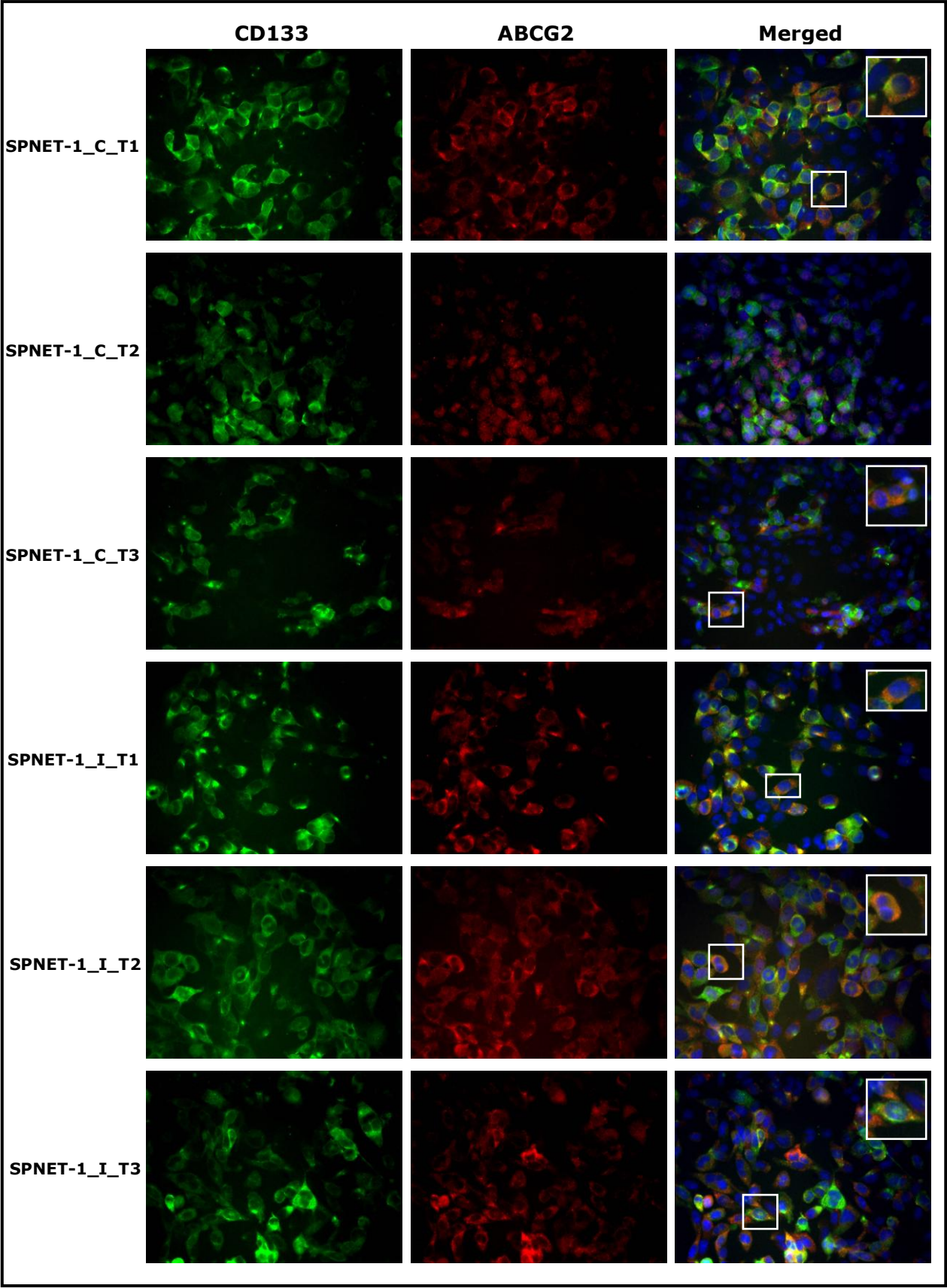


**Figure A3.9 Co-staining CD133 and ABCG2 immunofluorescence in the selected SPNET-1 sublines treated for less than 10 passages.** After the first round of treatment, the immunofluorescence results showed that cisplatin and irinotecan treated SPNET-1 monolayers were definitely negative for CD133 and ABCG2 co-staining. After multiple rounds of treatment, cells co-expressing CD133 and ABCG2 were however detected in all selected SPNET-1 sublines with the exception of SPNET-1\_C\_T2 subline, which was just CD133 positive. For each treatment a co-staining cell has been enlarged (x2) for clarity.

**A4: Co-staining immunofluorescence in the selected sublines after repeat treatment at later passage (more than 10 passages)**

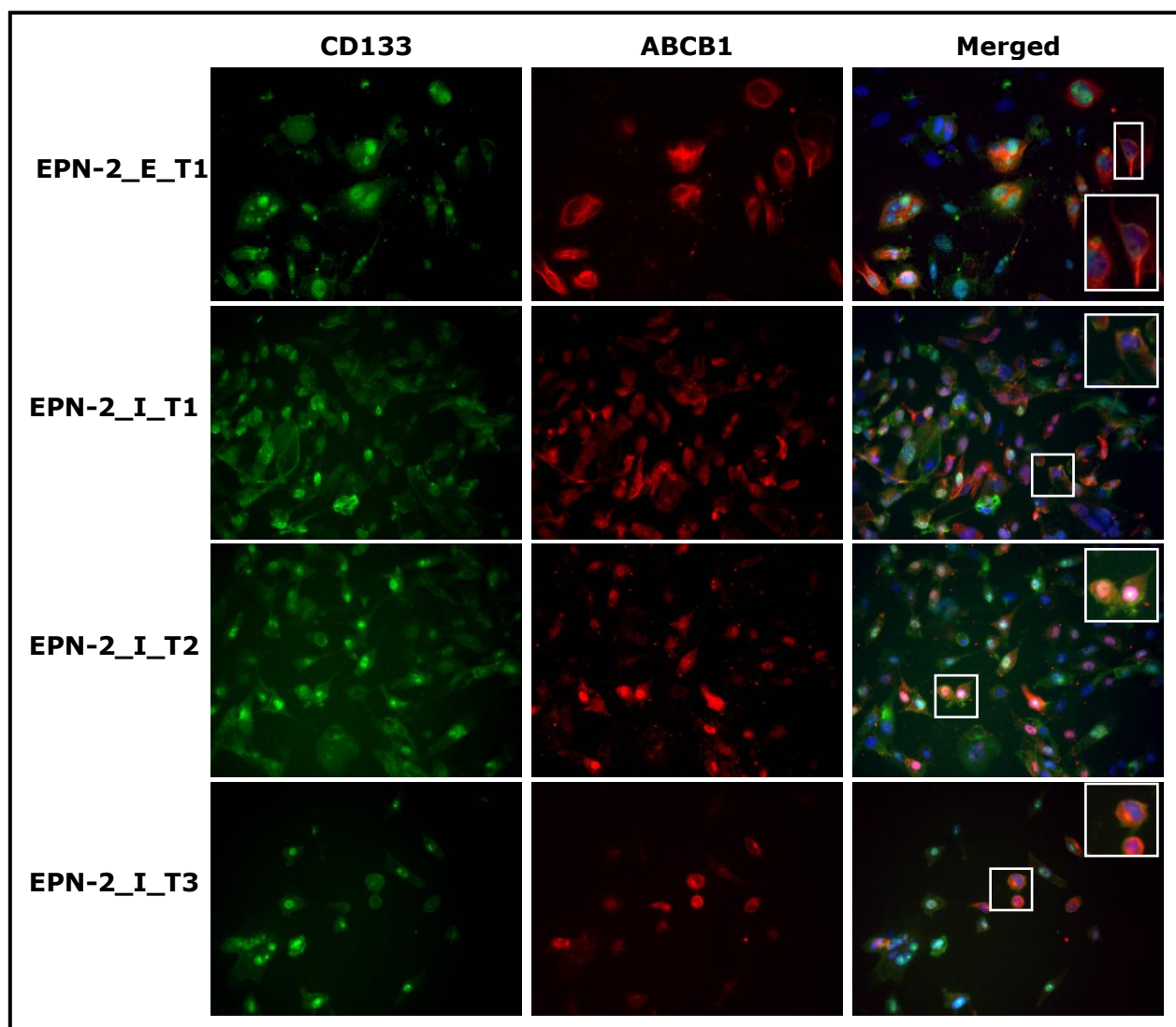


**Figure A4.1 Co-staining CD133 and ABCB1 immunofluorescence in the selected EPN-2 sublines treated for more than 10 passages.** After repeat treatment for more than 10 passages, a high level of CD133 and ABCB1 expression and a high proportion of cells expressing CD133 and ABCB1 were consistently observed in all selected EPN-2 sublines. For each treatment a co-staining cell has been enlarged (x2) for clarity.



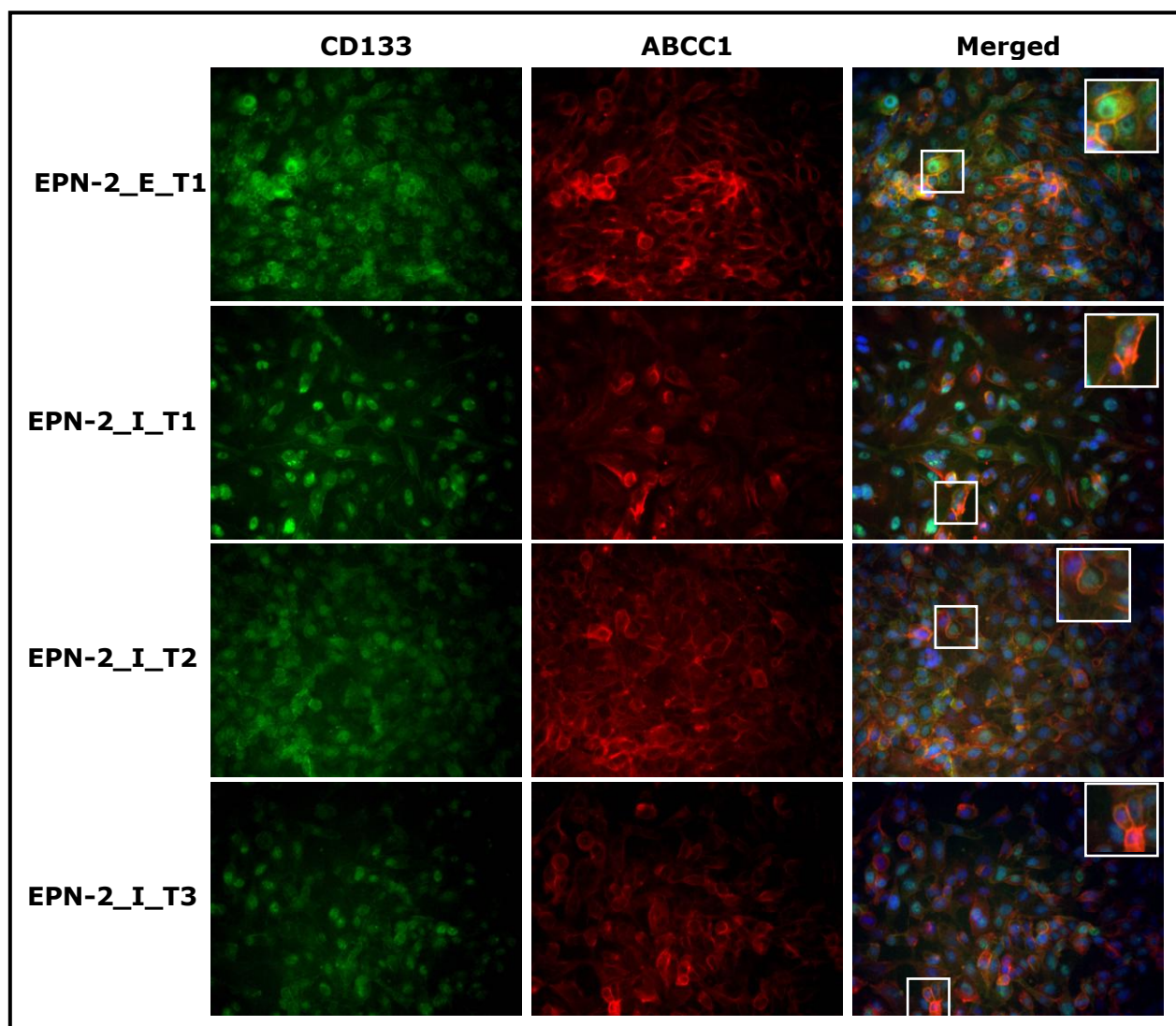


**Figure A4.2 Co-staining CD133 and ABCC1 immunofluorescence in the selected EPN-2 sublines treated for more than 10 passages.** Previous co-staining immunofluorescence results showed that all selected EPN-2 sublines were negative for CD133 and ABCC1 co-staining. However, all those sublines now obviously expressed a high level of CD133 and ABCC1 and comprised a high proportion of cells co-expressing CD133 and ABCC1 after prolonged treatment. For each treatment a co-staining cell has been enlarged (x2) for clarity.

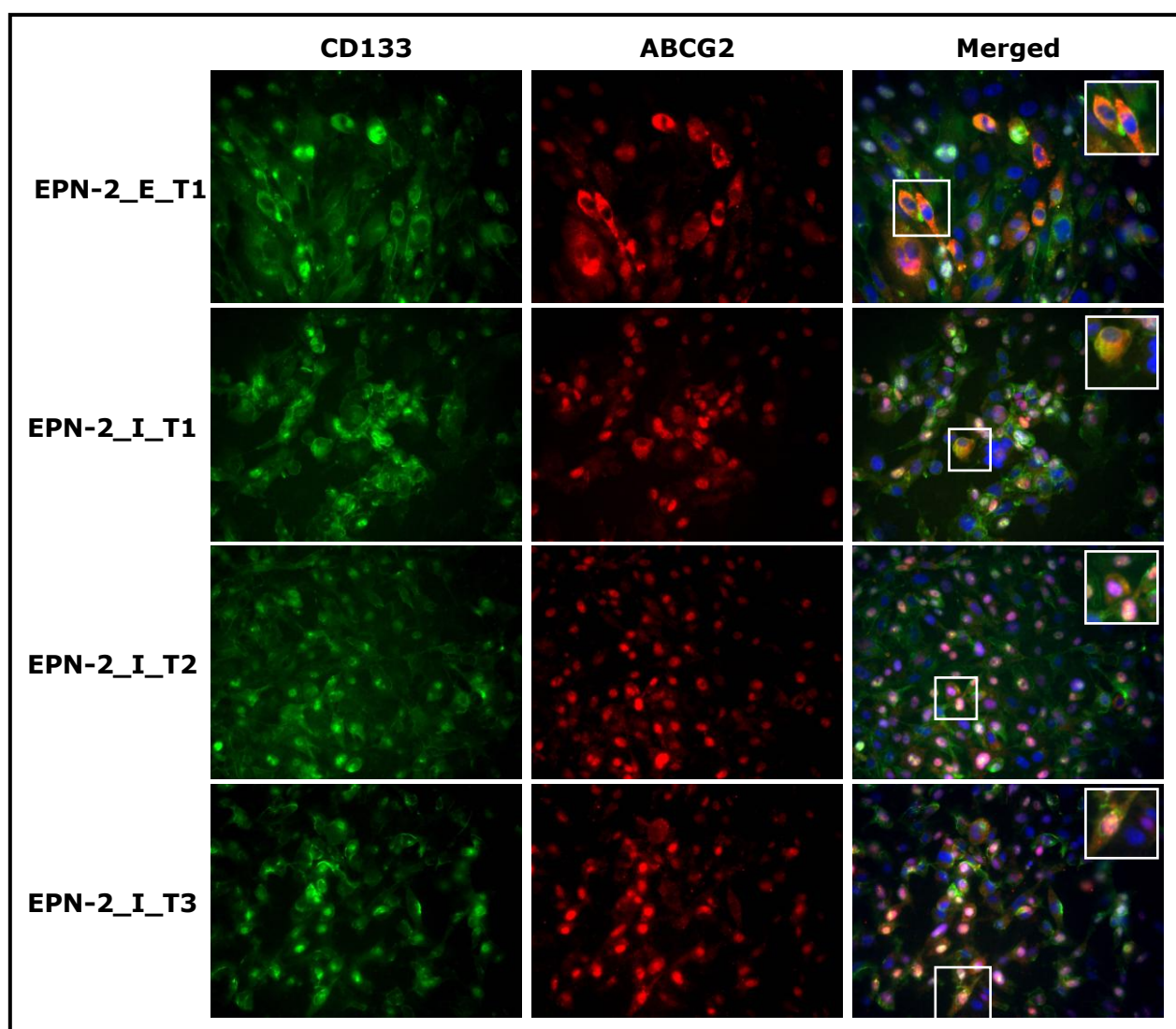


**Figure A4.3 Co-staining CD133 and ABCG2 immunofluorescence in the selected EPN-2 sublines treated for more than 10 passages.** Similar to the previous immunofluorescence results, cells co-expressing CD133 and ABCG2 were detected in all selected EPN-2 sublines. For each treatment a co-staining cell has been enlarged (x2) for clarity.



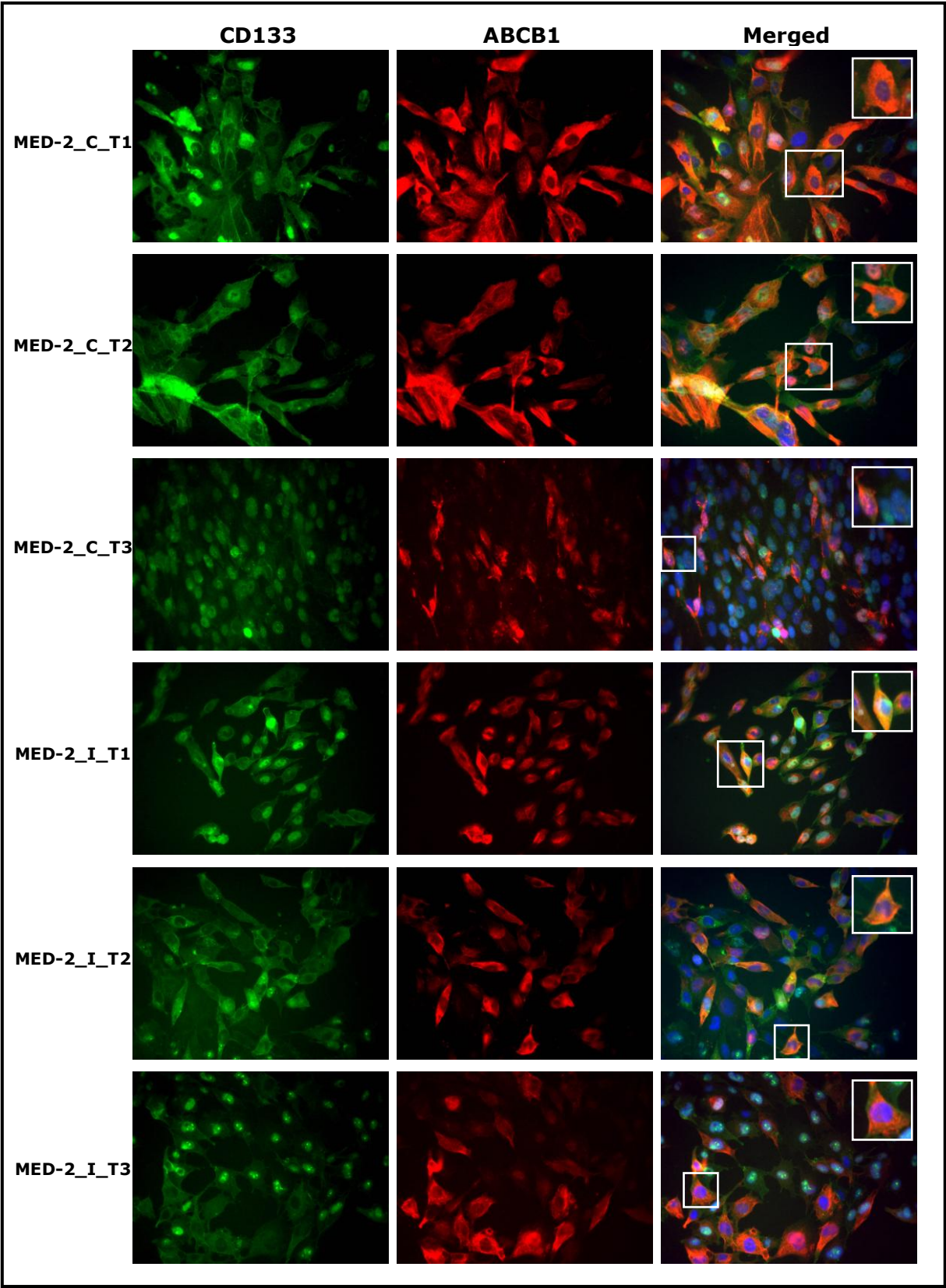


**Figure A4.4 Co-staining CD133 and ABCB1 immunofluorescence in the selected MED-2 sublines treated for more than 10 passages.** After multiple rounds of treatment for more than 10 passages, cells co-expressing CD133 and ABCB1 at a high level were consistently observed in all selected MED-2 sublines. Additionally, a high proportion of cells co-expressing CD133 and ABCB1 was also observed. For each treatment a co-staining cell has been enlarged (x2) for clarity.

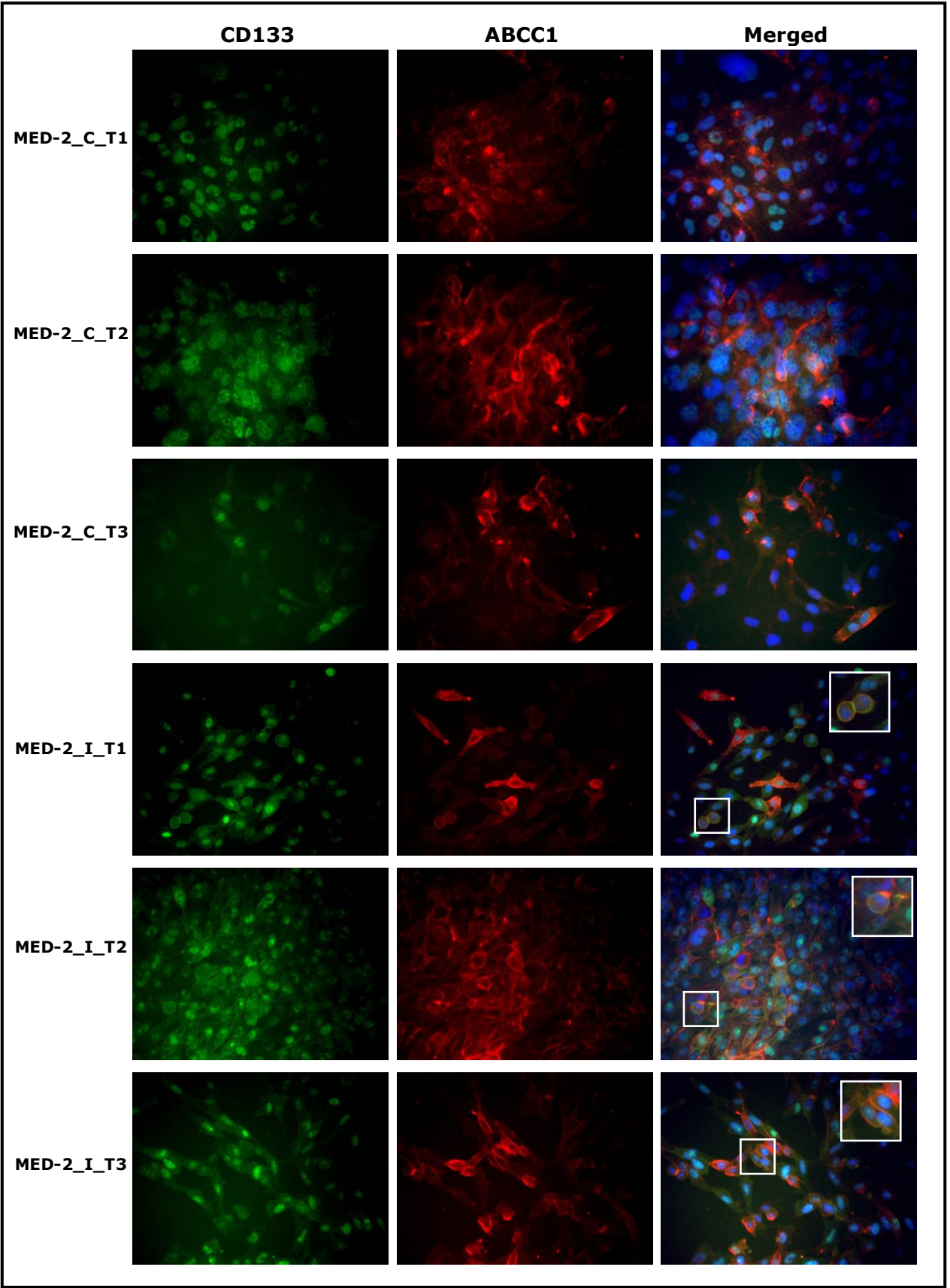


**Figure A4.5 Co-staining CD133 and ABCC1 immunofluorescence in the selected MED-2 sublines treated for more than 10 passages.** CD133 and ABCC1 co-expressing cells were observed in all selected irinotecan MED-2 sublines whereas all selected cisplatin MED-2 sublines expressed ABCC1, which was not co-stained with CD133. For each treatment a co-staining cell has been enlarged (x2) for clarity.



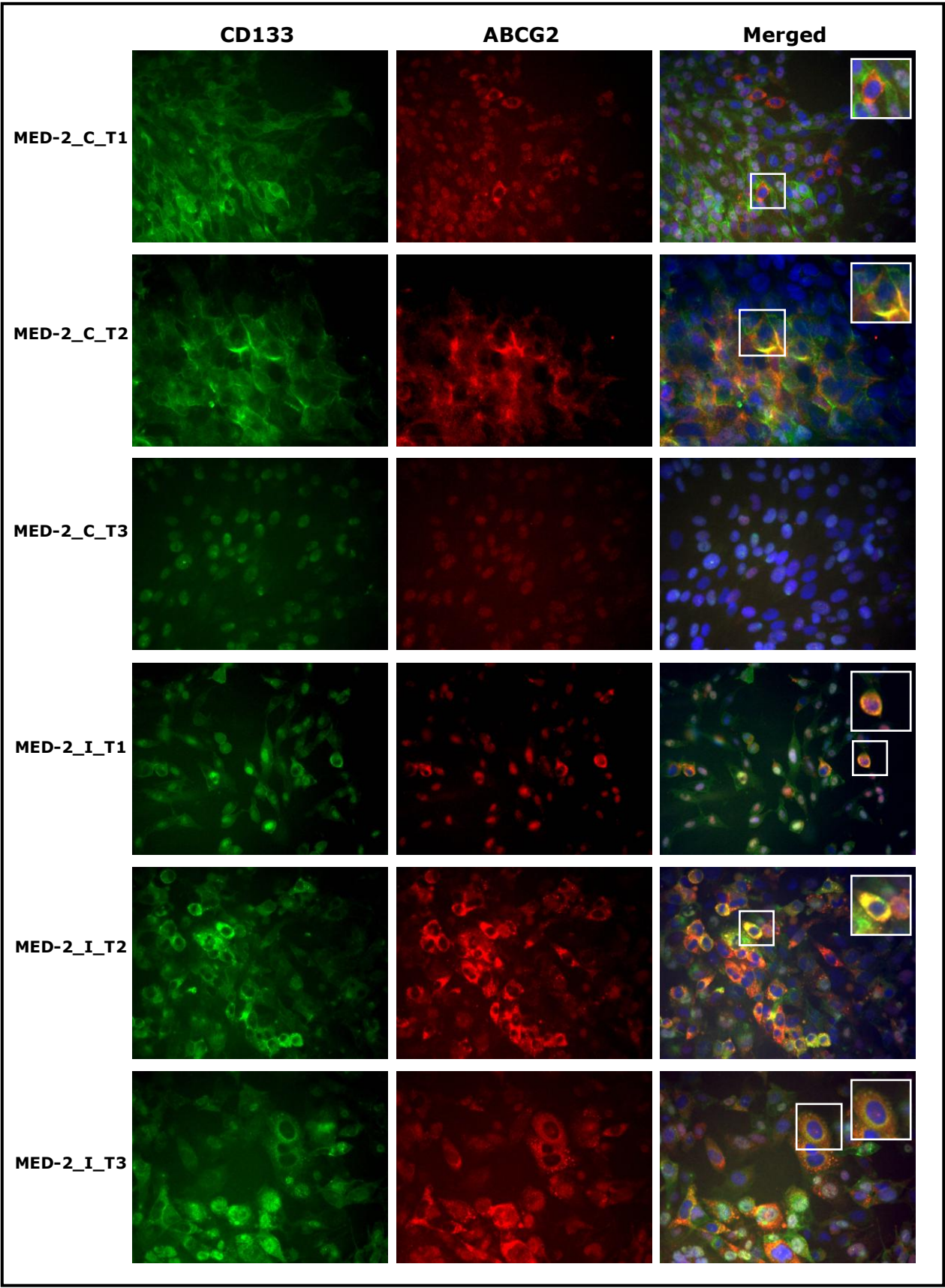


**Figure A4.6 Co-staining CD133 and ABCG2 immunofluorescence in the selected MED-2 sublines treated for more than 10 passages.** A high level of CD133 and ABCG2 co-expression was detected in all selected MED-2 sublines with the exception of MED-2\_C\_T3 subline. A high proportion of cells expressing CD133 and ABCG2 was observed in the selected irinotecan MED-2 sublines. For each treatment a co-staining cell has been enlarged (x2) for clarity.

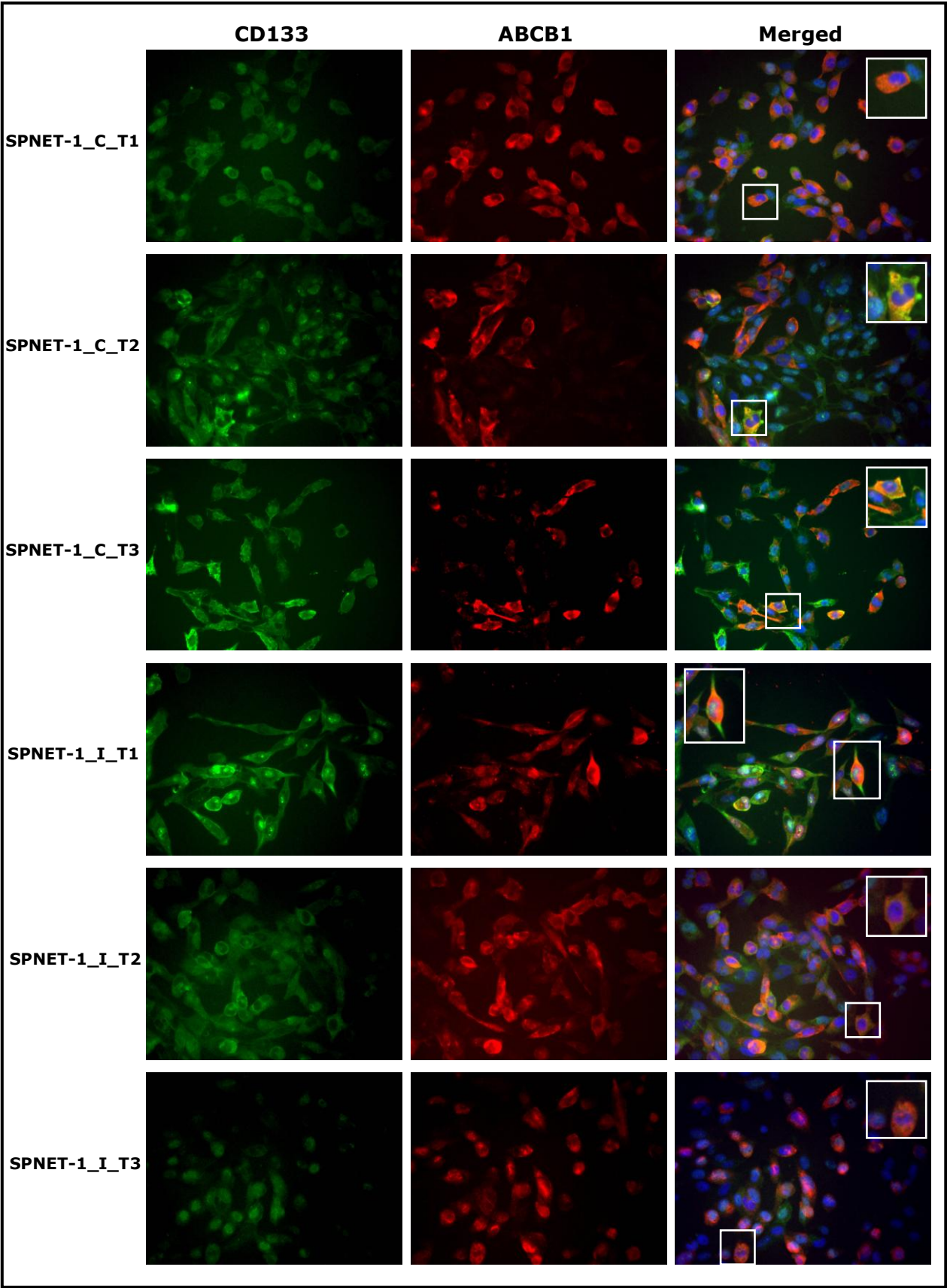


**Figure A4.7 Co-staining CD133 and ABCB1 immunofluorescence in the selected SPNET-1 sublines treated for more than 10 passages.** Cells co-expressing CD133 and ABCB1 were consistently detected at high level of co-expression in all selected SPNET-1 sublines and those sublines also comprised a high proportion of cells co-expressing CD133 and ABCB1. For each treatment a co-staining cell has been enlarged (x2) for clarity.



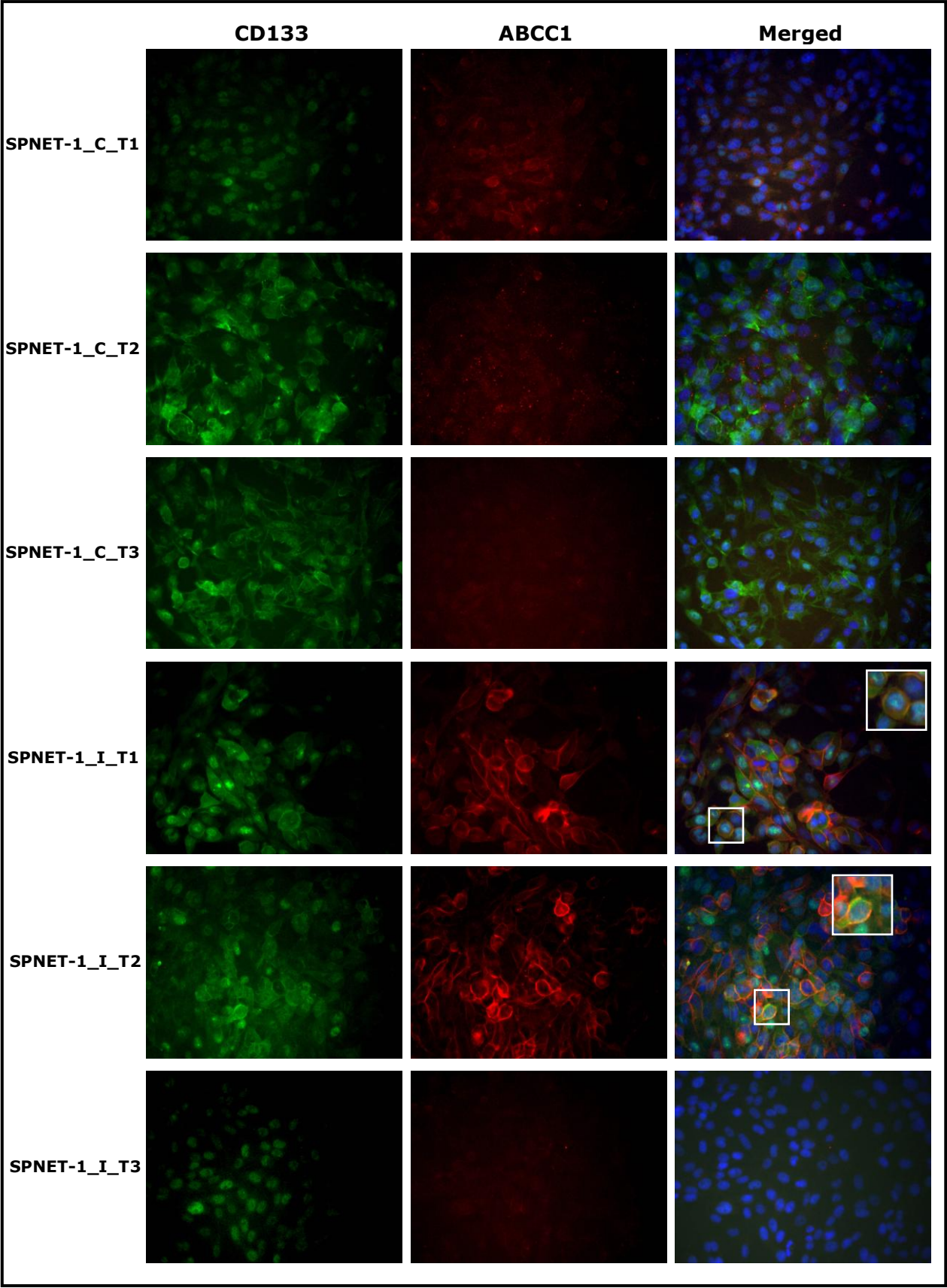


**Figure A4.8 Co-staining CD133 and ABCC1 immunofluorescence in the selected SPNET-1 sublines treated for more than 10 passages.** Most of selected SPNET-1 sublines were negative for CD133 and ABCC1 co-staining whilst SPNET-1\_I\_T1 and SPNET-1\_I\_T2 sublines co-expressed CD133 and ABCC1 at a high level. For each treatment a co-staining cell has been enlarged (x2) for clarity.

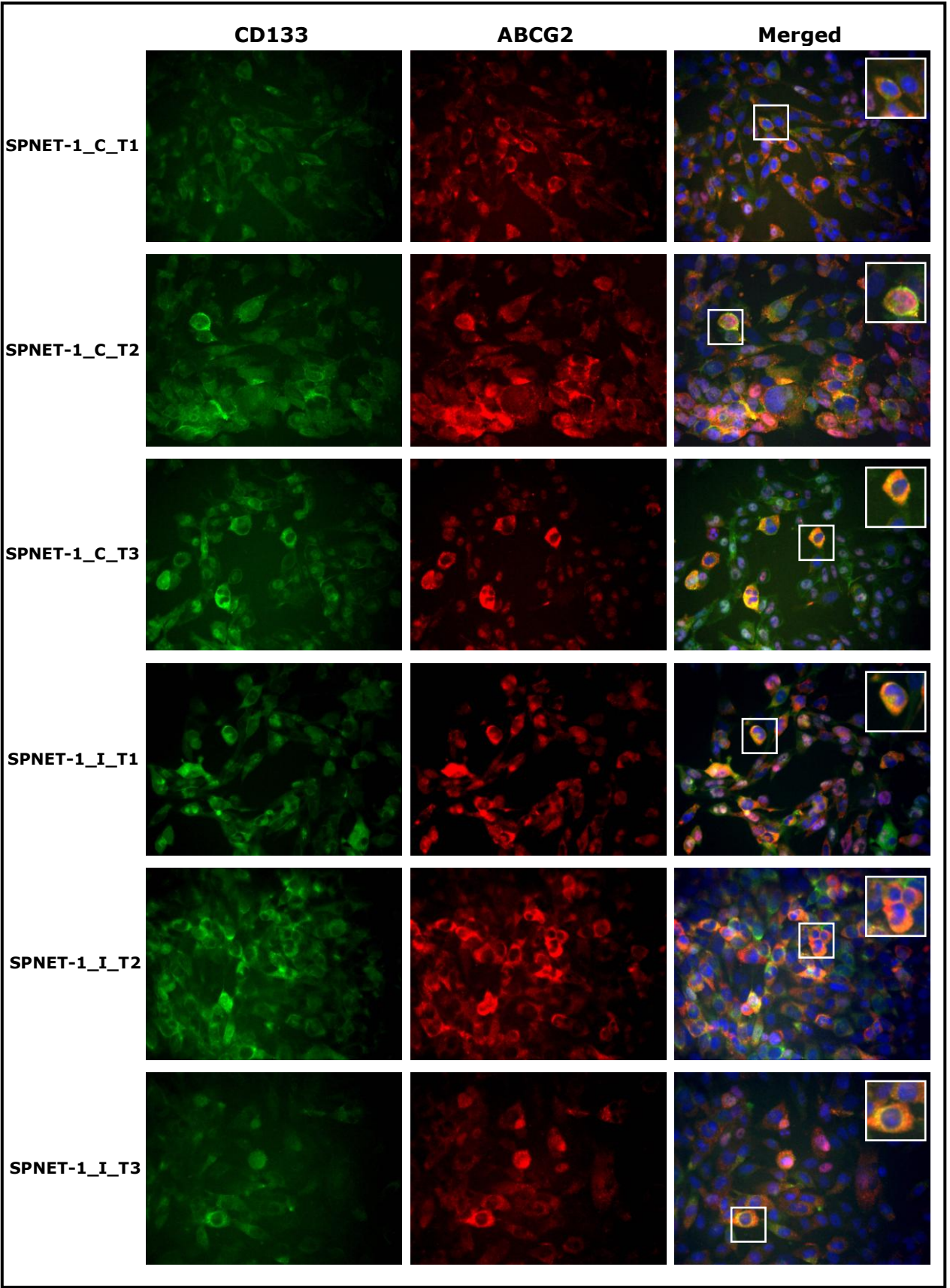


**Figure A4.9 Co-staining CD133 and ABCG2 immunofluorescence in the selected SPNET-1 sublines treated for more than 10 passages.** Similar to previous immunofluorescence results, which were performed on cells, treated for less than 10 passages, a high level of CD133 and ABCG2 co-expression and a high proportion of CD133 and ABCG2 co-expressing cells were observed in all selected SPNET-1 sublines. For each treatment a co-staining cell has been enlarged (x2) for clarity.

## Appendix B: Materials and Methods

### B1: Cell culture

**Table B1.1 Cell culture media**

Media	Composition
<b>1. Stem cell media</b>	- 5% of 1× Heparin (Sigma, T1027) + 2% of B27 (Fisher, 17504-044) + 23.4% of F12 (Gibco, 21765) in High glucose Dulbecco's Modified Eagle's Medium (DMEM) (Sigma, D6429) - <b>Before use:</b> 20 ng/ml of both Fibroblast Growth Factor (FGF) (Invitrogen, PHG0026) and Epidermal Growth Factor (EGF) (Fisher, 13247-051) were added to stem cell media
<b>2. Tumour media</b>	- 15% of Fetal Bovine Serum (FBS) (Fisher, VX10108-165) + 1% of L-glutamine (Fisher, VX25030-024) in 500 ml of Low glucose Dulbecco's Modified Eagle's Medium (DMEM) (Sigma, D6429)
<b>3. PFSK media</b>	- 10-15% of Fetal Bovine Serum (FBS) (Fisher, VX10108-165) in 500 ml of RPMI 1640 medium with L-glutamine (Sigma, R8758)
<b>4. NTERA media</b>	- 10% of FBS in 500 ml of High glucose DMEM - <b>Before use:</b> 1:100 Gentamicin was added to NTERA media

### B2: Immunofluorescence analysis

**Table B2.1 Solution for fixation**

Solutions	Composition
<b>1. Fixative reagent</b>	- 0.4% Paraformaldehyde (PFA) in HBSS
<b>2. Resuspended solution for NS</b>	- 30% Sucrose in HBSS

**Table B2.2 Solution for immunofluorescent staining**

Solutions	Composition
<b>1. Blocking reagent for membranous antigen</b> (single staining)	- 5% Normal Goat Serum (NGS) (Vector, S-1000) in Phosphate Buffer Saline (PBS)
<b>2. Blocking reagent for internal antigen</b> (single staining)	- 5% NGS + 0.25% Triton X-100 (Sigma, T9284) in PBS
<b>3. Blocking reagent for double staining</b>	- 10% NGS + 1% Bovine serum albumin (BSA) (Sigma, B4287) + 0.1% Triton X-100 in PBS
<b>4. Antibody solution for membranous antigen</b>	- 2% NGS in PBS
<b>5. Antibody solution for internal antigen</b>	- 2% NGS + 0.1% Triton X-100 in PBS
<b>6. Antibody solution for double staining</b>	- 2% NGS + 0.1% Triton X-100 + 1% BSA in PBS
<b>7. Washing solution for single staining</b>	- PBS
<b>8. Washing solution for double staining</b>	- 1% BSA in PBS or PBS

### B3: Western blot analysis

**Table B3.1 General solution for Western blotting analysis**

Solutions	Compositions
<b>1. Protease cocktail inhibitor (50X concentration)</b>	- 1 tablet of Complete mini protease inhibitor (Roche, 10946900) dissolved in 200µl of distilled water
<b>2. Lysis buffer for standard protein extraction</b>	- 150 mM of NaCl + 50 mM of Tris + 0.1% SDS (W/V) + 1% Triton X-100
<b>3. Lysis buffer for microsomal membrane extraction</b>	- 250mM of sucrose + 10mM of Tris pH7.4 + 0.2mM of CaCl <sub>2</sub>
<b>4. Lower gel buffer</b>	- 1.5M of Tris + 0.4% of SDS then filtered through 0.45µm filter, pH8.8
<b>5. Upper gel buffer</b>	- 0.5M of Tris + 0.4% of SDS then filtered through 0.45µm filter, pH6.7
<b>6. Electrode buffer</b>	- 25mM of Tris + 193mM of Glycine + 1% of SDS
<b>7. Transfer buffer</b>	- 25mM of Tris + 193mM of Glycine + 20% Methanol
<b>8. 10X Tris buffered saline (TBS)</b>	- 20mM of Tris + 135mM of NaCl ** pH 7.6
<b>9. TBS-T</b>	- 1X TBS + 0.1% Tween (MERCK, 437082Q)
<b>10. Blocking solution</b>	- 5% of Dried semi skimmed milk power (Marvel) in TBS-T solution
<b>11. Sample buffer</b>	- 0.76% of Tris + 15% of Glycerol + 2% of SDS + 5% of β-mercaptoethanol + 0.05% of Bromophenol blue pH 6.8

**Table B3.2 Lower gel (Resolving gel)**

Chemicals	Percentage of lower gel				
	5%	7%	10%	13%	15%
<b>Lower gel buffer</b>	1ml	1ml	1ml	1ml	1ml
<b>Acrylamide</b> (Severn Biotech, 20-2100-05)	0.67ml	0.93ml	1.33ml	1.73ml	2ml
<b>dH<sub>2</sub>O</b>	2.33ml	2.07ml	1.67ml	1.27ml	1ml
<b>10%APS</b> (Sigma, A3678)	25µl	25µl	25µl	25µl	25µl
<b>Temed</b>	3.3µl	3.3µl	3.3µl	3.3µl	3.3µl

**Table B3.3 Upper gel (Stacking gel)**

Chemicals	Amount of gel			
	X1	X2	X3	X4
<b>Upper gel buffer</b>	625 µl	1,250 µl	1,875 µl	2,500 µl
<b>Acrylamide</b>	312 µl	624 µl	936 µl	1,248 µl
<b>dH<sub>2</sub>O</b>	1,500 µl	3,000 µl	4500 µl	6,000 µl
<b>10% APS</b>	12.5 µl	25 µl	37.5 µl	50 µl
<b>Temed</b>	2.5 µl	5 µl	7.5 µl	10 µl

**B4: DNA extraction****Table B4.1 Lysis buffer**

Solutions	Compositions
<b>1. DNA lysis buffer (500 ml)</b>	- 50mM Tris, pH 8.0 + 100mM EDTA, pH 8.0 + 1% SDS + 100mM NaCl in 500 ml distilled water

**B5: TRF assay****Table B5.1 Solution for TRF assay**

Solutions	Compositions
<b>1. Denaturing solution</b> (1 litre)	- 1.5M NaCl + 0.5M NaOH in 1 litre distilled water
<b>2. Neutralising solution</b> (2 litres)	- 0.5M Tris + 1.5M NaCl in 2 litres distilled water
<b>3. 20x SSC</b> (1 litre)	- 3M NaCl + 0.3M Tri-Sodium Citrate in 1 litre distilled water
<b>4. 1x TAE</b>	- 40 mM Tris-acetate + 1mM EDTA <b>50x TAE:</b> 242 g of Tris base + 57.1 ml of glacial acetic acid in 100 ml of 0.5 M EDTA (pH 8.0)
<b>5. Washing buffer</b> (100 ml)	- 10 ml TRF solution (#1) (DIG wash & block buffer set 1, 10 conc.) + 90 ml distil water
<b>6. Blocking solution</b> (200 ml)	- 20 ml TRF solution (#2)* (DIG wash & block buffer set 2, 10 conc.) + 20 ml blocking serum + 160 ml distil water
<b>7. Anti-DIG-AP solution</b> (100 ml)	- 100 ml blocking solution* + 10 µl of anti-DIG-AP*
<b>8. Detection solution</b> (100 ml)	- 10 ml TRF solution (#4)* + 90 ml distil water

(\* Supplied with Telo TAGGG Telomere Length assay kit (Roche, 12209136001)

**B6: TRAP assay****Table B6.1 Solution for TRAP assay**

<b>Solutions</b>	<b>Compositions</b>
<b>1. Coomassie reagent</b>	- 0.05% Coomassie G-250 powder + 25% ethanol + 50% Perchloric acid
<b>2. 5xTBE (Tris-borate) buffer</b>	- 5.4% Tris + 2.75% Boric acid + 10mM Na <sub>2</sub> EDTA (pH 8.0) in distilled water <i>*Filter through 0.45 µm filter*</i>
<b>3. 1xTE buffer</b>	- 10 mM Tris (pH 8.0, 7.6 or 7.4) + 1 mM Na <sub>2</sub> EDTA (pH 8.0) in distilled water <i>*Store at room temperature*</i>
<b>4. 10% Polyacrylamide gel</b>	- 40% Acrylamide mix (Fisher Scientific, BP1406-1) + 10% 0.5xTBE buffer + 0.1% TEMED + 0.1% APS in nuclease free water
<b>5. Gel running buffer</b>	- 0.5xTBE buffer
<b>6. DNA molecular marker</b>	- 1.25% DNA marker VIII (Roche, 11336045001) + 18.75% loading buffer in nuclease free water
<b>7. Staining solution</b>	- 0.01% SyBR Green1 in 1x TE buffer

**B7: FACS functional analysis****Table B7.1 Buffer for FACS**

<b>Solutions</b>	<b>Compositions</b>
<b>1. FACS buffer</b>	- 0.5% BSA (albumin bovine serum) in Delbucco's modified Eagle's medium (DMEM) with 1000mg glucose without phenol red (Sigma, D5921)
<b>2. 10 mM EDTA</b>	- 372 g of EDTA in 100 ml of DPBS